

Altair® AcuSolve® 2025

Altair AcuSolve Validation Manual

Updated: 11/14/2024

Contents

AcuSolve Validation Manual 6

Turbulent Flow 8

Single-Phase Nucleate Boiling in a Rectangular Channel 9
Turbulent Flow Through a Pipe 14
Turbulent Flow Behind an Open-Slit V 18
Turbulent Flow with Separation in an Asymmetric Diffuser 25
Turbulent Flow Over a Backward-Facing Step 33
Turbulent Flow Past a Convex Curve in a Channel 40
Turbulent Natural Convection Inside a Tall Cavity 47
Turbulent Flow Over a NACA 0012 Airfoil 55
Turbulent Flow Through a 180 Degree Curved Channel 63
Turbulent Flow Through a Wavy Channel 69
Turbulent Flow Through a Heated Periodic Channel 77
Turbulent Mixing Layers in an Open Channel 83
Two-Phase Nucleate Boiling in a Cylindrical Pipe 88
Supersonic Flow Through a Converging-Diverging Nozzle 92
Turbulent Flow Past a Wall-Mounted Hump 97
Turbulent Flow Over an Oscillating Rigid Body Assembly 104

Steady Flow 111

Flow Between Concentric Cylinders 112
Turbulent Flow Through a Pipe 118
Laminar Couette Flow with Imposed Pressure Gradient 122
Flow Inside a Rotating Cavity 128
Natural Convection in a Concentric Annulus 136
Laminar Flow Past a 90° T-Junction 142
Laminar Flow Through a Channel with Heated Walls 147
Turbulent Flow Behind an Open-Slit V 152
Turbulent Flow Over a NACA 0012 Airfoil 159
Turbulent Natural Convection Inside a Tall Cavity 167
Viscous Heating Inside a Rotating Annulus 175
Separated Laminar Flow Over a Blunt Plate 183
Turbulent Flow with Separation in an Asymmetric Diffuser 190
Turbulent Flow Over a Backward-Facing Step 198
Turbulent Flow Past a Convex Curve in a Channel 205
Heat Transfer Between Radiating Concentric Cylinders 212
Turbulent Mixing Layers in an Open Channel 218

Laminar to Turbulent Transition Over an Airfoil....223
Turbulent Flow Through a 180 Degree Curved Channel.... 228
Heat Transfer Between Radiating Concentric Spheres.... 234
Single-Phase Nucleate Boiling in a Rectangular Channel.... 239
Turbulent Flow Past a Wall-Mounted Hump.... 244
Turbulent Flow Through a Heated Periodic Channel....251
Laminar Couette Flow with Imposed Pressure Gradient and Heated Walls....257

Laminar Flow....263

Circumferential Flow in a Cylinder Induced by a Rotating Solid....264
Laminar Couette Flow with Imposed Pressure Gradient.... 270
Flow Inside a Rotating Cavity.... 276
Laminar Flow Past a 90° T-Junction....284
Laminar Poiseuille Flow Through a Pipe....289
Oscillating Laminar Flow Around a Circular Cylinder....293
Separated Laminar Flow Over a Blunt Plate....298
Natural Convection in a Concentric Annulus....305
Flow Between Concentric Cylinders....311
Heat Transfer Between Radiating Concentric Cylinders....317
Laminar Couette Flow with Imposed Pressure Gradient and Heated Walls....323

Internal Flow....329

Flow Between Concentric Cylinders....330
Turbulent Flow Through a Pipe....336
Laminar Couette Flow with Imposed Pressure Gradient.... 340
Flow Inside a Rotating Cavity.... 346
Natural Convection in a Concentric Annulus....354
Laminar Flow Past a 90° T-Junction....360
Laminar Flow Through a Channel with Heated Walls.... 365
Turbulent Natural Convection Inside a Tall Cavity.... 370
Turbulent Flow with Separation in an Asymmetric Diffuser.... 378
Turbulent Flow Over a Backward-Facing Step....386
Turbulent Flow Past a Convex Curve in a Channel.... 393
Heat Transfer Between Radiating Concentric Cylinders....400
Turbulent Flow Through a 180 Degree Curved Channel.... 406
Circumferential Flow in a Cylinder Induced by a Rotating Solid....412
Heat Transfer Between Radiating Concentric Spheres.... 418
Two-Phase Nucleate Boiling in a Cylindrical Pipe....423
Single-Phase Nucleate Boiling in a Rectangular Channel.... 427
Supersonic Flow Through a Converging-Diverging Nozzle....432
Turbulent Flow Past a Wall-Mounted Hump.... 437
Laminar Couette Flow with Imposed Pressure Gradient and Heated Walls....444

External Flow 450

Turbulent Flow Behind an Open-Slit V 451
Turbulent Flow Over a NACA 0012 Airfoil 458
Oscillating Laminar Flow Around a Circular Cylinder 466
Separated Laminar Flow Over a Blunt Plate 471
Turbulent Mixing Layers in an Open Channel 478
Laminar to Turbulent Transition Over an Airfoil 483
Turbulent Flow Over an Oscillating Rigid Body Assembly 488
Turbulent Flow Through a Heated Periodic Channel 495

Transitional Flow 501

Laminar to Turbulent Transition Over an Airfoil 502

Transient Flow 507

Oscillating Laminar Flow Around a Circular Cylinder 508
Circumferential Flow in a Cylinder Induced by a Rotating Solid 513
Two-Phase Nucleate Boiling in a Cylindrical Pipe 519
Supersonic Flow Through a Converging-Diverging Nozzle 523
Turbulent Flow Over an Oscillating Rigid Body Assembly 528
Ideal Gas Compression in an Actuating Piston 535

Heat Transfer/Radiation 544

Natural Convection in a Concentric Annulus 545
Laminar Flow Through a Channel with Heated Walls 551
Laminar Flow Through a Pipe with Constant Wall Temperature 556
Laminar Flow Through a Pipe With Imposed Heat Flux 561
Turbulent Natural Convection Inside a Tall Cavity 566
Viscous Heating Inside a Rotating Annulus 574
Heat Transfer Between Radiating Concentric Cylinders 582
Heat Transfer Between Radiating Concentric Spheres 588
Two-Phase Nucleate Boiling in a Cylindrical Pipe 593
Single-Phase Nucleate Boiling in a Rectangular Channel 597
Supersonic Flow Through a Converging-Diverging Nozzle 602
Ideal Gas Compression in an Actuating Piston 607
Turbulent Flow Through a Heated Periodic Channel 616
Laminar Couette Flow with Imposed Pressure Gradient and Heated Walls 622

Moving Mesh 628

Circumferential Flow in a Cylinder Induced by a Rotating Solid 629
Turbulent Flow Over an Oscillating Rigid Body Assembly 635

Ideal Gas Compression in an Actuating Piston....642

Reference Frame....651

Flow Between Concentric Cylinders....652
Flow Inside a Rotating Cavity....658

Multiphase....666

Multiphase Flow of a 2D Dam Break....667
Two-Phase Nucleate Boiling in a Cylindrical Pipe....671

Compressible....675

Supersonic Flow Through a Converging-Diverging Nozzle....676
Ideal Gas Compression in an Actuating Piston....681

Intellectual Property Rights Notice....690
Technical Support....696

Index....697

AcuSolve Validation Manual

Collection of AcuSolve simulation cases for which results are compared against analytical or experimental results to demonstrate the accuracy of AcuSolve results.

The accuracy of the solutions presented in this document validates the capability of AcuSolve to simulate complex flow and heat transfer for a variety of problems. The goal is to provide accurate results for each validation case. Grid sensitivity studies have been performed, however, the simulation settings have not been optimized to minimize computation time. Instead, the cases presented are intended to portray settings that show a good trade off between accuracy and compute time.

> **Important:** Supporting database files (`*.hm` and `*.slb` for HyperMesh CFD/HyperMesh and SimLab, respectively) are available for the validation cases in a compressed `.zip` archive, `validation.zip`.

Copy `validation.zip` to a working directory, then expand it for access to individual database files. These can be used to recreate the results for a particular validation case or can be examined to see the AcuSolve settings in detail.

Each validation contains information in the following sections:

Problem Description	A description of the geometry, physical properties, and specific AcuSolve modeling strategy.
AcuSolve Results	Results obtained from the AcuSolve simulation compared against theoretical or experimental results.
Summary	A summary of the validation case.
Simulation Settings	AcuSolve settings for the specific validation case and the name and location of the associated database file.
References	Sources of theoretical equations or experimental results.

AcuSolve Results Presentation

Results for each validation case are presented with one or more contour plots that represent the CFD solution. For each case a comparison with the representative reference is provided and the associated error is reported.

Recreating the Results

You can recreate the AcuSolve results by using the database files provided. The general process to recreate the results is as follows:

1. Start HyperMesh CFD or SimLab and open the database file (`*.hm` or `*.slb`) for a particular validation case.
2. Launch AcuSolve to generate a solution.
3. Post-process results with HyperMesh CFD, SimLab or AcuTrans.

Typographical Conventions

Simulation settings are presented so that you can recreate the simulation case. The presentation of the simulation settings reflects the AcuSolve commands that are modified from default values. Labels in the GUI are indicated with highlighting, for example, Problem Description. Tree items that can be renamed are presented in normal font. Settings selected from a list are indicated after a dash. Settings that are entered directly into a field are indicated by courier font.

As an example, the following would indicate that the Global settings tree item was expanded, the Problem Description panel was opened, the Analysis type was set to Steady State, and the Turbulence equation set to Laminar.

Global	Problem Description
Analysis type	Steady State
Turbulence equation	Laminar

The following would indicate that Global in the tree was expanded, Material Model was also expanded, Gas is a branch that can be renamed and the material properties panel is opened, and the Density is entered as `1.808` with the units of kg/m3.

Global	Material Model
Gas	Material Type - Fluid
	Density `1.808` kg/m3

Turbulent Flow

2

This section includes validation cases containing flow conditions that will cause turbulence to form, requiring that a turbulence model is used.

This chapter covers the following:

- Single-Phase Nucleate Boiling in a Rectangular Channel (p. 9)
- Turbulent Flow Through a Pipe (p. 14)
- Turbulent Flow Behind an Open-Slit V (p. 18)
- Turbulent Flow with Separation in an Asymmetric Diffuser (p. 25)
- Turbulent Flow Over a Backward-Facing Step (p. 33)
- Turbulent Flow Past a Convex Curve in a Channel (p. 40)
- Turbulent Natural Convection Inside a Tall Cavity (p. 47)
- Turbulent Flow Over a NACA 0012 Airfoil (p. 55)
- Turbulent Flow Through a 180 Degree Curved Channel (p. 63)
- Turbulent Flow Through a Wavy Channel (p. 69)
- Turbulent Flow Through a Heated Periodic Channel (p. 77)
- Turbulent Mixing Layers in an Open Channel (p. 83)
- Two-Phase Nucleate Boiling in a Cylindrical Pipe (p. 88)
- Supersonic Flow Through a Converging-Diverging Nozzle (p. 92)
- Turbulent Flow Past a Wall-Mounted Hump (p. 97)
- Turbulent Flow Over an Oscillating Rigid Body Assembly (p. 104)

Single-Phase Nucleate Boiling in a Rectangular Channel

In this application, AcuSolve is used to simulate the wall heat flux due to nucleate boiling at a heated wall inside a rectangular channel with water flow. Results are compared with experimental heat flux measurements as reported by Steiner, et al. (2005). The close agreement of AcuSolve results with experimental results validates the ability of AcuSolve to model single phase nucleate boiling problems.

Problem Description

The problem consists of a channel with a heated wall at the bottom. The temperature of the wall is selected to onset the nucleate boiling at the heated wall. The dimensions of the inlet are 0.03 x 0.04 m; the inlet velocity (v) is 0.39 m/s and the temperature (T) of the fluid entering the inlets is varied from 373.15 K (100 C) to 406.15 (133 C)), while the atmospheric pressure is specified to be 2 bar. The pre-heated water enters the inlets and heat is transferred into the fluid from the heated walls. The heat causes sub-cooled boiling to occur in the region close to the wall and leads to the formation of bubbles at nucleation sites. The surface tension and vapor phase models are specified to emulate the physical process of water changing state to water vapor.

The heat transfer in this regime is dominated by two effects, the macro convection due to the motion of the bulk liquid and the latent heat transport associated with the evaporation of the liquid micro-layer between the bubble and the heated wall. Each of these effects are modeled with AcuSolve and the prediction of their processes is demonstrated in the following results.

The AcuSolve simulation is prepared as a steady state heat transfer simulation to determine the temperature and heat flux on the heated walls of the model. AcuSolve computes the single-phase nucleate boiling by employing Chen’s model for two-phase boiling flow described in Chen (1966). The heat flux values for different wall temperatures are compared against the experimental measurements, as described in Steiner, et al. (2005).

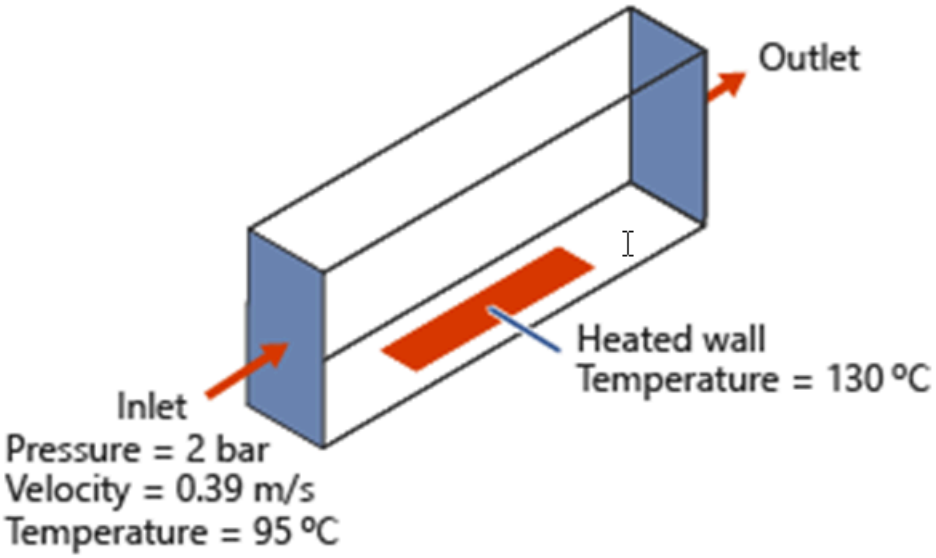


Figure 1: Critical Dimensions and Parameters for Simulating a Single-Phase Nucleate Boiling in a Rectangular Channel

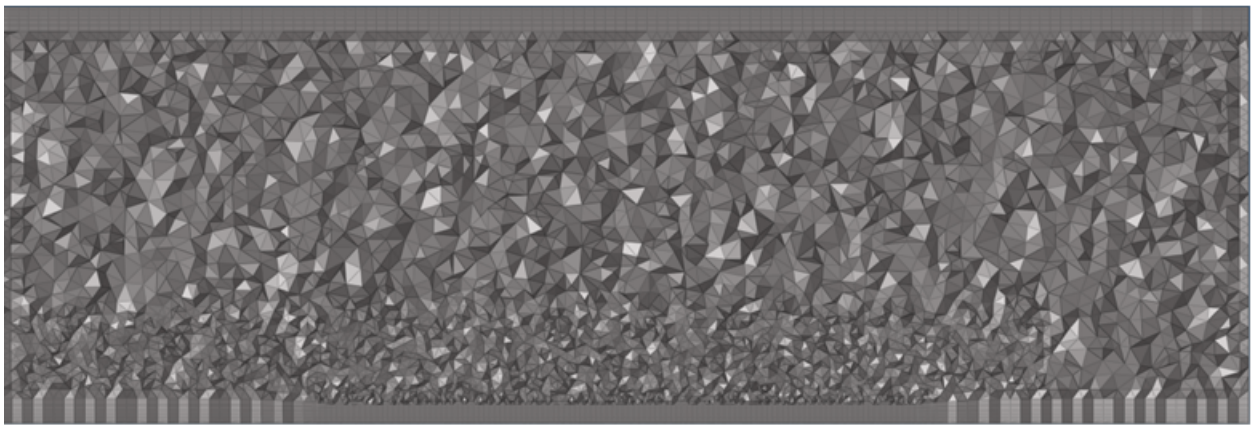


Figure 2: Mesh Used for Simulating a Single-Phase Nucleate Boiling in a Rectangular Channel

AcuSolve Results

The AcuSolve solution is run for heated wall temperature values of 100 C, 105 C, 110 C, 115 C, 120 C, 125 C, 130 C, 133 C and the results presented reflect the heat flux from the wall as the temperature nears the saturation temperature. The experimental values of heat flux (MW/m2) and wall temperature are presented with the corresponding AcuSolve results at seven temperature values. The AcuSolve results show good agreement with the experimental results for the heat flux, indicating that the single-phase nucleate boiling is properly captured.

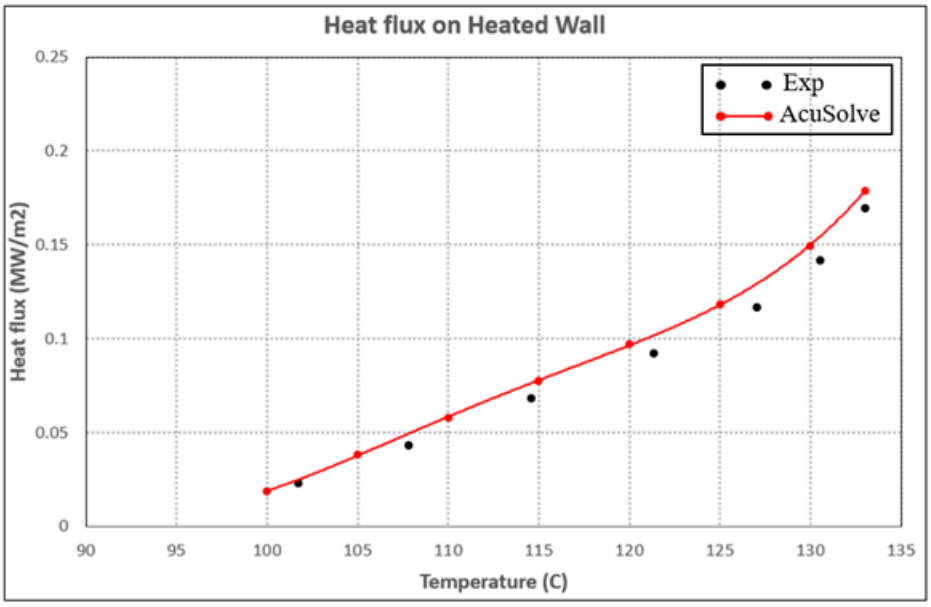


Figure 3: Heat Flux Values for Varying Wall Temperatures Compared to Experimental Data

Summary

The AcuSolve solution compares well with experimental results for single-phase nucleate boiling simulations. In this application, heat flux generated by the wall as the onset of boiling approaches are simulated with AcuSolve using the nucleate boiling feature and the RKE turbulence model. The experimental values of heat flux for the wall temperature range are presented with the corresponding AcuSolve results. A good agreement of simulation results with the experiment validates the ability to solve single-phase nucleate boiling using the nucleate boiling capabilities of AcuSolve.

Simulation Settings for Single-Phase Nucleate Boiling in a Rectangular Channel

HyperMesh CFD database file: `<your working directory>\channel_single_phase_boiling \channel_single_phase_boiling.hm`.

Global

- Problem Description
  - Analysis type – Steady
  - Turbulence equation – RKE
  - Temperature equation – Advective Diffusive
  - Nucleate Boiling Single Phase – On
- Auto Solution Strategy
  - Convergence Tolerance – `0.001`
  - Relaxation factor – `0.4`
- Surface Tension Model (“Water-srfTns”)
  - Type – Constant
  - Surface Tension – `0.07`

- Material Model
  - Vapor
    - Type – Constant
    - Density – `1.128` kg/m^3
    - Viscosity – `1.29e-5` kg/m-sec
    - Specific Heat – `2174.59` J/kg-K
    - Latent Heat – `2256000`
    - Latent Heat Temperature – `393.45` K
    - Conductivity – `0.02749` W/m-K
    - Turbulent Prandtl number – `1.0`
  - Water
    - Type – Constant
    - Density – `965.36` kg/m^3
    - Viscosity – `0.000314` kg/m-sec
    - Specific Heat – `4204.8` J/kg-K
    - Conductivity – `0.675` W/m-K
    - Turbulent Prandtl number – `0.91`
    - Vapor phase model – Vapor
    - Surface Tension model – Water-srfTns

Model

- Volumes
  - Fluid
    - Material– Water
- Surfaces
  - Inflow
    - Simple Boundary Condition – Inflow
    - Inflow type – Average Velocity
    - Average Velocity – `0.39` m/sec
    - Temperature – `368.15` K
  - Outflow
    - Simple Boundary Condition – Outflow
    - Back flow condition – On
    - Temperature back flow type – Mass flux average
    - Kinetic energy back flow type – Mass flux average
    - Dissipation rate back flow type – Mass flux average
  - Bottom
    - Simple Boundary Condition – Wall
  - Top

        - Simple Boundary Condition – Wall
    - Side_MinY
        - Simple Boundary Condition – Wall
    - Side_MaxY
        - Simple Boundary Condition – Wall
    - Heated Wall
        - Simple Boundary Condition – Wall
        - Temperature type – Value
        - Temperature – [373.15, 378.15, 383.15, 388.15, 393.15, 398.15, 403.15, 406.15] K

References

Helfried Steiner, Alexander Kobor, Ludwig Gebhard, 2005, "A wall heat transfer model for subcooled boiling flow", International Journal of Heat and Mass Transfer, Vol 48, pp. 4161- 4173.

Chen, J.C., 1966, "Correlation for Boiling Heat Transfer to Saturated Fluids in Convective Flow", United States: N. p., 1962. Web. doi:10.2172/4636495.

Turbulent Flow Through a Pipe

In this application, turbulent flow of air through a pipe is simulated. AcuSolve results are compared with experimental results as described in White (1991) and extracted from the Moody chart. The close agreement of AcuSolve results with experimental results validates the ability of AcuSolve to model turbulent flow within pipes.

Problem Description

The problem consists of air flowing through a pipe 0.004 m in diameter and 0.02 m long, as shown in the following image, which is not drawn to scale. The AcuSolve simulation utilizes periodic boundary conditions to obtain the fully developed profile within the pipe. The defined pressure drop, applied as a body force on the fluid volume, offsets the change in pressure due to the friction created by the no-slip walls of the pipe. The Reynolds number for this problem is approximately 8,250.

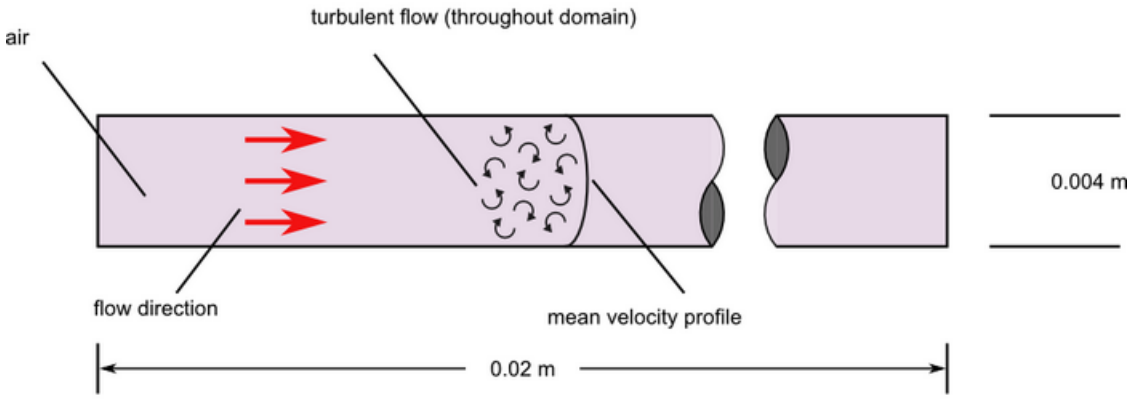


Figure 4: Critical Dimensions and Parameters for Simulating Turbulent Flow Through a Pipe

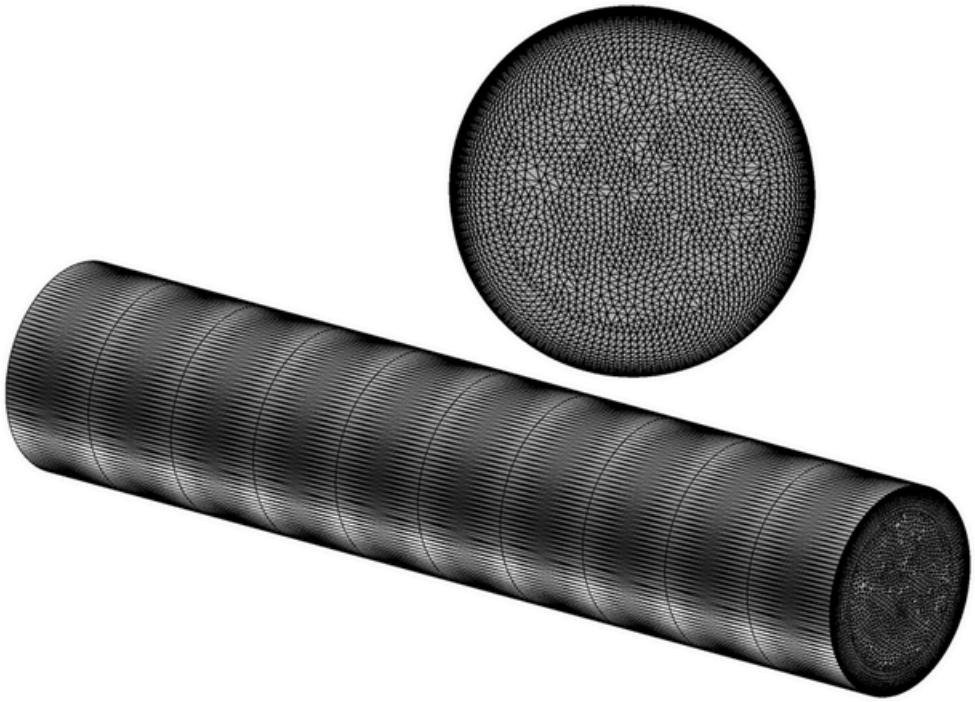


Figure 5: Mesh of a Periodic Segment Used for Simulating Turbulent Flow Through a Pipe

AcuSolve Results

The AcuSolve solution converged to a steady state and the results reflect the mean flow conditions with a turbulent velocity profile that is fully developed. The simulation was performed using the Spalart-Allmaras single-equation turbulence model. The velocity and eddy viscosity profiles are constant along the length of the pipe.

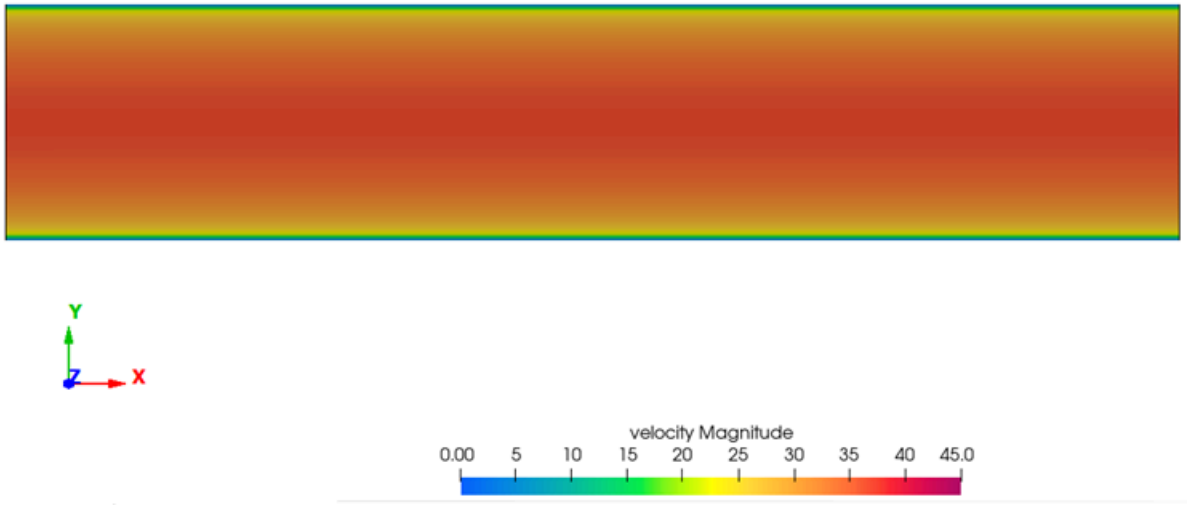


Figure 6: Velocity Contours for the Averaged Turbulent Flow

The experimental result for average velocity at the inlet is presented with the corresponding AcuSolve prediction in the following table.

Table 1:

	Experimental result	AcuSolve prediction	Percent deviation from experimental
Average inlet velocity	30.0	30.63	2.1

Summary

The AcuSolve solution compares well with the experimental result for average inlet velocity for turbulent flow through a pipe. In this application, the applied body force counteracts the change in pressure due to the viscous stresses near the pipe wall. The resulting friction factor for a smooth wall pipe and the specified Reynolds number is approximately 0.0326. With the imposed pressure drop defining the flow, the AcuSolve prediction of average inlet velocity is within 2.0 percent of the Darcy-Weisbach approximation.

Simulation Settings for Turbulent Flow Through a Pipe

SimLab database file: `<your working directory >\pipe_turbulent\pipe_turbulent.slb`.

Global

- Problem Description
  - Flow - Steady State
  - Turbulence equation - Spalart Allmaras
- Auto Solution Strategy
  - Relaxation factor - `0.4`

- Material Model
  - Air
    - Density - `1.225` kg/m3
    - Viscosity - `1.781e-05` kg/m-sec
- Body Force
  - dpdx
    - Gravity
      1. X-component - `3739.98` m/s2

  Model
- Volumes
  - Fluid
    - Element Set
      1. Material model - Air
      2. Body force - dpdx
- Surfaces
  - Inlet
    - Simple Boundary Condition - (disabled to allow for periodic conditions to be set)
  - Outlet
    - Simple Boundary Condition - (disabled to allow for periodic conditions to be set)
  - Wall
    - Simple Boundary Condition
      1. Type - Wall
      2. Roughness height - `0.0` mm
- Periodics
  - Periodic 1
    - Periodic Boundary Condition
      1. Type - Periodic

References

F. M. White. "Viscous Fluid Flow". Section 3-2.1. McGraw-Hill Book Co., Inc.. New York. 1991.

Experimental solution adapted from Darcy-Weisbach equation based on friction factor taken from the Moody chart with a Reynolds number of approximately 8,250.

Turbulent Flow Behind an Open-Slit V

In this application, AcuSolve is used to simulate turbulent flow of air through and behind a two dimensional open-slit V. AcuSolve results are compared with experimental results adapted from Yang and Tsai (1993). The close agreement of AcuSolve results with experimental results validates the ability of AcuSolve to model the Coandă effect.

Problem Description

The problem consists of air flowing through and past an open-slit V positioned within a flow domain, as shown in the following image, which is not drawn to scale. The flow domain is 0.3 m long and 0.1 m high. The narrow end of the V is positioned 0.05 m from the domain inlet. The slit in the V is 0.002 m high. The V widens to 0.022 m at 0.075 m from the domain inlet. Air enters the domain with a constant velocity of 20 m/s. The upper and lower limits of the domain are defined as no-slip boundary conditions.

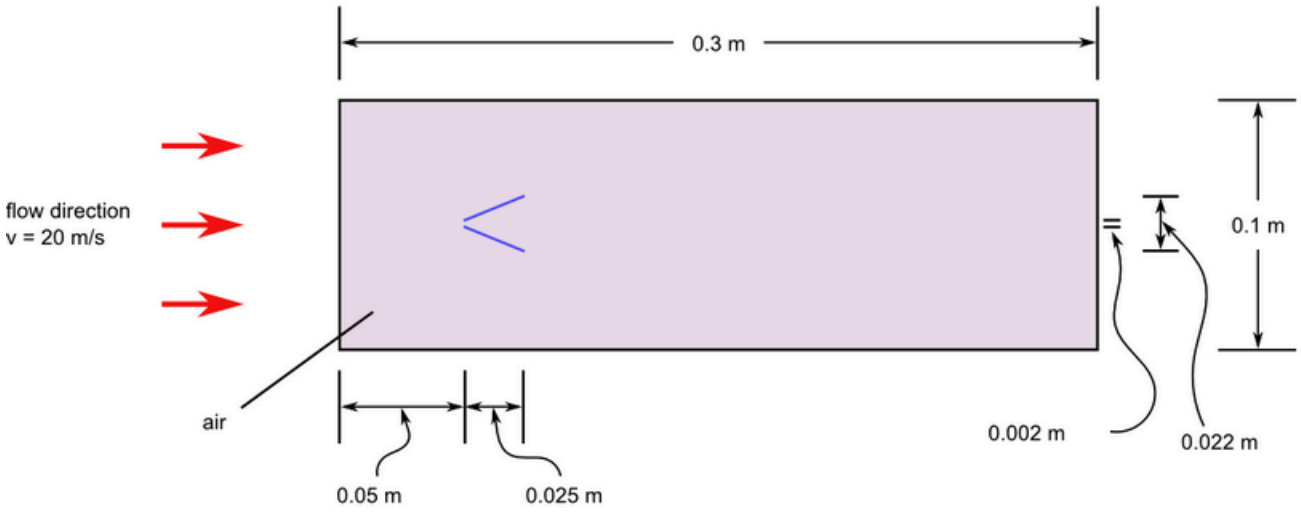


Figure 7: Critical Dimensions and Parameters for Simulating Turbulent Flow Behind an Open-Slit V

The simulation was performed as a two dimensional problem by restricting flow in the out-of-plane direction through the use of a mesh that is one element thick. A coarse mesh is used throughout much of the domain, with mesh refinement closer to the V.

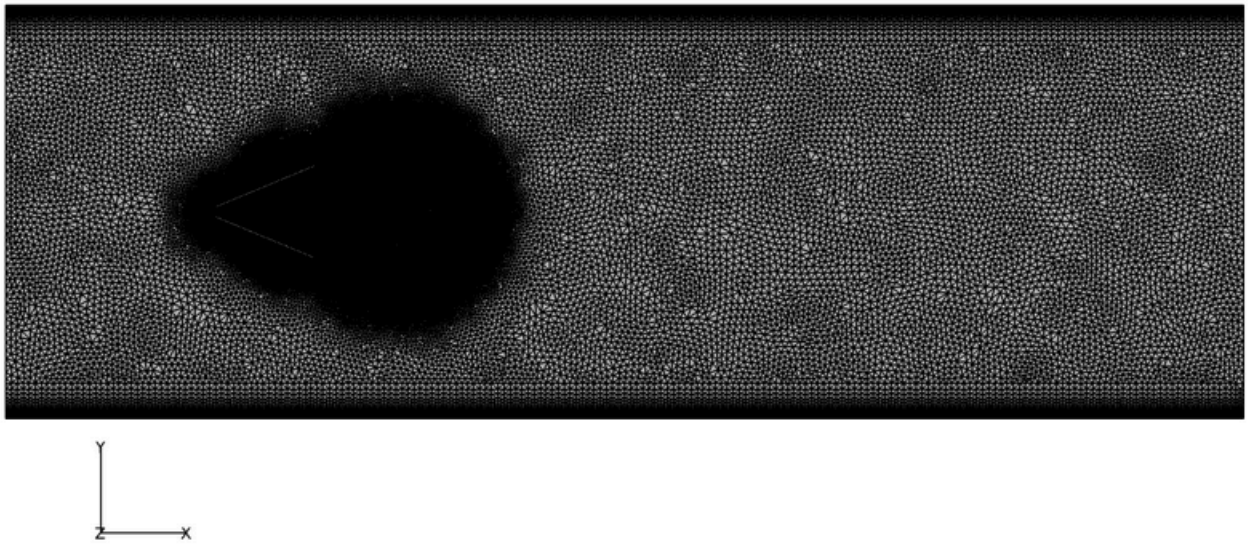


Figure 8: Mesh used for Simulating Turbulent Flow Behind an Open-Slit V (the V Lies Within the Dense Area of the Mesh)

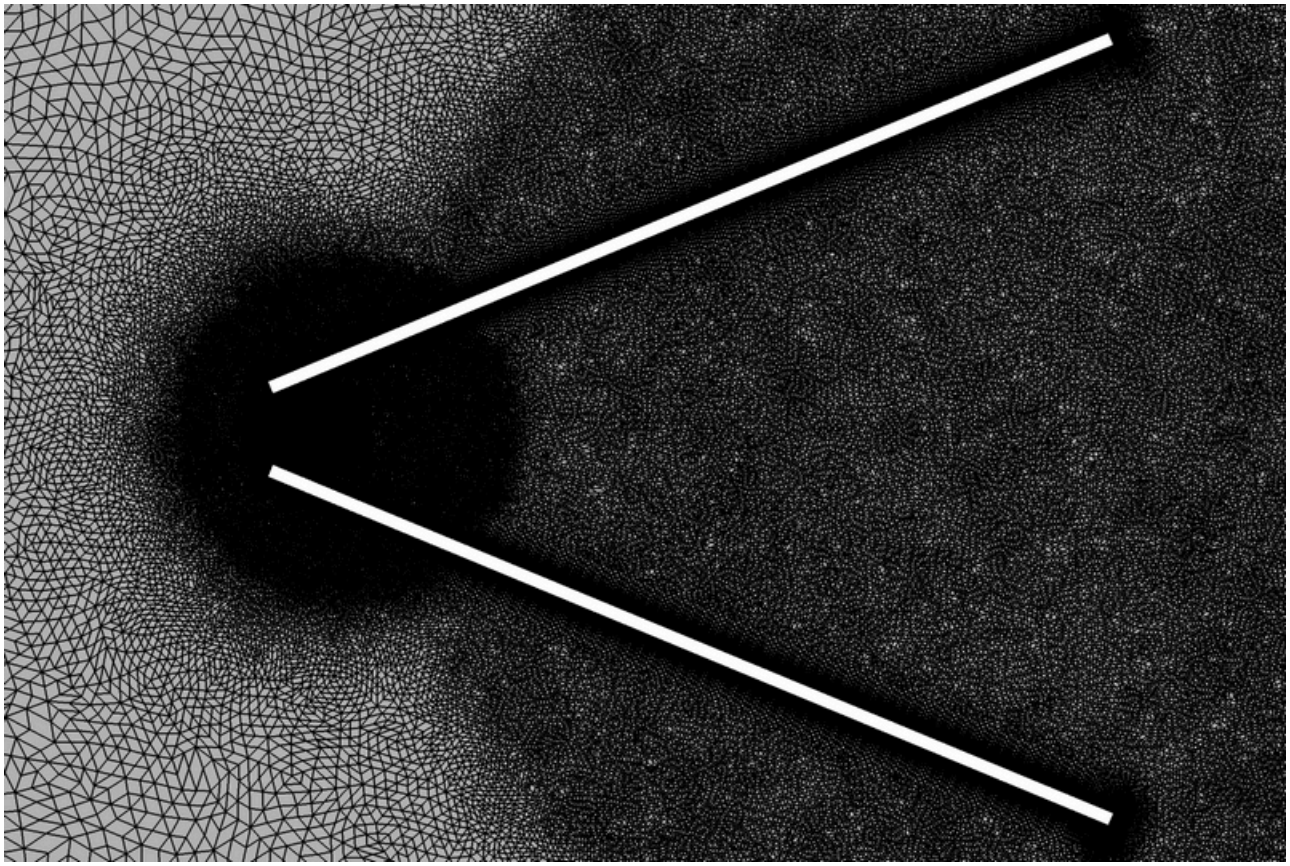


Figure 9: Mesh Surrounding the Open-Slit V

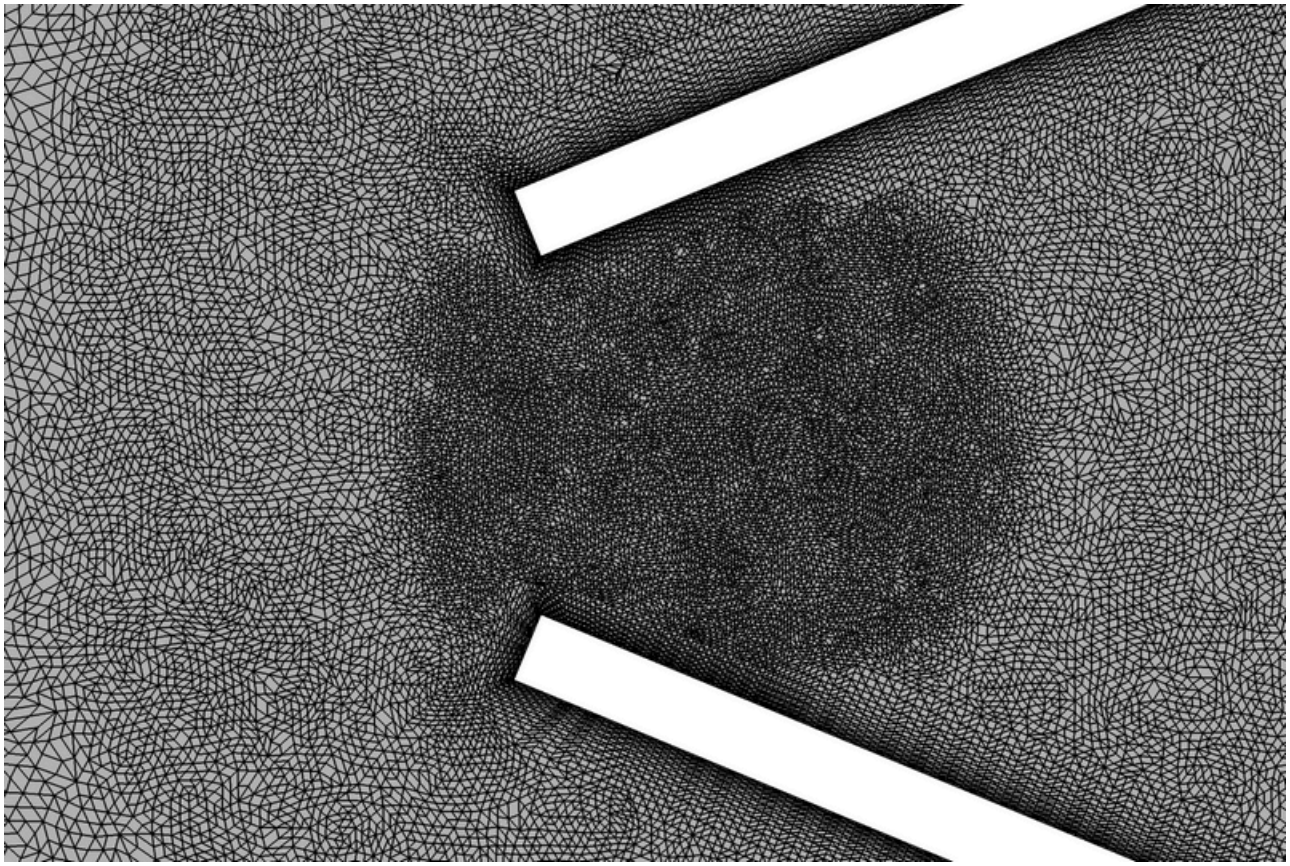


Figure 10: Mesh Near the Open Slit

AcuSolve Results

The AcuSolve solution converged to a steady state and the results reflect the mean flow conditions. Air flows through the open slit in the V and accelerates while being forced to one side due to the Coandă effect. As air encounters the exterior of the widening gutter, velocity increases and the wake induces recirculation near the exit of the V. The recirculation zone extends downstream of the V gutter.

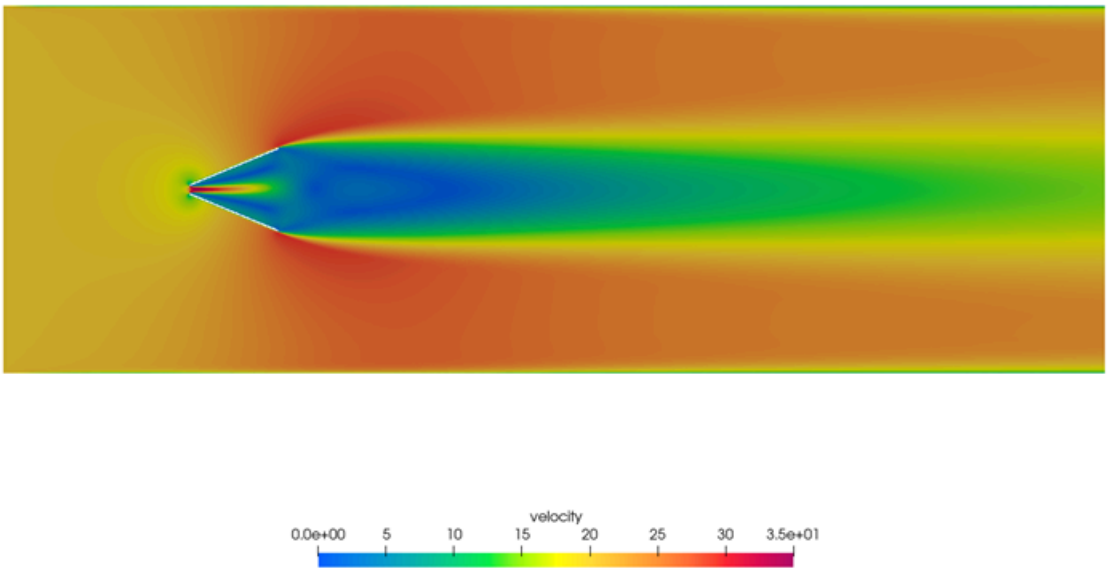


Figure 11: Contours of X-Velocity of Flow Through and Around an Open-Slit V (the Vertical Line Represents the Location, 0.022 m Downstream from the V exit, at Which Experimental Data is Compared to AcuSolve Results)

AcuSolve results were compared to experimental results at different heights 0.022 m behind the V exit. X-velocity is near zero at the bottom of the domain (height = -0.05 m), rising steeply with distance from the wall. The velocity gradient decreases until approximately 0.018 m below the center line of the domain, which is slightly below the bottom of the V exit. The velocity behind the V drops sharply with an increase in height, due to the blockage caused by the presence of the slanted walls. The lowest velocity is just above the center line of the domain.

The slight asymmetry in the velocity profile in the wake of the V is expected due to the Coandă effect.

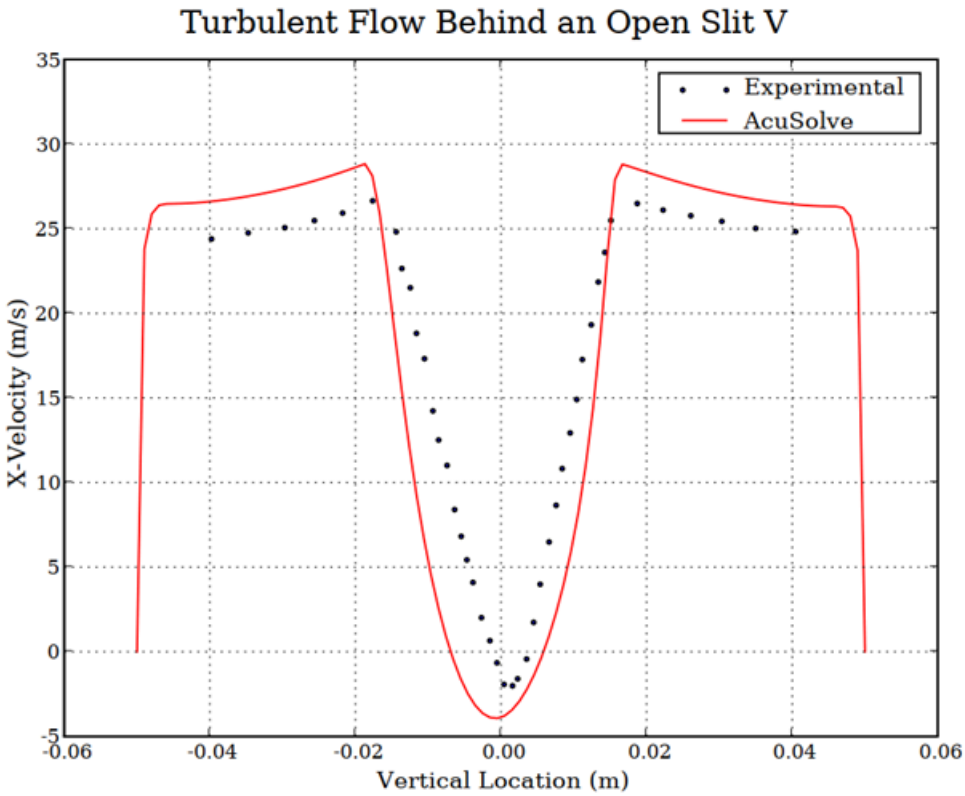


Figure 12: X-Velocity Plotted Against Vertical Location 0.0022 m Downstream of the V Exit

Summary

The AcuSolve results compare well with the experimental results for flow through and around an open-slit V. In this application, the V-shaped geometry diverts flow towards the side walls of the channel and also creates a high-velocity jet through the slit. The low pressure associated with the jet causes a deflection towards the walls of the V, resulting in an asymmetric flow field within the V shape. This application illustrates the ability of AcuSolve to accurately predict the Coandă effect. The acceleration of the flow due to the deflection along the V-shaped walls and the momentum deficit in the wake of the V is captured accurately.

Simulation Settings for Turbulent Flow Behind an Open-Slit V

HyperMesh CFD database file: `<your working directory>\v_gutter_turbulent\v_gutter_turbulent.hm`

Global

- Problem Description
  - Analysis type - Steady State
  - Turbulence equation - Spalart Allmaras
- Auto Solution Strategy
  - Relaxation factor - `0.5`
- Material Model

- Air
  - Density - `1.0` kg/m3
  - Viscosity - `1.8333e-05` kg/m-sec

Model

- Volumes
  - Fluid
    - Element Set
      1. Material model - Air
- Surfaces
  - Inlet
    - Simple Boundary Condition
      1. Type - Inflow
      2. Inflow type - Velocity
      3. X velocity - `20.0` m/sec
      4. Eddy viscosity - `0.000800426` m2/sec
  - LE_TE
    - Simple Boundary Condition
      1. Type - Wall
  - Outlet
    - Simple Boundary Condition
      1. Type - Outflow
  - Symm_MaxZ
    - Simple Boundary Condition
      1. Type - Slip
  - Symm_MinZ
    - Simple Boundary Condition
      1. Type - Slip
  - V_Walls
    - Simple Boundary Condition
      1. Type - Wall
  - Walls
    - Simple Boundary Condition
      1. Type - Wall

References

J.-T. Yang and G.-L. Tsai. "Near-wake flow of a v-gutter with slit bleed". Journal of Fluid Engineering. 115:13-20. March, 1993.

Turbulent Flow with Separation in an Asymmetric Diffuser

In this application, AcuSolve is used to simulate fully developed turbulent flow through an asymmetric diffuser with a divergent lower wall and a straight upper wall. AcuSolve results are compared with experimental results as described in Buice and Eaton (2000). The close agreement of AcuSolve results with experimental results validates the ability of AcuSolve to model cases with internal turbulent flow with flow separation and reattachment in an asymmetric diffuser.

Problem Description

The problem consists of air flowing through an asymmetric diffuser with a divergent lower wall and a straight upper wall, as shown in the following image, which is not drawn to scale. The diffuser inlet has a height of 1.5 cm (H) and extends 9 cm (6H) to the divergent section. The lower wall of the diffuser diverges at an angle of 10° and expands to 7.05 cm (4.7H). The divergent section has a horizontal length of 31.5 cm (21H). The expanded section of the diffuser extends 84 cm (56H) to the outlet. Air, with a density of 1.225 kg/m^3 and a viscosity of 1.8325 X 10^{-5} kg/m-s enters the diffuser through the inlet of the diffuser with a fully developed turbulent profile at a Reynolds's number of 20,000. The simulation was conducted with the Reynolds Averaged Navier-Stokes equations using four turbulence models, Spalart Allmaras, Shear Stress Transport (SST), K-ω and Realizable K-ε.

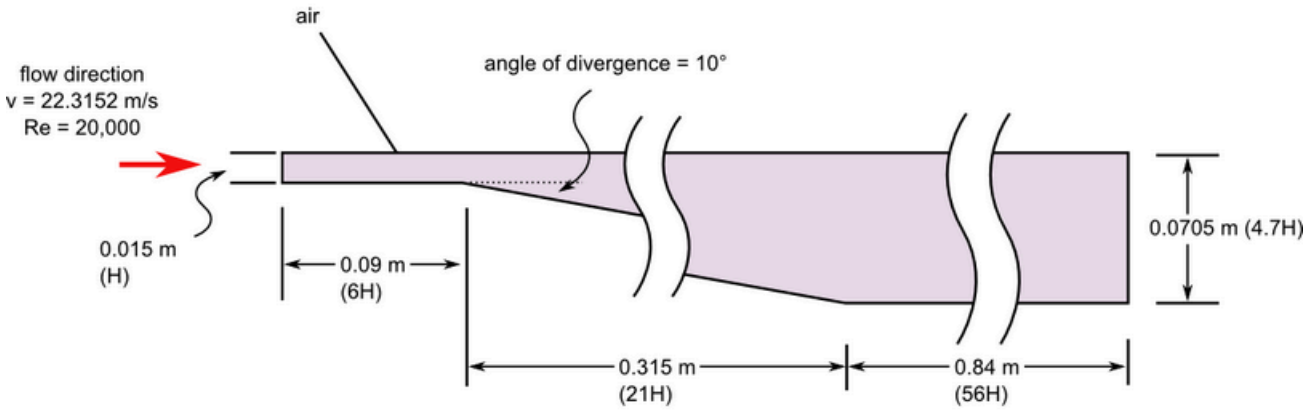


Figure 13: Critical Dimensions and Parameters for Simulating Turbulent Flow with Separation in an Asymmetric Diffuser

The simulation was performed as a two dimensional problem by constructing a volume mesh that contains a single layer of elements extruded in the cross stream direction (perpendicular to the flow plane) and by imposing symmetry boundary conditions on the extruded planes.



Figure 14: Mesh Details Near the Inlet and Divergent Section of Diffuser

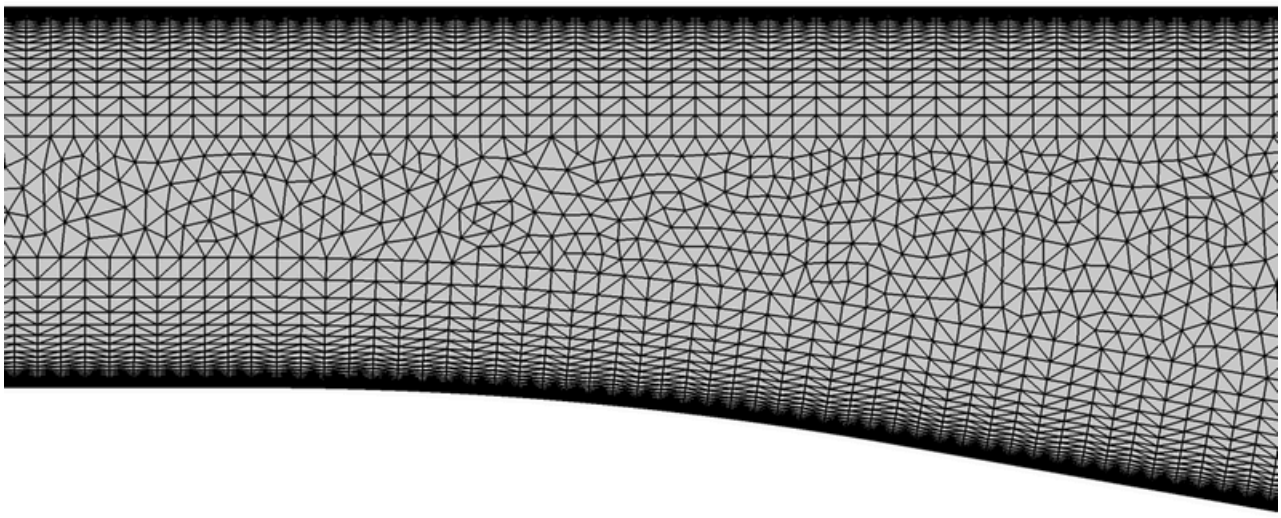


Figure 15: Mesh Details at the Beginning of the Divergence of the Lower Wall in the Diffuser

AcuSolve Results

The AcuSolve solution converged to a steady state and the results reflect the mean flow conditions. As the fully developed turbulent flow enters the divergent section, the peak velocity is maintained until the expansion of the cross-sectional height, forms an adverse pressure gradient. After the flow enters the divergent section, the velocity decreases significantly, due to the expansion of the cross-section height. This causes separation of the flow along the divergent wall and results in an area of recirculation.
The bulk of the flow above the divergent wall maintains its streamwise direction, while a portion of it reverses direction before reattaching further downstream of the divergent section. The following images show the steady state flow solution for flow within the diffuser.

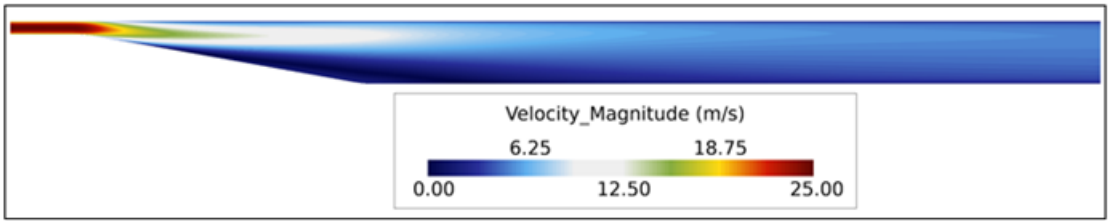


Figure 16: Velocity Contours Within the Diffuser

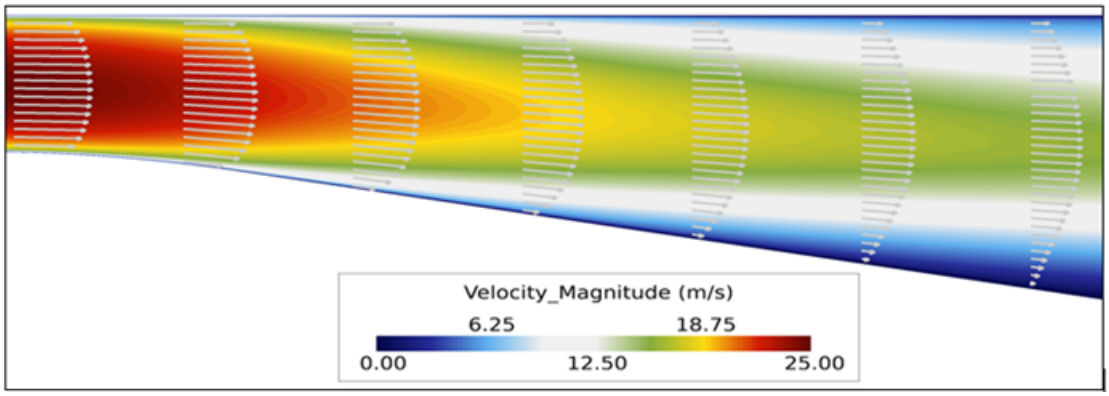


Figure 17: Close up View of Velocity Vectors and Contours of Velocity Magnitude in the Diffuser

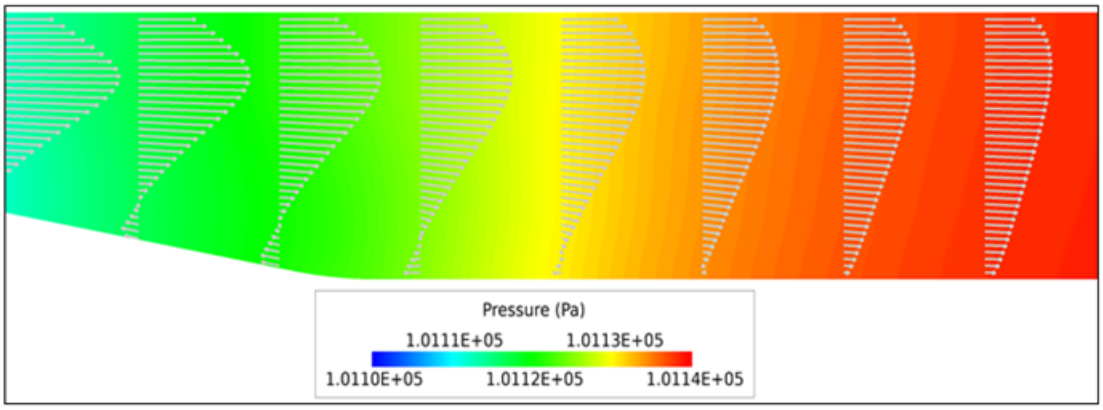


Figure 18: Close up View of Velocity Vectors and Contours of Pressure to Show Recirculation as it Approaches the Reattachment Point

Upstream of the diffuser section, the streamline velocity increases as the distance from the lower wall increases until it reaches the maximum velocity at the center of the channel. As the flow enters the divergent section of the channel, the streamwise velocity decreases near the bottom wall. The images below show the velocity profiles at three locations as measured from the midpoint of the curve where the bottom wall begins to diverge (X=0.0) for each of the tested turbulence models. The first location, where X/H = -5.944, is close to the inlet. The second location, where X/H = 13.468, is approximately 0.2 m downstream of the divergent section (~ 0.1 m from the fully expanded section). The third location, where X/H = 24.066, is approximately 0.16 m downstream of the point where the diffuser has reached the maximum height. In these plots the black circles represent the experimental measurements (Buice and Eaton 2000), the solid red lines for the prediction for the Spalart Allmaras model, solid blue lines for the prediction for the SST model, solid green lines for the prediction for the K-ω model and solid cyan lines for the K-ε model, representing the AcuSolve results. The non-dimensional height is represented by the fraction of the vertical height (Y) divided by the inlet height (H) and the velocity is normalized by the inlet velocity (Uref).

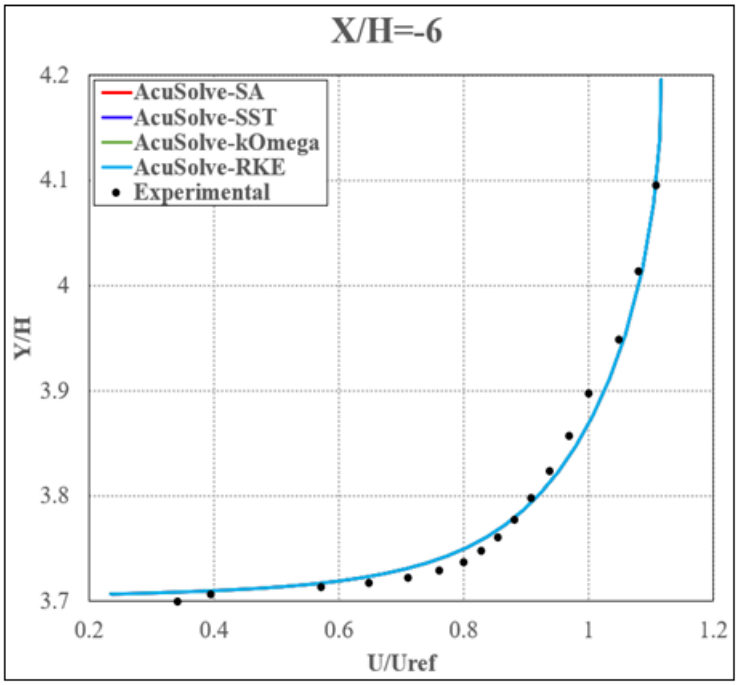


Figure 19: Non-Dimensional Streamwise Velocity Plotted Against Vertical Location Near the Inlet (X/H=-5.9442, Where the Reference Point is 6H Downstream of the Inlet)

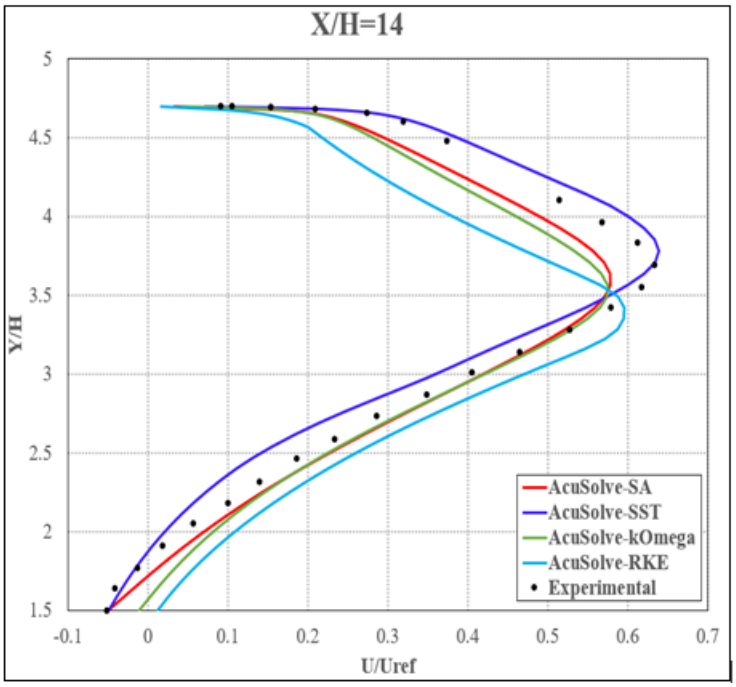


Figure 20: Non-Dimensional Streamwise Velocity Plotted Against Vertical Location Approximately 0.2 m Downstream of the Divergence (X/H = 13.468, Where the Reference Point is 6H Downstream of the Inlet)

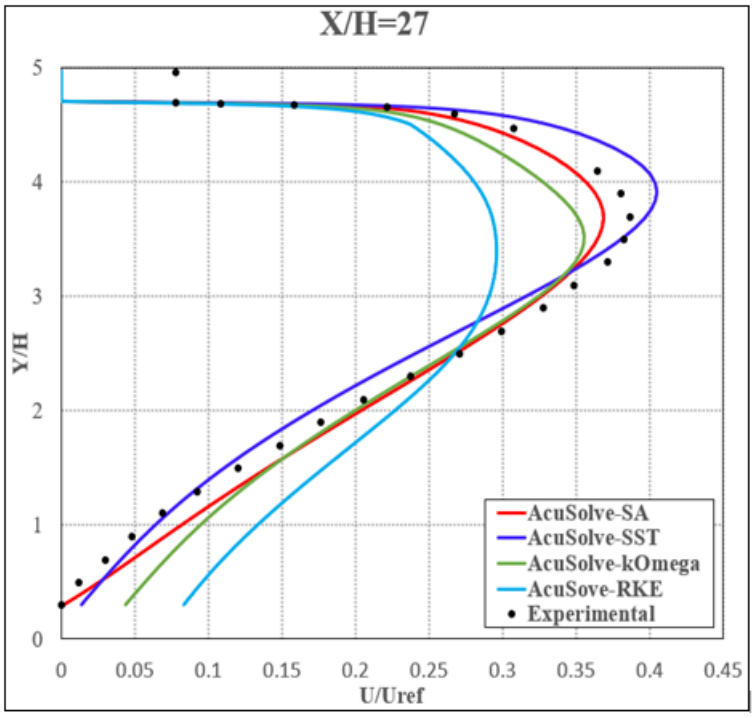


Figure 21: Non-Dimensional Streamwise Velocity Plotted Against Vertical Location Approximately 0.2 m Downstream of the Transition to the Fully Divergent Section (X/H = 27.066, Where the Reference Point is 6H Downstream of the Inlet)

The non-dimensional pressure coefficient (Cp) all along the inlet-bottom stretch of the diffuser is calculated using the reference pressure at X=-3H (at the bottom wall) and with reference velocity (Uref) at the inlet with the value of 22.3152 (m/s). The predicted non-dimensional pressure coefficients are compared to experimental results. The figure below shows Cp, along a constant vertical height, as a function of the streamwise distance from the inlet of the channel. The results demonstrate that AcuSolve is capable of accurately predicting the pressure within the diffuser within the expected range based on the type of turbulence model used. The performance of the three turbulence models were found to be consistent with previously published results for flow through the diffuser as published by Buice and Eaton (2000), with the SST model predicting the pressure distribution most accurately.

Note: The inlet of the experimental duct was 6H longer than that modeled - AcuSolve values where X/H < -6 are reported as the inlet value.

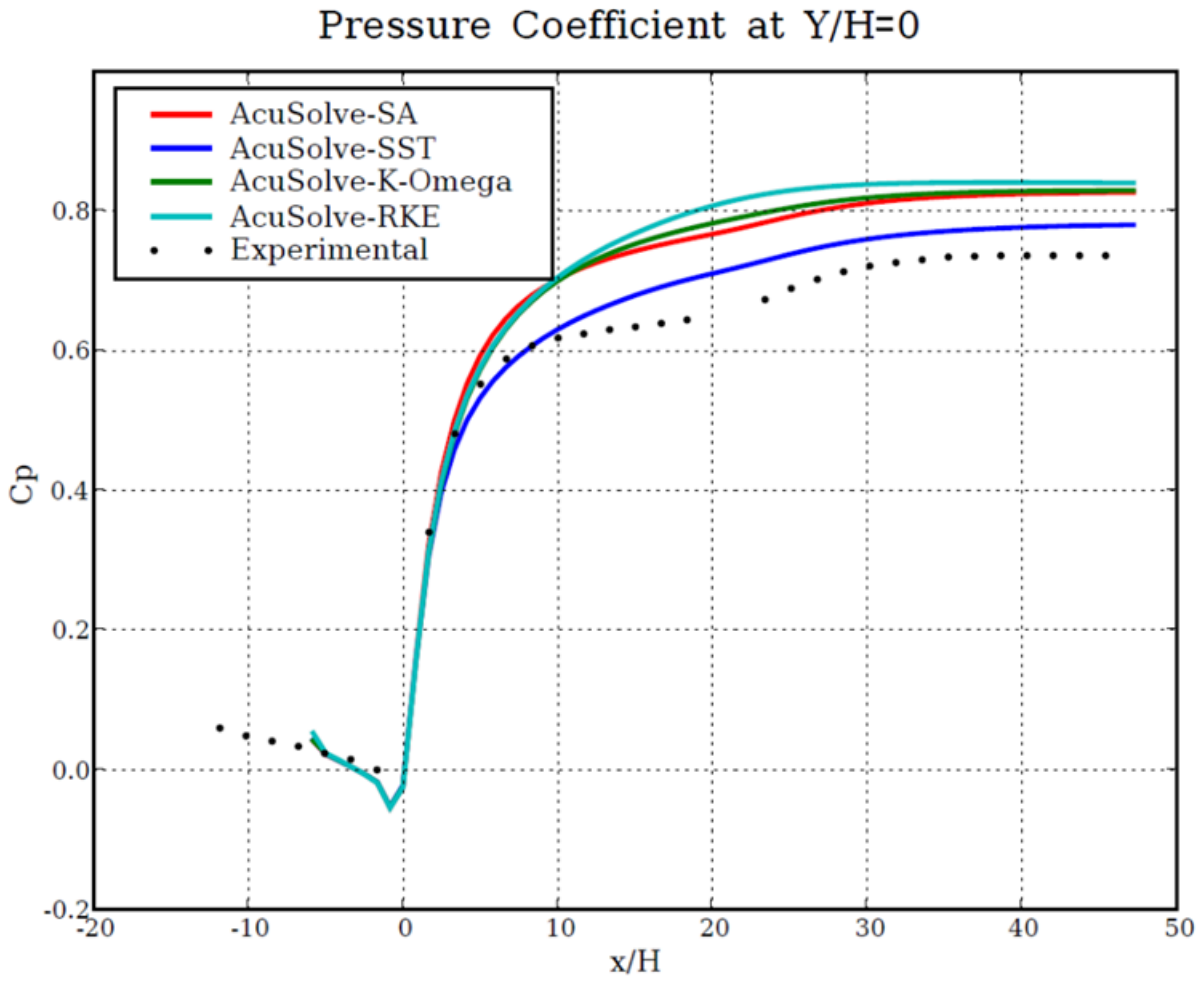


Figure 22: Non-Dimensional Pressure Coefficient (Cp) Plotted Against Relative Distance Along the Diffuser at a Constant Height Equal to the Bottom of the Inlet

Summary

In this application, a fully developed turbulent flow at a Reynolds number of 20,000 is studied. Due to the adverse pressure gradient, separation of flow occurs and causes recirculation in the divergent

section of the diffuser. The results were found to be consistent with previously published computational studies and experimental data. The results of this validation demonstrate the ability of AcuSolve to accurately predict the separation point, the recirculation that occurs along the divergent wall, and the reattachment point in the straight section of the diffuser.

Simulation Settings for Turbulent Flow with Separation in an Asymmetric Diffuser

HyperMesh CFD database file: `<your working directory>\asymmetric_diffuser_turbulent\asymmetric_diffuser_turbulent.hm`

Global

- Problem Description
  - Analysis type - Steady State
  - Turbulence equation - Spalart Allmaras
- Auto Solution Strategy
  - Max time steps - `150`
  - Relaxation Factor - `0.4`
- Material Model
  - Air
    - Density - `1.225.0` kg/m3
    - Viscosity - `1.8325e-5` kg/m-sec

  Model
- Volume
  - Volume
    - Element Set
      1. Material model - Air
- Surfaces
  - Bottom
    - Simple Boundary Condition
      1. Type - Wall
  - Inlet
    - Simple Boundary Condition (disabled to allow for nodal boundary conditions to be set)
    - Advanced Options
      1. Nodal Boundary Conditions
         1. X-Velocity
            1. Type - Linear
            2. Precedence - `2`
            3. Curve fit variable - Y coordinate
            4. Curve fit values (included in database)
         2. Y-Velocity

1. Type - Linear
2. Precedence - 2
3. Curve fit variable - Y coordinate
4. Curve fit values (included in database)

3. Eddy Viscosity
   1. Type - Linear
   2. Precedence - 2
   3. Curve fit variable - Y coordinate
   4. Curve fit values (included in database)

- Outlet
  - Simple Boundary Condition
    1. Type - Outflow - 101139.0 Pa
- Side 1
  - Simple Boundary Condition
    1. Type - Symmetry
- Side 2
  - Simple Boundary Condition
    1. Type - Symmetry
- Top
  - Simple Boundary Condition
    1. Type - Wall

References

C.U. Buice, and J.K., Eaton. "Experimental Investigation of Flow Through an Asymmetric Plane Diffuser". Journal of Fluids Engineering 122:433-435. June 2000.

S. Obi, K. Aoki and S. Masuda. "Experimental and Computational Study of Turbulent Separating Flow in an Asymmetric Plane Diffuser". Ninth Symposium on Turbulent Shear Flows. p. 305. Kyoto, Japan. August 16-19, 1993.

Turbulent Flow Over a Backward-Facing Step

In this application, AcuSolve is used to simulate fully developed turbulent flow over a backward-facing step. AcuSolve results are compared with experimental results as described in Driver (1985) and on the NASA Langley Research Center Turbulence Modeling Resource web page. The close agreement of AcuSolve results with experimental data and reference turbulence model performance validates the ability of AcuSolve to model cases with turbulent flow that forms a shear layer, recirculates and then reattaches downstream of the divergent step.

Problem Description

The problem consists of a fluid with material properties close to air flowing through a channel containing a sharp expansion, as shown in the following image, which is not drawn to scale. The step causes the flow to recirculate before reattaching downstream of the step. The inlet height of the channel is 8.0 m and expands as a step function to 9.0 m at a distance 20.0 m downstream of the inlet. This expanded section of the channel extends 50 m downstream of the step. The inflow of the channel is defined as fully developed at a Reynolds number (Re) of 36,000, based on the step height to match the experimental conditions. The density of the flow medium is 1.1837 kg/m^3 and the dynamic viscosity is 1.457 X 10^{-3} kg/m-s. The simulation was conducted with the Reynolds Averaged Navier-Stokes equations using four turbulence models, Spalart Allmaras, Shear Stress Transport (SST), K-ω and K-ε.

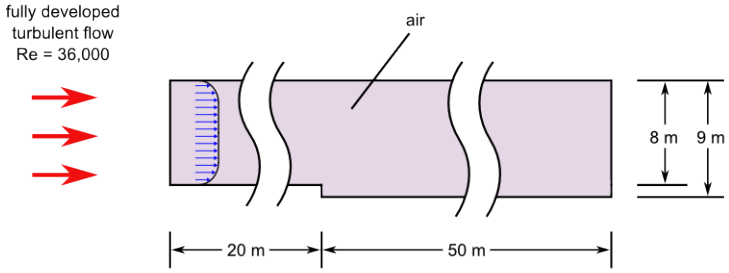


Figure 23: Critical Dimensions and Parameters for Simulating Turbulent Flow Through a Channel with a Backward-Facing Step

The simulation was performed as a two-dimensional problem by constructing a volume mesh that contains a single layer of elements extruded in the cross-stream direction, normal to the flow plane and by imposing symmetry boundary conditions on the extruded planes. The upper and lower walls are specified as no-slip, the inlet velocity and eddy viscosity are specified to match the conditions in the experiment (Driver 1985) at a distance of 20 m upstream of the step.

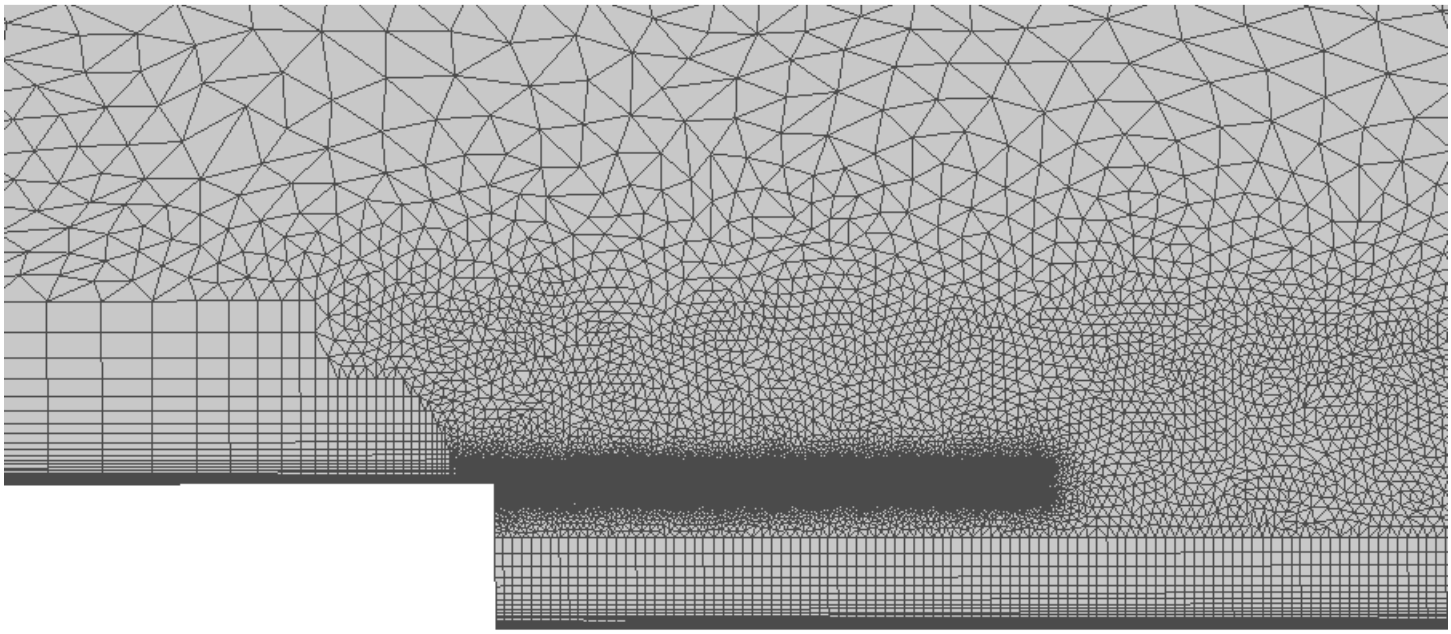


Figure 24: Detail of Mesh Near the Backward-Facing Step

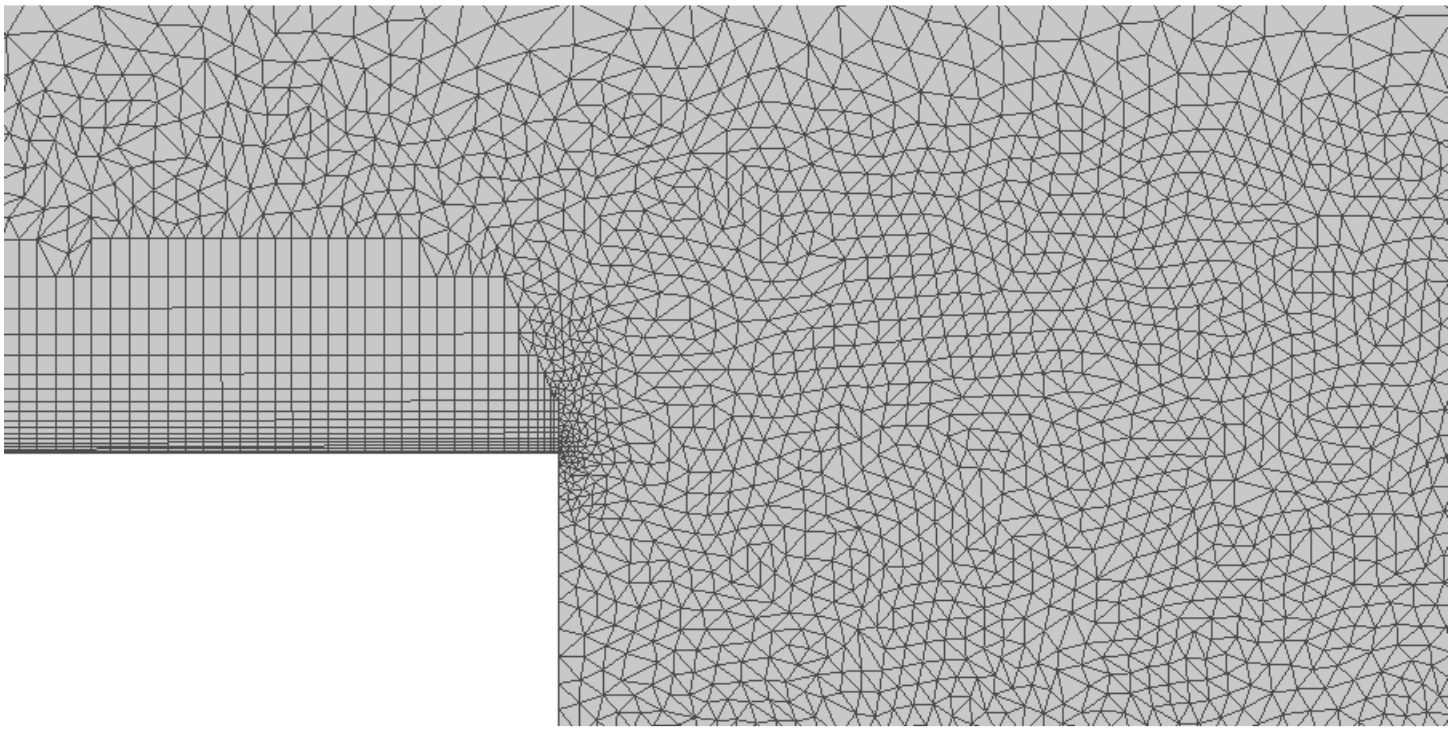


Figure 25: Finer Detail of Mesh Near the Backward-Facing Step

AcuSolve Results

The AcuSolve solution converged to a steady state and the results reflect the mean flow conditions. As the fully developed turbulent flow enters the divergent section, the expansion of the cross-sectional height causes a shear layer to develop above the lower wall. The expansion causes two recirculation zones; one immediately near the step wall and one that extends further downstream near the lower wall. The recirculation region eventually recovers downstream and the flow reattaches. The following images show the flow solution within the channel, demonstrating the recirculation region and reattachment point.

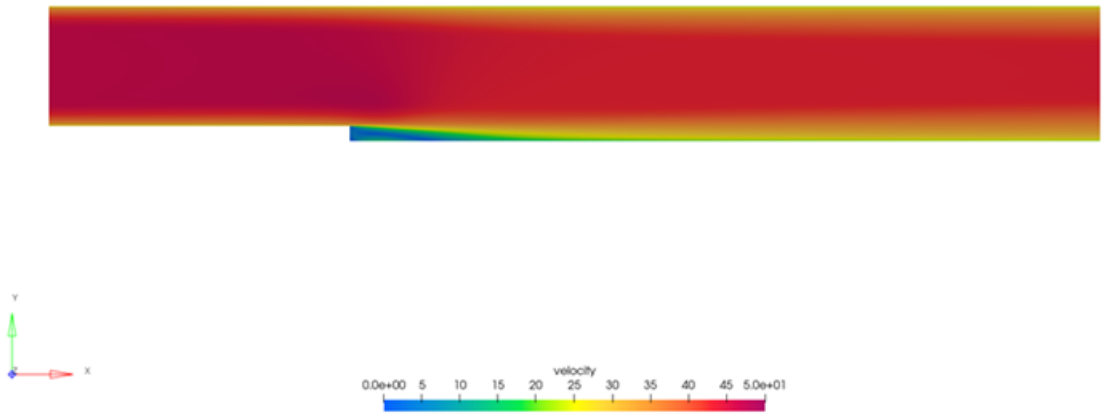


Figure 26: Velocity Contours Showing Low Velocity Near the Step Wall

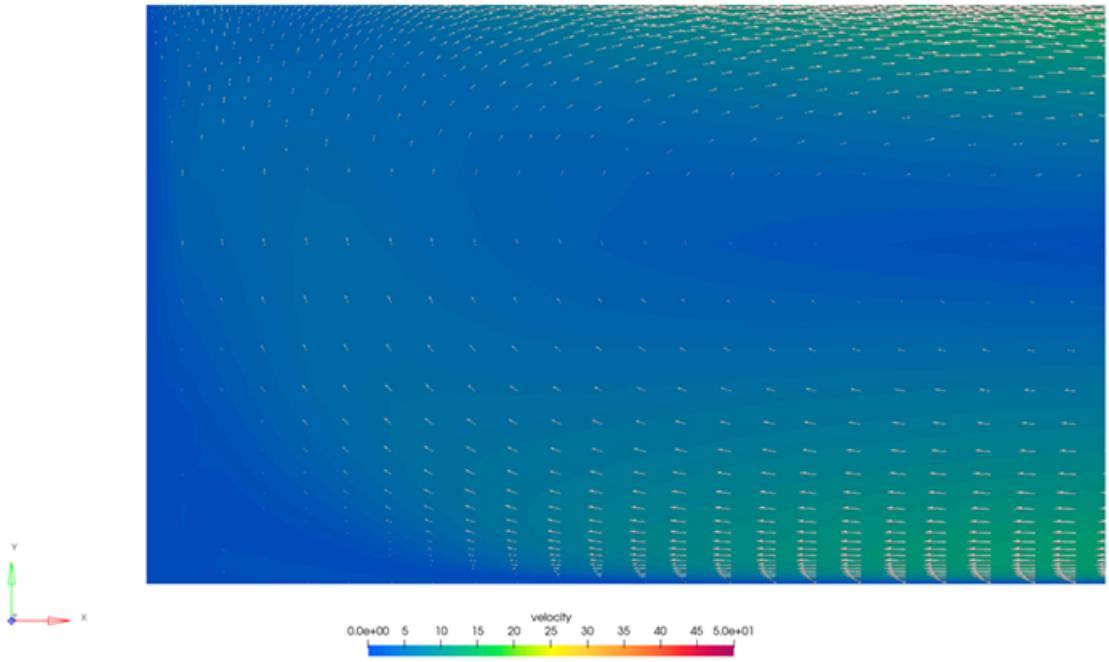


Figure 27: Close-Up View of Velocity Vectors and Contours in the Cross-Stream Plane Directly After the Step

Upstream of the expansion section, the streamwise velocity increases as the distance from the lower wall increases until it reaches the centerline of the channel and then begins decreasing until it reaches zero at the top wall. As the flow passes the step, it expands into the region directly downstream of the step wall, separating from the wall and recirculating until it recovers further downstream. The image below shows the coefficient of pressure along the lower wall of the step compared against experimental results. The coefficient of pressure is calculated using the reference velocity (Uref) obtained at x/H=-4 (centre of the channel) with the reference pressure (Pref) extracted at x/H = 40 (at the wall) so that Cp becomes 0 at x/H=40. The image shows black circles representing the experimental measurements (Driver 1985), a solid red line for the SA model, a solid blue line for the SST model, a solid green line for the K-ω model and a solid cyan line for the K-ε model, representing the AcuSolve results. The resulting pressure coefficient within the channel demonstrates minor differences between the three

turbulence models. The SA model predicts a slightly larger recirculation region and does not reach the peak pressure in the wake of the step, compared to the SST model.

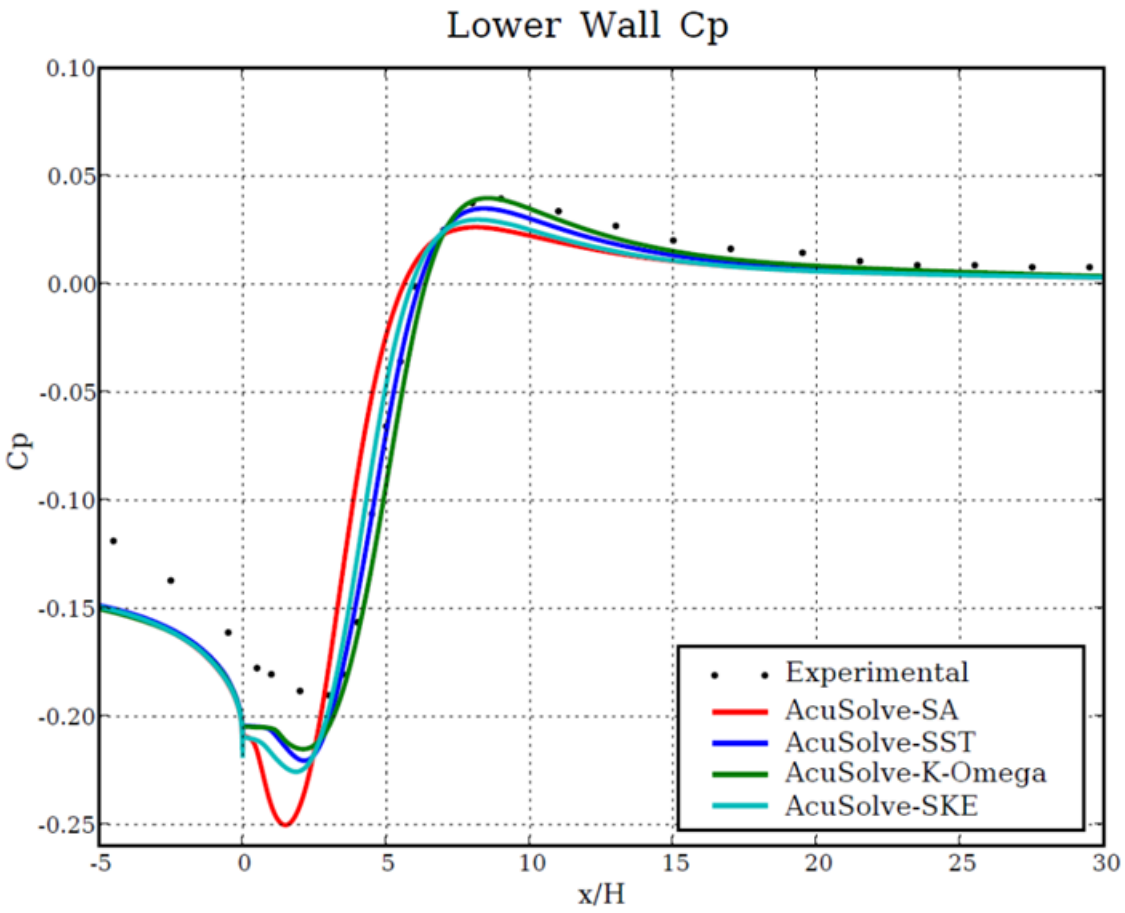


Figure 28: Coefficient of Pressure Plotted Against Location Along the Lower Wall Before and After the Step

Summary

In this application, a fully developed turbulent flow at a Reynolds number of 36,000 is studied and compared against experimental data. The AcuSolve results compare well with the experimental data for pressure coefficient. The performance of the Spalart Allmaras turbulence model was found to be consistent with previously published results for flow over a backward facing step (NASA 2015). The K-ω model appears to perform the best out of the three, predicting the reattachment and pressure distribution most accurately. AcuSolve demonstrates the ability to predict the shear layer in this type of application, the recirculation that occurs downstream of the step, as well as the reattachment point within the channel.

Simulation Settings for Turbulent Flow over a Backward-Facing Step

HyperMesh CFD database file: `<your working directory>\backstep_turbulent\backstep_turbulent.hm`

Global

- Problem Description
  - Analysis type - Steady State

- Turbulence equation - Shear Stress Transport
- Auto Solution Strategy
  - Max time steps - `100`
  - Relaxation Factor - `0.5`
- Material Model
  - Air
    - Density - `1.183` kg/m3
    - Viscosity - `1.4575e-3` kg/m-sec

Model

- Volume
  - Fluid
    - Element Set
      1. Material model - Air
- Surfaces
  - +Z
    - Simple Boundary Condition
      1. Type - Slip
  - -Z
    - Simple Boundary Condition
      1. Type - Slip
  - Inlet
    - Simple Boundary Condition - (disabled to allow for nodal boundary conditions to be set)
    - Advanced Options
      1. Nodal Boundary Conditions
         1. X-Velocity
            1. Type - Linear
            2. Precedence - Always
            3. Curve fit variable - Y reference coordinate
            4. Curve fit values - (included in database)
         2. Y-Velocity
            1. Type - Linear
            2. Precedence - Always
            3. Curve fit variable - Y reference coordinate
            4. Curve fit values - (included in database)
         3. Z-Velocity
            1. Type - Zero
         4. Kinetic Energy

1. Type - Linear
2. Precedence - Always
3. Curve fit variable - Y reference coordinate
4. Curve fit values - (included in database)

5. Eddy Frequency
   1. Type - Linear
   2. Precedence - Always
   3. Curve fit variable - Y reference coordinate
   4. Curve fit values - (included in database)

- Outlet
  - Simple Boundary Condition
    1. Type - Outflow
- Wall - Lower - Downstream
  - Simple Boundary Condition
    1. Type - Wall
    2. Turbulence wall type - Low Reynolds Number
- Wall - Lower - Upstream
  - Simple Boundary Condition
    1. Type - Wall
    2. Turbulence wall type - Low Reynolds Number
- Wall - Step
  - Simple Boundary Condition
    1. Type - Wall
    2. Turbulence wall type - Wall Function
- Wall - Upper
  - Simple Boundary Condition
    1. Type - Wall
    2. Turbulence wall type - Low Reynolds Number

References

D. M. Driver and H. L. Seegmiller. "Features of Reattaching Turbulent Shear Layer in Divergent Channel Flow". AIAA Journal, 23(2): 163-171. Feb 1985.

NASA Langley Research Center Turbulence Modeling Resource webpage. http://turbmodels.larc.nasa.gov/backstep_val.html. Accessed June 2021.

Turbulent Flow Past a Convex Curve in a Channel

In this application, AcuSolve is used to simulate fully developed turbulent flow through a channel containing a convex curve in the lower wall. AcuSolve results are compared with experimental results as described in Smits (1979) and on the NASA Langley Research Center Turbulence Modeling Resource webpage. The close agreement of AcuSolve results with experimental data and reference turbulence model performance validates the ability of AcuSolve to model cases with turbulent flow moving past a convex curved wall.

Problem Description

The problem consists of a fluid with material properties close to air flowing through a channel containing a 30° swept wall, with a lower convex wall. The inlet channel height and remaining duct height is 0.127 m. The bulk velocity (v) normal to the inlet is 31.9 m/s and an integrated outflow pressure is specified to allow the flow to pass through the channel. The flow develops into fully turbulent flow at a Reynolds's number (Re) of 2,100,000. The density of the flow medium is 1.225 kg/m3 and the dynamic viscosity is 1.8608 X 10-5 kg/m-s. The simulation is conducted with the Reynolds Averaged Navier-Stokes equations using the Spalart Allmaras, Shear Stress Transport (SST), K-ω and Realizable K-ε turbulence models. The flow conditions are compared against experimental data and the current state-of-the-art performance for coefficient of pressure and coefficient of friction.

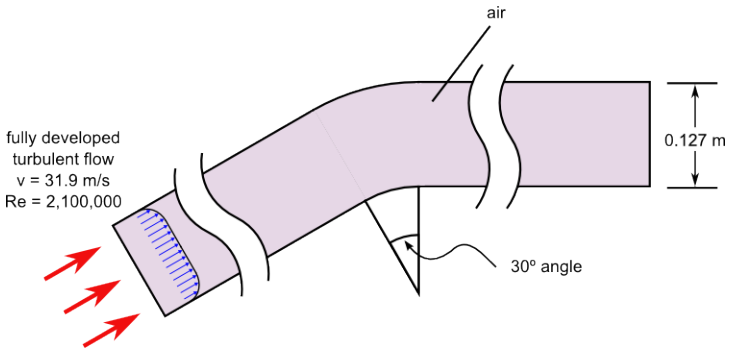


Figure 29: Critical Dimensions and Parameters for Simulating Turbulent Flow Through a Convex Channel

The simulation was performed as a two dimensional problem by restricting flow in the out-of-plane direction through the use of a mesh that is one element thick. The upper and lower walls are specified as no-slip, the inlet velocity and eddy viscosity are specified normal to the inlet face to match the experimental Reynolds Number.

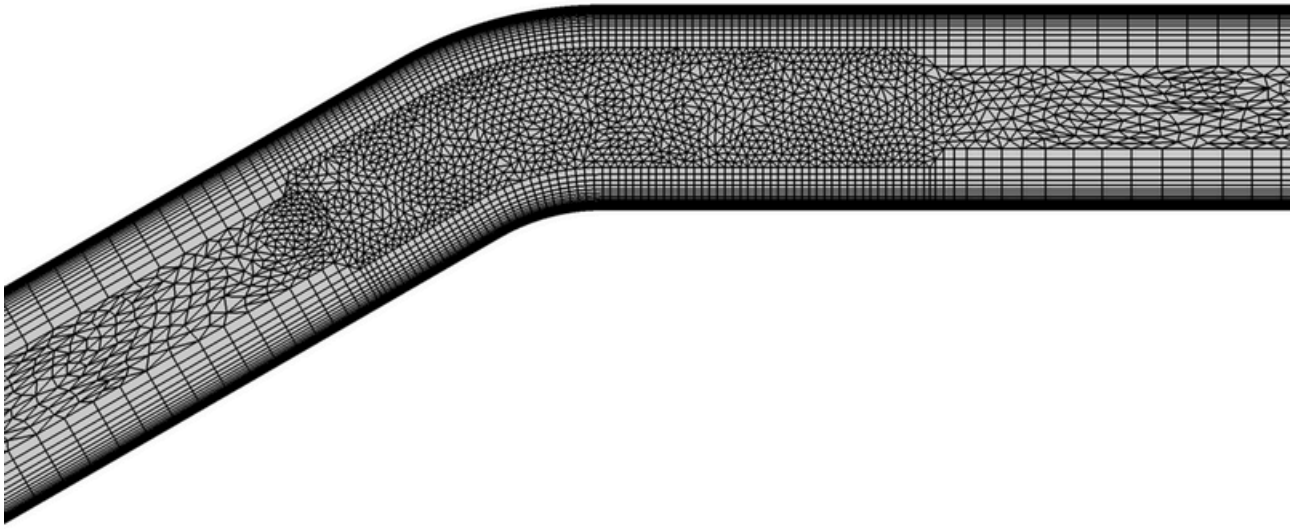


Figure 30: Detail of the Mesh used for Simulating Turbulent Flow Through a Convex Channel

AcuSolve Results

The AcuSolve solution converged to a steady state and the results reflect the mean flow conditions within the channel. As the fluid enters the channel it develops into fully turbulent flow exhibiting a steep parabolic velocity profile across the width of the channel. The flow begins to accelerate near the lower wall and decelerate near the top wall as it approaches the 30° bend. The results show that the upper (concave) wall destabilizes the boundary layer, increasing the eddy viscosity and forcing the flow velocity to decrease. The following figures show the flow conditions within the channel.

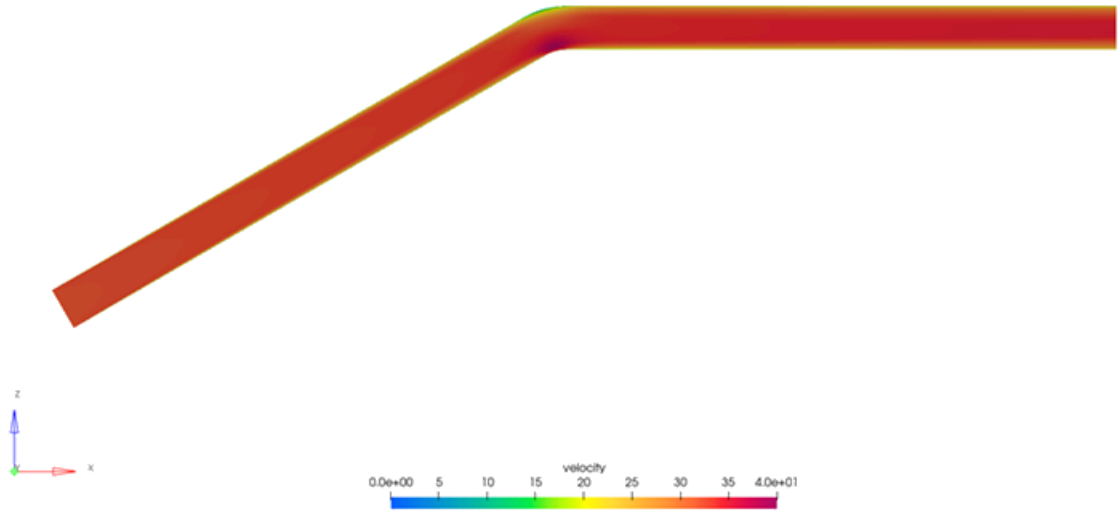


Figure 31: Velocity Contours in the Streamwise Plane

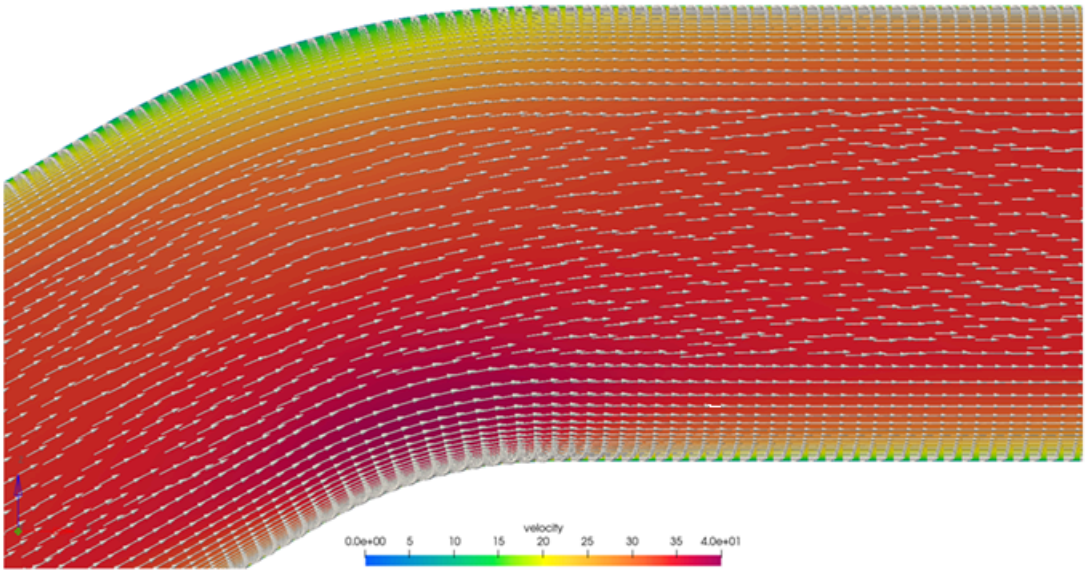


Figure 32: Close up View of Velocity Vectors and Velocity Contours at the 30° Bend

Upstream of the curved section of the channel, the flow normal to the channel opening increases as the distance from the lower wall increases until it reaches the centerline of the channel and then begins decreasing until it reaches zero at the top wall. As the flow approaches the curved section, it begins to accelerate, requiring that the flow velocity near the upper wall decrease to conserve momentum. The relatively low angle of curvature in the channel does not cause the accelerated fluid to recirculate. The images below show the coefficient of pressure (Cp) and coefficient of skin friction (Cf) along the lower wall of the channel. The images show black circles representing the experimental measurements (Smiths 1979), solid red lines for the SA model, solid blue lines for the SST model, solid green lines for the K-ω model and a solid cyan line for the K-ε model, representing the AcuSolve results. The coefficient of pressure within the channel is predicted nearly identically compared to the experiment for each of the turbulence models. It appears that the SST and K-ε models capture the low velocity region with the best accuracy, demonstrating that the flow velocity decreases significantly, but does not recirculate within the channel. This is shown in the friction coefficient plot, where the coefficient of friction, and subsequently the wall shear stress, does not decrease below zero.

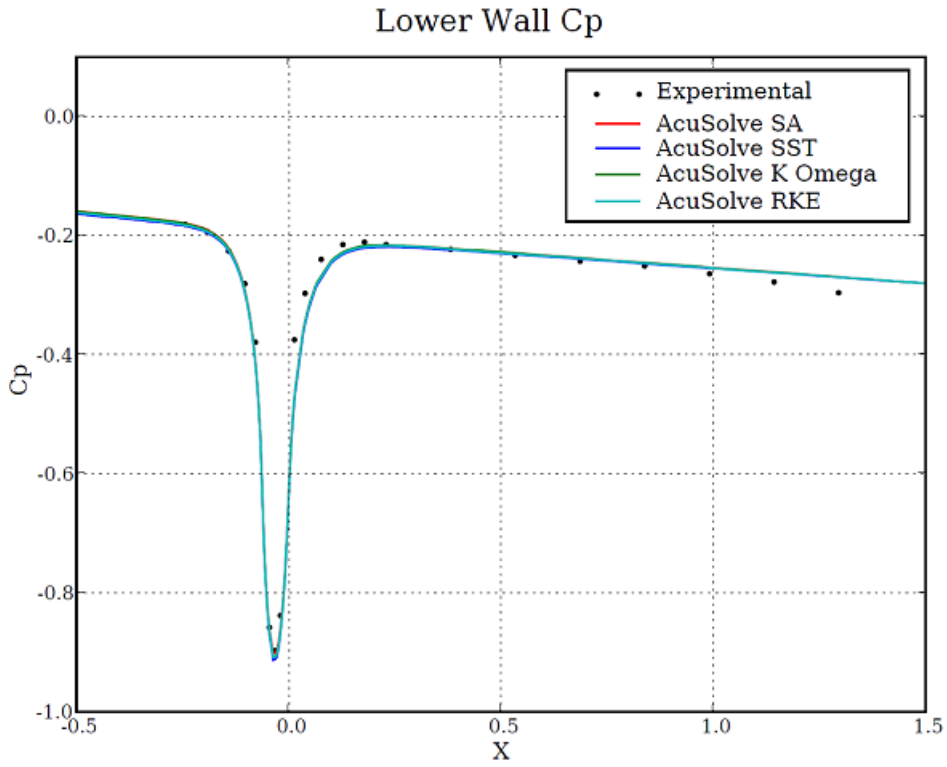


Figure 33: Coefficient of Pressure Plotted Against Relative Distance Along the Lower Wall from the Curve

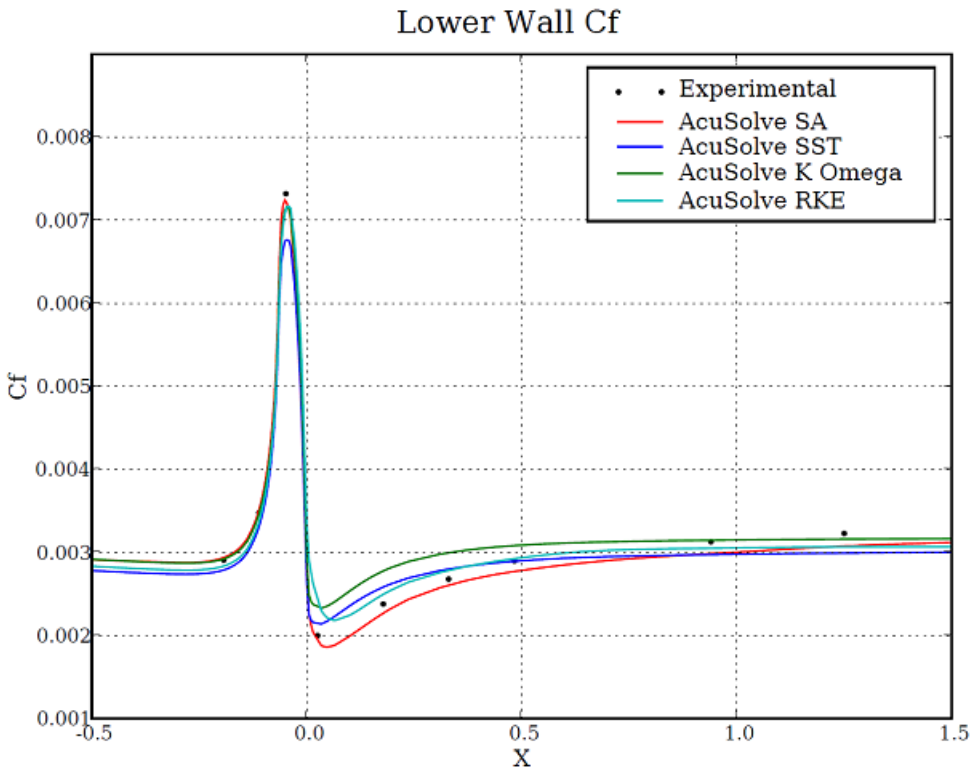


Figure 34: Skin Friction Coefficient Plotted Against Relative Distance Along the Lower Wall from the Curve

Summary

In this application, a turbulent flow through a curved channel at a Reynolds number of 2,100,000 is simulated and compared against experimental data. The AcuSolve results compare well with the experimental data for pressure coefficient and skin friction coefficient within the channel. The performance of the Spalart Allmaras turbulence model was found to be consistent with previously published results for flow through a convex-curved channel (NASA 2015) and the SST turbulence model appears to predict the shear stress on the lower wall most accurately. AcuSolve demonstrates the ability to predict the complex boundary layers resulting from the curvature of the channel and accurately predicts the propagation of the flow further downstream.

Simulation Settings for Turbulent Flow past a Convex Curve in a Channel

HyperMesh CFD database file: `<your working directory>\convex_curvature_turbulent \convex_curvature_turbulent.hm`

Global

- Problem Description
  - Analysis type - Steady State
  - Turbulence equation - Spalart Allmaras
- Auto Solution Strategy
  - Max time steps - `100`
  - Convergence tolerance - `0.0001`

    - Relaxation factor - `0.4`
- Material Model
    - Fluid
        - Density - `1.225` kg/m3
        - Viscosity - `1.8603e-5` kg/m-sec

  Model
- Volumes
    - Fluid - elbow
        - Element Set
            1. Material model - Fluid
    - Fluid - inlet
        - Element Set
            1. Material model - Fluid
    - Fluid - outlet
        - Element Set
            1. Material model - Fluid
- Surfaces
    - -Y
        - Simple Boundary Condition
            1. Type - Slip
    - +Y
        - 1. Type - Slip
    - Inlet
        - Simple Boundary Condition
            1. Type - Inflow
            2. Inflow type - Velocity
            3. Inflow velocity type - Normal
            4. Normal velocity - `31.9` m/sec
            5. Turbulence input type - Direct
            6. Eddy viscosity - `1.3671e-7` m2/sec
- Internal
    - Simple Boundary Condition - (disabled)
- Lower Wall
    - Simple Boundary Condition
        - Type - Wall
        - Turbulence wall type - Low Reynolds Number
- Outlet

    - Simple Boundary Condition
        - Type - Outflow
- Upper Wall
    - Simple Boundary Condition
        - Type - Wall
        - Turbulence wall type - Low Reynolds Number

References

A. J. Smits, S. T. B. Young, and P. Bradshaw. "The Effect of Short Regions of High Surface Curvature on Turbulent Boundary Layers". Journal of Fluid Mechanics. 94(2):209-242. 1979

NASA Langley Research Center Turbulence Modeling Resource webpage. http://turbmodels.larc.nasa.gov/smitscurve_val.html. Accessed May 2021.

Turbulent Natural Convection Inside a Tall Cavity

In this application, AcuSolve is used to simulate the natural convection of a turbulent flow field within a tall rectangular cavity. AcuSolve results are compared with experimental results as described in Betts and Bokhari (2000). The close agreement of AcuSolve results with experimental results validates the ability of AcuSolve to model cases with natural convection of turbulent flow within a tall cavity.

Problem Description

The problem consists of air within a tall cavity with a hot wall and a cold wall, as shown in the following image, which is not drawn to scale. The cavity is 2.18 m tall, 0.0762 m wide, and 0.52 m deep. The cavity's vertical walls differ in temperature, causing the fluid to transfer the heat, leading to natural convection. The temperature of the hot wall is 307.85 K, while the temperature of the cold wall is 288.25 K. The horizontal walls of the cavity are adiabatic. The length-to-width ratio of 28.6 and temperature difference of 19.6 K produce a turbulent flow field within the cavity with a Rayleigh number of $8.6X10^{5}$ (Betts and Bokhari 2000). The flow medium is air, with a Boussinesq approximation for density, a specific heat of 1005 J/kg-K, and a viscosity of $1.781 X 10^{-5}$ kg/m-s. Gravity is applied globally to the volume of air.

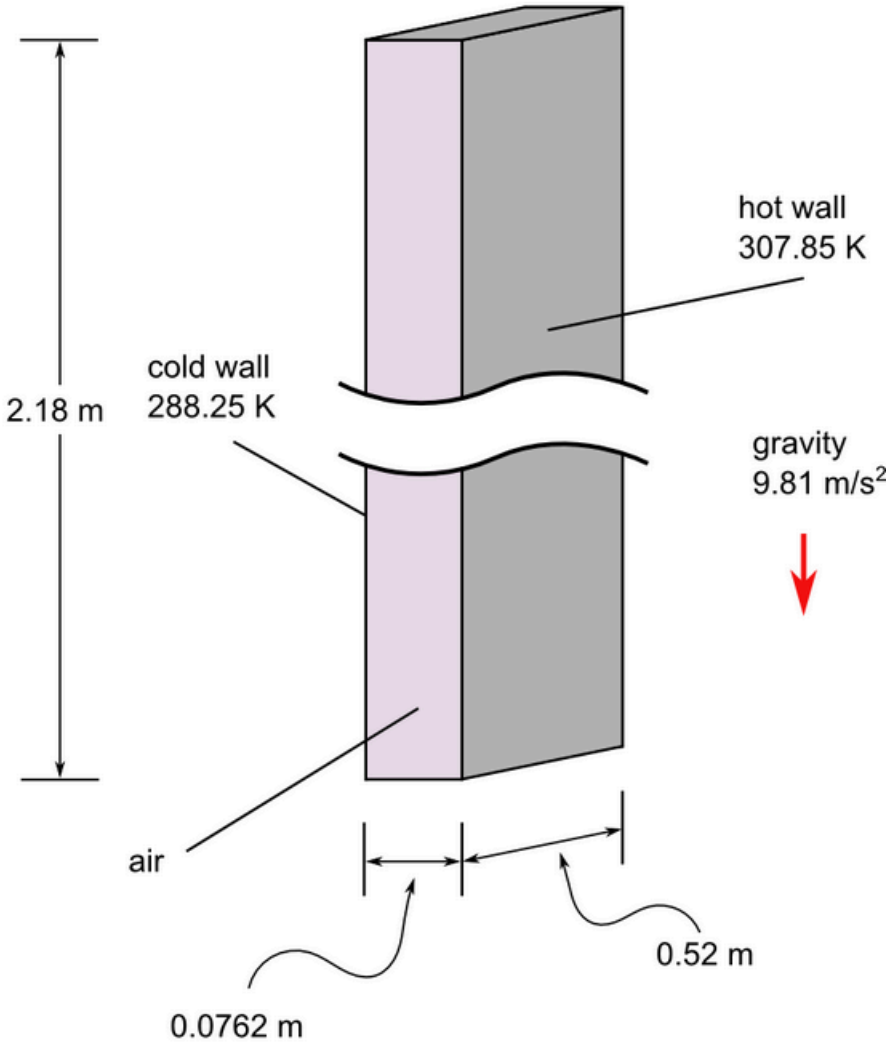


Figure 35: Critical Dimensions and Parameters for Simulating Turbulent Natural Convection in a Tall Cavity

The simulation was performed as a two dimensional problem by constructing a volume mesh that contains a single layer of elements in the extruded direction, normal to the flow plane and by imposing symmetry boundary conditions on the extruded planes.

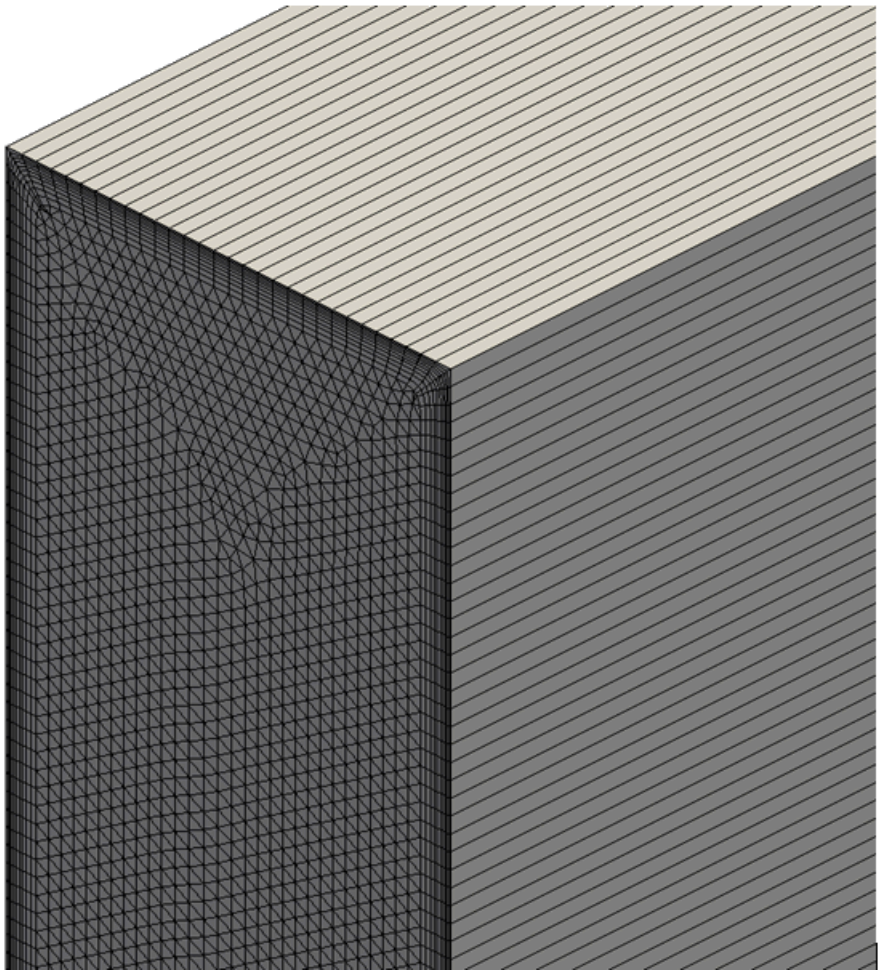


Figure 36: Mesh used for Simulating the Natural Convection of Turbulent Flow in a Tall Cavity

AcuSolve Results

The AcuSolve solution converged to a steady state and the results reflect the mean flow conditions. The natural convection of the flow is generated by heat transfer from the vertical walls to the fluid in the cavity. The temperature gradients created by this heat transfer cause differing densities within the flow region. The warmer air rises to the top of the cavity due to its lower density while the colder air sinks to the bottom of the cavity due to its higher density. This produces flow near the hot vertical wall in the positive vertical direction and flow near the cold wall in the negative vertical direction.

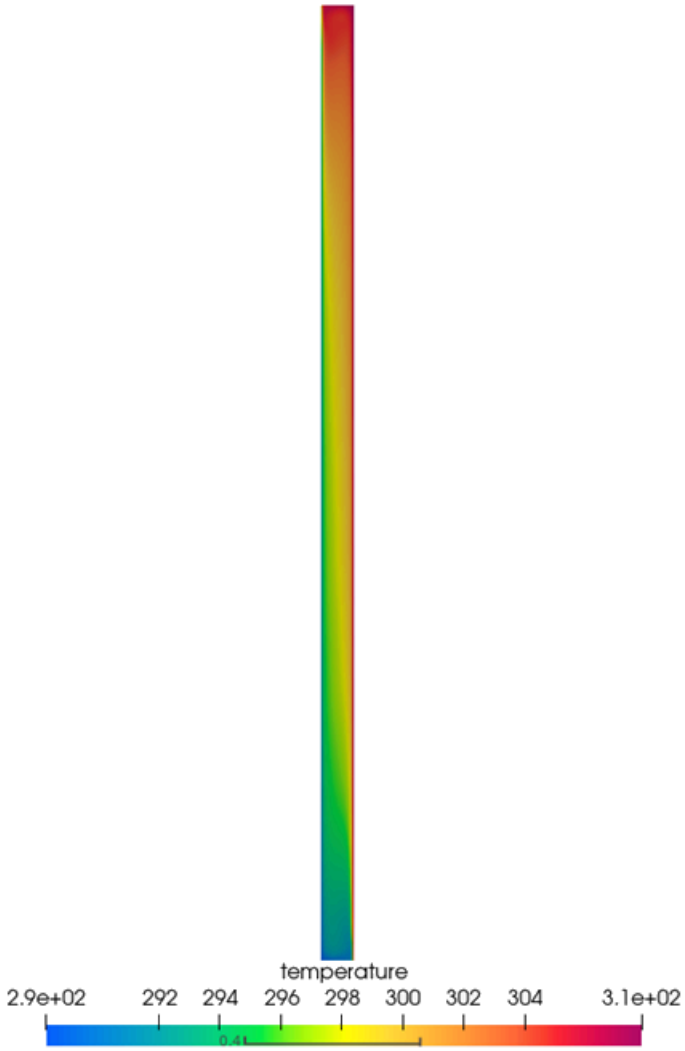


Figure 37: Temperature Contours Throughout Tall Cavity in the X-Y Plane

The AcuSolve results of the temperature and vertical velocity within the cavity are compared to the corresponding experimental values in the plots shown below. The temperature of the air is lowest near the cold vertical wall, remains relatively steady in the middle of the cavity, and then peaks near the hot vertical wall. Following a similar trend, the AcuSolve results show that the velocity is lowest near the cold vertical wall, due to the air sinking, and then steadily increases as the air begins to rise near the hot vertical wall. The velocity at the walls is zero due to the no-slip boundary condition. Additional comparisons are made to evaluate the performance of four turbulence models, Spalart-Allmaras (SA), shear stress transport (SST), K-Omega and K-ε.

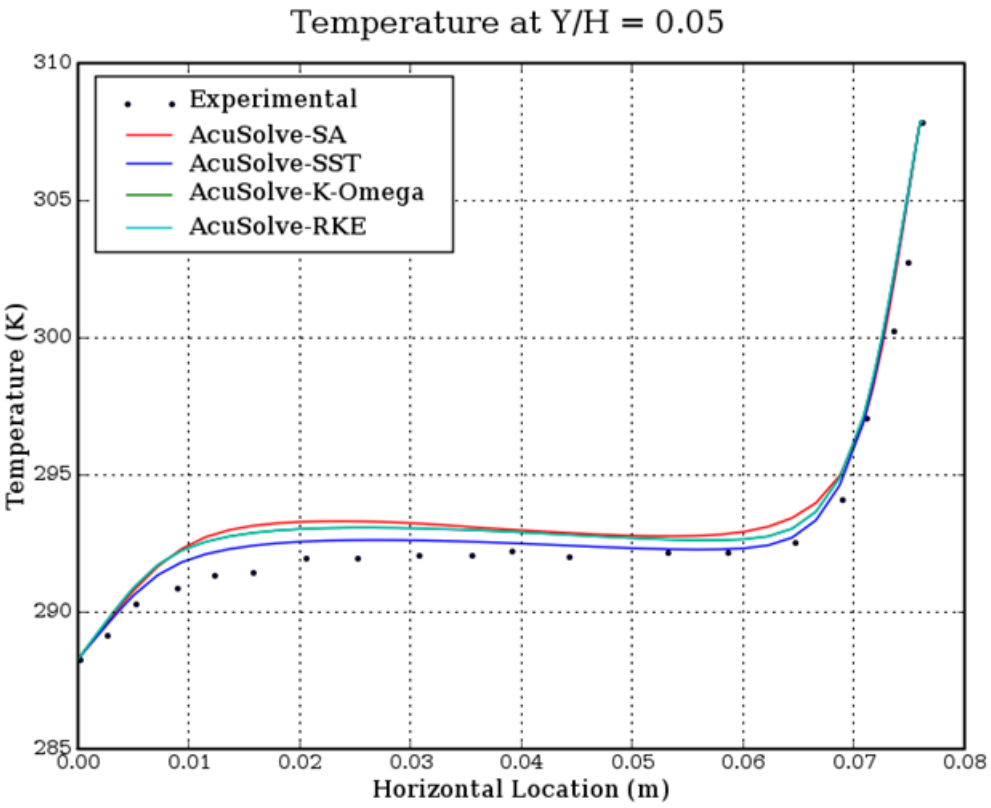


Figure 38: Temperature Plotted against Location along Horizontal at a Position of y/H=0.05 in the Cavity, where H is the Cavity Height and y is the Distance from the Bottom Wall

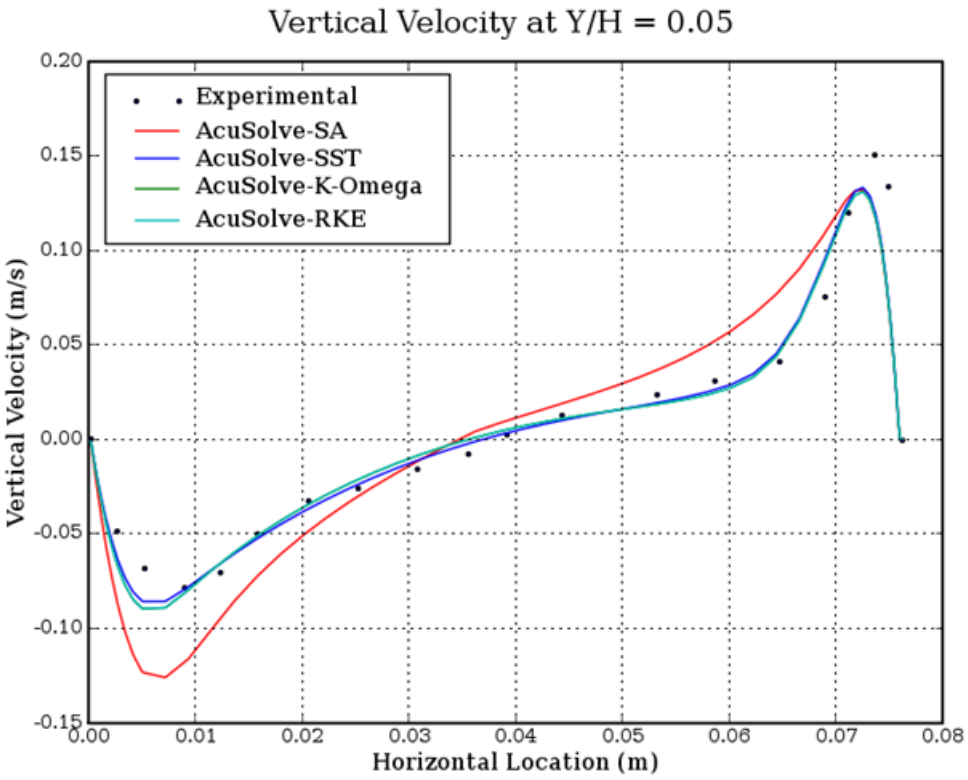


Figure 39: Vertical Velocity Plotted against Location along Horizontal at a Position of y/H=0.05 in the Cavity, where H is the Cavity Height and y is the Distance from the Bottom Wall

Summary

In this application, turbulent flow developed by natural convection, at a Rayleigh number of 8.6X105, is studied within a tall cavity. The AcuSolve results compare well with the experimental data for temperature and vertical velocity along a horizontal line at a location of y/H=0.05 in the tall cavity, with the two-equation models capturing the velocity gradient with greater accuracy. A temperature difference occurs within the flow region due to the heat transfer from the vertical walls of the cavity. The hotter, less-dense air rises to the top of the cavity while the colder, denser air sinks to the bottom, giving rise to recirculation. AcuSolve demonstrates the ability to accurately predict the natural convection of turbulent flow within a tall cavity.

Simulation Settings for Turbulent Natural Convection Inside a Tall Cavity

HyperMesh CFD database file: `<your working directory\cavity_turbulent_heat \cavity_turbulent_heat.hm`

Global

- Problem Description
  - Analysis type - Steady State
  - Turbulence equation - SST
- Auto Solution Strategy
  - Relaxation factor - `0.5`

- Convergence tolerance - `0.005`

- Material Model
  - Air
    - Type - Boussinesq
    - Density - `1.225` kg/m3
    - Specific Heat - `1005` J/kg-K
    - Viscosity - `1.781e-5` kg/m-sec

  Model
- Volumes
  - Volume
    - Element Set
      1. Material model - Air
- Surfaces
  - Back
    - Simple Boundary Condition
      1. Type - Symmetry
  - Bottom
    - **Simple Boundary Condition**
      1. Type - Wall
      2. Temperature BC type - Flux
      3. Heat Flux - `0.0` W/m2
  - Cold
    - **Simple Boundary Condition**
      1. Type - Wall
      2. Temperature BC type - Value
      3. Temperature - `288.25` K
  - Front
    - Simple Boundary Condition
      1. Type - Symmetry
  - Hot
    - Simple Boundary Condition
      1. Type - Wall
      2. Temperature BC type - Value
      3. Temperature - `307.85` K
  - Top
    - Simple Boundary Condition
      1. Type - Wall

2 Temperature BC type - Flux
3 Heat Flux - `0.0` W/m2

References

P.L. Betts and I.H. Bokhari. "Experiments on Turbulent Natural Convection in an Enclosed Tall Cavity". International Journal of Heat and Fluid Flow 21:675-683. 2000.

Turbulent Flow Over a NACA 0012 Airfoil

In this application, AcuSolve is used to simulate turbulent flow of a fluid over a NACA 0012 airfoil at 3 angles of attack, 0 degrees, 10 degrees, and 15 degrees. AcuSolve results are compared with experimental results for coefficients of pressure, lift, and drag reported by NASA. The close agreement of AcuSolve results with experimental results validates the ability of AcuSolve to model external aerodynamics.

Problem Description

The problem consists of a NACA 0012 airfoil located in the center of a cylindrical domain, as shown in the following image, which is not drawn to scale. Fluid enters the domain with a velocity of 1.0 m/s. The domain edges are distant, 500 chord lengths, from the airfoil to minimize any far field effects. The problem is set up to simulate high Reynolds number flow, with Re = 6,000,000.

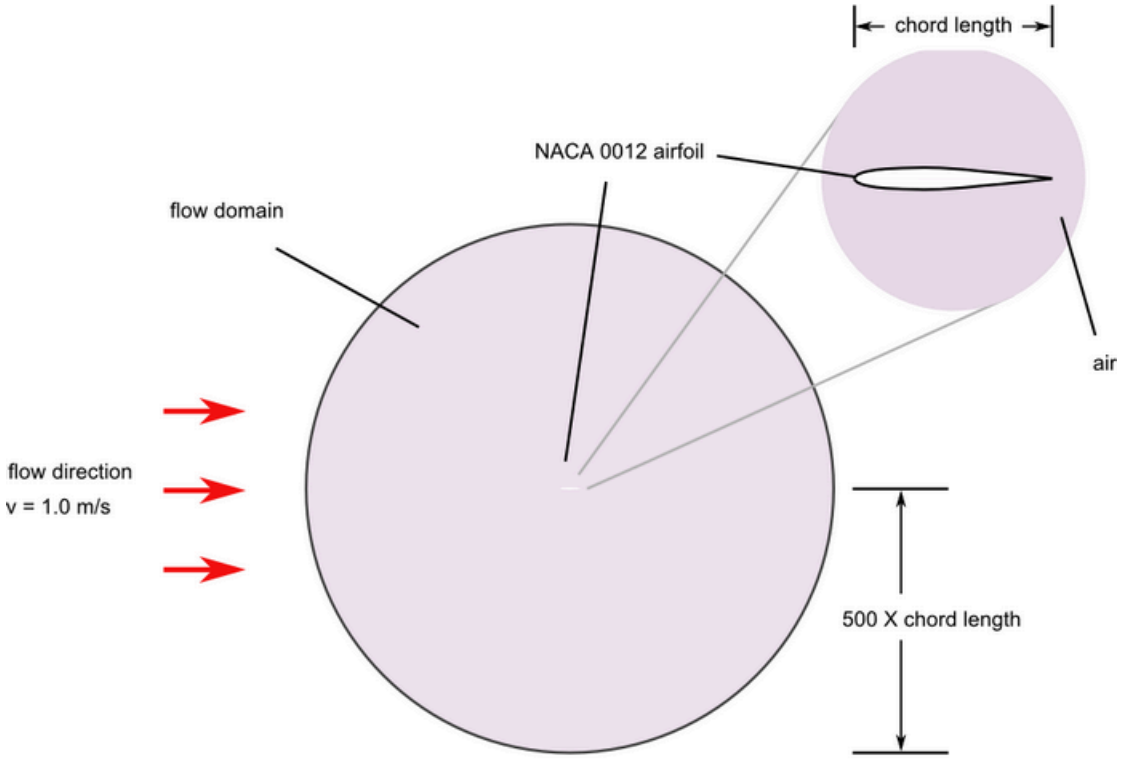


Figure 40: Critical Dimensions and Parameters for Simulating Turbulent Flow over a NACA 0012 Airfoil

The simulation was performed as a two dimensional problem by restricting flow in the out-of-plane direction through the use of a mesh that is one element thick.

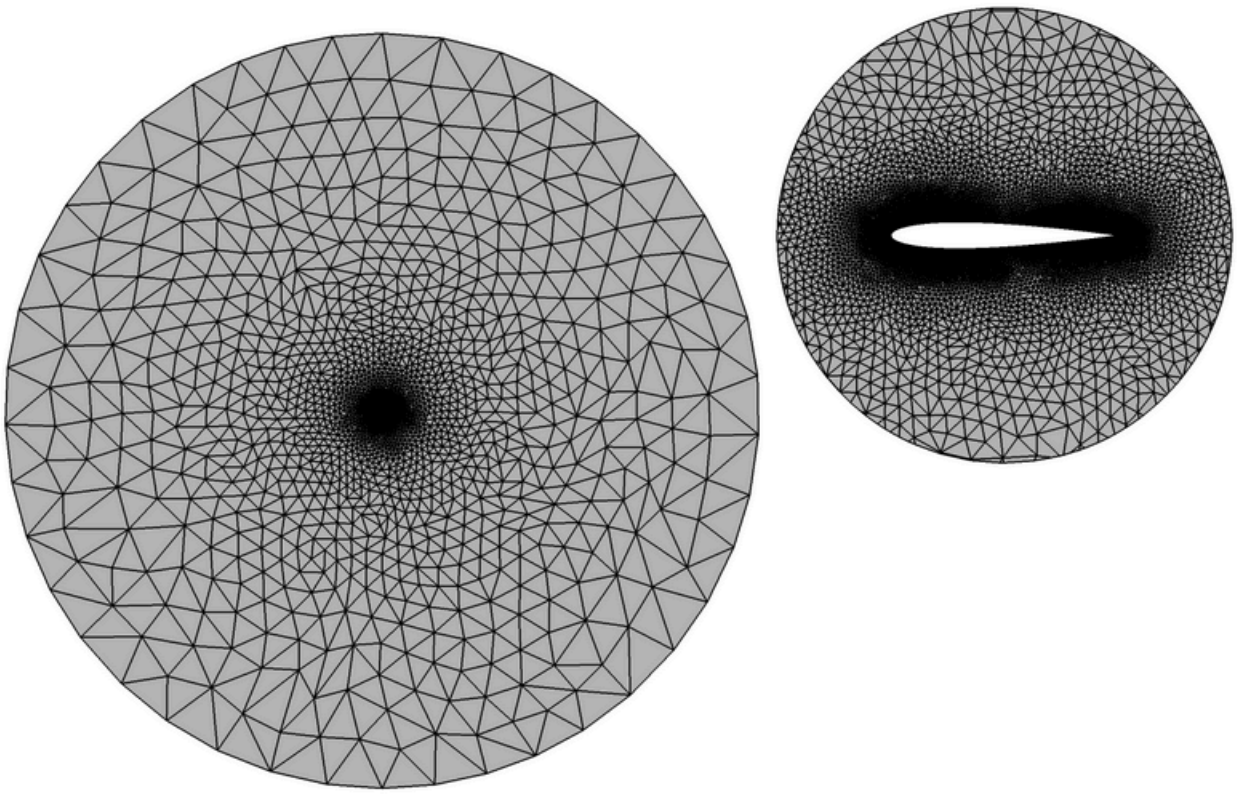


Figure 41: Mesh Used for Simulating Turbulent Flow over a NACA 0012 Airfoil (the Image on the Left Represents the Full Mesh, the Image on the Right Represents Mesh Details near the Airfoil)

AcuSolve Results

The AcuSolve solution converged to a steady state and the results reflect the mean flow conditions for each of the three angles of attack, 0 degrees, 10 degrees, and 15 degrees. For each case, the angle of attack was varied by changing the angle of the incident flow.

> **Note:** This enables the use of a single mesh for all of the simulations.

With a 0 degree angle of attack, the flow field is symmetric as the fluid flows over and under the airfoil. The airfoil impedes the flow, causing stagnation at the leading edge. As the fluid passes over and under the airfoil, velocity increases. As the fluid passes over the blunt trailing edge, a minor amount of flow separation occurs. The flow reattaches shortly after it passes the trailing edge and recovers the mean velocity in the distant far field.

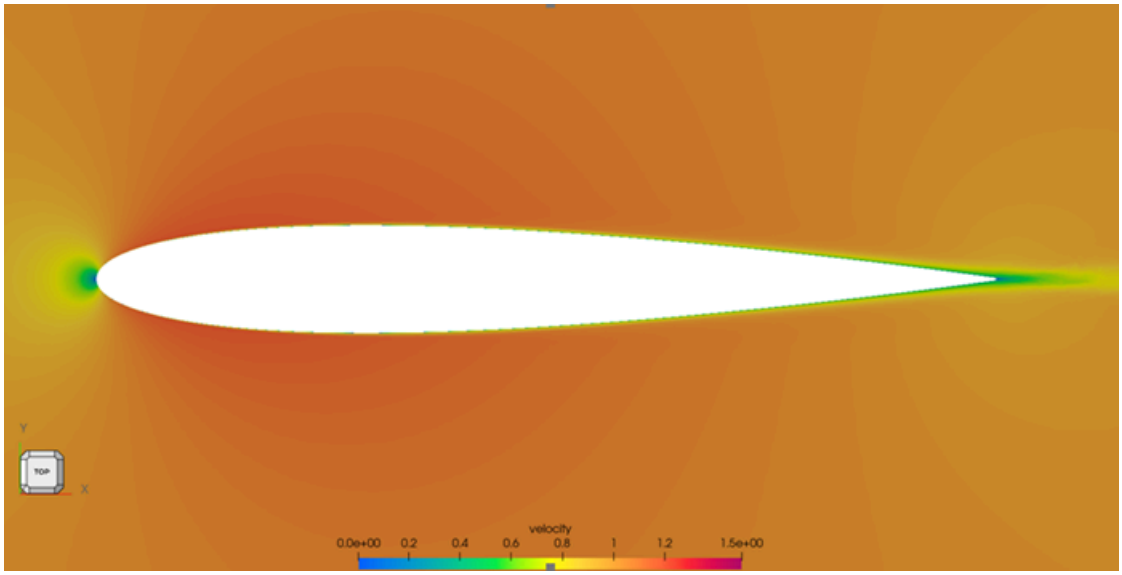


Figure 42: Contours of Velocity Magnitude Where Angle of Attack = 0 Degrees

With a 10 degree angle of attack, the stagnation point is shifted downward (relative to the airfoil), reflective of the shifted angle of attack. Fluid velocity above the airfoil is markedly different than that below the airfoil. A small low-velocity region is evident on the suction side of the airfoil, indicating some separation toward the trailing edge.

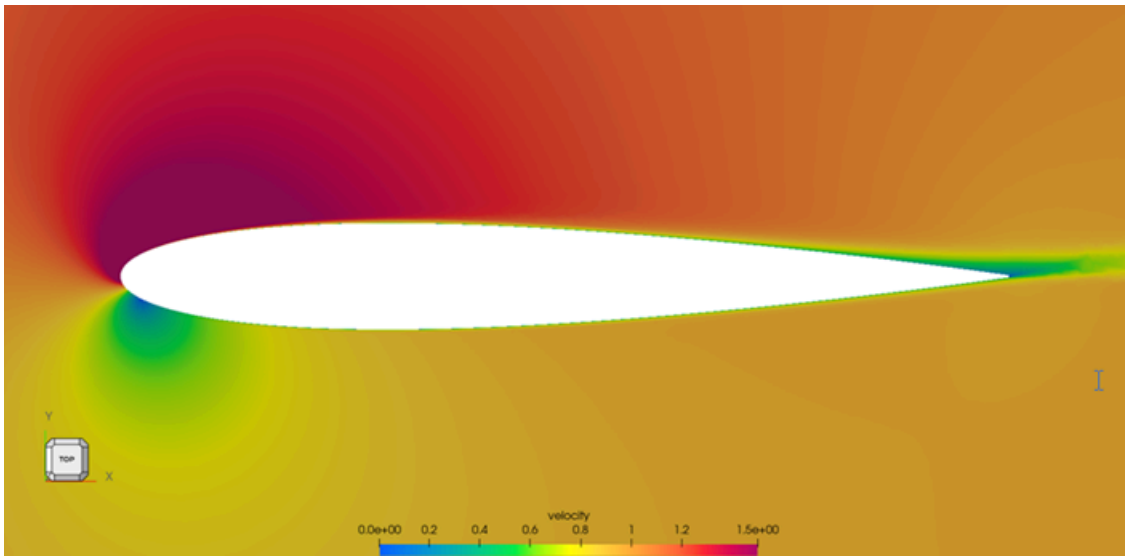


Figure 43: Contours of Velocity Magnitude Where Angle of Attack = 10 degrees

With a 15 degree angle of attack, the stagnation at the front of the airfoil is shifted even farther downward (relative to the airfoil), reflective of the shifted angle of attack. Additionally, the low-velocity wake increases in size, reflecting separation along the suction surface of the airfoil.

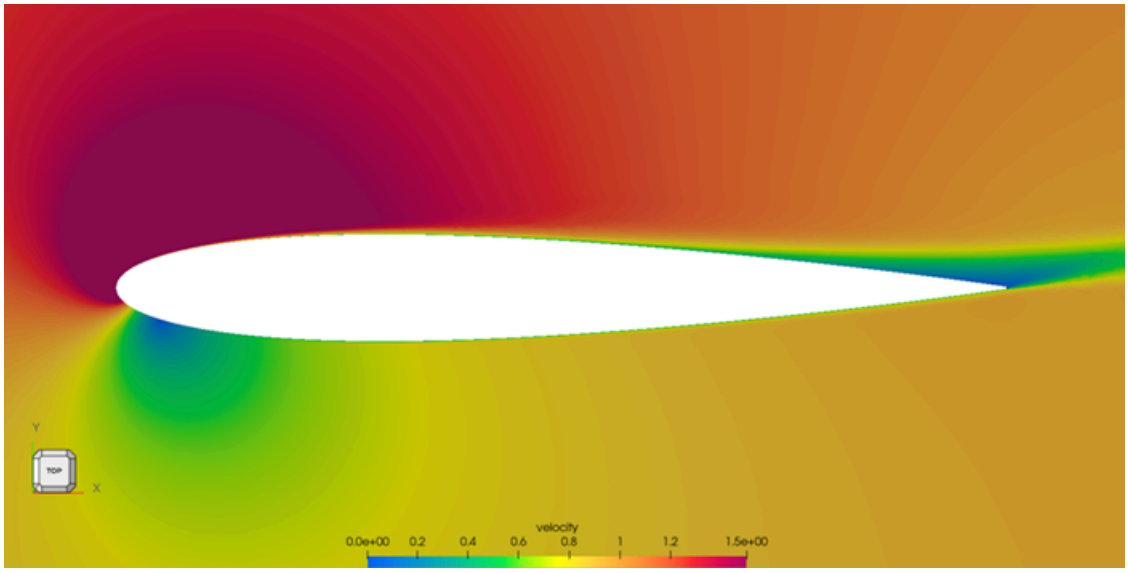


Figure 44: Contours of Velocity Magnitude Where Angle of Attack = 15 Degrees

Experimental values of coefficient of lift (CL) at angles of attack (α) of 10 degrees and 15 degrees and values of drag coefficient (cd) at angles of attack (α) of 0 degrees,10 degrees, and 15 degrees are presented with the corresponding AcuSolve results in the following table.

Table 2:

	CL (α=10)	**CL (α=15)**	**cd (α=0)**	**cd (α=10)**	**cd (α=15)**
Experimental	1.0941	1.5576	0.0082	0.0123	0.0207
AcuSolve	1.0905	1.5428	0.0081	0.0124	0.0208
Percent deviation from experimental	0.33	0.95	1.22	0.81	0.48

AcuSolve values for coefficient of pressure are plotted against experimental results for angles of attack (α) of 0 degrees, 10 degrees, and 15 degrees in the following plots. The results are presented for normalized distance along the airfoil, given by x/c, where x is the distance from the leading edge and c is the chord length.

For each case, AcuSolve is able to predict the flow characteristics at each point along the airfoil surface.

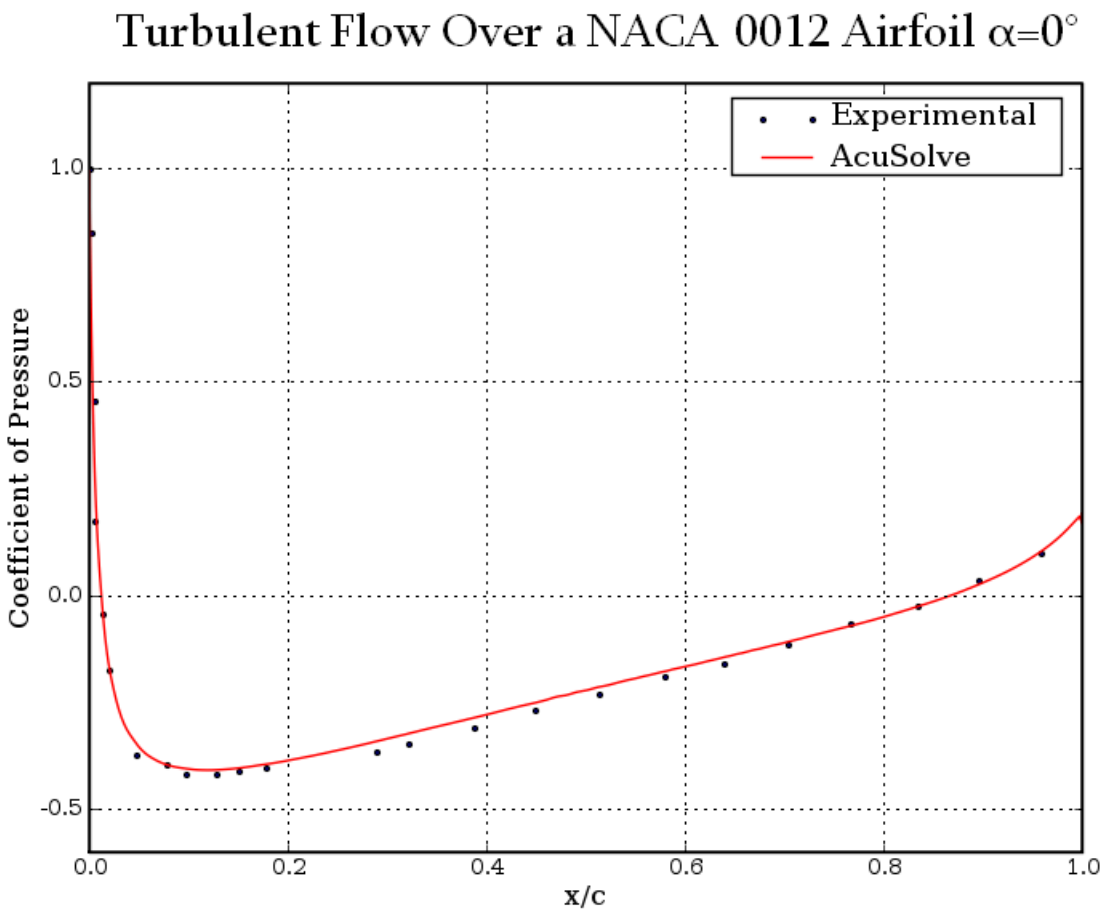


Figure 45: Coefficient of Pressure Plotted Against Normalized Distance Along the Airfoil for Angle of Attack (a) = 0 Degrees

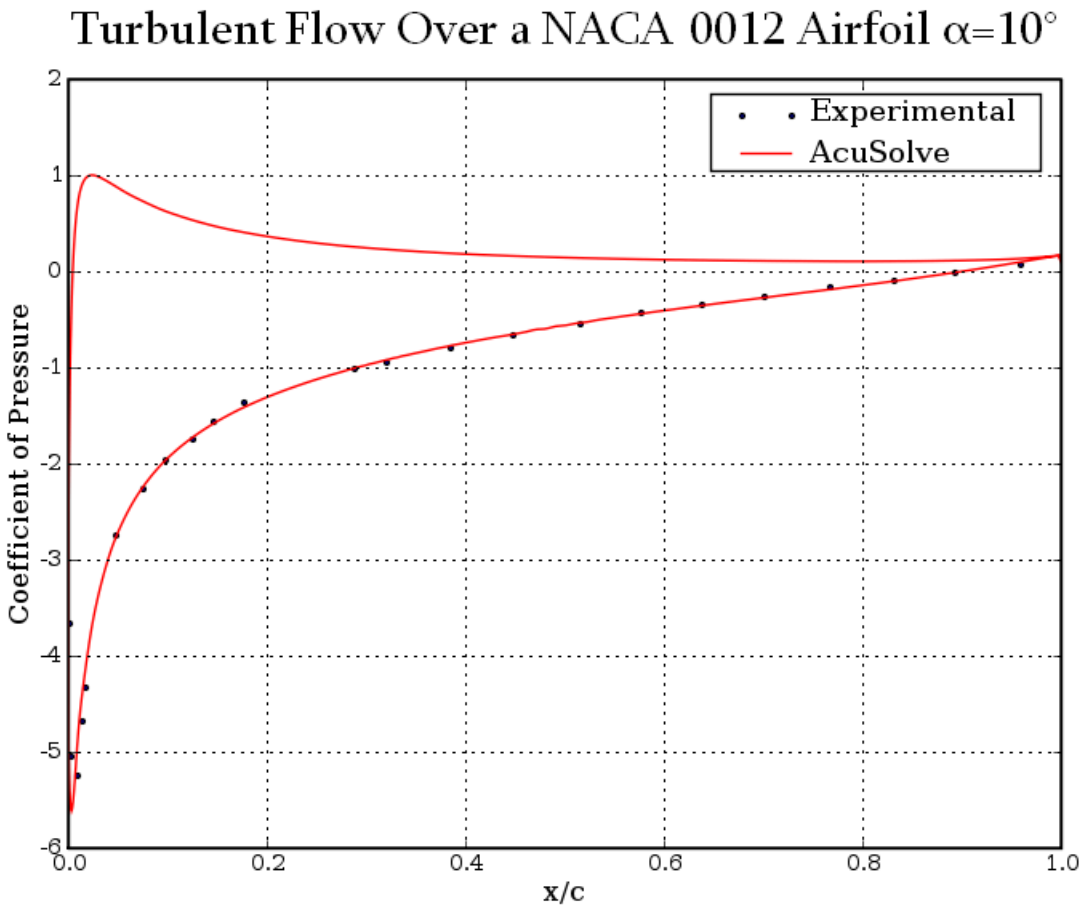


Figure 46: Coefficient of Pressure Plotted Against Normalized Distance Along the Airfoil For Angle of Attack (α) = 10 Degrees

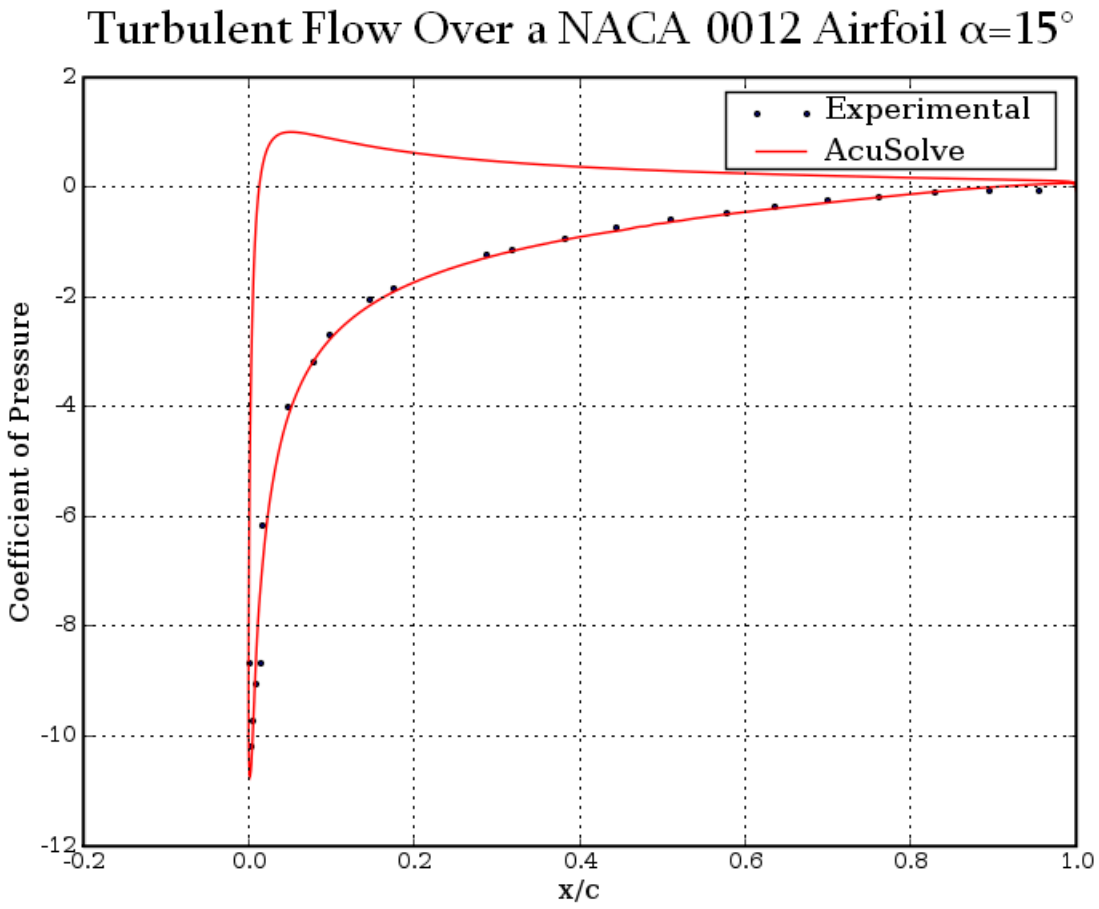


Figure 47: Coefficient of Pressure Plotted Against Normalized Distance Along the Airfoil for Angle of Attack (a) = 15 Degrees

Summary

The AcuSolve results compare well with the experimental results for flow over a NACA 0012 airfoil. In this application, a constant-velocity flow field impinges on the airfoil surface. As the flow convects in the streamwise direction along the airfoil surface, a boundary layer develops. The rate at which the boundary layer develops has significant impact on the viscous stresses present on the airfoil surface. At low angles of attack these stresses dominate the drag on the airfoil. As the angle of attack increases, the flow over the airfoil is no longer symmetric, which leads to the generation of lift. For non-zero angles of attack, the asymmetric pressure distribution on the airfoil creates another source of drag that is combined with the viscous stresses to determine the total drag on the airfoil. The AcuSolve results for coefficients of lift and drag at the 15 percent angle of attack are within 0.91 percent and 0.5 percent of experimental values, respectively. AcuSolve results for coefficient of pressure closely agree with experimental results along the length of the airfoil for all three angles of attack that were investigated.

Simulation Settings for Turbulent Flow Over a NACA0012 Airfoil

HyperMesh CFD database file: `<your working directory>\airfoil_turbulent\airfoil_turbulent.hm`

Global

- Problem Description
  - Analysis type - Steady State
  - Turbulence equation - Spalart Allmaras
- Auto Solution Strategy
  - Convergence tolerance - `0.0001`
  - Relaxation factor - `0.4`
- Material Model
  - Fluid
    - Density - `1.0` kg/m3
    - Viscosity - `1.667e-7` kg/m-sec

  Model
- Volumes
  - Fluid
    - Element Set
      1. Material model - Fluid
- Surfaces
  - +z slip
    - Simple Boundary Condition
      1. Type - Slip
  - -z slip
    - Simple Boundary Condition
      1. Type - Slip
  - airfoil surface
    - Simple Boundary Condition
      1. Type - Wall
  - farfield
    - Simple Boundary Condition
      1. Type - Far Field
      2. X velocity - cos(α) m/sec
      3. Y velocity - sin(α) m/sec
- Eddy viscosity - `1.0e-9` m2/sec

References

NASA - Langley Research Center. http://turbmodels.larc.nasa.gov/naca0012_val_sa.html

Turbulent Flow Through a 180 Degree Curved Channel

In this application, AcuSolve is used to simulate turbulent flow through a strongly curved two dimensional 180 degree U-duct channel. AcuSolve results are compared with experimental results adapted from Rumsey et al. (2000). The close agreement of AcuSolve results with experimental results validates the ability of AcuSolve to model turbulent cases with strong curvature effects.

Problem Description

The problem consists of a fluid with properties similar to air flowing through a curved channel, as shown in the following image, which is not drawn to scale. The inlet channel height and remaining duct height is 0.0381 m. The bulk velocity (v) normal to the inlet is 31.1 m/s and an integrated outflow pressure is specified to allow the flow to pass through the channel. The flow develops into fully turbulent flow at a Reynolds's number (Re) of approximately 1,000,000. The density of the flow medium is 1.0 kg/m3 and the dynamic viscosity is 1.1818 X 10-6 kg/m-s. The simulation is conducted with the Reynolds Averaged Navier-Stokes equations using the Spalart Allmaras, Shear Stress Transport (SST), K-ω and Realizable K-ε turbulence models. The velocity field from the simulations is compared against experimental data at select measurement locations.

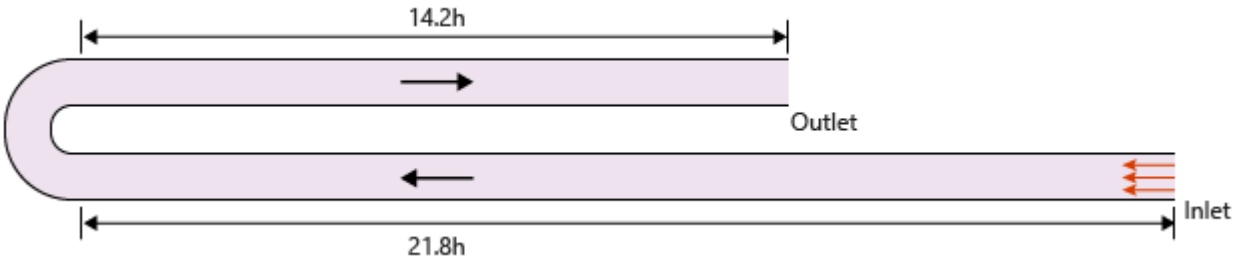
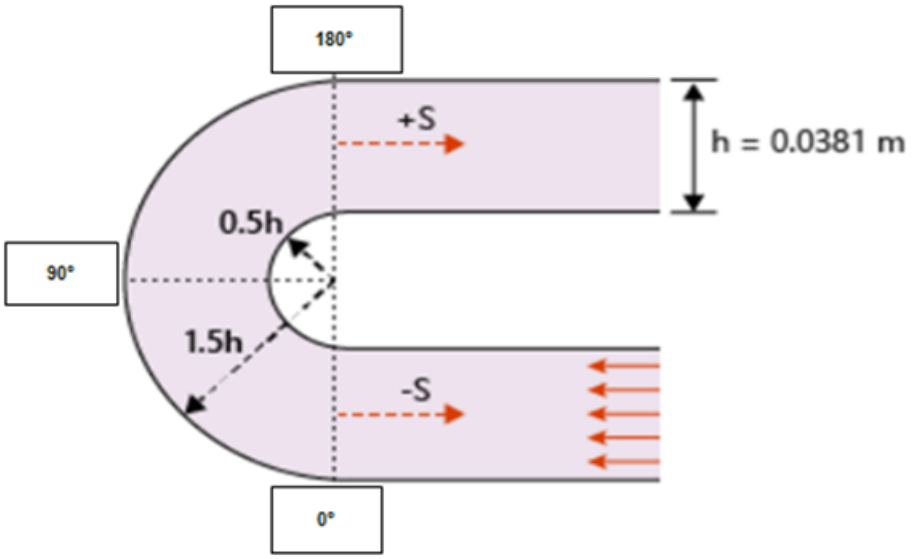


Figure 48: Critical Dimensions and Parameters for Simulating Turbulent Flow in the 180 degree U-Duct



The simulation was performed as a two dimensional problem by restricting flow in the out-of-plane direction through the use of a mesh that is one element thick. The upper and lower walls are specified as no-slip, the inlet velocity and eddy viscosity are specified normal to the inlet face to match the experimental Reynolds Number.

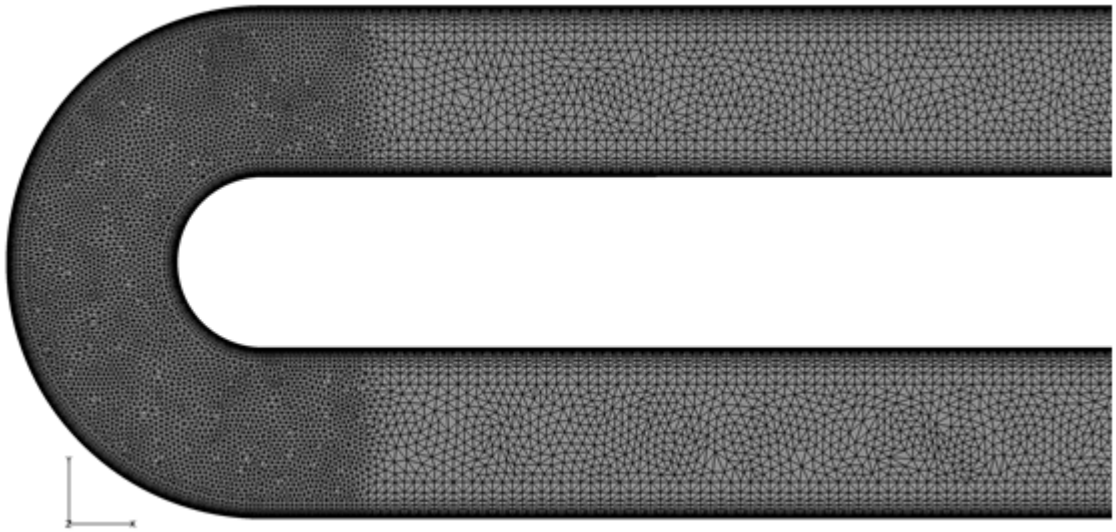


Figure 49: Mesh Used for Simulating Turbulent Flow in the 180 Degree U-Duct

AcuSolve Results

The AcuSolve solution converged to a steady state and the results reflect the mean flow conditions. As the flow passes the inner convex wall it begins to accelerate before decelerating directly past the curved section due to the adverse pressure gradient that eventually leads to a local recirculation zone. On the outer concave wall, the flow remains attached, but is influenced by the adverse pressure gradient above the recirculation region.

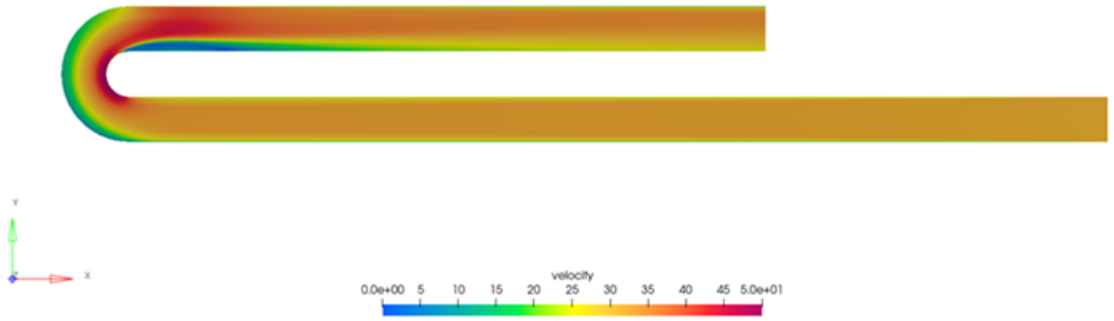


Figure 50: Velocity Contours in Stream Wise Plane

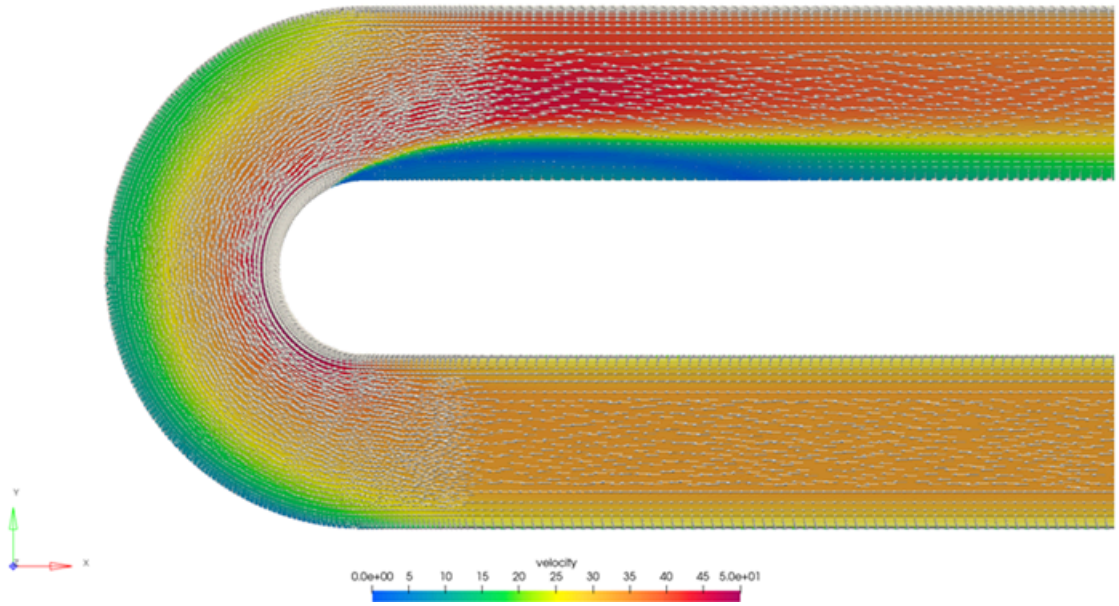


Figure 51: Close up View of Velocity Vectors and Velocity Contours at 180 Degree Bend

The experimental value for the ratio of Velocity magnitude (Vm) to inlet bulk velocity (Vb=31.1 m/s) at different sections of the U-duct is presented with the corresponding AcuSolve result for each of the turbulence models tested in the following images. The images show black circles representing the experimental measurements (Rumsey 2000), solid red lines for the SA model, solid blue lines for the SST model, solid green lines for the K-ω model and solid cyan lines for the K-ε model.

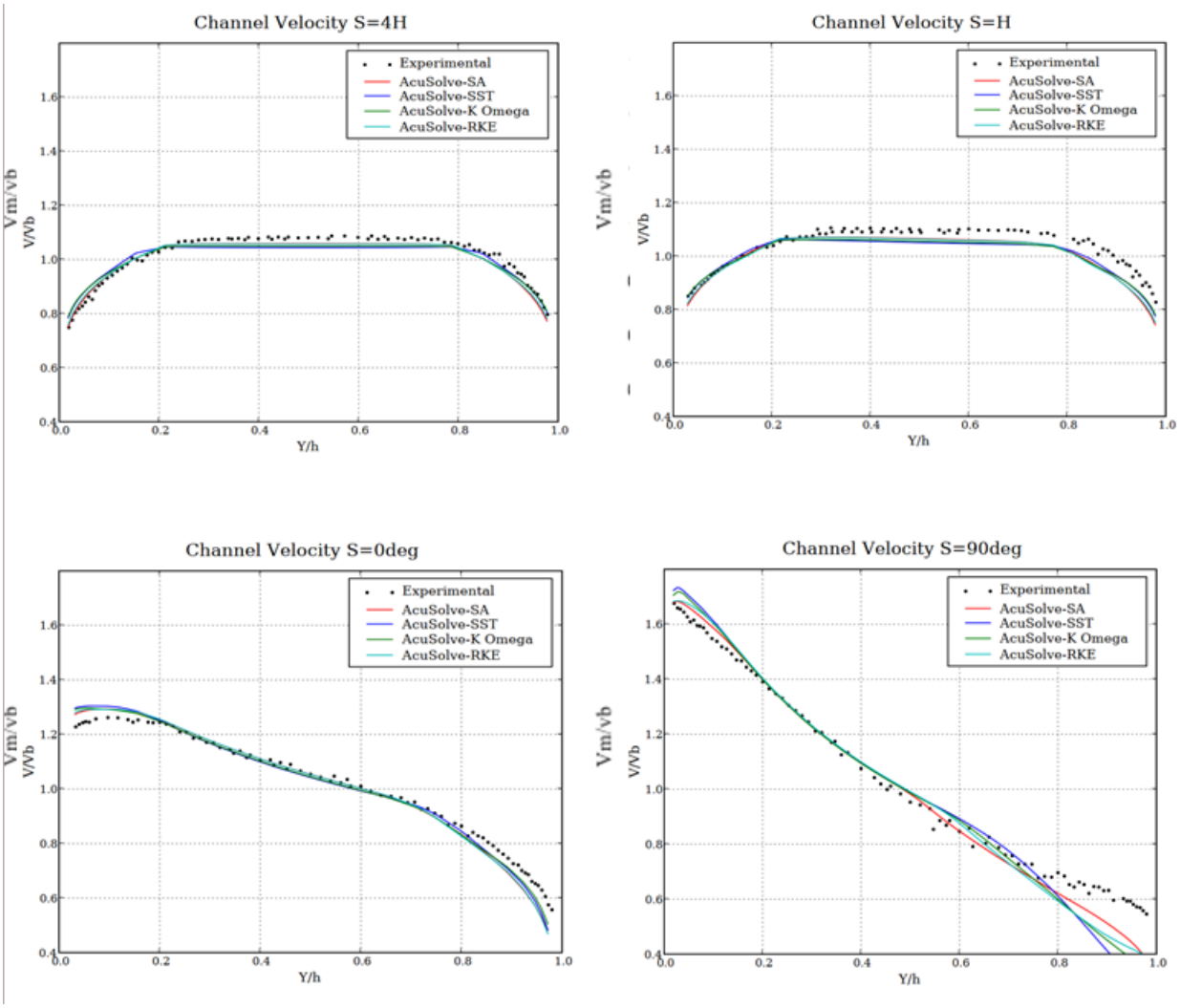


Figure 52:

Summary

The AcuSolve solution compares well with experimental results for flow past the 180 degree U-duct. The experimental value for the ratio of Velocity magnitude to inlet bulk velocity at different sections of the U-duct is presented with the corresponding AcuSolve result for various turbulence models. The performance of the Spalart Allmaras turbulence model was found to improve when the rotation curvature correction is included in the numerical formulation (enabled by default). In this application, AcuSolve demonstrates the ability to predict the complex boundary layer separation and reattachment resulting from the curvature of the channel.

Simulation Settings for Turbulent Flow Through a 180 Degree Curved Channel

HyperMesh CFD database file: `<your working directory>\curved_channel_simple_turbulent \curved_channel_simple_turbulent.hm`

Global

- Problem Description

- Analysis type - Steady State
- Turbulence equation - Realizable K-Epsilon

- Auto Solution Strategy
  - Relaxation factor - `0.4`
- Material Model
  - Air
    - Type- Constant
    - Density- `1.0` kg/m3
    - Viscosity- `1.1818e-006` kg/m-sec

  Model
- Volumes
  - Fluid
    - Element Set
      1. Material model- Air
- Surfaces
  - Inlet
    - Simple Boundary Condition
      1. Type- Wall
      2. Inflow type- Velocity
      3. Inflow velocity type- Normal
      4. Normal velocity- `31.1` m/sec
      5. Turbulence input type- Direct
      6. Eddy viscosity- `3.5547e-06` m2/sec
  - ext1
    - Simple Boundary Condition- Symmetry
  - ext2
    - Simple Boundary Condition- Symmetry
  - Outlet
    - Simple Boundary Condition
      1. Type- Outflow
  - wall-bottom
    - Simple Boundary Condition
      1. Type- Wall
      2. Turbulence wall type- Low Reynolds Number
  - wall-top
    - Simple Boundary Condition
      1. Type- Wall

2 Turbulence wall type- Low Reynolds Number

References

Christopher L. Rumsey, Thomas B. Gatski, and Joseph H. Morrison. "Turbulence Model Predictions of Strongly Curved Flow in a U-Duct", AIAA Journal, Vol. 38, No. 8 (2000), pp. 1394-1402.

Turbulent Flow Through a Wavy Channel

In this application, AcuSolve is used to simulate turbulent flow through a channel with a lower wall shaped as a sinusoidal wave. AcuSolve results are compared with experimental results adapted from Kuzan (1986). The close agreement of AcuSolve results with experimental results validates the ability of AcuSolve to model cases with internal flow through a channel with wavy walls.

Problem Description

The problem consists of air flowing through a channel with a wavy bottom wall. The channel is 1.1 m high, 1.0 m wide, and is modeled as a section 1.0 m in length, as shown in the following image, which is not drawn to scale. The bottom wall wave shape has an amplitude of 0.1 m and a wavelength of 1 m. The mass flow rate through the channel is set to a constant value of 0.816 kg/s. The flow field develops as a result of the non-planar bottom wall and viscous stresses acting near the top and bottom walls. Collision of air with the peak of the wave on the channel floor causes an acceleration of the flow, followed by recirculation as the flow area expands into the valley.

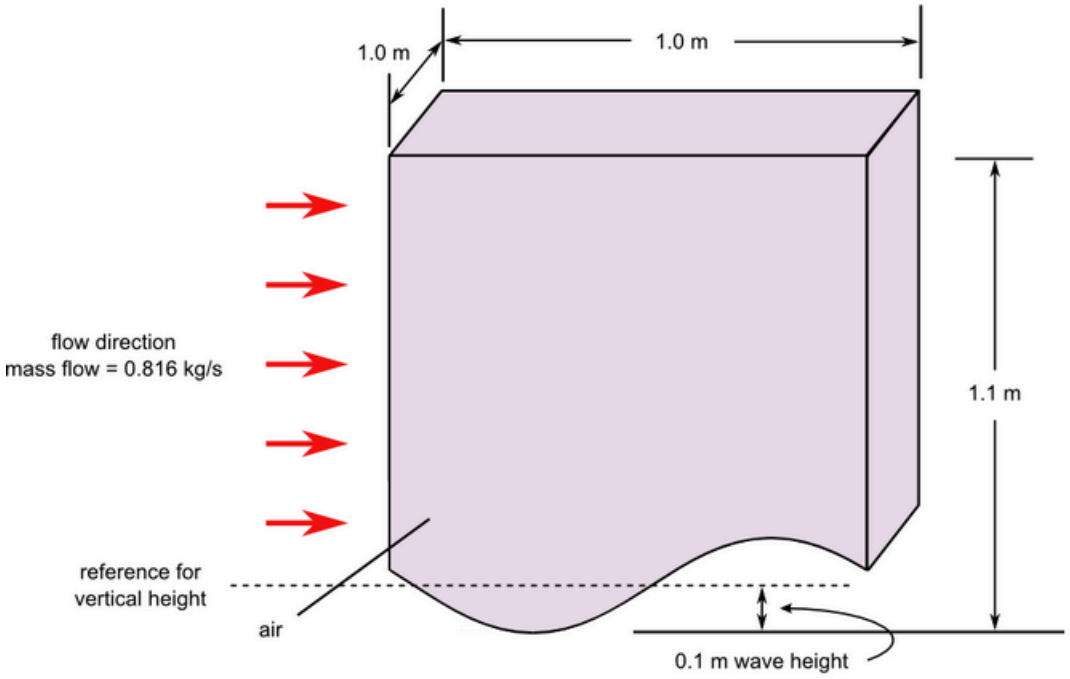


Figure 53: Critical Dimensions and Parameters for Simulating Turbulent Flow Through a Wavy Channel

The simulation was performed as a two dimensional problem by restricting flow in the out-of-plane direction through the use of a mesh that is one element thick. The elements were extruded to the width of the channel.

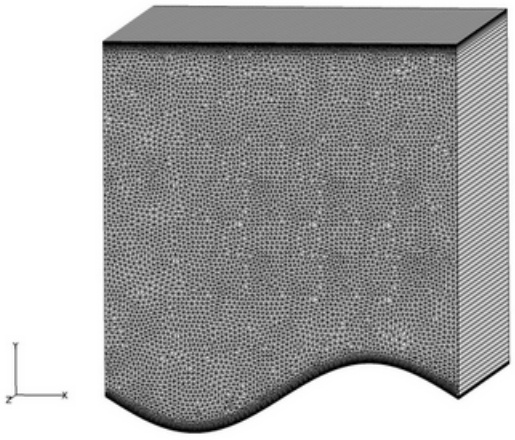


Figure 54: Mesh Used for Simulating Turbulent Flow Through a Wavy Channel

AcuSolve Results

The AcuSolve solution converged to a steady state and the results reflect the mean flow conditions. The expansion of the cross section as the air passes the trough in the wave causes an adverse pressure gradient to form. This results in separation of the flow along the downward-slanting walls of the wavy surfaces. The recirculation zone establishes itself within the troughs of the wave. The remaining flow above the troughs maintains its velocity in the streamwise direction and distributes throughout the channel. The flow accelerates as it travels over the wave peak and the velocity continues to increase as a function of distance from the wall until it reaches a maximum velocity approximately 0.3 m away from the upper wall.

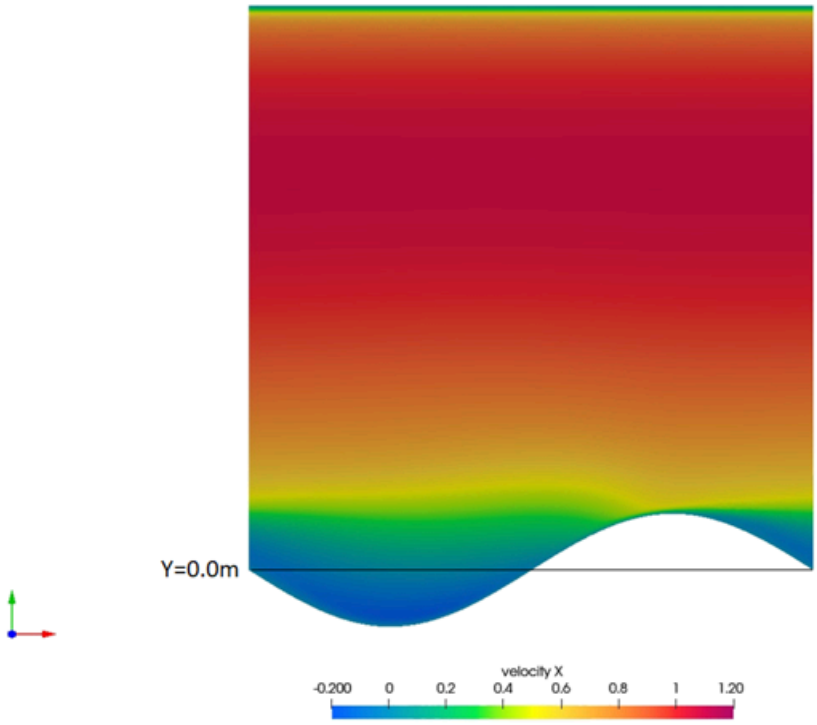


Figure 55: Velocity Contours in the X-Y Plane in a Wavy Channel (the Horizontal Line Represents the Reference for Wave Height - the Wave Crest is 0.1 m Above The Reference Height, and the Wave Valley is 0.1 m Below the Reference Height)

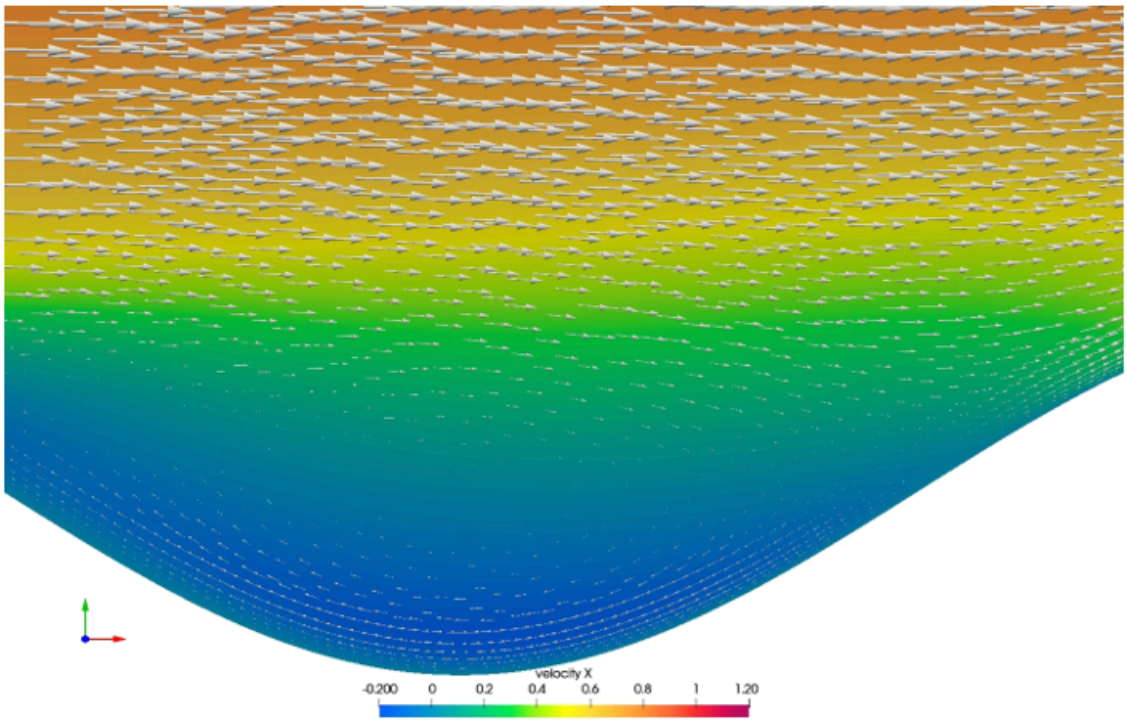


Figure 56: Close-Up View of Velocity Contours and Velocity Vectors in the X-Y Plane Near the Valley of a Wave

The X-velocity directly over the center of the wave valley initially decreases (backflow) as distance away from the bottom wall increases, with a maximum velocity in the -X direction at approximately 0.03 m above the valley floor. The X-velocity then increases to zero m/sec at 0.1 m above the valley, reflecting an end of the recirculation.

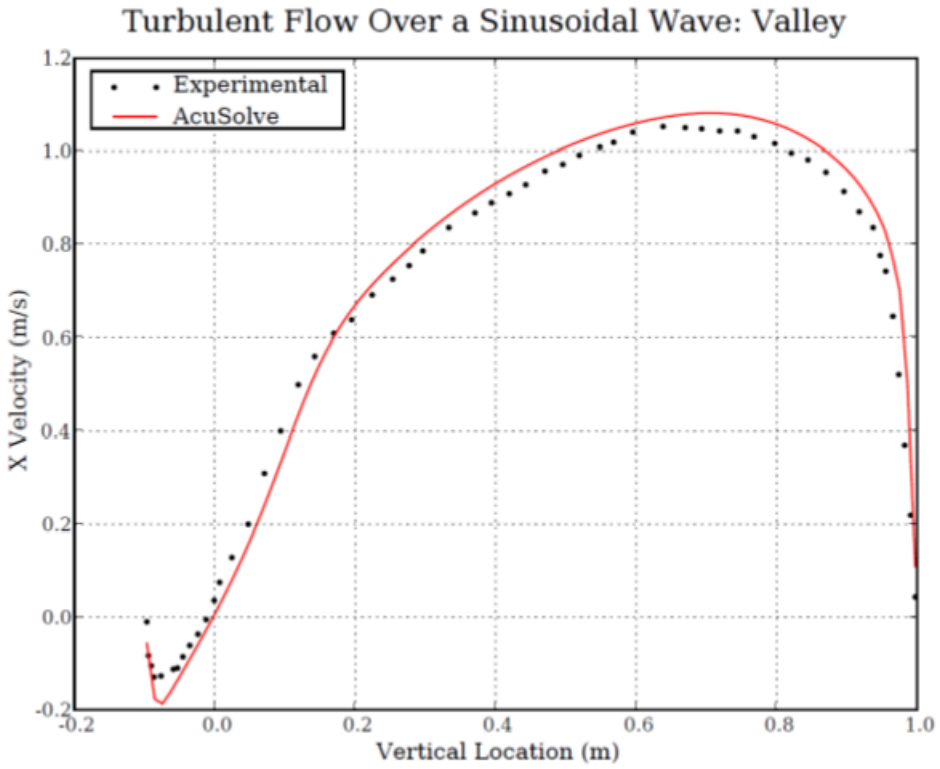


Figure 57: X-Velocity Plotted Against Vertical Location in the Channel Above the Valley Center (the Valley Floor is 0.1 m Below the Reference Height)

The X-velocity directly over the wave peak has different behavior due to the lack of recirculation. The velocity above the peak increases as distance away from the bottom wall increases, with a maximum velocity in the X direction at approximately 0.75 m. The velocity then decreases to zero at the top wall.

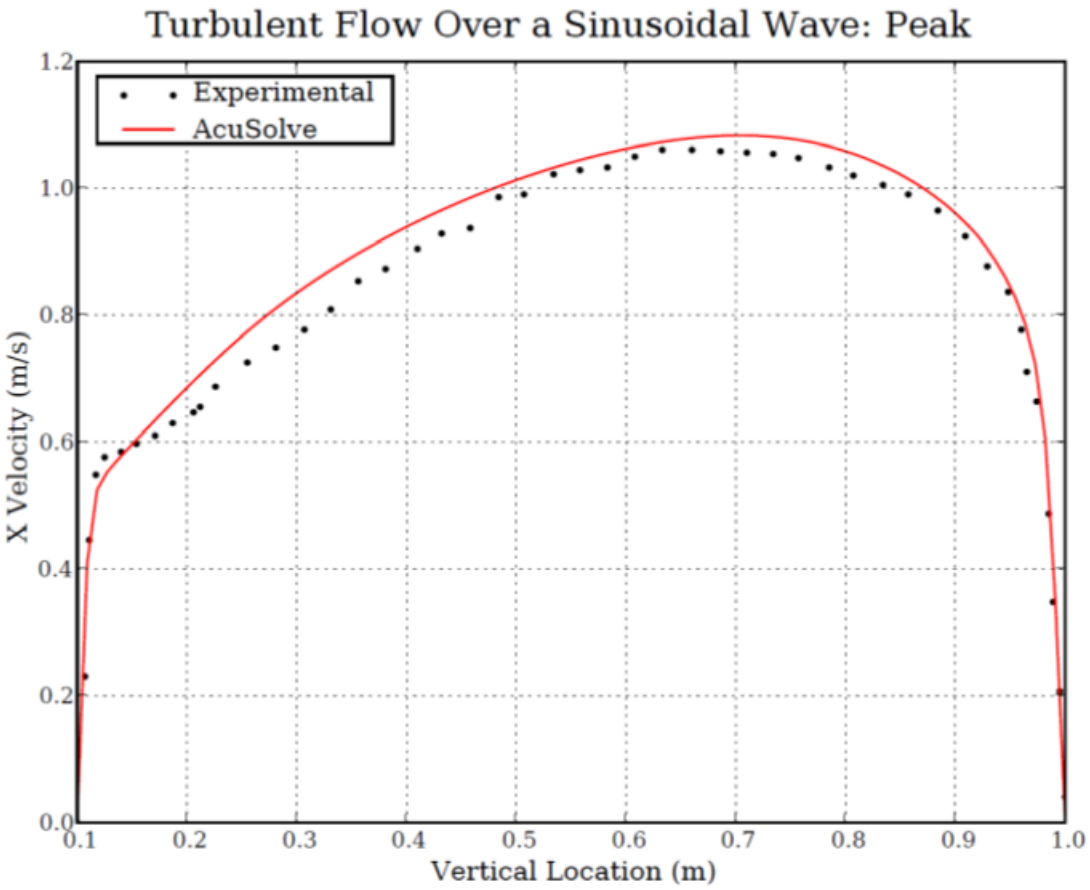


Figure 58: X-Velocity Plotted Against Vertical Location in the Channel Above the Wave Peak (the Wave Peak is 0.1 m Above the Reference Height)

Summary

The AcuSolve results compare well with the experimental data for X-velocity in a channel with a wavy bottom wall. In this application, the flow is driven with a constant mass flow rate and periodic constraints are used to model a repeating array of channel segments with a wavy bottom wall. Separation of the flow occurs as a result of the adverse pressure gradient created by the changes in area. This leads to recirculation within the wave valleys. The flow separation occurs along the smoothly tapered wave wall, illustrating the ability of AcuSolve to accurately predict the separation point in this type of application. The X-velocity predicted by AcuSolve matches the experimental results with an overall coefficient of determination (R2) of 0.99 for each location shown in the plots.

Simulation Settings for Turbulent Flow Through a Wavy Channel

SimLab database file: `<your working directory>\wavy_channel_turbulent \wavy_channel_turbulent.slb`

Global

- Problem Description
  - Flow Type - Steady State

- Turbulence - Spalart Allmaras
- Auto Solution Strategy
  - Relaxation factor - `0.4`
- Material Model
  - Air
    - Density - `1.0` kg/m3
    - Viscosity - `0.0001` kg/m-sec

  Model
- Volumes
  - Fluid
    - Element Set
      1. Material model - Air
- Surfaces
  - Max_X
    - Simple Boundary Condition - (disabled to allow for periodic conditions to be set)
  - Max_Y
    - Simple Boundary Condition
      1. Type - Wall
  - Max_Z
    - Simple Boundary Condition - (disabled to allow for periodic conditions to be set)
  - Min_X
    - Simple Boundary Condition - (disabled to allow for periodic conditions to be set)
    - Advanced Options
      1. Integrated Boundary Conditions
         1. Mass Flux
            1. Type - Constant
            2. Constant value - `-0.816` kg/sec
  - Min_Y
    - Simple Boundary Condition
      1. Type - Wall
  - Min_Z
    - Simple Boundary Condition - (disabled to allow for periodic conditions to be set)
- Periodics
  - Periodic-Crossflow
    - Periodic Boundary Condition
      1. Type - Periodic
  - Periodic-Streamwise

- Periodic Boundary Condition
  1. Type - Periodic
- Individual Periodic BCs
  1. Velocity
     1. Type - Periodic
  2. Pressure
     1. Type - Single Unknown Offset
  3. Eddy Viscosity
     1. Type - Periodic

References

J. D. Kuzan."Velocity Measurements for Turbulent Separated and Near-Separated Flows Over Solid Waves". Ph.D. thesis. Deptartment of Chemical Engineering. University of Illinois. University of Illinois. Urbana, IL. 1986

Turbulent Flow Through a Heated Periodic Channel

In this application, AcuSolve is used to solve for the flow and temperature field within a channel containing a heated wall. The wall is maintained at a constant temperature, inducing heat flux into the fluid, to predict the thermal law of the wall. The non-dimensional temperature versus the non-dimensional height above the wall is compared to the analytical correlation provided by Kader.

Problem Description

The problem consists of a fluid having material properties close to air with a density of 1.0 kg/m^3, molecular viscosity of 0.0001 kg/m-s, specific heat of 1005.0 J/kg-K and thermal conductivity of 0.139 W/m-K. The properties are specified to obtain a Prandtl number of 0.72. The velocity is defined as periodic and is driven by a constant acceleration body force equal to 2.0 m/s^2. The temperature is specified as periodic+unknown ratio allowing it to develop until it reaches a steady solution. The simulation description is shown in the following image, which is not drawn to scale. The model is simulated using the one equation Spalart Allmaras turbulence model along with the advective-diffusive temperature equation. The thermal wall distribution is validated against correlation data published by Kader 1981.

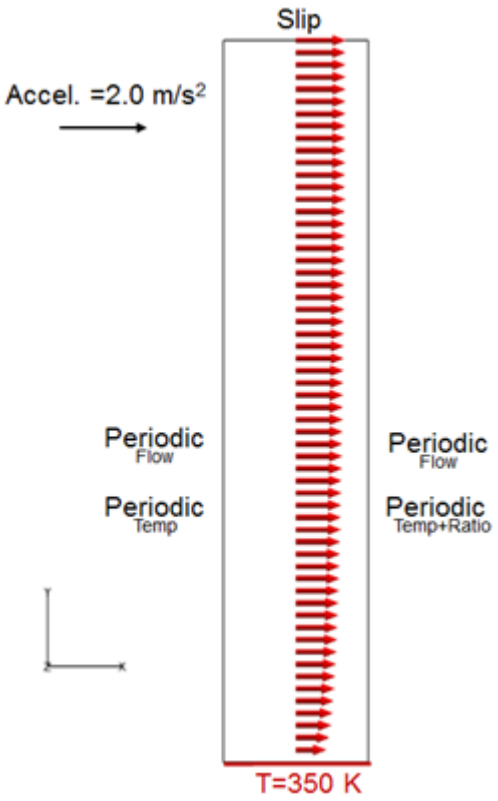


Figure 59: Critical Parameters used For Simulating Periodic Flow Within a Heated Channel

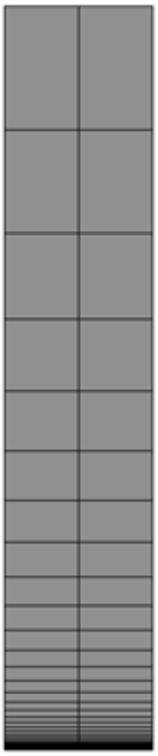


Figure 60: Mesh used For Simulating Periodic Flow Within a Heated Channel

The simulation was performed as a two-dimensional problem by constructing a volume mesh that contains a single layer of elements extruded in the cross-stream direction, normal to the flow plane and by imposing periodic boundary conditions on the extruded planes. The streamwise direction contains two elements allowing the flow and temperature solution to develop. Only the lower half of the channel is modeled, assuming the solution is mirror across the top slip plane.

AcuSolve Results

The AcuSolve solution converged to a steady state and the results reflect the mean flow conditions within the channel. The simulation results demonstrate that the channel wall induces a thermal flux into the flow field, producing a temperature distribution dependent on the distance from the wall. The thermal law of the wall computed from the AcuSolve results is compared with correlation data for the corresponding Prandtl number, as demonstrated in Kader 1981. The plot shown below gives the non-dimensional value of T+ as a function of Y+, where T+ and Y+ are computed per the following relationships:

$$T+ = \frac{(Tw - T)\rho C p u_\tau}{\dot{Q}} T \qquad (1)$$

$$Y+ = \frac{y u_\tau}{\nu} \qquad (2)$$

$$u_\tau = \sqrt{\tau w / \rho} \qquad (3)$$

Where $T+$, Tw is the fixed wall temperature, T is the temperature away from the wall, ρ is the fluid density, Cp is the fluid specific heat, uT is computed from the magnitude of the shear stress and $\dot{Q}_i$ is the local surface heat flux.

The image below shows black circles representing the correlation data and a solid red line for the AcuSolve results. The results demonstrate that the temperature distribution away from the wall is resolved properly and compares well with the correlation. Since an empirical relationship for T+ is used for comparison, there will be minor discrepancies compared with the simulation results. Additional comparisons have been made against DNS results for T+ from Kawamura et al. 1998.

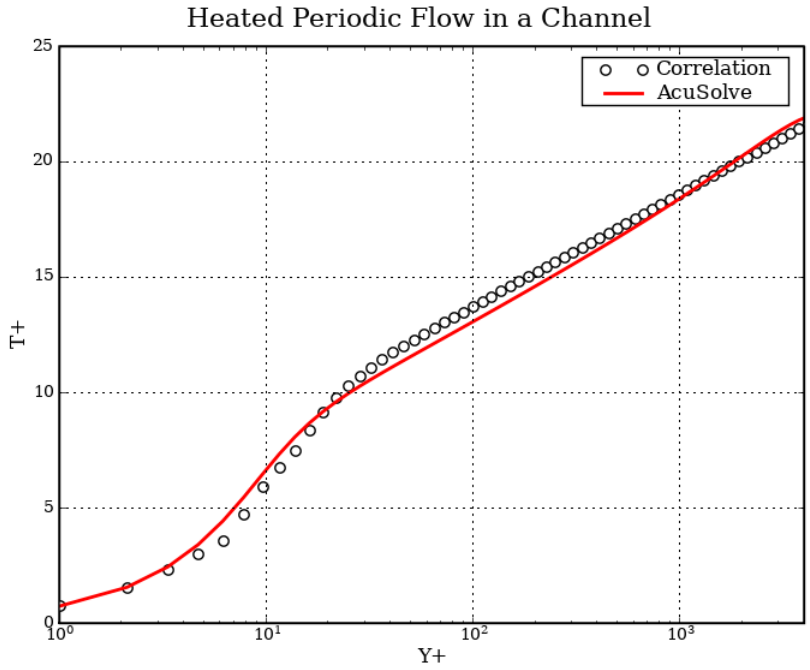


Figure 61: Thermal Boundary Layer Within the Heated Channel Compared Against the Correlation Data

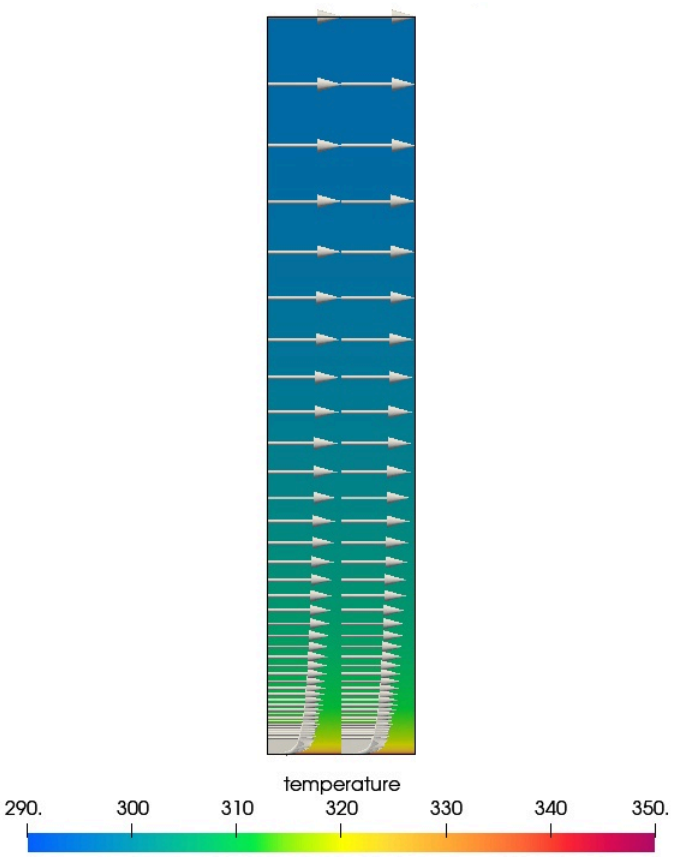


Figure 62: Contours of Temperature and Vectors Representing the Fluid Velocity Within the Channel

Summary

The AcuSolve solution compares well with the correlation data for turbulent flow within a heated channel. In this application, the constant temperature wall induces a surface heat flux, giving rise to a temperature gradient within the channel. AcuSolve can capture the correct temperature gradient at any location above the wall if an appropriate first layer height is selected to resolve a Y+ value of 1.0. The good agreement with correlation data for T+ demonstrates that AcuSolve can predict the locally varying temperature distribution within a turbulent channel.

Simulation Settings for Turbulent Flow Through a Heated Periodic Channel

SimLab database file: `<your working directory>\channel_periodic_heat\channel_periodic_heat.slb`

Global

- Problem Description
  - Flow type - Steady State
  - Temperature equation - Advective Diffusive
  - Turbulence equation - Spalart Allmaras
- Auto Solution Strategy
  - Max time steps - `50`

- Convergence tolerance - `0.0001`
- Relaxation Factor - `0.4`
- Temperature - On

- Material Model
  - Fluid
    - Type - Constant
    - Density - `1.0` kg/m3
    - Viscosity - `1.0e-4` kg/m*sec
    - Specific Heat - `1005.0` J/kg*K
    - Conductivity - `0.139` W/m*K
- Body Force
  - BodyForce
    - Gravity
      1. X-component - `2.0` m/sec2

Model

- Volumes
  - Fluid
    - Element Set
      1. Material model - Fluid
      2. Body force - BodyForce
- Surfaces
  - Symmetry_1
    - Simple Boundary Condition - (disabled to allow for periodic conditions to be set)
  - Symmetry_2
    - Simple Boundary Condition - (disabled to allow for periodic conditions to be set)
  - Inflow
    - Simple Boundary Condition - (combination of integrated BC and periodic BC set)
    - Advanced Options
      1. Integrated Boundary Conditions - Temperature - `300.0` K
  - Outflow
    - Simple Boundary Condition - (disabled to allow for periodic conditions to be set)
  - Slip_surface
    - Simple Boundary Condition
      1. Type- Slip
  - Wall_surface
    - Simple Boundary Condition
      1. Type- Wall

        2. Temperature BC type - Value
        3. Temperature - `350.0` K

- Periodics
  - 2D
    - Periodic Boundary Conditions
      1. Type - Periodic
  - Flow
    - Periodic Boundary Conditions
      1. Type - Periodic
  - Temperature
    - Individual Periodic BCs
      1. Temperature: Type - Single Unknown Ratio
- Nodes
  - Zero_z-velocity
    - Z-Velocity: Type - Zero

References

B.A. Kader, "Temperature and concentration profiles in fully turbulent boundary layers", International Journal of Heat and Mass Transfer, Volume 24, Issue 9, 1981, Pages 1541-1544.

H. Kawamura, K. Ohsaka, H. Abe and K. Yamamoto, "DNS of turbulent heat transfer in channel flow with low to medium-high Prandtl number fluid", International Journal of Heat and Mass Transfer, 19:482-491, 1998.

Turbulent Mixing Layers in an Open Channel

In this application, AcuSolve is used to simulate the mixing of two streams of fluid with different velocities moving past a splitter plate. AcuSolve results are compared with experimental results as described in J. Delville, et al. (1989). The close agreement of AcuSolve results with the experimental results validates the ability of AcuSolve to model mixing layers in the turbulent flow regime.

Problem Description

The problem consists of two streams of fluid having material properties of standard air with density of 1.2 kg /m^3 and molecular viscosity of 1.7189 kg/m-sec. The two fluid streams enter an open channel separated by a splitter plate at two streamwise locations with differing velocities. The length of the channel is 1.8 m for the top portion and 1.5 m for the bottom portion. The inlet velocity of the top section is 41.54 m/s, producing a Reynolds's number of 2900, based on l=1.0 mm, while the inlet velocity of the lower section is 22.4 m/s, giving a Reynolds's number of 1200, as shown in the following image, which is not drawn to scale. The model is simulated as steady state with constant inflow conditions, using the Spalart Allmaras (SA) turbulence model. The velocity profile is computed for several locations downstream of the splitter plate and compared against the experimental data, as described in Delville, 1989.

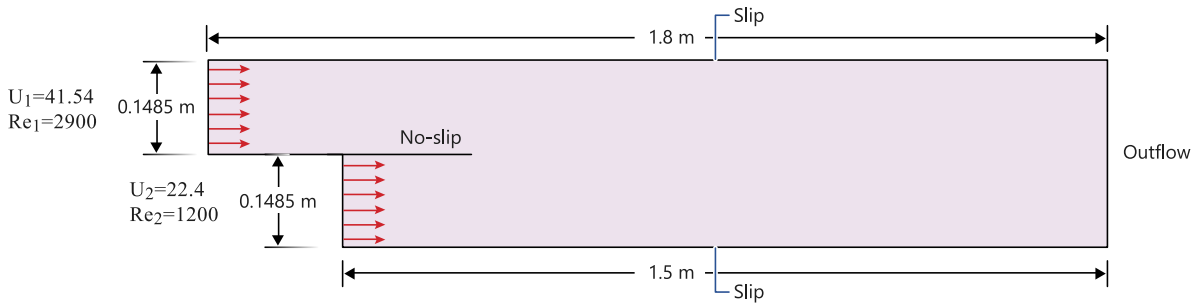


Figure 63: Critical Dimensions and Parameters Used for Simulating the Turbulent Mixing Layer

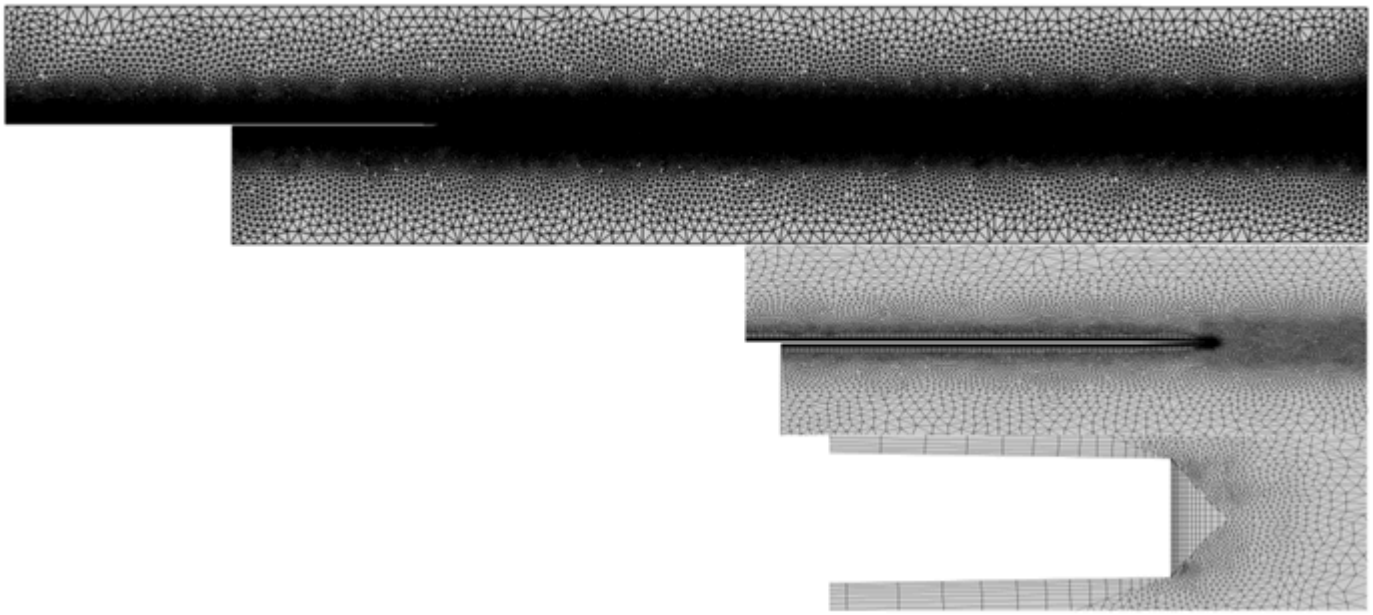


Figure 64: Mesh used for Simulating the Turbulent Mixing Layer Showing Close up Images Near the Trailing Edge of the Plate

The simulation was performed as a two dimensional problem by constructing a volume mesh that contains a single layer of elements extruded in the cross stream direction, normal to the flow plane and by imposing symmetry boundary conditions on the extruded planes. The upper and lower walls are specified as slip, the splitter plate is specified as no-slip and the inlet velocity and eddy viscosity are prescribed as constant values.

AcuSolve Results

The AcuSolve solution converged to a steady state and the results reflect the mean flow conditions within the open channel. The simulation result shows a developing flow field with the fluids fully separated as they pass the edge of the splitter plate. As the fluid travels downstream of the splitter plate, the dissimilar velocity fields produce a shear layer that results in momentum exchange between the two streams. The shear layer diffuses as the fluid travels further downstream. The relative velocity as a function of the normalized boundary layer height is computed from AcuSolve and compared with experimental data at three measurement stations, 0.2 m, 0.65 m and 0.95 m away from the trailing edge of the plate, as described in Delville, 1989. The image below shows black circles representing the experimental data and a solid red line for the AcuSolve results.

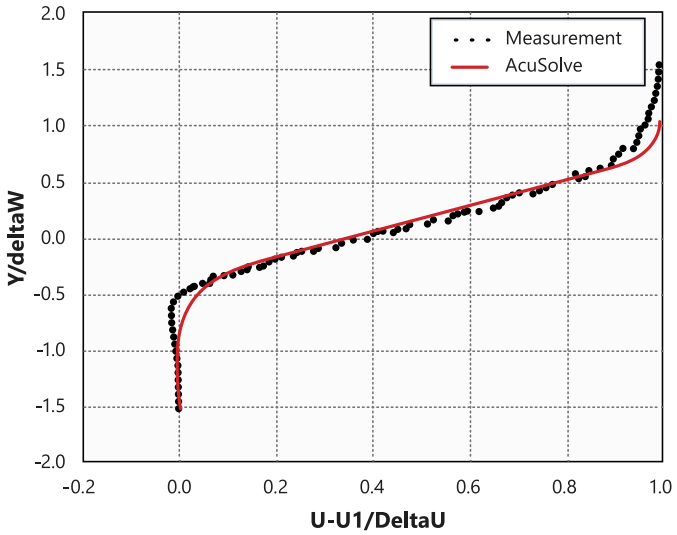


Figure 65: Relative Velocity within the Channel Compared Against Experimental Data Showing Experimental and Simulated Results for the SA Turbulence Model

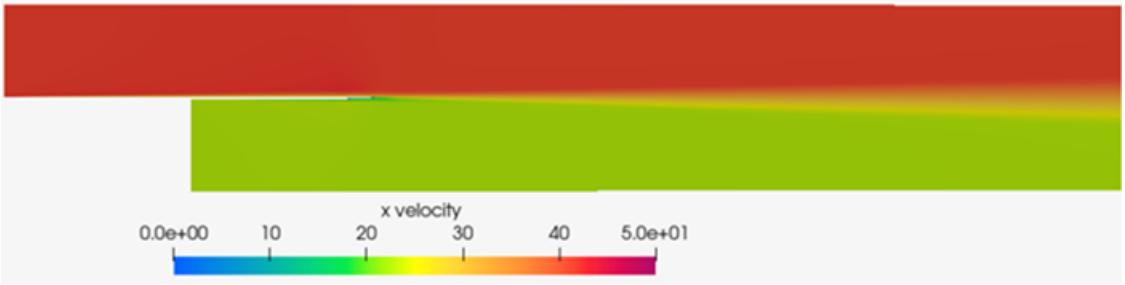


Figure 66: Velocity Magnitude Within the Channel

Summary

The AcuSolve solution compares well with experimental data for turbulent mixing within an open channel. In this application, the shear layer resulting from the dissimilar velocities of the incoming fluid streams results in an exchange of momentum within the channel. The amount of numerical dissipation from the grid is kept to a minimum to produce a good agreement with the experimental data. The good agreement with experimental results for the simulated turbulence model compares well with the measurement and previously published results, demonstrating that AcuSolve is capable of predicting turbulent mixing layers with relatively modest grid levels and the one equation turbulence model.

Simulation Settings for Turbulent Mixing Layers in an Open Channel

HyperMesh CFD database file: `<your working directory>\mixing_layer_turbulent \mixing_layer_turbulent.hm`

Global

- Problem Description
  - Analysis type - Steady State
  - Turbulence equation - Spalart Allmaras

- Auto Solution Strategy
  - Max time steps - `100`
  - Convergence tolerance - `0.001`
  - Relaxation Factor- `0.4`
- Material Model
  - Air
    - Type - Constant
    - Density - `1.2` kg/m3
    - Viscosity - `1.7189e-5` kg/m*sec

  Model
- Volumes
  - Volume
    - Element Set
      1. Material model - Air
- Surfaces
  - Back
    - Simple Boundary Condition
      1. Type- Symmetry
  - Front
    - Simple Boundary Condition
      1. Type- Symmetry
  - InletLower
    - Simple Boundary Condition
      1. Type- Inflow
      2. Inflow type- Velocity
      3. X Velocity- `22.4` m/sec
      4. Turbulence input type- Direct
      5. Eddy Viscosity- `0.0001432`
  - InletUpper
    - Simple Boundary Condition
      1. Type- Inflow
      2. Inflow type- Velocity
      3. X Velocity- `41.54` m/sec
      4. Turbulence input type- Direct
      5. Eddy Viscosity- `0.0001432`
  - Outlet
    - Simple Boundary Condition
      1. Type - Outflow

- Slip
  - Simple Boundary Condition
    1. Type- Slip
- SplitterPlate
  - Simple Boundary Condition
    1. Type - Wall
- TE
  - Simple Boundary Condition
    1. Type- Wall

References

Delville, J., Bellin, S., Garem, J. H., and Bonnet J. P., "Analysis of Structures in a Turbulent, Plane Mixing Layer by Use of a Pseudo Flow Visualization Method Based on Hot-Wire Anemometry," in: Advances in Turbulence 2, eds: H.-H. Fernholz and H. E. Fiedler, Proceedings of the Second European Turbulence Conference, Berlin, Aug. 30-Sept. 2, 1988, Springer Verlag, Berlin, 1989, pp. 251-256.

Two-Phase Nucleate Boiling in a Cylindrical Pipe

In this application, AcuSolve is used to simulate the changes in wall temperature due to two-phase nucleate boiling at the heated walls of a pipe with water flowing through it. AcuSolve results are compared with experimental results adapted from Koncar and others (2015). The close agreement of AcuSolve results with experimental results validates the ability of AcuSolve to model two-phase nucleate boiling problems.

Problem Description

The problem consists of a pipe with heated surrounding walls, as shown in the following image, which is not drawn to scale. The length of the pipe is 2 m and the radius is 0.0017 m. Mass flux at the inlet is 900 kg/m^2 and the temperature of the fluid entering the pipe is 473 K. A heat flux of 570,000 W/m^2 is applied on the walls. The preheated water enters the inlet and heat is transferred to the fluid from the walls. The heat causes sub-cooled boiling to occur in the region close to the wall and leads to the formation of bubbles at nucleation sites.

During sub-cooled boiling flow, heat and mass exchange between the phases takes place on the heated wall and in sub-cooled liquid flow. On the heated surface the vapor bubbles are generated and as they move through the sub-cooled liquid they condense and release the latent heat.

The AcuSolve simulation is set up to model transient state heat transfer to determine the temperature along the centerline of the pipe and along the heated pipe walls of the model. AcuSolve computes the two-phase nucleate boiling by simulating the three-dimensional flow in a heated pipe for two-phase boiling flow, as described in Koncar (2005). The temperatures along the centerline of the pipe and along the pipe walls are compared against the experimental measurements, as described in Koncar, et al. (2005).

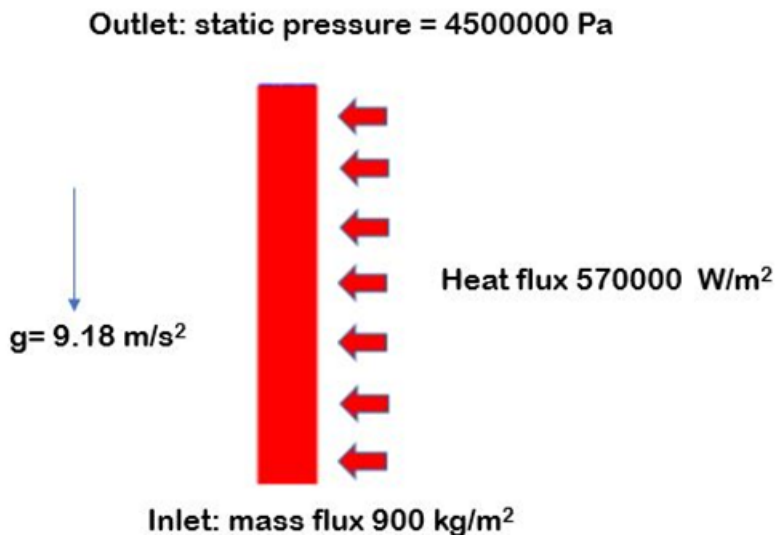


Figure 67: Parameters for Simulating a Two-Phase Nucleate Boiling Problem of a Pipe

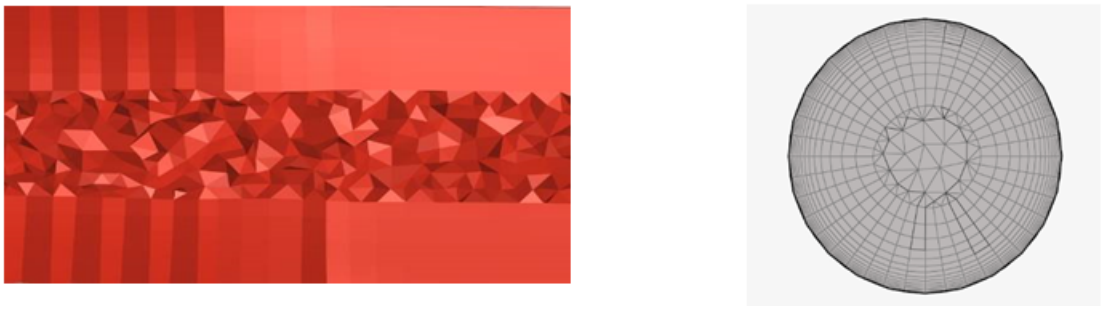


Figure 68: Mesh used for Simulating Two-Phase Flow in a Pipe

AcuSolve Results

The AcuSolve solution is run for a heat flux of 570,000 W/m^2 and the results are presented in the following image. The experimental values of wall temperature are presented with the corresponding AcuSolve results along the centerline of the pipe and along the pipe wall. The AcuSolve results show good agreement with the experimental results for the temperature, indicating that the two-phase nucleate boiling is properly captured.

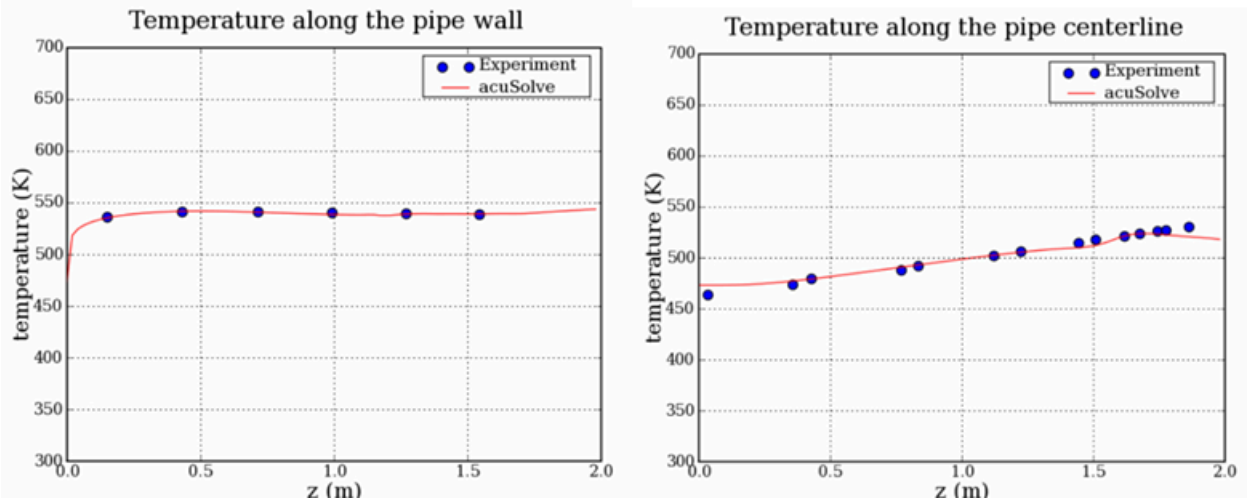


Figure 69: Temperature Values for Varying Streamwise Distance Compared to Experimental Data

Summary

The AcuSolve solution compares well with experimental results for two-phase nucleate boiling simulations. In this application, the temperature of the wall as the onset of boiling approaches are simulated with AcuSolve using the nucleate boiling feature and the SA turbulence model. The experimental values of temperature are presented with the corresponding AcuSolve results. A good agreement of simulation results with the experiment validates the ability to solve two-phase nucleate boiling using the nucleate boiling capabilities of AcuSolve.

Simulation Settings for Two-Phase Nucleate Boiling in a Cylindrical Pipe

HyperMesh CFD database file: `<your working directory>\pipe_two_phase_boiling \pipe_two_phase_boiling.hm`.

Global

- Problem Description
  - Analysis type – Transient
  - Turbulence equation – SA
  - Temperature equation – Advective Diffusive
- Auto Solution Strategy
  - Maximum time steps – `500`
  - Initial time increment – `0.003`
  - Convergence Tolerance – `0.001` sec
  - Relaxation factor – `0.3`
- Surface Tension Model (“Water_NB-Vapor_NB”)
  - Type – Constant
  - Surface Tension – `0.02382`
- Material Model
  - Vapor_NB
    - Type – Constant
    - Density – `23.75` kg/m^3
    - Viscosity – `1.79e-05` kg/m-sec
    - Specific Heat – `4225` J/kg-K
    - Latent Heat – `1675570`
    - Latent Heat Temperature – `530.55` K
    - Conductivity – `0.02528` W/m-K
  - Water_NB
    - Type – Constant
    - Density – `800` kg/m3
    - Viscosity – `0.0001339` kg/m-sec
    - Specific Heat – `4500` J/kg-K
    - Conductivity – `0.65` W/m-K
- Multifield parameter (Field interaction model)
  - Type – Algebraic Eulerian
  - Phase change type – Wall Boiling
  - Carrier field - Water
  - Disperse field – Vapor
  - Disperse field diameter type – Boiling kurul exponential
  - Drag model – Ishii zuber
  - Lift Model – Legendre Magnaudet

Model

- Volumes
  - Fluid
    - Material – Vapor_Water
- Surfaces
  - Inflow
    - Simple Boundary Condition – Inflow
    - Inflow type – Mass Flux Rate
    - Mass Flux Rate – `0.167634` kg/sec
    - Temperature – `473` K
  - Outflow
    - Simple Boundary Condition – Outflow
    - Pressure – `4500000` N/m2
  - Wall
    - Simple Boundary Condition – Wall
    - Temperature type – Flux
    - Heat Flux – `570000` W/m2

References

B. Koncar, E. Krapper, Y. Egorov, 2005, "CFD MODELING OF SUBCOOLED FLOW BOILING FOR NUCLEAR ENGINEERING APPLICATIONS", International Conference Nuclear Energy for New Europe 2005, Bled, Slovenia, September 5-8,2005.

Supersonic Flow Through a Converging-Diverging Nozzle

In this application, AcuSolve is used to simulate the high-speed turbulent flow in a converging and then diverging nozzle. The flow within the nozzle enters as subsonic, reaches sonic at the throat and shortly after develops a normal shock. AcuSolve results are compared with experimental results adapted from Bogar and Sajben (1983). The close agreement of AcuSolve results to experimental measurements validates the ability of AcuSolve to simulate internal supersonic flows where normal shocks are present.

Problem Description

The problem consists of a converging and then diverging nozzle represented as an extruded planar surface, as shown in the image below, which is not drawn to scale. The length of the domain is 0.213 m with a throat height of 0.044 m. The stagnation pressure and static temperature are constrained at the inlet to 135,000 Pa and 265.98 K, respectively. The static pressure is defined using the outflow boundary condition, where P_{static}=97216.08 Pa. The flow in the diffuser has an inlet Reynolds number of $6.5x10^5$. The upper and lower walls are set to no-slip and the side walls are set to slip, while the exterior walls are specified to be adiabatic. Images of the numerical mesh are shown below.

The AcuSolve simulation is prepared to model the pseudo-transient state to determine the shock location and corresponding scalar quantities within the diffuser. AcuSolve computes the flow and thermal solution by simulating a planar, two-dimensional flow problem with physical dimensions and input quantities as described in the Sajben Diffuser case presented by Bogar and Sajben (1983). The gas in the simulation domain enters at subsonic conditions and is forced to accelerate beyond Mach=1.0 as it passes through the throat. After reaching supersonic speed a normal shock wave develops causing the flow speed to reduce back below sonic. The pressure along the bottom wall of the diffuser is compared against experimental measurements to demonstrate the solver's capability to solve supersonic cases.

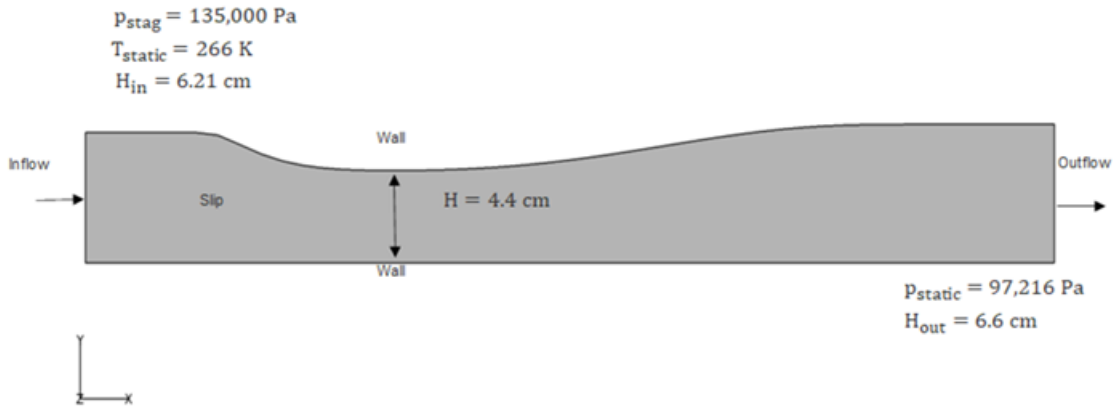


Figure 70: Parameters for Simulating Compressible Flow within a Converging-Diverging Nozzle

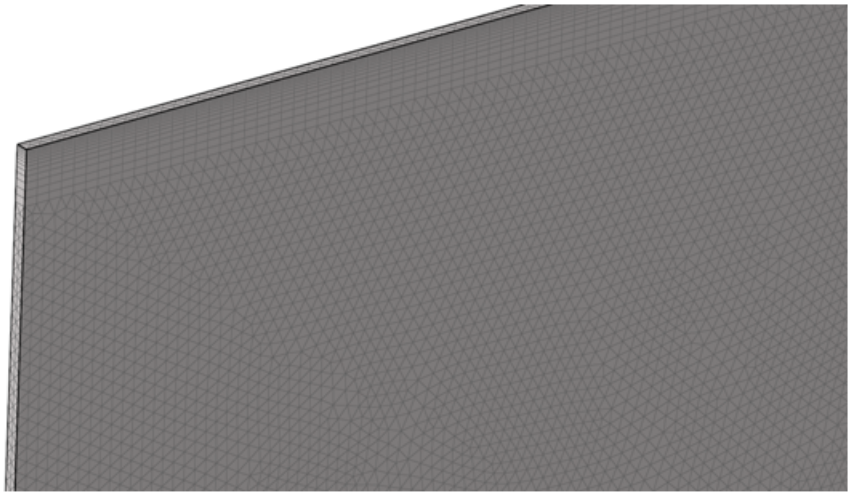


Figure 71: Mesh used for Simulating Compressible Flow in a Converging-Diverging Nozzle

AcuSolve Results

The AcuSolve solution is run for 0.025 seconds (6,250 timesteps with dt=4.0x10^{-6}sec) and converges to a pseudo-steady solution. The change in pressure from the inlet to outlet causes the flow to accelerate within the throat of the diffuser until it reaches approximately Mach=1.35. A normal shock is present just downstream of where the cross-sectional area of the nozzle increases, as shown in the image below. The numerical solution can be compared with the reference after normalizing the pressure along the wall by the inlet stagnation pressure (135 kPa) and the distance along the bottom wall by the nozzle throat height (0.044 m). The image below shows the normalized pressure versus normalized distance in comparison to NASA reference and experimental results. The image shows black circles representing the experimental measurements (Bogar and Sajben 1983), a dashed blue line representing the SA solution as obtained through NASA publication (Mohler 2005) and a solid red line representing the AcuSolve results with the Spalart-Allmaras turbulence model. The non-dimensional pressure within the diffuser agrees well with the reference data, demonstrating the correct physical location of the normal shock and expected moderate flow speed reduction within the constant cross-section diffuser portion of the nozzle.

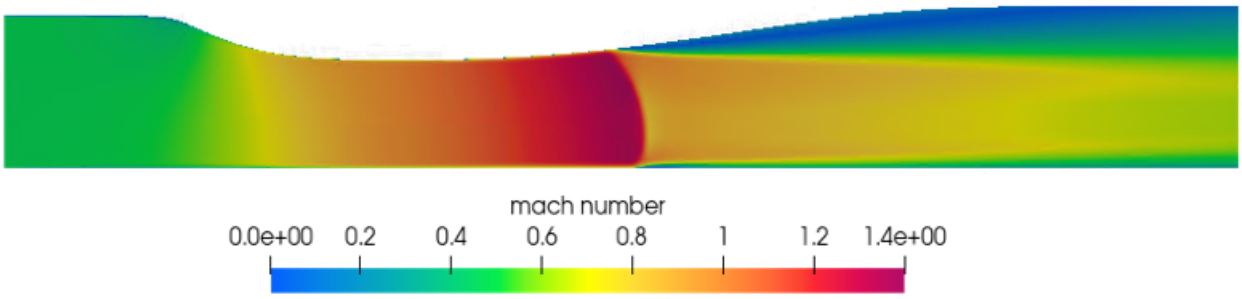


Figure 72: Contours of Mach Number within a Converging-Diverging Nozzle

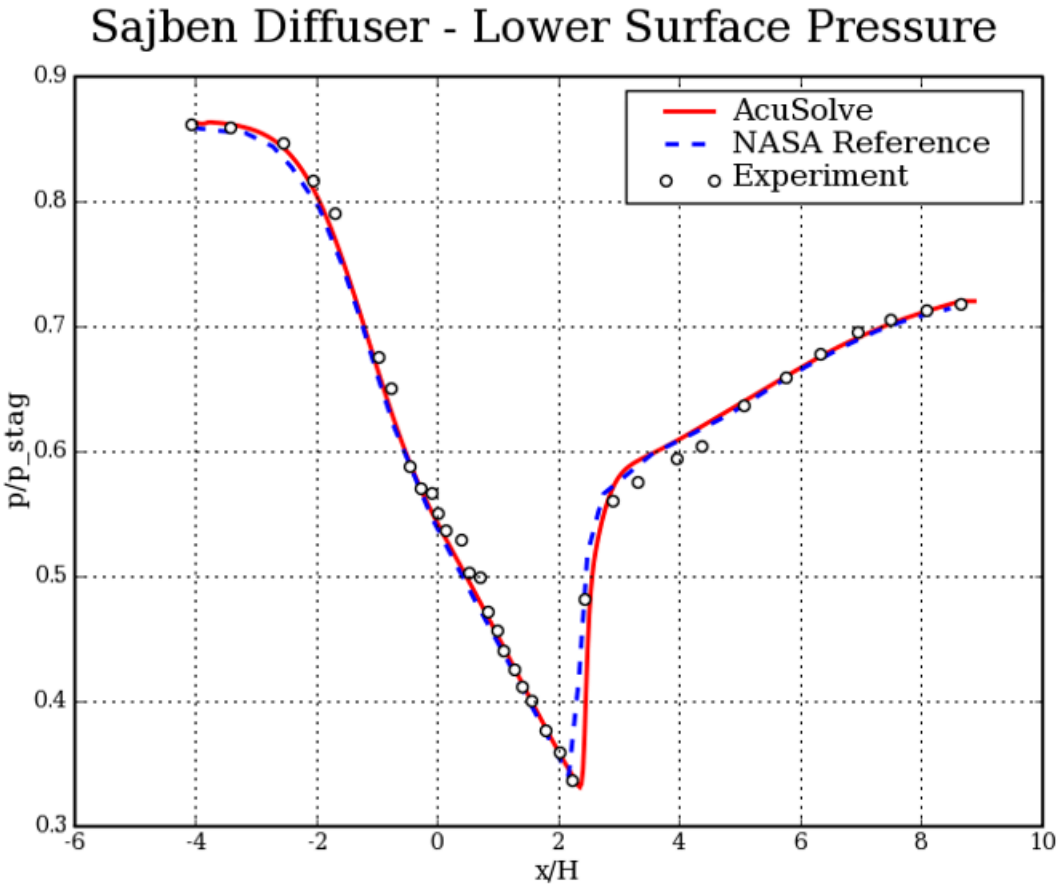


Figure 73: Normalized Pressure Versus Normalized Distance in Comparison to NASA Reference and Experimental Results

Summary

The AcuSolve solution compares well with experimental and numerical results for the described simulation. In this application, compressibility effects are accounted for using the coupled compressible flow solver with the ideal gas material definition. The thermal and momentum exchange within the nozzle is computed with AcuSolve using the compressible Navier-Stokes solver with the Spalart-Allmaras turbulence model. The experimental values of pressure are presented with the corresponding AcuSolve results and show good agreement, validating the ability to solve compressible cases with the presence of normal shocks. The results indicate that AcuSolve is able to properly predict the peak pressure magnitude and location within the diffuser while maintaining the normal shock when the time-step is selected to result in a maximum CFL of approximately 30.

Simulation Settings for Supersonic Flow Through a Converging-Diverging Nozzle

HyperMesh CFD database file: `<your working directory>\diffuser_compressible\diffuser_compressible.hm`

Global

- Problem Description

    - Flow – Compressible Navier Stokes
    - Analysis type – Transient
    - Turbulence equation – SA
    - Temperature equation – Advective Diffusive
- Auto Solution Strategy
    - Initial time increment – `4.0E-6`
    - Final time – `0.025` sec
    - Convergence Tolerance – `0.001` sec
    - Relaxation factor – `0.5`
- Material Model
    - Air-Ideal Gas
        - Type – Ideal_Gas
        - Viscosity – `1.781e-05` kg/m-sec
        - Specific Heat – `1005` J/kg-K
        - Conductivity – `0.02521` W/m-K
        - Gas Constant – `287.058` J/kg-K

Model

- Volumes
    - Fluid
        - Material – Air-Ideal Gas
- Surfaces
    - Inflow
        - Simple Boundary Condition – Inflow
        - Inflow type – Stagnation Pressure
        - Stagnation Pressure – `135000.0` N/m2
        - Turbulence_input_type – Direct
        - Eddy Viscosity – `1e-6` m^2/s
        - Temperature – `265.98` K
    - Outflow
        - Simple Boundary Condition – Outflow
        - Pressure – `97216.08` N/m2
    - Wall_1
        - Simple Boundary Condition – Wall
        - Type – auto_wall
    - Wall_2
        - Simple Boundary Condition – Wall
        - Type – auto_wall
    - Slip_1

        - Simple Boundary Condition – Slip
    - Slip_2
        - Simple Boundary Condition – Slip

References

Bogar, T. J., Sajben, M., and Kroutil, J. C. (1983) "Characteristic Frequencies of Transonic Diffuser Flow Oscillations," AIAA Journal, Vol. 21, No. 9, pp. 1232-1240.

Mohler, S.R., "Wind-US Unstructured Flow Solutions for a Transonic Diffuser," NASA CR-2005-213417, January 2005.

Turbulent Flow Past a Wall-Mounted Hump

In this application, AcuSolve is used to simulate fully developed turbulent flow past a smooth hump on the lower wall of a flow domain. AcuSolve results are compared with experimental results as described in Seifert and Pack (2002) and on the NASA Langley Research Center Turbulence Modeling Resource web page. The close agreement of AcuSolve results with experimental data and reference turbulence model performance validates the ability of AcuSolve to model cases with turbulent flow moving past a wall protrusion resulting in flow separation and recovery.

Problem Description

The problem consists of a fluid with material properties close to air flowing through a flow domain containing a well-defined smooth hump with a slit opening at approximately 65 percent of the hump chord. The inlet of the domain is defined with an inflow velocity in the streamwise direction that develops into fully turbulent flow at a Reynolds number (Re) of 936,000, based on the hump chord length of 1.0 m. The density of the flow medium is 1.0 kg/m^3 and the dynamic viscosity is 1.0684 X 10^{-6} kg/m-s. The simulation is conducted with the Reynolds Averaged Navier-Stokes equations using the Spalart Allmaras turbulence model, shear stress transport (SST) model, the K-ω model and Realizable K-ε model to evaluate the performance of the turbulence models. The flow predictions from AcuSolve are compared against experimental data and previously published turbulence model performance for pressure and friction coefficients within the domain.

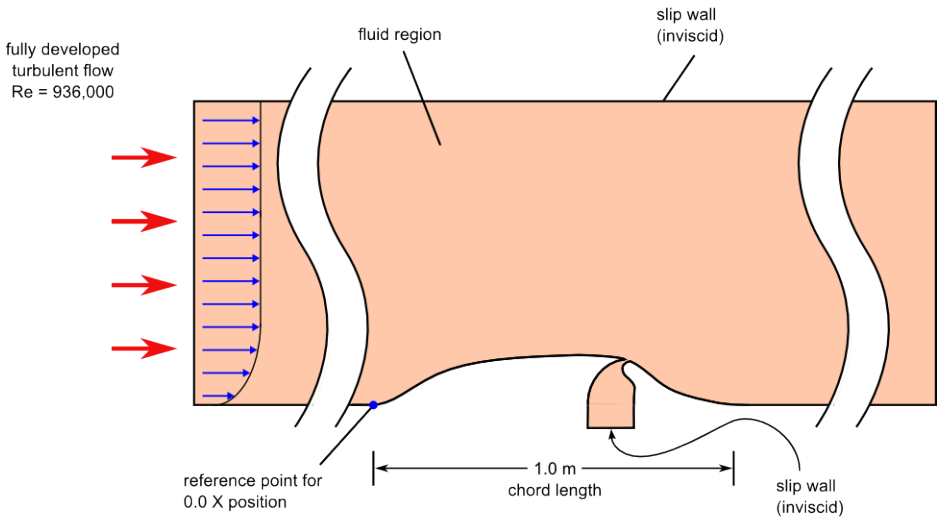


Figure 74: Critical Dimensions and Parameters for Simulating Turbulent Flow Through a Domain with a Wall-Mounted Hump

The upper walls of the domain are specified as slip (inviscid) and the lower walls are specified as no-slip. The inlet velocity and appropriate turbulence parameters are specified in the streamwise direction to match the desired Reynolds Number of 936,000. The outflow pressure is set to zero, and the lower wall on cavity below the hump is set to slip. The problem is simulated as two dimensional with a single layer of elements extruded in the cross stream direction and by defining the side walls as slip.

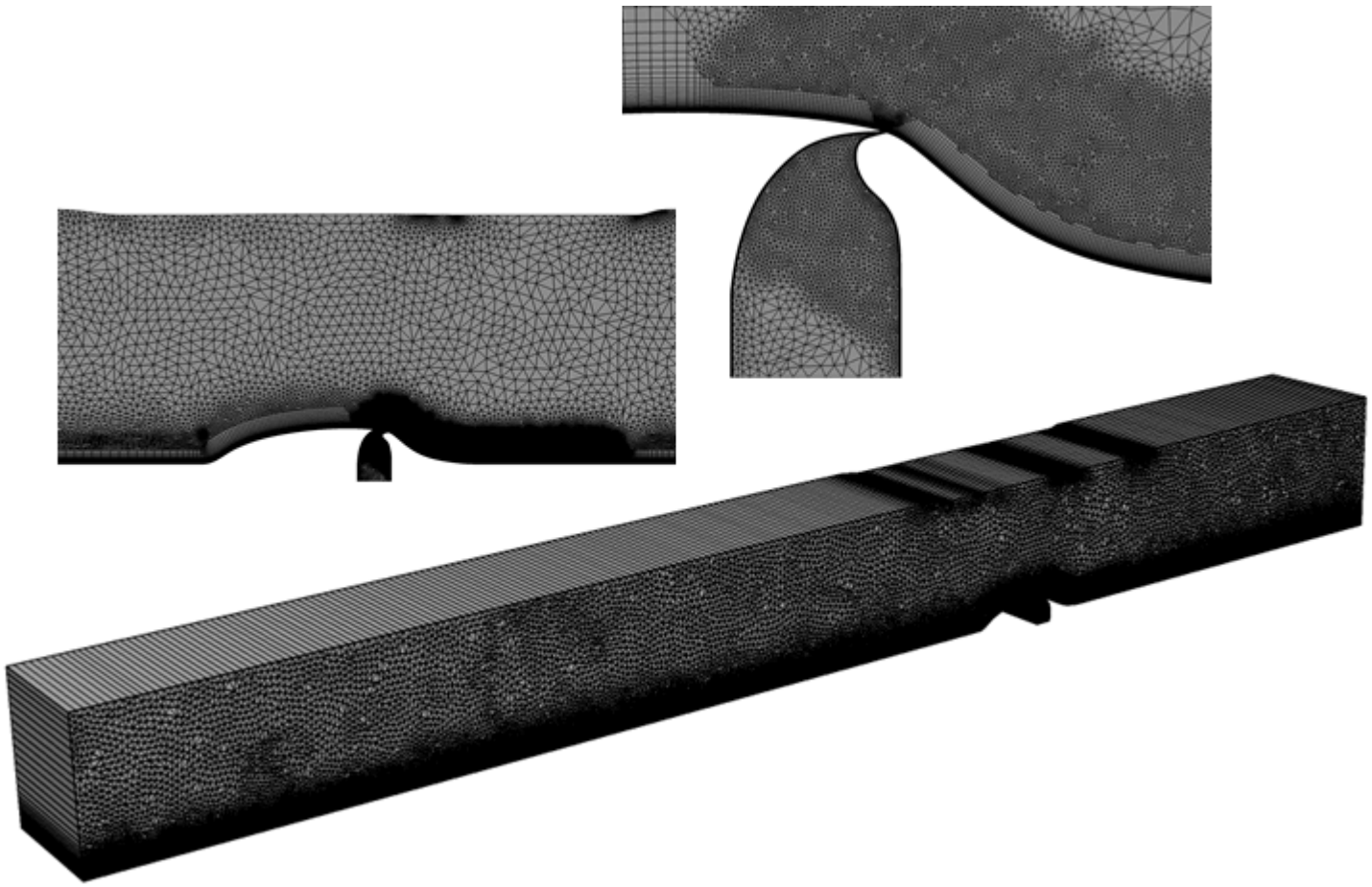


Figure 75: Three Views of the Mesh Used for Simulating Turbulent Flow over a Wall-Mounted Hump (Full Mesh is Shown on the Bottom, with Increased Resolution in Clockwise Views)

AcuSolve Results

The AcuSolve solution converged to a steady state and the results reflect the mean flow conditions within the domain. The images below show contours of velocity within the domain as well as the recirculation region directly downstream of the hump. As the flow enters the domain with a bulk velocity, it begins to develop a turbulent boundary layer near the lower wall prior to reaching the hump. As the flow approaches the hump section, the velocity near the lower wall decreases, but does not recirculate in front of the hump. It then accelerates over the top of the hump and separates immediately after reaching the cavity opening. The recirculation region propagates downstream, before the flow recovers and reattaches to the lower wall.

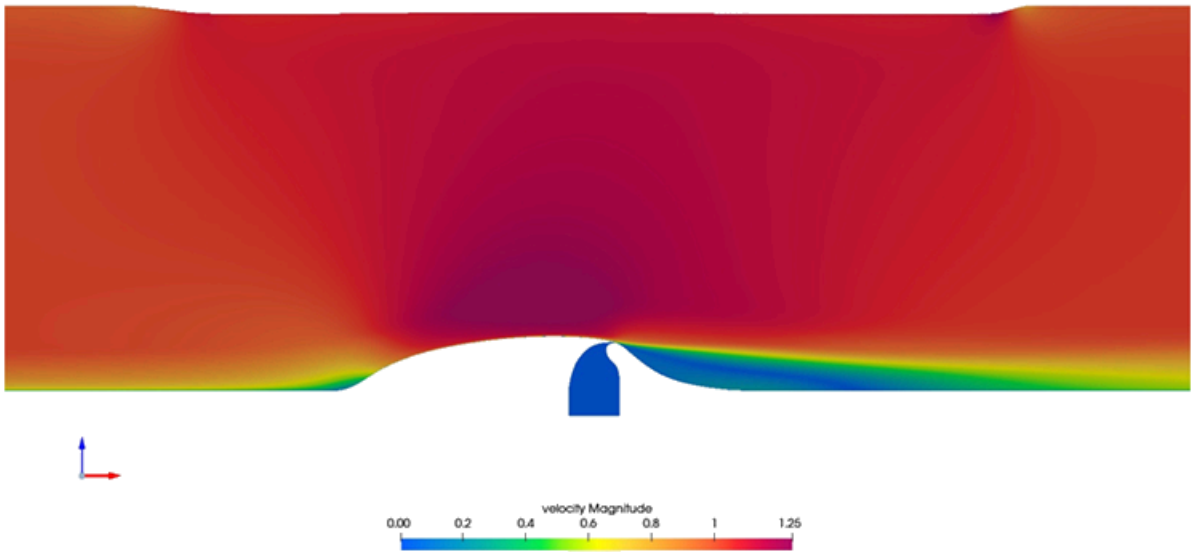


Figure 76: Velocity Contours on the Boundaries of the Domain, Showing Velocity Magnitude

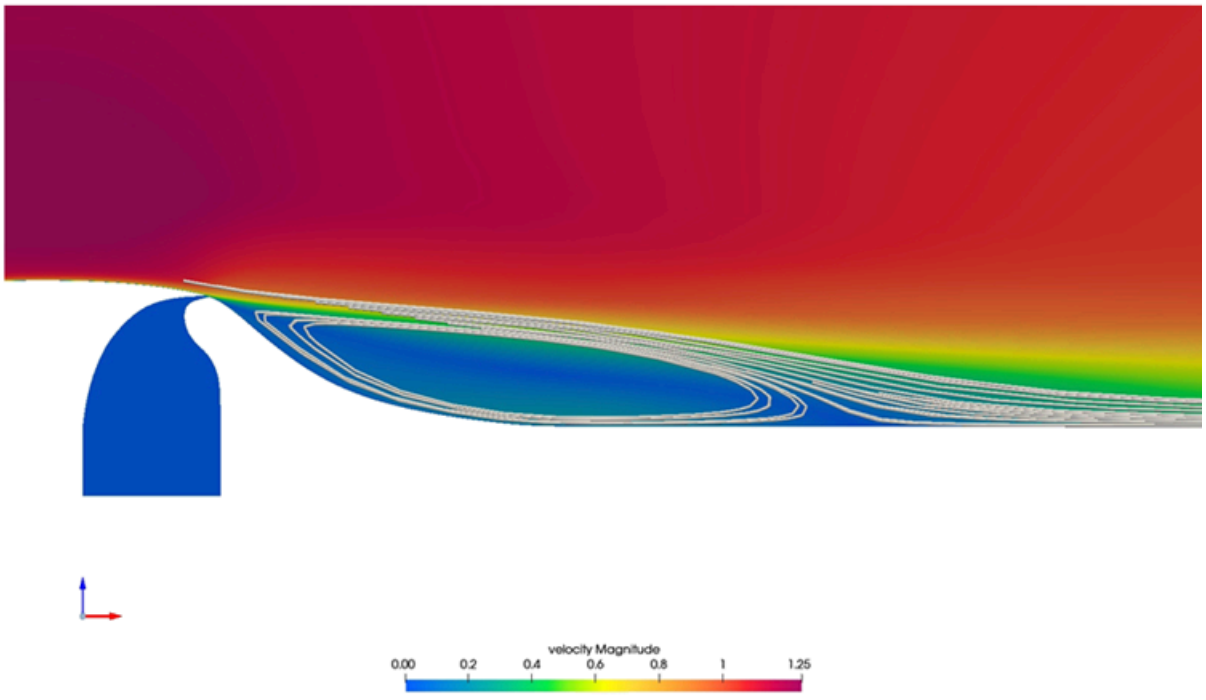


Figure 77: Close up View of Velocity Contours Showing the Recirculation Region with Streamlines (White Lines) Representing the Region of Backflow

The images below show the coefficient of pressure and coefficient of skin friction along the lower wall of the flow domain plotted with experimental results. The non-dimensional values are defined by the integrated inlet pressure and the magnitude of the inlet velocity. The images show black circles representing the experimental measurements (Seifert and Pack 2002), solid red lines for the SA model, solid blue lines for the SST model, solid green lines for the K-ω model and solid cyan lines for the Realizable K-ε model, representing the AcuSolve results. The resulting pressure coefficient within the domain demonstrates that there are minor differences between the four turbulence models. All four

models are shown to perform accurately in predicting the increase in surface pressure on the front of the hump but tend to over predict the skin friction in the wake of the hump, leading to a minor over prediction of the reattachment location. The SA model predicts a slightly larger recirculation region and does not meet the expected recovery pressure compared to SST, K- ω and K-ε models. This performance was found to be consistent with comparisons to other one equation models (NASA 2015).

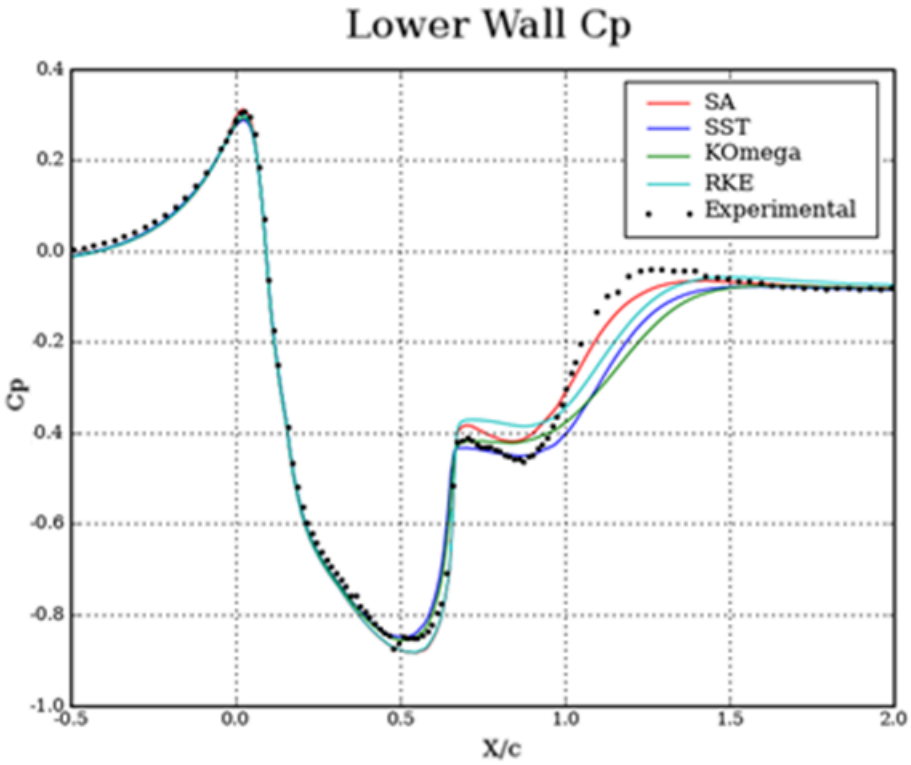


Figure 78: Coefficient of Pressure Along the Lower Wall as the Flow Moves Past the Hump, Where c is the Hump Chord Length and 0.0 is the Reference Location at the Front of the Hump in the X-Direction (Streamwise)

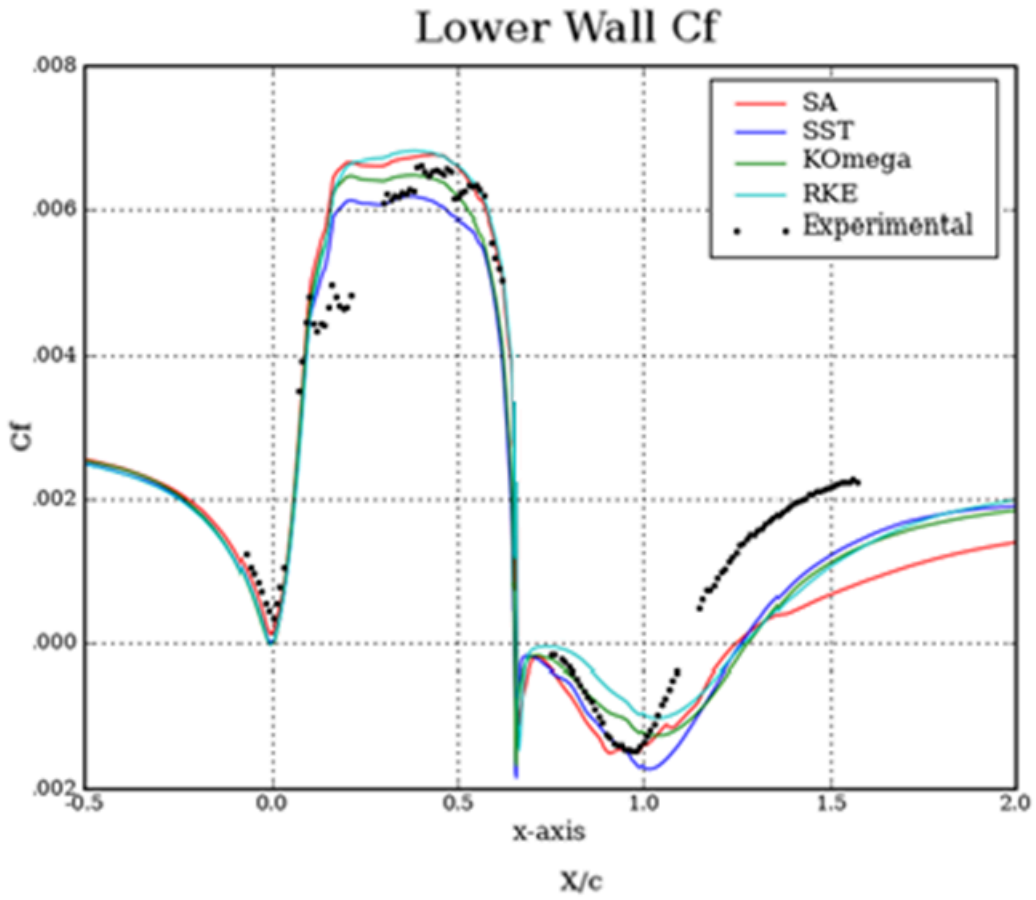


Figure 79: Skin Friction Coefficient Along the Lower Wall as the Flow Moves Past the Hump, Where c is the Hump Chord Length and 0.0 is the Reference Location at the Front of the Hump in the X-Direction (Streamwise)

Summary

In this application, a bulk turbulent flow at a Reynolds number of 936,000 within a flow domain containing a wall-mounted hump is studied and compared against experimental data. The AcuSolve results compare well with the experimental data for pressure coefficient and skin friction coefficient near the hump and downstream. The performance of the four turbulence models were found to be consistent with previously published results for flow over a wall-mounted hump (NASA 2015). For this application, the two equation models appear to outperform the one equation turbulence model, with better agreement for the downstream pressure on the wall. This application demonstrates AcuSolve's ability to predict the distribution of pressure and shear stress on protruding bodies within a turbulent flow field and serves to validate current turbulence modeling capabilities.

Simulation Settings for Turbulent Flow past a Wall-Mounted Hump

SimLab database file: `<your working directory>\wall_mounted_hump_turbulent\wall_mounted_hump_turbulent.slb`

Global

- Problem Description

    - Flow - Steady State
    - Turbulence equation - Spalart Allmaras
- Auto Solution Strategy
    - Max time steps - `100`
    - Convergence tolerance - `0.001`
    - Relaxation factor - `0.4`
- Material Model
    - Fluid
        - Density - `1.0` kg/m3
        - Viscosity - `1.0684e-6` kg/m-sec

  Model
- Volumes
    - Fluid
        - Element Set
            1. Material model - Fluid
- Surfaces
    - +Y
        - Simple Boundary Condition
            1. Type - Slip
    - -Y
        - Simple Boundary Condition
            1. Type - Slip
    - Cavity walls
        - Simple Boundary Condition
            1. Type - Wall
            2. Turbulence wall type - Wall Function
    - Hump walls
        - Simple Boundary Condition
            1. Type - Wall
            2. Turbulence wall type - Wall Function
    - Hump walls - downstream
        - Simple Boundary Condition
            1. Type - Wall
            2. Turbulence wall type - Wall Function
    - Inlet
        - Simple Boundary Condition
            1. Type - Inflow

2. Inflow type - Velocity
3. Inflow velocity type - Cartesian
4. X Velocity - `1.0` m/sec
5. Turbulence input type - Direct
6. Kinetic energy 1.2615e-5 m^2/s^2
7. Dissipation rate 0.00106 m^2/s^3

- Lower slip
  - Simple Boundary Condition
    1. Type - Slip
- Lower wall
  - Simple Boundary Condition
    1. Type - Wall
    2. Turbulence wall type - Wall Function
- Nozzle walls
  - Simple Boundary Condition
    1. Type - Wall
    2. Turbulence wall type - Wall Function

- Outlet
  - Simple Boundary Condition
    - Type - Outflow
- Slip
  - Simple Boundary Condition
    - Type - Slip

References

A Seifert and L.G. Pack. "Active Flow Separation Control on Wall-Mounted Hump at High Reynolds Numbers". AIAA Journal. 40(7). 2002.

NASA Langley Research Center Turbulence Modeling Resource web page. http://turbmodels.larc.nasa.gov/nasahump_val.html. Accessed June 2015.

Turbulent Flow Over an Oscillating Rigid Body Assembly

In this application, AcuSolve is used to simulate the fluid-structure interaction of a fluid moving over a cylinder/plate assembly. AcuSolve results are compared with experimental results as described in Gomes and Lienhart (2009). The close agreement of AcuSolve results with the experimental results validates the ability of AcuSolve to model cases in which the fluid forces lead to structural motions.

Problem Description

The problem consists of a fluid having material properties of standard water with density of 998 kg / m^3 and kinematic viscosity of 0.97e-6 m^2/sec through a two dimensional channel over a cylinder and plate assembly. The diameter of the cylinder is 0.022 m and the plate length is 0.042 m, while the inlet velocity is specified to match experimental conditions with a max velocity of 1.07 m/sec, as is shown in the following image, which is not drawn to scale. The model is simulated as transient with constant inflow conditions, allowing an oscillatory motion of the assembly to develop. The Shear Stress Transport (SST) turbulence model is used to model the turbulent portion of the flow and AcuSolve's internal rigid body motion is used to capture the motion of the oscillating assembly.

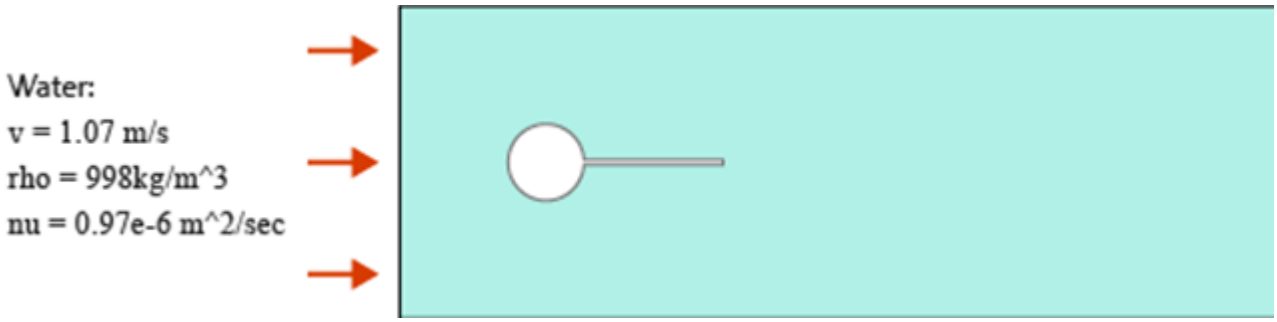


Figure 80: Critical Dimensions and Parameters used for Simulating Rigid Body Motion of Flow Past a Cylinder/Plate Assembly

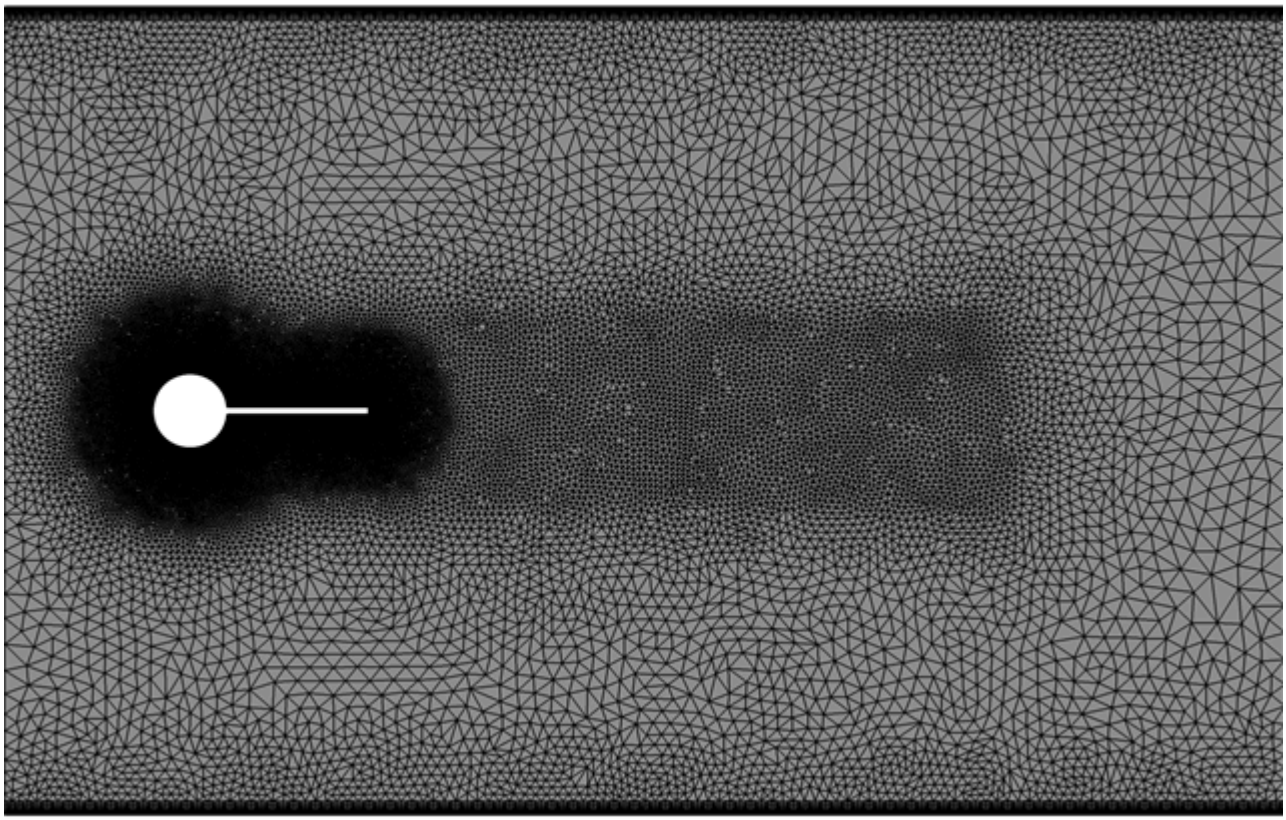


Figure 81: Mesh used for Simulating Rigid Body Motion of Flow Past a Cylinder/Plate Assembly

The simulation was performed as a two dimensional problem by constructing a volume mesh that contains a single layer of elements extruded in the cross stream direction, normal to the flow plane and by imposing symmetry boundary conditions on the extruded planes. The upper and lower walls are specified as no-slip and the inlet velocity is specified to match the conditions of the experiment (Gomes and Lienhart 2009).

AcuSolve Results

The AcuSolve solution reached a regularly repeating oscillatory state and the simulation was allowed to proceed for 10 seconds of physical time to obtain enough cycles for statistical analysis. The motion of the cylinder/plate assembly is directly attributed to the vortices shedding in its wake. The fluctuating loads on the assembly that result from the vortex shedding lead to a repeating cycle of structural rotation. The dominant oscillation frequency from the simulation was found to match well with the experimental measurements, within approximately 3.5 percent. The images below show the rigid body displacement of the assembly as it oscillates within the flow. Contours of velocity magnitude demonstrate the forcing on the assembly, while the mesh motion around the structure is captured and plotted for a single time step. Two dimensional plots showing the angular displacement demonstrate the motion, showing a single red line for the AcuSolve results.

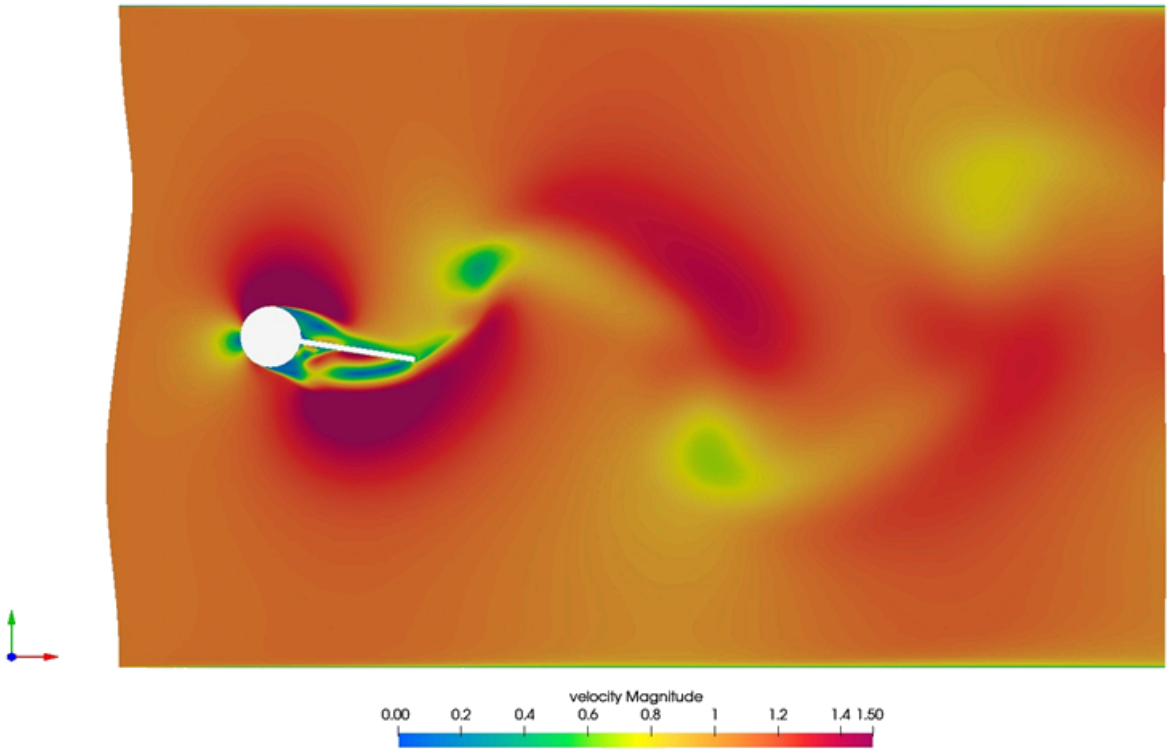


Figure 82: Velocity Contours Near the Assembly for a Single Time Step During the Simulation

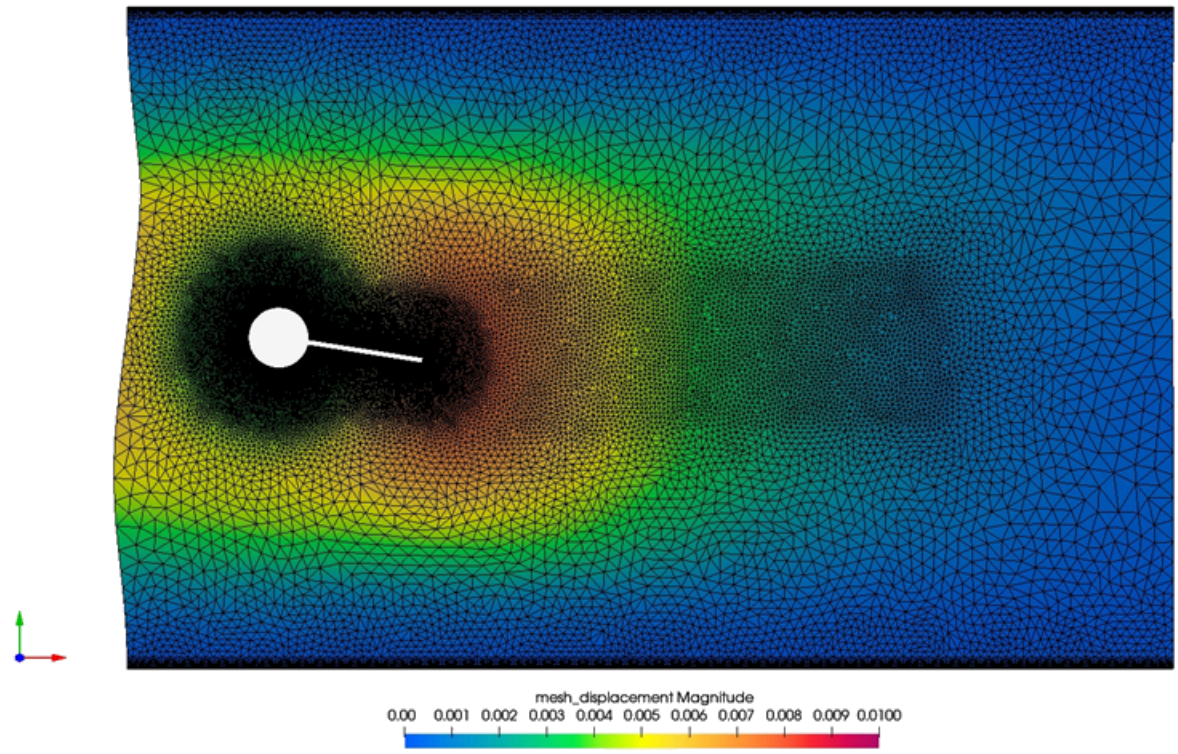


Figure 83: Mesh Displacement Contours Near the Assembly for a Single Time Step During the Simulation

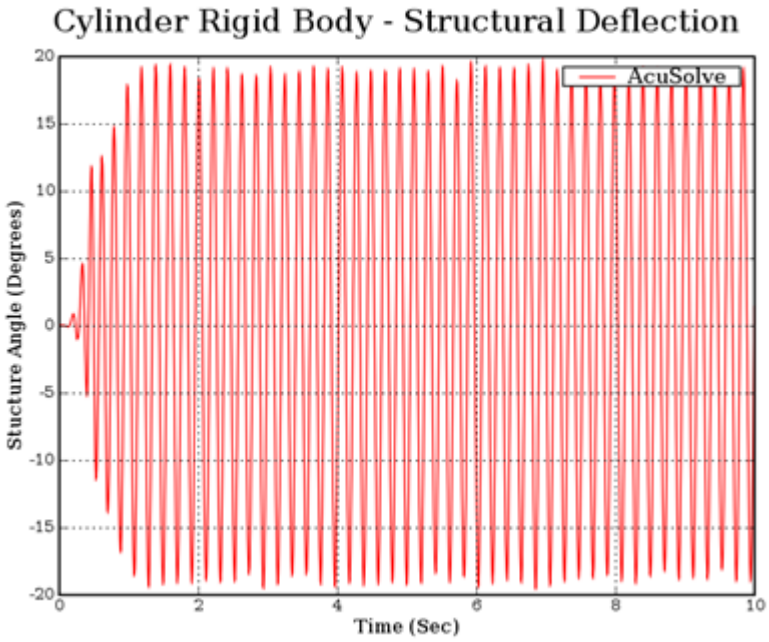


Figure 84: Rigid Body Displacement of the Assembly as a Function of Time, Showing the Oscillation Develop into the Pseudo-Steady Motion

The dominant frequency of the oscillation is easily identified in the Fast Fourier Transform (FFT) of the deflection angle, shown in the plot below.

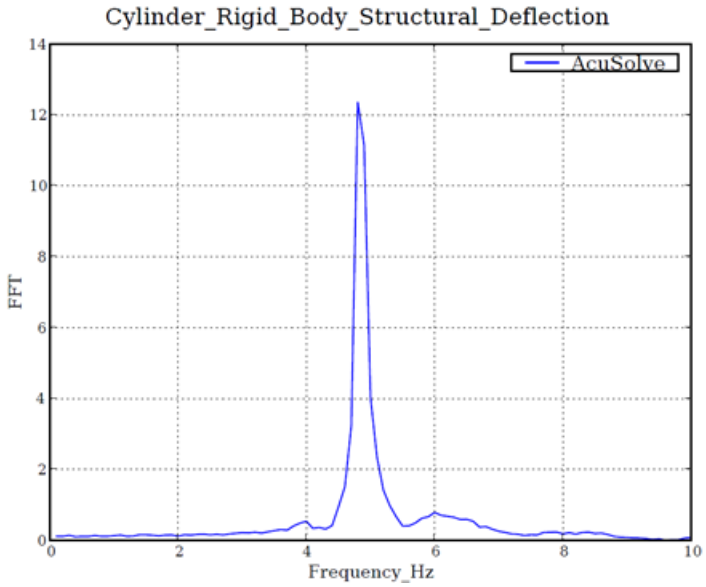


Figure 85: FFT of the Rigid Body Displacement Angle, Showing Power Spectral Density as a Function of Frequency

Summary

The AcuSolve solution compares well with experimental data for flow past an oscillating cylinder/plate assembly. In this application, water moves over the cylinder/plate assembly, giving rise to unsteady

loading that causes the body to rotate as a rigid body. The good agreement with the natural frequency of oscillation compared to the experimental data demonstrates that AcuSolve is capable of predicting fluid forced motion with an internal rigid body dynamic solver.

Simulation Settings for Turbulent Flow Over an Oscillating Rigid Body Assembly

SimLab database file: `<your working directory>\cylinder_rigidbody_turbulent\cylinder_rigidbody_turbulent.slb`

Global

- Problem Description
  - Flow - Transient
  - Turbulence equation - SST
  - Moving Mesh - Computed
- Auto Solution Strategy
  - Final Time - `10.0`
  - Initial Time Increment- `0.005`
  - Convergence tolerance- `0.001`
  - Max stagger iterations- `3`
- Material Model
  - Water
    - Type- Constant
    - Density- `998.0` kg/m3
    - Viscosity- `0.00096806` kg/m*sec
- Mesh Motion
  - RigidBody
    - Type- Rigid Body Dynamic
      1. Z rotation- Active
      2. Mass- `0.2089` kg
      3. Dyadic
         1. X-X - `3.7 e-5` kg-m2
         2. Y-Y- `3.7 e-5` kg-m2
         3. Z-Z - `3.7 e-5` kg-m2

  Model
- Volumes
  - Volume
    - Element Set
      1. Material model- Water
- Surfaces
  - Body

- Simple Boundary Condition
  1. Type- Wall
  2. Mesh displacement BC type- Fixed
  3. Mesh motion- RigidBody
- Interpolated Motion Surface

◦ Bottom
- Simple Boundary Condition
  1. Type- Wall
  2. Mesh displacement BC type- Fixed
- Interpolated Motion Surface

◦ Inflow
- Simple Boundary Condition
  1. Type- Inflow
  2. Inflow type- Velocity
  3. X Velocity- `1.07` m/sec
  4. Turbulence input type- Auto
  5. Turbulence intensity type- High
- Advanced Options
  1. Nodal Boundary Conditions
  2. X-velocity
     1. Type- Linear
     2. Precedence- `2`
     3. Curve fit variable- Y coordinate
     4. Curve fit values- Provided
  3. Y-velocity
     1. Type- Zero
  4. Z-velocity
     1. Type- Zero

◦ Bottom
- Simple Boundary Condition
  1. Type- Wall
  2. Mesh displacement BC type- Fixed
  3. Mesh motion- RigidBody

◦ Outflow
- Simple Boundary Condition
  1. Type- Outflow

◦ Top
- Simple Boundary Condition

1 Type- Wall
2 Mesh displacement BC type- Fixed

- maxZ
  - Simple Boundary Condition
    1 Type- Slip
- minZ
  - Simple Boundary Condition
    1 Type- Slip

References

Gomes, J. P. and Lienhart, H. (2009) Experimental Benchmark: Self-excited Fluid-structure Interaction Test Cases, in Fluid-Structure Interaction II: Modeling, Simulation, Optimization, Bungartz, H. J., Mehl, M., Schafer, M. (eds.), 383-412, Springer-Verlag.Ryhming.

Steady Flow

3

This section includes validation cases that consider steady state flow simulations.

This chapter covers the following:

- Flow Between Concentric Cylinders (p. 112)
- Turbulent Flow Through a Pipe (p. 118)
- Laminar Couette Flow with Imposed Pressure Gradient (p. 122)
- Flow Inside a Rotating Cavity (p. 128)
- Natural Convection in a Concentric Annulus (p. 136)
- Laminar Flow Past a 90° T-Junction (p. 142)
- Laminar Flow Through a Channel with Heated Walls (p. 147)
- Turbulent Flow Behind an Open-Slit V (p. 152)
- Turbulent Flow Over a NACA 0012 Airfoil (p. 159)
- Turbulent Natural Convection Inside a Tall Cavity (p. 167)
- Viscous Heating Inside a Rotating Annulus (p. 175)
- Separated Laminar Flow Over a Blunt Plate (p. 183)
- Turbulent Flow with Separation in an Asymmetric Diffuser (p. 190)
- Turbulent Flow Over a Backward-Facing Step (p. 198)
- Turbulent Flow Past a Convex Curve in a Channel (p. 205)
- Heat Transfer Between Radiating Concentric Cylinders (p. 212)
- Turbulent Mixing Layers in an Open Channel (p. 218)
- Laminar to Turbulent Transition Over an Airfoil (p. 223)
- Turbulent Flow Through a 180 Degree Curved Channel (p. 228)
- Heat Transfer Between Radiating Concentric Spheres (p. 234)
- Single-Phase Nucleate Boiling in a Rectangular Channel (p. 239)
- Turbulent Flow Past a Wall-Mounted Hump (p. 244)
- Turbulent Flow Through a Heated Periodic Channel (p. 251)
- Laminar Couette Flow with Imposed Pressure Gradient and Heated Walls (p. 257)

Flow Between Concentric Cylinders

In this application, AcuSolve is used to simulate the flow of water between concentric cylinders. The outer cylinder is held stationary while the inner cylinder rotates with a constant speed. AcuSolve results are compared with analytical results as described in White (1991). The close agreement of AcuSolve results with analytical results validates the ability of AcuSolve to model cases containing thin annular gaps with flow induced by rotating walls.

Problem Description

The problem consists of two concentric pipes with water filling the void between them, as shown in the following image, which is not drawn to scale. The radius of the outer pipe is 0.0468 m and the radius of the inner pipe is 0.0178 m. The inner cylinder rotates at 1 rad/sec and the outer cylinder is fixed. The induced flow is laminar and exhibits a steady state behavior. The rotation of the inner cylinder causes the fluid to rotate due to viscous shearing near the wall. As the outer cylinder is fixed, a velocity gradient is generated as a function of radius within the flow domain.

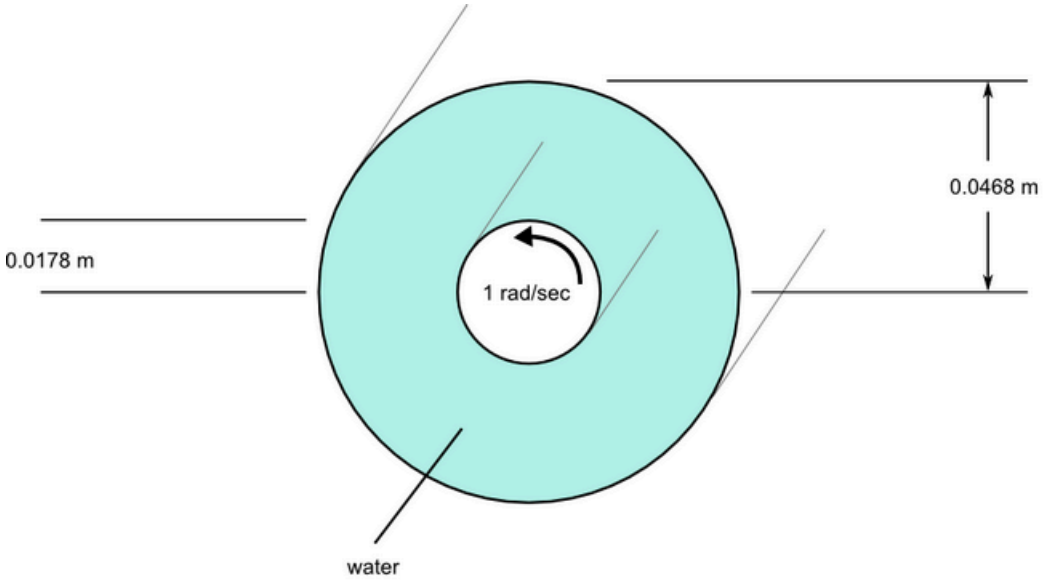


Figure 86: Critical Dimensions and Parameters for Simulating Flow Between Concentric Cylinders

The simulation was performed as a two dimensional problem by restricting flow in the out-of-plane direction through the use of a mesh that is one element thick.

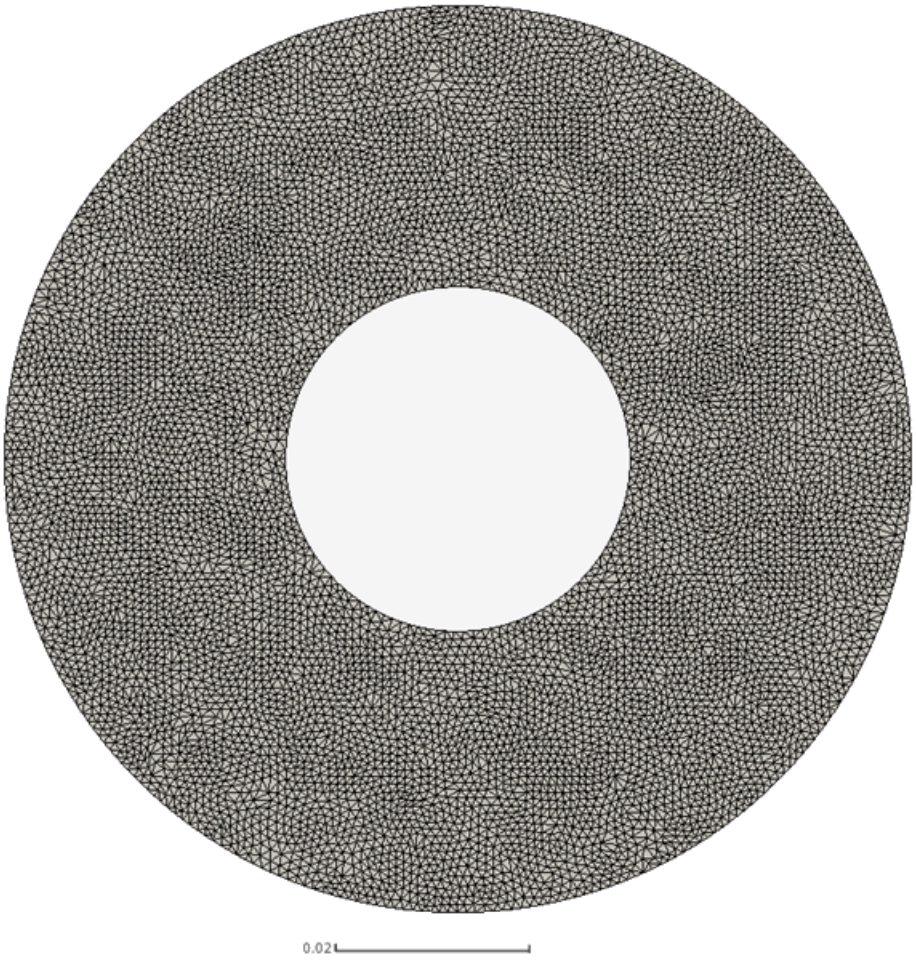


Figure 87: Mesh Used for Simulating Flow Between Concentric Cylinders

AcuSolve Results

The AcuSolve solution converged to a steady state and the results reflect the mean flow conditions. The velocity of the fluid within the cavity is greatest near the rotating inner cylinder. There is a nonlinear decrease in velocity as a function of distance away from the inner cylinder.

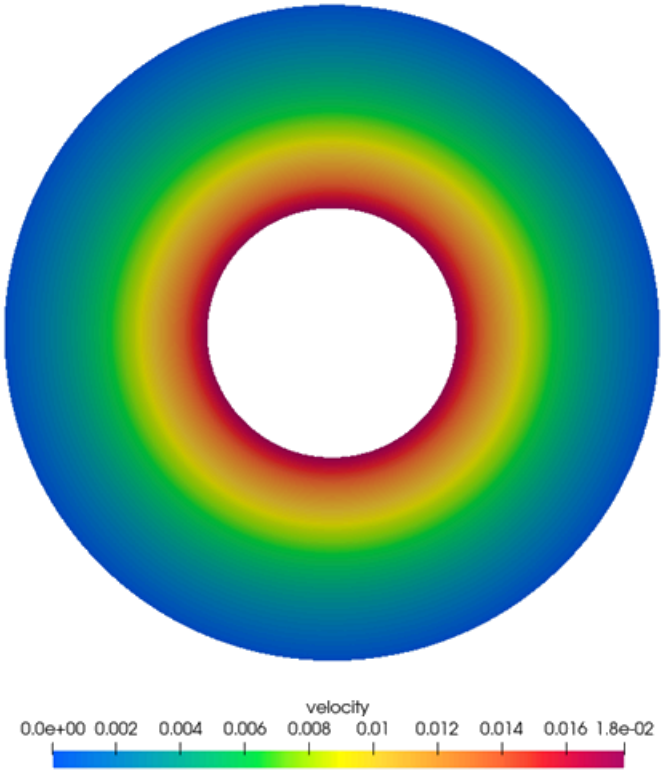


Figure 88: Contours of Tangential Velocity Between the Concentric Cylinders

Analytical tangential velocity at four distances away from the center of the rotating inner cylinder are presented with the corresponding AcuSolve results in the following table.

Table 3:

Distance from the center of rotating cylinder (m)	Analytical tangential velocity (m/s)	AcuSolve tangential velocity (m/s)	Percent deviation from analytical
0.020	0.01514	0.01514	0.04
0.025	0.01059	0.01058	0.10
0.030	0.00727	0.00727	0.06
0.035	0.00466	0.00466	0.10

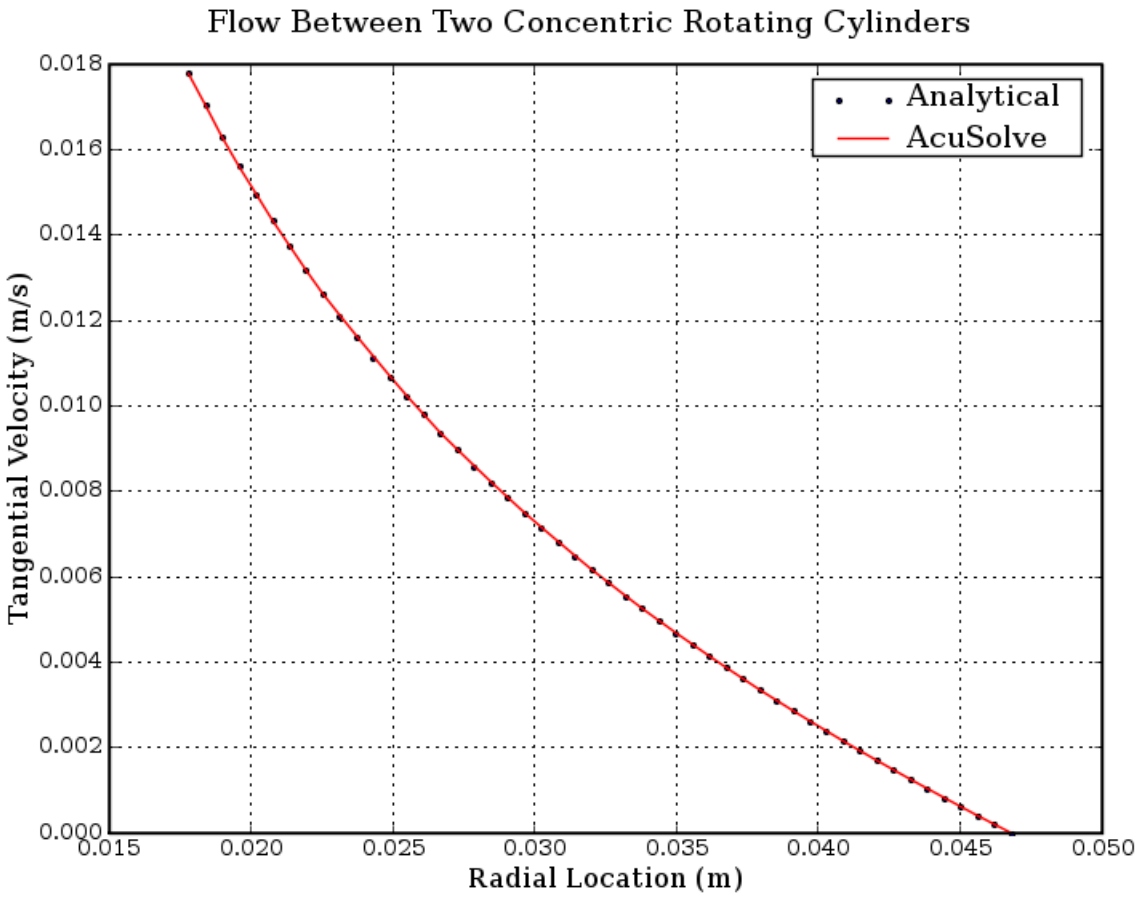


Figure 89: Tangential Velocity Plotted Against Distance from the Center of the Rotating Cylinder

Summary

The AcuSolve solution compares well with analytical results for the flow between concentric cylinders. In this application, the velocity in the annular fluid region is driven by the viscous stresses on the rotating wall. The AcuSolve tangential velocity is within 0.1 percent of the analytical solution at all radial locations.

Simulation Settings for Flow Between Concentric Cylinders

HyperMesh CFD database file: `<your working directory>\annulus_rotating\annulus_rotating.hm`

Global

- Problem Description
  - Analysis type - Steady State
  - Turbulence equation - Laminar
- Auto Solution Strategy
  - Relaxation Factor - `0.2`
- Material Model

- Water
  - Density - `1000.0` kg/m3
  - Viscosity - `0.001` kg/m-sec
- Reference Frame
  - Rotating_Cylinder
    - Rotation center
      1. X-coordinate - `0.0` m
      2. Y-coordinate - `0.0` m
      3. Z-coordinate - `0.0` m
    - Angular velocity
      1. X-component - `0.0` rad/sec
      2. Y-component - `0.0` rad/sec
      3. Z-component - `-1.0` rad/sec

Model

- Volumes
  - Volume
    - Element set
      1. Material model - Water
- Surfaces
  - Boundary1
    - Simple Boundary Condition
      1. Type - Symmetry
  - Boundary2
    - Simple Boundary Condition
      1. Type - Symmetry
  - Inner
    - Simple Boundary Condition
      1. Type - Wall
      2. Reference Frame - Rotating_Cylinder
  - Outer
    - Simple Boundary Condition
      1. Type - Wall
- Nodes
  - Fixed
    - Pressure
      1. Type - Zero

References

F. M. White. "Viscous Fluid Flow". Section 3-2.3. McGraw-Hill Book Co., Inc. New York. 1991.

Turbulent Flow Through a Pipe

In this application, turbulent flow of air through a pipe is simulated. AcuSolve results are compared with experimental results as described in White (1991) and extracted from the Moody chart. The close agreement of AcuSolve results with experimental results validates the ability of AcuSolve to model turbulent flow within pipes.

Problem Description

The problem consists of air flowing through a pipe 0.004 m in diameter and 0.02 m long, as shown in the following image, which is not drawn to scale. The AcuSolve simulation utilizes periodic boundary conditions to obtain the fully developed profile within the pipe. The defined pressure drop, applied as a body force on the fluid volume, offsets the change in pressure due to the friction created by the no-slip walls of the pipe. The Reynolds number for this problem is approximately 8,250.

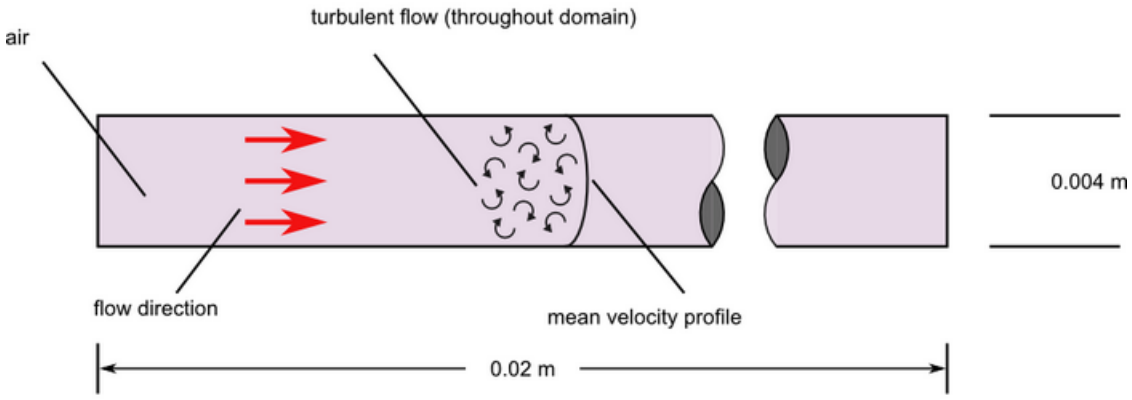


Figure 90: Critical Dimensions and Parameters for Simulating Turbulent Flow Through a Pipe

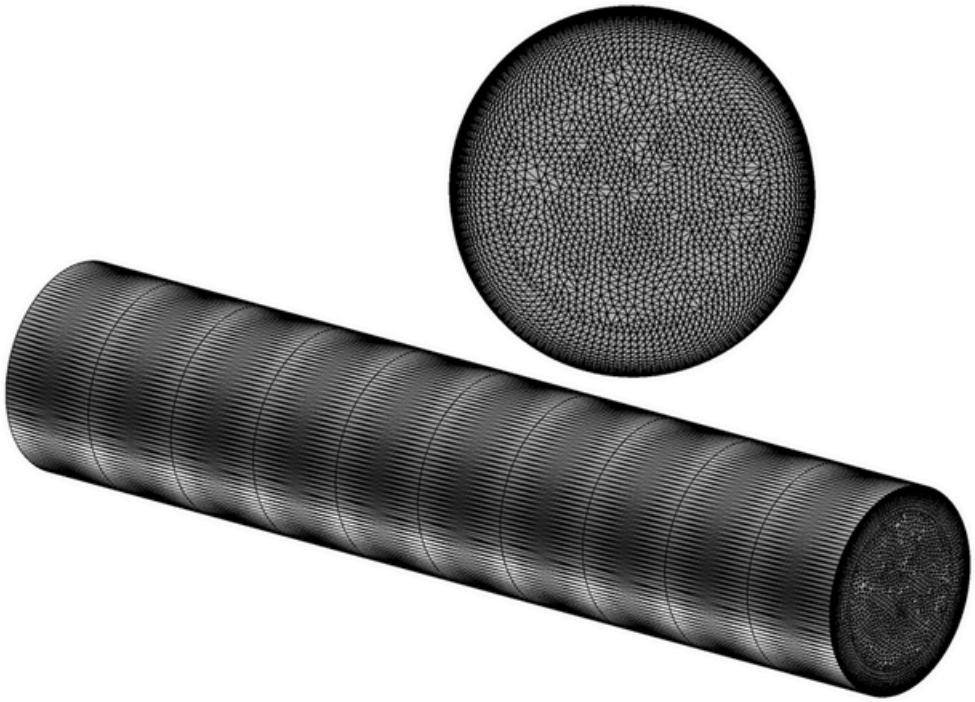


Figure 91: Mesh of a Periodic Segment Used for Simulating Turbulent Flow Through a Pipe

AcuSolve Results

The AcuSolve solution converged to a steady state and the results reflect the mean flow conditions with a turbulent velocity profile that is fully developed. The simulation was performed using the Spalart-Allmaras single-equation turbulence model. The velocity and eddy viscosity profiles are constant along the length of the pipe.

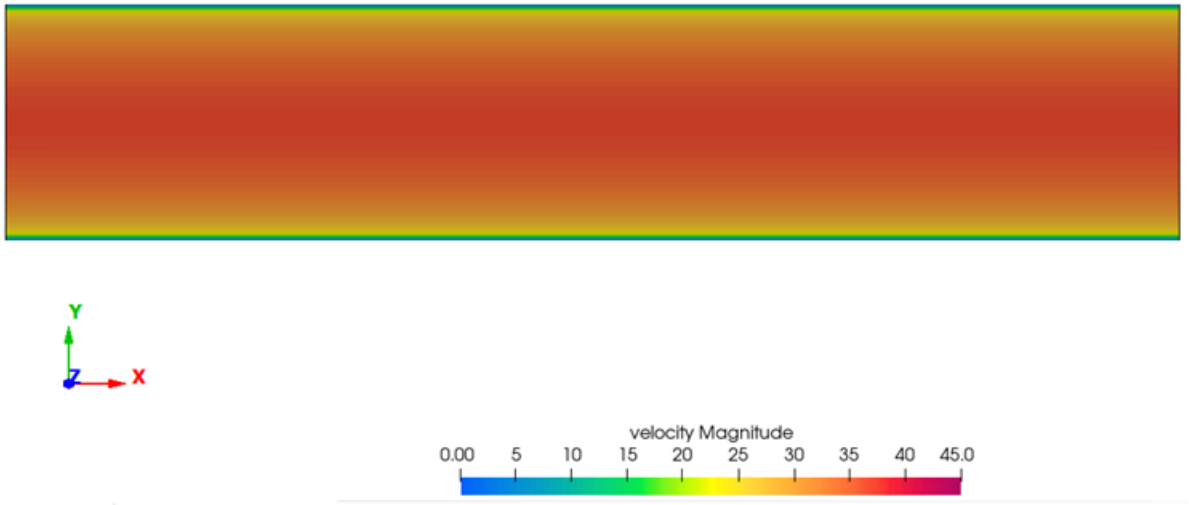


Figure 92: Velocity Contours for the Averaged Turbulent Flow

The experimental result for average velocity at the inlet is presented with the corresponding AcuSolve prediction in the following table.

Table 4:

	Experimental result	AcuSolve prediction	Percent deviation from experimental
Average inlet velocity	30.0	30.63	2.1

Summary

The AcuSolve solution compares well with the experimental result for average inlet velocity for turbulent flow through a pipe. In this application, the applied body force counteracts the change in pressure due to the viscous stresses near the pipe wall. The resulting friction factor for a smooth wall pipe and the specified Reynolds number is approximately 0.0326. With the imposed pressure drop defining the flow, the AcuSolve prediction of average inlet velocity is within 2.0 percent of the Darcy-Weisbach approximation.

Simulation Settings for Turbulent Flow Through a Pipe

SimLab database file: `<your working directory >\pipe_turbulent\pipe_turbulent.slb`.

Global

- Problem Description
  - Flow - Steady State
  - Turbulence equation - Spalart Allmaras
- Auto Solution Strategy
  - Relaxation factor - `0.4`

- Material Model
  - Air
    - Density - `1.225` kg/m3
    - Viscosity - `1.781e-05` kg/m-sec
- Body Force
  - dpdx
    - Gravity
      1. X-component - `3739.98` m/s2

  Model
- Volumes
  - Fluid
    - Element Set
      1. Material model - Air
      2. Body force - dpdx
- Surfaces
  - Inlet
    - Simple Boundary Condition - (disabled to allow for periodic conditions to be set)
  - Outlet
    - Simple Boundary Condition - (disabled to allow for periodic conditions to be set)
  - Wall
    - Simple Boundary Condition
      1. Type - Wall
      2. Roughness height - `0.0` mm
- Periodics
  - Periodic 1
    - Periodic Boundary Condition
      1. Type - Periodic

References

F. M. White. "Viscous Fluid Flow". Section 3-2.1. McGraw-Hill Book Co., Inc.. New York. 1991.

Experimental solution adapted from Darcy-Weisbach equation based on friction factor taken from the Moody chart with a Reynolds number of approximately 8,250.

Laminar Couette Flow with Imposed Pressure Gradient

In this application, AcuSolve is used to simulate the viscous flow of water between a moving and a stationary plate with an imposed pressure gradient. AcuSolve results are compared with analytical results described in White (1991). The close agreement of AcuSolve results with analytical results validates the ability of AcuSolve to model cases with imposed pressure gradients.

Problem Description

The problem consists of air between two plates in a two dimensional domain, as shown in the following image, which is not drawn to scale. The domain is 1.0 m high and 1.5 m long. The top plate moves with a constant velocity of 3.0 m/sec and the bottom plate is fixed. There is a mean-pressure gradient of -12 Pa/m applied to the bulk fluid in the streamwise direction. The problem is simulated with periodic boundaries in the streamwise direction. The induced flow field is laminar and exhibits a steady state behavior. The flow field develops from the pressure gradient, the motion of the top plate, and the viscous shear stresses near the plates.

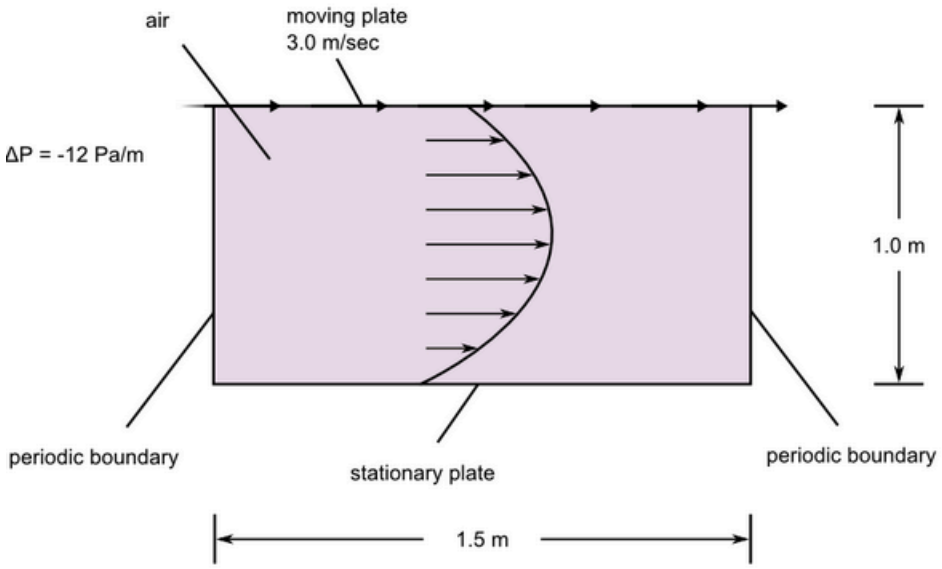


Figure 93: Critical Dimensions and Parameters for Simulating Laminar Couette Flow with an Imposed Pressure Gradient

The simulation was performed as a two dimensional problem by restricting flow in the out-of-plane direction through the use of a mesh that is one element thick.

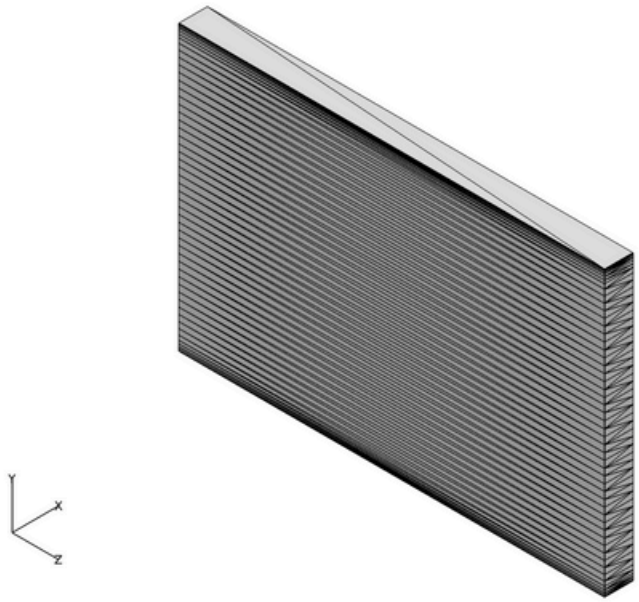


Figure 94: Mesh used for Simulating Laminar Couette Flow with an Imposed Pressure Gradient

AcuSolve Results

The AcuSolve solution converged to a steady state and the results reflect the mean flow conditions. The greatest velocity is located at approximately 40 percent of the channel height, closer to the moving plate. The flow develops as a result of the pressure gradient and the shear stress acting on the fluid near both the moving plate and the stationary plate.

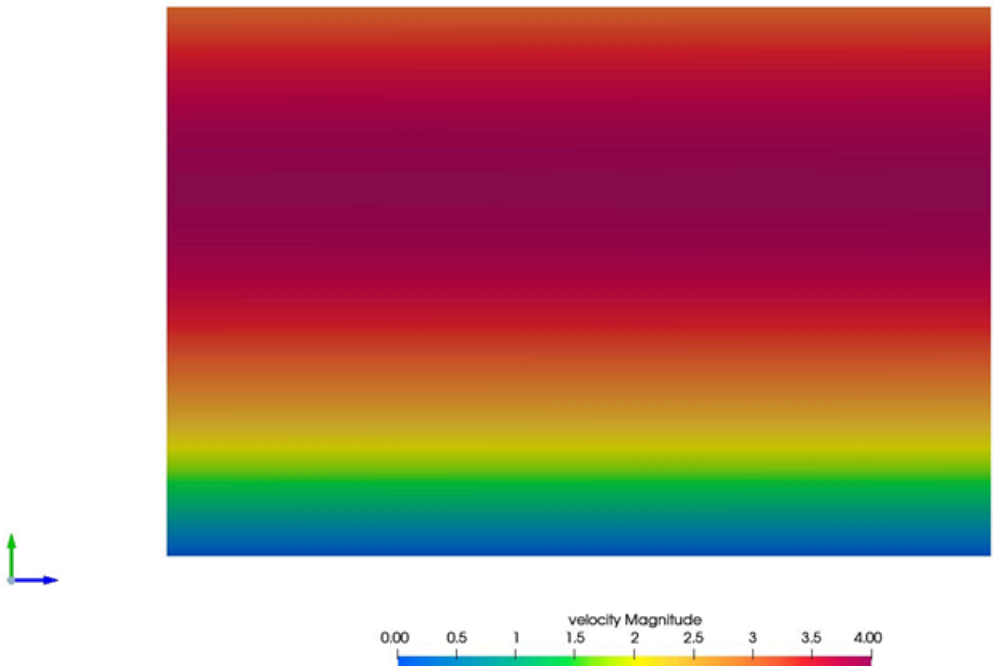


Figure 95: Z-Velocity Contours and Velocity Vectors

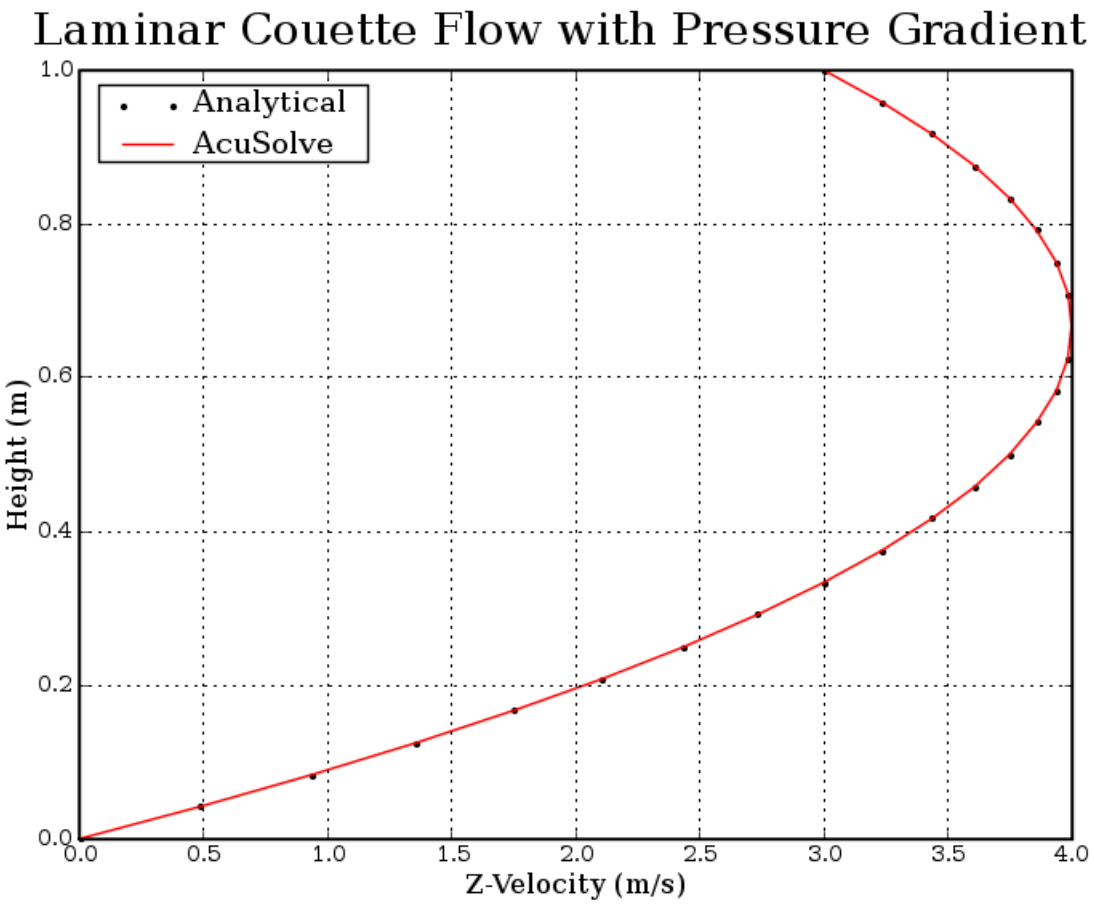


Figure 96: Z Velocity Plotted Against Height Above the Bottom of the Flow Field (Z Velocity is Presented on the X Axis to Better Represent the Velocity Profile in the Direction of Flow)

Summary

The velocity profile computed by AcuSolve agrees well with the analytical solution for this application. The velocity profile arises due to the combination of the imposed pressure gradient and the constant upper-wall velocity.

Note: The combination of these effects results in the asymmetric velocity profile that is reflected in the results.

Simulation Settings for Laminar Couette Flow with Imposed Pressure Gradient

SimLab database file: `<your working directory>\couette_flow\couette_flow.slb`

Global

- Problem Description
  - Solution Type - Steady State
  - Flow - Laminar

- Auto Solution Strategy
  - Relaxation factor - `0.2`
- Material Model
  - Air
    - Density - `1.0` kg/m3
    - Viscosity - `1.0` kg/m-sec
- Body Force
  - DP/DL
    - Gravity
      1. Z-component - `18.0` m/sec2

  Model
- Volumes
  - Fluid
    - Element set
      1. Material model - Air
      2. Body force - DP/DL
- Surfaces
  - Max_X
    - Simple Boundary Condition
      1. Type - Symmetry
  - Max_Y
    - Simple Boundary Condition
      1. Type - Wall
      2. Wall velocity type - Cartesian
      3. Z-velocity - `3.0` m/s
  - Max_Z
    - Simple Boundary Condition - (disabled to allow for periodic conditions to be set)
  - Min_X
    - Simple Boundary Condition
      1. Type - Symmetry
  - Min_Y
    - Simple Boundary Condition
      1. Type - Wall
  - Min_Z
    - Simple Boundary Condition - (disabled to allow for periodic conditions to be set)
- Periodics
  - Periodic 1

- Periodic Boundary Conditions
  1. Type - Periodic

References

F. M. White. "Viscous Fluid Flow". Section 3-2.3. McGraw-Hill Book Co., Inc. New York. 1991.

Flow Inside a Rotating Cavity

In this application, AcuSolve is used to simulate the flow of air in an enclosed cylindrical cavity with a rotating top and a fixed bottom. AcuSolve results are compared with experimental data adapted from Michelsen (1986). The close agreement of AcuSolve results with experimental data validates the ability of AcuSolve to model cases containing enclosed cavities with flow induced by rotating walls.

Problem Description

The problem consists of air in an enclosed cylinder 1.0 m tall with a radius of 1.0 m, as shown in the following image, which is not drawn to scale. The top of the cylinder rotates about its center at 1 rad/s, while the bottom of the cylinder is fixed. As the container top spins, the viscous stresses on the fluid induce a circumferential (swirl) velocity throughout the height of the cylinder. To conserve mass and momentum, the fluid generates a radial velocity that changes direction based on distance away from the rotation center of the cylinder.

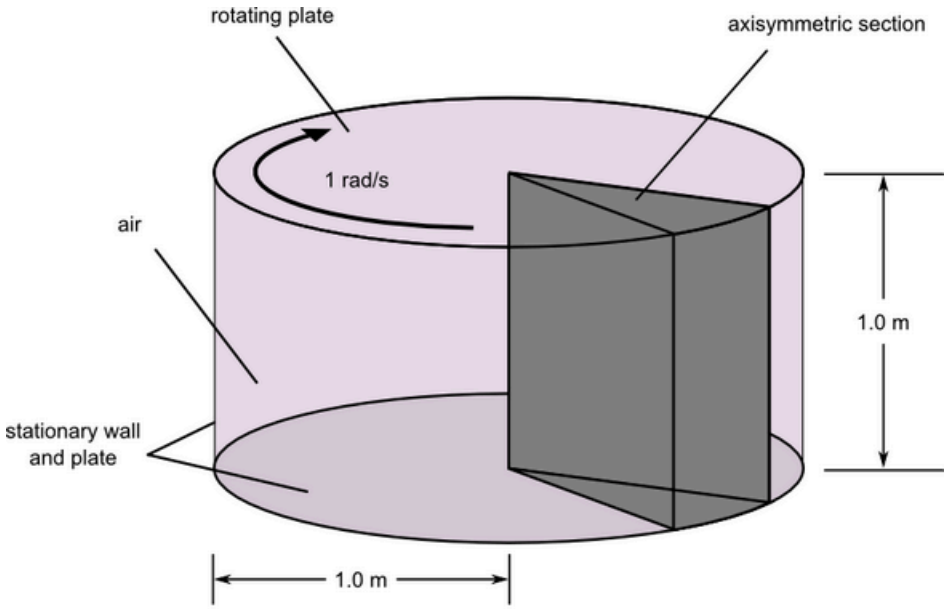


Figure 97: Critical Dimensions and Parameters for Simulating Flow Inside a Rotating Cavity

The flow domain is modeled with axisymmetric periodicity in the circumferential direction, which allows for accurate simulation of the flow while minimizing computational time.

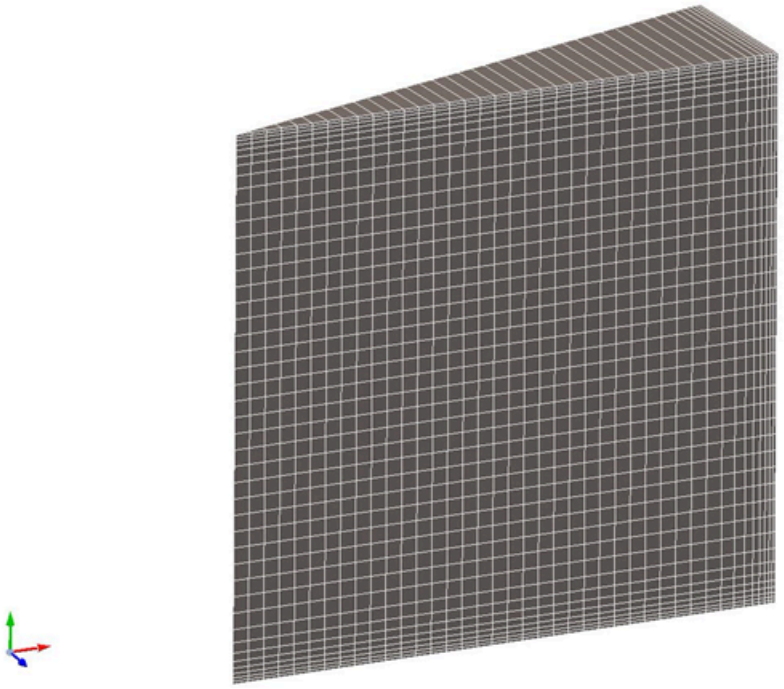


Figure 98: Mesh of Periodic Section Used for Simulating Flow Inside a Rotating Cylinder

AcuSolve Results

The AcuSolve solution converged to a steady state and the results reflect the mean flow conditions. The velocity varies with both vertical location and with distance from the rotation center. The complex flow field develops from a combination of the viscous stresses acting at the rotating cylinder top and at the stationary bottom.

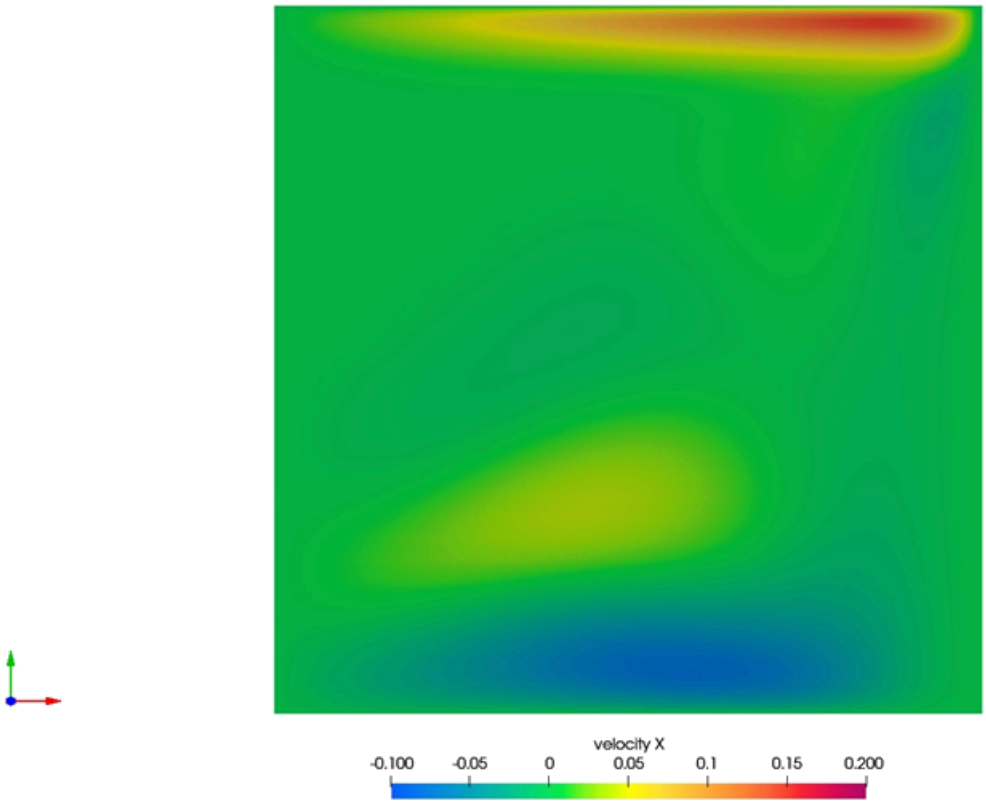


Figure 99: Contours of Radial Velocity with Velocity Vectors. This Image Shows the Front Face of the Modeled Cylinder Wedge, with the Center of Rotation on the Left Edge. The Vertical Line Represents a Radial Location 0.6 m From the Center of Rotation.

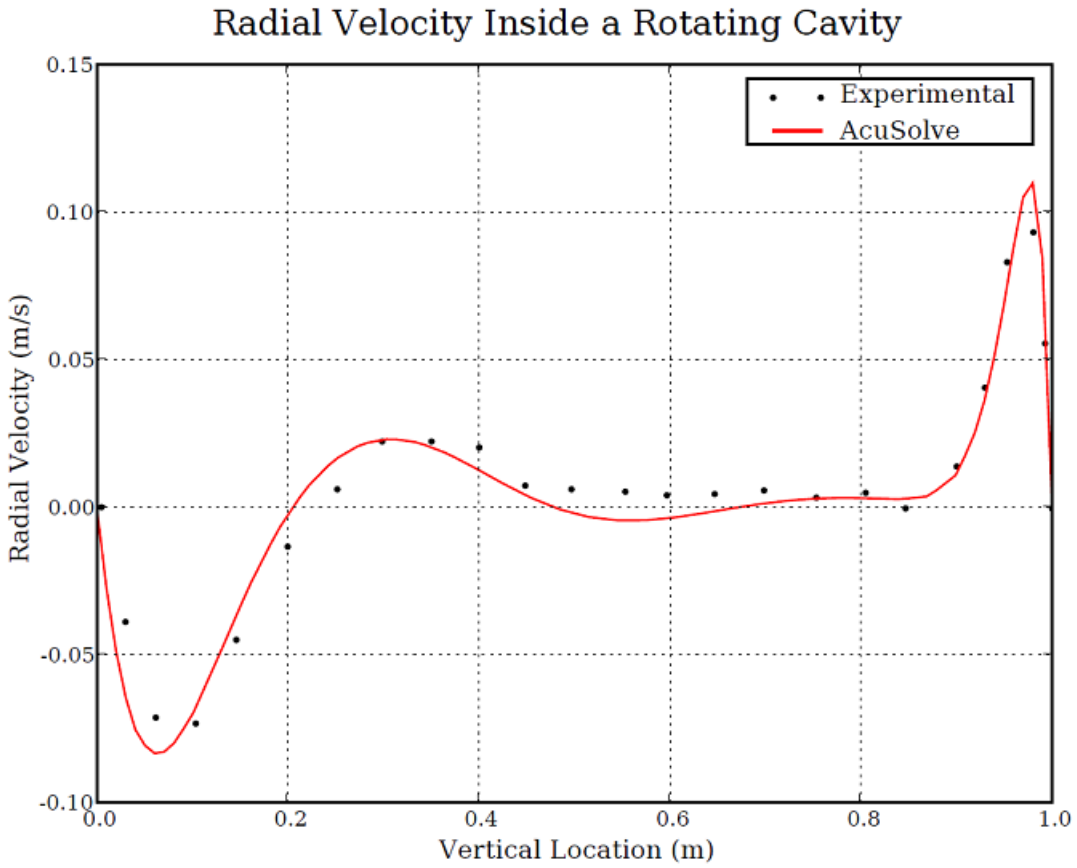


Figure 100: Radial Velocity (at 0.6 m From the Center of Rotation) as a Function of Vertical Location From Cylinder Bottom

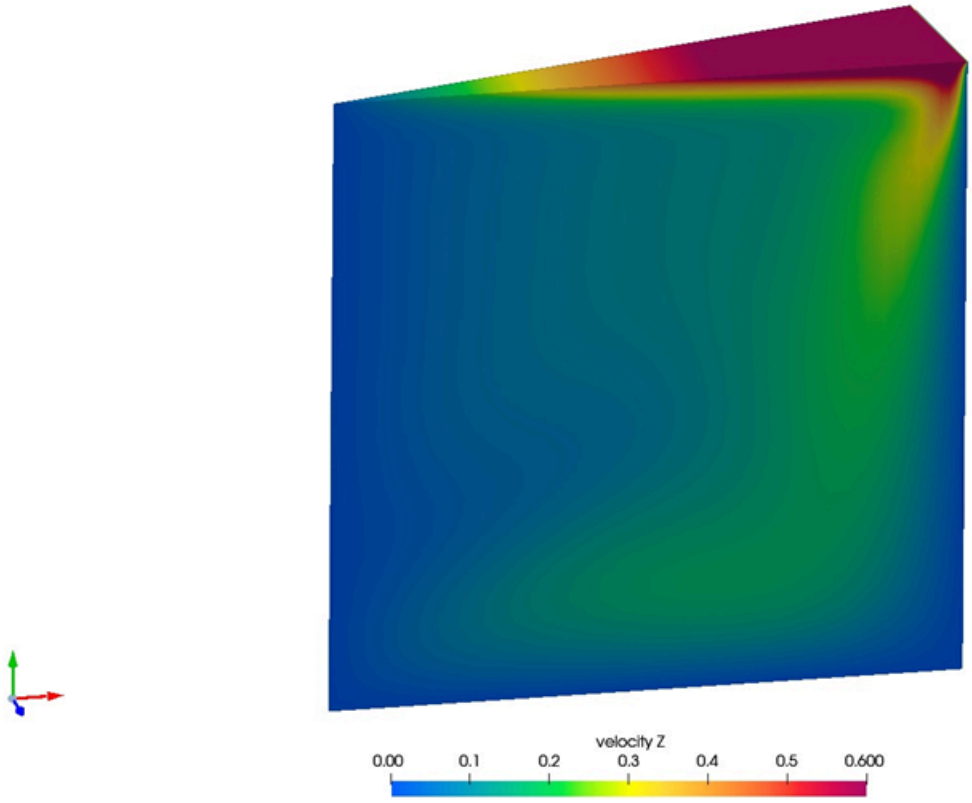


Figure 101: Contours of Swirl Velocity with Velocity Vectors

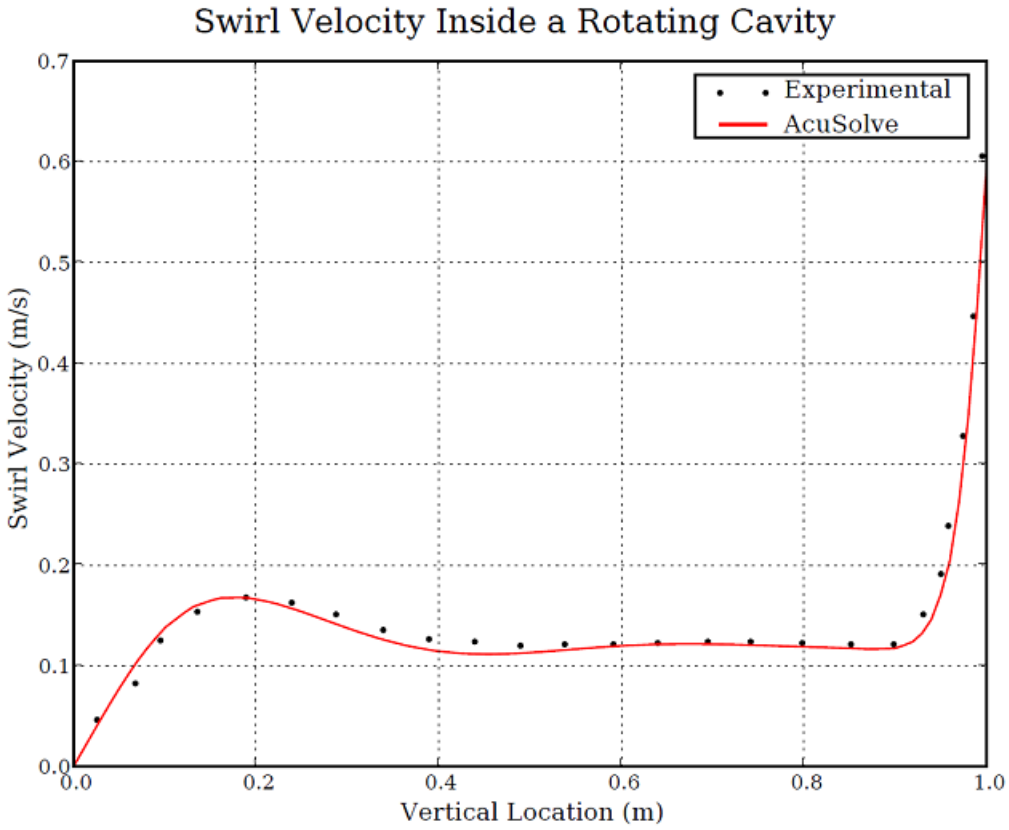


Figure 102: Swirl Velocity (at 0.6 m From Center of Rotation) as a Function of Vertical Location From the Cylinder Bottom

Summary

The AcuSolve solution compares well with the experimental data for flow induced by a rotating top of an enclosed cylinder. In this application, the flow in the fluid region is driven by the viscous stresses near the rotating top. Viscous stresses drag the fluid in a circular direction near the spinning wall. The angular velocity of the fluid decreases as distance from the top wall increases. Radial velocity develops as a result of the migration of the fluid toward the outer wall in regions of high angular velocity. The AcuSolve radial and swirl velocities compare very closely with the experimental data.

Simulation Settings for Flow Inside a Rotating Cavity

SimLab database file: `<your working directory>\cavity_rotating\cavity_rotating.slb`

Global

- Problem Description
  - Solution type - Steady State
  - Flow - Laminar
- Auto Solution Strategy
  - Relaxation Factor - `0.4`
- Material Model

- Air
  - Density - `1.0` kg/m3
  - Viscosity - `0.000556` kg/m-sec
- Reference Frame
  - Cavity Rotation
    - Rotation center
      1. X-coordinate - `0.0`
      2. Y-coordinate - `0.0`
      3. Z-coordinate - `0.0`
    - Angular velocity
      1. X-component - `0.0`
      2. Y-component - `-1.0` rad/sec
      3. Z-component - `0.0`

Model

- Volumes
  - Fluid
    - Element Set
      1. Material model - Air
- Surfaces
  - Bottom
    - Simple Boundary Condition
      1. Type - Wall
  - Max_X
    - Simple Boundary Condition
      1. Type - Wall
  - Max_Z
    - Simple Boundary Condition - (disabled to allow for periodic conditions to be set)
  - Min_Z
    - Simple Boundary Condition - (disabled to allow for periodic conditions to be set)
  - Top
    - Simple Boundary Condition
      1. Type - Wall
      2. Reference frame - Cavity Rotation
- Periodics
  - Periodic 1
    - Periodic Boundary Condition
      1. Type - Axisymmetric

2 Rotation axis
  1 point 1
    1 X-coordinate - `0.0` m
    2 Y-coordinate - `0.0` m
    3 Z-coordinate - `0.0` m
  2 point 2
    1 X-coordinate - `0.0` m
    2 Y-coordinate - `1.0` m
    3 Z-coordinate - `0.0` m

References

J. A. Michelsen. "Modeling of Laminar Incompressible Rotating Fluid Flow". AFM 86-05. Ph.D. thesis, Department of Fluid Mechanics, Technical University of Denmark. 1986.

Natural Convection in a Concentric Annulus

In this application, AcuSolve is used to simulate natural convection in the annular space between a heated inner pipe and an outer concentric pipe. AcuSolve results are compared with experimental results adapted from Kuehn and Goldstein (1978). The close agreement of AcuSolve results with experimental results validates the ability of AcuSolve to model cases with flow induced by natural convection.

Problem Description

The problem consists of two concentric cylinders with air filling the void between them, as shown in the following image, which is not drawn to scale. The radius of the inner cylinder is 0.0178 m and the radius of the outer cylinder is 0.0463 m. The inner cylinder is held at a fixed temperature of 373 K while the outer cylinder is held at 327 K. The temperature gradient drives the flow due to buoyancy effects.

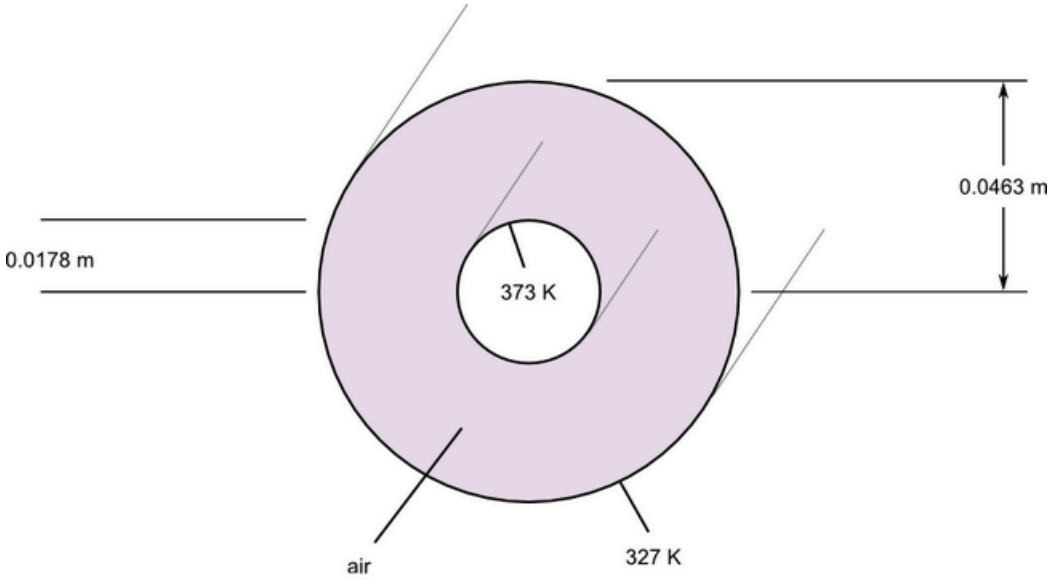


Figure 103: Critical Dimensions and Parameters for Simulating Natural Convection in a Concentric Annulus

The simulation was performed as a two dimensional problem by restricting flow in the out-of-plane direction through the use of a mesh that is one element thick. In addition, the half symmetry of the geometry is exploited to allow for modeling only half of the geometry. These characteristics allow for accurate simulation of the flow while minimizing computational time.

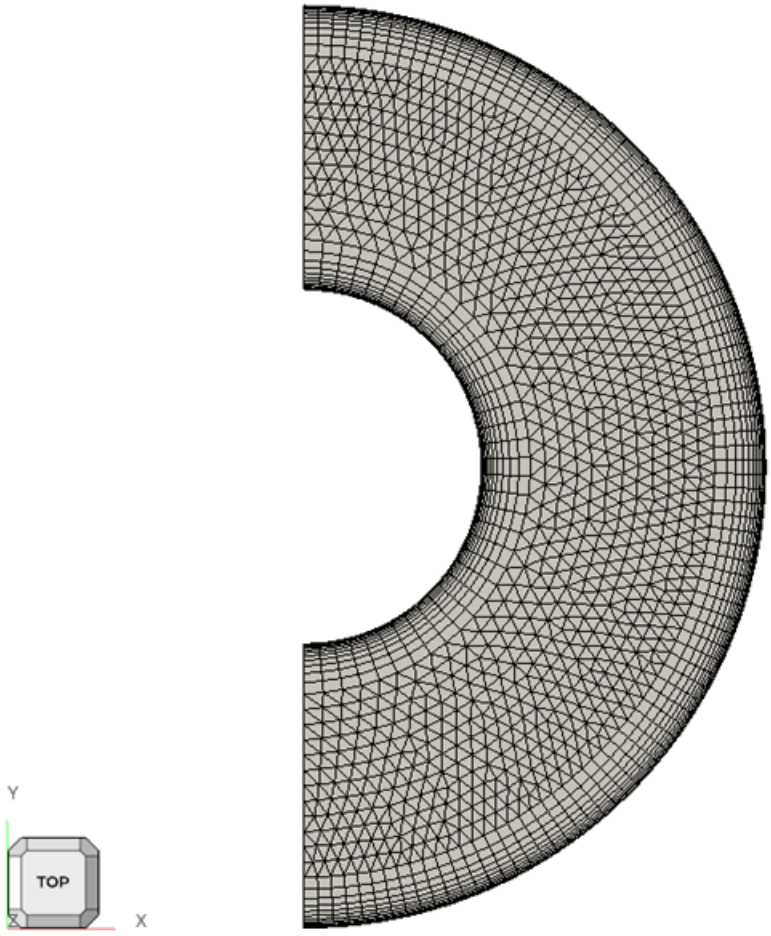


Figure 104: Mesh (Half of a Concentric Annulus) used for Simulating Natural Convection in a Concentric Annulus

AcuSolve Results

The AcuSolve solution converged to a steady state and the results reflect the mean flow conditions. Air density decreases due to heating by the inner cylinder, leading to convective currents within the annulus. As air approaches the outer cylinder, it is cooled by the outer wall, causing the density to increase. This results in heavier air sinking toward the bottom of the assembly.

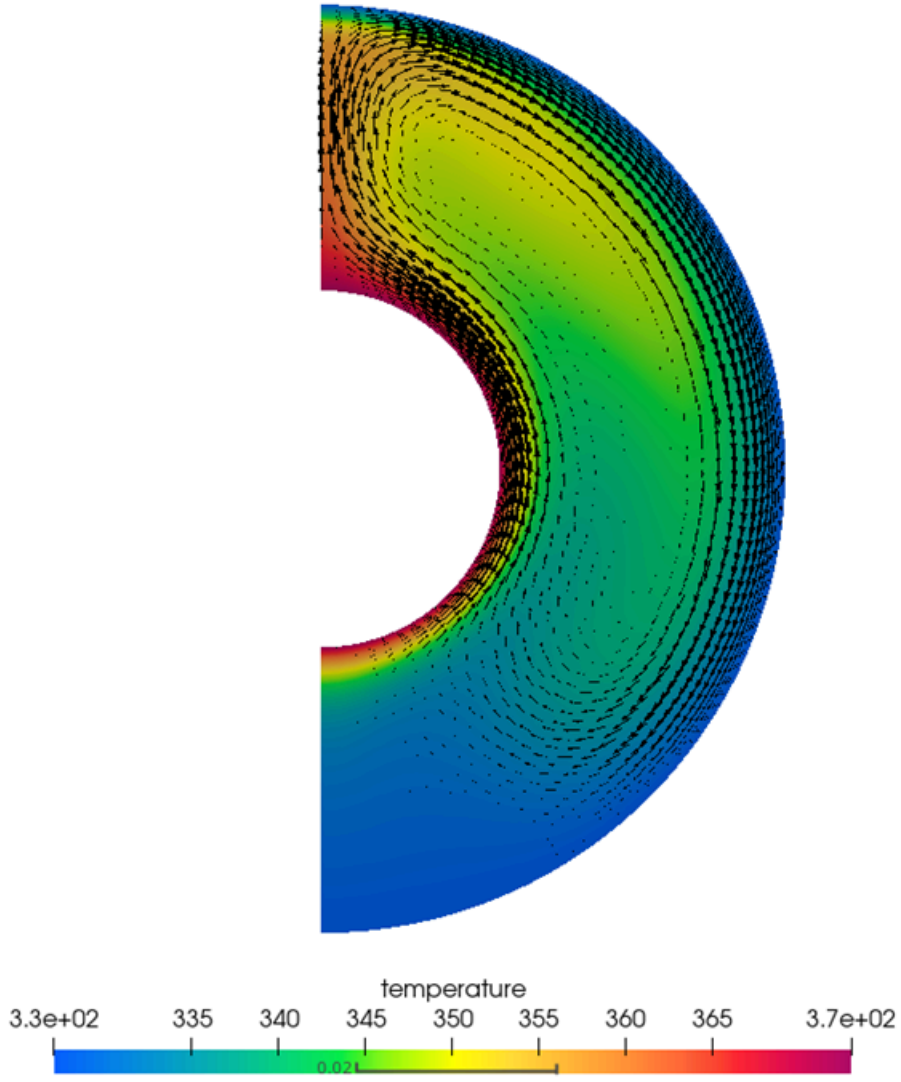


Figure 105: Temperature Contours and Velocity Vectors

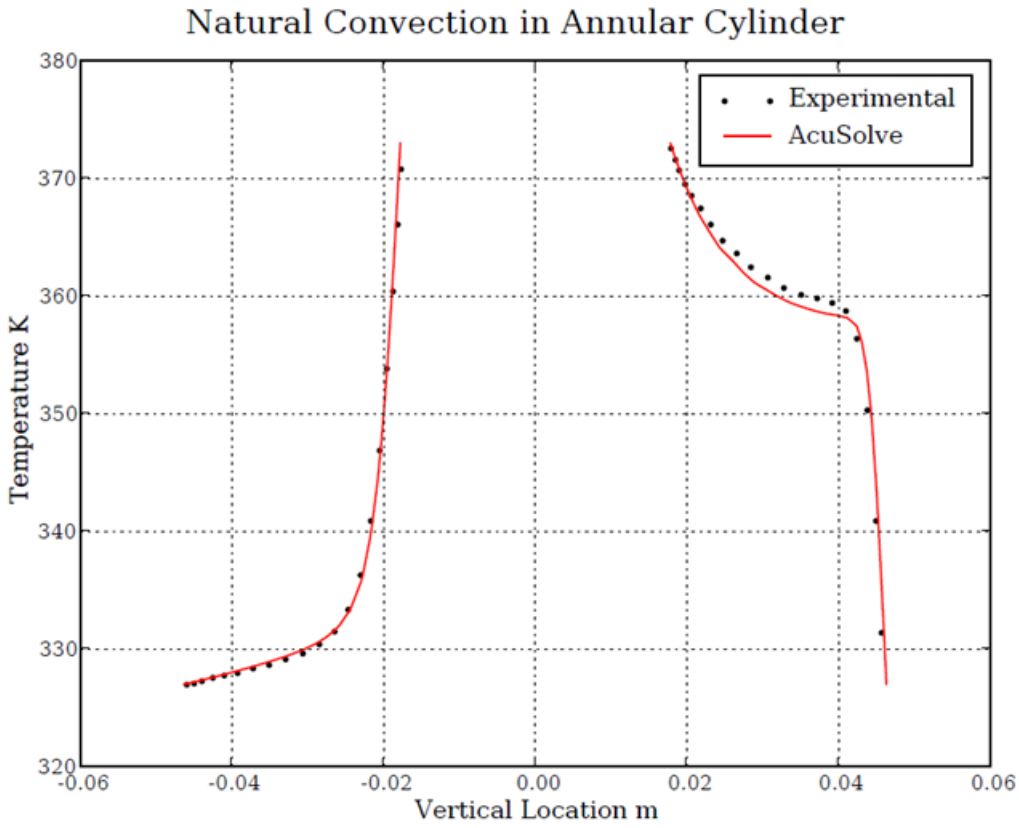


Figure 106: Temperature as a Function of Distance From the Center of the Inner Cylinder

Summary

The AcuSolve solution compares well with analytical results for natural convection in a concentric annulus. In this application, flow is driven by a decrease in density as air is heated. The local variations in density result in the higher density fluid sinking to the bottom of the annulus while the lower density fluid rises to the top. This transfer of momentum is a continuous process which results in the convective currents that are visible in the solution. The AcuSolve temperature results compare very closely with the experimental results.

Simulation Settings for Natural Convection in a Concentric Annulus

HyperMesh CFD database file: `<your working directory>\annulus_heat\annulus_heat.hm`

Global

- Problem Description
  - Analysis type - Steady State
  - Abs. pressure offset - `101325.0` N/m2
  - Temperature equation - Advective Diffusive
  - Turbulence equation - Laminar
  - Gravitational acceleration - { 0, -9.80665, 0 }
- Auto Solution Strategy

- Relaxation factor - `0.2`
- Flow - On
- Temperature - On

- Material Model
  - Air
    - Type - Boussinesq
    - Density - `1.225` kg/m3
    - Expansivity - `0.0034722` 1/K
    - Reference temperature - `288` K
    - Isothermal compressibility - `0.0` m2/N
    - Viscosity - `2.081e-5` kg/m-sec

  Model
- Volumes
  - Fluid
    - Element Set
      1. Material model - Air
  - Surfaces
    - ID
      1. Simple Boundary Condition
         1. Type - Wall
         2. Temperature BC type - Value
         3. Temperature - `373.0` K
    - Max_Z
      1. Simple Boundary Condition
      2. Type - Symmetry
    - Min_Z
      1. Simple Boundary Condition
      2. Type - Symmetry
    - OD
      1. Simple Boundary Condition
         1. Type - Wall
         2. Temperature BC type - Value
         3. Temperature - `327.0` K
    - Symmetry
      1. Simple Boundary Condition
      2. Type - Symmetry
  - Nodes
    - Node 1

1 Pressure

1 Type - Zero

References

T.H. Kuehn and R. J. Goldstein. "An Experimental Study of Natural Convection Heat Transfer in Concentric and Eccentric Horizontal Cylindrical Annuli". Journal of Heat Transfer 100:635-640. 1978.

Laminar Flow Past a 90° T-Junction

In this application, AcuSolve is used to simulate laminar flow through a channel with two outlets forming a T-junction. AcuSolve results are compared with experimental results adapted from Hayes and others (1989). The close agreement of AcuSolve results with experimental results validates the ability of AcuSolve to model cases with multiple outlet paths.

Problem Description

The problem consists of air flowing past a T-junction in a channel, as shown in the following image, which is not drawn to scale. Air enters the channel with an average velocity of 0.667 m/s and travels past the T-junction 2.0 m from the inlet. A portion of the flow will travel out of the branch of the channel due to the pressure difference between the bulk flow and the outlet of the branch.

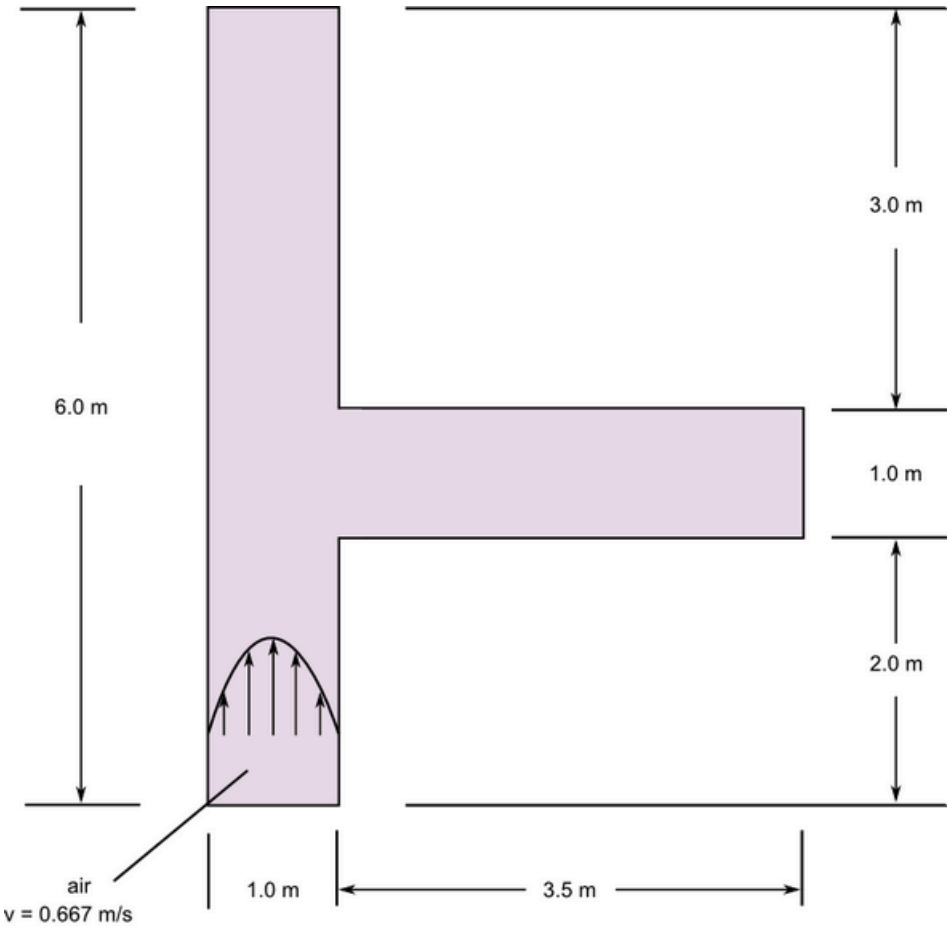


Figure 107: Critical Dimensions and Parameters for Simulating Laminar Flow Past a 90° T-Junction

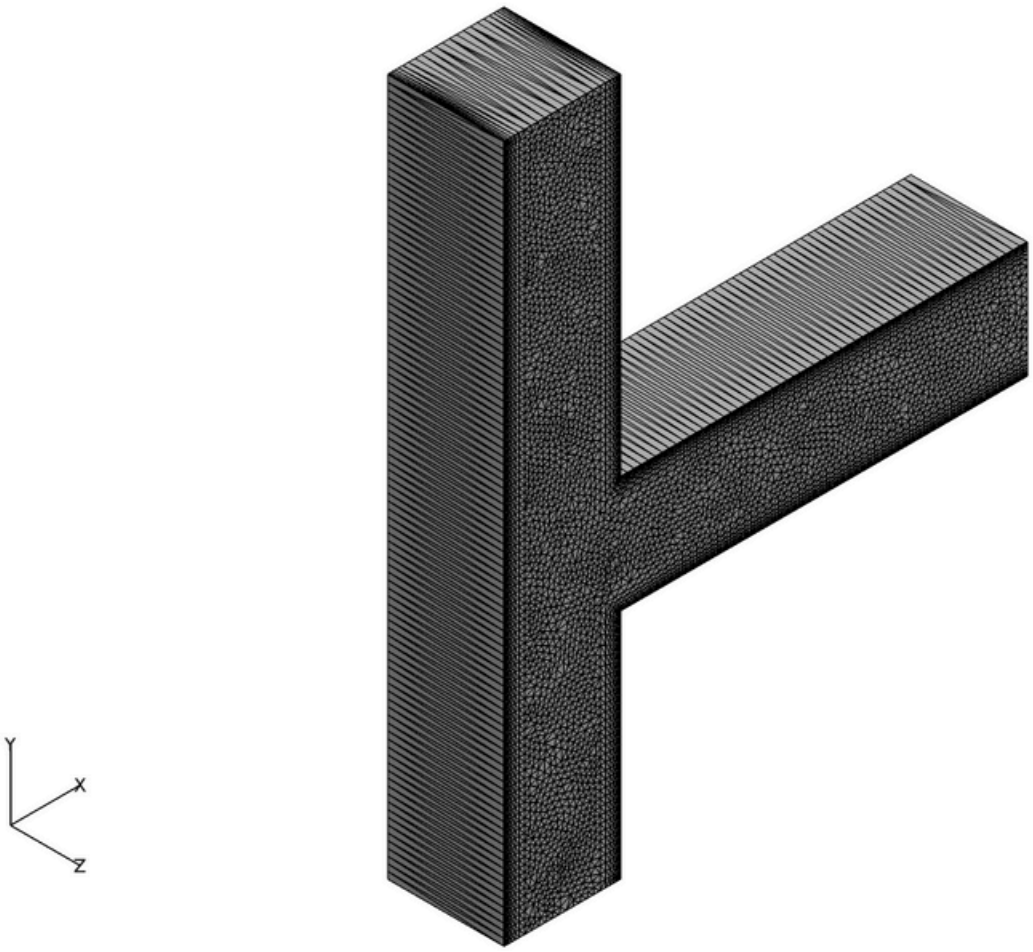


Figure 108: Mesh Used for Simulating Laminar Flow past a 90° T-Junction

AcuSolve Results

The AcuSolve solution converged to a steady state and the results reflect the mean flow conditions. As the air flows past the junction, a portion of it is diverted into the branch. A small recirculation region develops at the top of the junction and collapses before the flow exits the domain through the right branch.

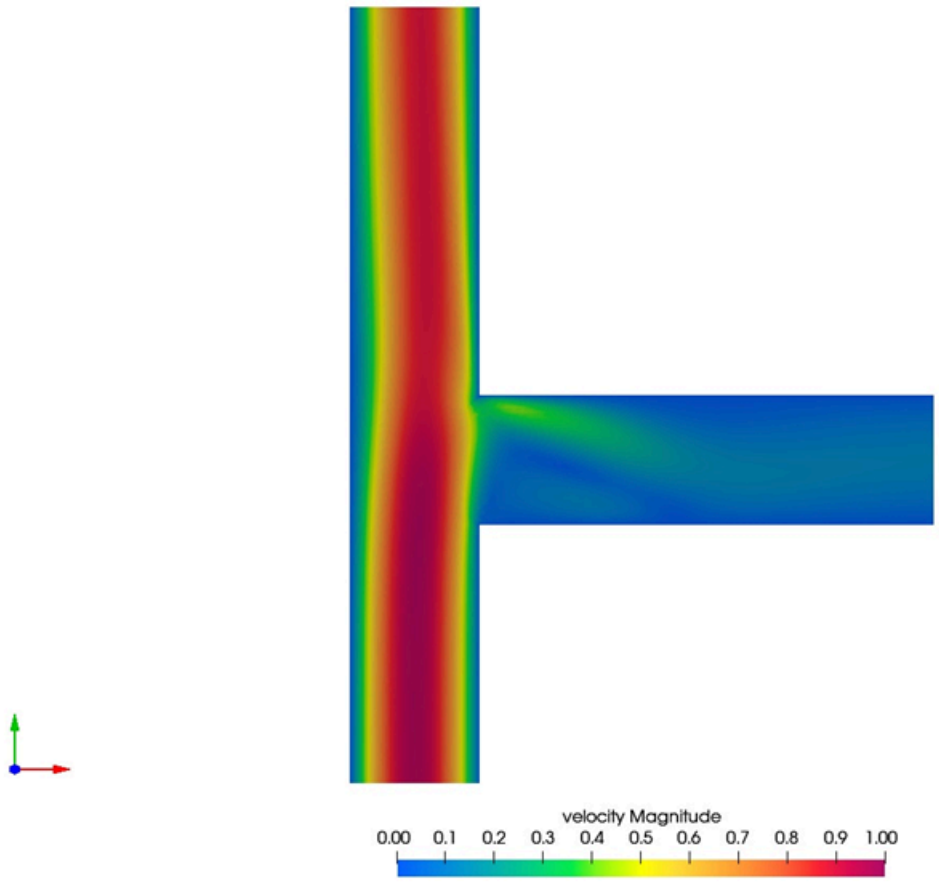


Figure 109: Velocity Contours in a T-Junction

The experimental value for the fraction of flow exiting the top branch of the channel is presented with the corresponding AcuSolve result in the following table.

Table 5:

	Experimental fractional flow	**AcuSolve fractional flow**	**Percent deviation from experimental**
Fractional flow exiting the upper branch	0.887	0.889	0.332

Summary

The AcuSolve solution compares well with experimental results for flow past a T-junction. In this application, flow is driven by a fixed flow rate at the inlet to the main branch. A portion of the flow from the main branch is diverted into the right branch of the T-junction, giving rise to recirculation just downstream of the junction. This recirculation collapses before the flow exits the side branch. The AcuSolve result for fractional flow exiting the top branch is within 0.33 percent of the experimental results.

Simulation Settings for Laminar Flow Past a 90° T-Junction

SimLab database file: `<your working directory>\T_junction_laminar\T_junction_laminar.slb`

Global

- Problem Description
  - Solution type - Steady State
  - Flow - Laminar
- Auto Solution Strategy
  - Relaxation factor - `0.2`
- Material Model
  - Air
    - Type - Constant
    - Density - `1.0` kg/m3
    - Viscosity - `0.003333` kg/m-sec

  Model
- Volumes
  - Fluid
    - Element Set
      1. Material model - Air
- Surfaces
  - Inflow
    - Simple Boundary Condition
      1. Type - Inflow
      2. Inflow type - Average Velocity
      3. Average velocity - `0.6667` m/sec
  - Max_Z
    - Simple Boundary Condition - (disabled to allow for periodic conditions to be set)
  - Min_Z
    - Simple Boundary Condition - (disabled to allow for periodic conditions to be set)
  - Outflow
    - Simple Boundary Condition
      1. Type - Outflow
  - T_Out
    - Simple Boundary Condition
      1. Type - Outflow
  - Walls
    - Simple Boundary Condition
      1. Type - Wall

- Periodics
  - Periodic 1
    - Periodic Boundary Condition
      1 Type - Periodic

References

R. E. Hayes, K. Nandkumar, and H. Nasr-El-Din. "Steady Laminar Flow in a 90 Degree Planar Branch". Computers and Fluids 17(4): 537-553. 1989.

Laminar Flow Through a Channel with Heated Walls

In this application, AcuSolve is used to simulate high Peclet number laminar flow through a channel with heated walls. AcuSolve results are compared with analytical results adapted from Hua and Pillai (2010). The close agreement of AcuSolve results with analytical results validates the ability of AcuSolve to model cases involving heat transfer to a moving fluid with a high Peclet number.

Problem Description

The problem consists of water at 20 °C flowing through a channel of infinite width with top and bottom walls heated to 75 °C. The channel is 0.2 m high and 0.8 m long, as shown in the following image, which is not drawn to scale. A centrally located slice 0.02 m wide is modeled with slip boundary conditions so that side-wall influences can be ignored. Water enters the channel with an average velocity of 0.003 m/s. As the fluid flows through the channel, it is heated by the top and bottom plates.

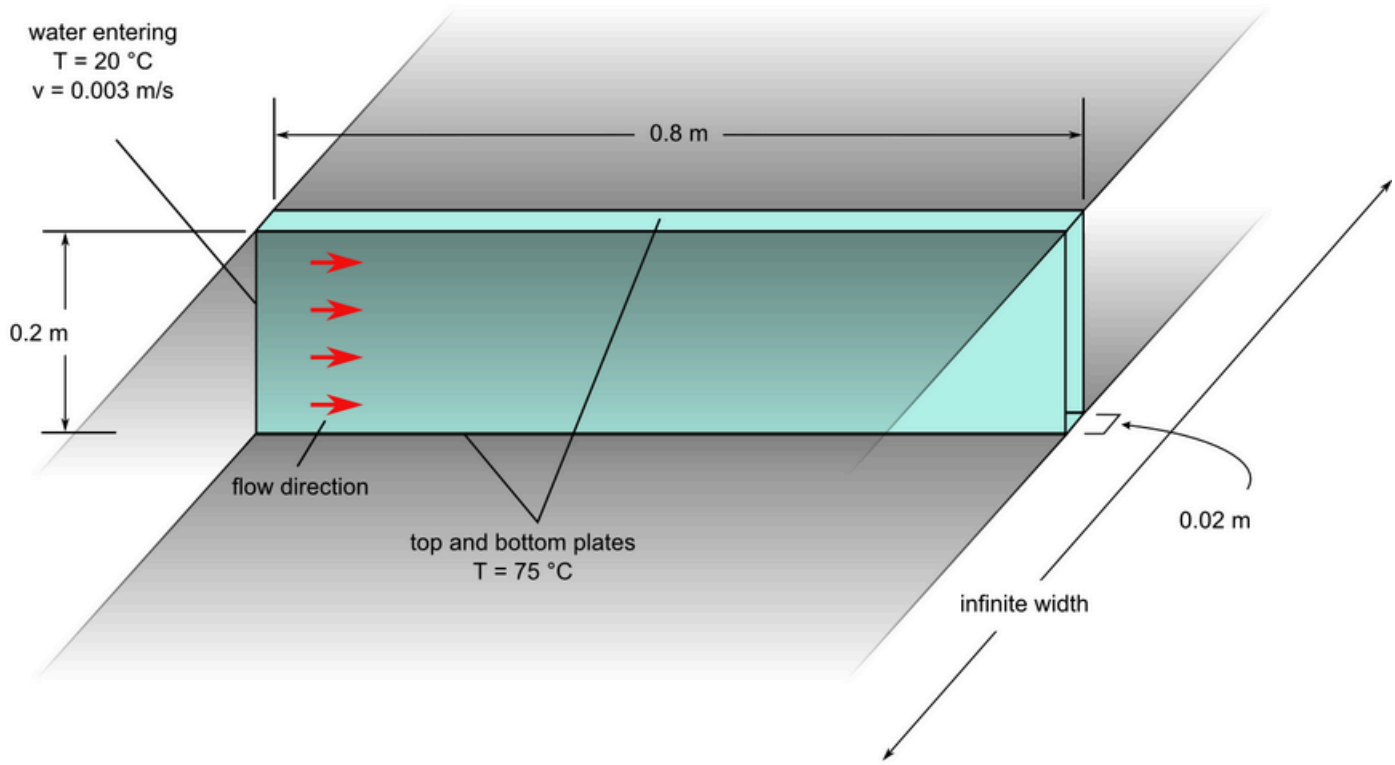


Figure 110: Critical Dimensions and Parameters for Simulating Laminar Flow Through a Channel with Heated Walls

The simulation was performed as a two dimensional problem by restricting flow in the out-of-plane direction through the use of a mesh that is one element thick. In addition, the symmetry of the geometry in the height direction is exploited to allow for modeling only half of the geometry. These characteristics allow for accurate simulation of flow while minimizing computational time.

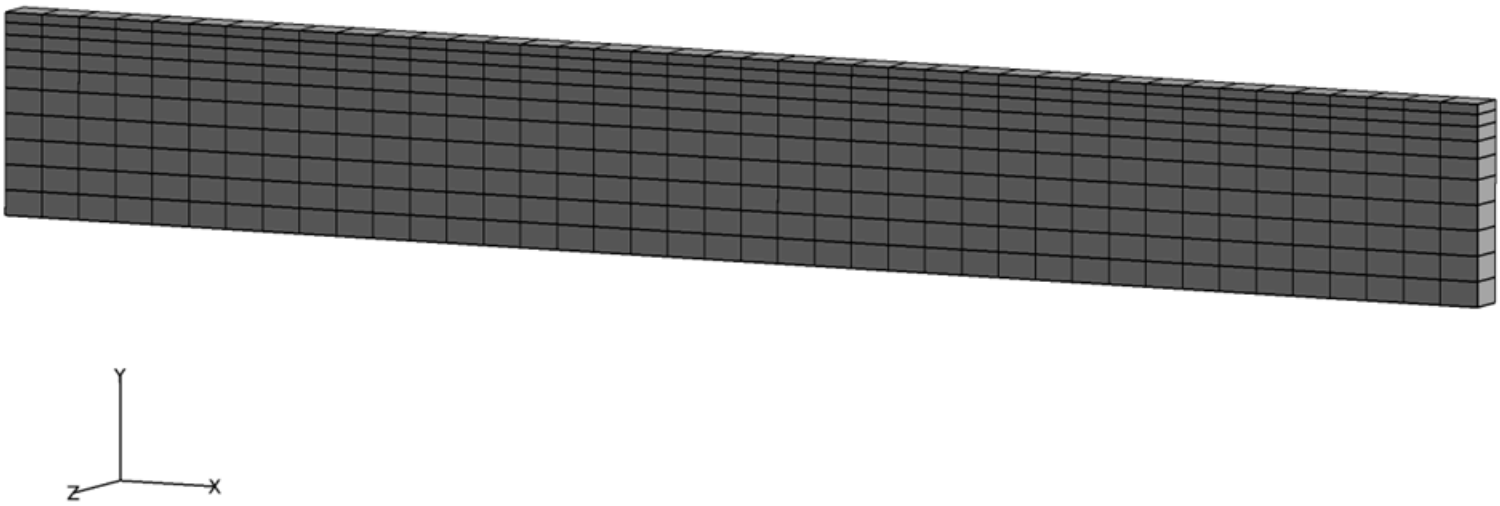


Figure 111: Mesh (Top Half of the Channel) used for Simulating Laminar Flow Through a Channel with Heated Walls

AcuSolve Results

The AcuSolve solution converged to a steady state and the results reflect the mean flow conditions. As the cool water enters the channel at temperature less than that of the walls, heat is transferred to the water by conduction. As the fluid travels along the channel, the temperature differential between the wall and the adjacent water decreases. The thermal boundary layer within the water develops as the flow propagates downstream.

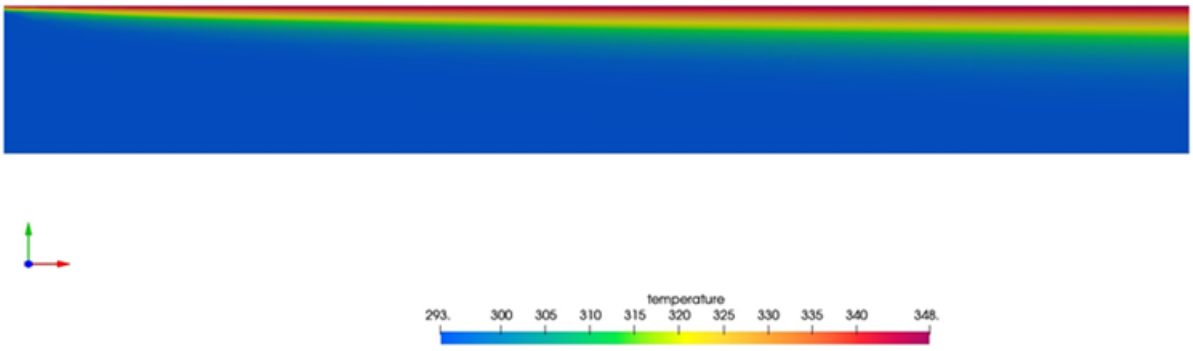


Figure 112: Temperature Contours Along the Top Half of a Heated Channel

Temperature at a specified vertical position in the channel increases along the length of the channel. The nature of that temperature change is dependent on proximity to the heated wall. Water in the center of the flow will have the least temperature change. Since this problem was solved for symmetrical flow, only the top half of the flow region was modeled. The vertical position for results shown in the following figure are based on the center of flow having a Y-position of 0.

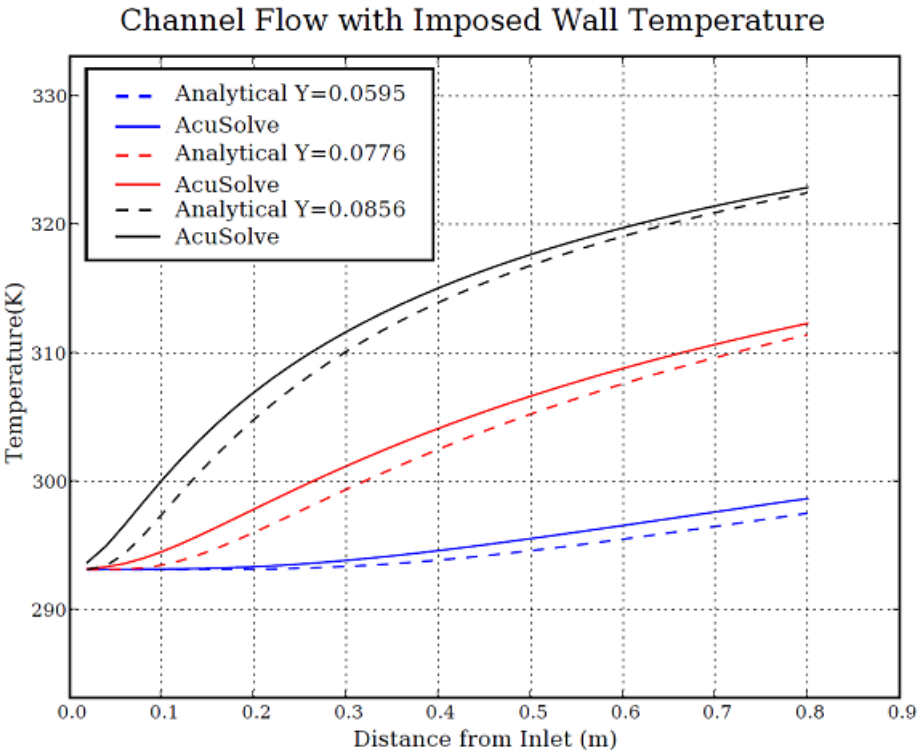


Figure 113: Temperature Plotted Against Distance from Inlet for 3 Different Heights from the Channel Center Line

Summary

The AcuSolve results compare well with the analytical results for the development of a thermal boundary layer in a heated channel. In this application, the model is set up to yield large gradients as the flow convects away from the inlet. The boundary conditions and mesh size were chosen specifically to yield a high Peclet number. The element Peclet number in the flow direction in this case is Pe=30.0, as calculated from the following equation.

$$Pe = \frac{\rho Cp|v|he}{k} \tag{4}$$

where ρ is the density, Cp the heat capacity, v the velocity, he the length, and k the thermal conductivity.

This example shows the robustness of the stabilized technique in AcuSolve when element Peclet number is high.

> **Note:** Standard Galerkin finite element formulations become unstable when the element Peclet number is greater than 1.0.

Simulation Settings for Laminar Flow Through a Channel with Heated Walls

SimLab database file: `<your working directory>\channel_laminar_heat\channel_laminar_heat.slb`

Global

- Problem Description
  - Flow - Steady State
  - Temperature equation - Advective Diffusive
  - Turbulence equation - Laminar
- Auto Solution Strategy
  - Relaxation factor - `0.4`
- Material Model
  - Fluid_Material
    - Density - `1000.0` kg/m3
    - Specific Heat - `1000` J/kg-K
    - Viscosity - `1.0e-12` kg/m-sec
    - Conductivity - 1.0 W/m-K

  Model
- Volumes
  - Fluid
    - Element Set
      1. Material model - Fluid_Material
- Surfaces
  - Inlet
    - Simple Boundary Condition
      1. Type - Inflow
      2. Inflow type - Velocity
      3. X velocity - `0.003` m/sec
      4. Temperature - `293.15` K
  - Outlet
    - Simple Boundary Condition
      1. Type - Outflow
  - Symm_MaxZ
    - Simple Boundary Condition
      1. Type - Slip
  - Symm_MinY
    - Simple Boundary Condition
      1. Type - Slip
  - Symm_MinZ
    - Simple Boundary Condition
      1. Type - Slip
  - Wall

- Simple Boundary Condition
  1. Type - Wall
  2. Temperature BC type - Value
  3. Temperature - `348.15` K

References

Hua Tan and K. M. Pillai. "Numerical Simulation of Reactive Flow in Liquid Composite Molding Using Flux-Corrected Transport (FCT) Based Finite Element/Control Volume (FE/CV) Method". International Journal of Heat and Mass Transfer. 53:2256-2271, 2010.

Turbulent Flow Behind an Open-Slit V

In this application, AcuSolve is used to simulate turbulent flow of air through and behind a two dimensional open-slit V. AcuSolve results are compared with experimental results adapted from Yang and Tsai (1993). The close agreement of AcuSolve results with experimental results validates the ability of AcuSolve to model the Coandă effect.

Problem Description

The problem consists of air flowing through and past an open-slit V positioned within a flow domain, as shown in the following image, which is not drawn to scale. The flow domain is 0.3 m long and 0.1 m high. The narrow end of the V is positioned 0.05 m from the domain inlet. The slit in the V is 0.002 m high. The V widens to 0.022 m at 0.075 m from the domain inlet. Air enters the domain with a constant velocity of 20 m/s. The upper and lower limits of the domain are defined as no-slip boundary conditions.

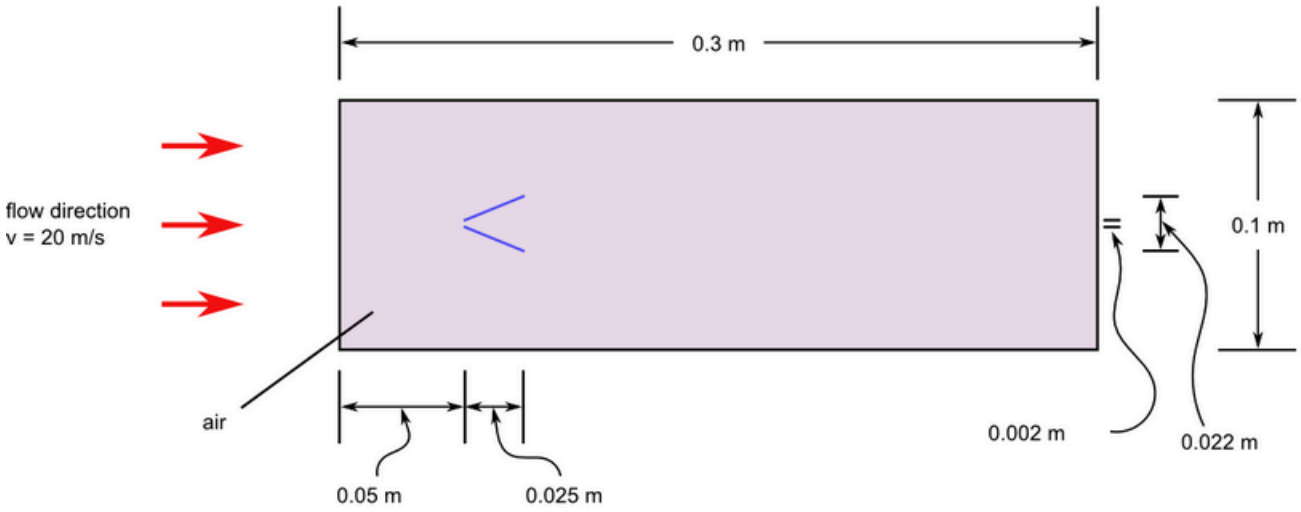


Figure 114: Critical Dimensions and Parameters for Simulating Turbulent Flow Behind an Open-Slit V

The simulation was performed as a two dimensional problem by restricting flow in the out-of-plane direction through the use of a mesh that is one element thick. A coarse mesh is used throughout much of the domain, with mesh refinement closer to the V.

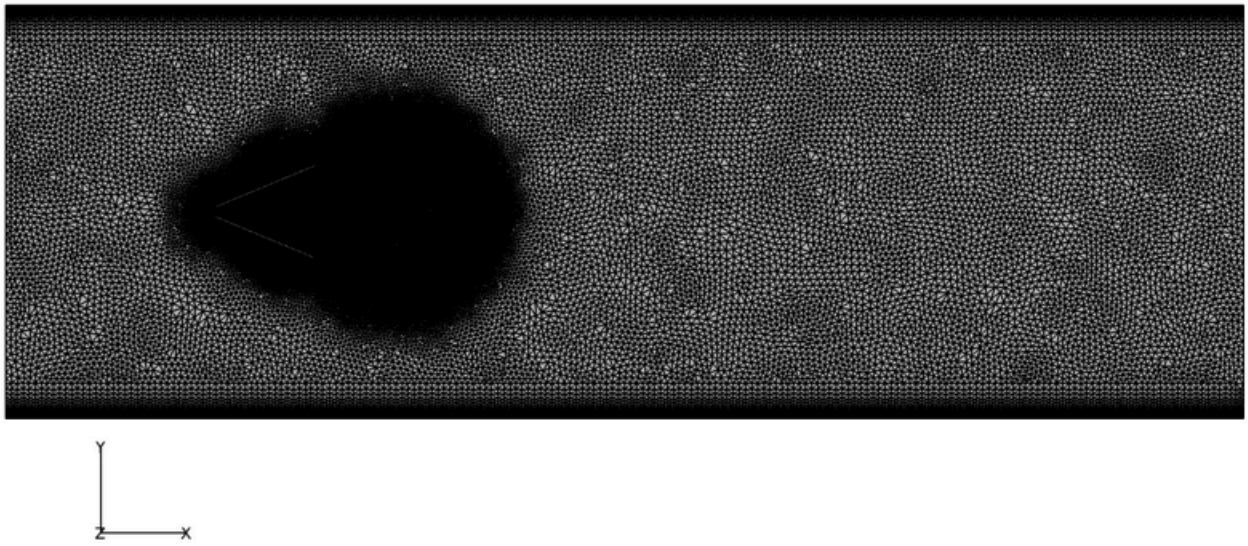


Figure 115: Mesh used for Simulating Turbulent Flow Behind an Open-Slit V (the V Lies Within the Dense Area of the Mesh)

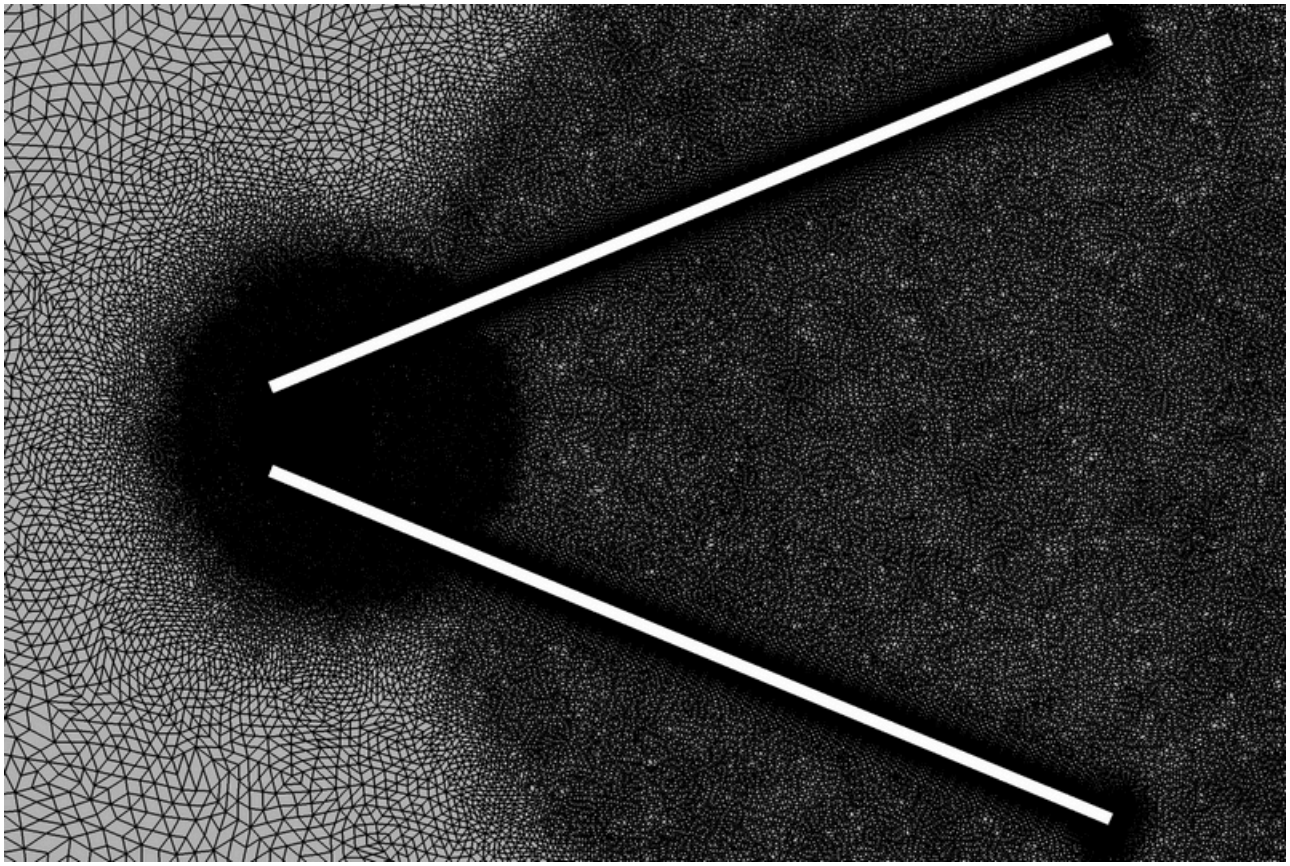


Figure 116: Mesh Surrounding the Open-Slit V

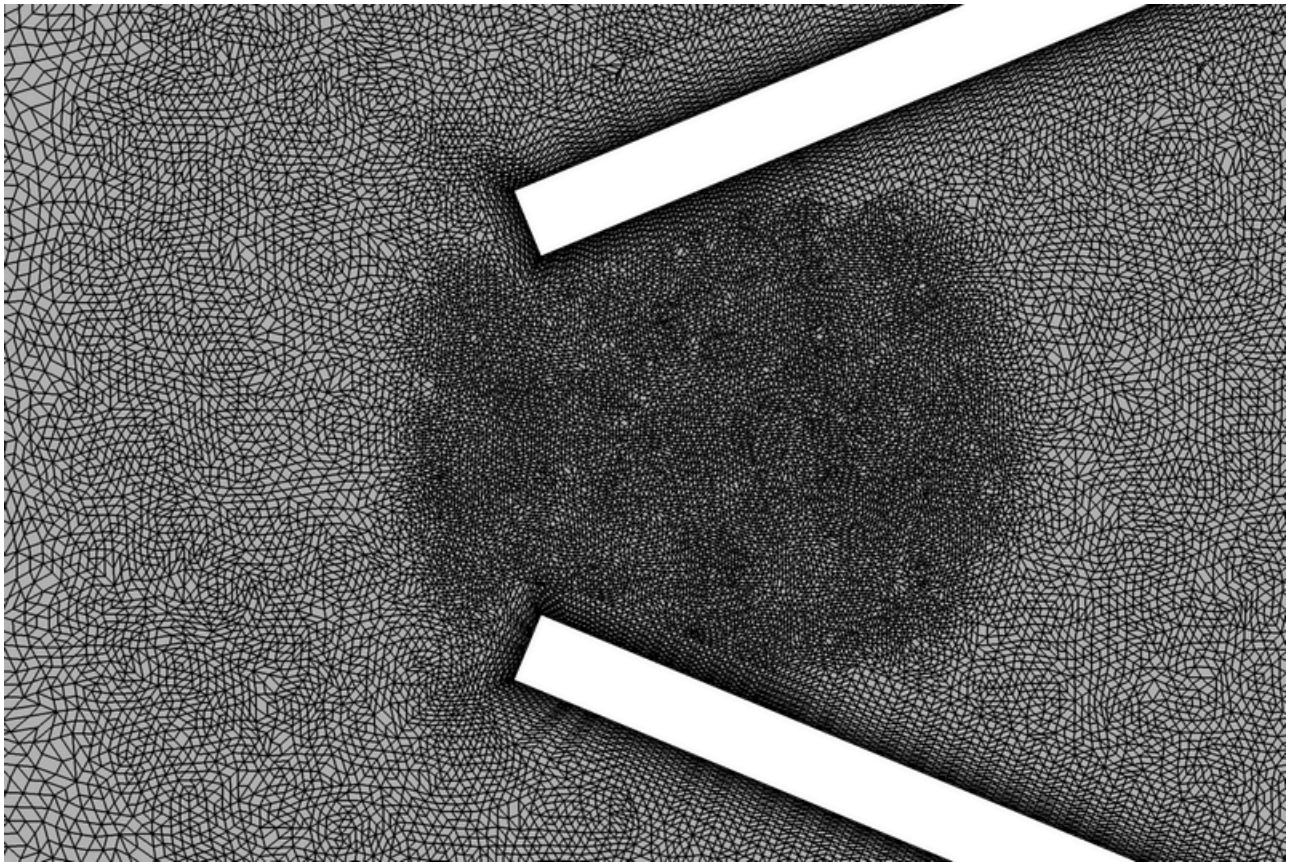


Figure 117: Mesh Near the Open Slit

AcuSolve Results

The AcuSolve solution converged to a steady state and the results reflect the mean flow conditions. Air flows through the open slit in the V and accelerates while being forced to one side due to the Coandă effect. As air encounters the exterior of the widening gutter, velocity increases and the wake induces recirculation near the exit of the V. The recirculation zone extends downstream of the V gutter.

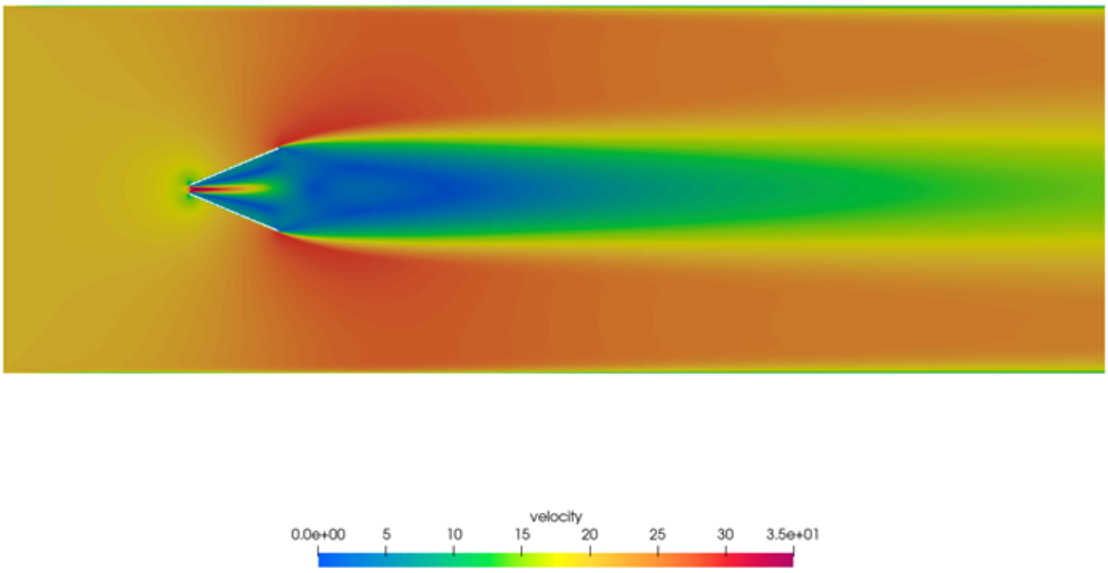


Figure 118: Contours of X-Velocity of Flow Through and Around an Open-Slit V (the Vertical Line Represents the Location, 0.022 m Downstream from the V exit, at Which Experimental Data is Compared to AcuSolve Results)

AcuSolve results were compared to experimental results at different heights 0.022 m behind the V exit. X-velocity is near zero at the bottom of the domain (height = -0.05 m), rising steeply with distance from the wall. The velocity gradient decreases until approximately 0.018 m below the center line of the domain, which is slightly below the bottom of the V exit. The velocity behind the V drops sharply with an increase in height, due to the blockage caused by the presence of the slanted walls. The lowest velocity is just above the center line of the domain.

The slight asymmetry in the velocity profile in the wake of the V is expected due to the Coandă effect.

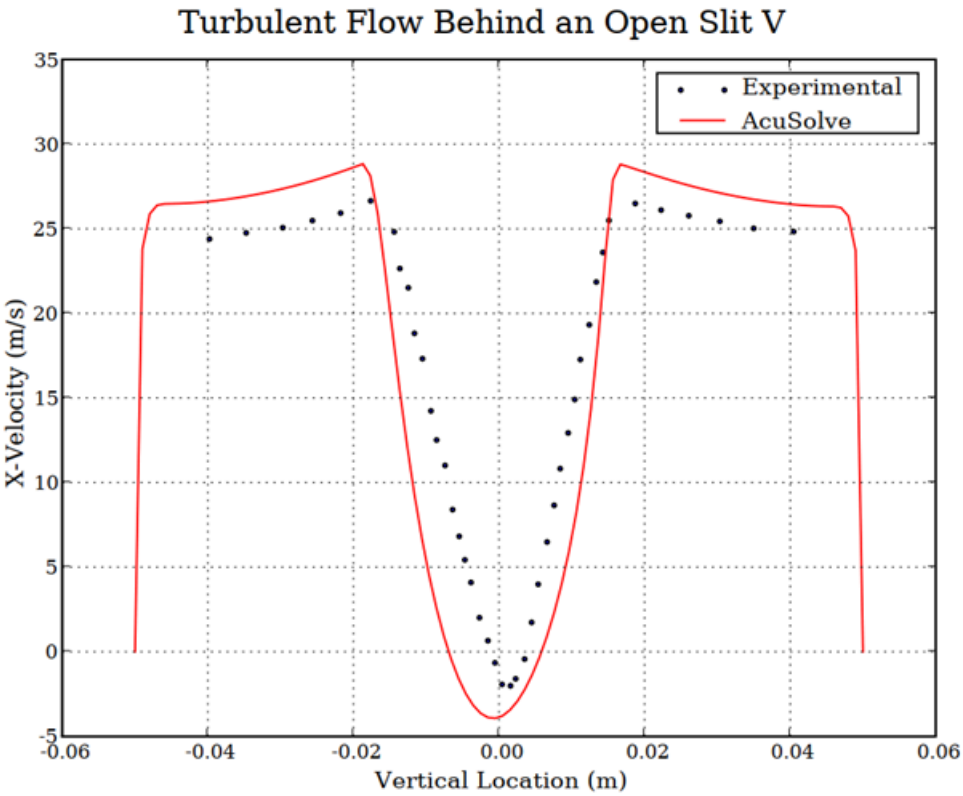


Figure 119: X-Velocity Plotted Against Vertical Location 0.0022 m Downstream of the V Exit

Summary

The AcuSolve results compare well with the experimental results for flow through and around an open-slit V. In this application, the V-shaped geometry diverts flow towards the side walls of the channel and also creates a high-velocity jet through the slit. The low pressure associated with the jet causes a deflection towards the walls of the V, resulting in an asymmetric flow field within the V shape. This application illustrates the ability of AcuSolve to accurately predict the Coandă effect. The acceleration of the flow due to the deflection along the V-shaped walls and the momentum deficit in the wake of the V is captured accurately.

Simulation Settings for Turbulent Flow Behind an Open-Slit V

HyperMesh CFD database file: `<your working directory>\v_gutter_turbulent \v_gutter_turbulent.hm`

Global

- Problem Description
  - Analysis type - Steady State
  - Turbulence equation - Spalart Allmaras
- Auto Solution Strategy
  - Relaxation factor - `0.5`
- Material Model

    - Air
        - Density - `1.0` kg/m3
        - Viscosity - `1.8333e-05` kg/m-sec

  Model
- Volumes
    - Fluid
        - Element Set
            1. Material model - Air
- Surfaces
    - Inlet
        - Simple Boundary Condition
            1. Type - Inflow
            2. Inflow type - Velocity
            3. X velocity - `20.0` m/sec
            4. Eddy viscosity - `0.000800426` m2/sec
    - LE_TE
        - Simple Boundary Condition
            1. Type - Wall
    - Outlet
        - Simple Boundary Condition
            1. Type - Outflow
    - Symm_MaxZ
        - Simple Boundary Condition
            1. Type - Slip
    - Symm_MinZ
        - Simple Boundary Condition
            1. Type - Slip
    - V_Walls
        - Simple Boundary Condition
            1. Type - Wall
    - Walls
        - Simple Boundary Condition
            1. Type - Wall

References

J.-T. Yang and G.-L. Tsai. "Near-wake flow of a v-gutter with slit bleed". Journal of Fluid Engineering. 115:13-20. March, 1993.

Turbulent Flow Over a NACA 0012 Airfoil

In this application, AcuSolve is used to simulate turbulent flow of a fluid over a NACA 0012 airfoil at 3 angles of attack, 0 degrees, 10 degrees, and 15 degrees. AcuSolve results are compared with experimental results for coefficients of pressure, lift, and drag reported by NASA. The close agreement of AcuSolve results with experimental results validates the ability of AcuSolve to model external aerodynamics.

Problem Description

The problem consists of a NACA 0012 airfoil located in the center of a cylindrical domain, as shown in the following image, which is not drawn to scale. Fluid enters the domain with a velocity of 1.0 m/s. The domain edges are distant, 500 chord lengths, from the airfoil to minimize any far field effects. The problem is set up to simulate high Reynolds number flow, with Re = 6,000,000.

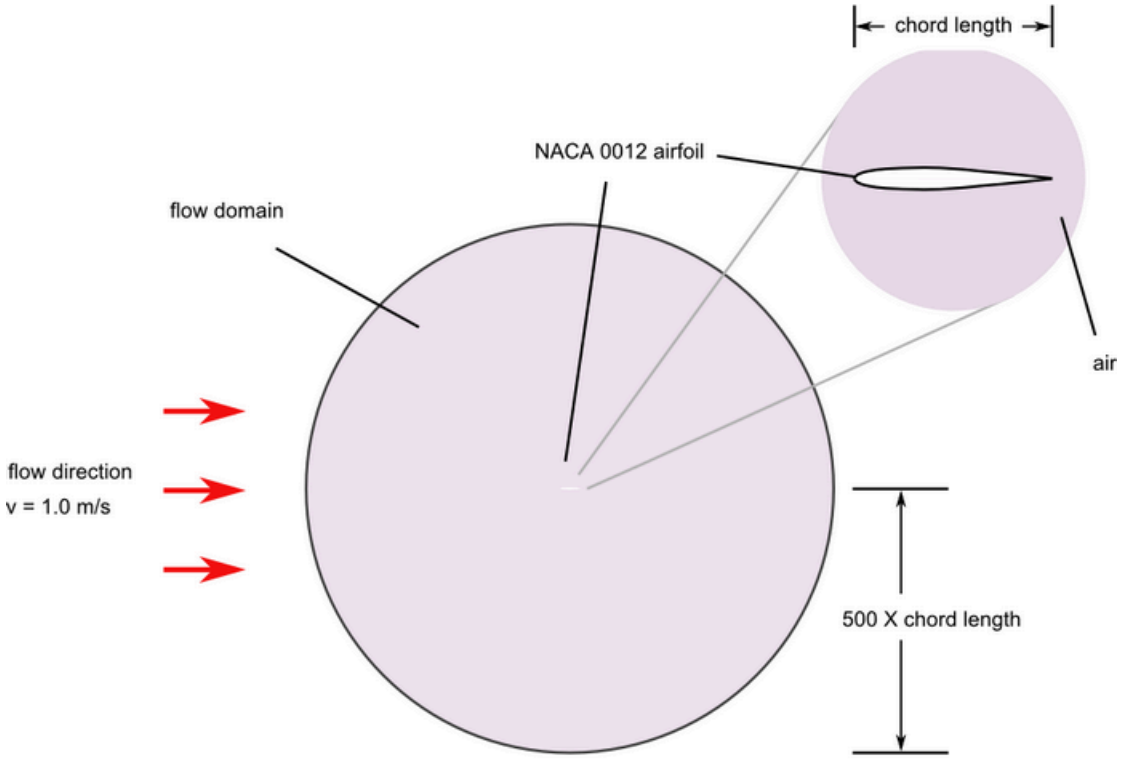


Figure 120: Critical Dimensions and Parameters for Simulating Turbulent Flow over a NACA 0012 Airfoil

The simulation was performed as a two dimensional problem by restricting flow in the out-of-plane direction through the use of a mesh that is one element thick.

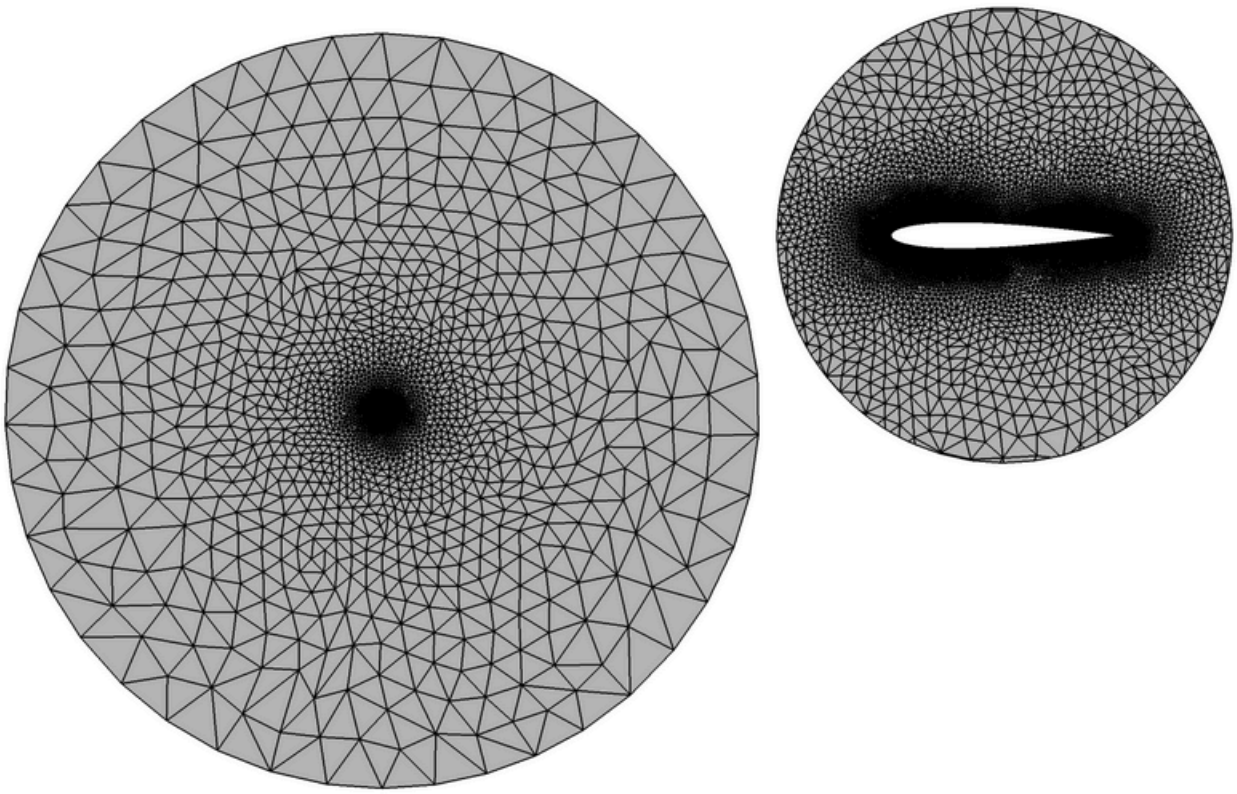


Figure 121: Mesh Used for Simulating Turbulent Flow over a NACA 0012 Airfoil (the Image on the Left Represents the Full Mesh, the Image on the Right Represents Mesh Details near the Airfoil)

AcuSolve Results

The AcuSolve solution converged to a steady state and the results reflect the mean flow conditions for each of the three angles of attack, 0 degrees, 10 degrees, and 15 degrees. For each case, the angle of attack was varied by changing the angle of the incident flow.

> **Note:** This enables the use of a single mesh for all of the simulations.

With a 0 degree angle of attack, the flow field is symmetric as the fluid flows over and under the airfoil. The airfoil impedes the flow, causing stagnation at the leading edge. As the fluid passes over and under the airfoil, velocity increases. As the fluid passes over the blunt trailing edge, a minor amount of flow separation occurs. The flow reattaches shortly after it passes the trailing edge and recovers the mean velocity in the distant far field.

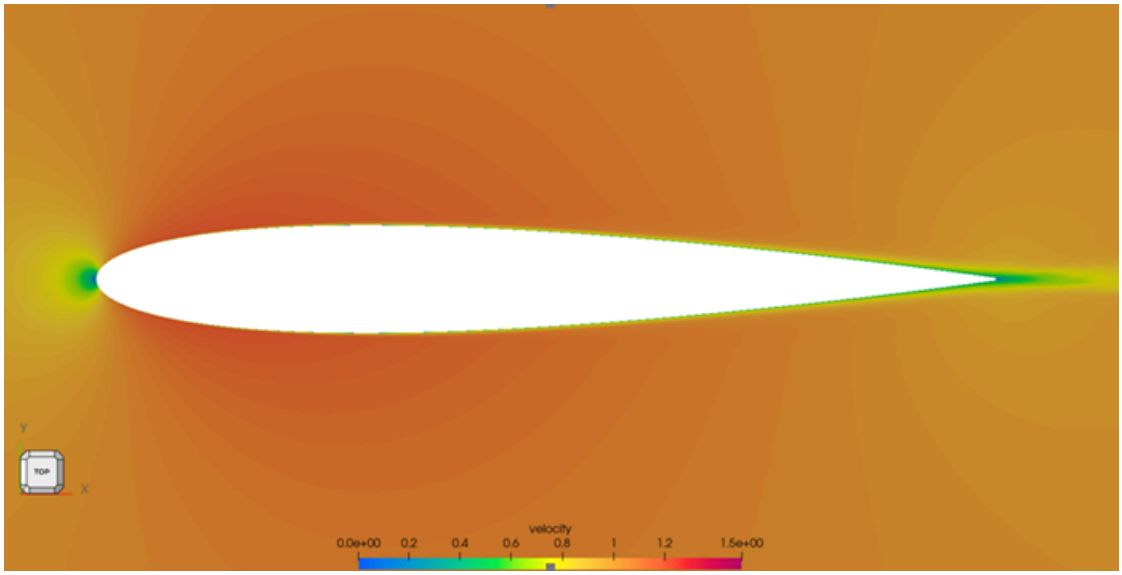


Figure 122: Contours of Velocity Magnitude Where Angle of Attack = 0 Degrees

With a 10 degree angle of attack, the stagnation point is shifted downward (relative to the airfoil), reflective of the shifted angle of attack. Fluid velocity above the airfoil is markedly different than that below the airfoil. A small low-velocity region is evident on the suction side of the airfoil, indicating some separation toward the trailing edge.

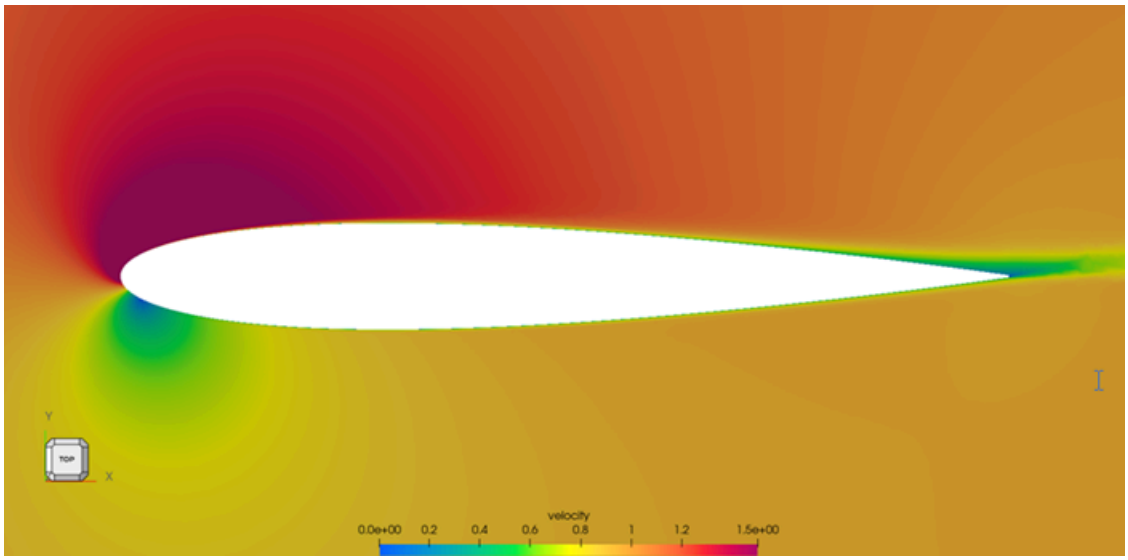


Figure 123: Contours of Velocity Magnitude Where Angle of Attack = 10 degrees

With a 15 degree angle of attack, the stagnation at the front of the airfoil is shifted even farther downward (relative to the airfoil), reflective of the shifted angle of attack. Additionally, the low-velocity wake increases in size, reflecting separation along the suction surface of the airfoil.

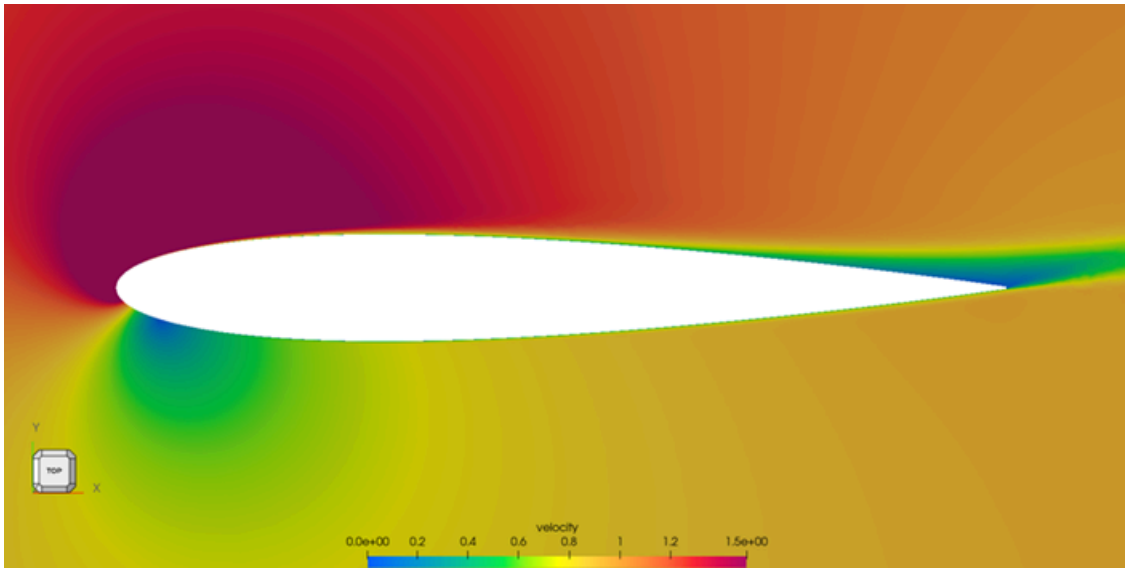


Figure 124: Contours of Velocity Magnitude Where Angle of Attack = 15 Degrees

Experimental values of coefficient of lift (CL) at angles of attack (α) of 10 degrees and 15 degrees and values of drag coefficient (cd) at angles of attack (α) of 0 degrees,10 degrees, and 15 degrees are presented with the corresponding AcuSolve results in the following table.

Table 6:

	CL (α=10)	**CL (α=15)**	**cd (α=0)**	**cd (α=10)**	**cd (α=15)**
Experimental	1.0941	1.5576	0.0082	0.0123	0.0207
AcuSolve	1.0905	1.5428	0.0081	0.0124	0.0208
Percent deviation from experimental	0.33	0.95	1.22	0.81	0.48

AcuSolve values for coefficient of pressure are plotted against experimental results for angles of attack (α) of 0 degrees, 10 degrees, and 15 degrees in the following plots. The results are presented for normalized distance along the airfoil, given by x/c, where x is the distance from the leading edge and c is the chord length.

For each case, AcuSolve is able to predict the flow characteristics at each point along the airfoil surface.

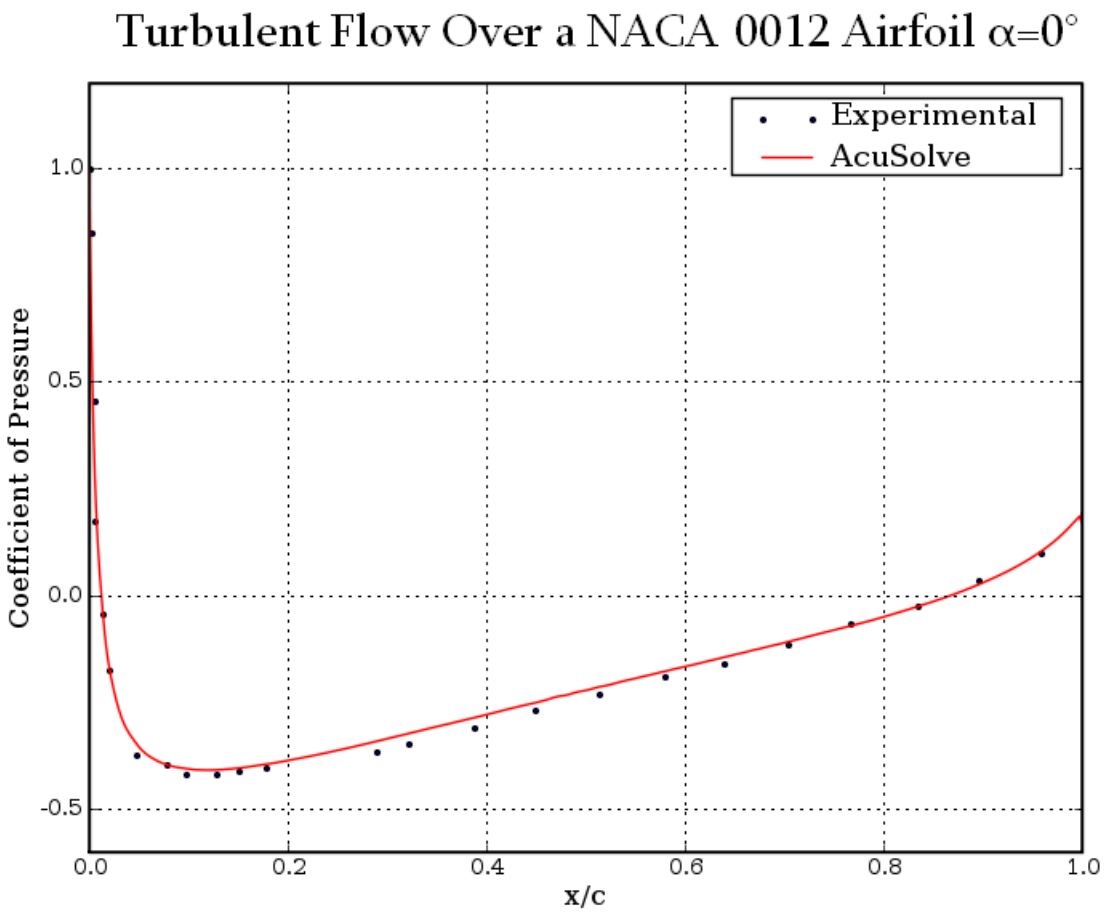


Figure 125: Coefficient of Pressure Plotted Against Normalized Distance Along the Airfoil for Angle of Attack (a) = 0 Degrees

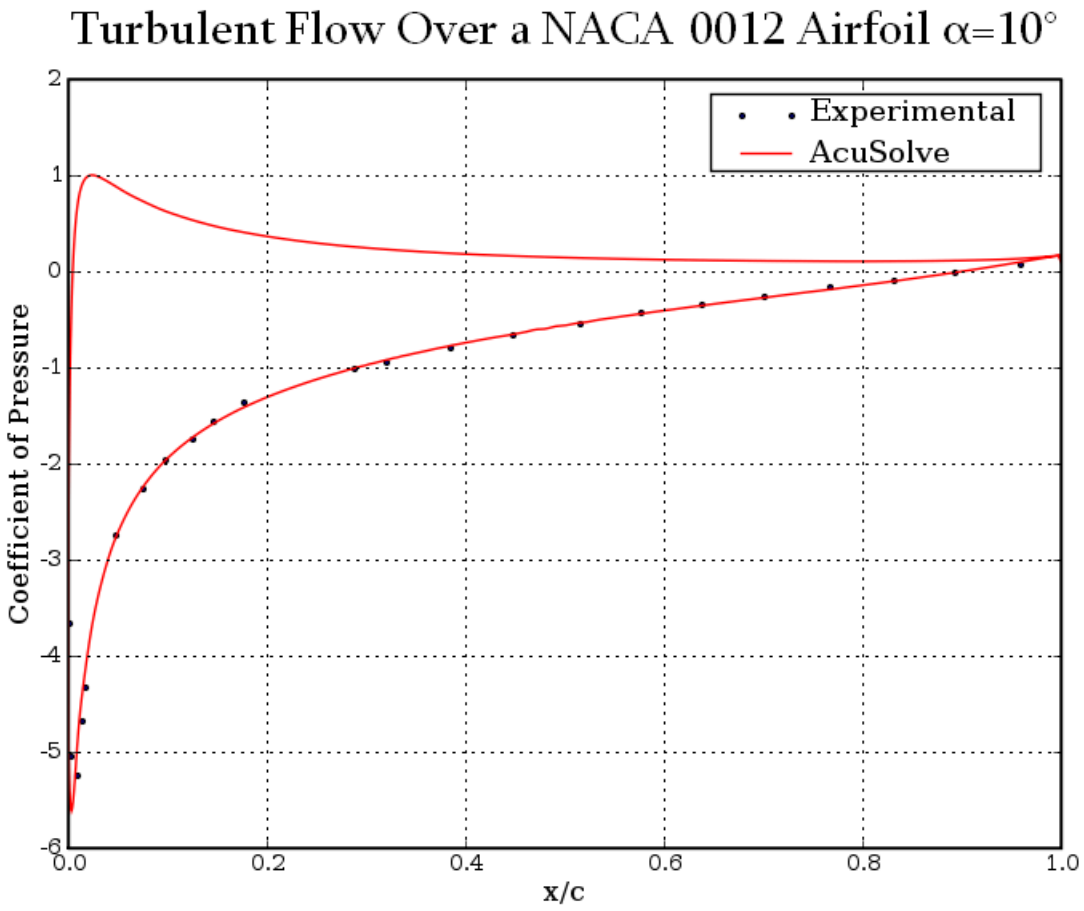


Figure 126: Coefficient of Pressure Plotted Against Normalized Distance Along the Airfoil For Angle of Attack (a) = 10 Degrees

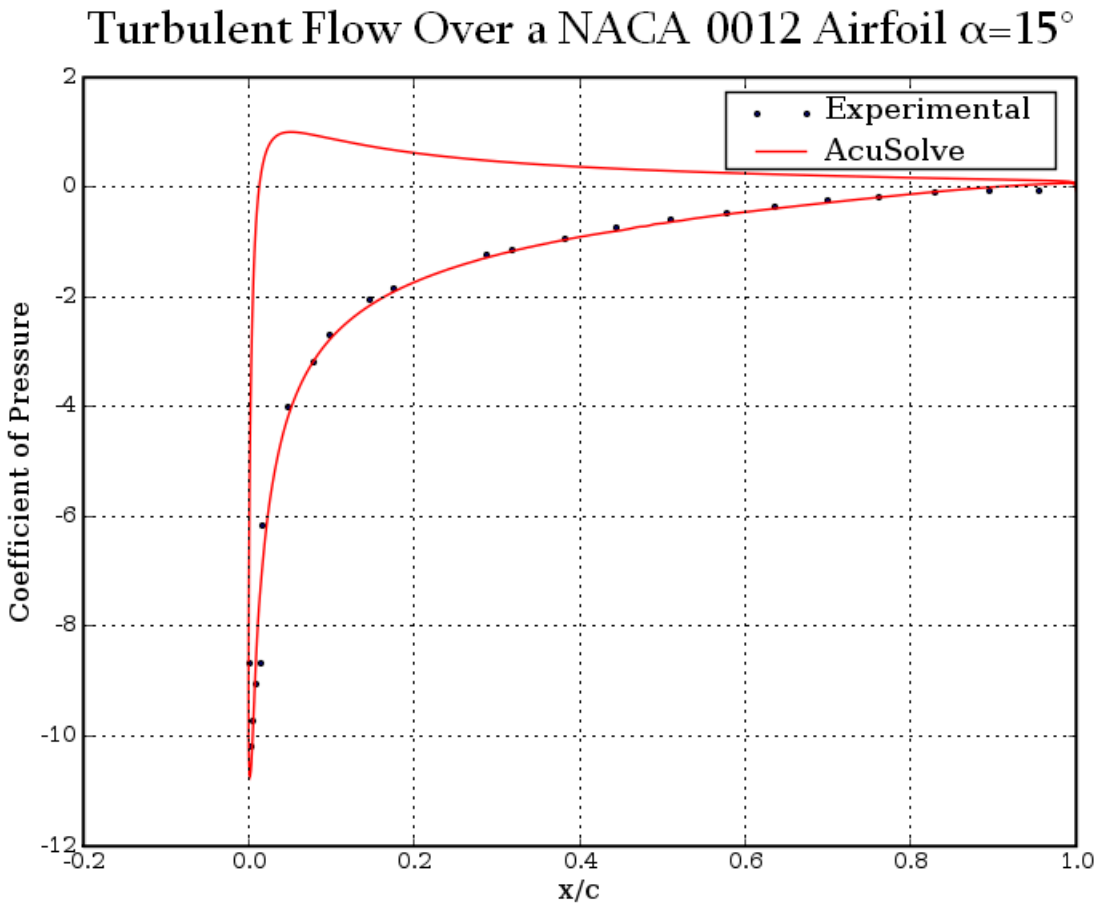


Figure 127: Coefficient of Pressure Plotted Against Normalized Distance Along the Airfoil for Angle of Attack (a) = 15 Degrees

Summary

The AcuSolve results compare well with the experimental results for flow over a NACA 0012 airfoil. In this application, a constant-velocity flow field impinges on the airfoil surface. As the flow convects in the streamwise direction along the airfoil surface, a boundary layer develops. The rate at which the boundary layer develops has significant impact on the viscous stresses present on the airfoil surface. At low angles of attack these stresses dominate the drag on the airfoil. As the angle of attack increases, the flow over the airfoil is no longer symmetric, which leads to the generation of lift. For non-zero angles of attack, the asymmetric pressure distribution on the airfoil creates another source of drag that is combined with the viscous stresses to determine the total drag on the airfoil. The AcuSolve results for coefficients of lift and drag at the 15 percent angle of attack are within 0.91 percent and 0.5 percent of experimental values, respectively. AcuSolve results for coefficient of pressure closely agree with experimental results along the length of the airfoil for all three angles of attack that were investigated.

Simulation Settings for Turbulent Flow Over a NACA0012 Airfoil

HyperMesh CFD database file: `<your working directory>\airfoil_turbulent\airfoil_turbulent.hm`

Global

- Problem Description
  - Analysis type - Steady State
  - Turbulence equation - Spalart Allmaras
- Auto Solution Strategy
  - Convergence tolerance - `0.0001`
  - Relaxation factor - `0.4`
- Material Model
  - Fluid
    - Density - `1.0` kg/m3
    - Viscosity - `1.667e-7` kg/m-sec

  Model
- Volumes
  - Fluid
    - Element Set
      1. Material model - Fluid
- Surfaces
  - +z slip
    - Simple Boundary Condition
      1. Type - Slip
  - -z slip
    - Simple Boundary Condition
      1. Type - Slip
  - airfoil surface
    - Simple Boundary Condition
      1. Type - Wall
  - farfield
    - Simple Boundary Condition
      1. Type - Far Field
      2. X velocity - cos(α) m/sec
      3. Y velocity - sin(α) m/sec
- Eddy viscosity - `1.0e-9` m2/sec

References

NASA - Langley Research Center. http://turbmodels.larc.nasa.gov/naca0012_val_sa.html

Turbulent Natural Convection Inside a Tall Cavity

In this application, AcuSolve is used to simulate the natural convection of a turbulent flow field within a tall rectangular cavity. AcuSolve results are compared with experimental results as described in Betts and Bokhari (2000). The close agreement of AcuSolve results with experimental results validates the ability of AcuSolve to model cases with natural convection of turbulent flow within a tall cavity.

Problem Description

The problem consists of air within a tall cavity with a hot wall and a cold wall, as shown in the following image, which is not drawn to scale. The cavity is 2.18 m tall, 0.0762 m wide, and 0.52 m deep. The cavity's vertical walls differ in temperature, causing the fluid to transfer the heat, leading to natural convection. The temperature of the hot wall is 307.85 K, while the temperature of the cold wall is 288.25 K. The horizontal walls of the cavity are adiabatic. The length-to-width ratio of 28.6 and temperature difference of 19.6 K produce a turbulent flow field within the cavity with a Rayleigh number of $8.6X10^{5}$ (Betts and Bokhari 2000). The flow medium is air, with a Boussinesq approximation for density, a specific heat of 1005 J/kg-K, and a viscosity of $1.781 X 10^{-5}$ kg/m-s. Gravity is applied globally to the volume of air.

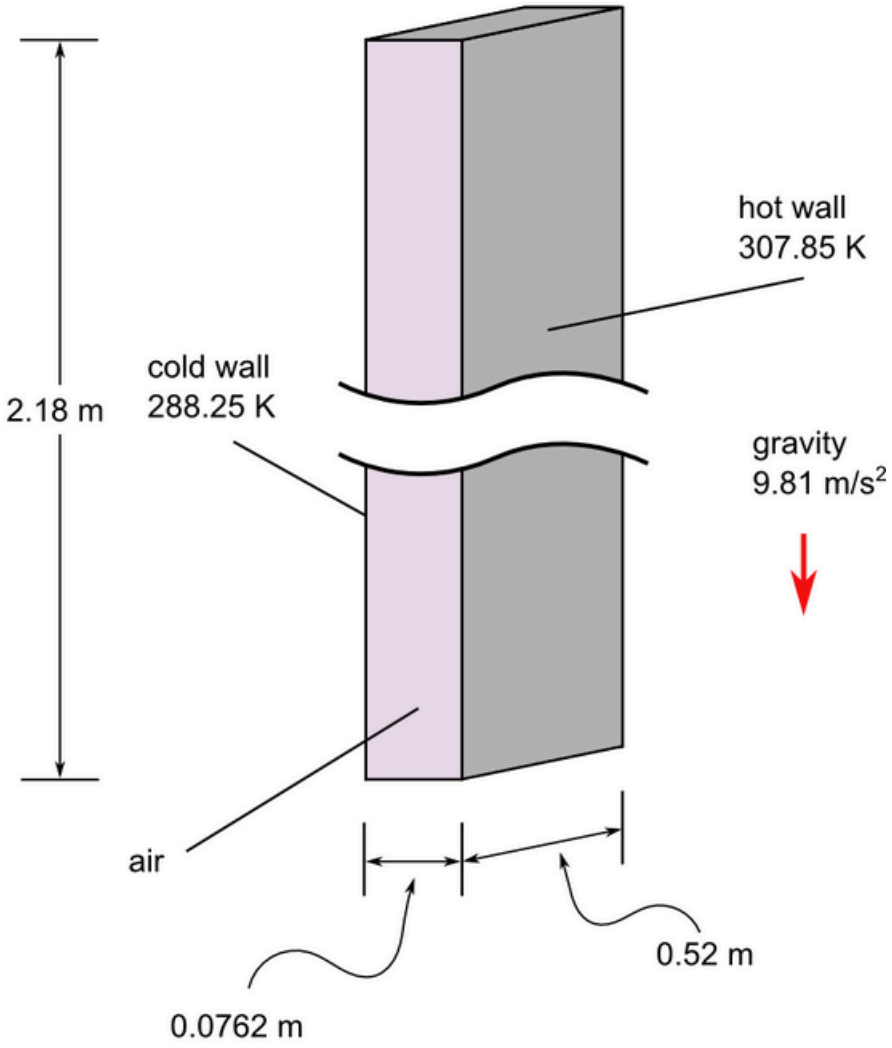


Figure 128: Critical Dimensions and Parameters for Simulating Turbulent Natural Convection in a Tall Cavity

The simulation was performed as a two dimensional problem by constructing a volume mesh that contains a single layer of elements in the extruded direction, normal to the flow plane and by imposing symmetry boundary conditions on the extruded planes.

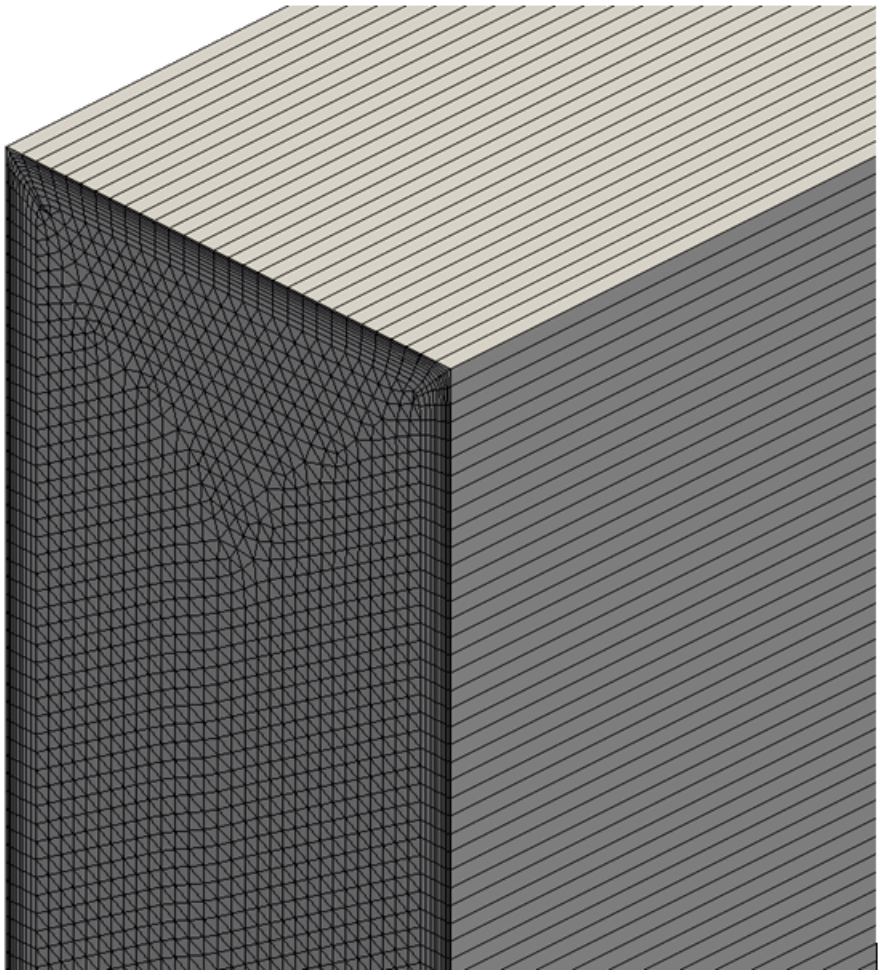


Figure 129: Mesh used for Simulating the Natural Convection of Turbulent Flow in a Tall Cavity

AcuSolve Results

The AcuSolve solution converged to a steady state and the results reflect the mean flow conditions. The natural convection of the flow is generated by heat transfer from the vertical walls to the fluid in the cavity. The temperature gradients created by this heat transfer cause differing densities within the flow region. The warmer air rises to the top of the cavity due to its lower density while the colder air sinks to the bottom of the cavity due to its higher density. This produces flow near the hot vertical wall in the positive vertical direction and flow near the cold wall in the negative vertical direction.

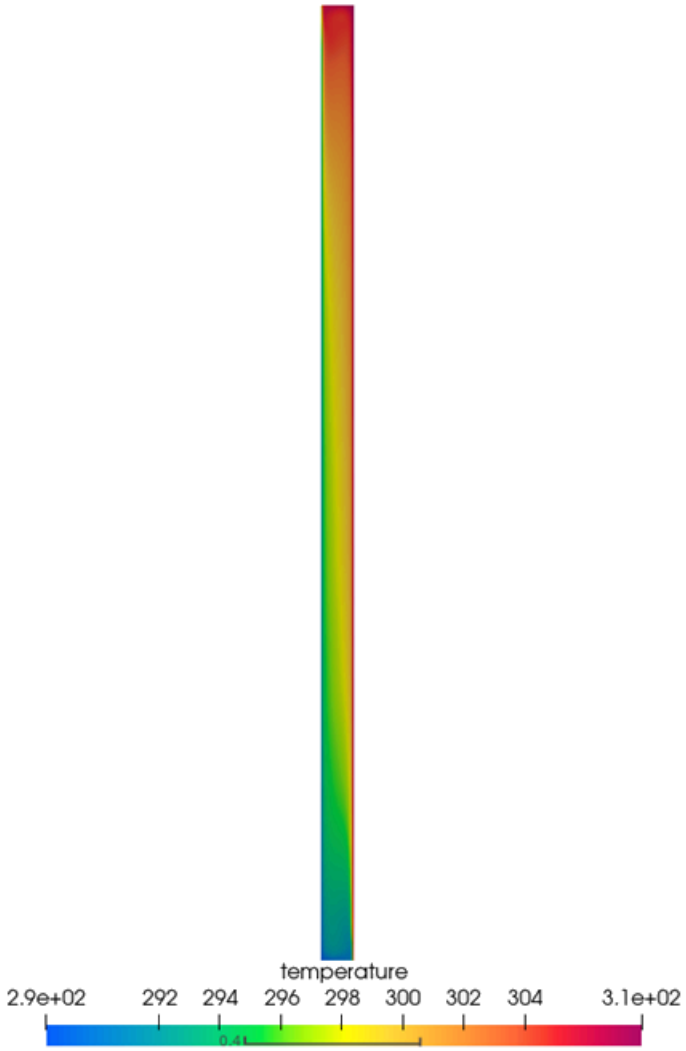


Figure 130: Temperature Contours Throughout Tall Cavity in the X-Y Plane

The AcuSolve results of the temperature and vertical velocity within the cavity are compared to the corresponding experimental values in the plots shown below. The temperature of the air is lowest near the cold vertical wall, remains relatively steady in the middle of the cavity, and then peaks near the hot vertical wall. Following a similar trend, the AcuSolve results show that the velocity is lowest near the cold vertical wall, due to the air sinking, and then steadily increases as the air begins to rise near the hot vertical wall. The velocity at the walls is zero due to the no-slip boundary condition. Additional comparisons are made to evaluate the performance of four turbulence models, Spalart-Allmaras (SA), shear stress transport (SST), K-Omega and K-ε.

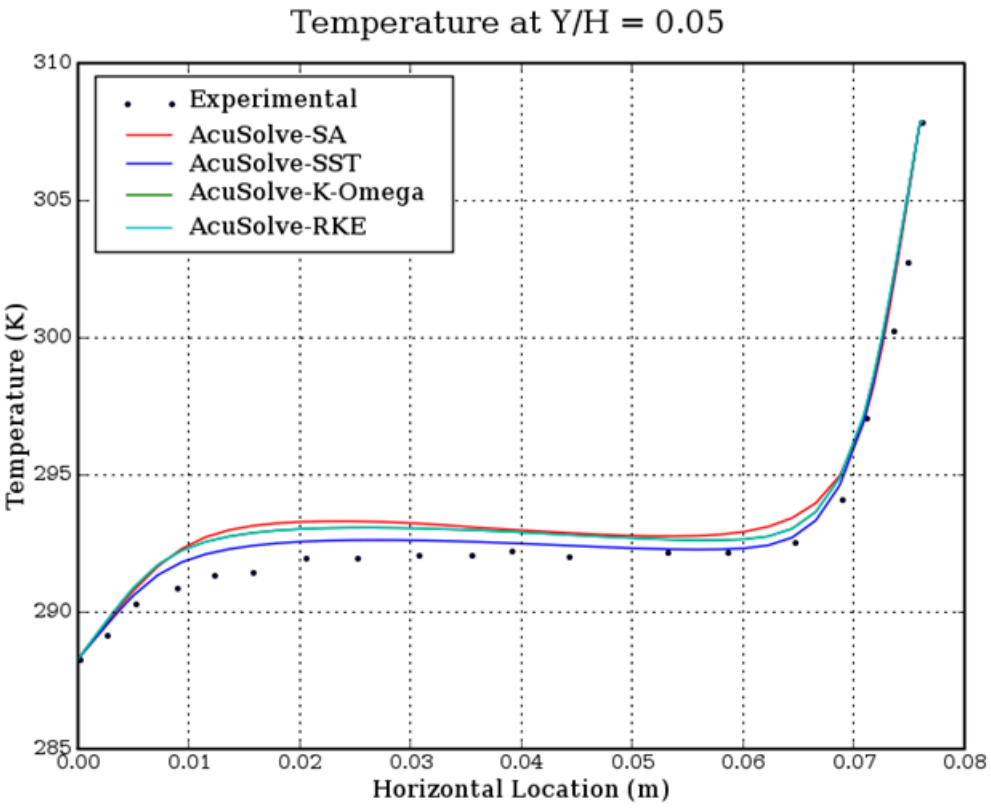


Figure 131: Temperature Plotted against Location along Horizontal at a Position of y/H=0.05 in the Cavity, where H is the Cavity Height and y is the Distance from the Bottom Wall

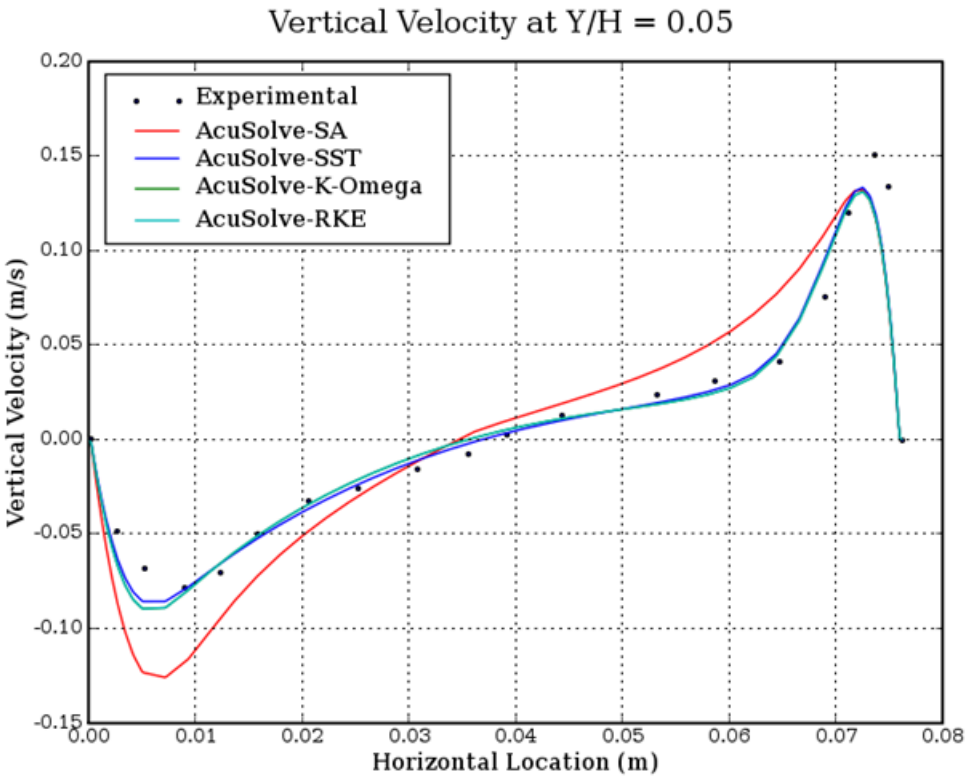


Figure 132: Vertical Velocity Plotted against Location along Horizontal at a Position of y/H=0.05 in the Cavity, where H is the Cavity Height and y is the Distance from the Bottom Wall

Summary

In this application, turbulent flow developed by natural convection, at a Rayleigh number of 8.6X105, is studied within a tall cavity. The AcuSolve results compare well with the experimental data for temperature and vertical velocity along a horizontal line at a location of y/H=0.05 in the tall cavity, with the two-equation models capturing the velocity gradient with greater accuracy. A temperature difference occurs within the flow region due to the heat transfer from the vertical walls of the cavity. The hotter, less-dense air rises to the top of the cavity while the colder, denser air sinks to the bottom, giving rise to recirculation. AcuSolve demonstrates the ability to accurately predict the natural convection of turbulent flow within a tall cavity.

Simulation Settings for Turbulent Natural Convection Inside a Tall Cavity

HyperMesh CFD database file: `<your working directory\cavity_turbulent_heat \cavity_turbulent_heat.hm`

Global

- Problem Description
  - Analysis type - Steady State
  - Turbulence equation - SST
- Auto Solution Strategy
  - Relaxation factor - `0.5`

- Convergence tolerance - `0.005`

- Material Model
  - Air
    - Type - Boussinesq
    - Density - `1.225` kg/m3
    - Specific Heat - `1005` J/kg-K
    - Viscosity - `1.781e-5` kg/m-sec

  Model
- Volumes
  - Volume
    - Element Set
      1. Material model - Air
- Surfaces
  - Back
    - Simple Boundary Condition
      1. Type - Symmetry
  - Bottom
    - **Simple Boundary Condition**
      1. Type - Wall
      2. Temperature BC type - Flux
      3. Heat Flux - `0.0` W/m2
  - Cold
    - **Simple Boundary Condition**
      1. Type - Wall
      2. Temperature BC type - Value
      3. Temperature - `288.25` K
  - Front
    - Simple Boundary Condition
      1. Type - Symmetry
  - Hot
    - Simple Boundary Condition
      1. Type - Wall
      2. Temperature BC type - Value
      3. Temperature - `307.85` K
  - Top
    - Simple Boundary Condition
      1. Type - Wall

2 Temperature BC type - Flux
3 Heat Flux - `0.0` W/m2

References

P.L. Betts and I.H. Bokhari. "Experiments on Turbulent Natural Convection in an Enclosed Tall Cavity". International Journal of Heat and Fluid Flow 21:675-683. 2000.

Viscous Heating Inside a Rotating Annulus

In this application, AcuSolve is used to simulate fluid flow and viscous heating in an annulus formed by concentric cylinders. AcuSolve results are compared with analytical results adapted from Bird and others (1960). The close agreement of AcuSolve results with analytical results validates the ability of AcuSolve to model cases with viscous heating.

Problem Description

The problem consists of a viscous fluid filling the annulus between two concentric cylinders, as shown in the following image, which is not drawn to scale. The inner cylinder has a radius of 1.0 m and is fixed in place. The outer cylinder has a radius of 2.0 m and rotates with a constant angular velocity of 0.5 rad/s. The inner cylinder is held at a constant temperature of 273 K and the outer cylinder is held at 274 K.

The rotation of the outer cylinder causes the fluid to rotate due to the viscous shearing near the wall. As the inner cylinder is fixed, a velocity gradient is generated as a function of distance from the inner cylinder center. Viscous stresses within the domain generate significant amounts of heat, leading to a substantial increase in the fluid temperature in regions of high shear.

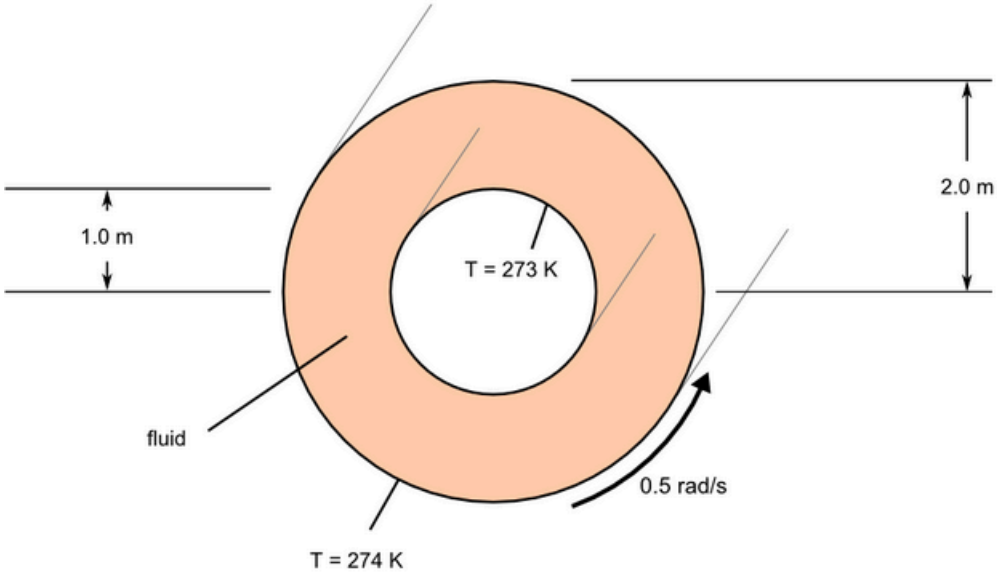


Figure 133: Critical Dimensions and Parameters for Simulating Viscous Heating Inside a Rotating Annulus

The simulation was performed as a two-dimensional problem by constructing a volume mesh that contains a single layer of elements in the extruded direction, normal to the flow plane, and by imposing symmetry boundary conditions on the extruded planes.

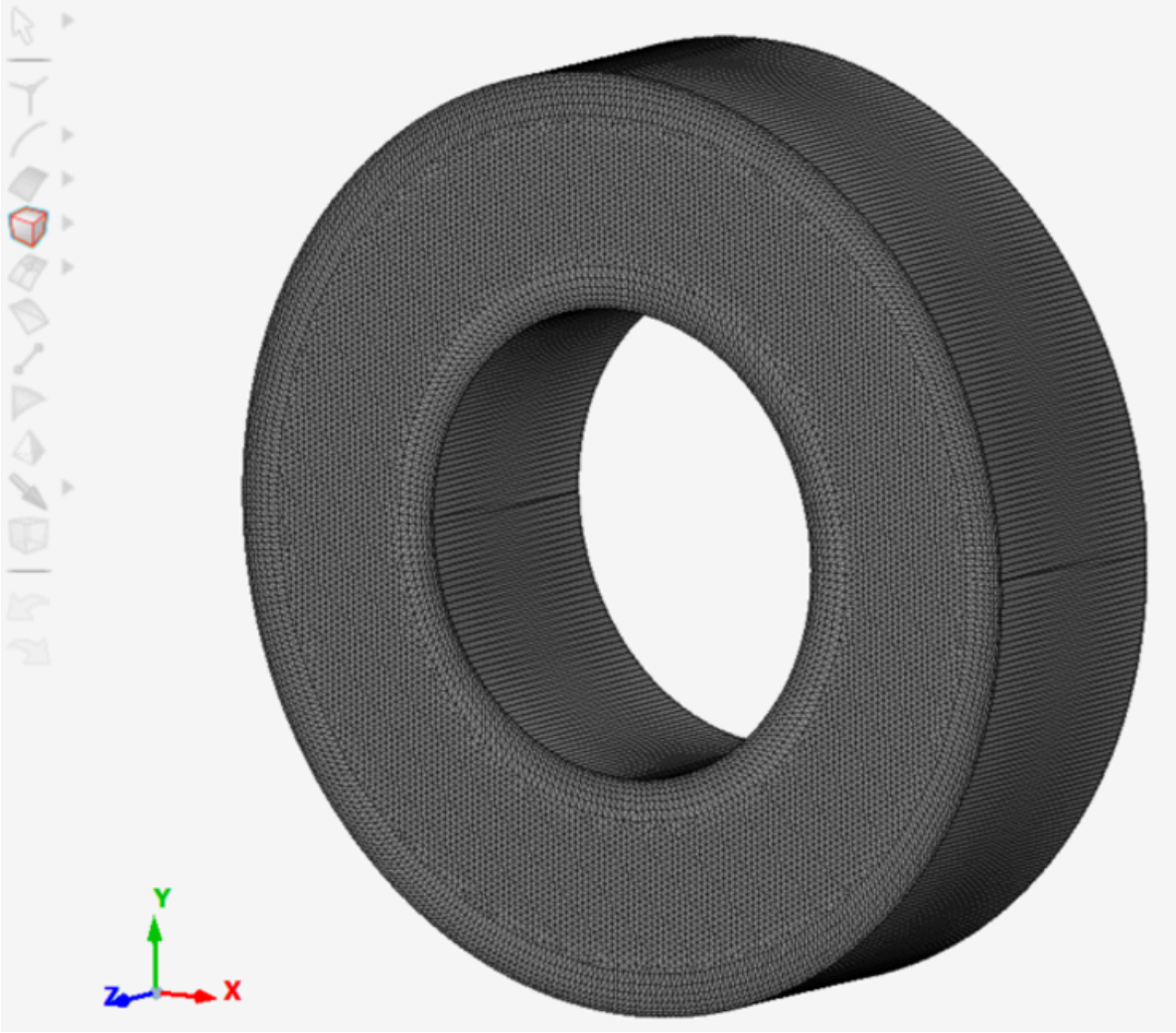


Figure 134: Mesh used for Simulating Viscous Heating Inside a Rotating Annulus

AcuSolve Results

The AcuSolve solution converged to a steady state and the results reflect the mean flow conditions. Flow is induced by the viscous shearing near the outer wall, creating a velocity gradient with the highest velocity near the moving wall.

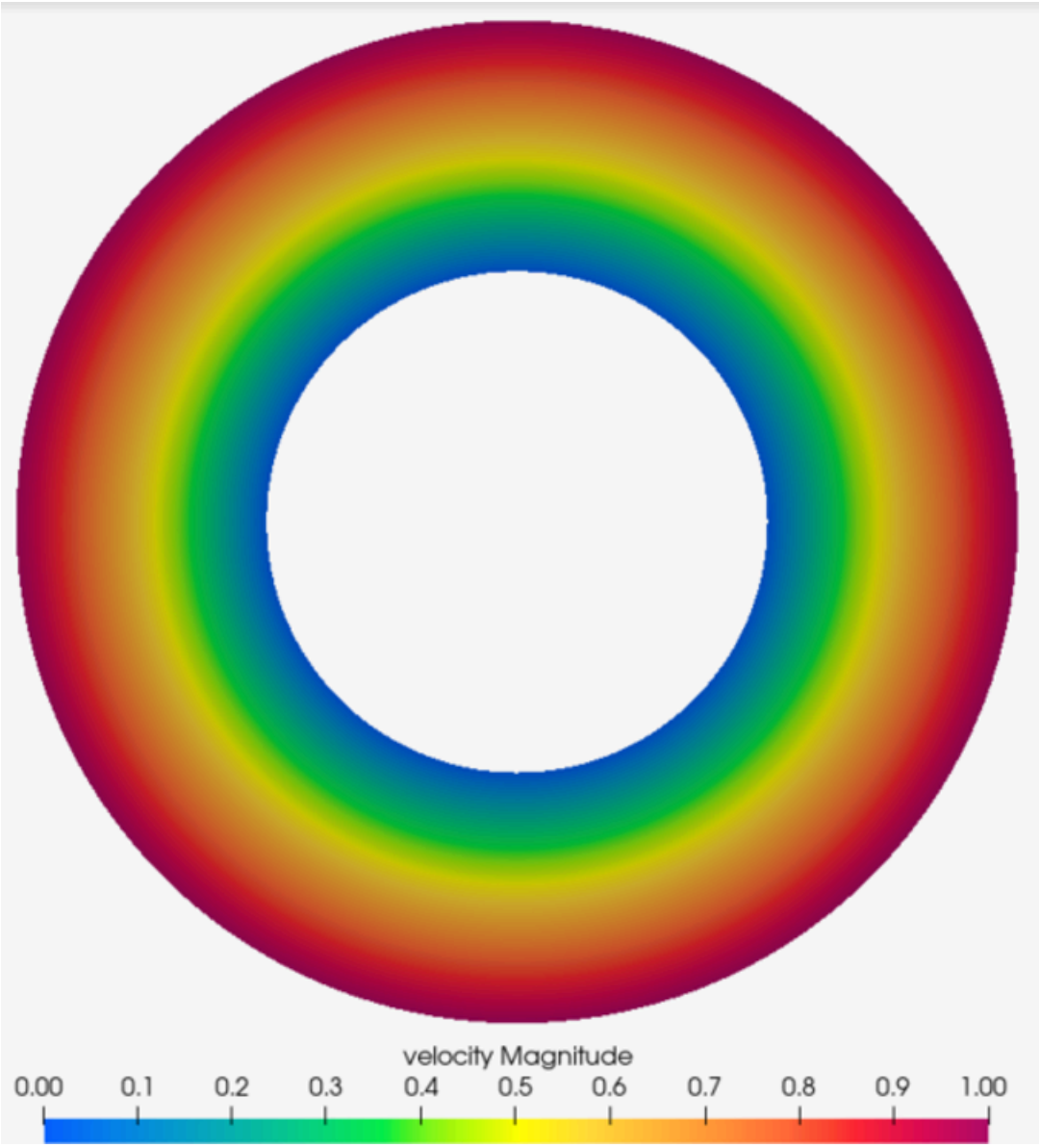


Figure 135: Contours of Velocity Magnitude (m/s)

The velocity gradient causes viscous heating, causing the fluid temperature to increase. The resulting temperature profile is nonlinear with the highest temperatures occurring in the space between the cylinders.

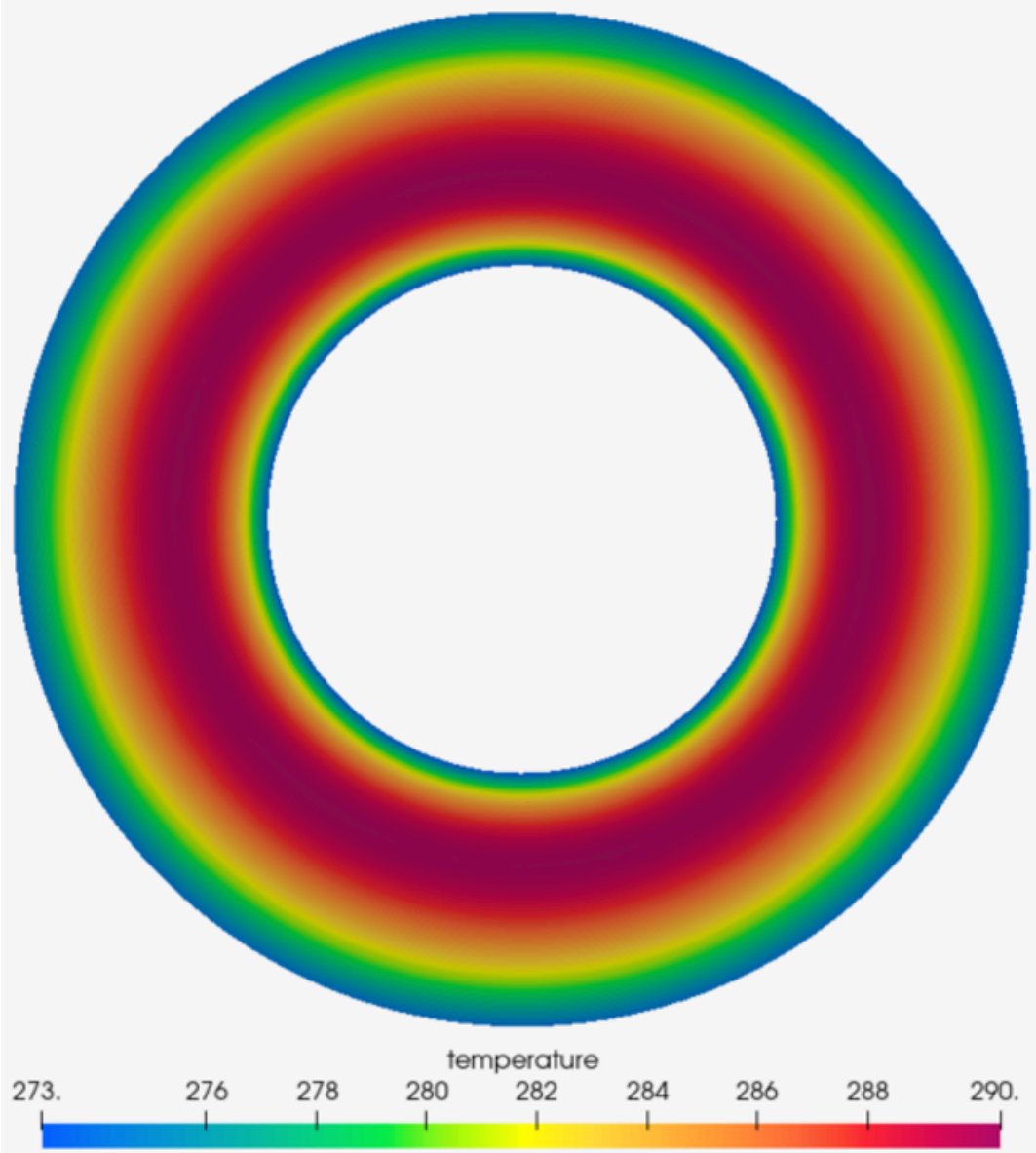


Figure 136: Contours of Temperature (K)

AcuSolve results were compared to analytical results for velocity and for temperature across a range of radial locations.

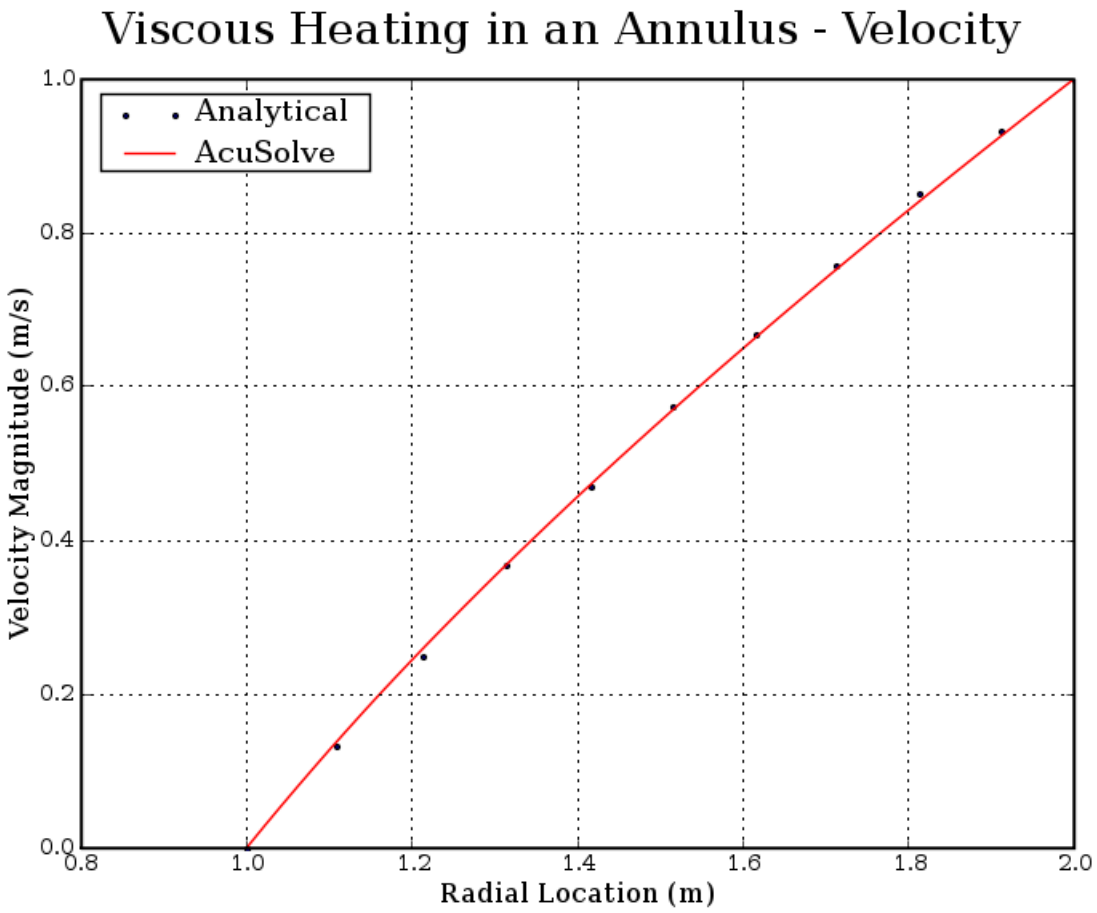


Figure 137: Velocity Magnitude Plotted Against Radial Location from the Center of the Inner Cylinder

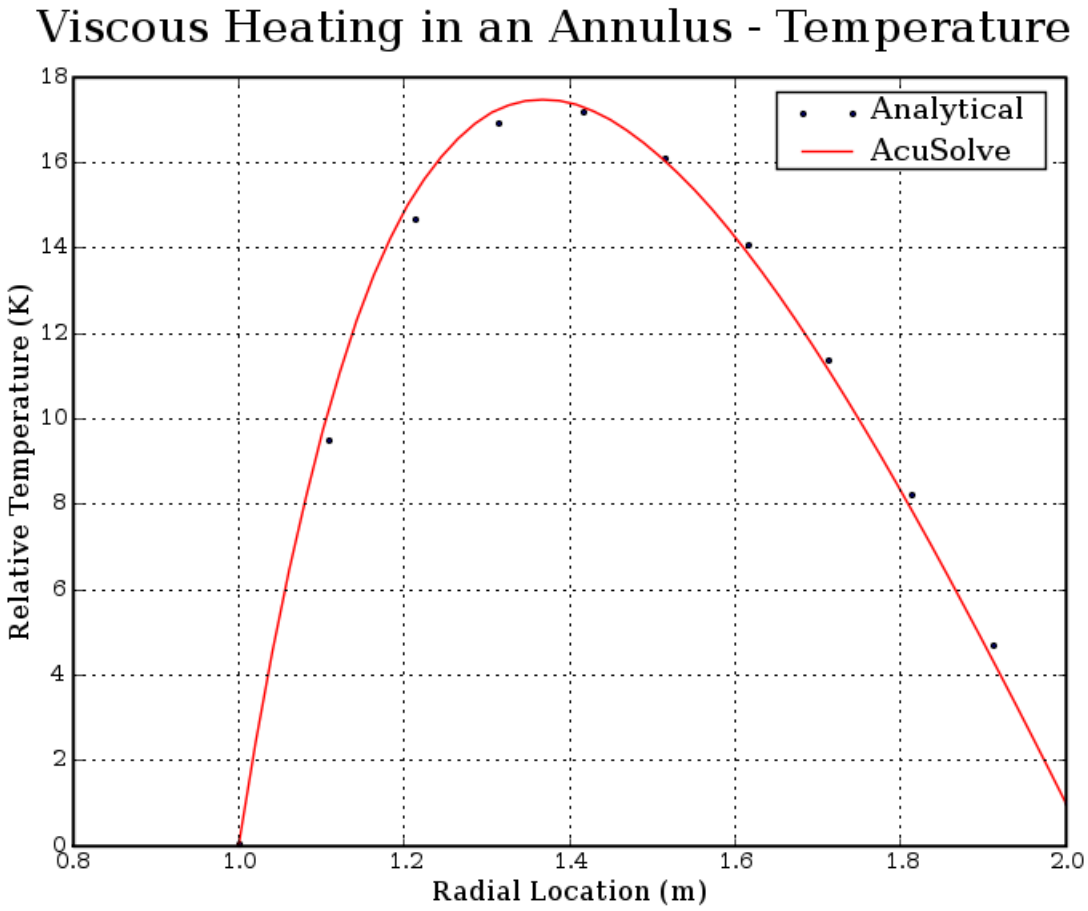


Figure 138: Temperature (Relative to the Inner Cylinder Wall Temperature) Plotted Against Radial Location from the Center of the Inner Pipe

Summary

The AcuSolve results compare well with the analytical results for both the flow field and the temperature across the annulus. In this application, flow is induced due to the viscous stresses generated by the rotation of the exterior cylinder. Velocity gradients between the cylinders give rise to shear stresses that induce frictional heating of the fluid. Due to the high viscosity of the fluid, the viscous heating is significant and leads to large increases in the temperature between the cylinders. This application validates the ability of AcuSolve to simulate flows where the viscous heating contribution is significant.

Simulation Settings for Viscous Heating Inside a Rotating Annulus

SimLab database file: `<your working directory>\annulus_rotating_heat\annulus_rotating_heat.slb`

Global

- Problem Description
  - Analysis type - Steady State
  - Temperature equation - Advective Diffusive

- Turbulence equation - Laminar

- Auto Solution Strategy
  - Relaxation factor - `0.2`
- Material Model
  - Fluid
    - Density - `1.0` kg/m3
    - Viscosity - `300` kg/m-sec
    - Conductivity - `1.0` W/m-K
- Reference Frame
  - Outer_Rotation
    - Angular Velocity
      1. X-component - `0.0` rad/sec
      2. Y-component - `0.0` rad/sec
      3. Z-component - `0.5` rad/sec

Model

- Volumes
  - Fluid
    - Element Set
      1. Material model - Fluid
      2. Viscous heating - On
- Surfaces
  - Inner_Cylinder
    - Simple Boundary Condition
      1. Type - Wall
      2. Temperature BC type - Value
      3. Temperature - `273.0` K
  - Outer_Cylinder
    - Simple Boundary Condition
      1. Type - Wall
      2. Reference frame - Outer_Rotation
      3. Temperature BC type - Value
      4. Temperature - `274.0` K
  - Symm_MaxZ
    - Simple Boundary Condition
      1. Type - Symmetry
  - Symm_MinZ
    - Simple Boundary Condition

1 Type - Symmetry

- Nodes
  - Node 1
    - Pressure
      1 Type - Zero

References

R. B. Bird, W. E. Stewart, and E. N. Lightfoot. "Transport phenomena". New York, John Wiley and Sons, 1960

Separated Laminar Flow Over a Blunt Plate

In this application, AcuSolve is used to simulate the separation of laminar flow over a blunt plate. AcuSolve results are compared with experimental results as described in J.C. Lane and R.I. Loehrke (1980). The close agreement of AcuSolve results with the experimental results validates the ability of AcuSolve to model cases with external laminar flow including separation.

Problem Description

The problem consists of external, laminar flow over a blunt plate 1.5 m long and 0.09 m thick, as shown in the following image, which is not drawn to scale. The fluid flows with a uniform horizontal velocity (v) of 0.045133 m/s. The fluid material used for the simulation has a density of 1.0 kg/m^3 and a dynamic viscosity of 1.7894 X 10^{-5} kg/m-s. The resulting Reynolds number for the flow, based on the plate thickness, is approximately 227. This indicates that the flow over the plate is laminar. As the fluid flows past the leading edge of the plate, the pressure decreases, resulting in a separation region downstream of the leading edge. At some distance downstream from the leading edge, the pressure gradient decreases, and viscous forces cause the recirculation zone to dissipate, allowing the flow to reattach to the plate.

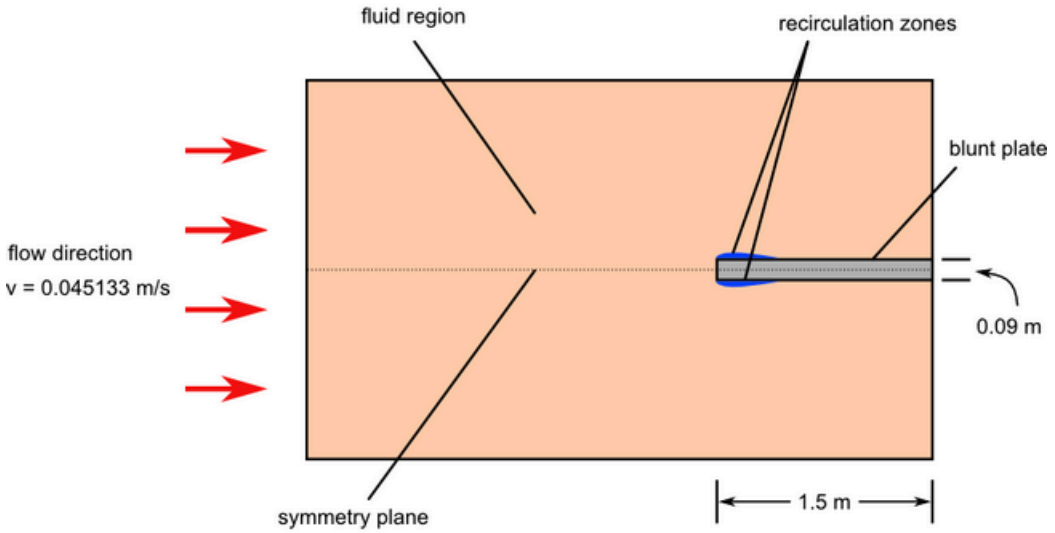


Figure 139:

The simulation was performed as a two dimensional problem by constructing a volume mesh that contains a single layer of elements in the extruded direction, normal to the flow plane, and by imposing symmetry boundary conditions on the extruded planes. In addition, the half symmetry of the geometry was exploited to allow for modeling only the top half of the geometry. These characteristics allow for accurate simulation of the flow while minimizing computational time. The following images show the mesh distribution and a refined mesh zone around the blunt plate.

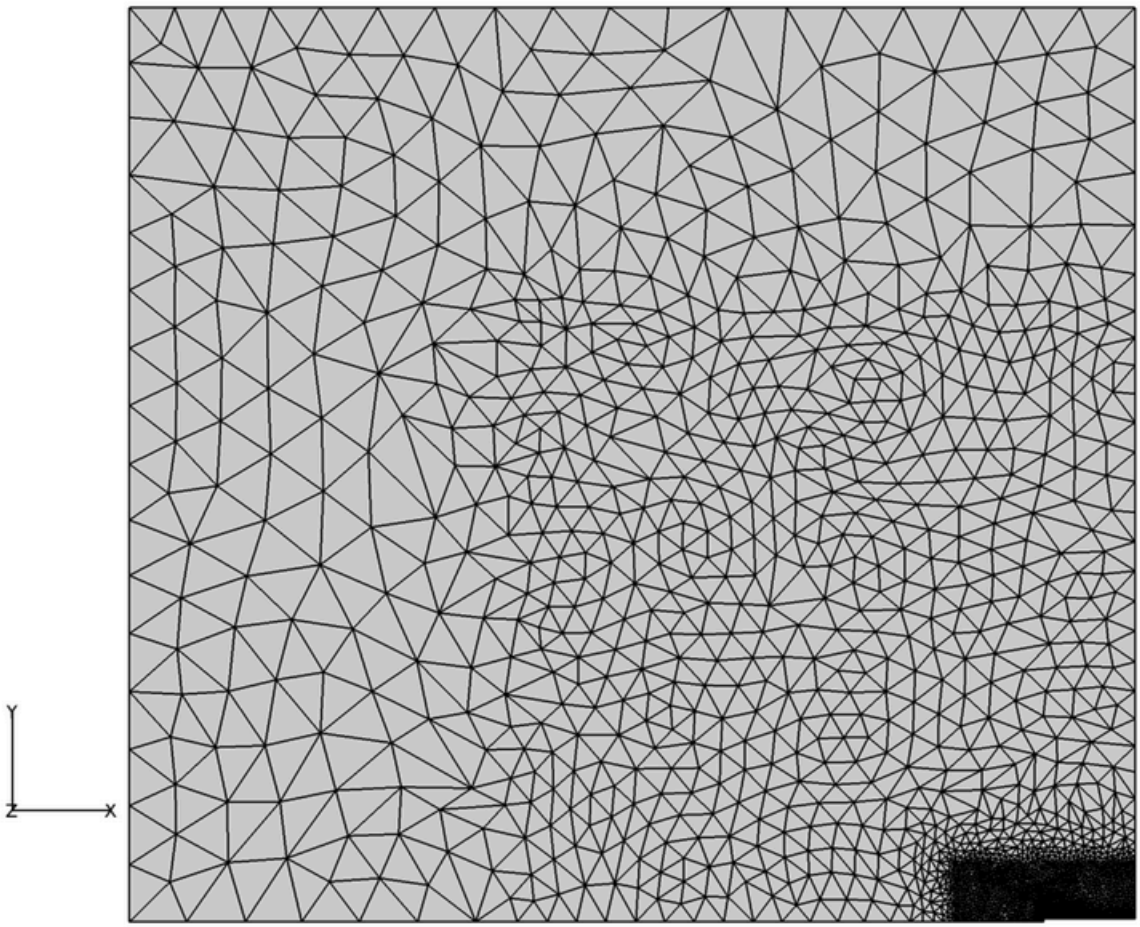


Figure 140: Mesh used for Simulating Separated Laminar Flow over a Blunt Plate

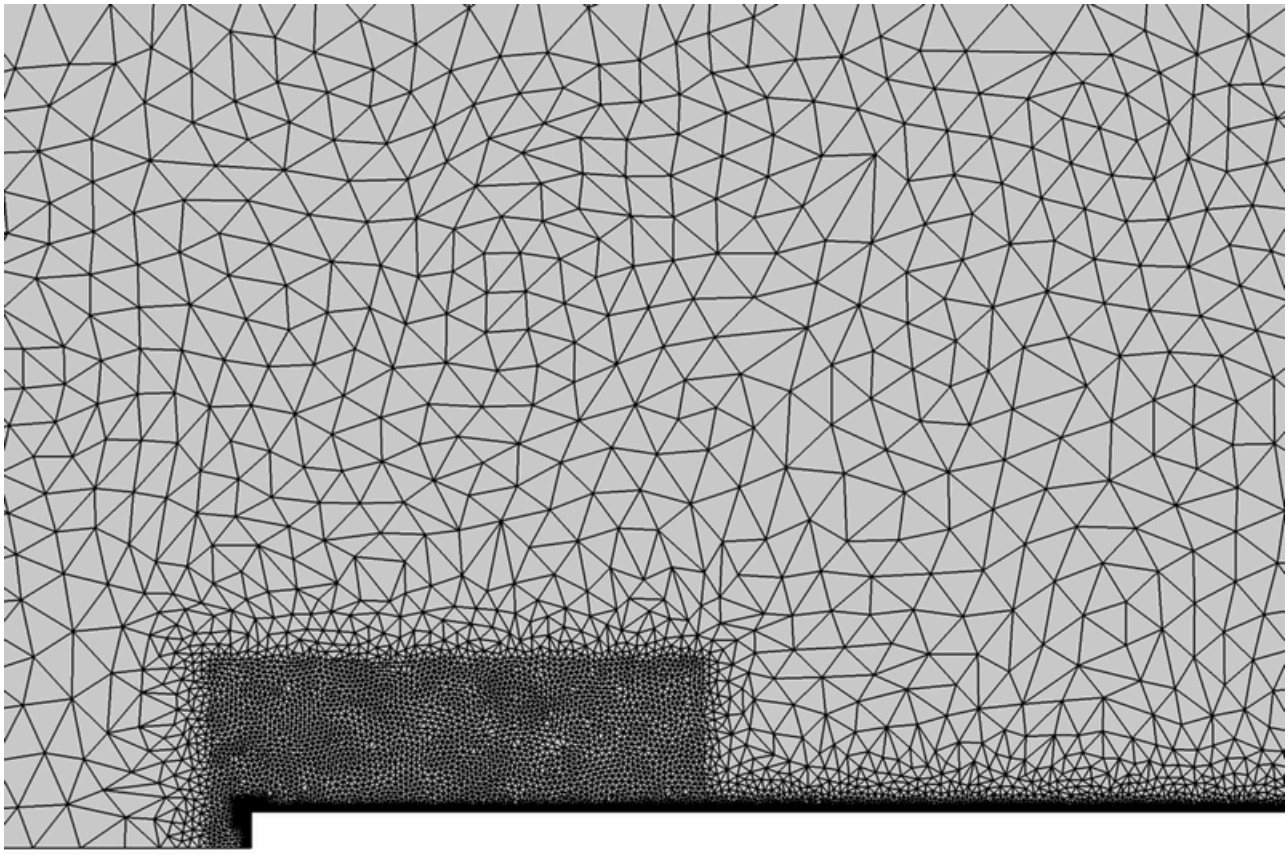


Figure 141: Mesh Detail Showing Refinement Zones at the Leading Edge of the Blunt Plate

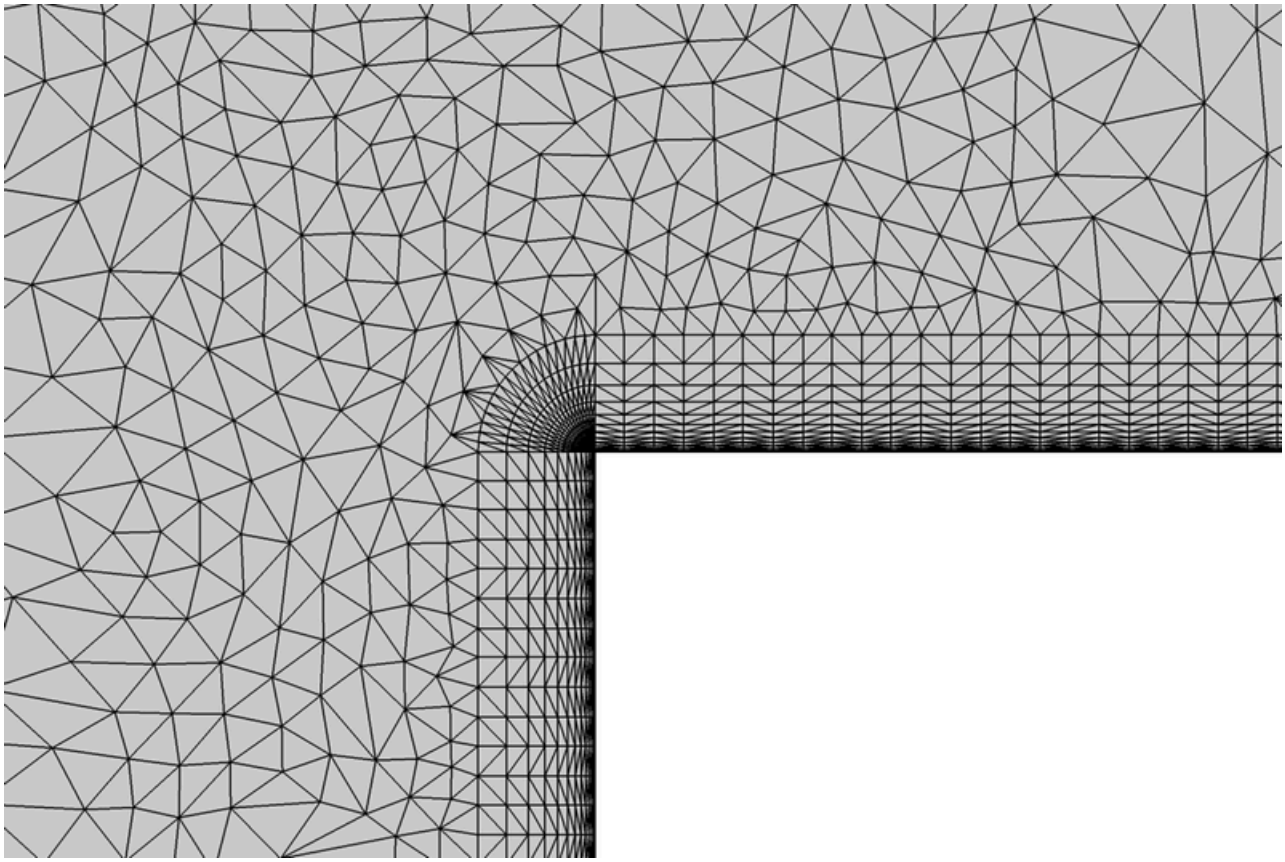


Figure 142: Mesh Detail Showing Mesh Elements Near the Leading Edge of the Blunt Plate

AcuSolve Results

The AcuSolve solution converged to a steady state and the results reflect the mean flow conditions over the blunt plate. The flow velocity is reduced to zero at the leading face, forming a stagnation point at the center. The flow reaches a maximum velocity as it flows around the leading edges and separates from the plate. Flow separation (shear stress parallel to the wall becomes negative) occurs downstream of the leading edge, leading to a recirculation zone. The flow reattaches 0.37 m downstream of the leading edge. The velocity in the laminar boundary layer increases from zero at the wall to free-stream velocity at the boundary layer edge. Along the plate length, the boundary layer slowly grows in thickness. The following image shows the contours of the flow velocity parallel to the streamwise direction and the recirculation region in the wake of the plate edge.

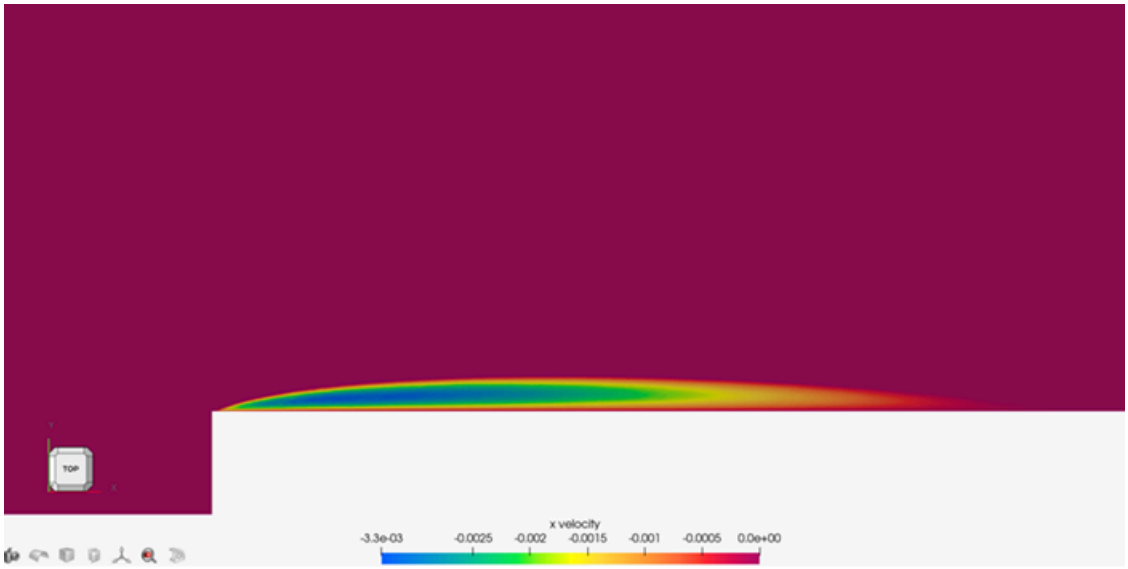


Figure 143: X-Velocity Contours Near the Leading Edge of the Blunt Plate

Downstream of the leading edge, the flow eventually reattaches to the plate at the point where the shear stress parallel to the wall passes from negative through zero to positive. The reattachment point is 0.37 m from the leading edge of the plate and corresponds to the trailing edge of the contours.

The results for the predicted and experimental reattachment length (xreattach) are presented in the table below. T represents the plate thickness.

Table 7:

AcuSolve xreattach	AcuSolve xreattach/T	Experimental xreattach/T	Percent error (%)
0.37	4.11	4.0	2.8

Summary

In this application, a constant flow inlet velocity and symmetric boundary conditions were used to model 2D flow over a blunt plate. The AcuSolve solution compares well with experimental results for the separation of laminar flow over a blunt plate. The non-dimensional reattachment length obtained from the AcuSolve steady state solution compares well with the experimental solution, with an error of less than 3.0 percent. The results of this simulation validate the ability of AcuSolve to accurately predict the reattachment point in cases with external, laminar flow with separation.

Simulation Settings for Separated Laminar Flow over a Blunt Plate

HyperMesh CFD database file: `<your working directory>\blunt_plate_laminar\blunt_plate_laminar.hm`

Global

- Problem Description

- Analysis type - Steady State
- Turbulence equation - Laminar

- Auto Solution Strategy
  - Relaxation Factor - `0.2`
- Material Model
  - Fluid
    - Density - `1.0` kg/m3
    - Viscosity - `1.7894e-005` kg/m-sec

  Model
- Volumes
  - Fluid
    - Element Set
      1. Material model - Fluid
- Surfaces
  - Back
    - Simple Boundary Condition
      1. Type - Symmetry
  - Freestream
    - Simple Boundary Condition
      1. Type - Slip
  - Front
    - Simple Boundary Condition
      1. Type - Symmetry
  - Inlet
    - Simple Boundary Condition
      1. Type - Inflow
      2. Inflow type - Velocity
      3. Inflow velocity type - Cartesian
      4. X Velocity - `0.045133` m/s
  - Outflow
    - Simple Boundary Condition
      1. Type - Outflow
  - Plate
    - Simple Boundary Condition
      1. Type - Wall
  - Symmetry
    - Simple Boundary Condition

1 Type - Symmetry

References

J.C. Lane and R.I. Loehrke. "Leading Edge Separation from a Blunt Plate at Low Reynolds Number". Journal of Fluids Engineering. 102(4):494-496. 1980.

Turbulent Flow with Separation in an Asymmetric Diffuser

In this application, AcuSolve is used to simulate fully developed turbulent flow through an asymmetric diffuser with a divergent lower wall and a straight upper wall. AcuSolve results are compared with experimental results as described in Buice and Eaton (2000). The close agreement of AcuSolve results with experimental results validates the ability of AcuSolve to model cases with internal turbulent flow with flow separation and reattachment in an asymmetric diffuser.

Problem Description

The problem consists of air flowing through an asymmetric diffuser with a divergent lower wall and a straight upper wall, as shown in the following image, which is not drawn to scale. The diffuser inlet has a height of 1.5 cm (H) and extends 9 cm (6H) to the divergent section. The lower wall of the diffuser diverges at an angle of 10° and expands to 7.05 cm (4.7H). The divergent section has a horizontal length of 31.5 cm (21H). The expanded section of the diffuser extends 84 cm (56H) to the outlet. Air, with a density of 1.225 kg/m^3 and a viscosity of 1.8325 X 10^{-5} kg/m-s enters the diffuser through the inlet of the diffuser with a fully developed turbulent profile at a Reynolds's number of 20,000. The simulation was conducted with the Reynolds Averaged Navier-Stokes equations using four turbulence models, Spalart Allmaras, Shear Stress Transport (SST), K-ω and Realizable K-ε.

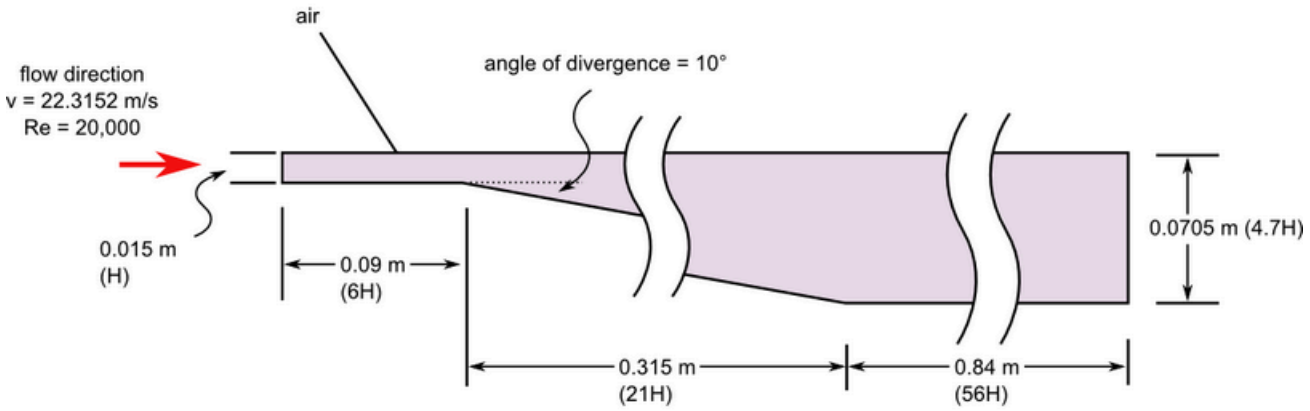


Figure 144: Critical Dimensions and Parameters for Simulating Turbulent Flow with Separation in an Asymmetric Diffuser

The simulation was performed as a two dimensional problem by constructing a volume mesh that contains a single layer of elements extruded in the cross stream direction (perpendicular to the flow plane) and by imposing symmetry boundary conditions on the extruded planes.



Figure 145: Mesh Details Near the Inlet and Divergent Section of Diffuser

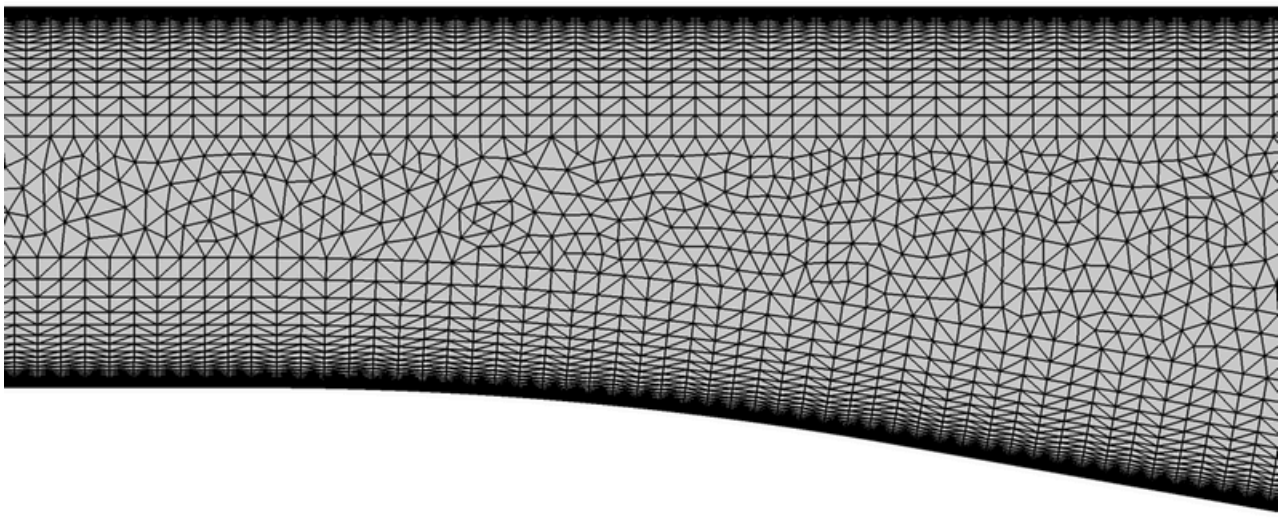


Figure 146: Mesh Details at the Beginning of the Divergence of the Lower Wall in the Diffuser

AcuSolve Results

The AcuSolve solution converged to a steady state and the results reflect the mean flow conditions. As the fully developed turbulent flow enters the divergent section, the peak velocity is maintained until the expansion of the cross-sectional height, forms an adverse pressure gradient. After the flow enters the divergent section, the velocity decreases significantly, due to the expansion of the cross-section height. This causes separation of the flow along the divergent wall and results in an area of recirculation.
The bulk of the flow above the divergent wall maintains its streamwise direction, while a portion of it reverses direction before reattaching further downstream of the divergent section. The following images show the steady state flow solution for flow within the diffuser.

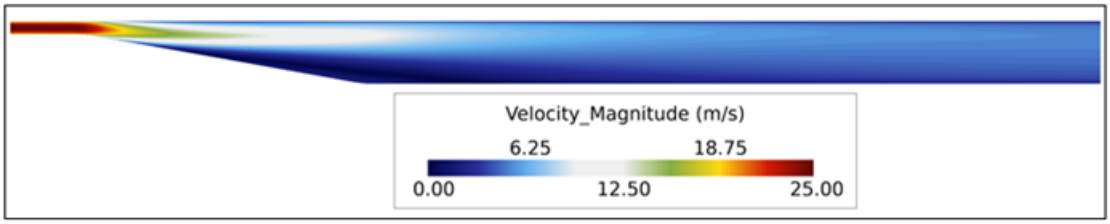


Figure 147: Velocity Contours Within the Diffuser

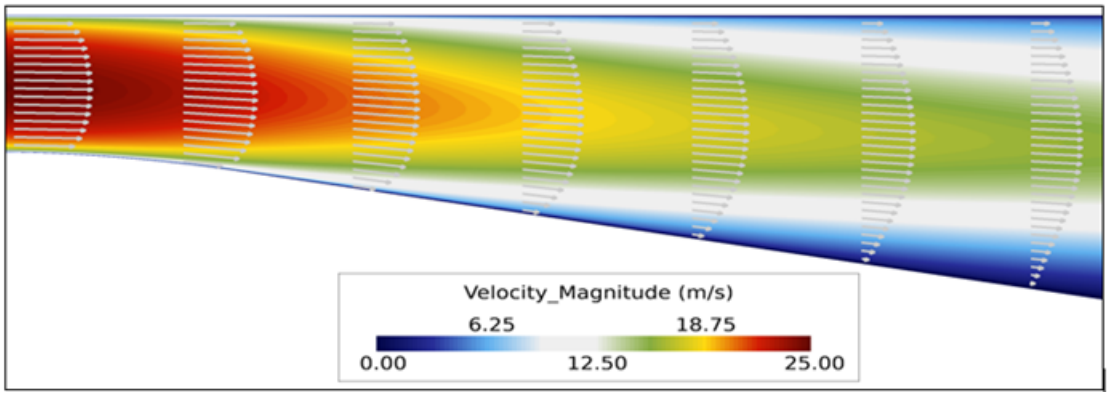


Figure 148: Close up View of Velocity Vectors and Contours of Velocity Magnitude in the Diffuser

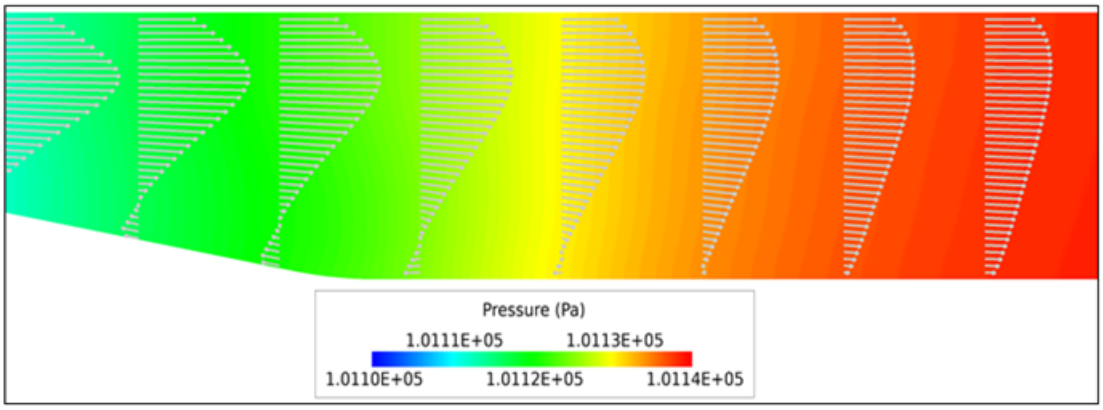


Figure 149: Close up View of Velocity Vectors and Contours of Pressure to Show Recirculation as it Approaches the Reattachment Point

Upstream of the diffuser section, the streamline velocity increases as the distance from the lower wall increases until it reaches the maximum velocity at the center of the channel. As the flow enters the divergent section of the channel, the streamwise velocity decreases near the bottom wall. The images below show the velocity profiles at three locations as measured from the midpoint of the curve where the bottom wall begins to diverge (X=0.0) for each of the tested turbulence models. The first location, where X/H = -5.944, is close to the inlet. The second location, where X/H = 13.468, is approximately 0.2 m downstream of the divergent section (~ 0.1 m from the fully expanded section). The third location, where X/H = 24.066, is approximately 0.16 m downstream of the point where the diffuser has reached the maximum height. In these plots the black circles represent the experimental measurements (Buice and Eaton 2000), the solid red lines for the prediction for the Spalart Allmaras model, solid blue lines for the prediction for the SST model, solid green lines for the prediction for the K-ω model and solid cyan lines for the K-ε model, representing the AcuSolve results. The non-dimensional height is represented by the fraction of the vertical height (Y) divided by the inlet height (H) and the velocity is normalized by the inlet velocity (Uref).

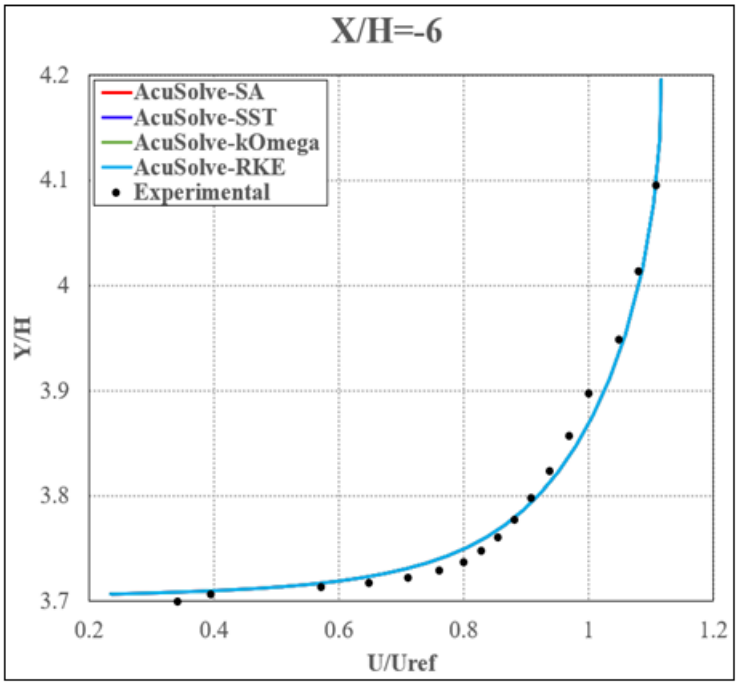


Figure 150: Non-Dimensional Streamwise Velocity Plotted Against Vertical Location Near the Inlet (X/H=-5.9442, Where the Reference Point is 6H Downstream of the Inlet)

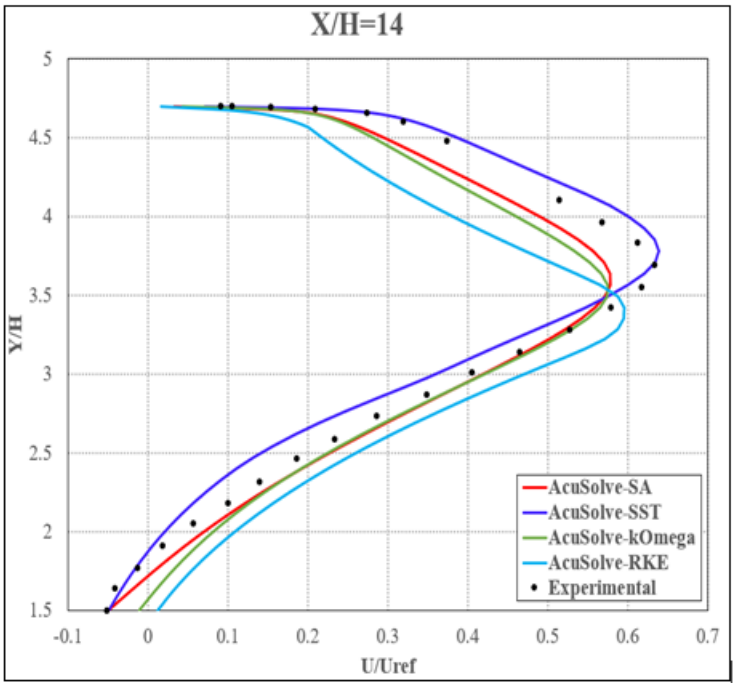


Figure 151: Non-Dimensional Streamwise Velocity Plotted Against Vertical Location Approximately 0.2 m Downstream of the Divergence (X/H = 13.468, Where the Reference Point is 6H Downstream of the Inlet)

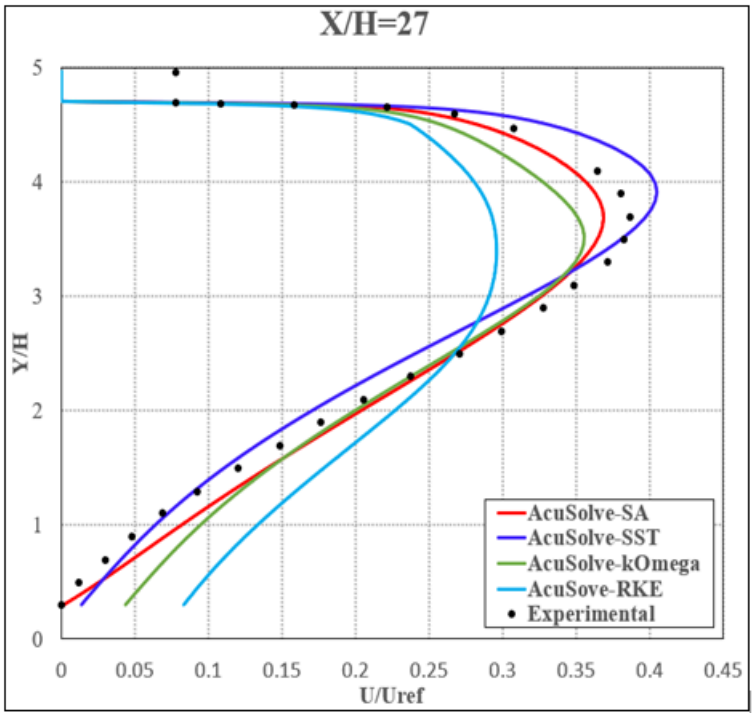


Figure 152: Non-Dimensional Streamwise Velocity Plotted Against Vertical Location Approximately 0.2 m Downstream of the Transition to the Fully Divergent Section (X/H = 27.066, Where the Reference Point is 6H Downstream of the Inlet)

The non-dimensional pressure coefficient (Cp) all along the inlet-bottom stretch of the diffuser is calculated using the reference pressure at X=-3H (at the bottom wall) and with reference velocity (Uref) at the inlet with the value of 22.3152 (m/s). The predicted non-dimensional pressure coefficients are compared to experimental results. The figure below shows Cp, along a constant vertical height, as a function of the streamwise distance from the inlet of the channel. The results demonstrate that AcuSolve is capable of accurately predicting the pressure within the diffuser within the expected range based on the type of turbulence model used. The performance of the three turbulence models were found to be consistent with previously published results for flow through the diffuser as published by Buice and Eaton (2000), with the SST model predicting the pressure distribution most accurately.

Note: The inlet of the experimental duct was 6H longer than that modeled - AcuSolve values where X/H < -6 are reported as the inlet value.

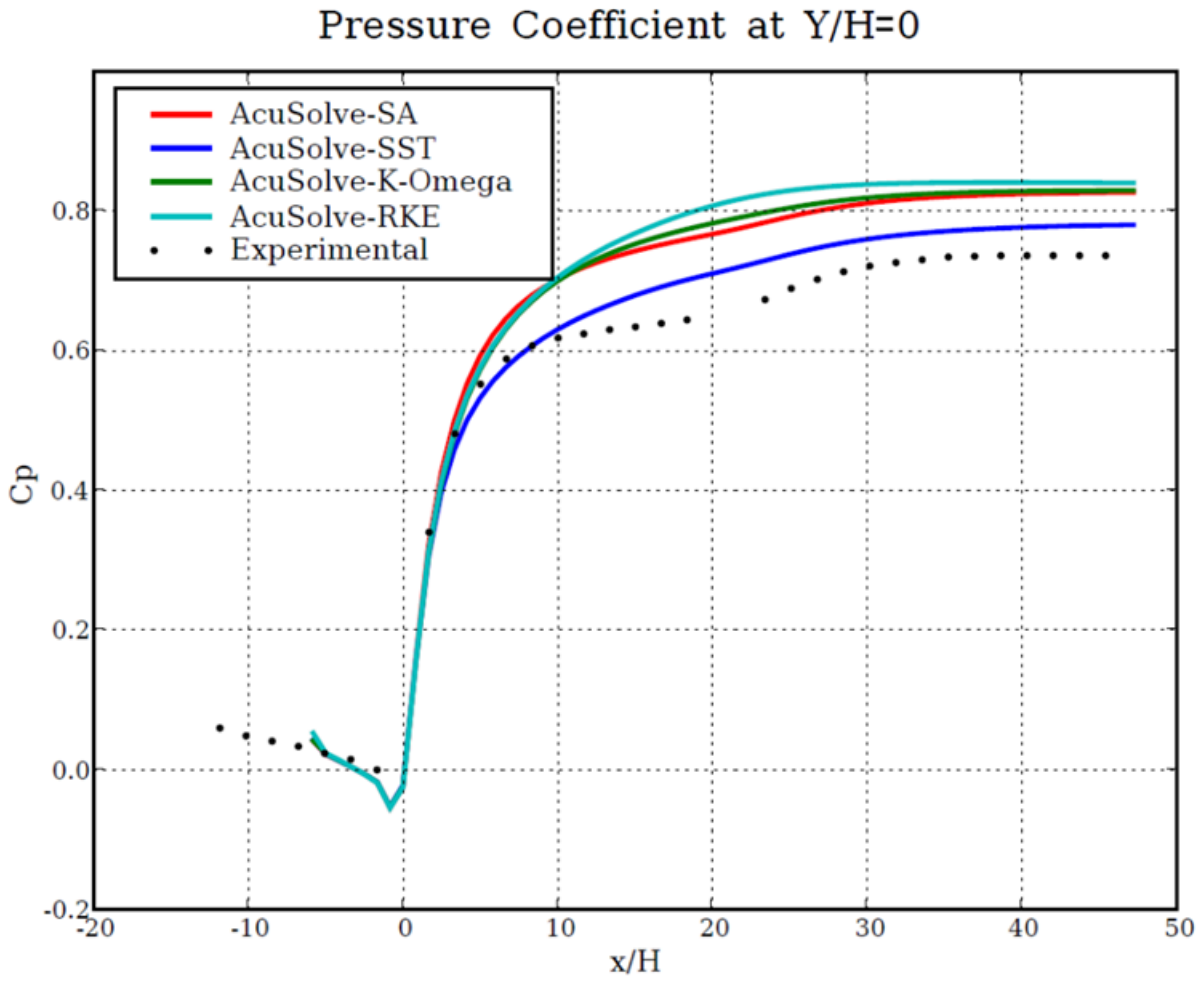


Figure 153: Non-Dimensional Pressure Coefficient (Cp) Plotted Against Relative Distance Along the Diffuser at a Constant Height Equal to the Bottom of the Inlet

Summary

In this application, a fully developed turbulent flow at a Reynolds number of 20,000 is studied. Due to the adverse pressure gradient, separation of flow occurs and causes recirculation in the divergent

section of the diffuser. The results were found to be consistent with previously published computational studies and experimental data. The results of this validation demonstrate the ability of AcuSolve to accurately predict the separation point, the recirculation that occurs along the divergent wall, and the reattachment point in the straight section of the diffuser.

Simulation Settings for Turbulent Flow with Separation in an Asymmetric Diffuser

HyperMesh CFD database file: `<your working directory>\asymmetric_diffuser_turbulent\asymmetric_diffuser_turbulent.hm`

Global

- Problem Description
  - Analysis type - Steady State
  - Turbulence equation - Spalart Allmaras
- Auto Solution Strategy
  - Max time steps - `150`
  - Relaxation Factor - `0.4`
- Material Model
  - Air
    - Density - `1.225.0` kg/m3
    - Viscosity - `1.8325e-5` kg/m-sec

  Model
- Volume
  - Volume
    - Element Set
      1. Material model - Air
- Surfaces
  - Bottom
    - Simple Boundary Condition
      1. Type - Wall
  - Inlet
    - Simple Boundary Condition (disabled to allow for nodal boundary conditions to be set)
    - Advanced Options
      1. Nodal Boundary Conditions
         1. X-Velocity
            1. Type - Linear
            2. Precedence - `2`
            3. Curve fit variable - Y coordinate
            4. Curve fit values (included in database)
         2. Y-Velocity

1 Type - Linear
2 Precedence - 2
3 Curve fit variable - Y coordinate
4 Curve fit values (included in database)

3 Eddy Viscosity
1 Type - Linear
2 Precedence - 2
3 Curve fit variable - Y coordinate
4 Curve fit values (included in database)

- Outlet
  - Simple Boundary Condition
    1 Type - Outflow - 101139.0 Pa
- Side 1
  - Simple Boundary Condition
    1 Type - Symmetry
- Side 2
  - Simple Boundary Condition
    1 Type - Symmetry
- Top
  - Simple Boundary Condition
    1 Type - Wall

References

C.U. Buice, and J.K., Eaton. "Experimental Investigation of Flow Through an Asymmetric Plane Diffuser". Journal of Fluids Engineering 122:433-435. June 2000.

S. Obi, K. Aoki and S. Masuda. "Experimental and Computational Study of Turbulent Separating Flow in an Asymmetric Plane Diffuser". Ninth Symposium on Turbulent Shear Flows. p. 305. Kyoto, Japan. August 16-19, 1993.

Turbulent Flow Over a Backward-Facing Step

In this application, AcuSolve is used to simulate fully developed turbulent flow over a backward-facing step. AcuSolve results are compared with experimental results as described in Driver (1985) and on the NASA Langley Research Center Turbulence Modeling Resource web page. The close agreement of AcuSolve results with experimental data and reference turbulence model performance validates the ability of AcuSolve to model cases with turbulent flow that forms a shear layer, recirculates and then reattaches downstream of the divergent step.

Problem Description

The problem consists of a fluid with material properties close to air flowing through a channel containing a sharp expansion, as shown in the following image, which is not drawn to scale. The step causes the flow to recirculate before reattaching downstream of the step. The inlet height of the channel is 8.0 m and expands as a step function to 9.0 m at a distance 20.0 m downstream of the inlet. This expanded section of the channel extends 50 m downstream of the step. The inflow of the channel is defined as fully developed at a Reynolds number (Re) of 36,000, based on the step height to match the experimental conditions. The density of the flow medium is 1.1837 kg/m^3 and the dynamic viscosity is 1.457 X 10^{-3} kg/m-s. The simulation was conducted with the Reynolds Averaged Navier-Stokes equations using four turbulence models, Spalart Allmaras, Shear Stress Transport (SST), K-ω and K-ε.

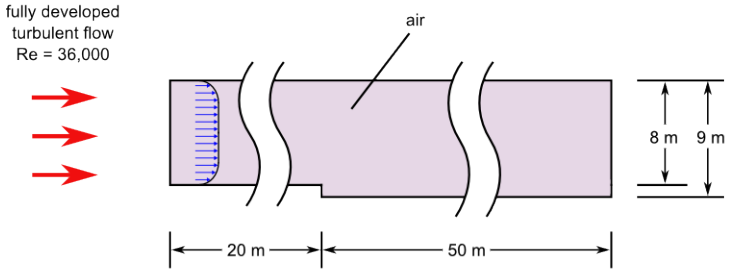


Figure 154: Critical Dimensions and Parameters for Simulating Turbulent Flow Through a Channel with a Backward-Facing Step

The simulation was performed as a two-dimensional problem by constructing a volume mesh that contains a single layer of elements extruded in the cross-stream direction, normal to the flow plane and by imposing symmetry boundary conditions on the extruded planes. The upper and lower walls are specified as no-slip, the inlet velocity and eddy viscosity are specified to match the conditions in the experiment (Driver 1985) at a distance of 20 m upstream of the step.

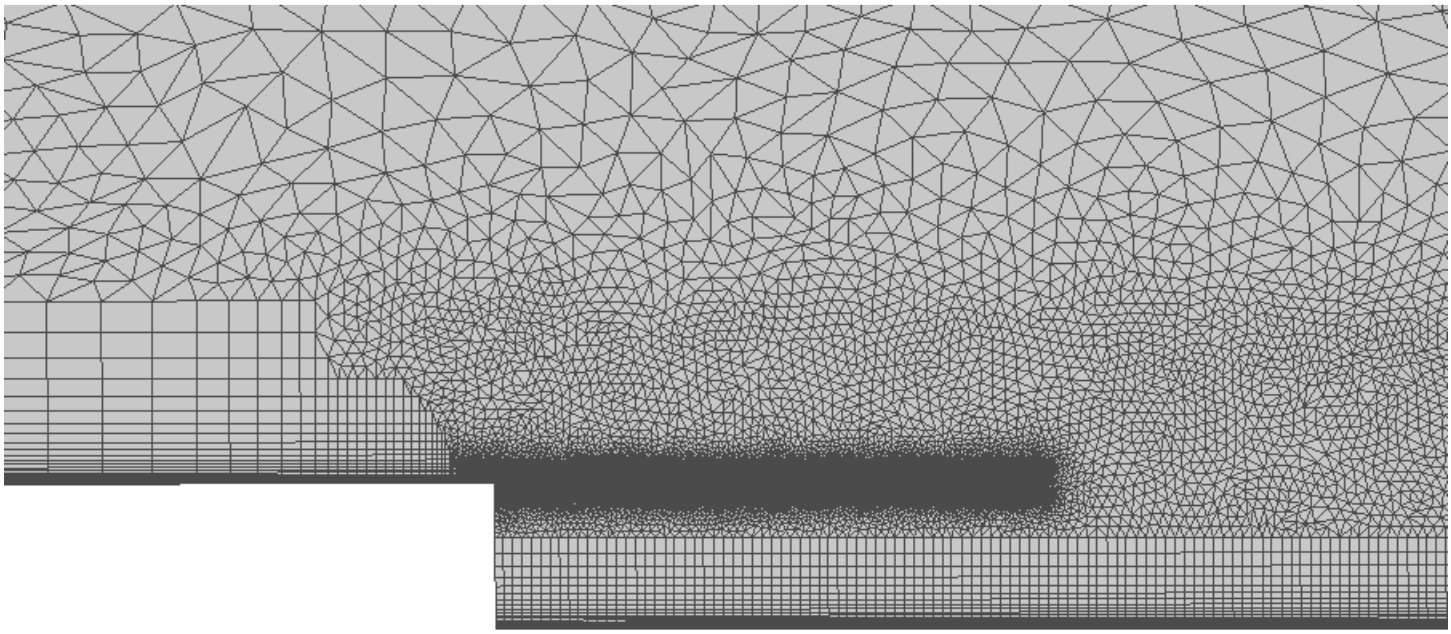


Figure 155: Detail of Mesh Near the Backward-Facing Step

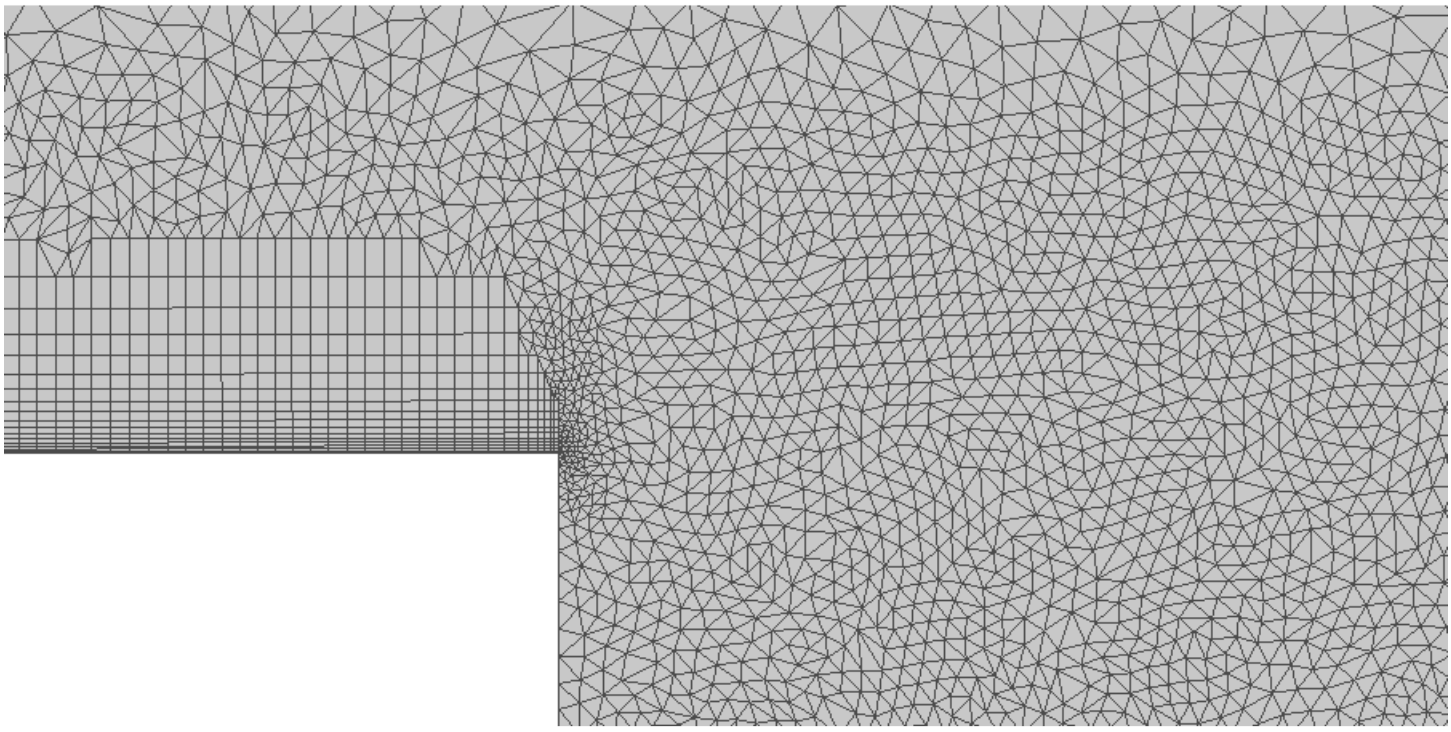


Figure 156: Finer Detail of Mesh Near the Backward-Facing Step

AcuSolve Results

The AcuSolve solution converged to a steady state and the results reflect the mean flow conditions. As the fully developed turbulent flow enters the divergent section, the expansion of the cross-sectional height causes a shear layer to develop above the lower wall. The expansion causes two recirculation zones; one immediately near the step wall and one that extends further downstream near the lower wall. The recirculation region eventually recovers downstream and the flow reattaches. The following images show the flow solution within the channel, demonstrating the recirculation region and reattachment point.

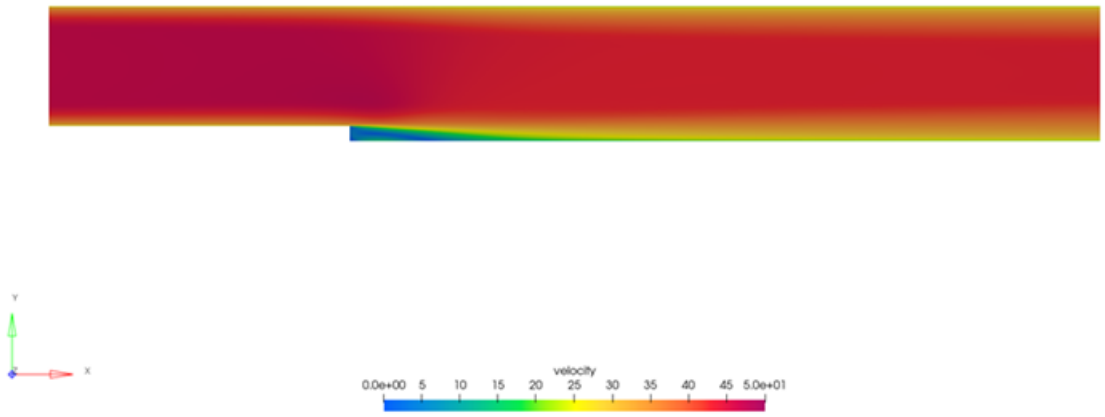


Figure 157: Velocity Contours Showing Low Velocity Near the Step Wall

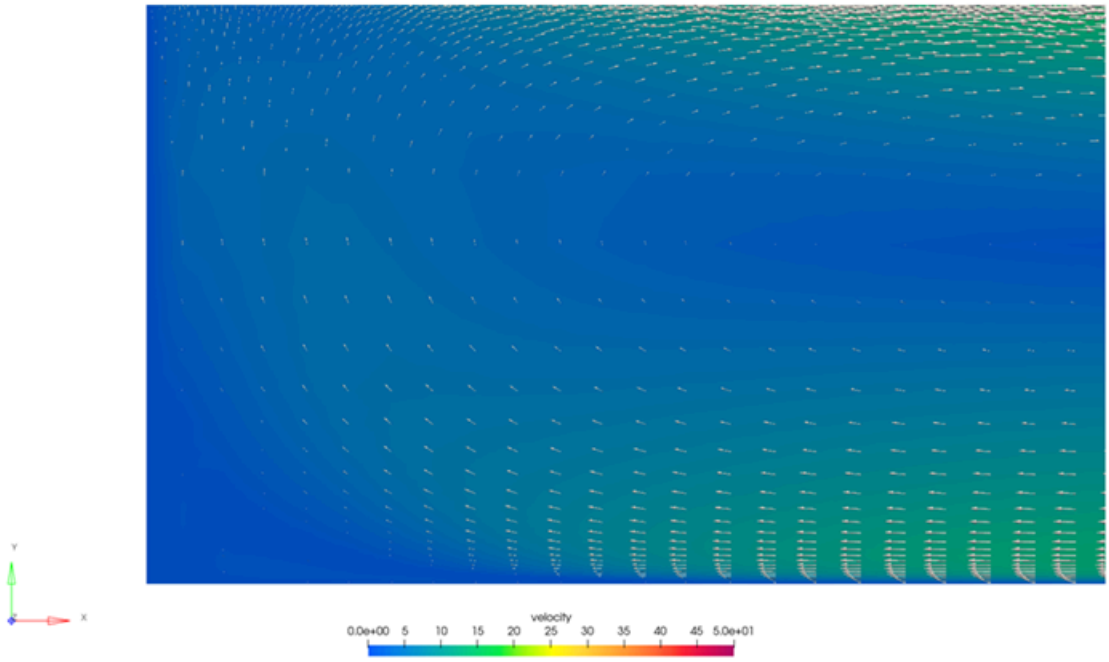


Figure 158: Close-Up View of Velocity Vectors and Contours in the Cross-Stream Plane Directly After the Step

Upstream of the expansion section, the streamwise velocity increases as the distance from the lower wall increases until it reaches the centerline of the channel and then begins decreasing until it reaches zero at the top wall. As the flow passes the step, it expands into the region directly downstream of the step wall, separating from the wall and recirculating until it recovers further downstream. The image below shows the coefficient of pressure along the lower wall of the step compared against experimental results. The coefficient of pressure is calculated using the reference velocity (Uref) obtained at x/H=-4 (centre of the channel) with the reference pressure (Pref) extracted at x/H = 40 (at the wall) so that Cp becomes 0 at x/H=40. The image shows black circles representing the experimental measurements (Driver 1985), a solid red line for the SA model, a solid blue line for the SST model, a solid green line for the K-ω model and a solid cyan line for the K-ε model, representing the AcuSolve results. The resulting pressure coefficient within the channel demonstrates minor differences between the three

turbulence models. The SA model predicts a slightly larger recirculation region and does not reach the peak pressure in the wake of the step, compared to the SST model.

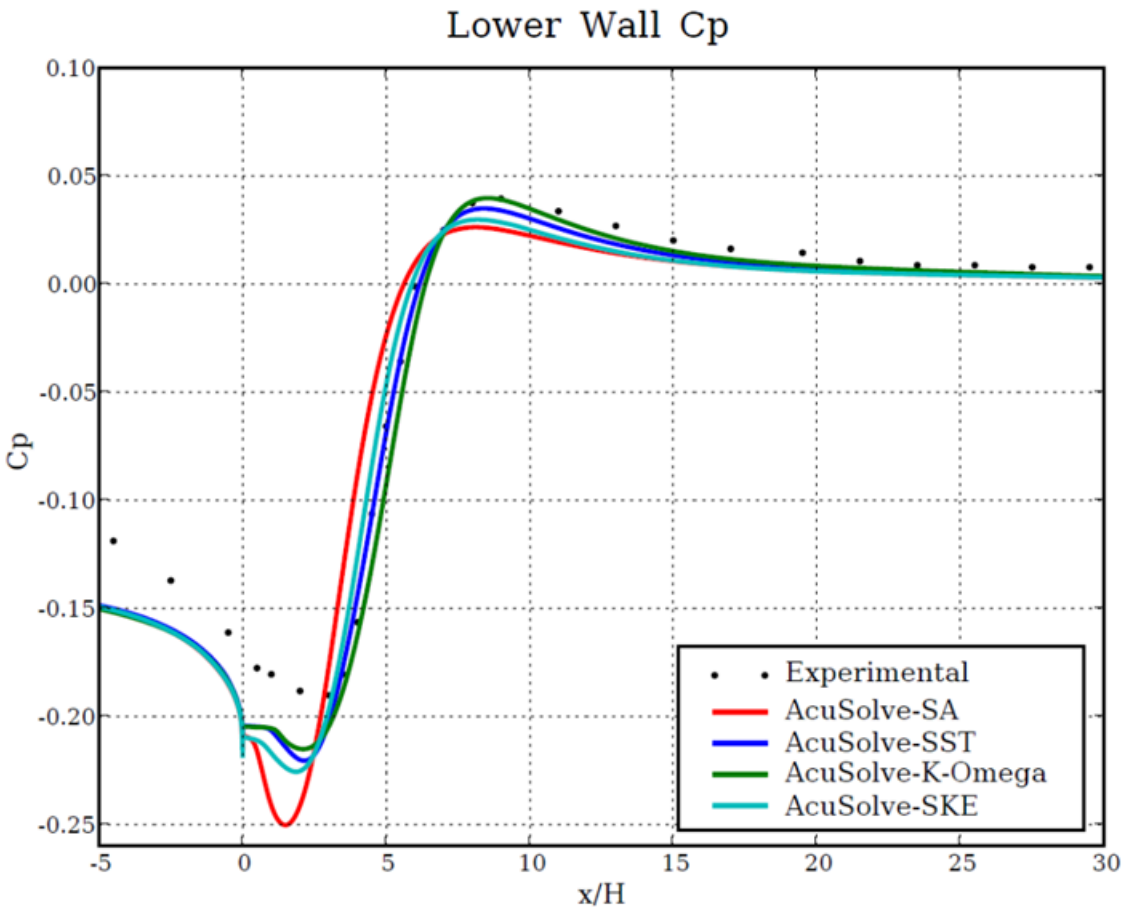


Figure 159: Coefficient of Pressure Plotted Against Location Along the Lower Wall Before and After the Step

Summary

In this application, a fully developed turbulent flow at a Reynolds number of 36,000 is studied and compared against experimental data. The AcuSolve results compare well with the experimental data for pressure coefficient. The performance of the Spalart Allmaras turbulence model was found to be consistent with previously published results for flow over a backward facing step (NASA 2015). The K-ω model appears to perform the best out of the three, predicting the reattachment and pressure distribution most accurately. AcuSolve demonstrates the ability to predict the shear layer in this type of application, the recirculation that occurs downstream of the step, as well as the reattachment point within the channel.

Simulation Settings for Turbulent Flow over a Backward-Facing Step

HyperMesh CFD database file: `<your working directory>\backstep_turbulent\backstep_turbulent.hm`

Global

- Problem Description
  - Analysis type - Steady State

- Turbulence equation - Shear Stress Transport
- Auto Solution Strategy
  - Max time steps - `100`
  - Relaxation Factor - `0.5`
- Material Model
  - Air
    - Density - `1.183` kg/m3
    - Viscosity - `1.4575e-3` kg/m-sec

  Model
- Volume
  - Fluid
    - Element Set
      1. Material model - Air
- Surfaces
  - +Z
    - Simple Boundary Condition
      1. Type - Slip
  - -Z
    - Simple Boundary Condition
      1. Type - Slip
  - Inlet
    - Simple Boundary Condition - (disabled to allow for nodal boundary conditions to be set)
    - Advanced Options
      1. Nodal Boundary Conditions
         1. X-Velocity
            1. Type - Linear
            2. Precedence - Always
            3. Curve fit variable - Y reference coordinate
            4. Curve fit values - (included in database)
         2. Y-Velocity
            1. Type - Linear
            2. Precedence - Always
            3. Curve fit variable - Y reference coordinate
            4. Curve fit values - (included in database)
         3. Z-Velocity
            1. Type - Zero
         4. Kinetic Energy

1. Type - Linear
2. Precedence - Always
3. Curve fit variable - Y reference coordinate
4. Curve fit values - (included in database)

5. Eddy Frequency
   1. Type - Linear
   2. Precedence - Always
   3. Curve fit variable - Y reference coordinate
   4. Curve fit values - (included in database)

- Outlet
  - Simple Boundary Condition
    1. Type - Outflow
- Wall - Lower - Downstream
  - Simple Boundary Condition
    1. Type - Wall
    2. Turbulence wall type - Low Reynolds Number
- Wall - Lower - Upstream
  - Simple Boundary Condition
    1. Type - Wall
    2. Turbulence wall type - Low Reynolds Number
- Wall - Step
  - Simple Boundary Condition
    1. Type - Wall
    2. Turbulence wall type - Wall Function
- Wall - Upper
  - Simple Boundary Condition
    1. Type - Wall
    2. Turbulence wall type - Low Reynolds Number

References

D. M. Driver and H. L. Seegmiller. "Features of Reattaching Turbulent Shear Layer in Divergent Channel Flow". AIAA Journal, 23(2): 163-171. Feb 1985.

NASA Langley Research Center Turbulence Modeling Resource webpage. http://turbmodels.larc.nasa.gov/backstep_val.html. Accessed June 2021.

Turbulent Flow Past a Convex Curve in a Channel

In this application, AcuSolve is used to simulate fully developed turbulent flow through a channel containing a convex curve in the lower wall. AcuSolve results are compared with experimental results as described in Smits (1979) and on the NASA Langley Research Center Turbulence Modeling Resource webpage. The close agreement of AcuSolve results with experimental data and reference turbulence model performance validates the ability of AcuSolve to model cases with turbulent flow moving past a convex curved wall.

Problem Description

The problem consists of a fluid with material properties close to air flowing through a channel containing a 30° swept wall, with a lower convex wall. The inlet channel height and remaining duct height is 0.127 m. The bulk velocity (v) normal to the inlet is 31.9 m/s and an integrated outflow pressure is specified to allow the flow to pass through the channel. The flow develops into fully turbulent flow at a Reynolds's number (Re) of 2,100,000. The density of the flow medium is 1.225 kg/m3 and the dynamic viscosity is 1.8608 X 10-5 kg/m-s. The simulation is conducted with the Reynolds Averaged Navier-Stokes equations using the Spalart Allmaras, Shear Stress Transport (SST), K-ω and Realizable K-ε turbulence models. The flow conditions are compared against experimental data and the current state-of-the-art performance for coefficient of pressure and coefficient of friction.

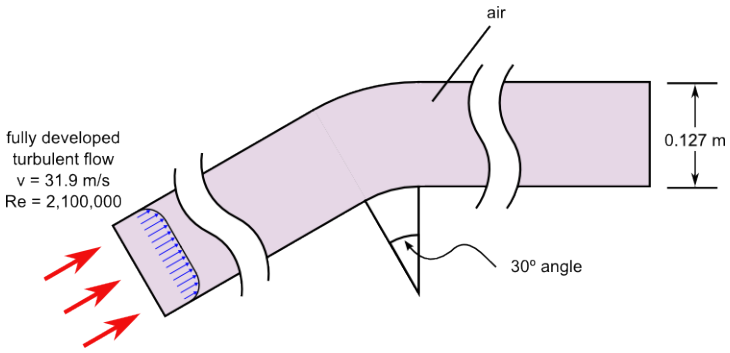


Figure 160: Critical Dimensions and Parameters for Simulating Turbulent Flow Through a Convex Channel

The simulation was performed as a two dimensional problem by restricting flow in the out-of-plane direction through the use of a mesh that is one element thick. The upper and lower walls are specified as no-slip, the inlet velocity and eddy viscosity are specified normal to the inlet face to match the experimental Reynolds Number.

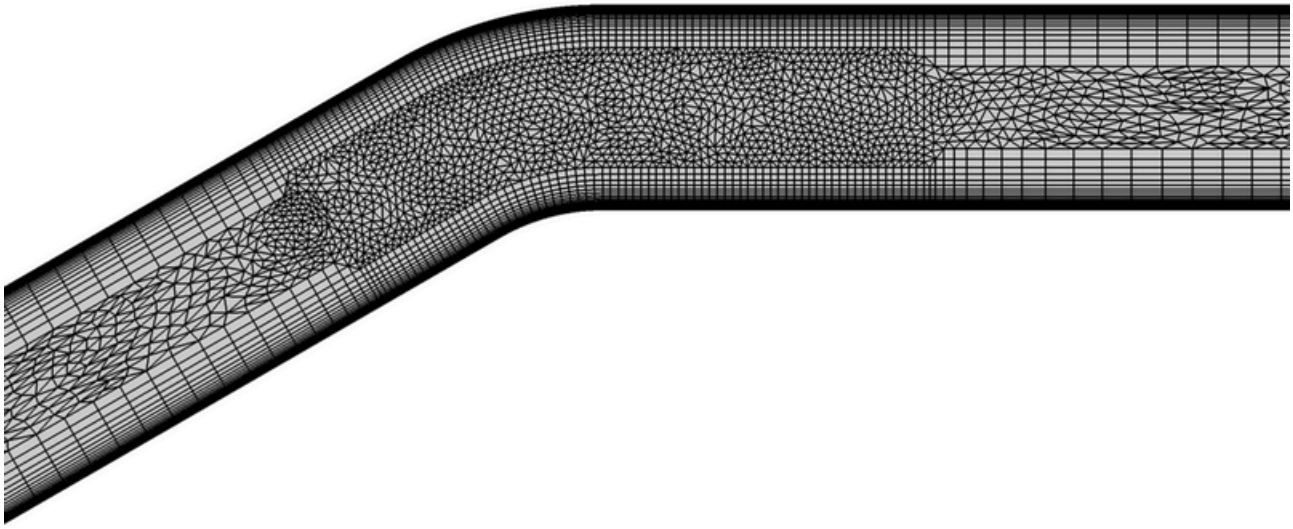


Figure 161: Detail of the Mesh used for Simulating Turbulent Flow Through a Convex Channel

AcuSolve Results

The AcuSolve solution converged to a steady state and the results reflect the mean flow conditions within the channel. As the fluid enters the channel it develops into fully turbulent flow exhibiting a steep parabolic velocity profile across the width of the channel. The flow begins to accelerate near the lower wall and decelerate near the top wall as it approaches the 30° bend. The results show that the upper (concave) wall destabilizes the boundary layer, increasing the eddy viscosity and forcing the flow velocity to decrease. The following figures show the flow conditions within the channel.

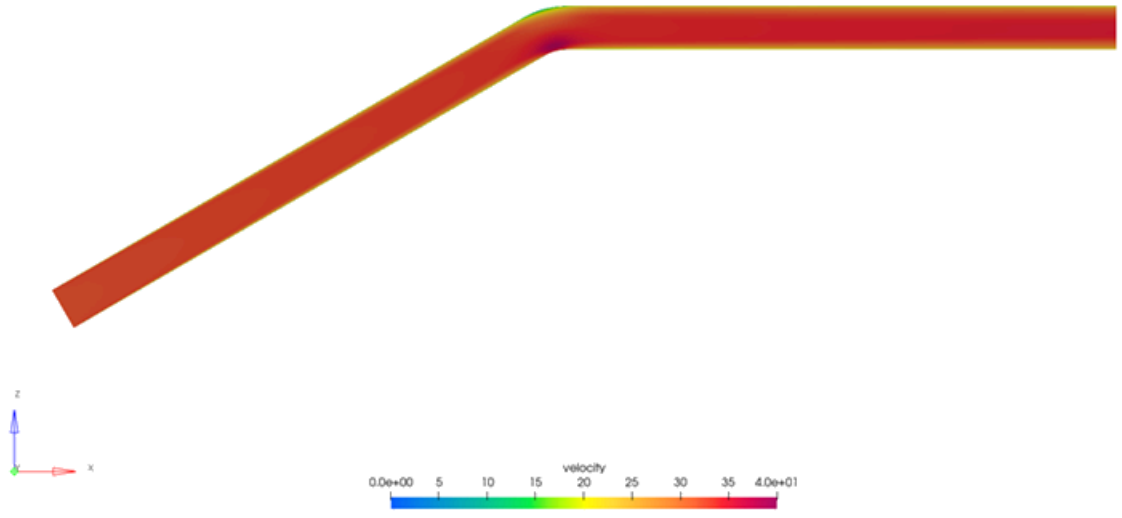


Figure 162: Velocity Contours in the Streamwise Plane

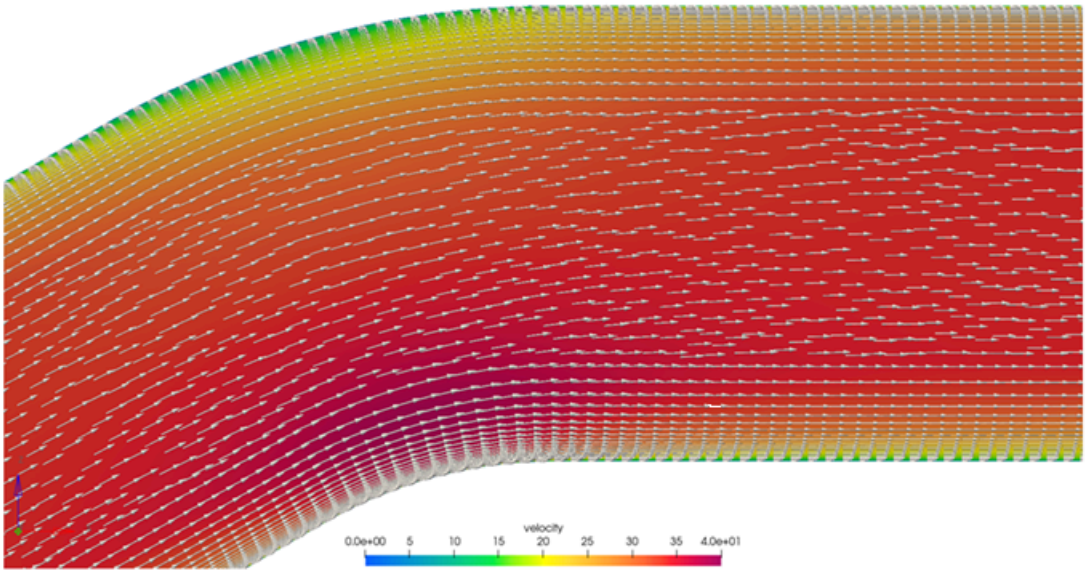


Figure 163: Close up View of Velocity Vectors and Velocity Contours at the 30° Bend

Upstream of the curved section of the channel, the flow normal to the channel opening increases as the distance from the lower wall increases until it reaches the centerline of the channel and then begins decreasing until it reaches zero at the top wall. As the flow approaches the curved section, it begins to accelerate, requiring that the flow velocity near the upper wall decrease to conserve momentum. The relatively low angle of curvature in the channel does not cause the accelerated fluid to recirculate. The images below show the coefficient of pressure (Cp) and coefficient of skin friction (Cf) along the lower wall of the channel. The images show black circles representing the experimental measurements (Smiths 1979), solid red lines for the SA model, solid blue lines for the SST model, solid green lines for the K-ω model and a solid cyan line for the K-ε model, representing the AcuSolve results. The coefficient of pressure within the channel is predicted nearly identically compared to the experiment for each of the turbulence models. It appears that the SST and K-ε models capture the low velocity region with the best accuracy, demonstrating that the flow velocity decreases significantly, but does not recirculate within the channel. This is shown in the friction coefficient plot, where the coefficient of friction, and subsequently the wall shear stress, does not decrease below zero.

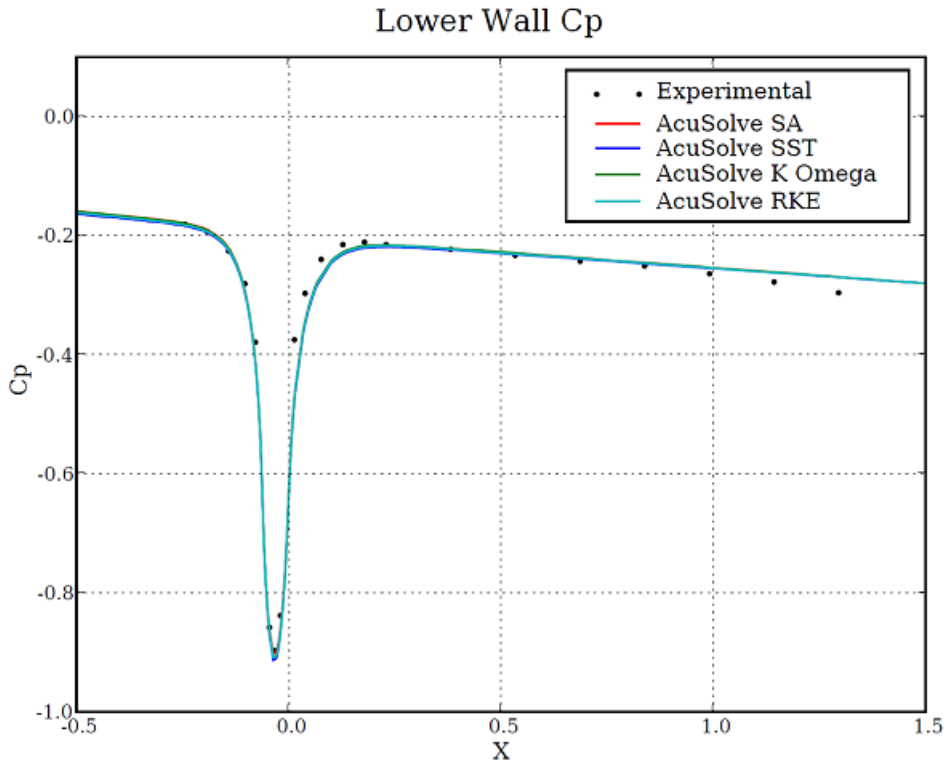


Figure 164: Coefficient of Pressure Plotted Against Relative Distance Along the Lower Wall from the Curve

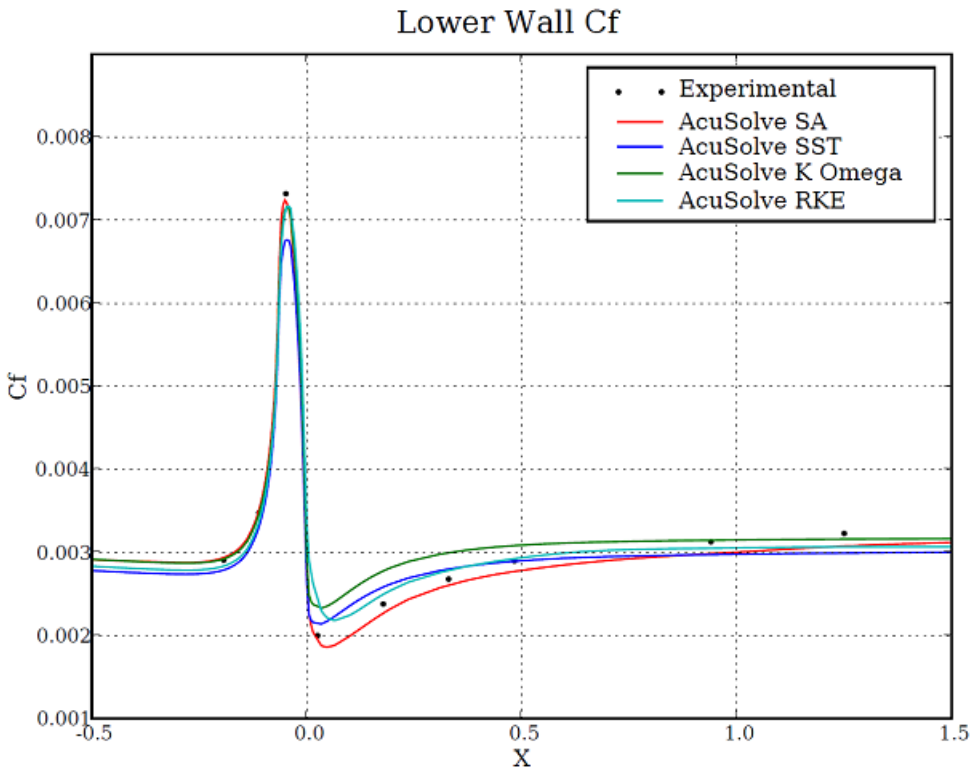


Figure 165: Skin Friction Coefficient Plotted Against Relative Distance Along the Lower Wall from the Curve

Summary

In this application, a turbulent flow through a curved channel at a Reynolds number of 2,100,000 is simulated and compared against experimental data. The AcuSolve results compare well with the experimental data for pressure coefficient and skin friction coefficient within the channel. The performance of the Spalart Allmaras turbulence model was found to be consistent with previously published results for flow through a convex-curved channel (NASA 2015) and the SST turbulence model appears to predict the shear stress on the lower wall most accurately. AcuSolve demonstrates the ability to predict the complex boundary layers resulting from the curvature of the channel and accurately predicts the propagation of the flow further downstream.

Simulation Settings for Turbulent Flow past a Convex Curve in a Channel

HyperMesh CFD database file: `<your working directory>\convex_curvature_turbulent \convex_curvature_turbulent.hm`

Global

- Problem Description
  - Analysis type - Steady State
  - Turbulence equation - Spalart Allmaras
- Auto Solution Strategy
  - Max time steps - `100`
  - Convergence tolerance - `0.0001`

    - Relaxation factor - `0.4`
- Material Model
    - Fluid
        - Density - `1.225` kg/m3
        - Viscosity - `1.8603e-5` kg/m-sec

  Model
- Volumes
    - Fluid - elbow
        - Element Set
            1. Material model - Fluid
    - Fluid - inlet
        - Element Set
            1. Material model - Fluid
    - Fluid - outlet
        - Element Set
            1. Material model - Fluid
- Surfaces
    - -Y
        - Simple Boundary Condition
            1. Type - Slip
    - +Y
        - 1. Type - Slip
    - Inlet
        - Simple Boundary Condition
            1. Type - Inflow
            2. Inflow type - Velocity
            3. Inflow velocity type - Normal
            4. Normal velocity - `31.9` m/sec
            5. Turbulence input type - Direct
            6. Eddy viscosity - `1.3671e-7` m2/sec
- Internal
    - Simple Boundary Condition - (disabled)
- Lower Wall
    - Simple Boundary Condition
        - Type - Wall
        - Turbulence wall type - Low Reynolds Number
- Outlet

    - Simple Boundary Condition
        - Type - Outflow
- Upper Wall
    - Simple Boundary Condition
        - Type - Wall
        - Turbulence wall type - Low Reynolds Number

References

A. J. Smits, S. T. B. Young, and P. Bradshaw. "The Effect of Short Regions of High Surface Curvature on Turbulent Boundary Layers". Journal of Fluid Mechanics. 94(2):209-242. 1979

NASA Langley Research Center Turbulence Modeling Resource webpage. http://turbmodels.larc.nasa.gov/smitscurve_val.html. Accessed May 2021.

Heat Transfer Between Radiating Concentric Cylinders

In this application, AcuSolve is used to simulate the heat transfer due to radiation between concentric cylinders. The inner and outer cylinders are held at constant temperature and are defined to be radiation surfaces. AcuSolve results are compared with analytical results for temperature as described in Incropera (2006). The close agreement of AcuSolve results with analytical results validates the ability of AcuSolve to model cases with radiation heat transfer requiring view factor computation.

Problem Description

The problem consists of a fluid with arbitrary material properties between two infinitely long concentric cylinders, as shown in the following image, which is not drawn to scale. The radius of the outer cylinder is 0.0468 m and the radius of the inner cylinder is 0.0178 m. The inner cylinder is defined to have a constant wall temperature at 773.0 K (500 °C). The outer cylinder is defined to have a constant wall temperature at 300.0 K (27 °C). Both cylinders are specified to radiate as grey bodies, with emissivity set to 0.03778.

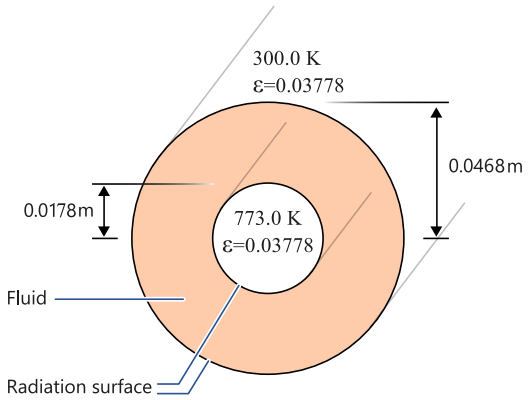


Figure 166: Critical Dimensions and Parameters Used for Simulating Radiation Between Two Concentric Cylinders

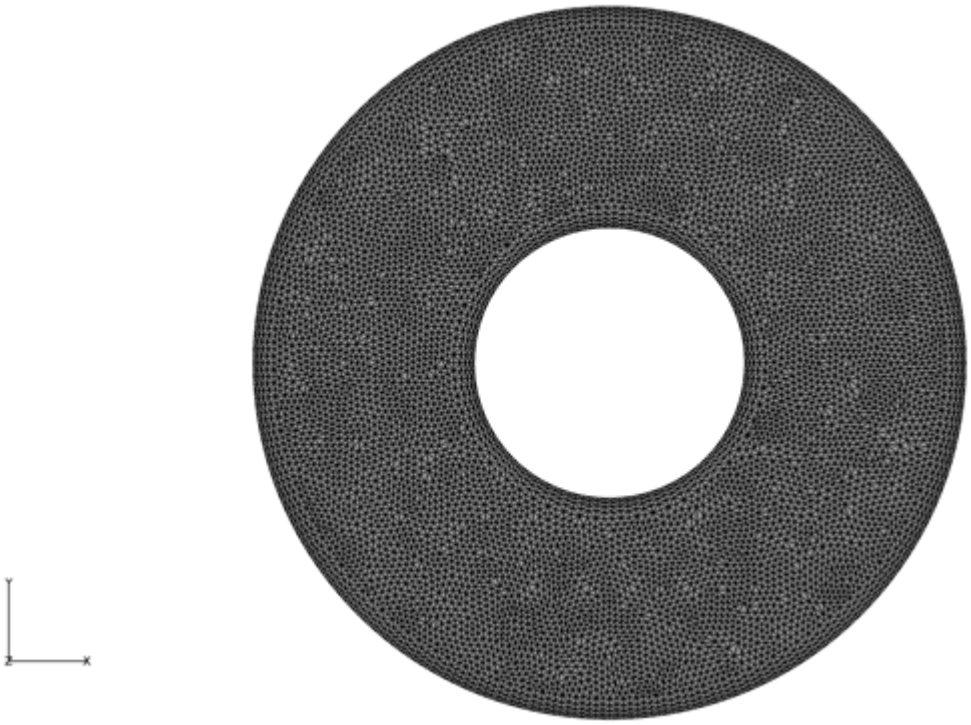


Figure 167: Mesh used for Simulating Radiation Between Two Concentric Cylinders

The simulation was performed as a two-dimensional problem by constructing a volume mesh that contains a single layer of elements normal to the radial and circumferential directions.

AcuSolve Results

The AcuSolve solution converges to a steady state and the results reflect the mean temperature distribution. As the inner diameter is considerably hotter than the outer, a heat flux, due to radiation, is present between the cylinders. The temperature within the medium reduces logarithmically as a function of the radius. The following images show the temperature with the medium as a function of radius from the center. The temperature is compared with the analytical solution as described in Incropera (2006). The image below shows black circles representing the analytical solution and a solid red line for the AcuSolve results.

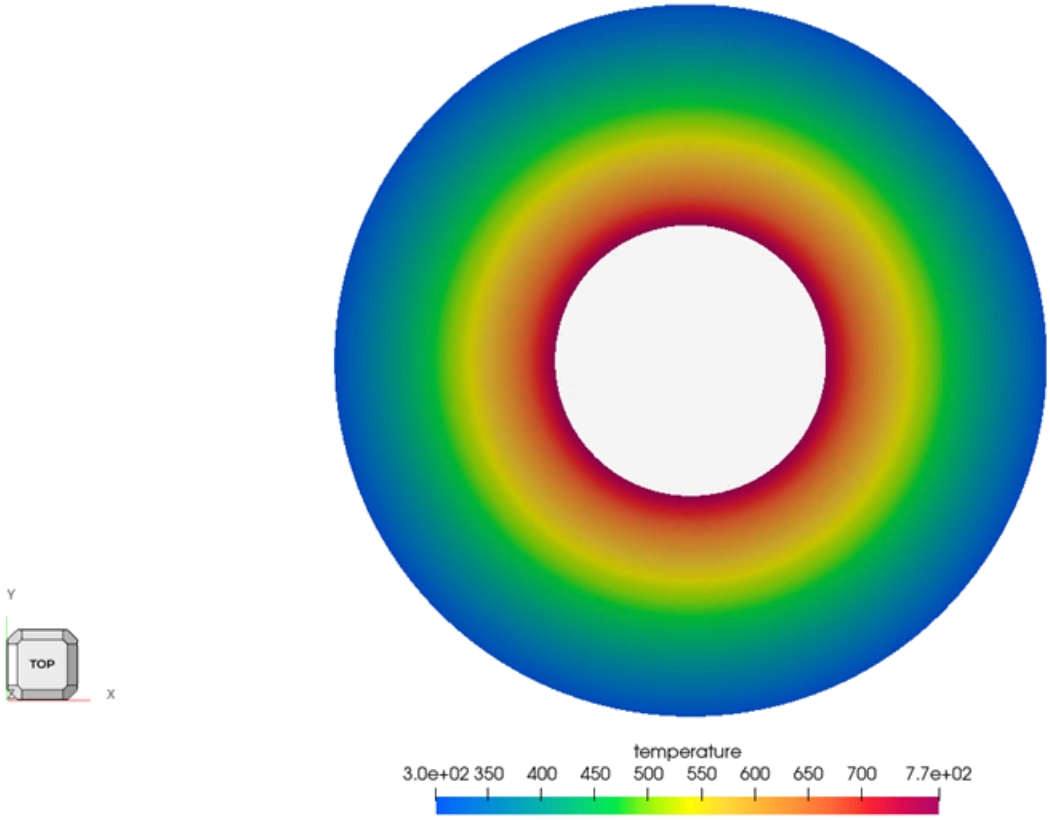


Figure 168: Contours of Temperature Between the Concentric Cylinders

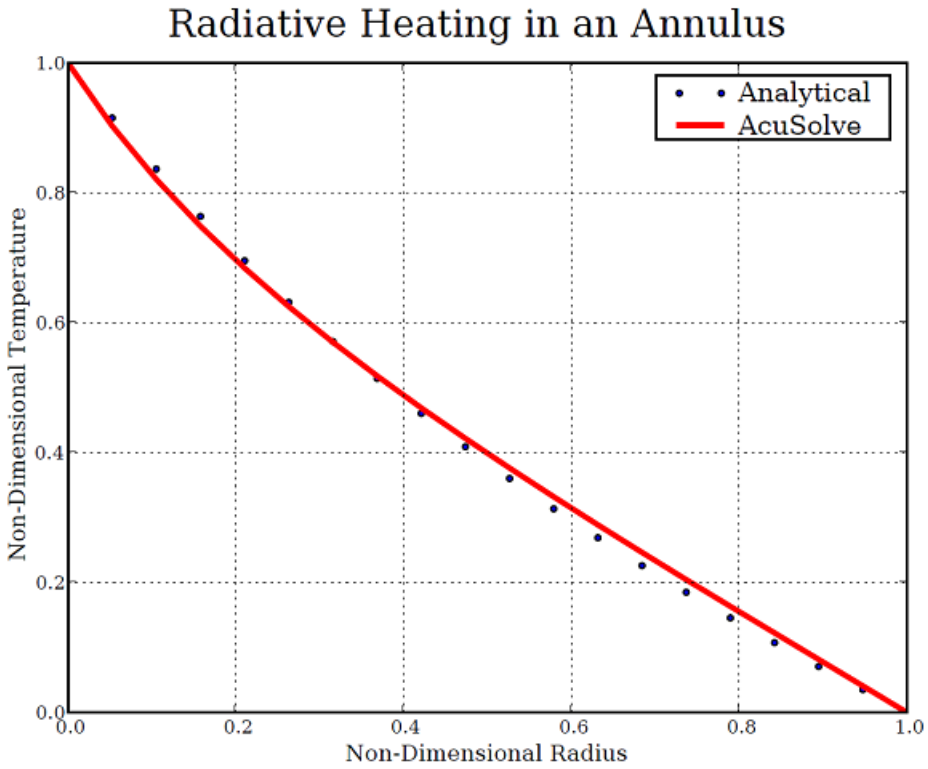


Figure 169: Non Dimensional Temperature Distribution Within the Annulus as a Function of Non Dimensional Radius

Summary

The AcuSolve solution compares well with analytical results for heat transfer due to radiation between two concentric cylinders. In this application, an arbitrary material is subjected to a heat flux that is calculated based on the view factors within the model. As a result of radiative heat flux a temperature distribution between the two cylinders develops. The AcuSolve solution for the temperature as a function of radius matches well compared to the analytical solution.

Heat Transfer Between Radiating Concentric Cylinders

HyperMesh CFD database file: `<your working directory>\annulus_radiation \annulus_radiation.hm`

Global

- Problem Description
  - Analysis type - Steady State
  - Temperature equation - Advective Diffusive
  - Radiation equation- Enclosure
- Auto Solution Strategy
  - Convergence tolerance - `0.0001`
  - Relaxation Factor- `0.4`
  - Flow- off

    - Enclosure radiation- on
- Material Model
    - Material
        - Conductivity
            1. Type - Constant
            2. Conductivity- `1.0`
- Emissivity Model
    - Grey Body
        - Emissivity- `0.03778`
    - Black Body
        - Emissivity- `1.0`

  Model
- Volumes
    - Medium
        - Element Set
            1. Medium - Fluid
            2. Material model- Material
- Surfaces
    - ID
        - Simple Boundary Condition
            1. Type- Wall
            2. Temperature BC type- Value
            3. Temperature- `773.0` K
        - Radiation Surface
            1. Type- Wall
            2. Emissivity model- Grey Body
    - Max_Z
        - Simple Boundary Condition
            1. Type- Symmetry
        - Radiation Surface
            1. Type- Wall
            2. Emissivity model- Black Body
    - Min_Z
        - Simple Boundary Condition
            1. Type- Symmetry
        - Radiation Surface
            1. Type- Wall

2. Emissivity model- Black Body

- OD
  - Simple Boundary Condition
    1. Type- Wall
    2. Temperature BC type- Value
    3. Temperature- `300.0` K
  - Radiation Surface
    1. Type- Wall
    2. Emissivity model- Grey Body

References

F. P. Incropera and D. P. DeWitt. "Fundamentals of Heat Transfer - Sixth Edition". John Wiley & Sons. New York. 2006.

Turbulent Mixing Layers in an Open Channel

In this application, AcuSolve is used to simulate the mixing of two streams of fluid with different velocities moving past a splitter plate. AcuSolve results are compared with experimental results as described in J. Delville, et al. (1989). The close agreement of AcuSolve results with the experimental results validates the ability of AcuSolve to model mixing layers in the turbulent flow regime.

Problem Description

The problem consists of two streams of fluid having material properties of standard air with density of 1.2 kg /m^3 and molecular viscosity of 1.7189 kg/m-sec. The two fluid streams enter an open channel separated by a splitter plate at two streamwise locations with differing velocities. The length of the channel is 1.8 m for the top portion and 1.5 m for the bottom portion. The inlet velocity of the top section is 41.54 m/s, producing a Reynolds's number of 2900, based on l=1.0 mm, while the inlet velocity of the lower section is 22.4 m/s, giving a Reynolds's number of 1200, as shown in the following image, which is not drawn to scale. The model is simulated as steady state with constant inflow conditions, using the Spalart Allmaras (SA) turbulence model. The velocity profile is computed for several locations downstream of the splitter plate and compared against the experimental data, as described in Delville, 1989.

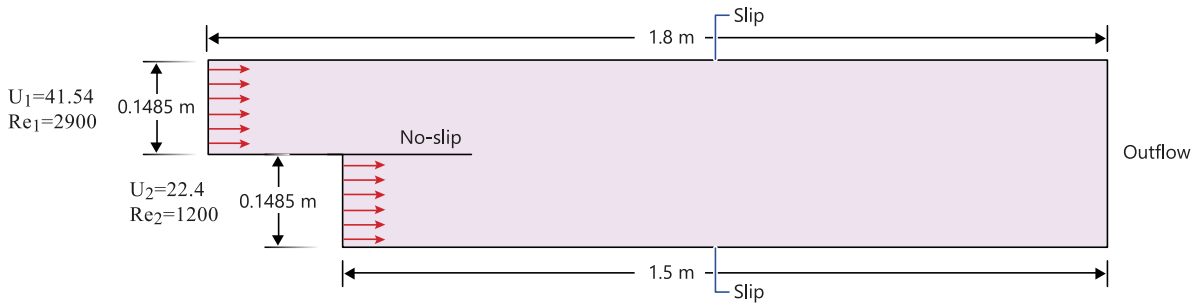


Figure 170: Critical Dimensions and Parameters Used for Simulating the Turbulent Mixing Layer

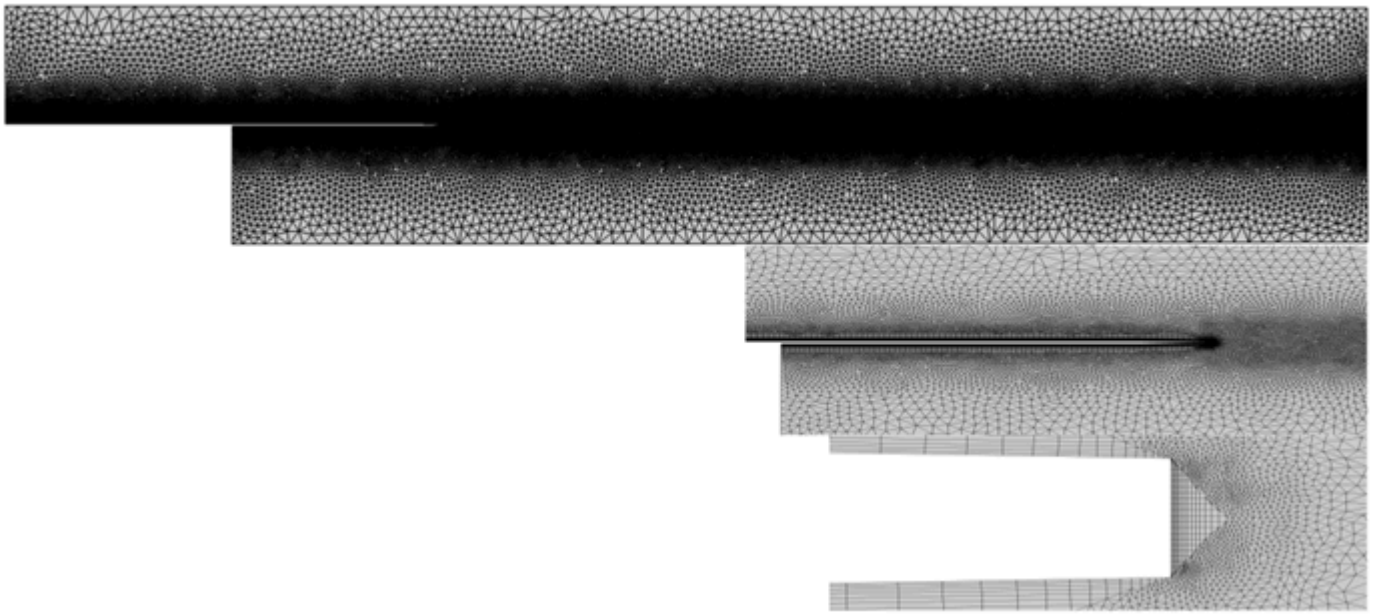


Figure 171: Mesh used for Simulating the Turbulent Mixing Layer Showing Close up Images Near the Trailing Edge of the Plate

The simulation was performed as a two dimensional problem by constructing a volume mesh that contains a single layer of elements extruded in the cross stream direction, normal to the flow plane and by imposing symmetry boundary conditions on the extruded planes. The upper and lower walls are specified as slip, the splitter plate is specified as no-slip and the inlet velocity and eddy viscosity are prescribed as constant values.

AcuSolve Results

The AcuSolve solution converged to a steady state and the results reflect the mean flow conditions within the open channel. The simulation result shows a developing flow field with the fluids fully separated as they pass the edge of the splitter plate. As the fluid travels downstream of the splitter plate, the dissimilar velocity fields produce a shear layer that results in momentum exchange between the two streams. The shear layer diffuses as the fluid travels further downstream. The relative velocity as a function of the normalized boundary layer height is computed from AcuSolve and compared with experimental data at three measurement stations, 0.2 m, 0.65 m and 0.95 m away from the trailing edge of the plate, as described in Delville, 1989. The image below shows black circles representing the experimental data and a solid red line for the AcuSolve results.

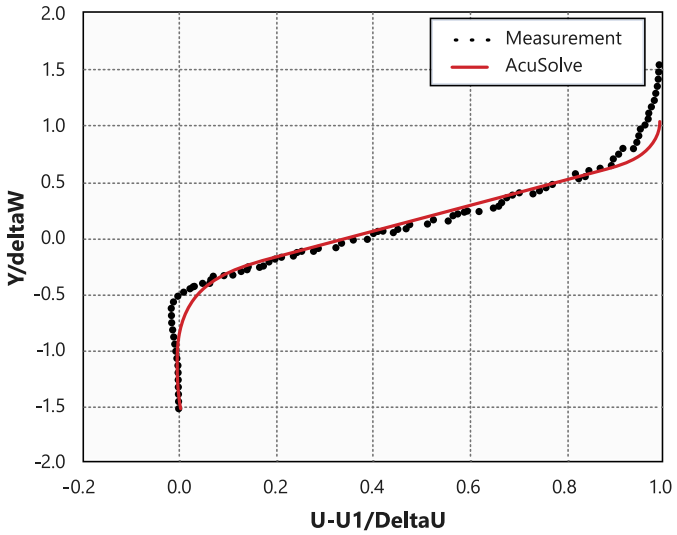


Figure 172: Relative Velocity within the Channel Compared Against Experimental Data Showing Experimental and Simulated Results for the SA Turbulence Model

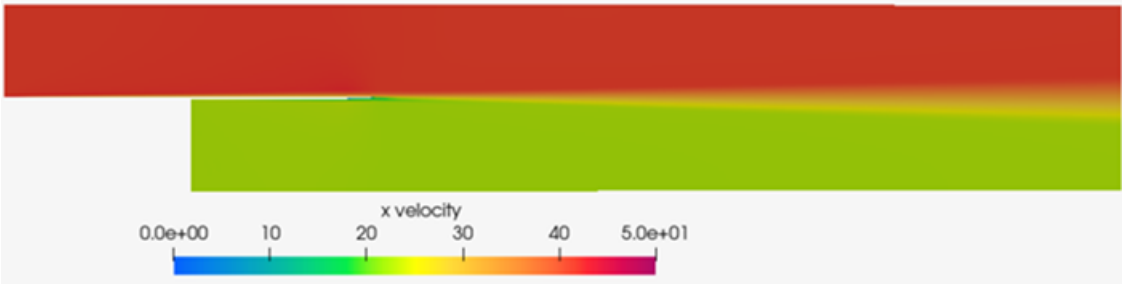


Figure 173: Velocity Magnitude Within the Channel

Summary

The AcuSolve solution compares well with experimental data for turbulent mixing within an open channel. In this application, the shear layer resulting from the dissimilar velocities of the incoming fluid streams results in an exchange of momentum within the channel. The amount of numerical dissipation from the grid is kept to a minimum to produce a good agreement with the experimental data. The good agreement with experimental results for the simulated turbulence model compares well with the measurement and previously published results, demonstrating that AcuSolve is capable of predicting turbulent mixing layers with relatively modest grid levels and the one equation turbulence model.

Simulation Settings for Turbulent Mixing Layers in an Open Channel

HyperMesh CFD database file: `<your working directory>\mixing_layer_turbulent \mixing_layer_turbulent.hm`

Global

- Problem Description
  - Analysis type - Steady State
  - Turbulence equation - Spalart Allmaras

- Auto Solution Strategy
  - Max time steps - `100`
  - Convergence tolerance - `0.001`
  - Relaxation Factor- `0.4`
- Material Model
  - Air
    - Type - Constant
    - Density - `1.2` kg/m3
    - Viscosity - `1.7189e-5` kg/m*sec

  Model
- Volumes
  - Volume
    - Element Set
      1. Material model - Air
- Surfaces
  - Back
    - Simple Boundary Condition
      1. Type- Symmetry
  - Front
    - Simple Boundary Condition
      1. Type- Symmetry
  - InletLower
    - Simple Boundary Condition
      1. Type- Inflow
      2. Inflow type- Velocity
      3. X Velocity- `22.4` m/sec
      4. Turbulence input type- Direct
      5. Eddy Viscosity- `0.0001432`
  - InletUpper
    - Simple Boundary Condition
      1. Type- Inflow
      2. Inflow type- Velocity
      3. X Velocity- `41.54` m/sec
      4. Turbulence input type- Direct
      5. Eddy Viscosity- `0.0001432`
  - Outlet
    - Simple Boundary Condition
      1. Type - Outflow

- Slip
  - Simple Boundary Condition
    1. Type- Slip
- SplitterPlate
  - Simple Boundary Condition
    1. Type - Wall
- TE
  - Simple Boundary Condition
    1. Type- Wall

References

Delville, J., Bellin, S., Garem, J. H., and Bonnet J. P., "Analysis of Structures in a Turbulent, Plane Mixing Layer by Use of a Pseudo Flow Visualization Method Based on Hot-Wire Anemometry," in: Advances in Turbulence 2, eds: H.-H. Fernholz and H. E. Fiedler, Proceedings of the Second European Turbulence Conference, Berlin, Aug. 30-Sept. 2, 1988, Springer Verlag, Berlin, 1989, pp. 251-256.

Laminar to Turbulent Transition Over an Airfoil

In this application, AcuSolve is used to solve for the flow field around a high lift airfoil with inflow conditions that lead to transitional flow on the pressure and suction side of the airfoil's surface. The moderate level of turbulence intensity at the inlet, low angle of attack and shape of the airfoil induce a transition to turbulent flow after a separation bubble develops on the surface. The coefficient of pressure is compared against experimental data from laboratory experiments.

Problem Description

The problem consists of a fluid having material properties close to air with density of 1.0 kg /m3 and molecular viscosity specified to produce a Reynolds number of 2.0e6, assuming a chord length of 1.0 m and an inlet velocity of 1.0 m/s, as is shown in the following image, which is not drawn to scale. The inflow velocity is oriented to simulate a 1 degree angle of attack. The model is simulated as steady state with constant inflow conditions using the farfield boundary condition. The two-equation gamma-ReTheta (γ- Reθ) transition model, used with the one equation Spalart Allmaras turbulence model, is validated against experimental data obtained from the experimental studies conducted by Somers, 1997.

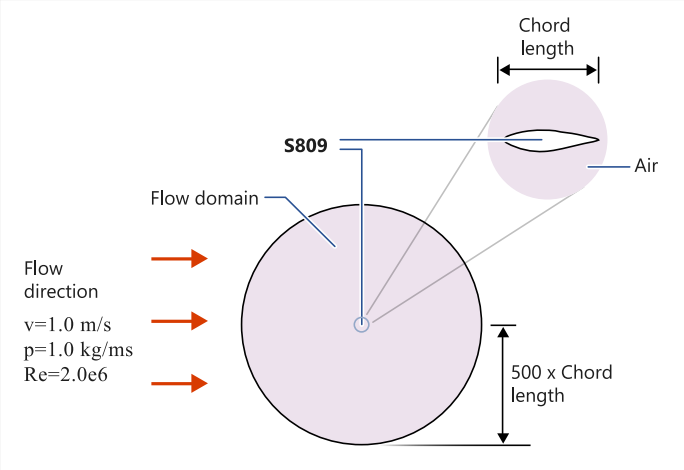


Figure 174: Critical Dimensions and Parameters used for Simulating Transitional Flow over the S809 Airfoil

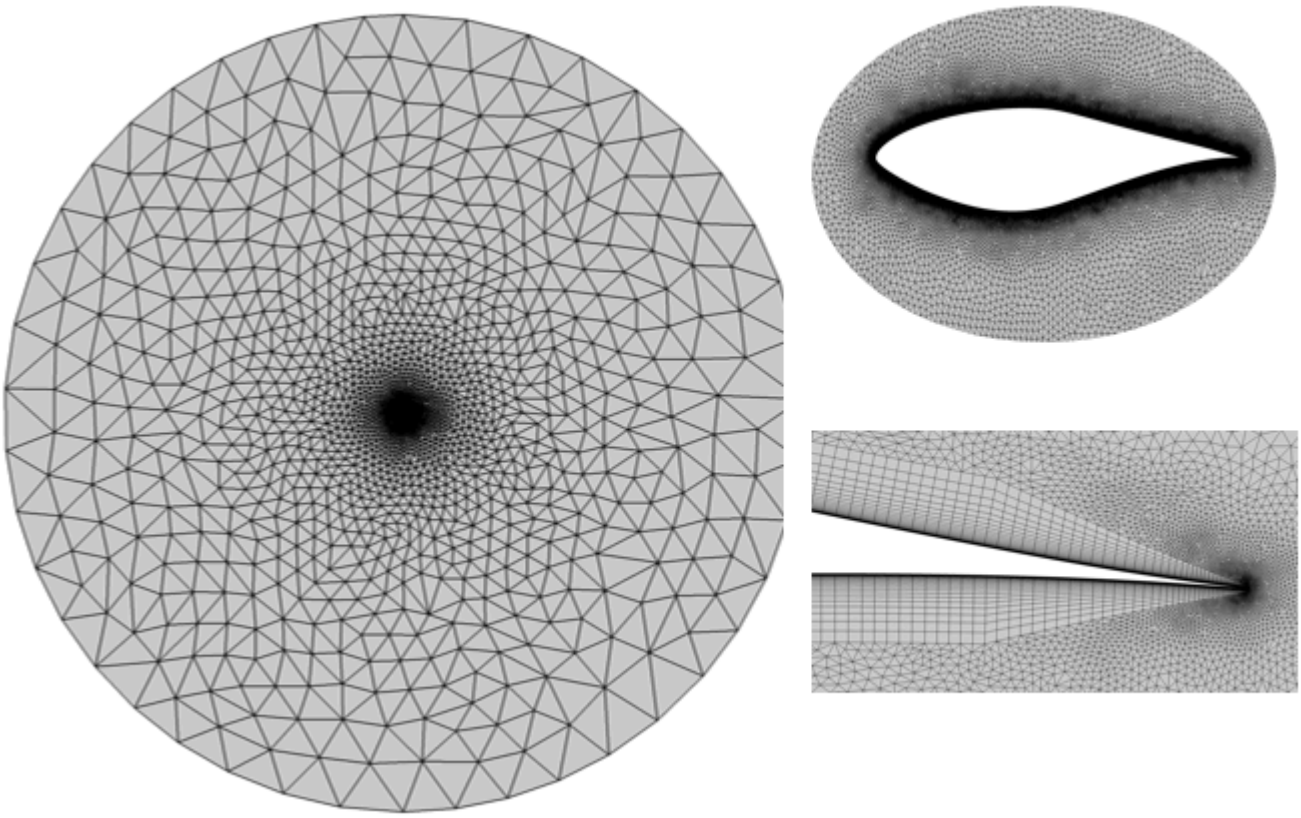


Figure 175: Mesh Used for Simulating Transitional over the S809 Airfoil

The simulation was performed as a two-dimensional problem by constructing a volume mesh that contains a single layer of elements extruded in the cross-stream direction, normal to the flow plane and by imposing symmetry boundary conditions on the extruded planes. The airfoil walls are specified as no-slip and the inlet velocity and eddy viscosity are specified at the farfield boundary.

AcuSolve Results

The AcuSolve solution converged to a steady state and the results reflect the mean flow conditions over the airfoil. The simulation results show that the flow field is laminar at the leading edge until approximately 50 percent chord on the pressure side and until approximately 55 percent on the suction side, then transitions to turbulent as it moves further downstream. The onset is caused by small separation bubbles at these locations. The following images show the negative pressure coefficient (-Cp) on the surface of the airfoil. The mean pressure at a reference point upstream of the airfoil is subtracted from the surface pressure and divided by the inlet velocity and air density to arrive at Cp. The Cp computed from AcuSolve is compared with experimental data, as described in Somers, 1997. The image shows black circles representing the experimental data and a solid red line for the AcuSolve results. Additional plots show contours of intermittency that illustrate the transition from laminar to turbulent flow.

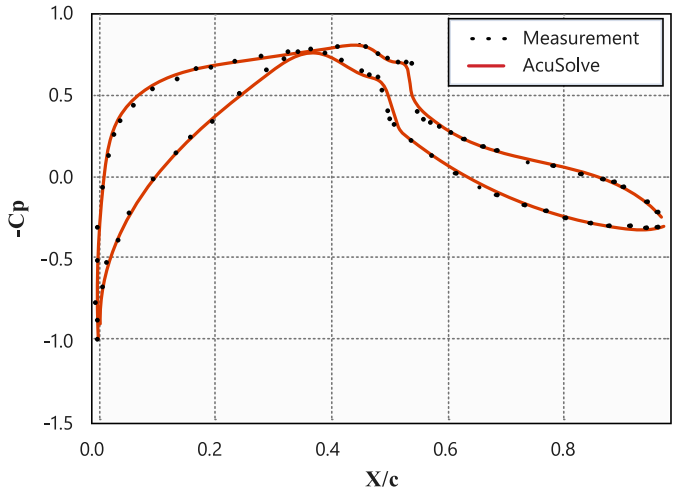


Figure 176: Negative pressure coefficient on the airfoil surface showing experimental and simulated results for the SA two equation (γ- Reθ) transition model

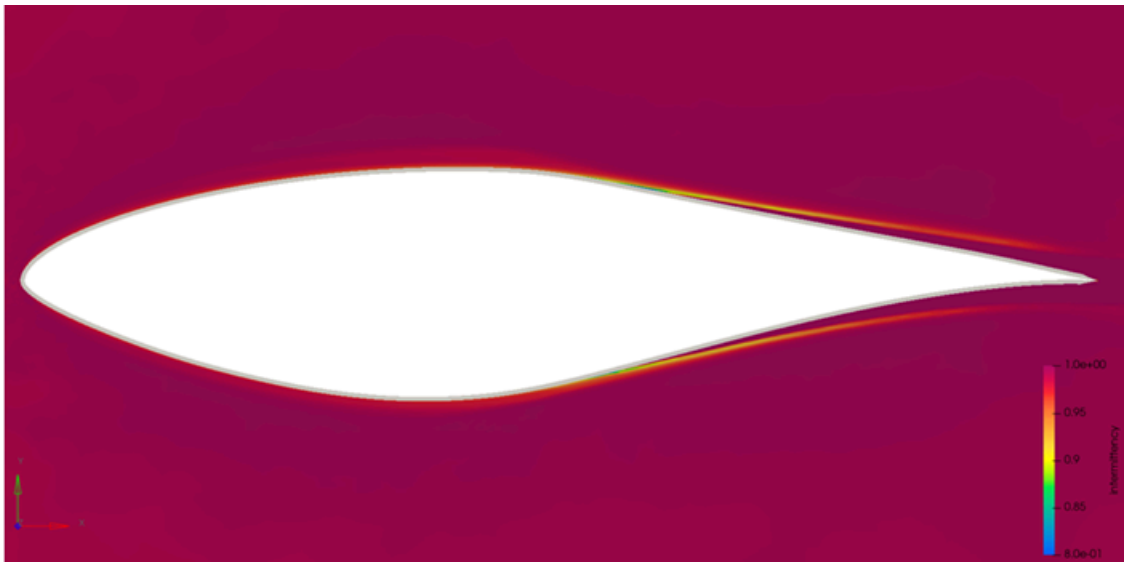


Figure 177: Contours of Intermittency Demonstrate the Onset Location from Laminar to Turbulent over the Airfoil

Summary

The AcuSolve solution compares well with experimental data for transitional flow over the S809 airfoil at a low angle of attack. Additional simulations and measurements for the full drag polar have been tested and compare well with considerably better accuracy when transition closure is included into the RANS solution. The good agreement with experimental results for the transition location and magnitude of expected pressure demonstrate that AcuSolve can predict the transition onset location for flow over surfaces with mild to moderate pressure gradients.

Simulation Settings for Laminar to Turbulent Transition Over an Airfoil

HyperMesh CFD database file: `<your working directory>\airfoil_transition\airfoil_transition.hm`

Global

- Problem Description
  - Analysis type - Steady State
  - Turbulence equation - Spalart Allmaras
  - Turbulence transition model- Gamma-ReTheta
- Auto Solution Strategy
  - Max time steps - `100`
  - Convergence tolerance - `0.0001`
  - Relaxation Factor- `0.5`
  - Turbulence transition- on
- Material Model
  - Air
    - Type - Constant
    - Density - `1.0` kg/m3
    - Viscosity - `5.0e-7` kg/m*sec

  Model
- Volumes
  - Fluid
    - Element Set
      1. Material model - Air
- Surfaces
  - +z slip
    - Simple Boundary Condition
      1. Type- Slip
  - -z slip
    - Simple Boundary Condition
      1. Type- Slip
  - farfield
    - Simple Boundary Condition
      1. Type- Far Field
      2. X velocity = `1.0` *cos(α), where α is the angle of attack in radians
      3. Y velocity = `1.0` *sin(α), where α is the angle of attack in radians
      4. Turbulence input type- Auto
      5. Turbulence intensity type- Value
      6. Turbulence intensity percent- `0.025`
  - airfoil surface
    - Simple Boundary Condition

1 Type- Wall

References

Somers, D., Design and Experimental Results for the S809 Airfoil. NREL/SR-440-6918. 1997

Turbulent Flow Through a 180 Degree Curved Channel

In this application, AcuSolve is used to simulate turbulent flow through a strongly curved two dimensional 180 degree U-duct channel. AcuSolve results are compared with experimental results adapted from Rumsey et al. (2000). The close agreement of AcuSolve results with experimental results validates the ability of AcuSolve to model turbulent cases with strong curvature effects.

Problem Description

The problem consists of a fluid with properties similar to air flowing through a curved channel, as shown in the following image, which is not drawn to scale. The inlet channel height and remaining duct height is 0.0381 m. The bulk velocity (v) normal to the inlet is 31.1 m/s and an integrated outflow pressure is specified to allow the flow to pass through the channel. The flow develops into fully turbulent flow at a Reynolds's number (Re) of approximately 1,000,000. The density of the flow medium is 1.0 kg/m3 and the dynamic viscosity is 1.1818 X 10-6 kg/m-s. The simulation is conducted with the Reynolds Averaged Navier-Stokes equations using the Spalart Allmaras, Shear Stress Transport (SST), K-ω and Realizable K-ε turbulence models. The velocity field from the simulations is compared against experimental data at select measurement locations.

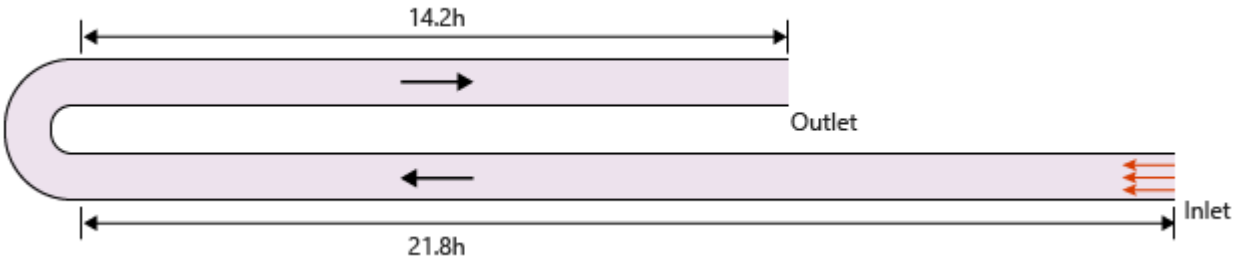
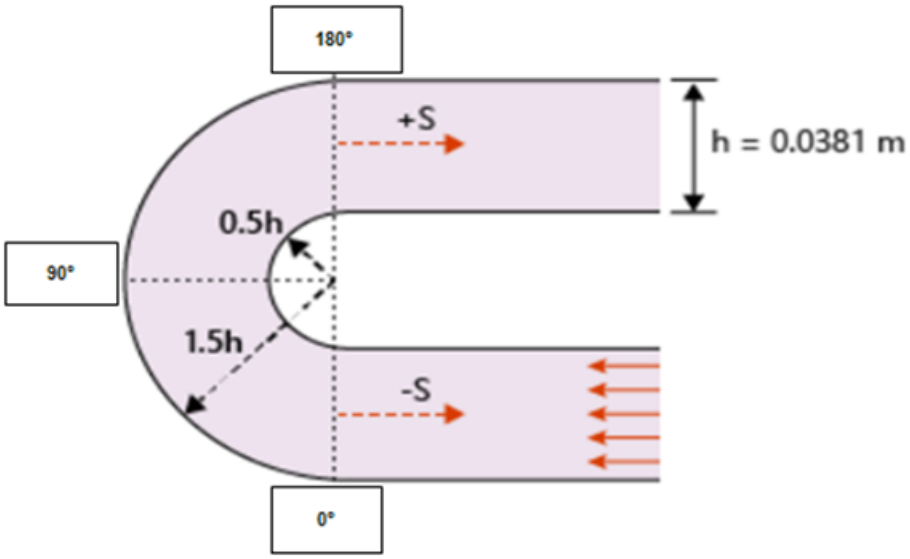


Figure 178: Critical Dimensions and Parameters for Simulating Turbulent Flow in the 180 degree U-Duct



The simulation was performed as a two dimensional problem by restricting flow in the out-of-plane direction through the use of a mesh that is one element thick. The upper and lower walls are specified as no-slip, the inlet velocity and eddy viscosity are specified normal to the inlet face to match the experimental Reynolds Number.

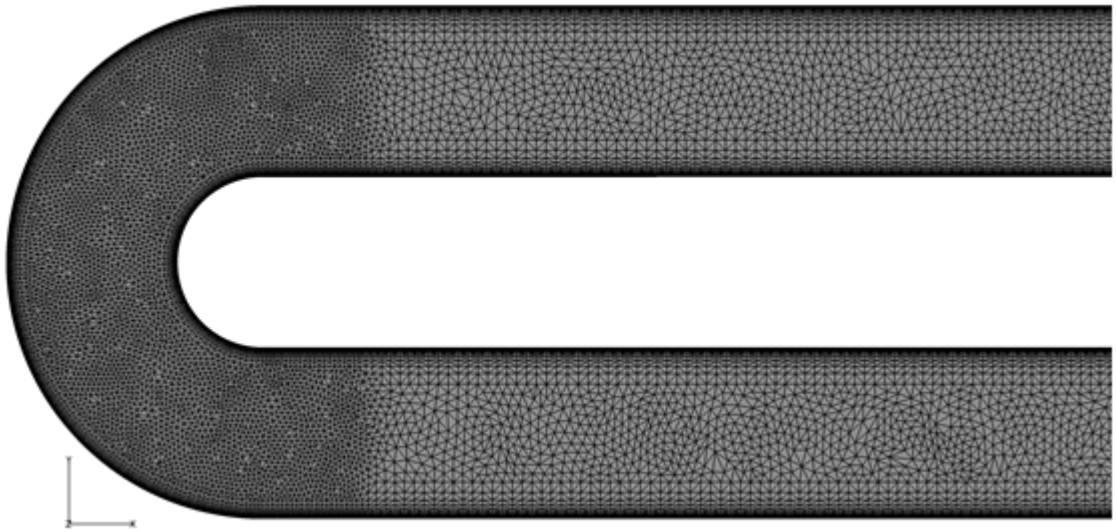


Figure 179: Mesh Used for Simulating Turbulent Flow in the 180 Degree U-Duct

AcuSolve Results

The AcuSolve solution converged to a steady state and the results reflect the mean flow conditions. As the flow passes the inner convex wall it begins to accelerate before decelerating directly past the curved section due to the adverse pressure gradient that eventually leads to a local recirculation zone. On the outer concave wall, the flow remains attached, but is influenced by the adverse pressure gradient above the recirculation region.

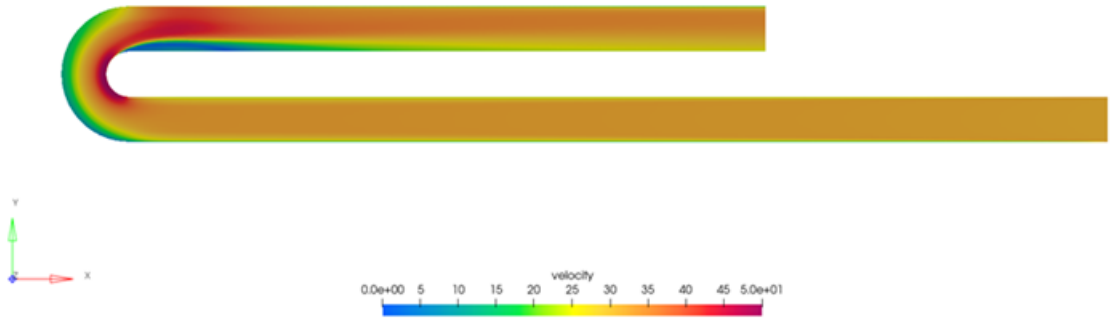


Figure 180: Velocity Contours in Stream Wise Plane

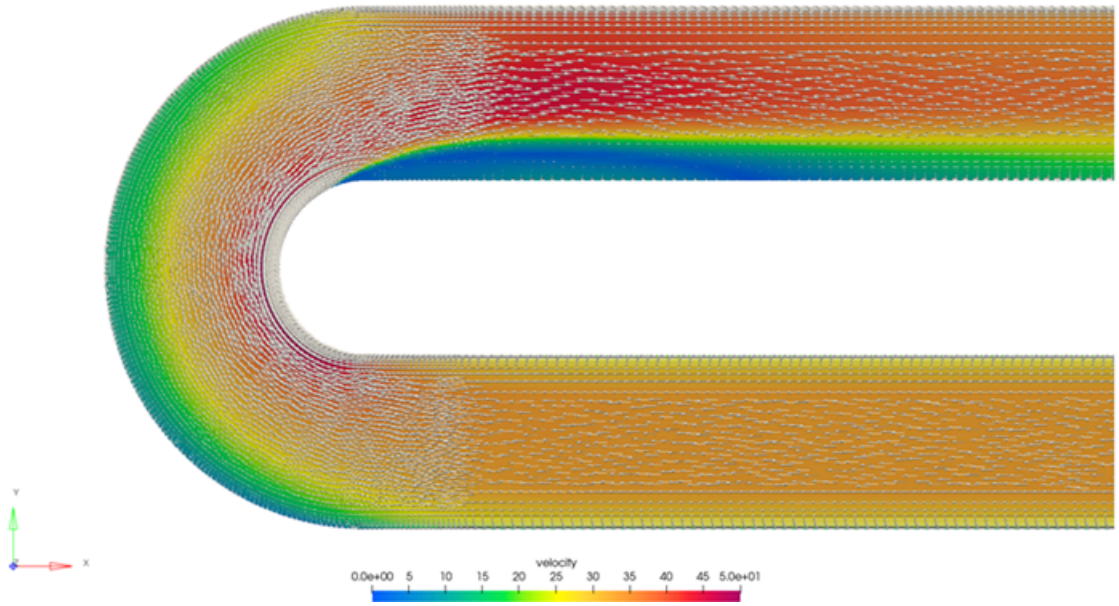


Figure 181: Close up View of Velocity Vectors and Velocity Contours at 180 Degree Bend

The experimental value for the ratio of Velocity magnitude (Vm) to inlet bulk velocity (Vb=31.1 m/s) at different sections of the U-duct is presented with the corresponding AcuSolve result for each of the turbulence models tested in the following images. The images show black circles representing the experimental measurements (Rumsey 2000), solid red lines for the SA model, solid blue lines for the SST model, solid green lines for the K-ω model and solid cyan lines for the K-ε model.

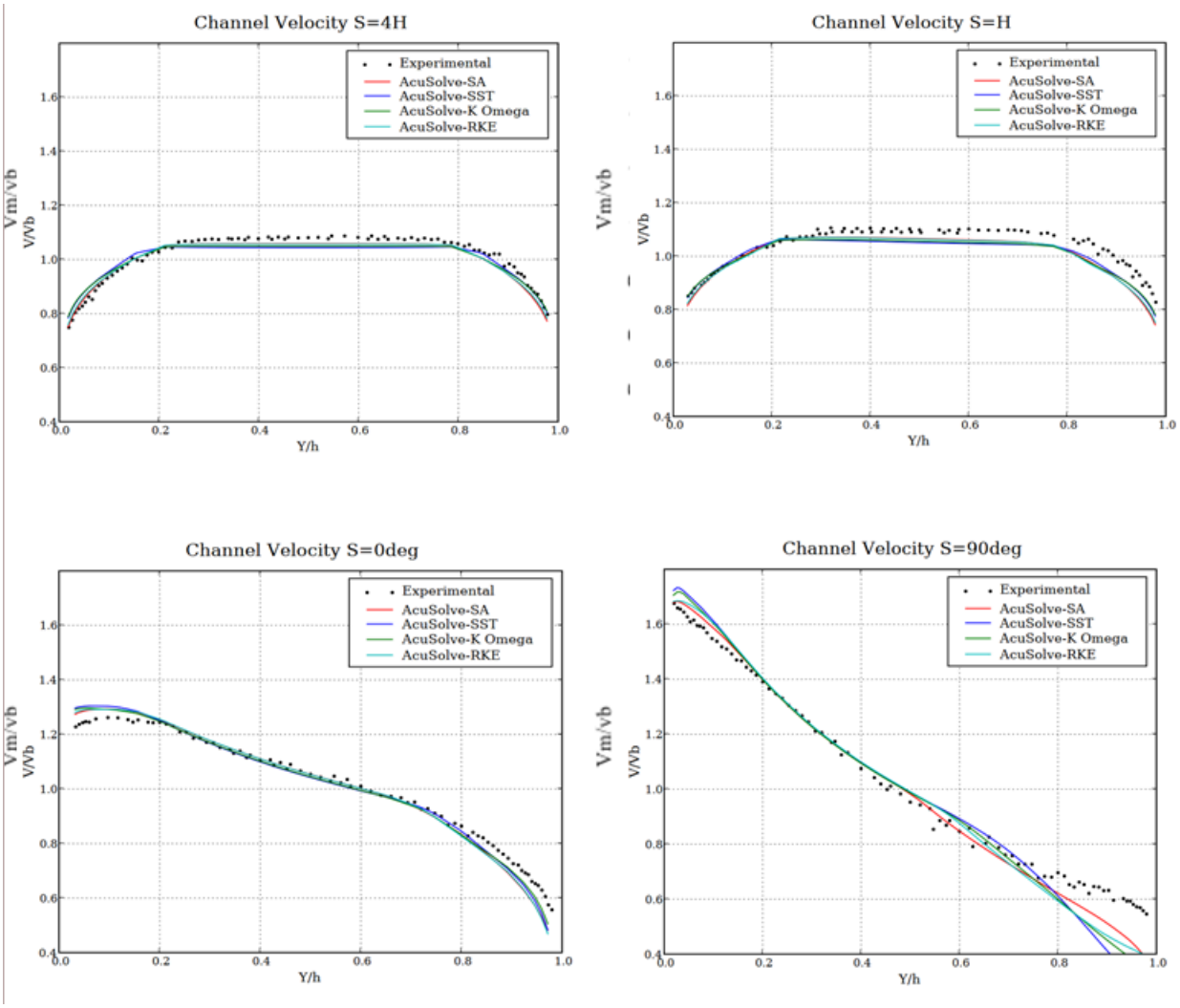


Figure 182:

Summary

The AcuSolve solution compares well with experimental results for flow past the 180 degree U-duct. The experimental value for the ratio of Velocity magnitude to inlet bulk velocity at different sections of the U-duct is presented with the corresponding AcuSolve result for various turbulence models. The performance of the Spalart Allmaras turbulence model was found to improve when the rotation curvature correction is included in the numerical formulation (enabled by default). In this application, AcuSolve demonstrates the ability to predict the complex boundary layer separation and reattachment resulting from the curvature of the channel.

Simulation Settings for Turbulent Flow Through a 180 Degree Curved Channel

HyperMesh CFD database file: `<your working directory>\curved_channel_simple_turbulent \curved_channel_simple_turbulent.hm`

Global

- Problem Description

- Analysis type - Steady State
- Turbulence equation - Realizable K-Epsilon

- Auto Solution Strategy
  - Relaxation factor - `0.4`
- Material Model
  - Air
    - Type- Constant
    - Density- `1.0` kg/m3
    - Viscosity- `1.1818e-006` kg/m-sec

  Model
- Volumes
  - Fluid
    - Element Set
      1. Material model- Air
- Surfaces
  - Inlet
    - Simple Boundary Condition
      1. Type- Wall
      2. Inflow type- Velocity
      3. Inflow velocity type- Normal
      4. Normal velocity- `31.1` m/sec
      5. Turbulence input type- Direct
      6. Eddy viscosity- `3.5547e-06` m2/sec
  - ext1
    - Simple Boundary Condition- Symmetry
  - ext2
    - Simple Boundary Condition- Symmetry
  - Outlet
    - Simple Boundary Condition
      1. Type- Outflow
  - wall-bottom
    - Simple Boundary Condition
      1. Type- Wall
      2. Turbulence wall type- Low Reynolds Number
  - wall-top
    - Simple Boundary Condition
      1. Type- Wall

2 Turbulence wall type- Low Reynolds Number

References

Christopher L. Rumsey, Thomas B. Gatski, and Joseph H. Morrison. "Turbulence Model Predictions of Strongly Curved Flow in a U-Duct", AIAA Journal, Vol. 38, No. 8 (2000), pp. 1394-1402.

Heat Transfer Between Radiating Concentric Spheres

In this application, AcuSolve is used to simulate the heat transfer due to conduction and radiation between concentric spheres. The inside surface of the inner and the outside surface of the outer sphere are both held at constant temperature, while the gap between them radiates the heat from one sphere to the other.

AcuSolve results are compared with analytical results for temperature and heat flux as described in Incropera (2006) and Salazar, et al. (2016). The close agreement of AcuSolve results with analytical results validates the ability of AcuSolve to model cases with radiation heat transfer and conjugate heat transfer with enclosure radiation modeling and the discrete ordinate (DO) radiation model.

Problem Description

The problem consists of a fluid region with arbitrary material properties between two concentric spheres with surfaces held at fixed temperature, as shown in the following image, which is not drawn to scale. The radius of the outer sphere is 0.04 m and the radius of the inner sphere is 0.01 m. The inner surface of the inner sphere is defined to have a constant wall temperature at 300.0 K (27 ºC). The outer surface of the outer sphere is defined to have a constant wall temperature at 1300.0 K (1027 ºC). The fluid within the spheres is defined as a non-conducting material, allowing heat to transfer via radiation only. The solid and fluid regions equilibrate to a steady temperature and can be compared with a semi-analytical solution for the temperature and heat flux at the fluid boundaries.

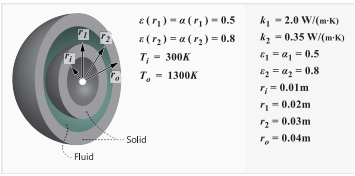


Figure 183: Critical Dimensions and Parameters used for Simulating Conduction and Radiation Between two Concentric Spheres



Figure 184: Mesh used for Simulating Radiation Between two Concentric Spheres

The simulation was performed as a three dimensional problem by constructing a volume mesh that contains a layer of boundary elements normal to the radial direction.

AcuSolve Results

The AcuSolve solution converges to a steady state and the results reflect the mean temperature distribution within the spheres. As the outer diameter is considerably hotter than the inner, a heat flux is present between the spheres. The temperature within the mediums increases as a function of the radius, with a slope corresponding to the temperature difference and the specified emissivity of the shells. The following image shows the temperature contour within the spheres along with the two-dimensional plot of the temperature versus radius in the solid mediums. The temperature and heat flux at the radiation surfaces are compared with the analytical solution as described in Salazar, et al. (2016).

Table 8: The Analytical Solution for the Temperature and Heat Flux at r1 and r2 are Presented with the Corresponding AcuSolve Results for the Enclosure (Surface to Surface) Model and the DO

	T(r1) (K)	T(r2) (K)	Q(r1) (W)	Q(r2) (W)
Analytical	578.2	1035.0	-27822.5	12365.6
AcuSolve (Enclosure)	578.4	1035.1	-27827	12364.2
AcuSolve (DO)	561.8	1023.6	-26175	12897.0
Percent Difference (Enclosure)	0.034%	0.010%	-0.015%	-0.011%
Percent Difference (DO)	2.8%	-1.11%	5.92%	4.3%

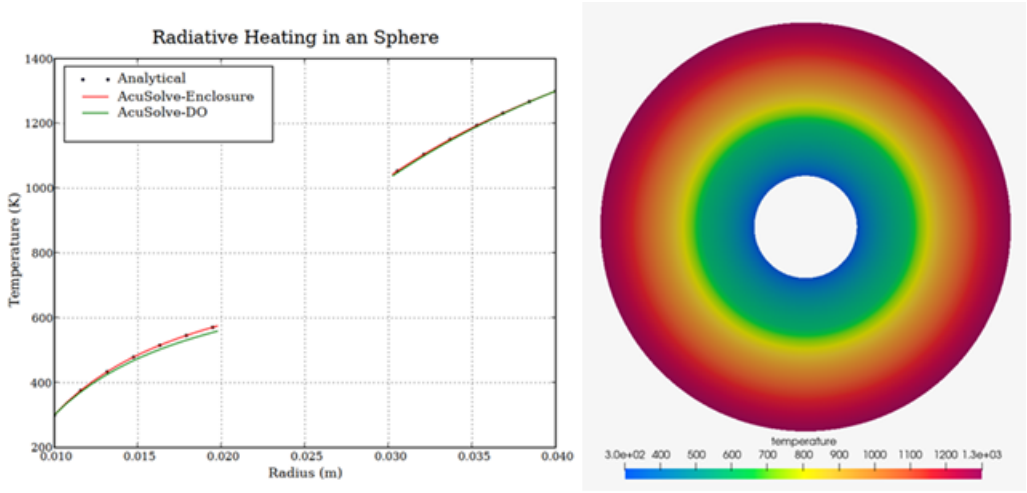


Figure 185: Two-Dimensional Plot and Contours of Temperature Between the Concentric Spheres

Summary

The AcuSolve solution compares well with analytical results for heat transfer due to conduction and radiation between two concentric spheres. In this application, an arbitrary material is subjected to a heat flux that is calculated based on the view factors or the DO model within the simulation. As a result of the conjugate heat transfer and the radiative heat flux a temperature distribution between the two spheres develops. The AcuSolve solution for the temperature and heat flux at the radiation surfaces matches well compared to the analytical solution with only a minor difference for the enclosure radiation model. The enclosure radiation model was found to have a higher accuracy for this application compared to the DO model, as expected due to the relatively low optical thickness in this simulation.

Heat Transfer Between Radiating Concentric Spheres

HyperMesh CFD database file: `<your working directory>\sphere_radiation\sphere_radiation.hm`.

Global

- Problem Description
  - Analysis type - Steady State
  - Temperature equation - Advective Diffusive
  - Radiation equation - Enclosure
- Auto Solution Strategy
  - Convergence tolerance - `1.0e-5`
  - Relaxation Factor - `0.4`
  - Flow - off
  - Enclosure radiation - on
- Material Model
  - Inner
  - Conductivity
    - Type - Constant

        - Conductivity - `2.0`
    - Outer
    - Conductivity
        - Type - Constant
        - Conductivity - `0.35`
    - Radiating
    - Conductivity
        - Type - Constant
        - Conductivity - `1.0e-6`
- Emissivity Model
- Inner
    - Emissivity - `0.5`
- Outer
    - Emissivity - `0.8`

  Model
- Volumes
    - Inner
        - Element Set
            1. Medium- Solid
            2. Material model - Inner
        - Outer
            1. Element Set
                1. Medium - Solid
                2. Material model - Outer
        - Radiating
            1. Element Set
                1. Medium - Fluid
                2. Material model - Radiating
- Surfaces
    - Inner_Inner_r1
        - Simple Boundary Condition - (disabled to allow for heat flux)
    - Inner_Inner_ri
        - Simple Boundary Condition
            1. Type - Wall
            2. Temperature BC type - Value
            3. Temperature - `300.0` K
    - Inner_Radiating_r1

- Simple Boundary Condition (disabled to allow for heat flux)
- Radiation Surface
  1. Type - Wall
  2. Emissivity model - Inner

- Outer_Outer_r2
  - Simple Boundary Condition (disabled to allow for heat flux)
- Inner_Outer_ro
  - Simple Boundary Condition
    1. Type - Wall
    2. Temperature BC type - Value
    3. Temperature - `1300.0` K
- Outer_Radiating_r2
  - Simple Boundary Condition (disabled to allow for heat flux)
  - Radiation Surface
    1. Type - Wall
    2. Emissivity model - Outer

References

F. P. Incropera and D. P. DeWitt. "Fundamentals of Heat Transfer – Sixth Edition". John Wiley & Sons. New York. 2006.

Salazar, G., Droba, J., Oliver, B., & Amar, A. J. (2016). Development and Verification of Enclosure Radiation Capabilities in the CHarring Ablator Response (CHAR) code. 46th AIAA Thermophysics Conference.

Single-Phase Nucleate Boiling in a Rectangular Channel

In this application, AcuSolve is used to simulate the wall heat flux due to nucleate boiling at a heated wall inside a rectangular channel with water flow. Results are compared with experimental heat flux measurements as reported by Steiner, et al. (2005). The close agreement of AcuSolve results with experimental results validates the ability of AcuSolve to model single phase nucleate boiling problems.

Problem Description

The problem consists of a channel with a heated wall at the bottom. The temperature of the wall is selected to onset the nucleate boiling at the heated wall. The dimensions of the inlet are 0.03 x 0.04 m; the inlet velocity (v) is 0.39 m/s and the temperature (T) of the fluid entering the inlets is varied from 373.15 K (100 C) to 406.15 (133 C)), while the atmospheric pressure is specified to be 2 bar. The pre-heated water enters the inlets and heat is transferred into the fluid from the heated walls. The heat causes sub-cooled boiling to occur in the region close to the wall and leads to the formation of bubbles at nucleation sites. The surface tension and vapor phase models are specified to emulate the physical process of water changing state to water vapor.

The heat transfer in this regime is dominated by two effects, the macro convection due to the motion of the bulk liquid and the latent heat transport associated with the evaporation of the liquid micro-layer between the bubble and the heated wall. Each of these effects are modeled with AcuSolve and the prediction of their processes is demonstrated in the following results.

The AcuSolve simulation is prepared as a steady state heat transfer simulation to determine the temperature and heat flux on the heated walls of the model. AcuSolve computes the single-phase nucleate boiling by employing Chen’s model for two-phase boiling flow described in Chen (1966). The heat flux values for different wall temperatures are compared against the experimental measurements, as described in Steiner, et al. (2005).

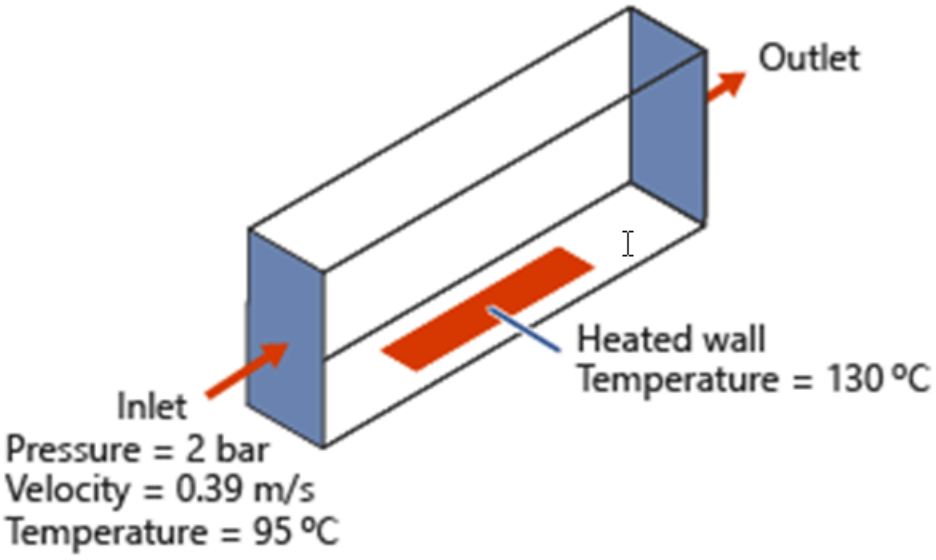


Figure 186: Critical Dimensions and Parameters for Simulating a Single-Phase Nucleate Boiling in a Rectangular Channel

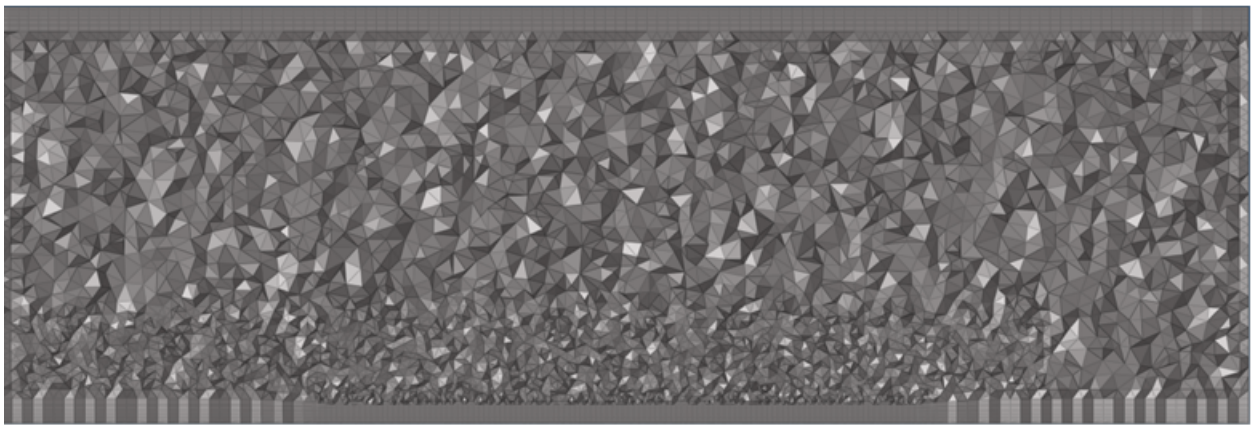


Figure 187: Mesh Used for Simulating a Single-Phase Nucleate Boiling in a Rectangular Channel

AcuSolve Results

The AcuSolve solution is run for heated wall temperature values of 100 C, 105 C, 110 C, 115 C, 120 C, 125 C, 130 C, 133 C and the results presented reflect the heat flux from the wall as the temperature nears the saturation temperature. The experimental values of heat flux (MW/m2) and wall temperature are presented with the corresponding AcuSolve results at seven temperature values. The AcuSolve results show good agreement with the experimental results for the heat flux, indicating that the single-phase nucleate boiling is properly captured.

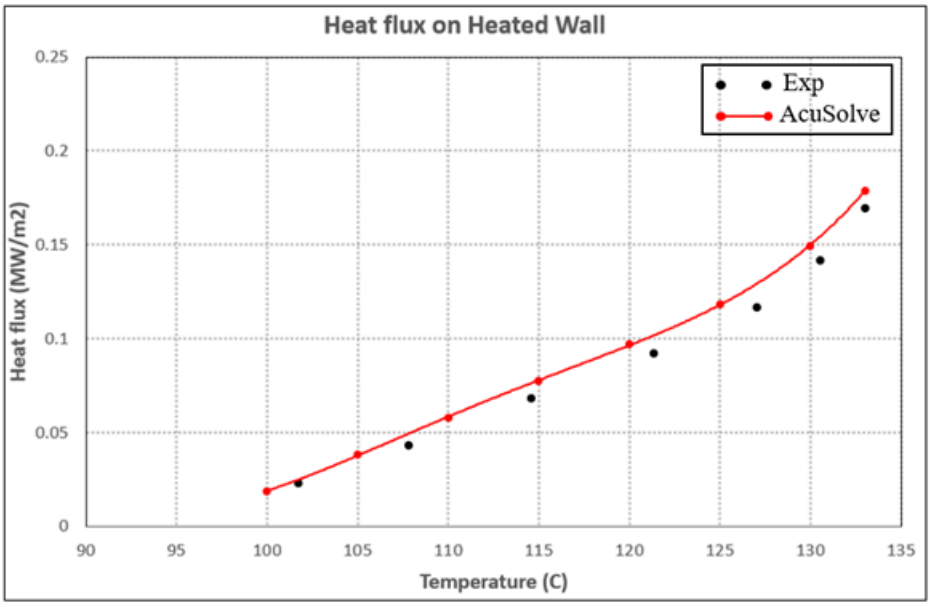


Figure 188: Heat Flux Values for Varying Wall Temperatures Compared to Experimental Data

Summary

The AcuSolve solution compares well with experimental results for single-phase nucleate boiling simulations. In this application, heat flux generated by the wall as the onset of boiling approaches are simulated with AcuSolve using the nucleate boiling feature and the RKE turbulence model. The experimental values of heat flux for the wall temperature range are presented with the corresponding AcuSolve results. A good agreement of simulation results with the experiment validates the ability to solve single-phase nucleate boiling using the nucleate boiling capabilities of AcuSolve.

Simulation Settings for Single-Phase Nucleate Boiling in a Rectangular Channel

HyperMesh CFD database file: `<your working directory>\channel_single_phase_boiling \channel_single_phase_boiling.hm`.

Global

- Problem Description
  - Analysis type – Steady
  - Turbulence equation – RKE
  - Temperature equation – Advective Diffusive
  - Nucleate Boiling Single Phase – On
- Auto Solution Strategy
  - Convergence Tolerance – `0.001`
  - Relaxation factor – `0.4`
- Surface Tension Model (“Water-srfTns”)
  - Type – Constant
  - Surface Tension – `0.07`

- Material Model
  - Vapor
    - Type – Constant
    - Density – `1.128` kg/m^3
    - Viscosity – `1.29e-5` kg/m-sec
    - Specific Heat – `2174.59` J/kg-K
    - Latent Heat – `2256000`
    - Latent Heat Temperature – `393.45` K
    - Conductivity – `0.02749` W/m-K
    - Turbulent Prandtl number – `1.0`
  - Water
    - Type – Constant
    - Density – `965.36` kg/m^3
    - Viscosity – `0.000314` kg/m-sec
    - Specific Heat – `4204.8` J/kg-K
    - Conductivity – `0.675` W/m-K
    - Turbulent Prandtl number – `0.91`
    - Vapor phase model – Vapor
    - Surface Tension model – Water-srfTns

Model

- Volumes
  - Fluid
    - Material– Water
- Surfaces
  - Inflow
    - Simple Boundary Condition – Inflow
    - Inflow type – Average Velocity
    - Average Velocity – `0.39` m/sec
    - Temperature – `368.15` K
  - Outflow
    - Simple Boundary Condition – Outflow
    - Back flow condition – On
    - Temperature back flow type – Mass flux average
    - Kinetic energy back flow type – Mass flux average
    - Dissipation rate back flow type – Mass flux average
  - Bottom
    - Simple Boundary Condition – Wall
  - Top

        - Simple Boundary Condition – Wall
    - Side_MinY
        - Simple Boundary Condition – Wall
    - Side_MaxY
        - Simple Boundary Condition – Wall
    - Heated Wall
        - Simple Boundary Condition – Wall
        - Temperature type – Value
        - Temperature – [373.15, 378.15, 383.15, 388.15, 393.15, 398.15, 403.15, 406.15] K

References

Helfried Steiner, Alexander Kobor, Ludwig Gebhard, 2005, "A wall heat transfer model for subcooled boiling flow", International Journal of Heat and Mass Transfer, Vol 48, pp. 4161- 4173.

Chen, J.C., 1966, "Correlation for Boiling Heat Transfer to Saturated Fluids in Convective Flow", United States: N. p., 1962. Web. doi:10.2172/4636495.

Turbulent Flow Past a Wall-Mounted Hump

In this application, AcuSolve is used to simulate fully developed turbulent flow past a smooth hump on the lower wall of a flow domain. AcuSolve results are compared with experimental results as described in Seifert and Pack (2002) and on the NASA Langley Research Center Turbulence Modeling Resource web page. The close agreement of AcuSolve results with experimental data and reference turbulence model performance validates the ability of AcuSolve to model cases with turbulent flow moving past a wall protrusion resulting in flow separation and recovery.

Problem Description

The problem consists of a fluid with material properties close to air flowing through a flow domain containing a well-defined smooth hump with a slit opening at approximately 65 percent of the hump chord. The inlet of the domain is defined with an inflow velocity in the streamwise direction that develops into fully turbulent flow at a Reynolds number (Re) of 936,000, based on the hump chord length of 1.0 m. The density of the flow medium is 1.0 kg/m^3 and the dynamic viscosity is 1.0684 X 10^{-6} kg/m-s. The simulation is conducted with the Reynolds Averaged Navier-Stokes equations using the Spalart Allmaras turbulence model, shear stress transport (SST) model, the K-ω model and Realizable K-ε model to evaluate the performance of the turbulence models. The flow predictions from AcuSolve are compared against experimental data and previously published turbulence model performance for pressure and friction coefficients within the domain.

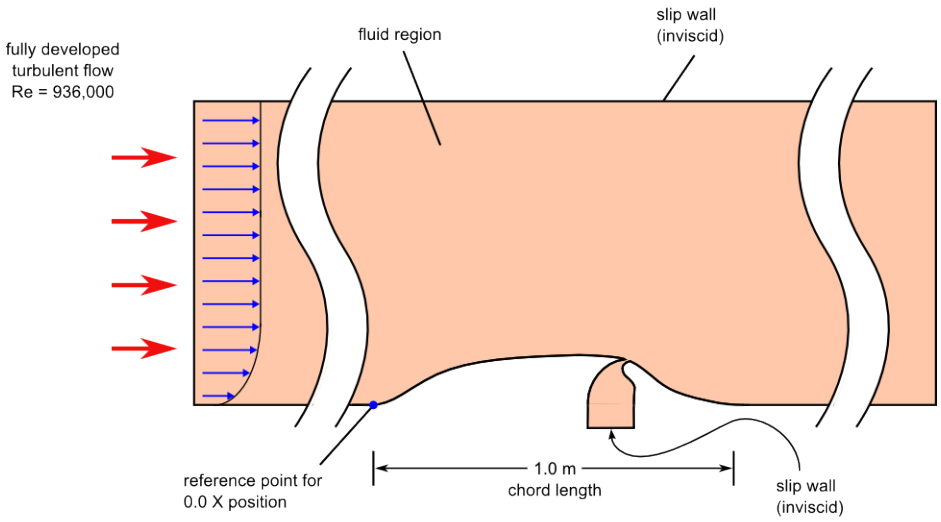


Figure 189: Critical Dimensions and Parameters for Simulating Turbulent Flow Through a Domain with a Wall-Mounted Hump

The upper walls of the domain are specified as slip (inviscid) and the lower walls are specified as no-slip. The inlet velocity and appropriate turbulence parameters are specified in the streamwise direction to match the desired Reynolds Number of 936,000. The outflow pressure is set to zero, and the lower wall on cavity below the hump is set to slip. The problem is simulated as two dimensional with a single layer of elements extruded in the cross stream direction and by defining the side walls as slip.

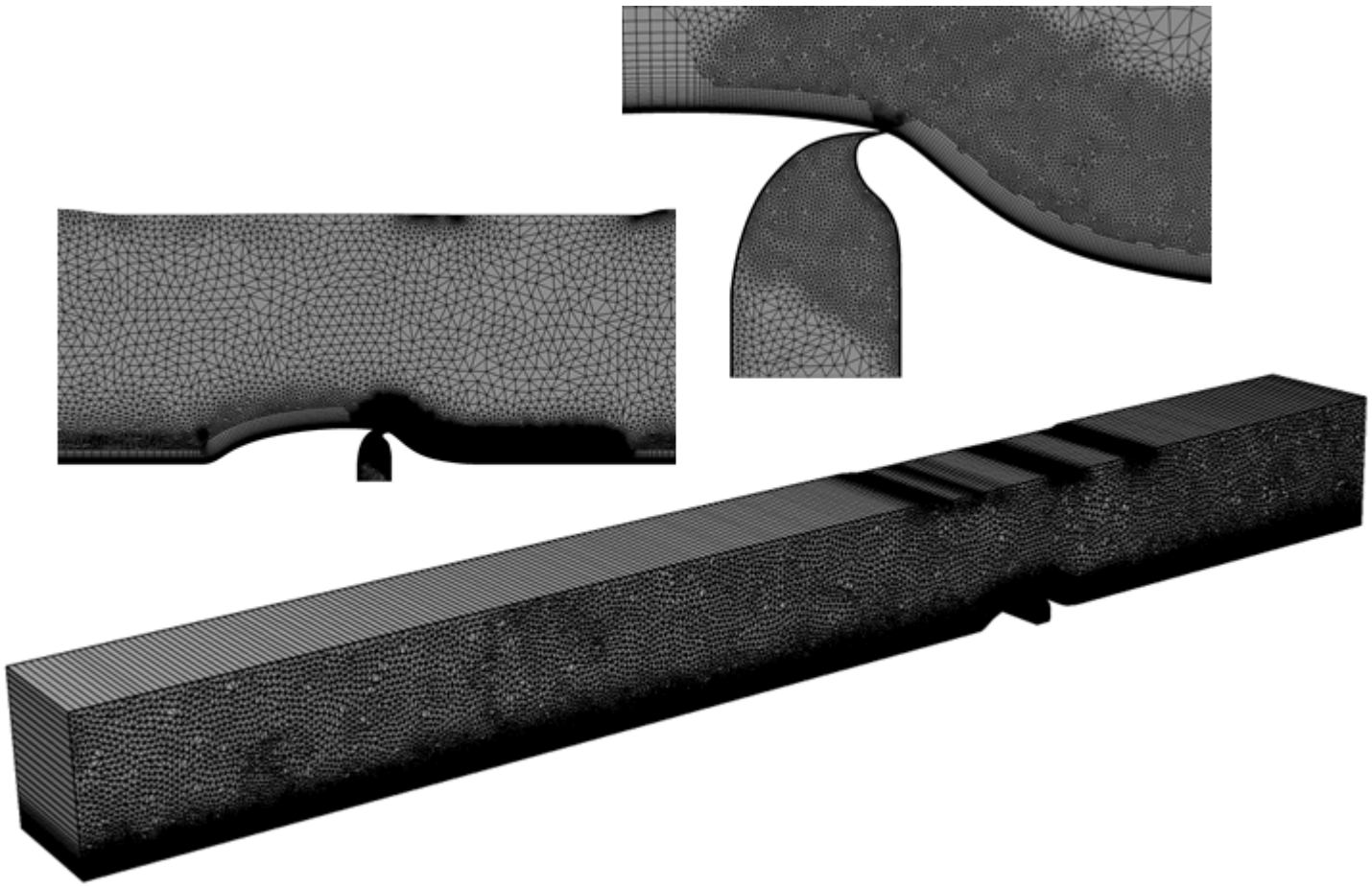


Figure 190: Three Views of the Mesh Used for Simulating Turbulent Flow over a Wall-Mounted Hump (Full Mesh is Shown on the Bottom, with Increased Resolution in Clockwise Views)

AcuSolve Results

The AcuSolve solution converged to a steady state and the results reflect the mean flow conditions within the domain. The images below show contours of velocity within the domain as well as the recirculation region directly downstream of the hump. As the flow enters the domain with a bulk velocity, it begins to develop a turbulent boundary layer near the lower wall prior to reaching the hump. As the flow approaches the hump section, the velocity near the lower wall decreases, but does not recirculate in front of the hump. It then accelerates over the top of the hump and separates immediately after reaching the cavity opening. The recirculation region propagates downstream, before the flow recovers and reattaches to the lower wall.

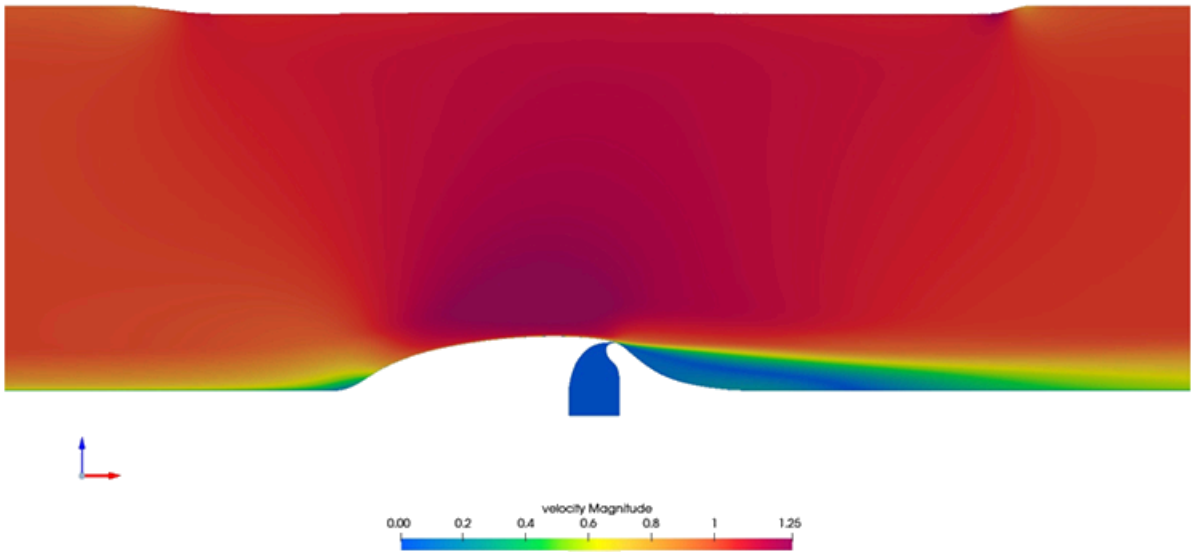


Figure 191: Velocity Contours on the Boundaries of the Domain, Showing Velocity Magnitude

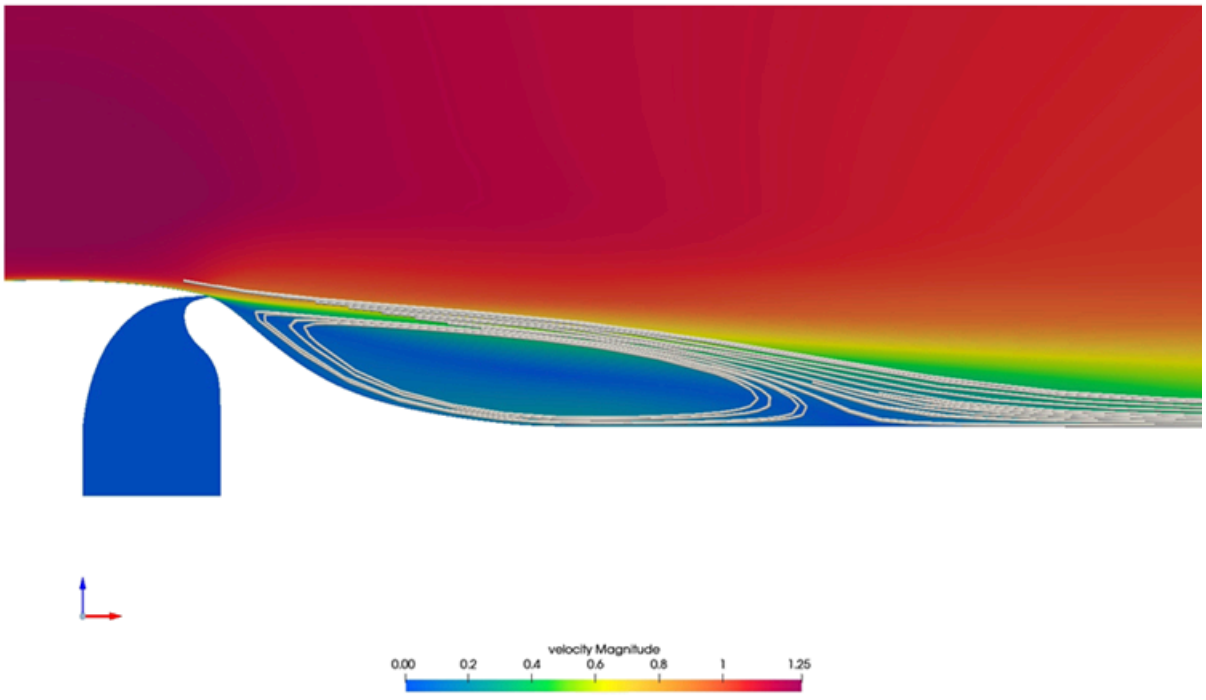


Figure 192: Close up View of Velocity Contours Showing the Recirculation Region with Streamlines (White Lines) Representing the Region of Backflow

The images below show the coefficient of pressure and coefficient of skin friction along the lower wall of the flow domain plotted with experimental results. The non-dimensional values are defined by the integrated inlet pressure and the magnitude of the inlet velocity. The images show black circles representing the experimental measurements (Seifert and Pack 2002), solid red lines for the SA model, solid blue lines for the SST model, solid green lines for the K-ω model and solid cyan lines for the Realizable K-ε model, representing the AcuSolve results. The resulting pressure coefficient within the domain demonstrates that there are minor differences between the four turbulence models. All four

models are shown to perform accurately in predicting the increase in surface pressure on the front of the hump but tend to over predict the skin friction in the wake of the hump, leading to a minor over prediction of the reattachment location. The SA model predicts a slightly larger recirculation region and does not meet the expected recovery pressure compared to SST, K- ω and K-ε models. This performance was found to be consistent with comparisons to other one equation models (NASA 2015).

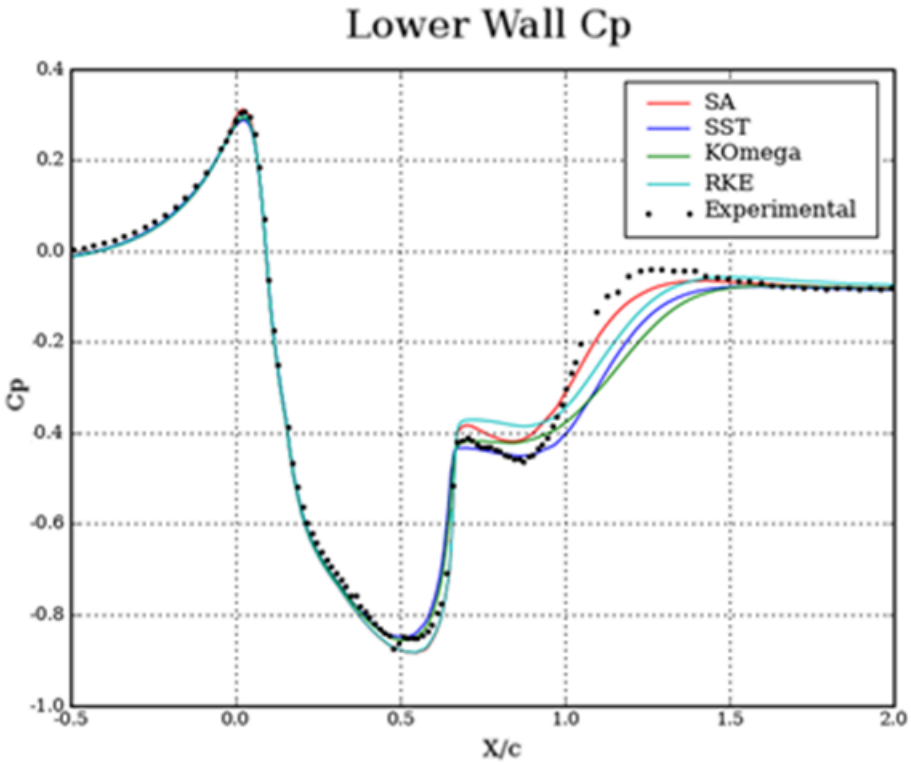


Figure 193: Coefficient of Pressure Along the Lower Wall as the Flow Moves Past the Hump, Where c is the Hump Chord Length and 0.0 is the Reference Location at the Front of the Hump in the X-Direction (Streamwise)

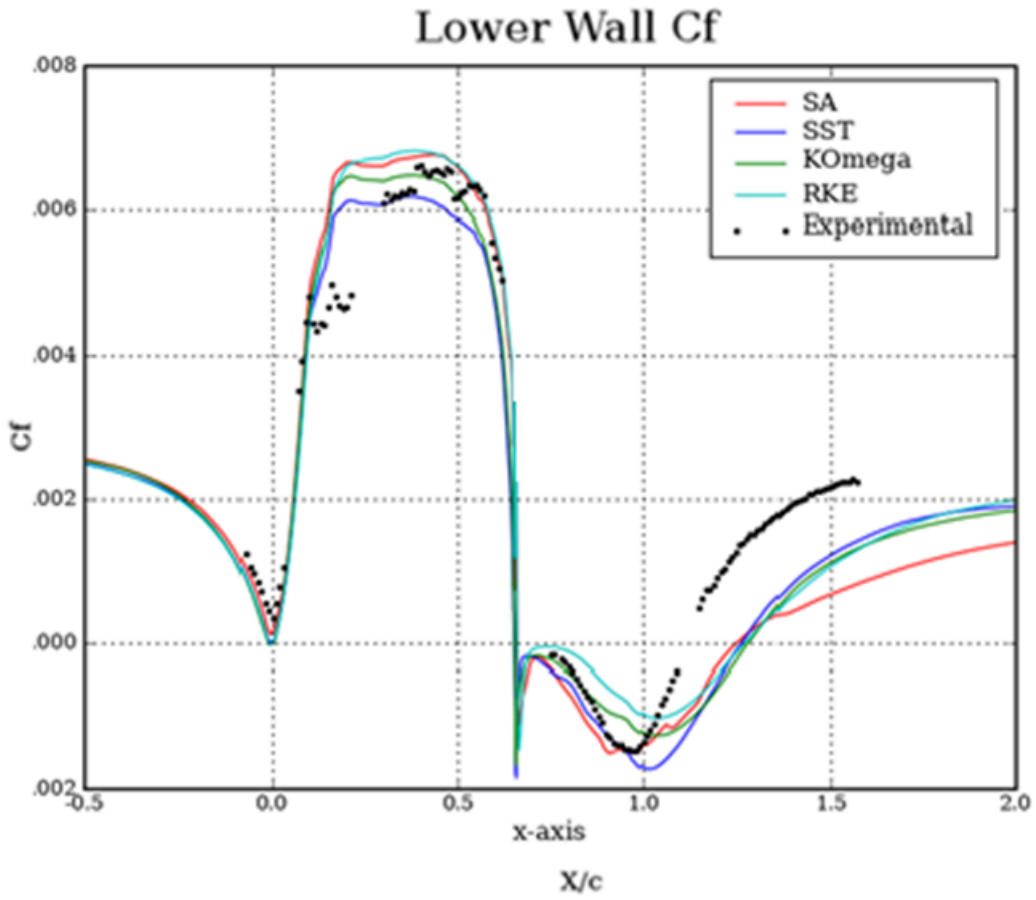


Figure 194: Skin Friction Coefficient Along the Lower Wall as the Flow Moves Past the Hump, Where c is the Hump Chord Length and 0.0 is the Reference Location at the Front of the Hump in the X-Direction (Streamwise)

Summary

In this application, a bulk turbulent flow at a Reynolds number of 936,000 within a flow domain containing a wall-mounted hump is studied and compared against experimental data. The AcuSolve results compare well with the experimental data for pressure coefficient and skin friction coefficient near the hump and downstream. The performance of the four turbulence models were found to be consistent with previously published results for flow over a wall-mounted hump (NASA 2015). For this application, the two equation models appear to outperform the one equation turbulence model, with better agreement for the downstream pressure on the wall. This application demonstrates AcuSolve's ability to predict the distribution of pressure and shear stress on protruding bodies within a turbulent flow field and serves to validate current turbulence modeling capabilities.

Simulation Settings for Turbulent Flow past a Wall-Mounted Hump

SimLab database file: `<your working directory>\wall_mounted_hump_turbulent\wall_mounted_hump_turbulent.slb`

Global

- Problem Description

- Flow - Steady State
- Turbulence equation - Spalart Allmaras

- Auto Solution Strategy
  - Max time steps - `100`
  - Convergence tolerance - `0.001`
  - Relaxation factor - `0.4`
- Material Model
  - Fluid
    - Density - `1.0` kg/m3
    - Viscosity - `1.0684e-6` kg/m-sec

  Model
- Volumes
  - Fluid
    - Element Set
      1. Material model - Fluid
- Surfaces
  - +Y
    - Simple Boundary Condition
      1. Type - Slip
  - -Y
    - Simple Boundary Condition
      1. Type - Slip
  - Cavity walls
    - Simple Boundary Condition
      1. Type - Wall
      2. Turbulence wall type - Wall Function
  - Hump walls
    - Simple Boundary Condition
      1. Type - Wall
      2. Turbulence wall type - Wall Function
  - Hump walls - downstream
    - Simple Boundary Condition
      1. Type - Wall
      2. Turbulence wall type - Wall Function
  - Inlet
    - Simple Boundary Condition
      1. Type - Inflow

2. Inflow type - Velocity
3. Inflow velocity type - Cartesian
4. X Velocity - `1.0` m/sec
5. Turbulence input type - Direct
6. Kinetic energy 1.2615e-5 m^2/s^2
7. Dissipation rate 0.00106 m^2/s^3

- Lower slip
  - Simple Boundary Condition
    1. Type - Slip
- Lower wall
  - Simple Boundary Condition
    1. Type - Wall
    2. Turbulence wall type - Wall Function
- Nozzle walls
  - Simple Boundary Condition
    1. Type - Wall
    2. Turbulence wall type - Wall Function

- Outlet
  - Simple Boundary Condition
    - Type - Outflow
- Slip
  - Simple Boundary Condition
    - Type - Slip

References

A Seifert and L.G. Pack. "Active Flow Separation Control on Wall-Mounted Hump at High Reynolds Numbers". AIAA Journal. 40(7). 2002.

NASA Langley Research Center Turbulence Modeling Resource web page. http://turbmodels.larc.nasa.gov/nasahump_val.html. Accessed June 2015.

Turbulent Flow Through a Heated Periodic Channel

In this application, AcuSolve is used to solve for the flow and temperature field within a channel containing a heated wall. The wall is maintained at a constant temperature, inducing heat flux into the fluid, to predict the thermal law of the wall. The non-dimensional temperature versus the non-dimensional height above the wall is compared to the analytical correlation provided by Kader.

Problem Description

The problem consists of a fluid having material properties close to air with a density of 1.0 kg/m^3, molecular viscosity of 0.0001 kg/m-s, specific heat of 1005.0 J/kg-K and thermal conductivity of 0.139 W/m-K. The properties are specified to obtain a Prandtl number of 0.72. The velocity is defined as periodic and is driven by a constant acceleration body force equal to 2.0 m/s^2. The temperature is specified as periodic+unknown ratio allowing it to develop until it reaches a steady solution. The simulation description is shown in the following image, which is not drawn to scale. The model is simulated using the one equation Spalart Allmaras turbulence model along with the advective-diffusive temperature equation. The thermal wall distribution is validated against correlation data published by Kader 1981.

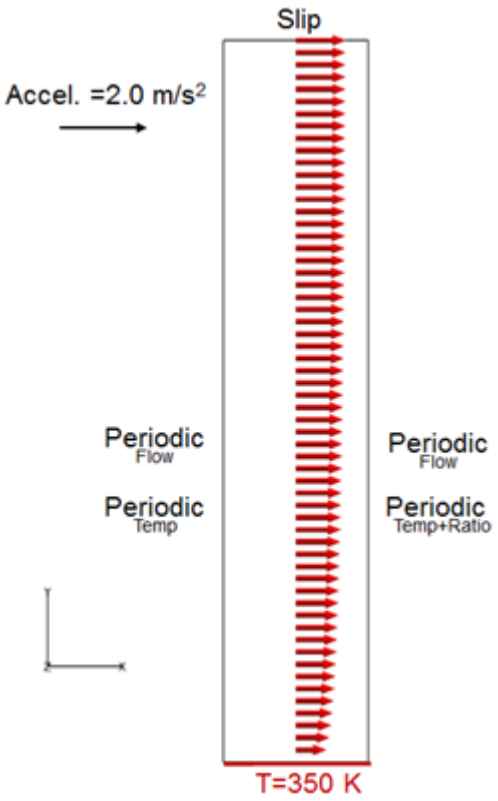


Figure 195: Critical Parameters used For Simulating Periodic Flow Within a Heated Channel

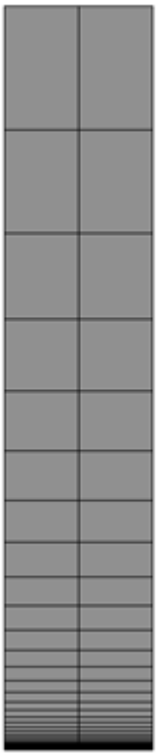


Figure 196: Mesh used For Simulating Periodic Flow Within a Heated Channel

The simulation was performed as a two-dimensional problem by constructing a volume mesh that contains a single layer of elements extruded in the cross-stream direction, normal to the flow plane and by imposing periodic boundary conditions on the extruded planes. The streamwise direction contains two elements allowing the flow and temperature solution to develop. Only the lower half of the channel is modeled, assuming the solution is mirror across the top slip plane.

AcuSolve Results

The AcuSolve solution converged to a steady state and the results reflect the mean flow conditions within the channel. The simulation results demonstrate that the channel wall induces a thermal flux into the flow field, producing a temperature distribution dependent on the distance from the wall. The thermal law of the wall computed from the AcuSolve results is compared with correlation data for the corresponding Prandtl number, as demonstrated in Kader 1981. The plot shown below gives the non-dimensional value of T+ as a function of Y+, where T+ and Y+ are computed per the following relationships:

$$T+ = \frac{(Tw - T)\rho C p u_\tau}{\dot{Q}} T \tag{5}$$

$$Y+ = \frac{y u_\tau}{v} \tag{6}$$

$$u_\tau = \sqrt{\tau w / \rho} \tag{7}$$

Where $T+$, Tw is the fixed wall temperature, T is the temperature away from the wall, ρ is the fluid density, Cp is the fluid specific heat, uT is computed from the magnitude of the shear stress and $\dot{Q}_i$ is the local surface heat flux.

The image below shows black circles representing the correlation data and a solid red line for the AcuSolve results. The results demonstrate that the temperature distribution away from the wall is resolved properly and compares well with the correlation. Since an empirical relationship for T+ is used for comparison, there will be minor discrepancies compared with the simulation results. Additional comparisons have been made against DNS results for T+ from Kawamura et al. 1998.

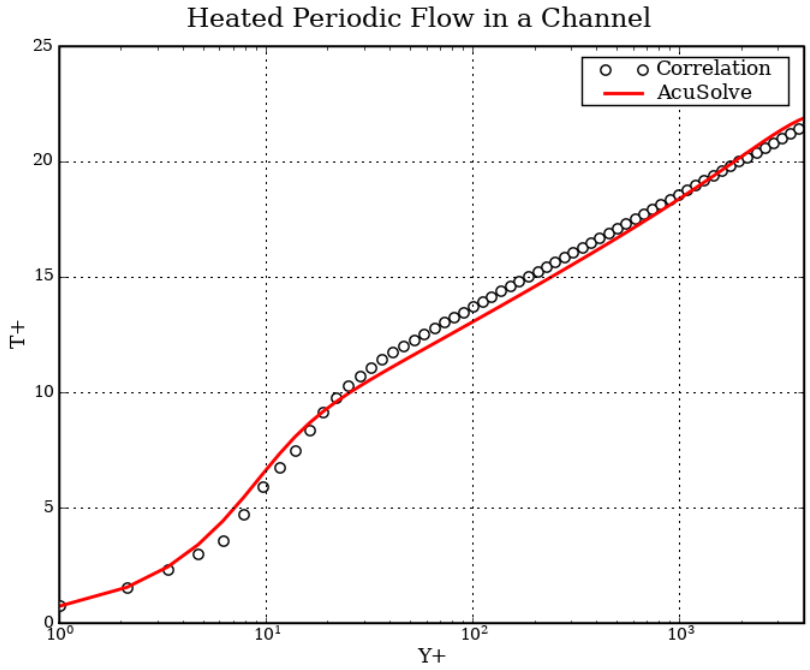


Figure 197: Thermal Boundary Layer Within the Heated Channel Compared Against the Correlation Data

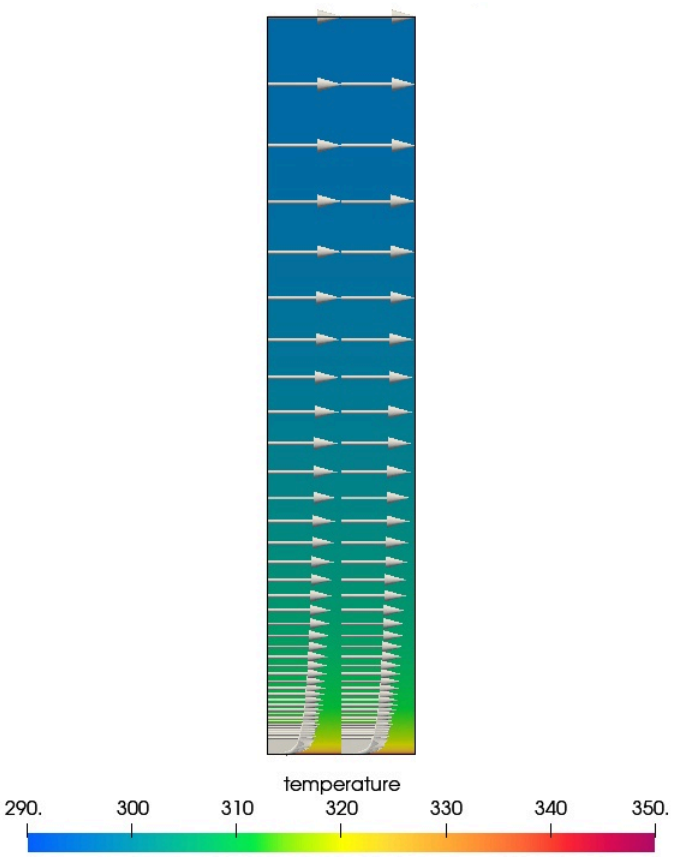


Figure 198: Contours of Temperature and Vectors Representing the Fluid Velocity Within the Channel

Summary

The AcuSolve solution compares well with the correlation data for turbulent flow within a heated channel. In this application, the constant temperature wall induces a surface heat flux, giving rise to a temperature gradient within the channel. AcuSolve can capture the correct temperature gradient at any location above the wall if an appropriate first layer height is selected to resolve a Y+ value of 1.0. The good agreement with correlation data for T+ demonstrates that AcuSolve can predict the locally varying temperature distribution within a turbulent channel.

Simulation Settings for Turbulent Flow Through a Heated Periodic Channel

SimLab database file: `<your working directory>\channel_periodic_heat\channel_periodic_heat.slb`

Global

- Problem Description
  - Flow type - Steady State
  - Temperature equation - Advective Diffusive
  - Turbulence equation - Spalart Allmaras
- Auto Solution Strategy
  - Max time steps - `50`

    - Convergence tolerance - `0.0001`
    - Relaxation Factor - `0.4`
    - Temperature - On
- Material Model
    - Fluid
        - Type - Constant
        - Density - `1.0` kg/m3
        - Viscosity - `1.0e-4` kg/m*sec
        - Specific Heat - `1005.0` J/kg*K
        - Conductivity - `0.139` W/m*K
- Body Force
    - BodyForce
        - Gravity
            1. X-component - `2.0` m/sec2

Model

- Volumes
    - Fluid
        - Element Set
            1. Material model - Fluid
            2. Body force - BodyForce
- Surfaces
    - Symmetry_1
        - Simple Boundary Condition - (disabled to allow for periodic conditions to be set)
    - Symmetry_2
        - Simple Boundary Condition - (disabled to allow for periodic conditions to be set)
    - Inflow
        - Simple Boundary Condition - (combination of integrated BC and periodic BC set)
        - Advanced Options
            1. Integrated Boundary Conditions - Temperature - `300.0` K
    - Outflow
        - Simple Boundary Condition - (disabled to allow for periodic conditions to be set)
    - Slip_surface
        - Simple Boundary Condition
            1. Type- Slip
    - Wall_surface
        - Simple Boundary Condition
            1. Type- Wall

2 Temperature BC type - Value
3 Temperature - `350.0` K

- Periodics
  - 2D
    - Periodic Boundary Conditions
      1 Type - Periodic
  - Flow
    - Periodic Boundary Conditions
      1 Type - Periodic
  - Temperature
    - Individual Periodic BCs
      1 Temperature: Type - Single Unknown Ratio
- Nodes
  - Zero_z-velocity
    - Z-Velocity: Type - Zero

References

B.A. Kader, "Temperature and concentration profiles in fully turbulent boundary layers", International Journal of Heat and Mass Transfer, Volume 24, Issue 9, 1981, Pages 1541-1544.

H. Kawamura, K. Ohsaka, H. Abe and K. Yamamoto, "DNS of turbulent heat transfer in channel flow with low to medium-high Prandtl number fluid", International Journal of Heat and Mass Transfer, 19:482-491, 1998.

Laminar Couette Flow with Imposed Pressure Gradient and Heated Walls

In this application, AcuSolve is used to simulate the flow of a highly viscous fluid between a moving and a stationary plate with an imposed pressure gradient and fixed temperature on the walls. AcuSolve results are compared with analytical results described in White (1991). The close agreement of AcuSolve results with analytical results validates the ability of AcuSolve to model cases with imposed pressure gradients and viscous heating.

Problem Description

The problem consists of a viscous fluid between two plates in a two-dimensional domain, as shown in the following image, which is not drawn to scale. The domain is 1.0 m high and 1.5 m long. The top plate moves with a constant velocity of 3.0 m/sec and the bottom plate is fixed. To simulate a fully developed flow with a relatively short length domain there is a mean-pressure gradient of -12 Pa/m applied to the fluid in the streamwise direction, defined as a body force acting on the entire fluid. The lower wall is held at a fixed temperature of 273.0 K, while the upper wall is held at a fixed temperature of 274.0 K. The problem is simulated with periodic boundaries in the streamwise direction. The Reynolds number of the flow, based on the distance between the plates is 0.3, indicating laminar flow. The flow field develops from the pressure gradient, the motion of the top plate, and the viscous shear stresses near the plates. The shear stress within the domain causes the temperature to increase within the channel.

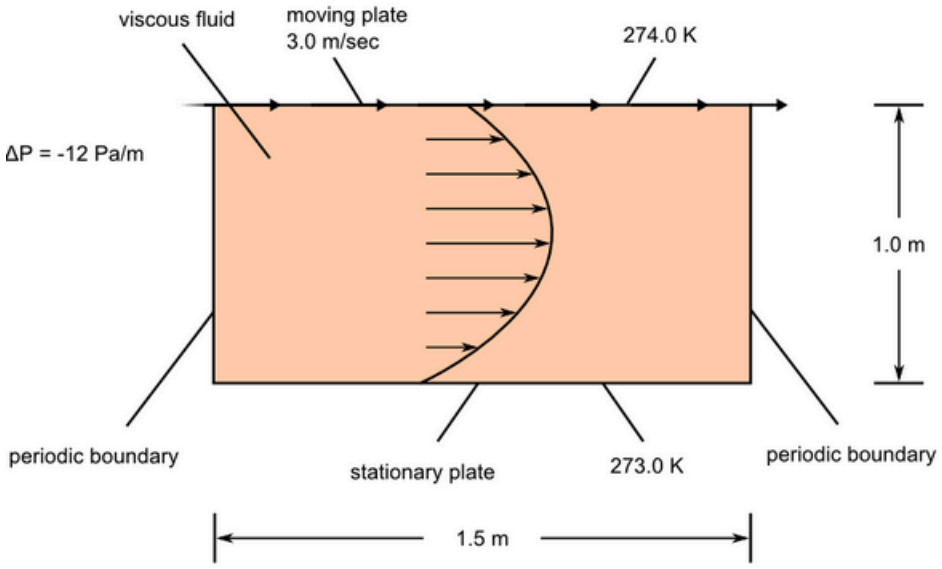


Figure 199: Critical Dimensions and Parameters for Simulating Laminar Couette Flow with an Imposed Pressure Gradient and Heated Walls

The simulation was performed as a two dimensional problem by constructing a volume mesh that contains a single layer of elements extruded in the cross stream direction, normal to the flow plane and by imposing symmetry boundary conditions on the extruded planes. Due to the periodic natural of the flow, a single element extrusion in the streamwise direction is used to reduce the model size.

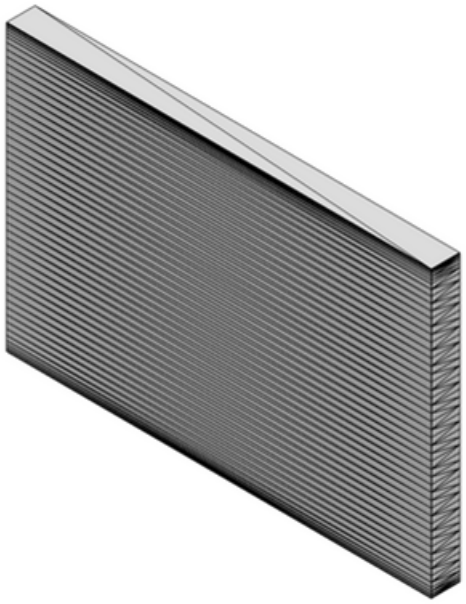


Figure 200: Mesh used for Simulating Laminar Couette Flow with an Imposed Pressure Gradient and Heated Walls

AcuSolve Results

The AcuSolve solution converged to a steady state and the results reflect the mean flow conditions. The simulation results show a flow field with a nearly linear distribution of velocity, with the peak at the top wall. The flow develops primarily because of the shear stress acting on the fluid near both the moving plate and the stationary plate. The temperature variation between the two plates develops due to the viscous heating effects that increase the temperature within the channel, with the maximum near the central height of the domain. The following figure shows the temperature distribution between the two plates and velocity vectors indicating the velocity profile.

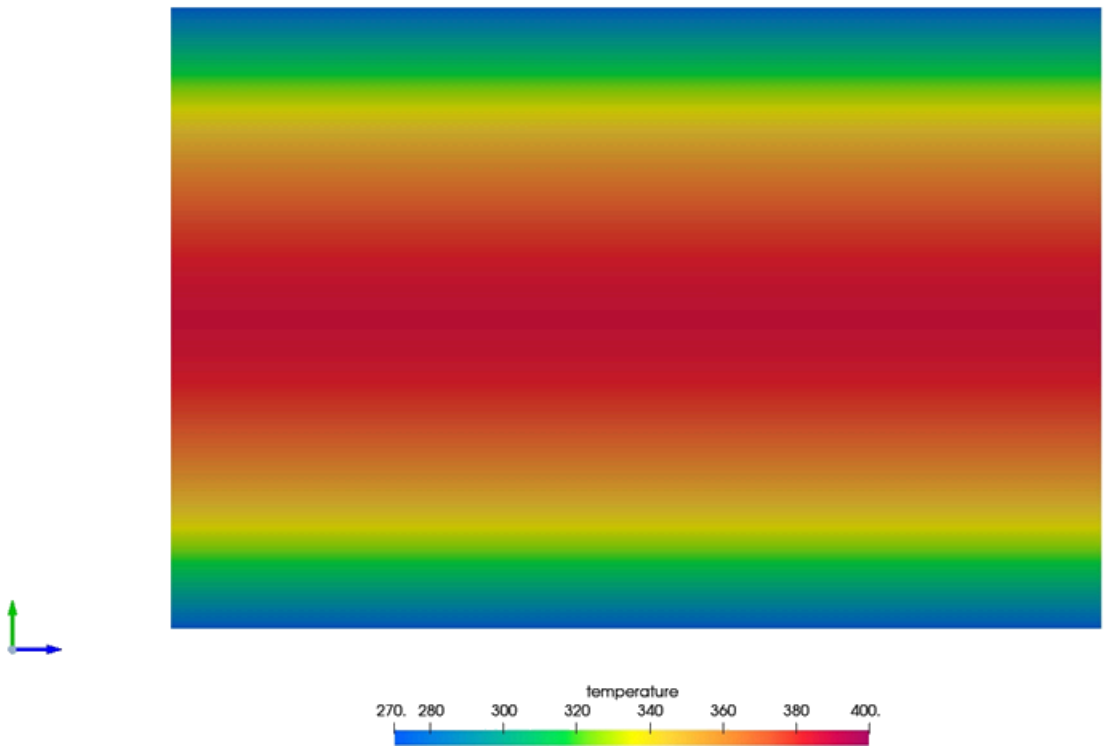


Figure 201: Contours of Temperature Between the Plates, with Velocity Vectors

The following image demonstrates the accuracy of the solution compared to the analytical results as computed by the solution for viscous heating within a channel with a moving upper boundary.

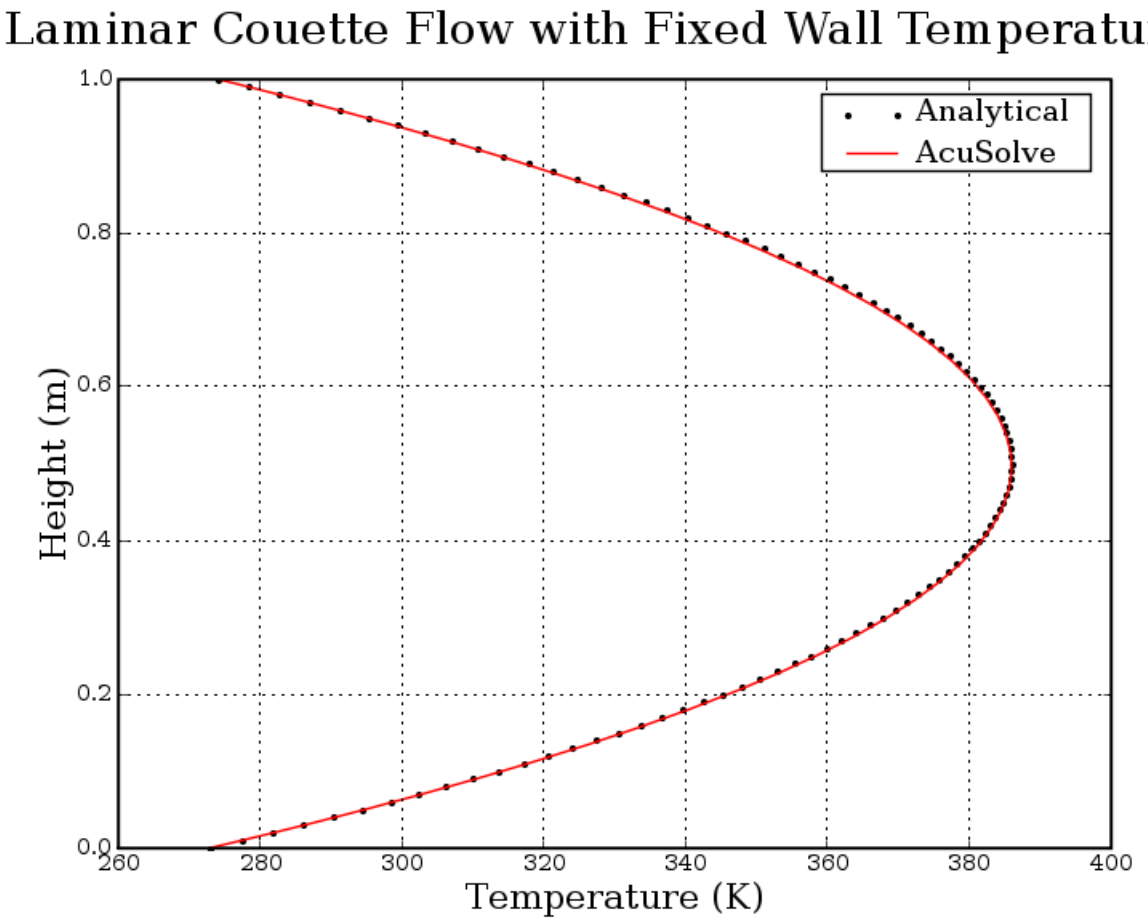


Figure 202: Temperature Plotted Against Height above the Bottom of the Flow Field (Temperature is Presented on the X Axis to Better Represent the Distribution Between the Plates in the Streamwise Direction)

Summary

In this application, a fully developed laminar flow between two plates with fixed temperature is studied and compared against analytical data. The AcuSolve results compare well with the analytical data for the temperature distribution between the two plates. The simulation indicates that the velocity profile arises due to the combination of the viscous shearing and the velocity of the upper plate. The velocity and temperature profiles computed by AcuSolve demonstrate how highly viscous fluids tend to direct the flow regime. AcuSolve demonstrates the ability to predict the analytical solution for viscous heating between two flat plates with moving and stationary boundaries and an imposed pressure gradient.

Simulation Settings for Laminar Couette Flow with Imposed Pressure Gradient and Heated Walls

SimLab database file: `<your working directory>\couette_laminar_heat\couette_laminar_heat.slb`

Global

- Problem Description

    - Flow - Steady State
    - Temperature equation - Advective Diffusive
    - Turbulence equation - Laminar
- Auto Solution Strategy
    - Relaxation factor - `0.2`
- Material Model
    - Fluid
        - Density - `1.0` kg/m3
        - Specific Heat - `1.0` J/kg-K
        - Viscosity - `100.0` kg/m-sec
- Body Force
    - DP/DL
        - Gravity
            1. Z-component - `18.0` m/sec2

Model

- Volumes
    - Fluid
        - Element set
            1. Material model - Fluid
            2. Body force - DP/DL
            3. Viscous heating - on
- Surfaces
    - Max_X
        - Simple Boundary Condition
            1. Type - Symmetry
    - Max_Y
        - Simple Boundary Condition
            1. Type - Wall
            2. Wall velocity type - Cartesian
            3. Z-velocity - `3.0` m/s
            4. Temperature - `274.0` K
    - Max_Z
        - Simple Boundary Condition - (disabled to allow for periodic conditions to be set)
    - Min_X
        - Simple Boundary Condition
            1. Type - Symmetry
    - Min_Y

        - Simple Boundary Condition
            1. Type - Wall
            2. Temperature - `273.0` K
    - Min_Z
        - Simple Boundary Condition - (disabled to allow for periodic conditions to be set)
- Periodics
    - Periodic 1 all
        - Periodic Boundary Conditions
            1. Type - Periodic

References

F. M. White. "Viscous Fluid Flow". Section 3-3.2. McGraw-Hill Book Co., Inc. New York. 1991.

Laminar Flow

4

This section includes validation cases that do not require a turbulence model to be used.

This chapter covers the following:

- Circumferential Flow in a Cylinder Induced by a Rotating Solid (p. 264)
- Laminar Couette Flow with Imposed Pressure Gradient (p. 270)
- Flow Inside a Rotating Cavity (p. 276)
- Laminar Flow Past a 90° T-Junction (p. 284)
- Laminar Poiseuille Flow Through a Pipe (p. 289)
- Oscillating Laminar Flow Around a Circular Cylinder (p. 293)
- Separated Laminar Flow Over a Blunt Plate (p. 298)
- Natural Convection in a Concentric Annulus (p. 305)
- Flow Between Concentric Cylinders (p. 311)
- Heat Transfer Between Radiating Concentric Cylinders (p. 317)
- Laminar Couette Flow with Imposed Pressure Gradient and Heated Walls (p. 323)

Circumferential Flow in a Cylinder Induced by a Rotating Solid

In this application, AcuSolve is used to simulate the flow of air between concentric cylinders that is initiated by the rotation of the solid inner cylinder. The outer cylinder is held stationary while the inner cylinder rotates with a constant speed. AcuSolve results are compared with analytical results as described in White (1991). The close agreement of AcuSolve results with analytical results validates the ability of AcuSolve to maintain a continuous velocity across a non-conformal guide surface interface.

Problem Description

The problem consists of a fluid with material properties of a viscous fluid with the density of air rotating between two infinitely long concentric cylinders, as shown in the following image, which is not drawn to scale. The radius of the outer cylinder is 3.0 m and the radius of the inner cylinder is 1.5 m. The inner cylinder is defined as a solid medium and rotates at 1 rad/sec. The inner cylinder's surface velocity is mapped to the adjacent surface within the fluid medium, while the outer cylinder is fixed. The induced flow is laminar and exhibits a steady state behavior after running for a short period of physical time. The rotation of the inner cylinder causes the fluid to rotate due to viscous shearing near the wall. As the outer cylinder is fixed, a velocity gradient is generated as a function of radius within the flow domain.

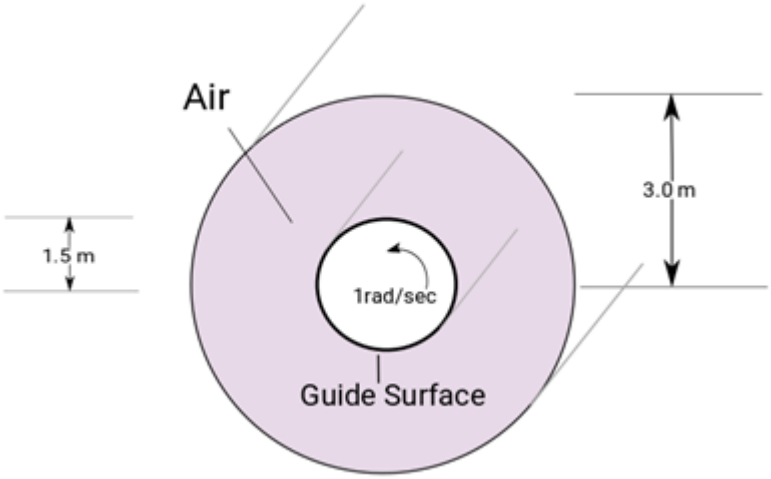


Figure 203: Critical Dimensions and Parameters Used for Simulating Flow Between Two Concentric Cylinders Split with a Guide Surface

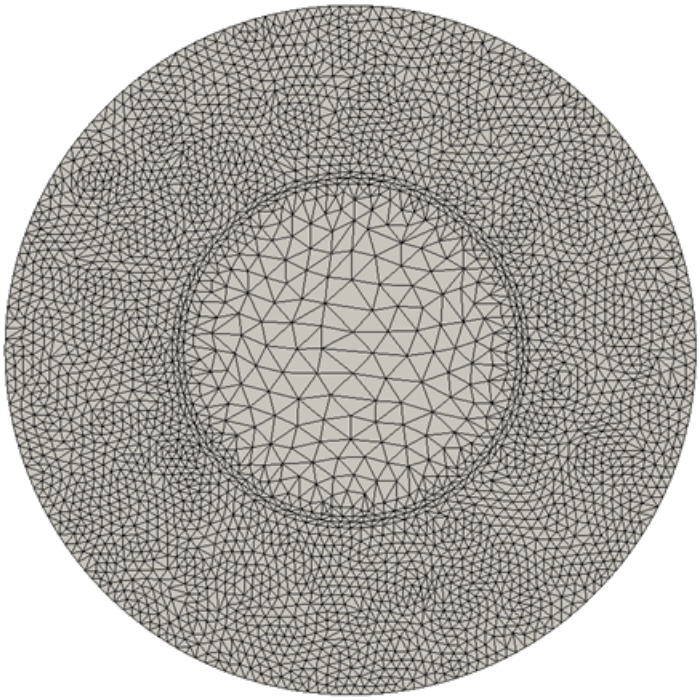


Figure 204: Mesh Used for Simulating Flow Between Two Concentric Cylinders

The simulation was performed as a two dimensional problem by constructing a volume mesh that contains a single layer of elements in the extruded direction, normal to the flow plane and by imposing slip flow and mesh boundary conditions on the extruded planes.

AcuSolve Results

The AcuSolve solution reaches a quasi-static result with the velocity between the two cylinders reaching a steady state at the simulation end time. As the solid inner cylinder rotates, it acts as a guide surface for the fluid elements to track and inherit the two velocity components. The velocity at the edge of the inner cylinder is equal to exactly the rotational speed multiplied by the radius. As the radius increases, the flow velocity reduces until it reaches zero at the outer diameter. The following images show the tangential velocity within the fluid as a function of radius from the center. The tangential velocity is compared with the analytical solution. The image below shows black circles representing the analytical solution and a solid red line for the AcuSolve results.

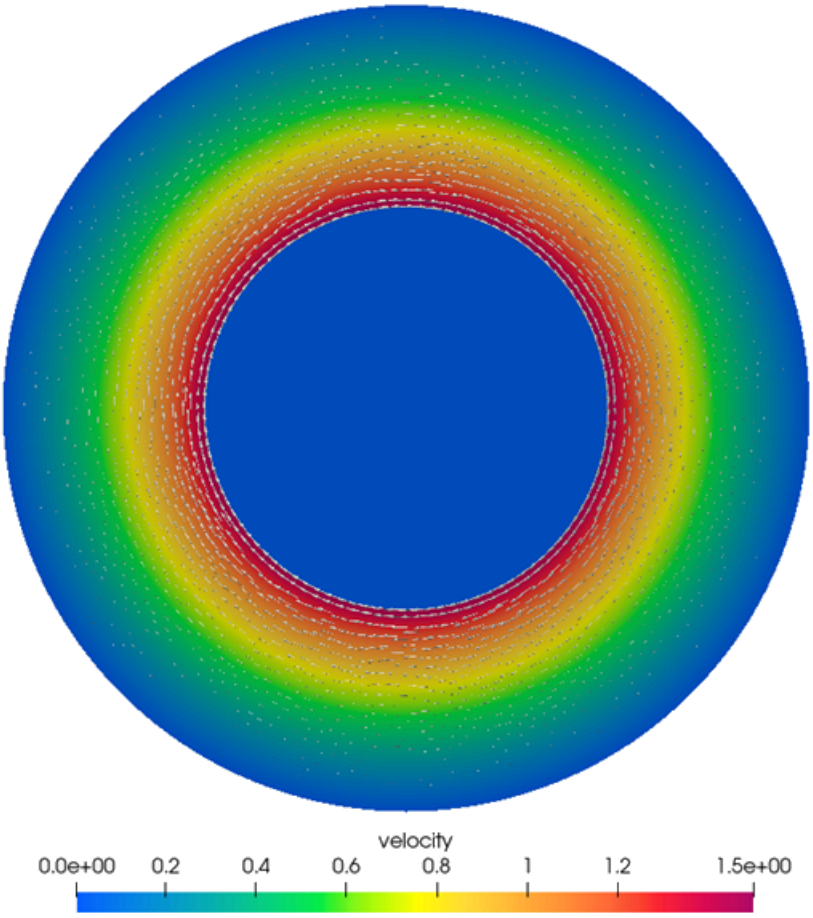


Figure 205: Contours and Vectors of Velocity Between the Concentric Cylinders

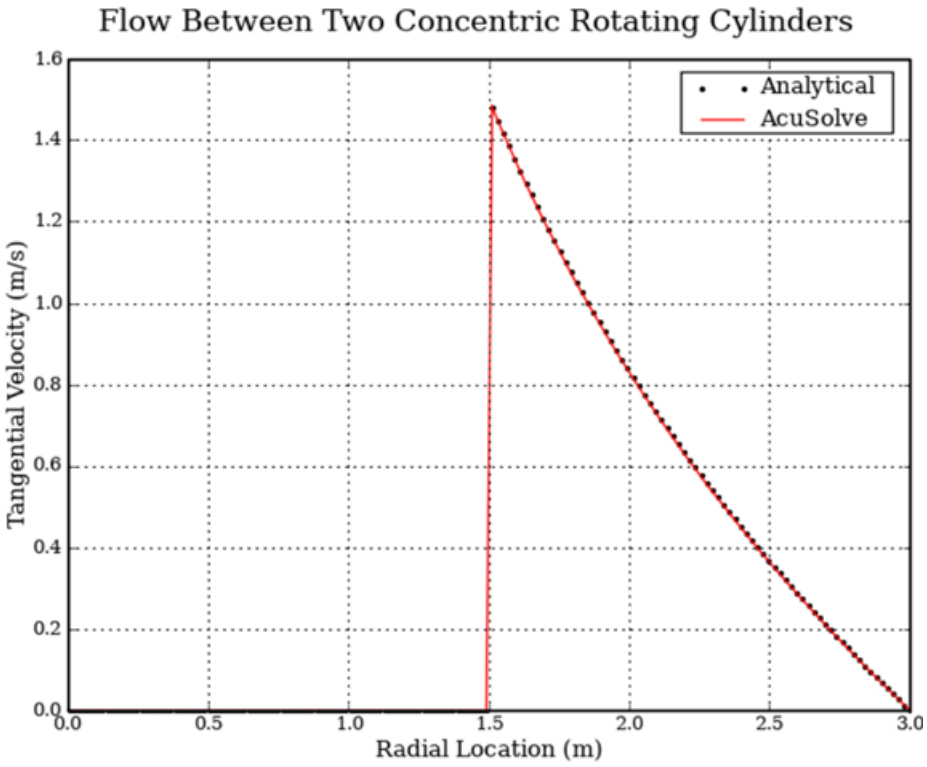


Figure 206: Tangential Velocity Within the Solid and Fluid as a Function of Radial Distance from the Center at the Final Timestep

Summary

The AcuSolve solution compares well with analytical results for laminar flow between concentric cylinders, where the inner cylinder guides the adjacent fluid elements. In this application, a fluid initially at rest inherits the angular velocity from the inner cylinder while the outer cylinder does not rotate. As a result of the inherited velocity and viscosity of the fluid, flow develops between the two cylinders. The AcuSolve solution for the tangential velocity as a function of radius matches exactly with the analytical results.

Simulation Settings for Flow Between Concentric Split Cylinders

HyperMesh CFD database file: `<your working directory>\annulus_split_rotating \annulus_split_rotating.hm`

- Problem Description
  - Analysis type - Transient
  - Flow equation - Navier Stokes
  - Turbulence equation - Laminar
  - Mesh type - Arbitrary Mesh Movement (ALE)
- Auto Solution Strategy
  - Max time steps - `40`
  - Initial time increment- `0.02` sec

- Convergence tolerance - `0.001`
- Min stagger iterations - `2`
- Max stagger iterations - `4`

- Material Model
  - Air
    - Density
      1. Type - Constant
      2. Density - `1.225` kg/m3
    - Viscosity
      1. Type - Constant
      2. Viscosity - `1.781` kg/m-sec
- Mesh Motion
  - Rotation
    - Rotation Center
      1. X-coordinate - `2.0` m
      2. Y-coordinate - `0.0` m
      3. Z-coordinate - `0.0` m
    - Angular velocity
      1. X-component - `1.0` rad/sec
      2. Y-component- `0.0` rad/sec
      3. Z-component - `0.0` rad/sec

  Model
- Volumes
  - CylinderInner
    - Element Set
      1. Medium - Solid
      2. Material model - Aluminum
  - CylinderOuter
    - Element Set
      1. Medium - Fluid
      2. Material model - Air
- Surfaces
  - InBottom
    - Simple Boundary Condition
      1. Type- Slip
      2. Mesh displacement type- Slip
  - InInterf

        - Simple Boundary Condition
            1. Type- Wall
            2. Mesh displacement type- Fixed
            3. Mesh motion- Rotation
        - Guide Surface
            1. Type- Faceted
    - InTop
        - Simple Boundary Condition
            1. Type- Slip
            2. Mesh displacement type- Slip
    - OutBottom
        - Simple Boundary Condition
            1. Type- Slip
            2. Mesh displacement type- Slip
    - OutInterf
        - Simple Boundary Condition
            1. Type- Wall
            2. Wall velocity type- Match Mesh Velocity
            3. Mesh displacement type- Guide surface
            4. Guide surface- InInterf
    - OutTop
        - Simple Boundary Condition
            1. Type- Slip
            2. Mesh displacement type- Slip
    - OutWall
        - Simple Boundary Condition
            1. Type- Wall
            2. Mesh displacement type- Fixed
- Nodes
    - PressurePoint
        - Pressure
            1. Type- Zero

References

F. M. White. "Viscous Fluid Flow". Section 3-2.3. McGraw-Hill Book Co., Inc. New York. 1991.

Laminar Couette Flow with Imposed Pressure Gradient

In this application, AcuSolve is used to simulate the viscous flow of water between a moving and a stationary plate with an imposed pressure gradient. AcuSolve results are compared with analytical results described in White (1991). The close agreement of AcuSolve results with analytical results validates the ability of AcuSolve to model cases with imposed pressure gradients.

Problem Description

The problem consists of air between two plates in a two dimensional domain, as shown in the following image, which is not drawn to scale. The domain is 1.0 m high and 1.5 m long. The top plate moves with a constant velocity of 3.0 m/sec and the bottom plate is fixed. There is a mean-pressure gradient of -12 Pa/m applied to the bulk fluid in the streamwise direction. The problem is simulated with periodic boundaries in the streamwise direction. The induced flow field is laminar and exhibits a steady state behavior. The flow field develops from the pressure gradient, the motion of the top plate, and the viscous shear stresses near the plates.

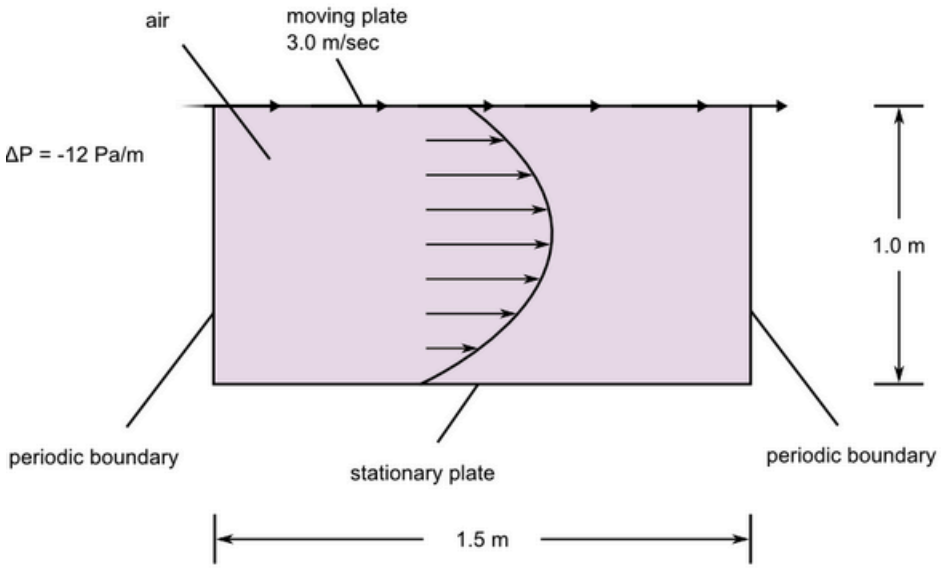


Figure 207: Critical Dimensions and Parameters for Simulating Laminar Couette Flow with an Imposed Pressure Gradient

The simulation was performed as a two dimensional problem by restricting flow in the out-of-plane direction through the use of a mesh that is one element thick.

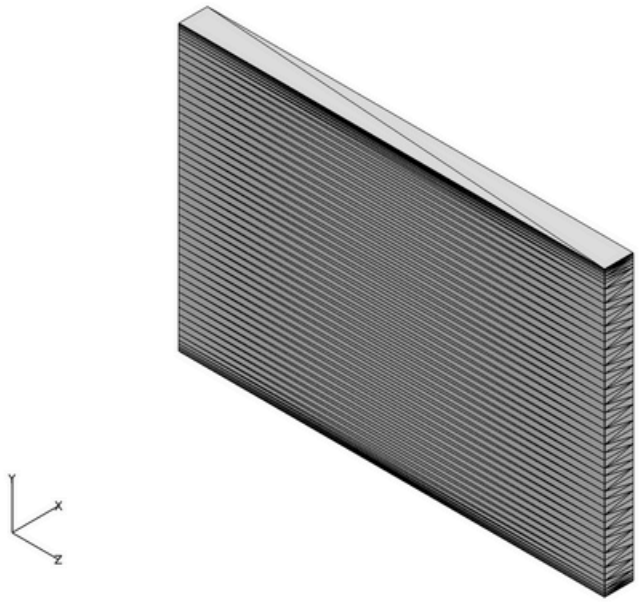


Figure 208: Mesh used for Simulating Laminar Couette Flow with an Imposed Pressure Gradient

AcuSolve Results

The AcuSolve solution converged to a steady state and the results reflect the mean flow conditions. The greatest velocity is located at approximately 40 percent of the channel height, closer to the moving plate. The flow develops as a result of the pressure gradient and the shear stress acting on the fluid near both the moving plate and the stationary plate.

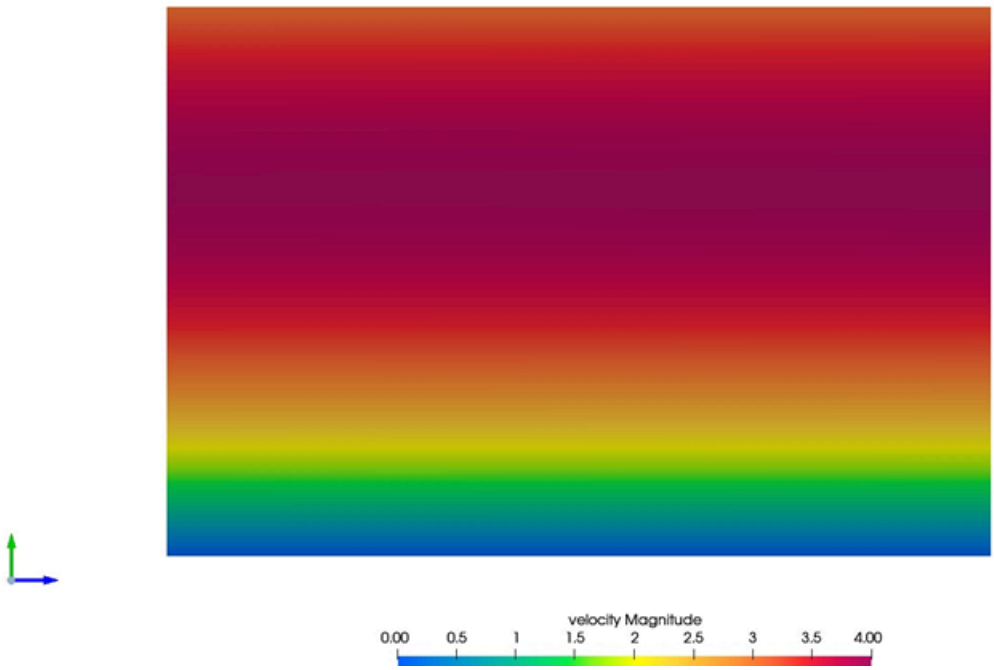


Figure 209: Z-Velocity Contours and Velocity Vectors

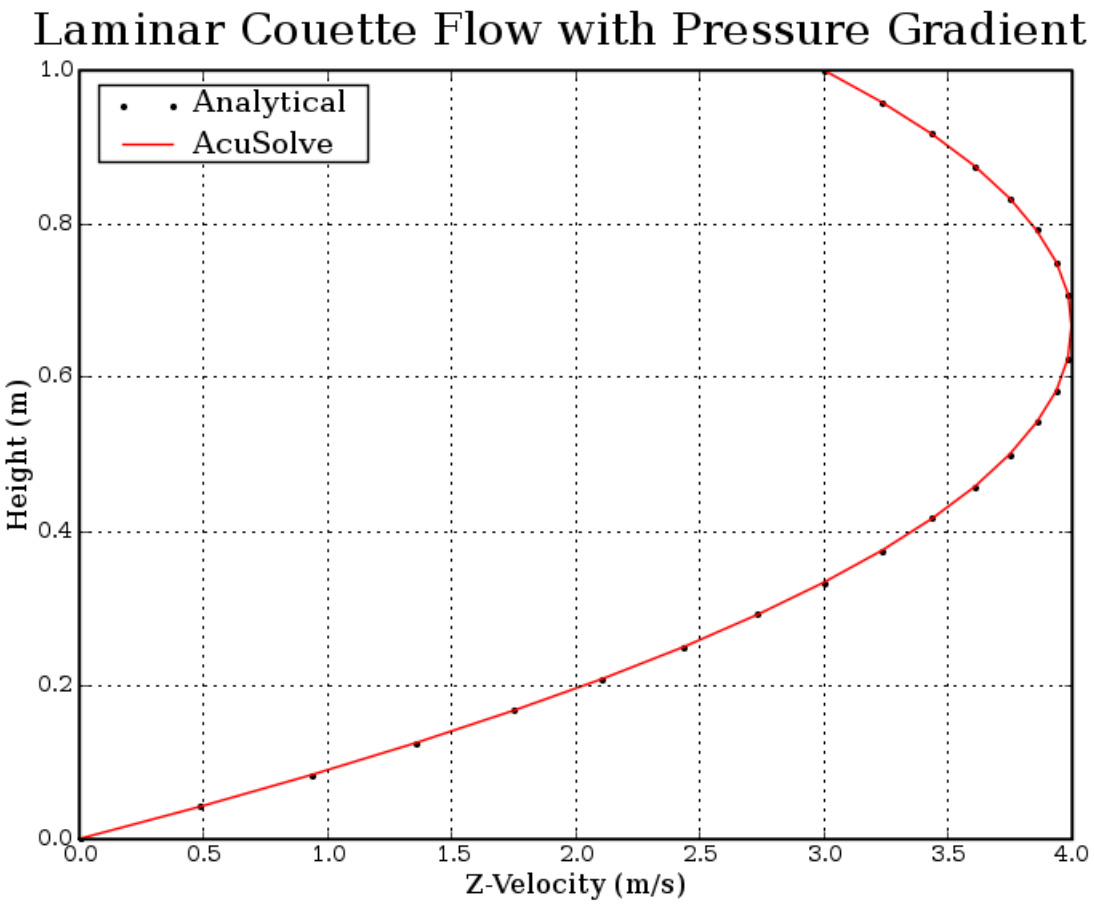


Figure 210: Z Velocity Plotted Against Height Above the Bottom of the Flow Field (Z Velocity is Presented on the X Axis to Better Represent the Velocity Profile in the Direction of Flow)

Summary

The velocity profile computed by AcuSolve agrees well with the analytical solution for this application. The velocity profile arises due to the combination of the imposed pressure gradient and the constant upper-wall velocity.

Note: The combination of these effects results in the asymmetric velocity profile that is reflected in the results.

Simulation Settings for Laminar Couette Flow with Imposed Pressure Gradient

SimLab database file: `<your working directory>\couette_flow\couette_flow.slb`

Global

- Problem Description
  - Solution Type - Steady State
  - Flow - Laminar

- Auto Solution Strategy
  - Relaxation factor - `0.2`
- Material Model
  - Air
    - Density - `1.0` kg/m3
    - Viscosity - `1.0` kg/m-sec
- Body Force
  - DP/DL
    - Gravity
      1. Z-component - `18.0` m/sec2

Model

- Volumes
  - Fluid
    - Element set
      1. Material model - Air
      2. Body force - DP/DL
- Surfaces
  - Max_X
    - Simple Boundary Condition
      1. Type - Symmetry
  - Max_Y
    - Simple Boundary Condition
      1. Type - Wall
      2. Wall velocity type - Cartesian
      3. Z-velocity - `3.0` m/s
  - Max_Z
    - Simple Boundary Condition - (disabled to allow for periodic conditions to be set)
  - Min_X
    - Simple Boundary Condition
      1. Type - Symmetry
  - Min_Y
    - Simple Boundary Condition
      1. Type - Wall
  - Min_Z
    - Simple Boundary Condition - (disabled to allow for periodic conditions to be set)
- Periodics
  - Periodic 1

- Periodic Boundary Conditions
  1. Type - Periodic

References

F. M. White. "Viscous Fluid Flow". Section 3-2.3. McGraw-Hill Book Co., Inc. New York. 1991.

Flow Inside a Rotating Cavity

In this application, AcuSolve is used to simulate the flow of air in an enclosed cylindrical cavity with a rotating top and a fixed bottom. AcuSolve results are compared with experimental data adapted from Michelsen (1986). The close agreement of AcuSolve results with experimental data validates the ability of AcuSolve to model cases containing enclosed cavities with flow induced by rotating walls.

Problem Description

The problem consists of air in an enclosed cylinder 1.0 m tall with a radius of 1.0 m, as shown in the following image, which is not drawn to scale. The top of the cylinder rotates about its center at 1 rad/s, while the bottom of the cylinder is fixed. As the container top spins, the viscous stresses on the fluid induce a circumferential (swirl) velocity throughout the height of the cylinder. To conserve mass and momentum, the fluid generates a radial velocity that changes direction based on distance away from the rotation center of the cylinder.

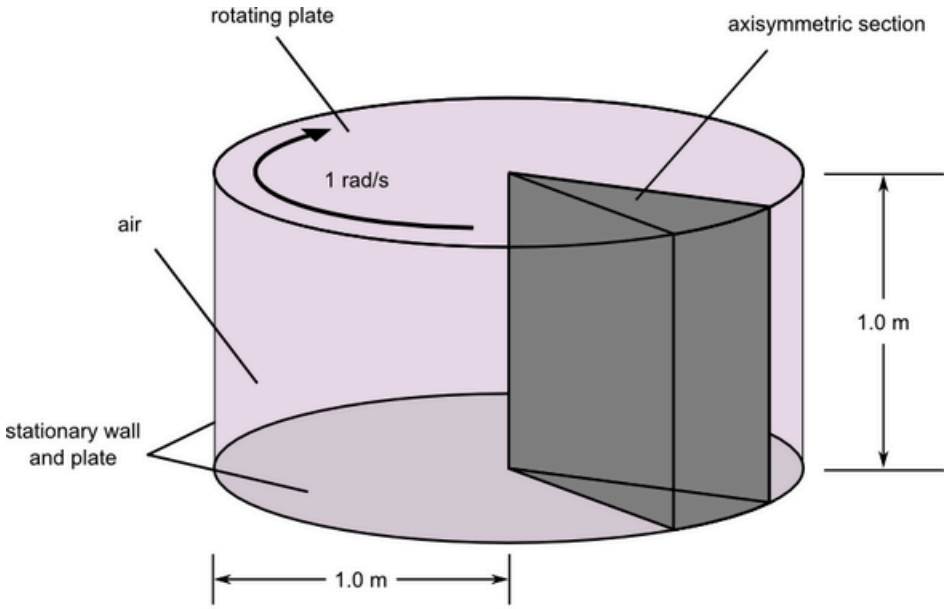


Figure 211: Critical Dimensions and Parameters for Simulating Flow Inside a Rotating Cavity

The flow domain is modeled with axisymmetric periodicity in the circumferential direction, which allows for accurate simulation of the flow while minimizing computational time.

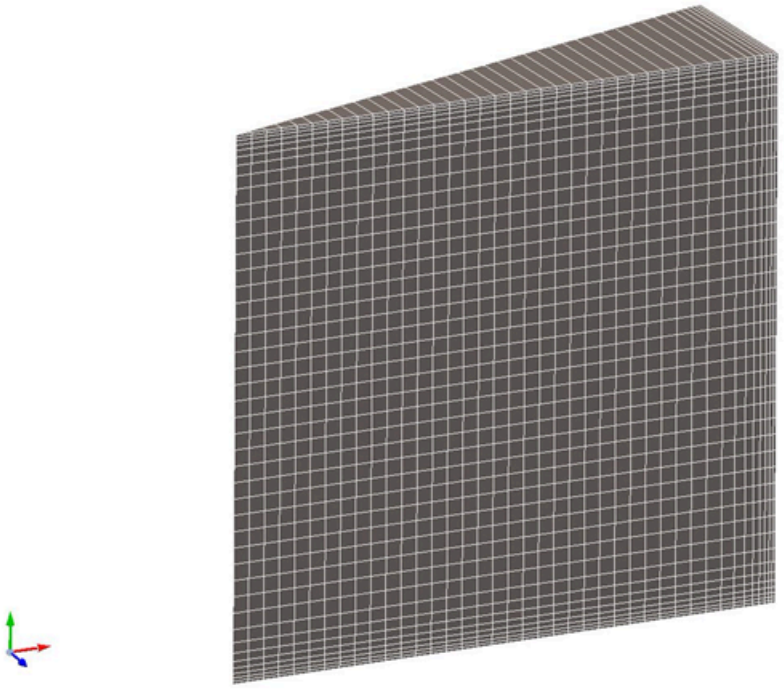


Figure 212: Mesh of Periodic Section Used for Simulating Flow Inside a Rotating Cylinder

AcuSolve Results

The AcuSolve solution converged to a steady state and the results reflect the mean flow conditions. The velocity varies with both vertical location and with distance from the rotation center. The complex flow field develops from a combination of the viscous stresses acting at the rotating cylinder top and at the stationary bottom.

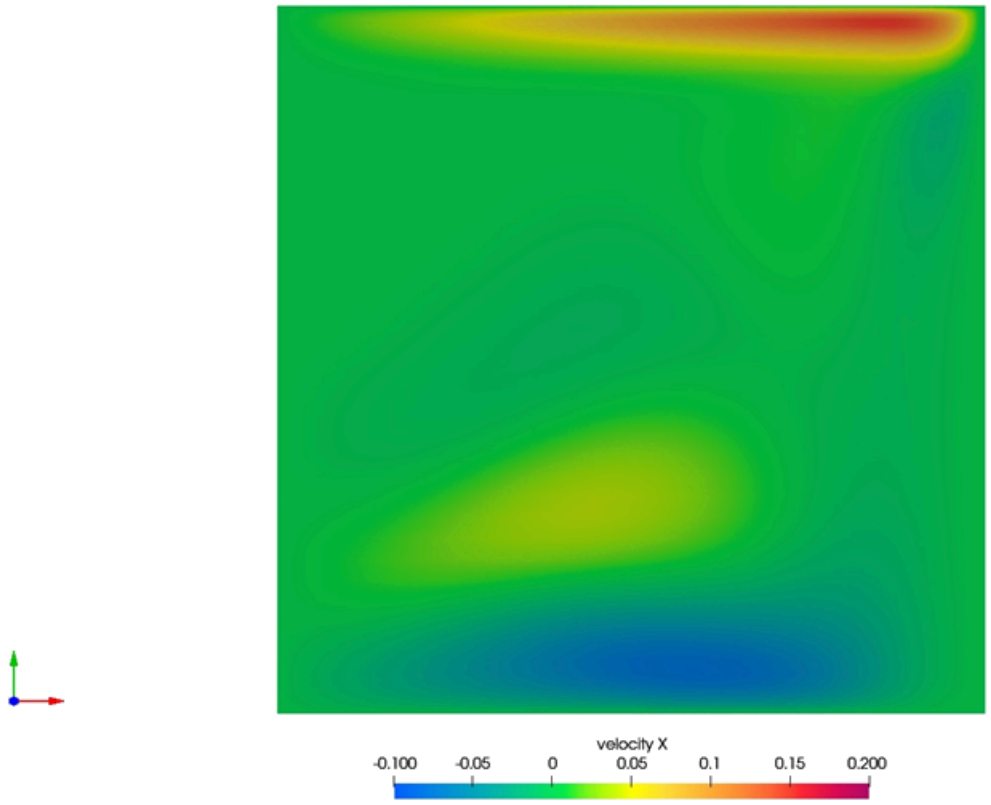


Figure 213: Contours of Radial Velocity with Velocity Vectors. This Image Shows the Front Face of the Modeled Cylinder Wedge, with the Center of Rotation on the Left Edge. The Vertical Line Represents a Radial Location 0.6 m From the Center of Rotation.

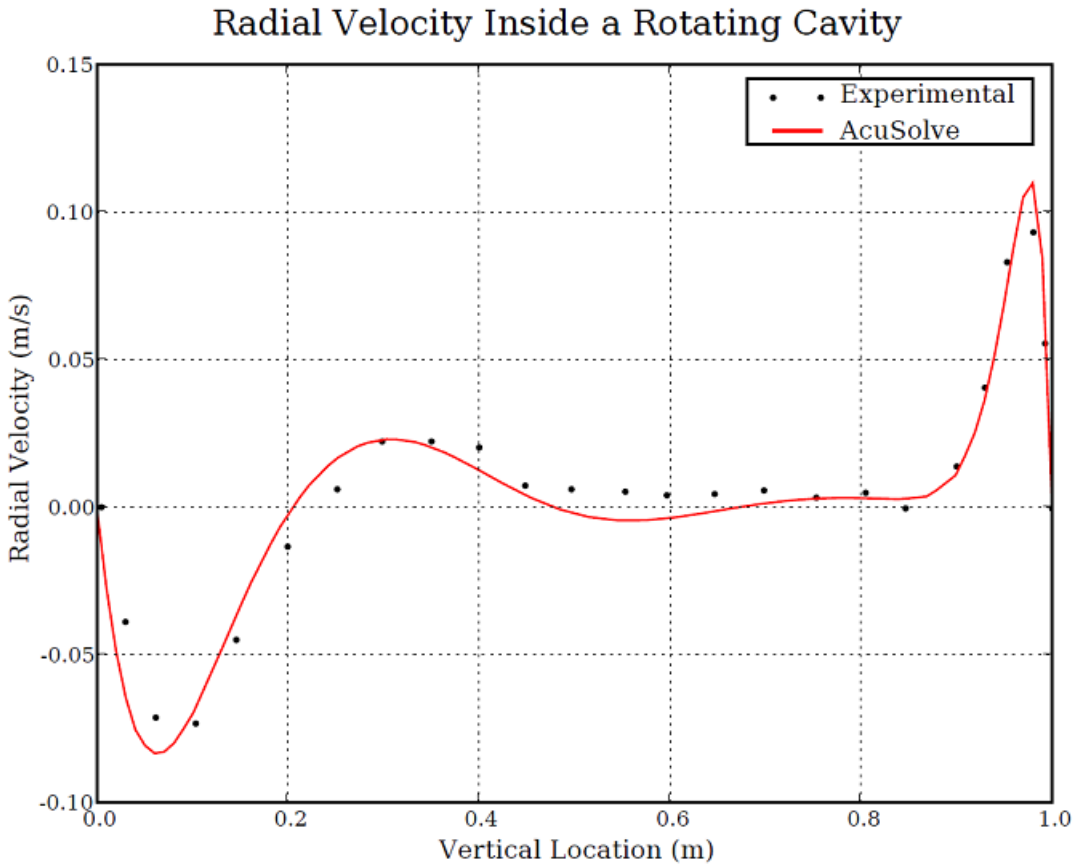


Figure 214: Radial Velocity (at 0.6 m From the Center of Rotation) as a Function of Vertical Location From Cylinder Bottom

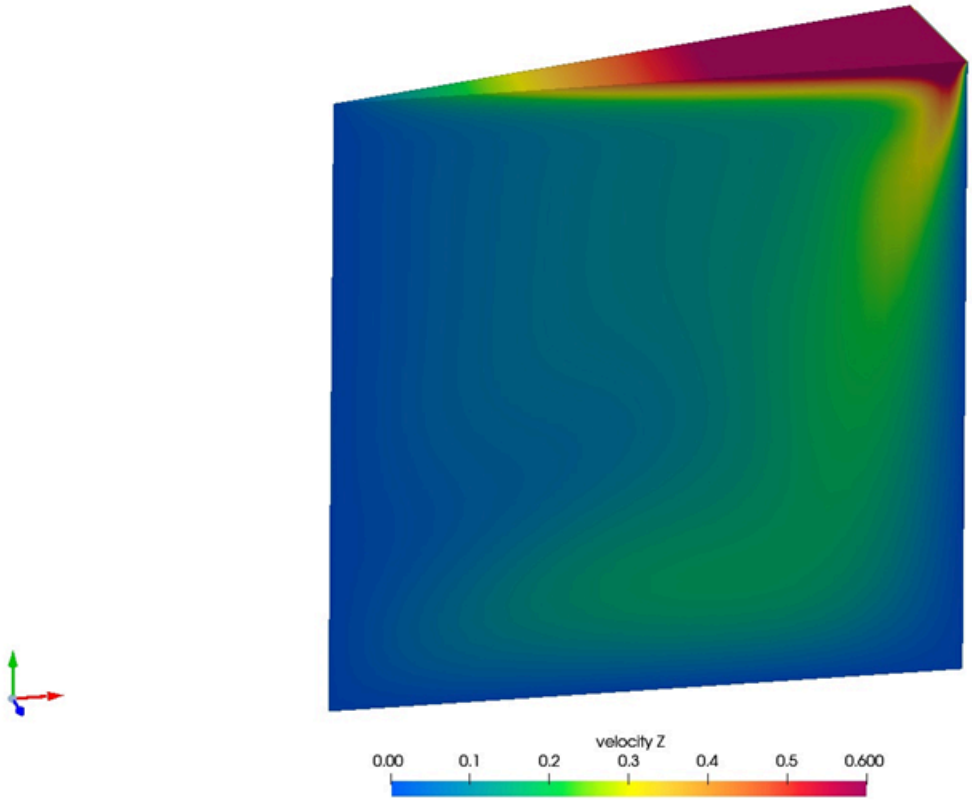


Figure 215: Contours of Swirl Velocity with Velocity Vectors

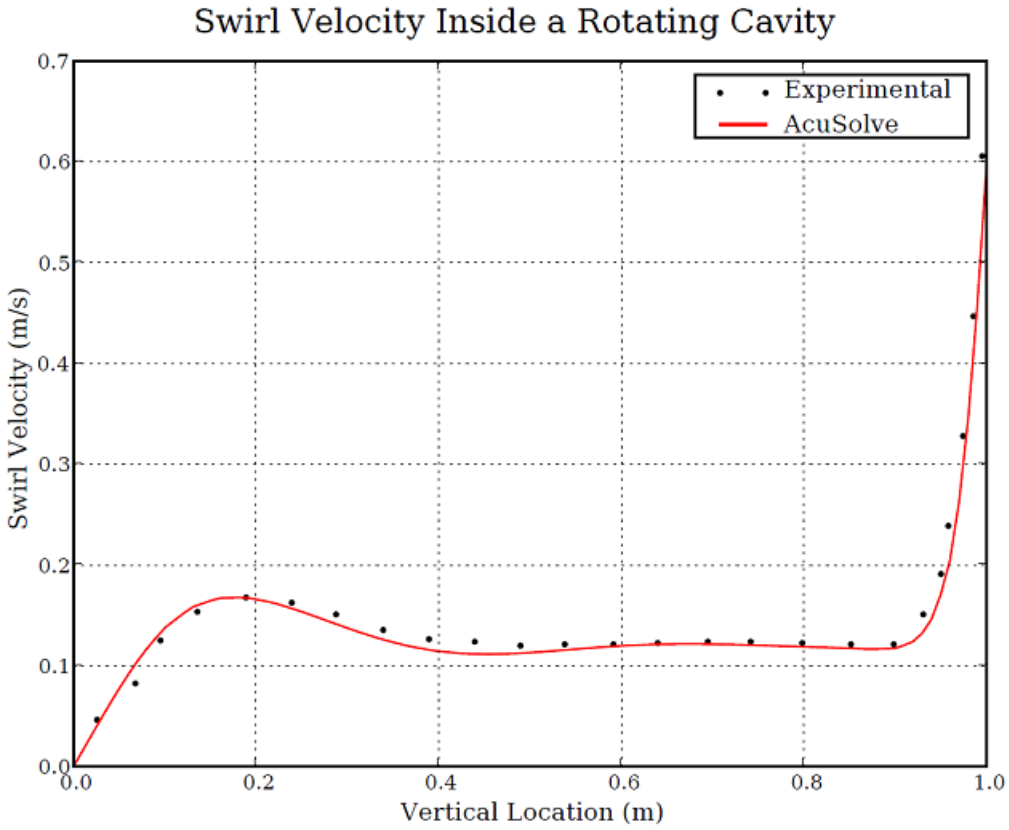


Figure 216: Swirl Velocity (at 0.6 m From Center of Rotation) as a Function of Vertical Location From the Cylinder Bottom

Summary

The AcuSolve solution compares well with the experimental data for flow induced by a rotating top of an enclosed cylinder. In this application, the flow in the fluid region is driven by the viscous stresses near the rotating top. Viscous stresses drag the fluid in a circular direction near the spinning wall. The angular velocity of the fluid decreases as distance from the top wall increases. Radial velocity develops as a result of the migration of the fluid toward the outer wall in regions of high angular velocity. The AcuSolve radial and swirl velocities compare very closely with the experimental data.

Simulation Settings for Flow Inside a Rotating Cavity

SimLab database file: `<your working directory>\cavity_rotating\cavity_rotating.slb`

Global

- Problem Description
  - Solution type - Steady State
  - Flow - Laminar
- Auto Solution Strategy
  - Relaxation Factor - `0.4`
- Material Model

- Air
  - Density - `1.0` kg/m3
  - Viscosity - `0.000556` kg/m-sec

- Reference Frame
  - Cavity Rotation
    - Rotation center
      1. X-coordinate - `0.0`
      2. Y-coordinate - `0.0`
      3. Z-coordinate - `0.0`
    - Angular velocity
      1. X-component - `0.0`
      2. Y-component - `-1.0` rad/sec
      3. Z-component - `0.0`

Model

- Volumes
  - Fluid
    - Element Set
      1. Material model - Air
- Surfaces
  - Bottom
    - Simple Boundary Condition
      1. Type - Wall
  - Max_X
    - Simple Boundary Condition
      1. Type - Wall
  - Max_Z
    - Simple Boundary Condition - (disabled to allow for periodic conditions to be set)
  - Min_Z
    - Simple Boundary Condition - (disabled to allow for periodic conditions to be set)
  - Top
    - Simple Boundary Condition
      1. Type - Wall
      2. Reference frame - Cavity Rotation
- Periodics
  - Periodic 1
    - Periodic Boundary Condition
      1. Type - Axisymmetric

2 Rotation axis
  1 point 1
    1 X-coordinate - `0.0` m
    2 Y-coordinate - `0.0` m
    3 Z-coordinate - `0.0` m
  2 point 2
    1 X-coordinate - `0.0` m
    2 Y-coordinate - `1.0` m
    3 Z-coordinate - `0.0` m

References

J. A. Michelsen. "Modeling of Laminar Incompressible Rotating Fluid Flow". AFM 86-05. Ph.D. thesis, Department of Fluid Mechanics, Technical University of Denmark. 1986.

Laminar Flow Past a 90° T-Junction

In this application, AcuSolve is used to simulate laminar flow through a channel with two outlets forming a T-junction. AcuSolve results are compared with experimental results adapted from Hayes and others (1989). The close agreement of AcuSolve results with experimental results validates the ability of AcuSolve to model cases with multiple outlet paths.

Problem Description

The problem consists of air flowing past a T-junction in a channel, as shown in the following image, which is not drawn to scale. Air enters the channel with an average velocity of 0.667 m/s and travels past the T-junction 2.0 m from the inlet. A portion of the flow will travel out of the branch of the channel due to the pressure difference between the bulk flow and the outlet of the branch.

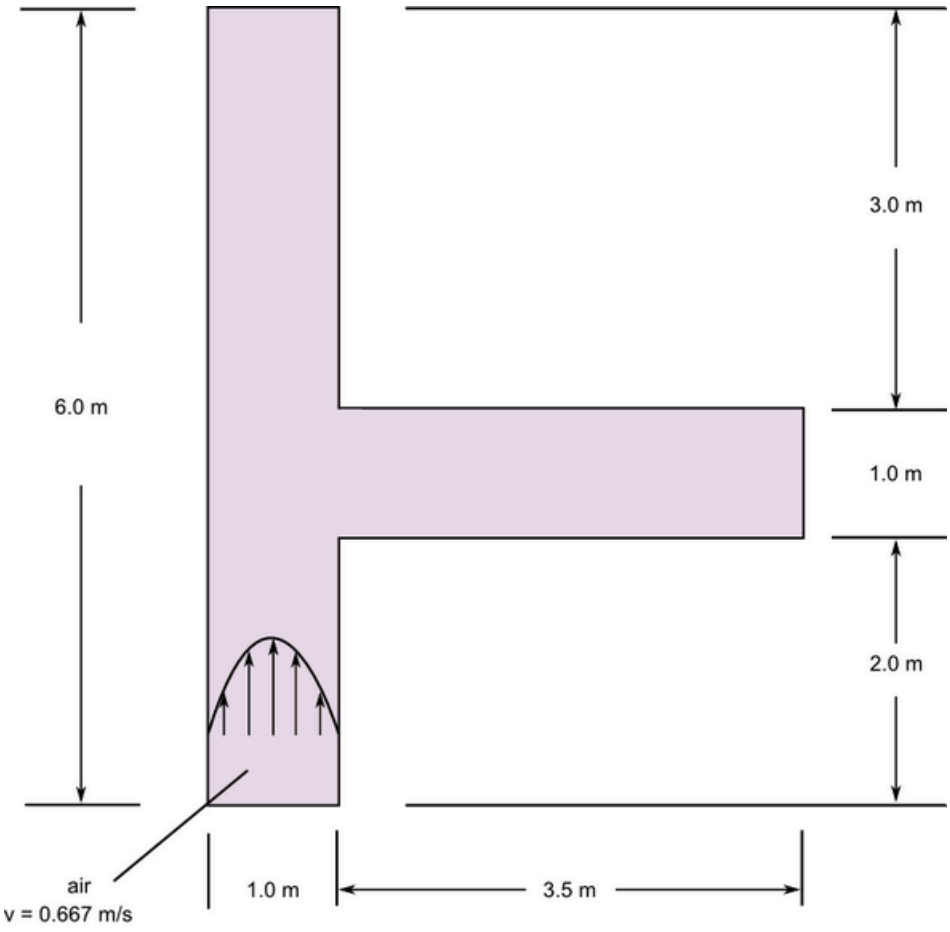


Figure 217: Critical Dimensions and Parameters for Simulating Laminar Flow Past a 90° T-Junction

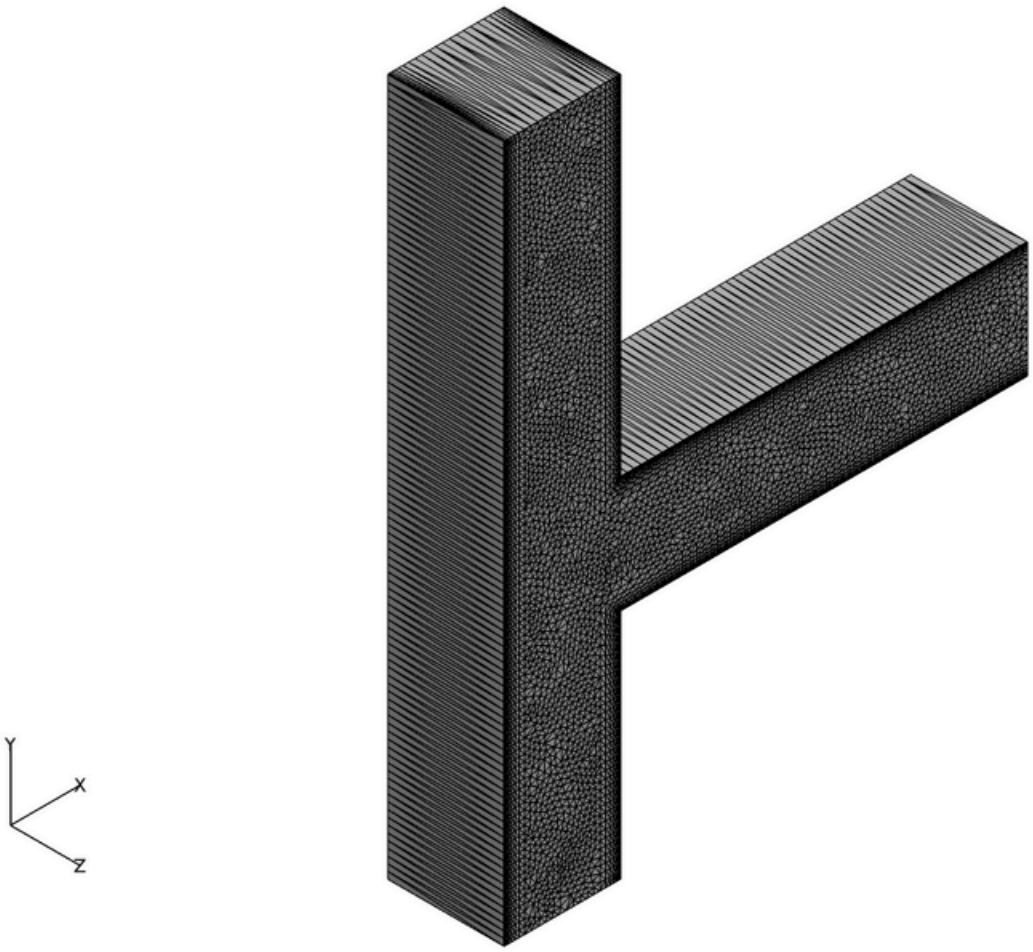


Figure 218: Mesh Used for Simulating Laminar Flow past a 90° T-Junction

AcuSolve Results

The AcuSolve solution converged to a steady state and the results reflect the mean flow conditions. As the air flows past the junction, a portion of it is diverted into the branch. A small recirculation region develops at the top of the junction and collapses before the flow exits the domain through the right branch.

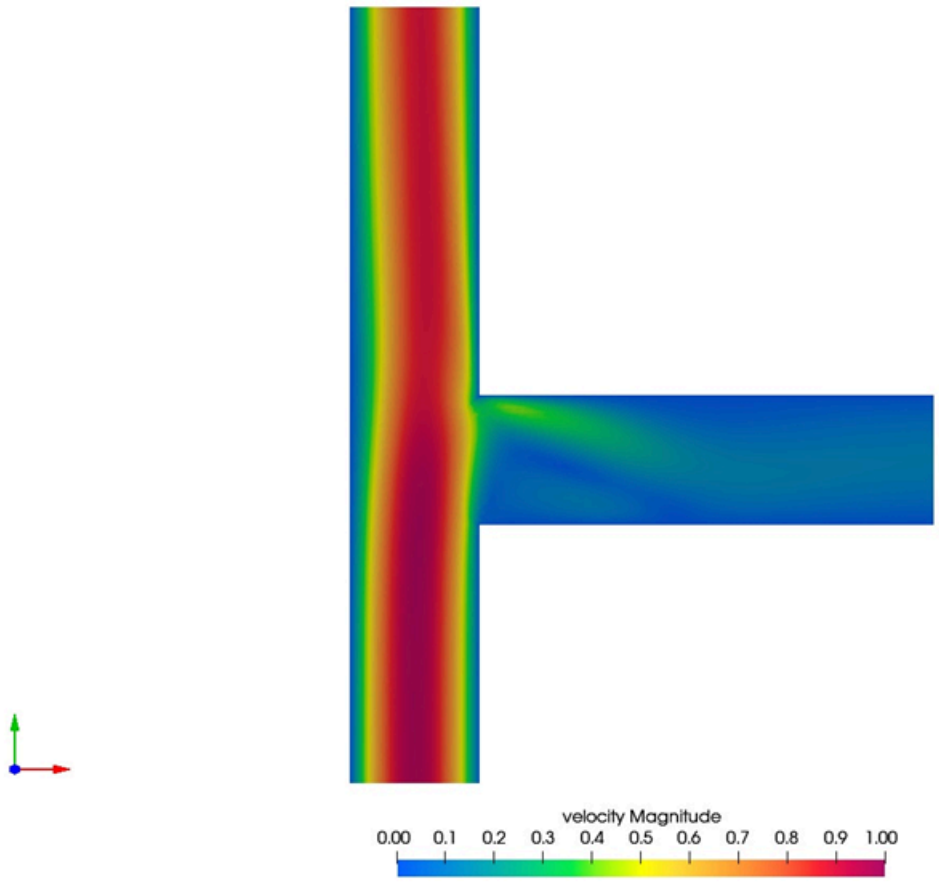


Figure 219: Velocity Contours in a T-Junction

The experimental value for the fraction of flow exiting the top branch of the channel is presented with the corresponding AcuSolve result in the following table.

Table 9:

	Experimental fractional flow	**AcuSolve fractional flow**	**Percent deviation from experimental**
Fractional flow exiting the upper branch	0.887	0.889	0.332

Summary

The AcuSolve solution compares well with experimental results for flow past a T-junction. In this application, flow is driven by a fixed flow rate at the inlet to the main branch. A portion of the flow from the main branch is diverted into the right branch of the T-junction, giving rise to recirculation just downstream of the junction. This recirculation collapses before the flow exits the side branch. The AcuSolve result for fractional flow exiting the top branch is within 0.33 percent of the experimental results.

Simulation Settings for Laminar Flow Past a 90° T-Junction

SimLab database file: `<your working directory>\T_junction_laminar\T_junction_laminar.slb`

Global

- Problem Description
  - Solution type - Steady State
  - Flow - Laminar
- Auto Solution Strategy
  - Relaxation factor - `0.2`
- Material Model
  - Air
    - Type - Constant
    - Density - `1.0` kg/m3
    - Viscosity - `0.003333` kg/m-sec

  Model
- Volumes
  - Fluid
    - Element Set
      1. Material model - Air
- Surfaces
  - Inflow
    - Simple Boundary Condition
      1. Type - Inflow
      2. Inflow type - Average Velocity
      3. Average velocity - `0.6667` m/sec
  - Max_Z
    - Simple Boundary Condition - (disabled to allow for periodic conditions to be set)
  - Min_Z
    - Simple Boundary Condition - (disabled to allow for periodic conditions to be set)
  - Outflow
    - Simple Boundary Condition
      1. Type - Outflow
  - T_Out
    - Simple Boundary Condition
      1. Type - Outflow
  - Walls
    - Simple Boundary Condition
      1. Type - Wall

- Periodics
  - Periodic 1
    - Periodic Boundary Condition
      1. Type - Periodic

References

R. E. Hayes, K. Nandkumar, and H. Nasr-El-Din. "Steady Laminar Flow in a 90 Degree Planar Branch". Computers and Fluids 17(4): 537-553. 1989.

Laminar Poiseuille Flow Through a Pipe

In this application, AcuSolve is used to simulate the flow of carbon dioxide (CO_2) entering a pipe with a fixed velocity. AcuSolve results are compared with analytical results using the Hagen-Poiseuille approach as described in White (1991). The close agreement of AcuSolve results with analytical results validates the ability of AcuSolve to model cases with constant flow velocity.

Problem Description

The problem consists of CO_2 flowing through a circular pipe 0.0025 m in diameter and 0.01 m long, as shown in the following image, which is not drawn to scale. The CO_2 enters the pipe with an average inlet velocity of 3.0 m/s. The flow field develops as a result of the viscous shearing on the fluid at the pipe wall.

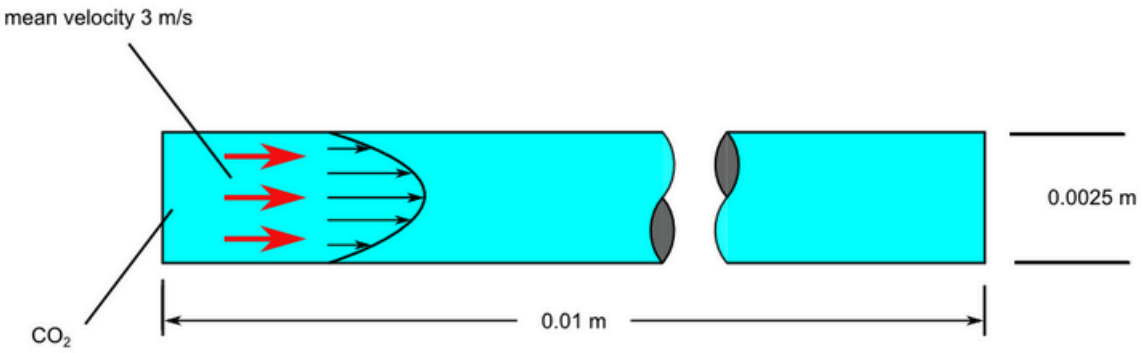


Figure 220: Critical Dimensions and Parameters for Simulating Laminar Poiseuille Flow Through a Pipe



Figure 221: Mesh Used for Simulating Laminar Poiseuille Flow Through a Pipe

AcuSolve Results

The AcuSolve solution converged to a steady state and the results reflect the mean flow conditions. The pressure decreases along the length of the pipe.

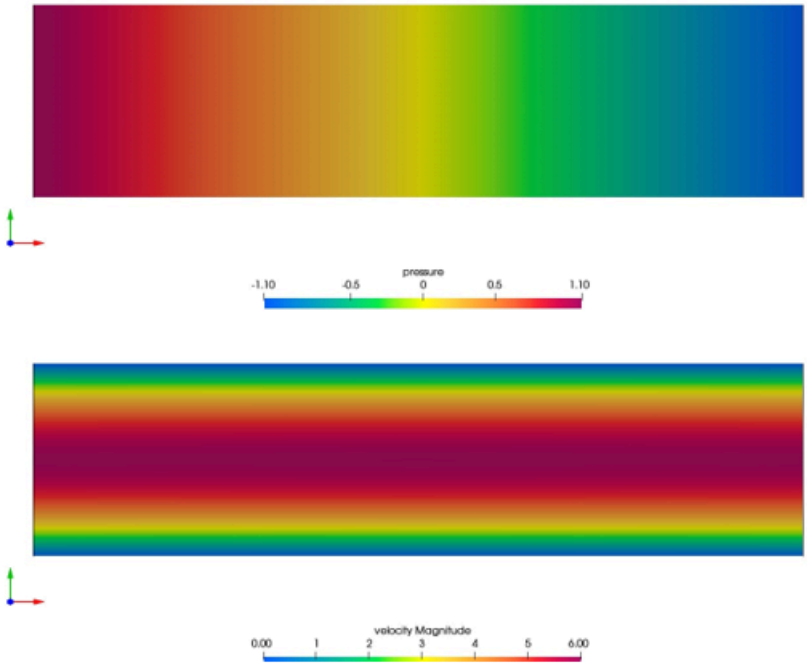


Figure 222: Pressure Contours and Velocity Magnitude Vectors

The analytical pressure drop between the inlet and the outlet is presented with the corresponding AcuSolve result in the following table.

Table 10:

	Analytical pressure drop (Pa)	**AcuSolve pressure drop (Pa)**	**Percent deviation from analytical**
Inlet to outlet pressure drop	2.242	2.245	0.099

Summary

The AcuSolve solution compares well with analytical results for laminar flow through a pipe. In this application, the pressure drop along the length of the pipe is caused by the viscous shearing near the pipe wall. The AcuSolve steady state solution compares well with the analytical solution, with less than 0.1 percent error. The computation cost of the solution is reduced significantly due to the use of extruded elements in the streamwise direction and the fully established flow profile that is assigned.

Simulation Settings for Laminar Poiseuille Flow Through a Pipe

SimLab database file: `<your working directory>\pipe_laminar\pipe_laminar.slb`

Global

- Problem Description

- Flow Type - Steady State
- Turbulence - Laminar

- Auto Solution Strategy
  - Relaxation factor - `0.2`
- Material Model
  - CO2
    - Density `1.808` kg/m3
    - Viscosity `1.46e-5` kg/m-sec

  Model
- Volumes
  - Fluid
    - Element Set
      1. Material Model - CO2
- Surfaces
  - Inflow
    - Simple Boundary Condition - (disabled to allow for periodic conditions to be set)
    - Advanced Options
      1. Integrated Boundary Conditions
         1. Mass Flux
            1. Type - Constant
            2. Constant value - `-2.6625e-05` kg/sec
  - Outflow
    - Simple Boundary Condition - (disabled to allow for periodic conditions to be set)
  - Wall
    - Simple Boundary Condition
      1. Type - Wall
- Periodics
  - Periodic 1
    - Individual Periodic BCs
      1. Velocity
         1. Type - Periodic
      2. Pressure
         1. Type - Single Unknown Offset

References

F. M. White. "Viscous Fluid Flow". Section 3-2.1. McGraw-Hill Book Co., Inc.. New York. 1991.

Oscillating Laminar Flow Around a Circular Cylinder

In this application, AcuSolve is used to simulate two dimensional, laminar flow over a cylinder to predict separation of flow from the cylinder surface and the flow in the wake area. AcuSolve results are compared with experimental results as described in Tritton (1959). The close agreement of AcuSolve results with experimental results validates the ability of AcuSolve to model cases with unsteady oscillating vortex streets.

Problem Description

The problem consists of a cylinder located in a rectangular domain, as shown in the following image, which is not drawn to scale. A fluid enters the domain with a low velocity (v) of 0.5 m/s. The diameter (D) of the cylinder is 20 cm. The domain extends 10 X D upstream of the cylinder center, 5D above and below the cylinder center, and 40D downstream of the cylinder center. The density of the working fluid is 1 kg/m^3 and the viscosity is 0.001 kg/m-s. The Reynolds number for this problem is 100.

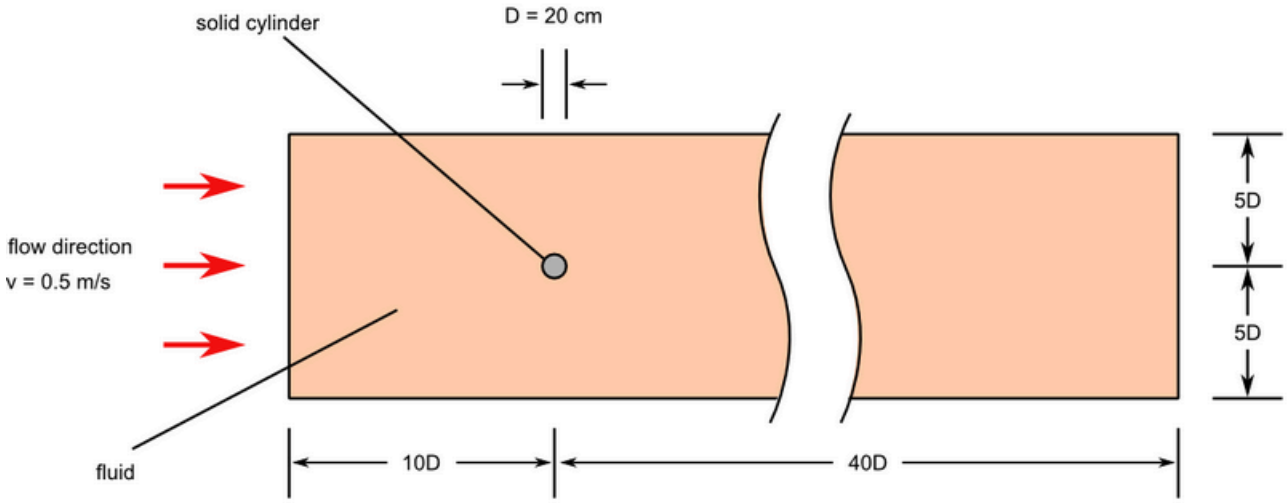


Figure 223: Critical Dimensions and Parameters for Simulating Oscillating Laminar Flow Around a Circular Cylinder

The simulation was performed as a two dimensional problem by constructing a volume mesh that contains a single layer of elements in the extruded direction, normal to the flow plane, and by imposing symmetry boundary conditions on the extruded planes.

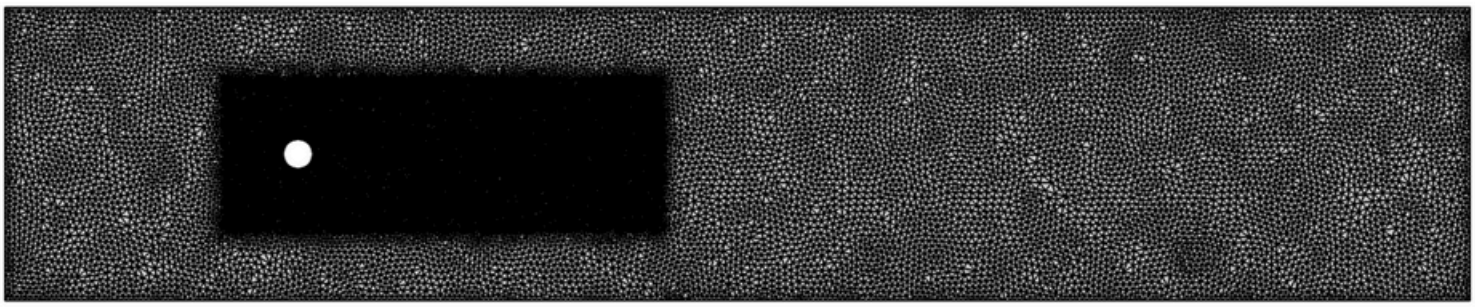


Figure 224: Mesh used for Simulating Oscillating Laminar Flow Around a Circular Cylinder

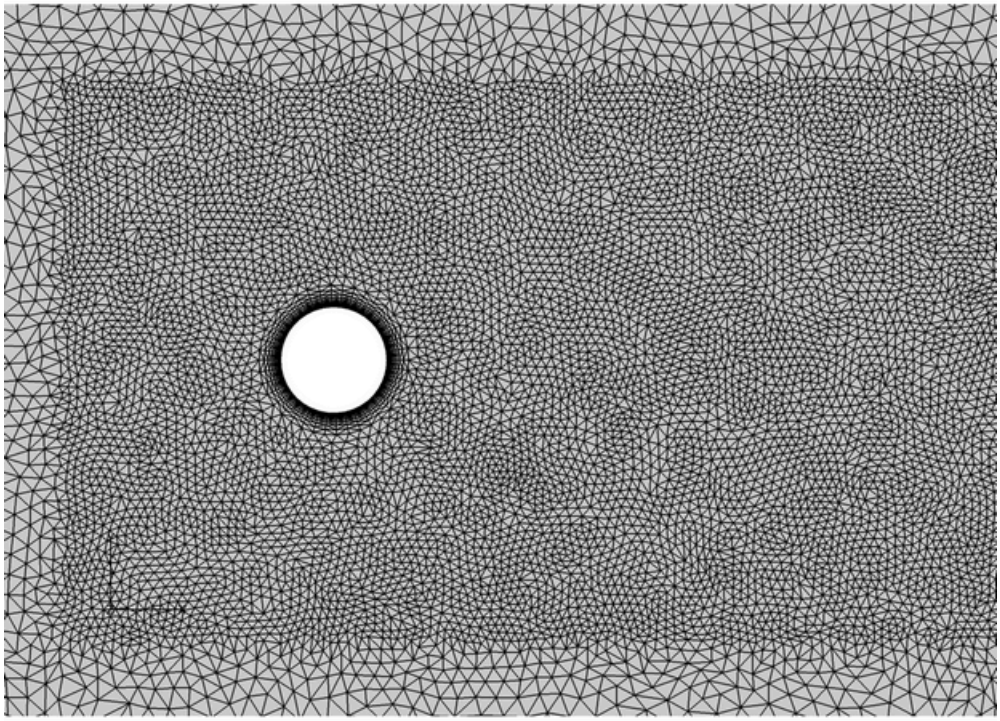


Figure 225: Details of the Mesh Showing Refinement Zone Around the Cylinder

AcuSolve Results

The simulation was run as transient for a time record sufficient to ensure that the vortex shedding in the wake reached a stabilized oscillation frequency. The AcuSolve solution shows an unsteady, oscillating flow field with flow around the cylinder separating from the cylinder surface. A wake area is developed downstream of the cylinder with alternating vortices shedding at a regular frequency from the top and bottom of the cylinder surface. This results in oscillating lift forces that act on the cylinder as shown in the following images.

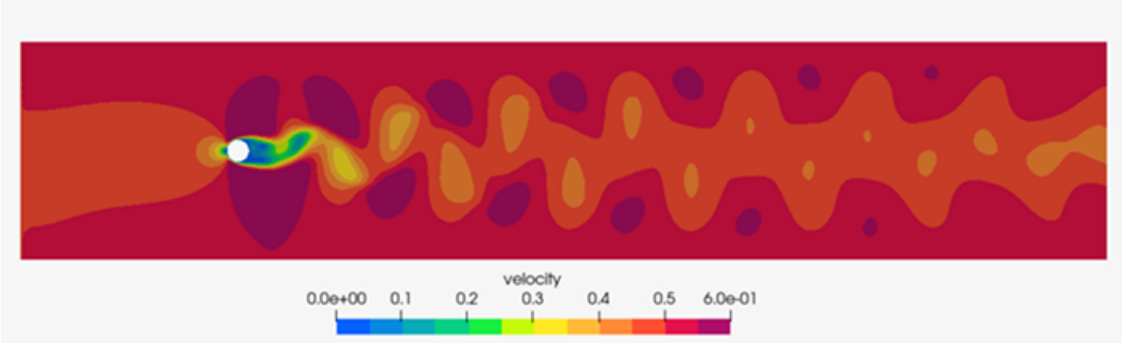


Figure 226: Contours of Velocity Magnitude

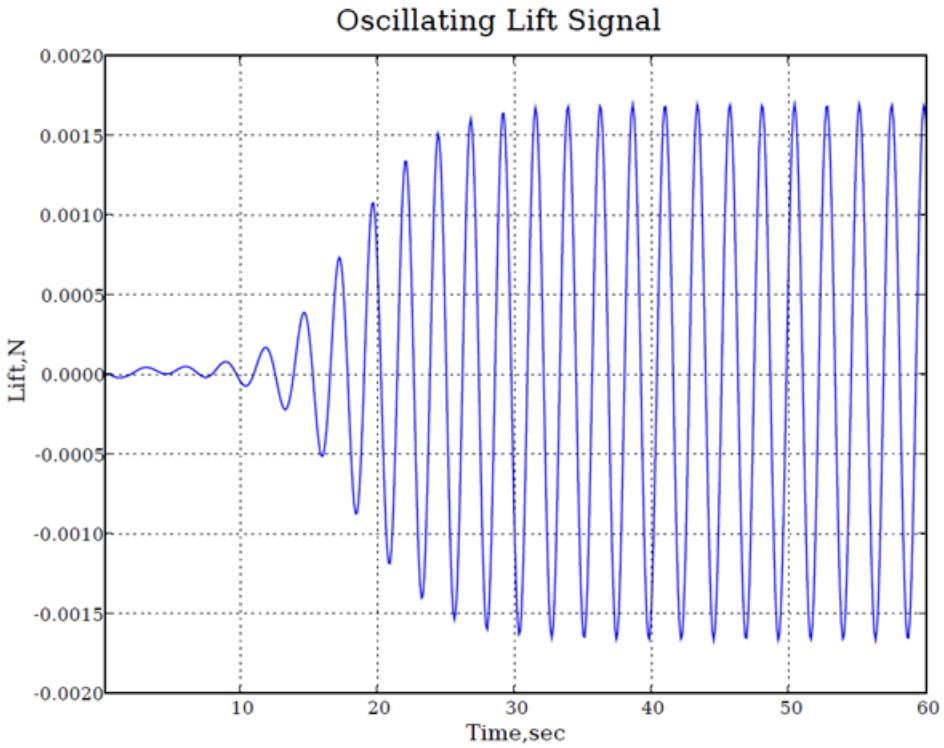


Figure 227: Lift Coefficient (lift force perpendicular to flow) plotted against time. Simulation was run for 600 time steps for a duration of 60 s

The Strouhal number for this simulation, a dimensionless number describing oscillating flows, is used to validate AcuSolve results. The experimental Strouhal number for this problem is given by

$$St = \frac{\omega * L}{V} = 0.165 \quad (8)$$

where ω is the dominant frequency of oscillations, L is the diameter of the cylinder, and v is the flow velocity.

The peak frequency of the oscillating lift force was computed by transforming the time dependent data into frequency space with a Fourier transform. From the Fourier transform, the AcuSolve-based Strouhal number was calculated. The table below shows the comparison of the Strouhal number provided by the AcuSolve prediction and the measurement given by Tritton (1959).

Table 11:

	Experimental	**AcuSolve**
Strouhal number	0.165	0.173

Summary

In this application, two dimensional flow over a cylinder is achieved by enforcing symmetry conditions on the front and back surfaces of the flow domain. The laminar, unsteady simulation shows the flow separation that leads to alternating vortex shedding. Frequency of the lift force acting on the cylinder is calculated to evaluate the Strouhal number. The AcuSolve solution compares well with results reported by Tritton (1959), differing slightly from the experimental results. In this application, AcuSolve demonstrates the ability to accurately predict oscillating laminar flow around a circular cylinder.

Simulation Settings for Oscillating Laminar Flow Around a Circular Cylinder

HyperMesh CFD database file: `<your working directory>\cylinder_laminar\cylinder_laminar.hm`

Global

- Problem Description
  - Analysis type - Transient
  - Turbulence equation - Laminar
- Auto Solution Strategy
  - Analysis type - Transient
  - Max time - `600` sec
  - Initial time increment - `0.1` sec
- Material Model
  - Fluid
    - Density - `1.0` kg/m3
    - Viscosity - `1.0e-3` kg/m-sec

  Model
- Volumes
  - Volume
    - Element Set
      1. Material model - Fluid
- Surfaces
  - Back
    - Simple Boundary Condition
      1. Type - Symmetry
  - Base

- Simple Boundary Condition
  1. Type - Slip
- Front
  - Simple Boundary Condition
    1. Type - Symmetry
- Inflow
  - Simple Boundary Condition
    1. Type - Inflow
    2. Inflow Type - Average velocity
    3. Average Velocity - `0.5` m/sec
- Outflow
  - Simple Boundary Condition
    1. Type - Outflow
- Top
  - Simple Boundary Condition
    1. Type - Slip

References

D.J. Tritton. "Experiments on the Flow around a Circular Cylinder at Low Reynolds Number". Journal of Fluid Mech. 6(04):547-567. 1959

Separated Laminar Flow Over a Blunt Plate

In this application, AcuSolve is used to simulate the separation of laminar flow over a blunt plate. AcuSolve results are compared with experimental results as described in J.C. Lane and R.I. Loehrke (1980). The close agreement of AcuSolve results with the experimental results validates the ability of AcuSolve to model cases with external laminar flow including separation.

Problem Description

The problem consists of external, laminar flow over a blunt plate 1.5 m long and 0.09 m thick, as shown in the following image, which is not drawn to scale. The fluid flows with a uniform horizontal velocity (v) of 0.045133 m/s. The fluid material used for the simulation has a density of 1.0 kg/m^3 and a dynamic viscosity of 1.7894 X 10^{-5} kg/m-s. The resulting Reynolds number for the flow, based on the plate thickness, is approximately 227. This indicates that the flow over the plate is laminar. As the fluid flows past the leading edge of the plate, the pressure decreases, resulting in a separation region downstream of the leading edge. At some distance downstream from the leading edge, the pressure gradient decreases, and viscous forces cause the recirculation zone to dissipate, allowing the flow to reattach to the plate.

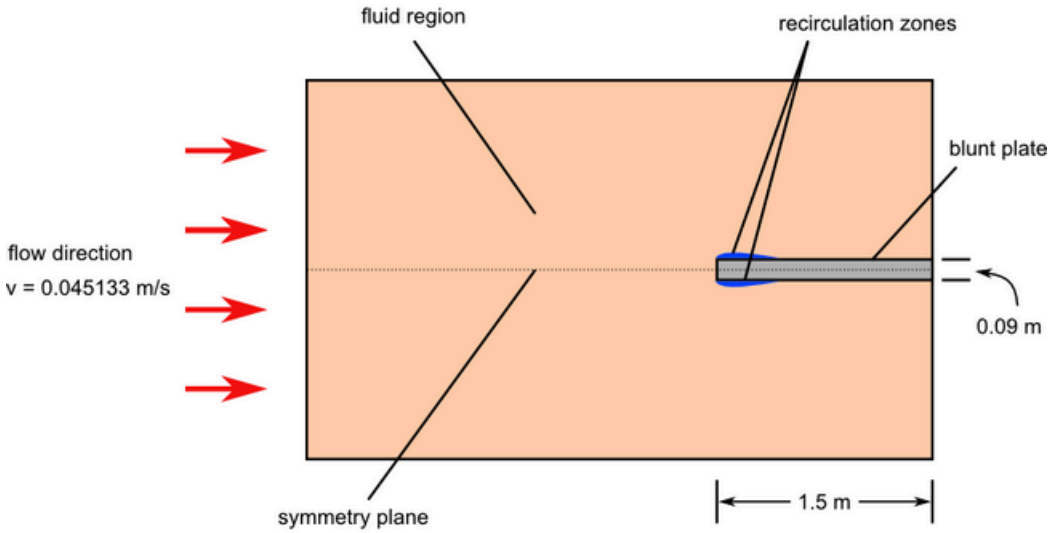


Figure 228:

The simulation was performed as a two dimensional problem by constructing a volume mesh that contains a single layer of elements in the extruded direction, normal to the flow plane, and by imposing symmetry boundary conditions on the extruded planes. In addition, the half symmetry of the geometry was exploited to allow for modeling only the top half of the geometry. These characteristics allow for accurate simulation of the flow while minimizing computational time. The following images show the mesh distribution and a refined mesh zone around the blunt plate.

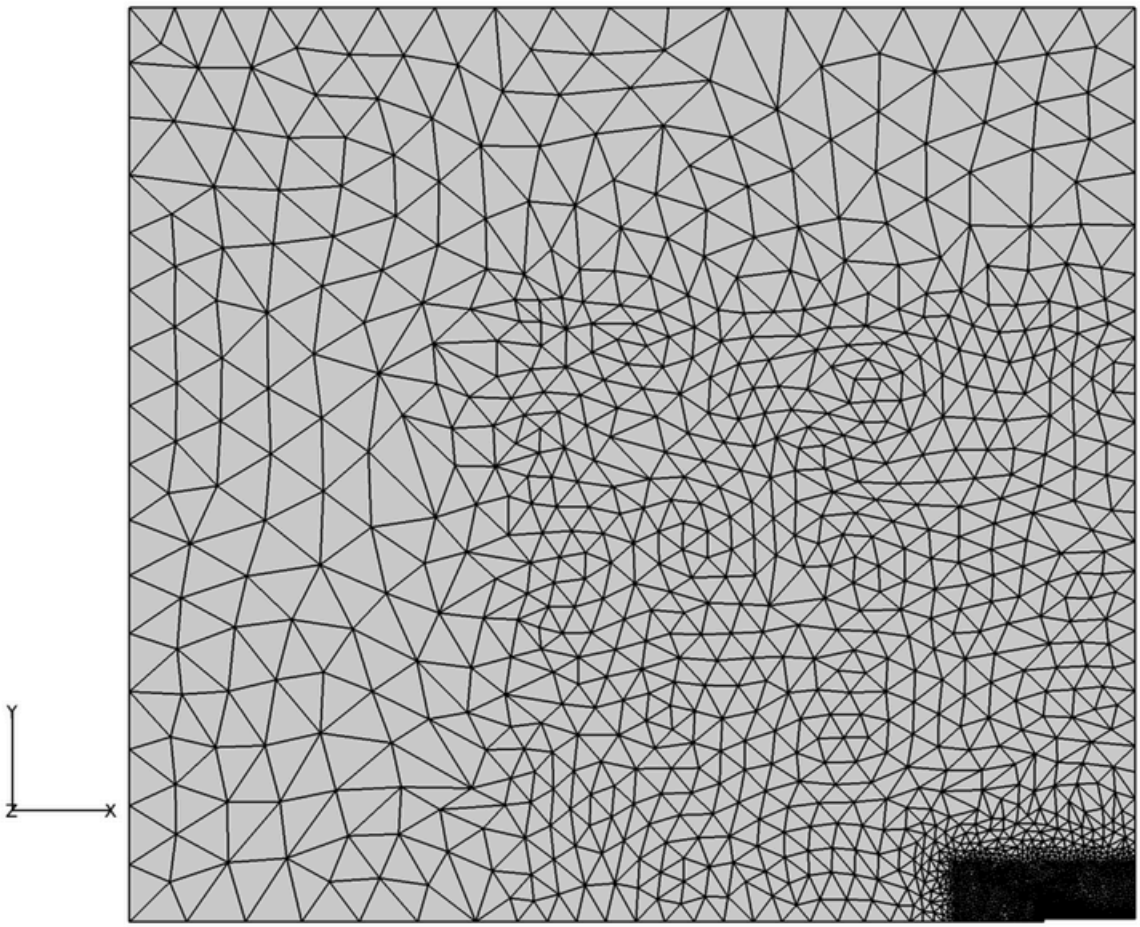


Figure 229: Mesh used for Simulating Separated Laminar Flow over a Blunt Plate

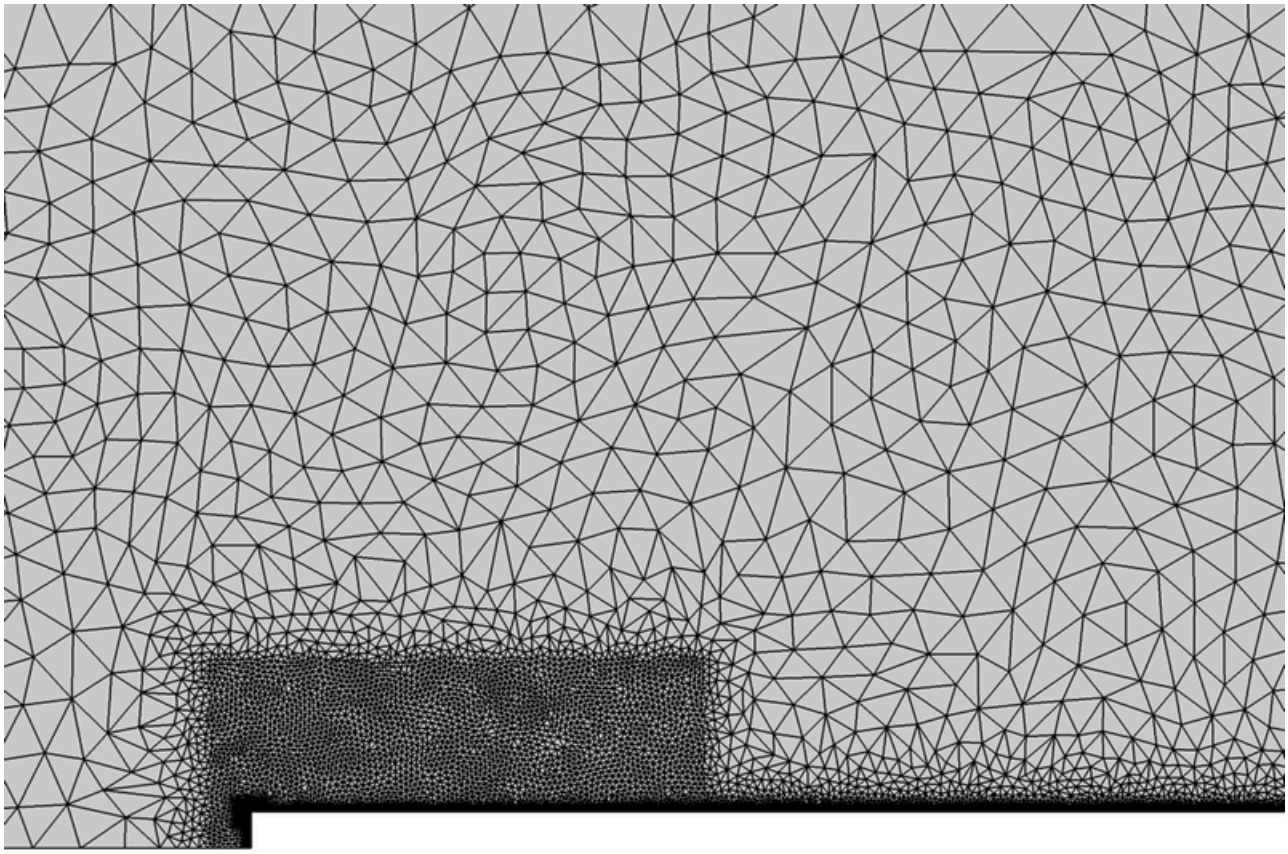


Figure 230: Mesh Detail Showing Refinement Zones at the Leading Edge of the Blunt Plate

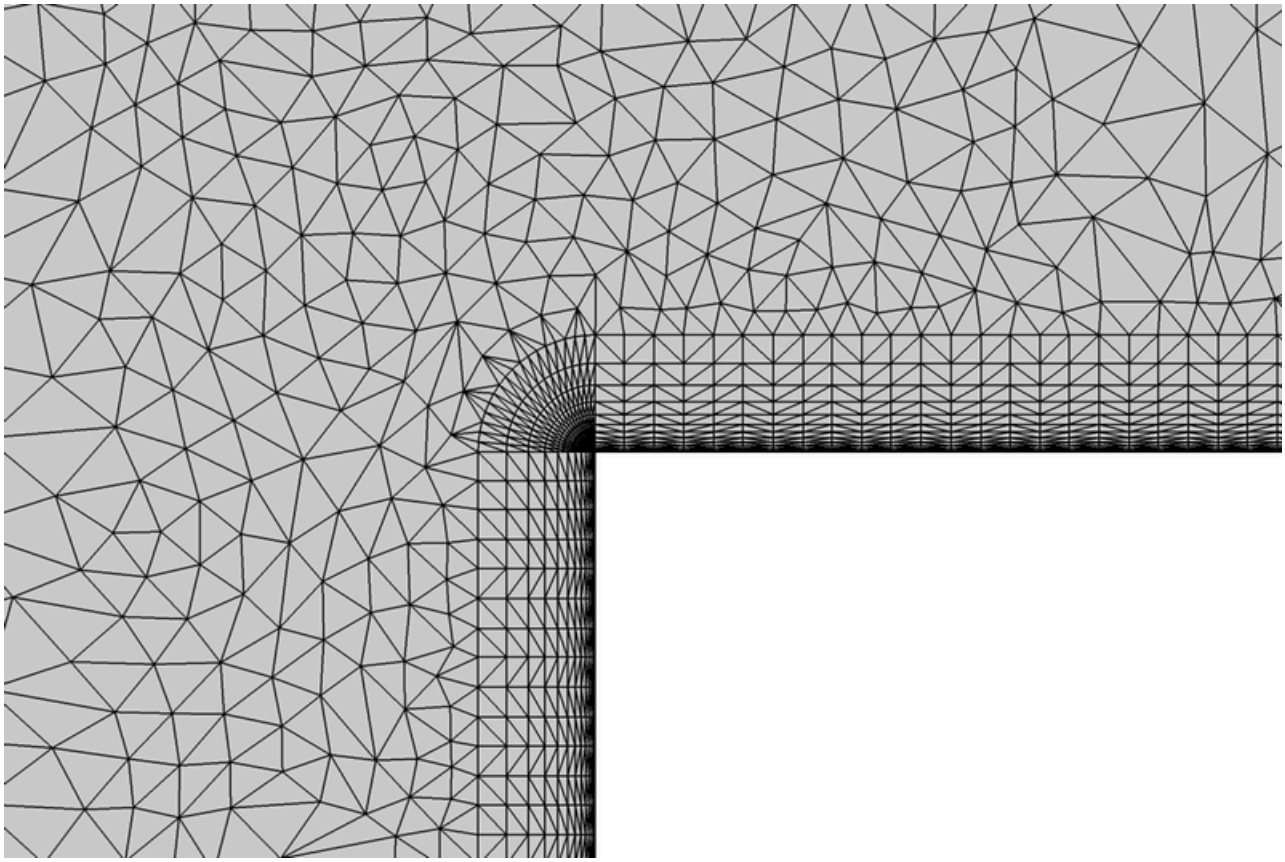


Figure 231: Mesh Detail Showing Mesh Elements Near the Leading Edge of the Blunt Plate

AcuSolve Results

The AcuSolve solution converged to a steady state and the results reflect the mean flow conditions over the blunt plate. The flow velocity is reduced to zero at the leading face, forming a stagnation point at the center. The flow reaches a maximum velocity as it flows around the leading edges and separates from the plate. Flow separation (shear stress parallel to the wall becomes negative) occurs downstream of the leading edge, leading to a recirculation zone. The flow reattaches 0.37 m downstream of the leading edge. The velocity in the laminar boundary layer increases from zero at the wall to free-stream velocity at the boundary layer edge. Along the plate length, the boundary layer slowly grows in thickness. The following image shows the contours of the flow velocity parallel to the streamwise direction and the recirculation region in the wake of the plate edge.

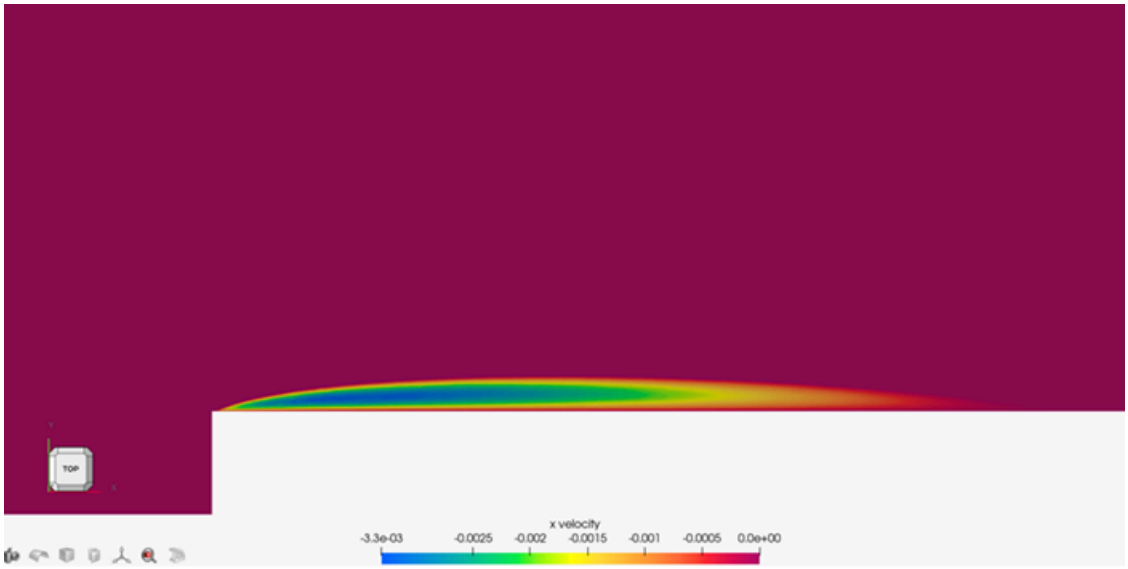


Figure 232: X-Velocity Contours Near the Leading Edge of the Blunt Plate

Downstream of the leading edge, the flow eventually reattaches to the plate at the point where the shear stress parallel to the wall passes from negative through zero to positive. The reattachment point is 0.37 m from the leading edge of the plate and corresponds to the trailing edge of the contours.

The results for the predicted and experimental reattachment length (xreattach) are presented in the table below. T represents the plate thickness.

Table 12:

AcuSolve xreattach	AcuSolve xreattach/T	Experimental xreattach/T	Percent error (%)
0.37	4.11	4.0	2.8

Summary

In this application, a constant flow inlet velocity and symmetric boundary conditions were used to model 2D flow over a blunt plate. The AcuSolve solution compares well with experimental results for the separation of laminar flow over a blunt plate. The non-dimensional reattachment length obtained from the AcuSolve steady state solution compares well with the experimental solution, with an error of less than 3.0 percent. The results of this simulation validate the ability of AcuSolve to accurately predict the reattachment point in cases with external, laminar flow with separation.

Simulation Settings for Separated Laminar Flow over a Blunt Plate

HyperMesh CFD database file: `<your working directory>\blunt_plate_laminar\blunt_plate_laminar.hm`

Global

- Problem Description

    - Analysis type - Steady State
    - Turbulence equation - Laminar
- Auto Solution Strategy
    - Relaxation Factor - `0.2`
- Material Model
    - Fluid
        - Density - `1.0` kg/m3
        - Viscosity - `1.7894e-005` kg/m-sec

  Model
- Volumes
    - Fluid
        - Element Set
            1. Material model - Fluid
- Surfaces
    - Back
        - Simple Boundary Condition
            1. Type - Symmetry
    - Freestream
        - Simple Boundary Condition
            1. Type - Slip
    - Front
        - Simple Boundary Condition
            1. Type - Symmetry
    - Inlet
        - Simple Boundary Condition
            1. Type - Inflow
            2. Inflow type - Velocity
            3. Inflow velocity type - Cartesian
            4. X Velocity - `0.045133` m/s
    - Outflow
        - Simple Boundary Condition
            1. Type - Outflow
    - Plate
        - Simple Boundary Condition
            1. Type - Wall
    - Symmetry
        - Simple Boundary Condition

1 Type - Symmetry

References

J.C. Lane and R.I. Loehrke. "Leading Edge Separation from a Blunt Plate at Low Reynolds Number". Journal of Fluids Engineering. 102(4):494-496. 1980.

Natural Convection in a Concentric Annulus

In this application, AcuSolve is used to simulate natural convection in the annular space between a heated inner pipe and an outer concentric pipe. AcuSolve results are compared with experimental results adapted from Kuehn and Goldstein (1978). The close agreement of AcuSolve results with experimental results validates the ability of AcuSolve to model cases with flow induced by natural convection.

Problem Description

The problem consists of two concentric cylinders with air filling the void between them, as shown in the following image, which is not drawn to scale. The radius of the inner cylinder is 0.0178 m and the radius of the outer cylinder is 0.0463 m. The inner cylinder is held at a fixed temperature of 373 K while the outer cylinder is held at 327 K. The temperature gradient drives the flow due to buoyancy effects.

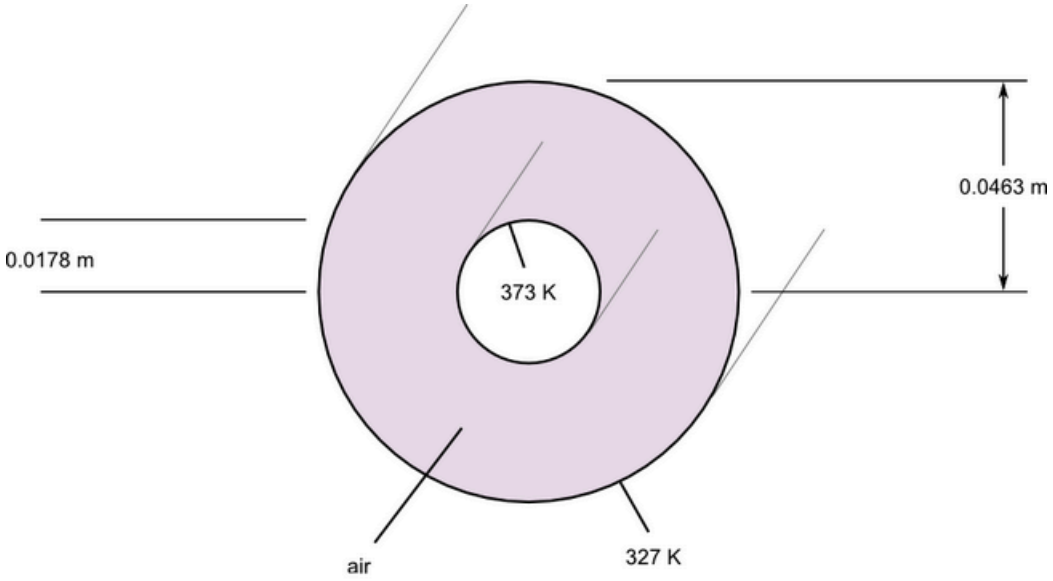


Figure 233: Critical Dimensions and Parameters for Simulating Natural Convection in a Concentric Annulus

The simulation was performed as a two dimensional problem by restricting flow in the out-of-plane direction through the use of a mesh that is one element thick. In addition, the half symmetry of the geometry is exploited to allow for modeling only half of the geometry. These characteristics allow for accurate simulation of the flow while minimizing computational time.

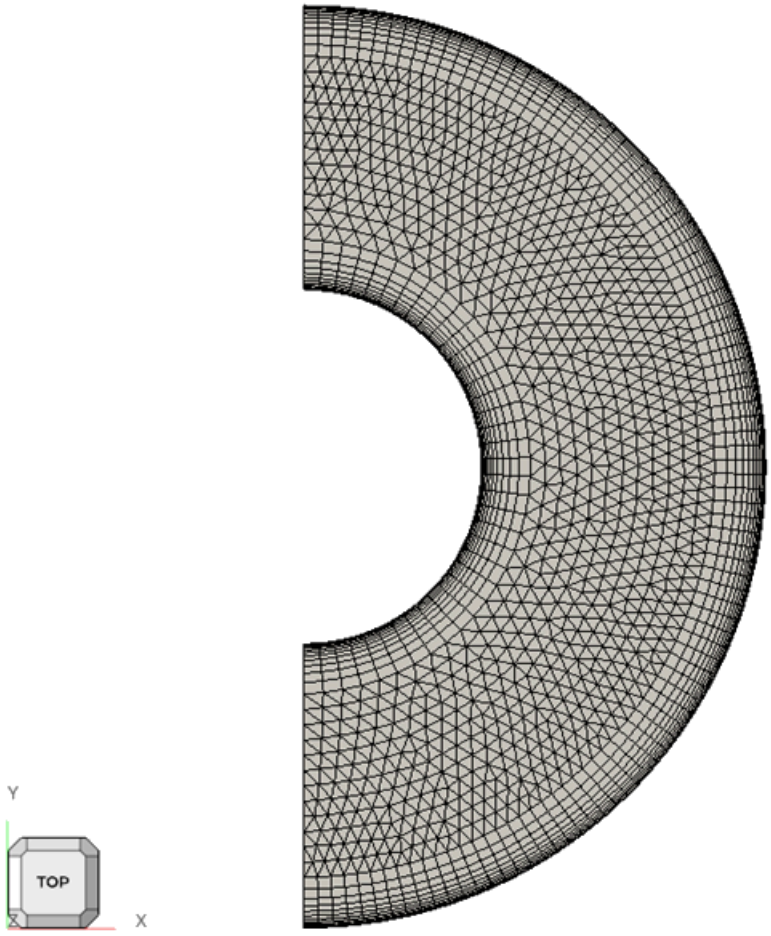


Figure 234: Mesh (Half of a Concentric Annulus) used for Simulating Natural Convection in a Concentric Annulus

AcuSolve Results

The AcuSolve solution converged to a steady state and the results reflect the mean flow conditions. Air density decreases due to heating by the inner cylinder, leading to convective currents within the annulus. As air approaches the outer cylinder, it is cooled by the outer wall, causing the density to increase. This results in heavier air sinking toward the bottom of the assembly.

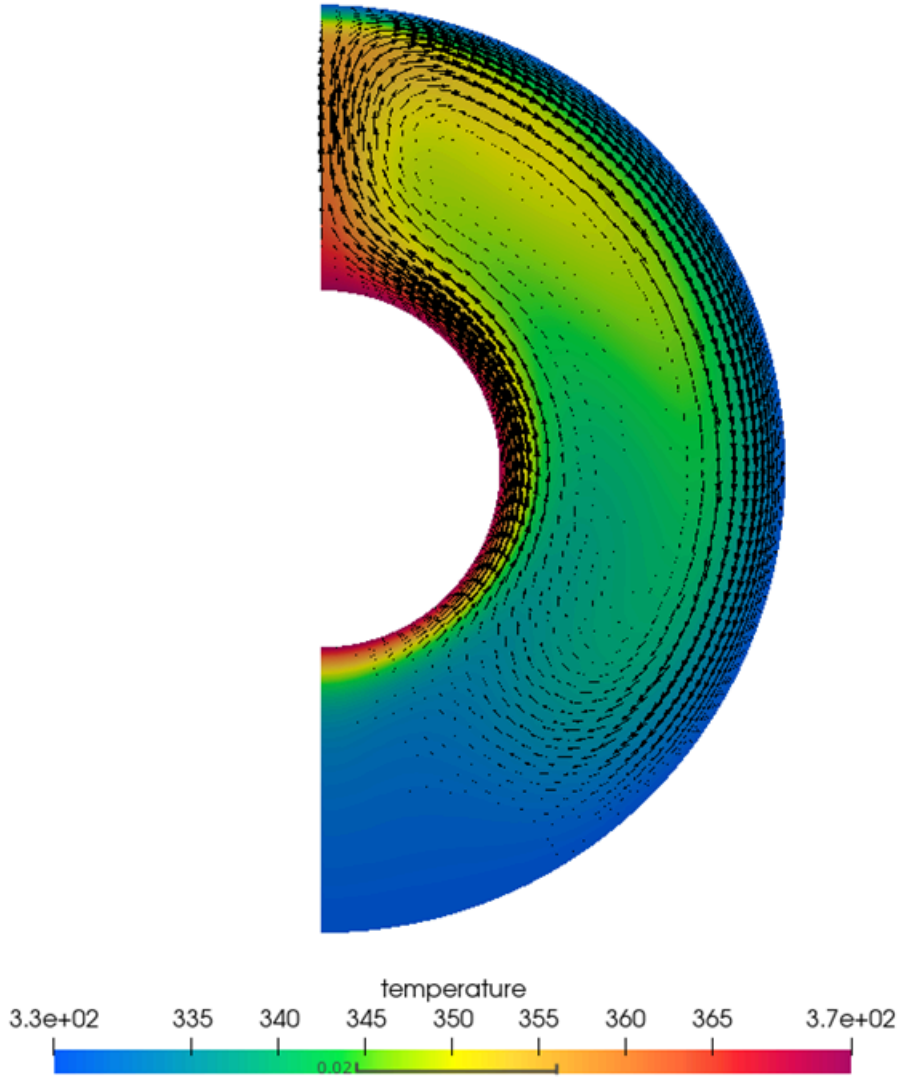


Figure 235: Temperature Contours and Velocity Vectors

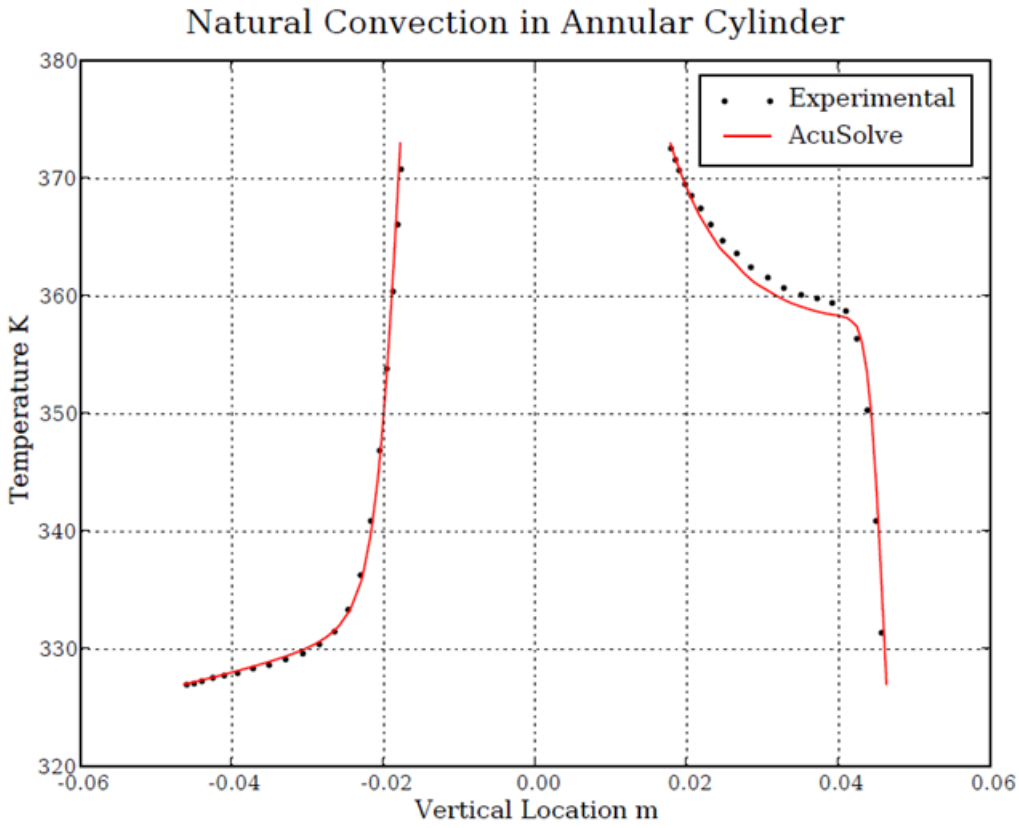


Figure 236: Temperature as a Function of Distance From the Center of the Inner Cylinder

Summary

The AcuSolve solution compares well with analytical results for natural convection in a concentric annulus. In this application, flow is driven by a decrease in density as air is heated. The local variations in density result in the higher density fluid sinking to the bottom of the annulus while the lower density fluid rises to the top. This transfer of momentum is a continuous process which results in the convective currents that are visible in the solution. The AcuSolve temperature results compare very closely with the experimental results.

Simulation Settings for Natural Convection in a Concentric Annulus

HyperMesh CFD database file: `<your working directory>\annulus_heat\annulus_heat.hm`

Global

- Problem Description
  - Analysis type - Steady State
  - Abs. pressure offset - `101325.0` N/m2
  - Temperature equation - Advective Diffusive
  - Turbulence equation - Laminar
  - Gravitational acceleration - { 0, -9.80665, 0 }
- Auto Solution Strategy

- Relaxation factor - `0.2`
- Flow - On
- Temperature - On

- Material Model
  - Air
    - Type - Boussinesq
    - Density - `1.225` kg/m3
    - Expansivity - `0.0034722` 1/K
    - Reference temperature - `288` K
    - Isothermal compressibility - `0.0` m2/N
    - Viscosity - `2.081e-5` kg/m-sec

  Model
- Volumes
  - Fluid
    - Element Set
      1. Material model - Air
  - Surfaces
    - ID
      1. Simple Boundary Condition
         1. Type - Wall
         2. Temperature BC type - Value
         3. Temperature - `373.0` K
    - Max_Z
      1. Simple Boundary Condition
      2. Type - Symmetry
    - Min_Z
      1. Simple Boundary Condition
      2. Type - Symmetry
    - OD
      1. Simple Boundary Condition
         1. Type - Wall
         2. Temperature BC type - Value
         3. Temperature - `327.0` K
    - Symmetry
      1. Simple Boundary Condition
      2. Type - Symmetry
  - Nodes
    - Node 1

1 Pressure

1 Type - Zero

References

T.H. Kuehn and R. J. Goldstein. "An Experimental Study of Natural Convection Heat Transfer in Concentric and Eccentric Horizontal Cylindrical Annuli". Journal of Heat Transfer 100:635-640. 1978.

Flow Between Concentric Cylinders

In this application, AcuSolve is used to simulate the flow of water between concentric cylinders. The outer cylinder is held stationary while the inner cylinder rotates with a constant speed. AcuSolve results are compared with analytical results as described in White (1991). The close agreement of AcuSolve results with analytical results validates the ability of AcuSolve to model cases containing thin annular gaps with flow induced by rotating walls.

Problem Description

The problem consists of two concentric pipes with water filling the void between them, as shown in the following image, which is not drawn to scale. The radius of the outer pipe is 0.0468 m and the radius of the inner pipe is 0.0178 m. The inner cylinder rotates at 1 rad/sec and the outer cylinder is fixed. The induced flow is laminar and exhibits a steady state behavior. The rotation of the inner cylinder causes the fluid to rotate due to viscous shearing near the wall. As the outer cylinder is fixed, a velocity gradient is generated as a function of radius within the flow domain.

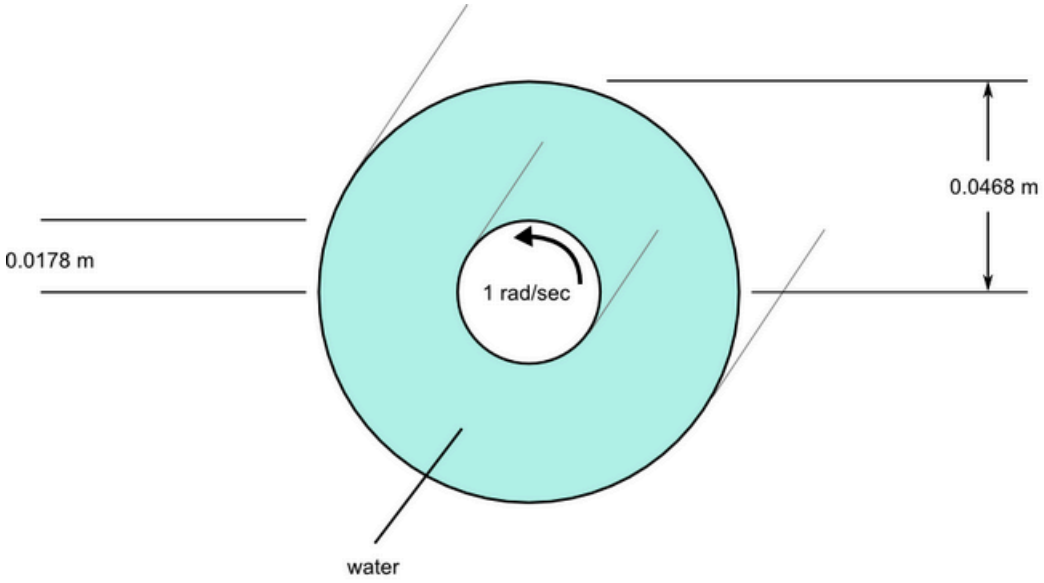


Figure 237: Critical Dimensions and Parameters for Simulating Flow Between Concentric Cylinders

The simulation was performed as a two dimensional problem by restricting flow in the out-of-plane direction through the use of a mesh that is one element thick.

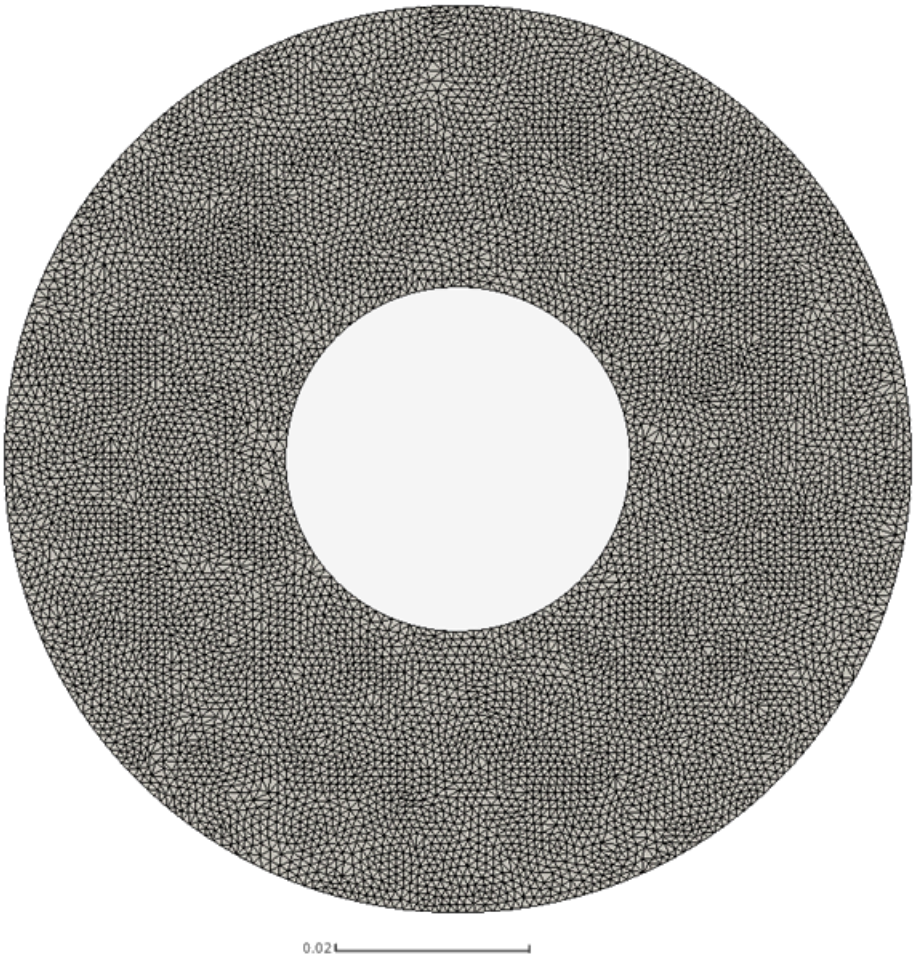


Figure 238: Mesh Used for Simulating Flow Between Concentric Cylinders

AcuSolve Results

The AcuSolve solution converged to a steady state and the results reflect the mean flow conditions. The velocity of the fluid within the cavity is greatest near the rotating inner cylinder. There is a nonlinear decrease in velocity as a function of distance away from the inner cylinder.

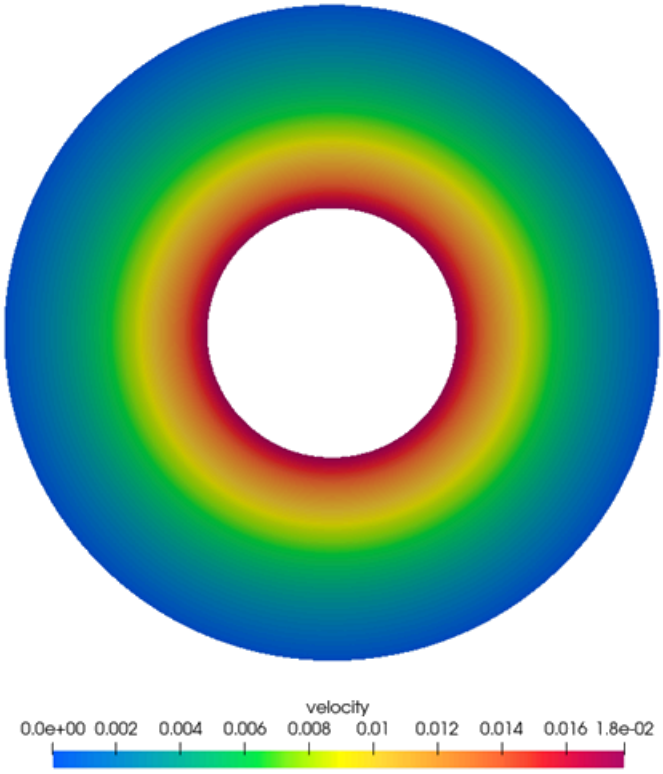


Figure 239: Contours of Tangential Velocity Between the Concentric Cylinders

Analytical tangential velocity at four distances away from the center of the rotating inner cylinder are presented with the corresponding AcuSolve results in the following table.

Table 13:

Distance from the center of rotating cylinder (m)	Analytical tangential velocity (m/s)	AcuSolve tangential velocity (m/s)	Percent deviation from analytical
0.020	0.01514	0.01514	0.04
0.025	0.01059	0.01058	0.10
0.030	0.00727	0.00727	0.06
0.035	0.00466	0.00466	0.10

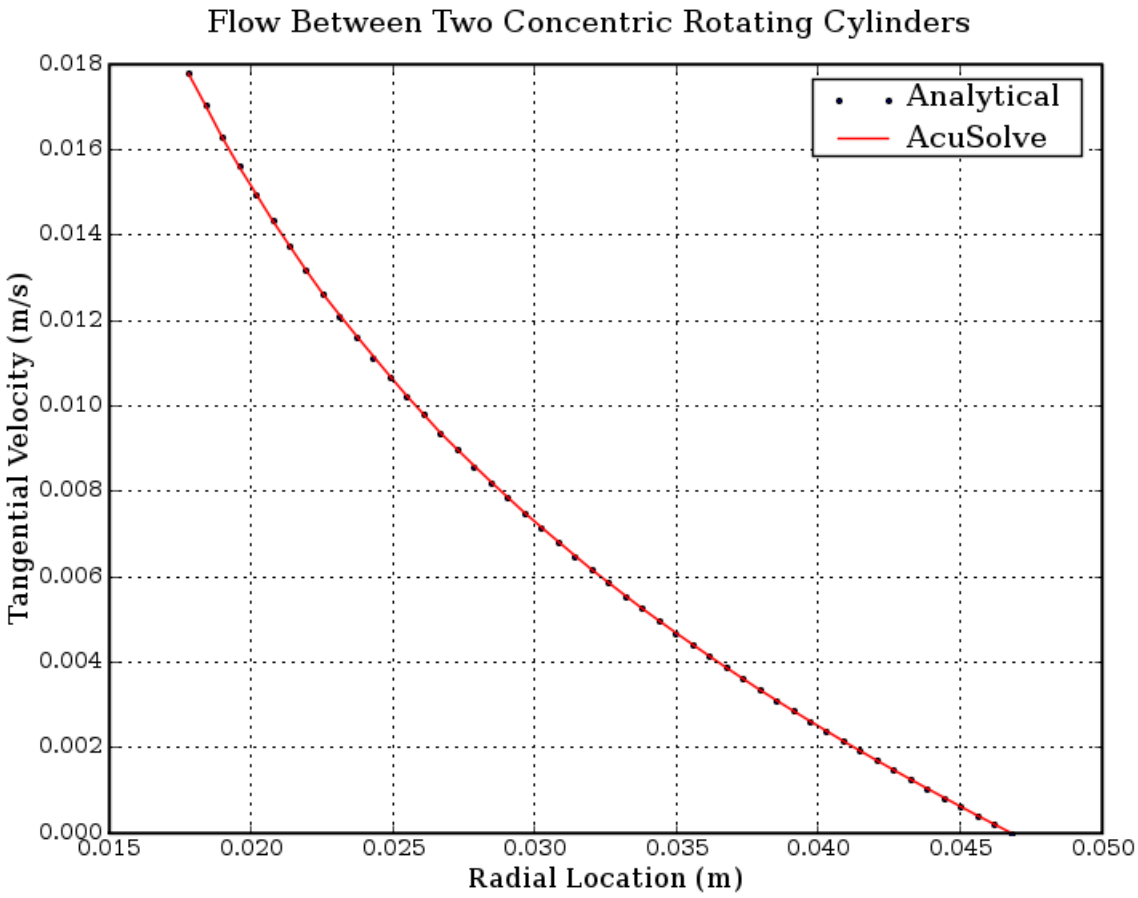


Figure 240: Tangential Velocity Plotted Against Distance from the Center of the Rotating Cylinder

Summary

The AcuSolve solution compares well with analytical results for the flow between concentric cylinders. In this application, the velocity in the annular fluid region is driven by the viscous stresses on the rotating wall. The AcuSolve tangential velocity is within 0.1 percent of the analytical solution at all radial locations.

Simulation Settings for Flow Between Concentric Cylinders

HyperMesh CFD database file: `<your working directory>\annulus_rotating\annulus_rotating.hm`

Global

- Problem Description
  - Analysis type - Steady State
  - Turbulence equation - Laminar
- Auto Solution Strategy
  - Relaxation Factor - `0.2`
- Material Model

    - Water
        - Density - `1000.0` kg/m3
        - Viscosity - `0.001` kg/m-sec
- Reference Frame
    - Rotating_Cylinder
        - Rotation center
            1. X-coordinate - `0.0` m
            2. Y-coordinate - `0.0` m
            3. Z-coordinate - `0.0` m
        - Angular velocity
            1. X-component - `0.0` rad/sec
            2. Y-component - `0.0` rad/sec
            3. Z-component - `-1.0` rad/sec

Model

- Volumes
    - Volume
        - Element set
            1. Material model - Water
- Surfaces
    - Boundary1
        - Simple Boundary Condition
            1. Type - Symmetry
    - Boundary2
        - Simple Boundary Condition
            1. Type - Symmetry
    - Inner
        - Simple Boundary Condition
            1. Type - Wall
            2. Reference Frame - Rotating_Cylinder
    - Outer
        - Simple Boundary Condition
            1. Type - Wall
- Nodes
    - Fixed
        - Pressure
            1. Type - Zero

References

F. M. White. "Viscous Fluid Flow". Section 3-2.3. McGraw-Hill Book Co., Inc. New York. 1991.

Heat Transfer Between Radiating Concentric Cylinders

In this application, AcuSolve is used to simulate the heat transfer due to radiation between concentric cylinders. The inner and outer cylinders are held at constant temperature and are defined to be radiation surfaces. AcuSolve results are compared with analytical results for temperature as described in Incropera (2006). The close agreement of AcuSolve results with analytical results validates the ability of AcuSolve to model cases with radiation heat transfer requiring view factor computation.

Problem Description

The problem consists of a fluid with arbitrary material properties between two infinitely long concentric cylinders, as shown in the following image, which is not drawn to scale. The radius of the outer cylinder is 0.0468 m and the radius of the inner cylinder is 0.0178 m. The inner cylinder is defined to have a constant wall temperature at 773.0 K (500 °C). The outer cylinder is defined to have a constant wall temperature at 300.0 K (27 °C). Both cylinders are specified to radiate as grey bodies, with emissivity set to 0.03778.

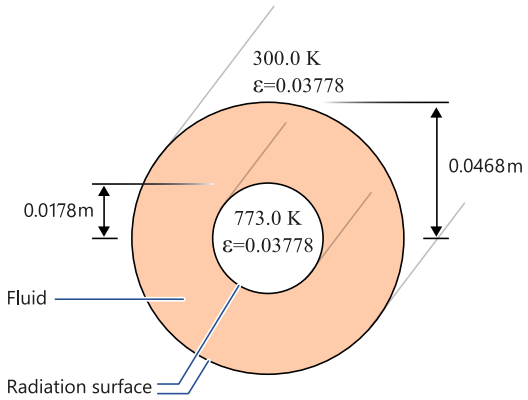


Figure 241: Critical Dimensions and Parameters Used for Simulating Radiation Between Two Concentric Cylinders

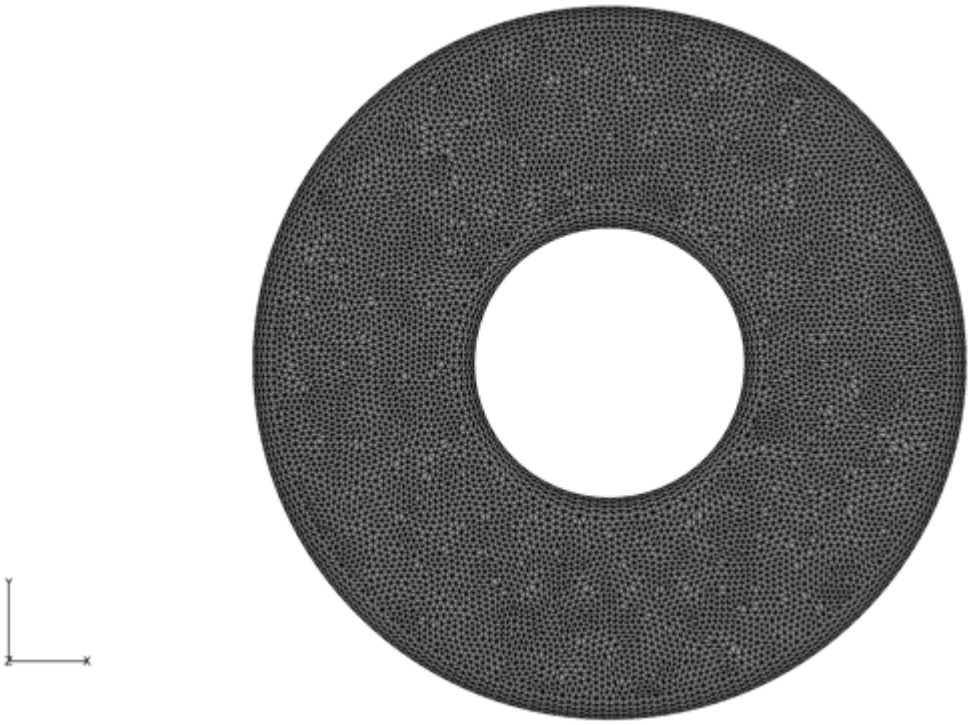


Figure 242: Mesh used for Simulating Radiation Between Two Concentric Cylinders

The simulation was performed as a two-dimensional problem by constructing a volume mesh that contains a single layer of elements normal to the radial and circumferential directions.

AcuSolve Results

The AcuSolve solution converges to a steady state and the results reflect the mean temperature distribution. As the inner diameter is considerably hotter than the outer, a heat flux, due to radiation, is present between the cylinders. The temperature within the medium reduces logarithmically as a function of the radius. The following images show the temperature with the medium as a function of radius from the center. The temperature is compared with the analytical solution as described in Incropera (2006). The image below shows black circles representing the analytical solution and a solid red line for the AcuSolve results.

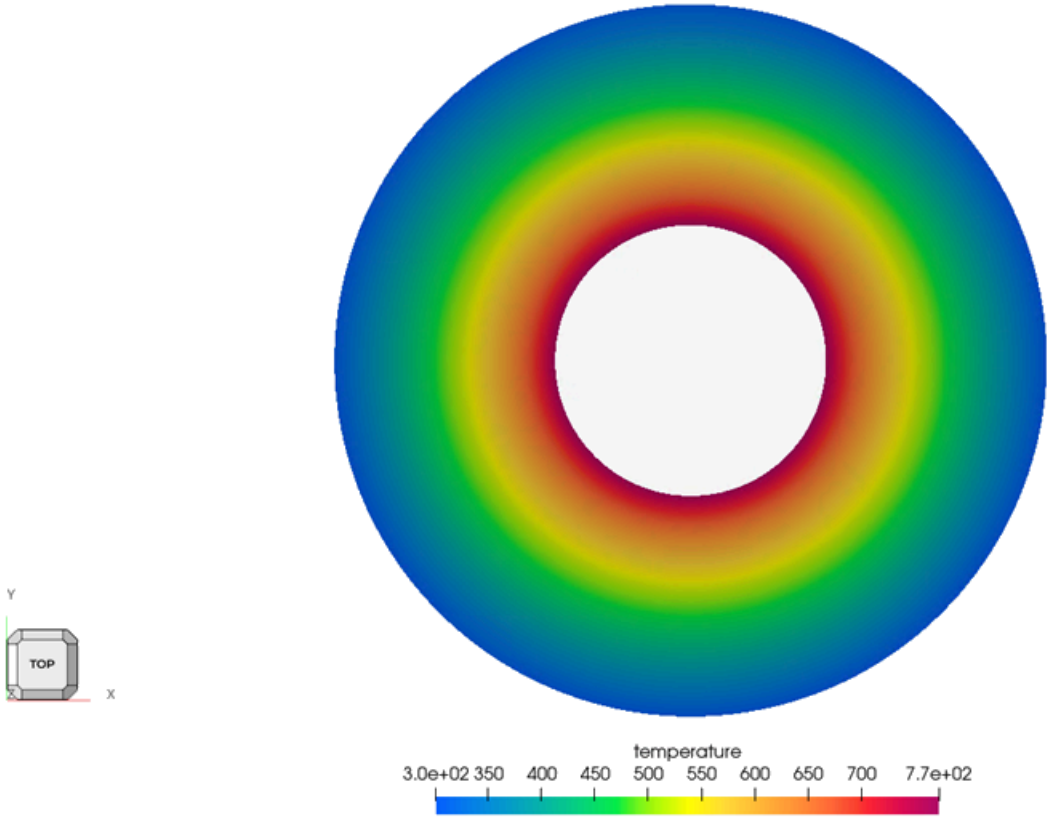


Figure 243: Contours of Temperature Between the Concentric Cylinders

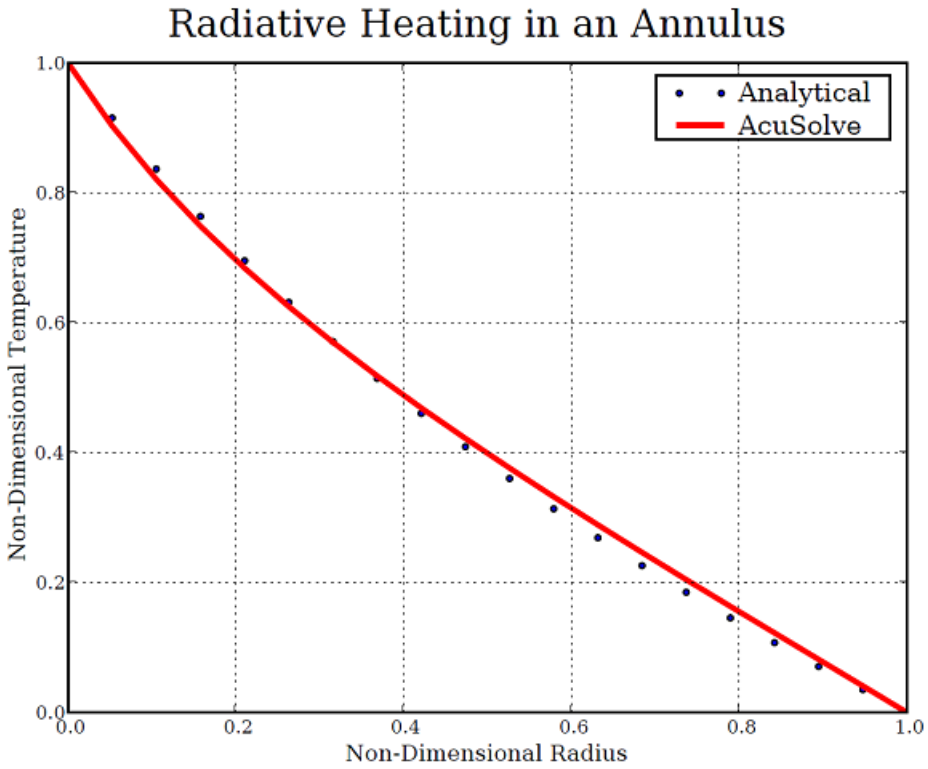


Figure 244: Non Dimensional Temperature Distribution Within the Annulus as a Function of Non Dimensional Radius

Summary

The AcuSolve solution compares well with analytical results for heat transfer due to radiation between two concentric cylinders. In this application, an arbitrary material is subjected to a heat flux that is calculated based on the view factors within the model. As a result of radiative heat flux a temperature distribution between the two cylinders develops. The AcuSolve solution for the temperature as a function of radius matches well compared to the analytical solution.

Heat Transfer Between Radiating Concentric Cylinders

HyperMesh CFD database file: `<your working directory>\annulus_radiation \annulus_radiation.hm`

Global

- Problem Description
  - Analysis type - Steady State
  - Temperature equation - Advective Diffusive
  - Radiation equation- Enclosure
- Auto Solution Strategy
  - Convergence tolerance - `0.0001`
  - Relaxation Factor- `0.4`
  - Flow- off

    - Enclosure radiation- on
- Material Model
    - Material
        - Conductivity
            1. Type - Constant
            2. Conductivity- `1.0`
- Emissivity Model
    - Grey Body
        - Emissivity- `0.03778`
    - Black Body
        - Emissivity- `1.0`

  Model
- Volumes
    - Medium
        - Element Set
            1. Medium - Fluid
            2. Material model- Material
- Surfaces
    - ID
        - Simple Boundary Condition
            1. Type- Wall
            2. Temperature BC type- Value
            3. Temperature- `773.0` K
        - Radiation Surface
            1. Type- Wall
            2. Emissivity model- Grey Body
    - Max_Z
        - Simple Boundary Condition
            1. Type- Symmetry
        - Radiation Surface
            1. Type- Wall
            2. Emissivity model- Black Body
    - Min_Z
        - Simple Boundary Condition
            1. Type- Symmetry
        - Radiation Surface
            1. Type- Wall

2. Emissivity model- Black Body

- OD
  - Simple Boundary Condition
    1. Type- Wall
    2. Temperature BC type- Value
    3. Temperature- `300.0` K
  - Radiation Surface
    1. Type- Wall
    2. Emissivity model- Grey Body

References

F. P. Incropera and D. P. DeWitt. "Fundamentals of Heat Transfer - Sixth Edition". John Wiley & Sons. New York. 2006.

Laminar Couette Flow with Imposed Pressure Gradient and Heated Walls

In this application, AcuSolve is used to simulate the flow of a highly viscous fluid between a moving and a stationary plate with an imposed pressure gradient and fixed temperature on the walls. AcuSolve results are compared with analytical results described in White (1991). The close agreement of AcuSolve results with analytical results validates the ability of AcuSolve to model cases with imposed pressure gradients and viscous heating.

Problem Description

The problem consists of a viscous fluid between two plates in a two-dimensional domain, as shown in the following image, which is not drawn to scale. The domain is 1.0 m high and 1.5 m long. The top plate moves with a constant velocity of 3.0 m/sec and the bottom plate is fixed. To simulate a fully developed flow with a relatively short length domain there is a mean-pressure gradient of -12 Pa/m applied to the fluid in the streamwise direction, defined as a body force acting on the entire fluid. The lower wall is held at a fixed temperature of 273.0 K, while the upper wall is held at a fixed temperature of 274.0 K. The problem is simulated with periodic boundaries in the streamwise direction. The Reynolds number of the flow, based on the distance between the plates is 0.3, indicating laminar flow. The flow field develops from the pressure gradient, the motion of the top plate, and the viscous shear stresses near the plates. The shear stress within the domain causes the temperature to increase within the channel.

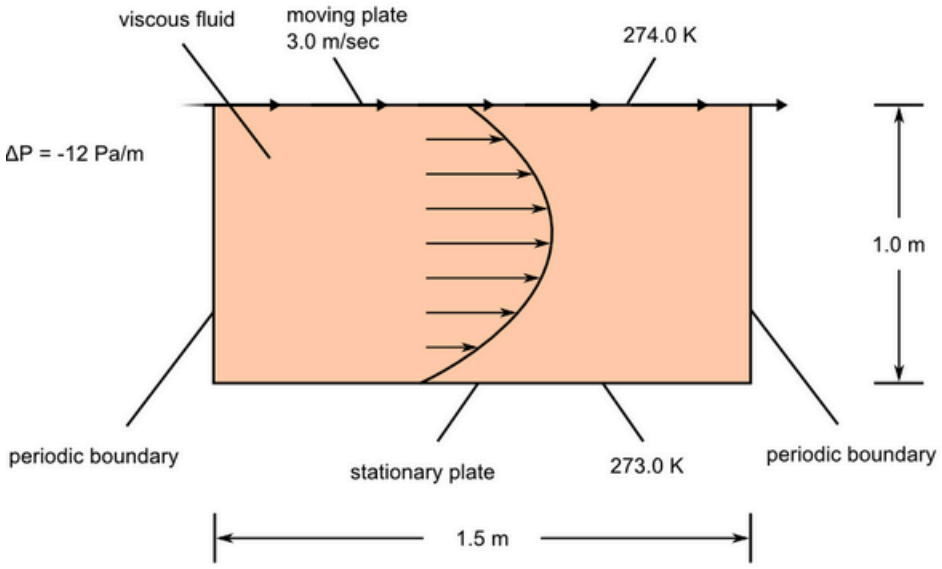


Figure 245: Critical Dimensions and Parameters for Simulating Laminar Couette Flow with an Imposed Pressure Gradient and Heated Walls

The simulation was performed as a two dimensional problem by constructing a volume mesh that contains a single layer of elements extruded in the cross stream direction, normal to the flow plane and by imposing symmetry boundary conditions on the extruded planes. Due to the periodic natural of the flow, a single element extrusion in the streamwise direction is used to reduce the model size.

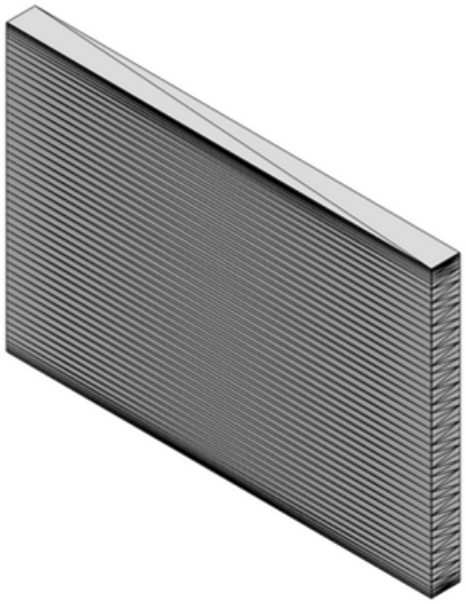


Figure 246: Mesh used for Simulating Laminar Couette Flow with an Imposed Pressure Gradient and Heated Walls

AcuSolve Results

The AcuSolve solution converged to a steady state and the results reflect the mean flow conditions. The simulation results show a flow field with a nearly linear distribution of velocity, with the peak at the top wall. The flow develops primarily because of the shear stress acting on the fluid near both the moving plate and the stationary plate. The temperature variation between the two plates develops due to the viscous heating effects that increase the temperature within the channel, with the maximum near the central height of the domain. The following figure shows the temperature distribution between the two plates and velocity vectors indicating the velocity profile.

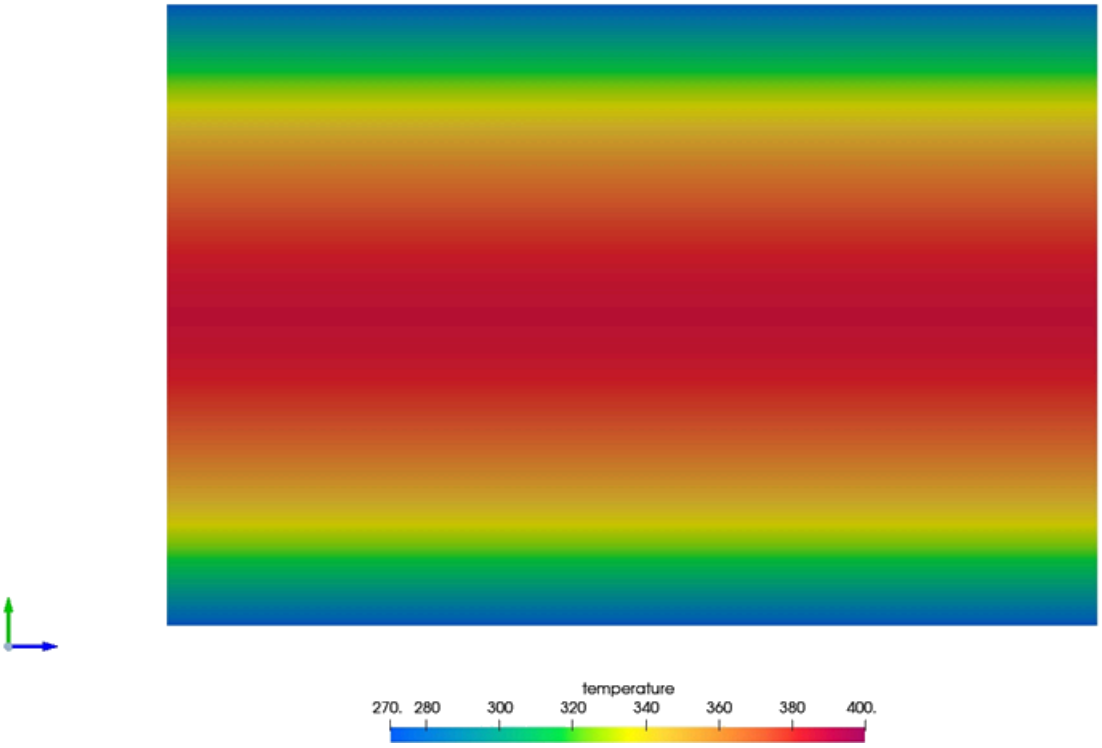


Figure 247: Contours of Temperature Between the Plates, with Velocity Vectors

The following image demonstrates the accuracy of the solution compared to the analytical results as computed by the solution for viscous heating within a channel with a moving upper boundary.

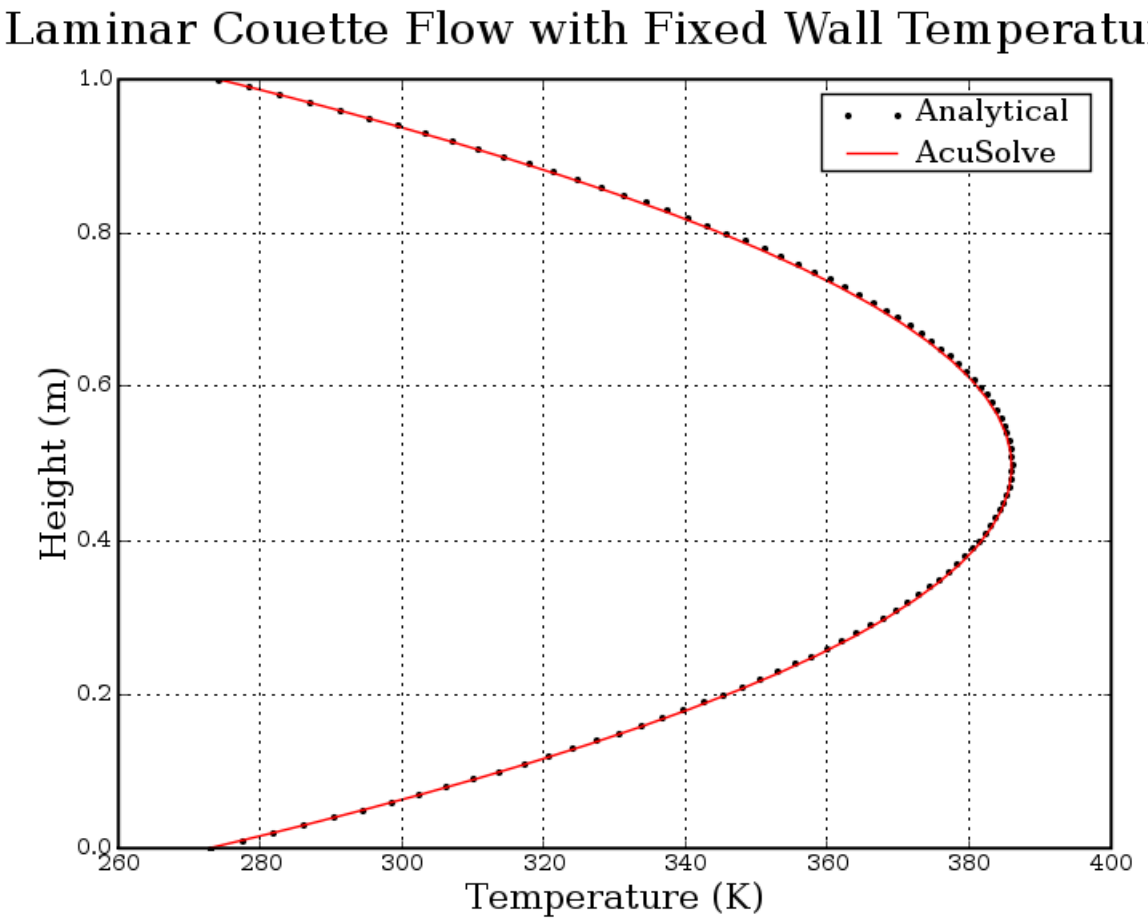


Figure 248: Temperature Plotted Against Height above the Bottom of the Flow Field (Temperature is Presented on the X Axis to Better Represent the Distribution Between the Plates in the Streamwise Direction)

Summary

In this application, a fully developed laminar flow between two plates with fixed temperature is studied and compared against analytical data. The AcuSolve results compare well with the analytical data for the temperature distribution between the two plates. The simulation indicates that the velocity profile arises due to the combination of the viscous shearing and the velocity of the upper plate. The velocity and temperature profiles computed by AcuSolve demonstrate how highly viscous fluids tend to direct the flow regime. AcuSolve demonstrates the ability to predict the analytical solution for viscous heating between two flat plates with moving and stationary boundaries and an imposed pressure gradient.

Simulation Settings for Laminar Couette Flow with Imposed Pressure Gradient and Heated Walls

SimLab database file: `<your working directory>\couette_laminar_heat\couette_laminar_heat.slb`

Global

- Problem Description

    - Flow - Steady State
    - Temperature equation - Advective Diffusive
    - Turbulence equation - Laminar
- Auto Solution Strategy
    - Relaxation factor - `0.2`
- Material Model
    - Fluid
        - Density - `1.0` kg/m3
        - Specific Heat - `1.0` J/kg-K
        - Viscosity - `100.0` kg/m-sec
- Body Force
    - DP/DL
        - Gravity
            1. Z-component - `18.0` m/sec2

    Model
- Volumes
    - Fluid
        - Element set
            1. Material model - Fluid
            2. Body force - DP/DL
            3. Viscous heating - on
- Surfaces
    - Max_X
        - Simple Boundary Condition
            1. Type - Symmetry
    - Max_Y
        - Simple Boundary Condition
            1. Type - Wall
            2. Wall velocity type - Cartesian
            3. Z-velocity - `3.0` m/s
            4. Temperature - `274.0` K
    - Max_Z
        - Simple Boundary Condition - (disabled to allow for periodic conditions to be set)
    - Min_X
        - Simple Boundary Condition
            1. Type - Symmetry
    - Min_Y

        - Simple Boundary Condition
            1. Type - Wall
            2. Temperature - `273.0` K
    - Min_Z
        - Simple Boundary Condition - (disabled to allow for periodic conditions to be set)
- Periodics
    - Periodic 1 all
        - Periodic Boundary Conditions
            1. Type - Periodic

References

F. M. White. "Viscous Fluid Flow". Section 3-3.2. McGraw-Hill Book Co., Inc. New York. 1991.

Internal Flow

5

This section includes validation cases that consider wall bounded simulation domains with internally constrained fluid medium.

This chapter covers the following:

- Flow Between Concentric Cylinders (p. 330)
- Turbulent Flow Through a Pipe (p. 336)
- Laminar Couette Flow with Imposed Pressure Gradient (p. 340)
- Flow Inside a Rotating Cavity (p. 346)
- Natural Convection in a Concentric Annulus (p. 354)
- Laminar Flow Past a 90° T-Junction (p. 360)
- Laminar Flow Through a Channel with Heated Walls (p. 365)
- Turbulent Natural Convection Inside a Tall Cavity (p. 370)
- Turbulent Flow with Separation in an Asymmetric Diffuser (p. 378)
- Turbulent Flow Over a Backward-Facing Step (p. 386)
- Turbulent Flow Past a Convex Curve in a Channel (p. 393)
- Heat Transfer Between Radiating Concentric Cylinders (p. 400)
- Turbulent Flow Through a 180 Degree Curved Channel (p. 406)
- Circumferential Flow in a Cylinder Induced by a Rotating Solid (p. 412)
- Heat Transfer Between Radiating Concentric Spheres (p. 418)
- Two-Phase Nucleate Boiling in a Cylindrical Pipe (p. 423)
- Single-Phase Nucleate Boiling in a Rectangular Channel (p. 427)
- Supersonic Flow Through a Converging-Diverging Nozzle (p. 432)
- Turbulent Flow Past a Wall-Mounted Hump (p. 437)
- Laminar Couette Flow with Imposed Pressure Gradient and Heated Walls (p. 444)

Flow Between Concentric Cylinders

In this application, AcuSolve is used to simulate the flow of water between concentric cylinders. The outer cylinder is held stationary while the inner cylinder rotates with a constant speed. AcuSolve results are compared with analytical results as described in White (1991). The close agreement of AcuSolve results with analytical results validates the ability of AcuSolve to model cases containing thin annular gaps with flow induced by rotating walls.

Problem Description

The problem consists of two concentric pipes with water filling the void between them, as shown in the following image, which is not drawn to scale. The radius of the outer pipe is 0.0468 m and the radius of the inner pipe is 0.0178 m. The inner cylinder rotates at 1 rad/sec and the outer cylinder is fixed. The induced flow is laminar and exhibits a steady state behavior. The rotation of the inner cylinder causes the fluid to rotate due to viscous shearing near the wall. As the outer cylinder is fixed, a velocity gradient is generated as a function of radius within the flow domain.

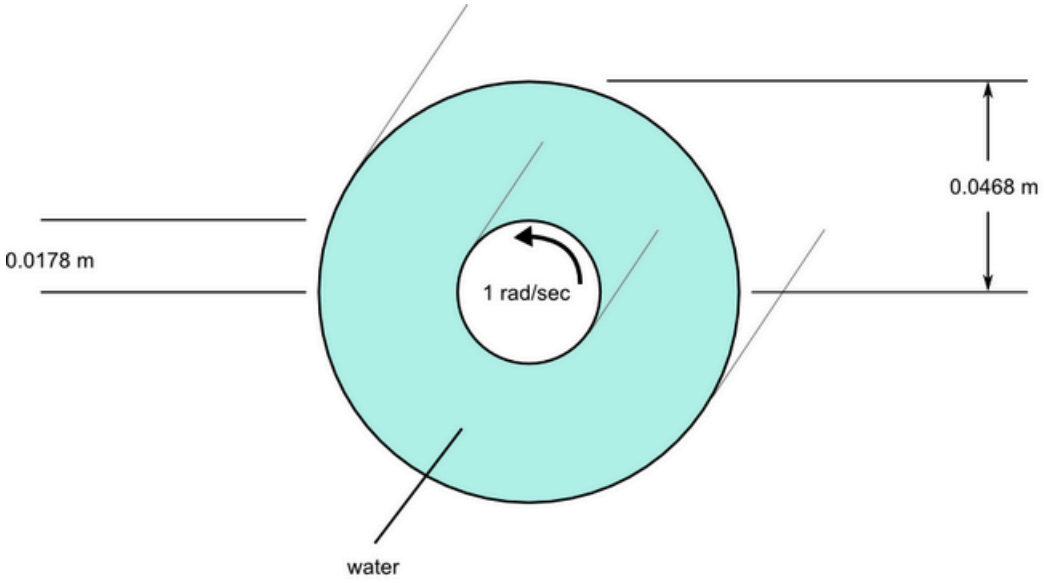


Figure 249: Critical Dimensions and Parameters for Simulating Flow Between Concentric Cylinders

The simulation was performed as a two dimensional problem by restricting flow in the out-of-plane direction through the use of a mesh that is one element thick.

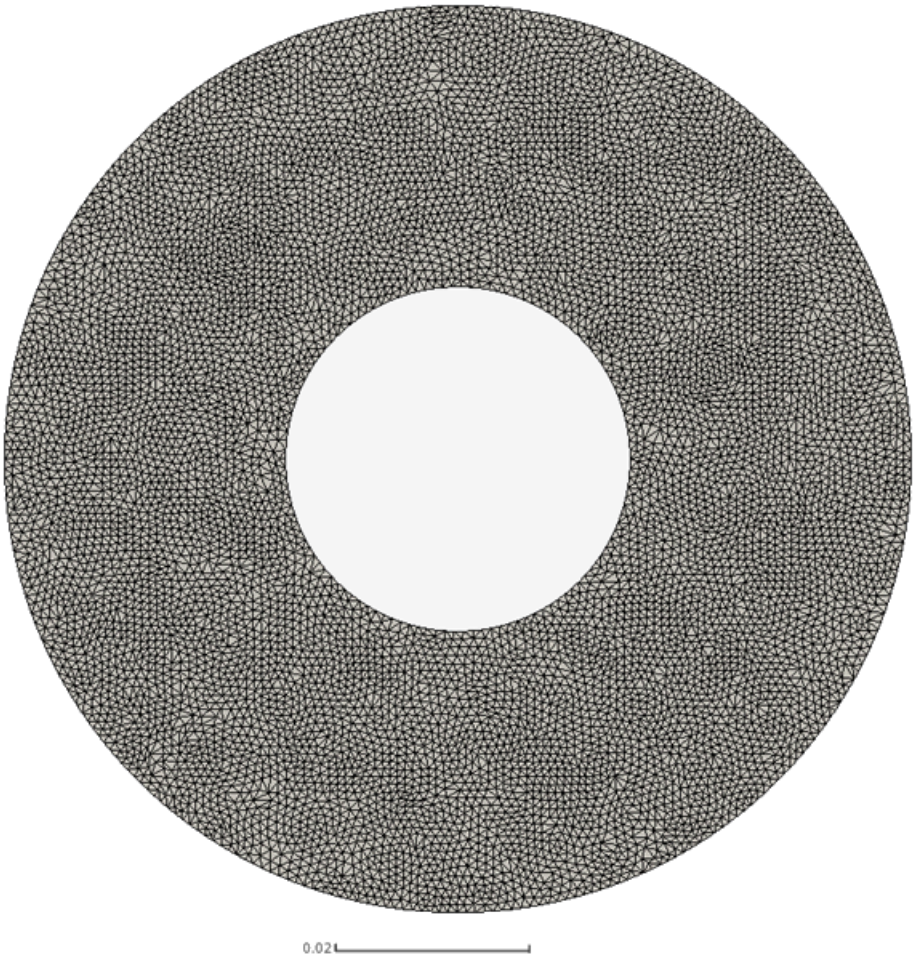


Figure 250: Mesh Used for Simulating Flow Between Concentric Cylinders

AcuSolve Results

The AcuSolve solution converged to a steady state and the results reflect the mean flow conditions. The velocity of the fluid within the cavity is greatest near the rotating inner cylinder. There is a nonlinear decrease in velocity as a function of distance away from the inner cylinder.

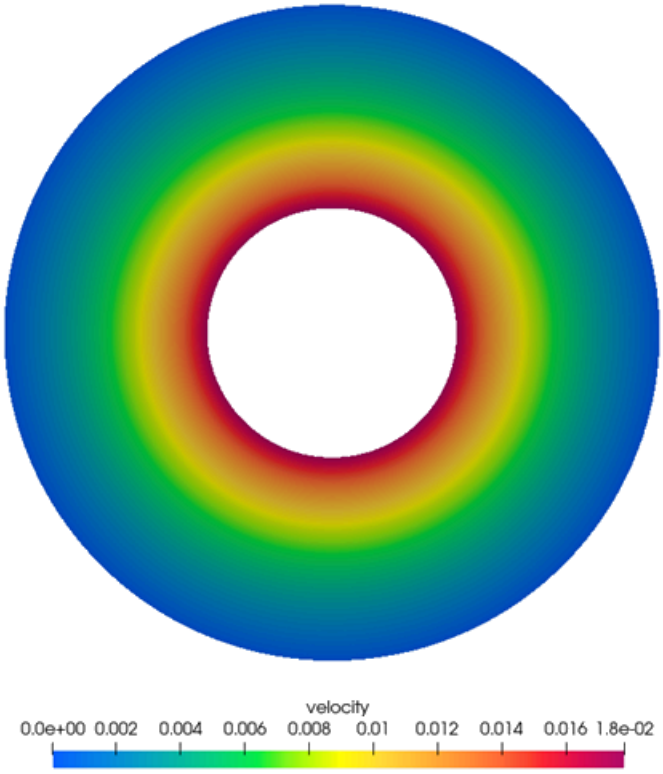


Figure 251: Contours of Tangential Velocity Between the Concentric Cylinders

Analytical tangential velocity at four distances away from the center of the rotating inner cylinder are presented with the corresponding AcuSolve results in the following table.

Table 14:

Distance from the center of rotating cylinder (m)	Analytical tangential velocity (m/s)	AcuSolve tangential velocity (m/s)	Percent deviation from analytical
0.020	0.01514	0.01514	0.04
0.025	0.01059	0.01058	0.10
0.030	0.00727	0.00727	0.06
0.035	0.00466	0.00466	0.10

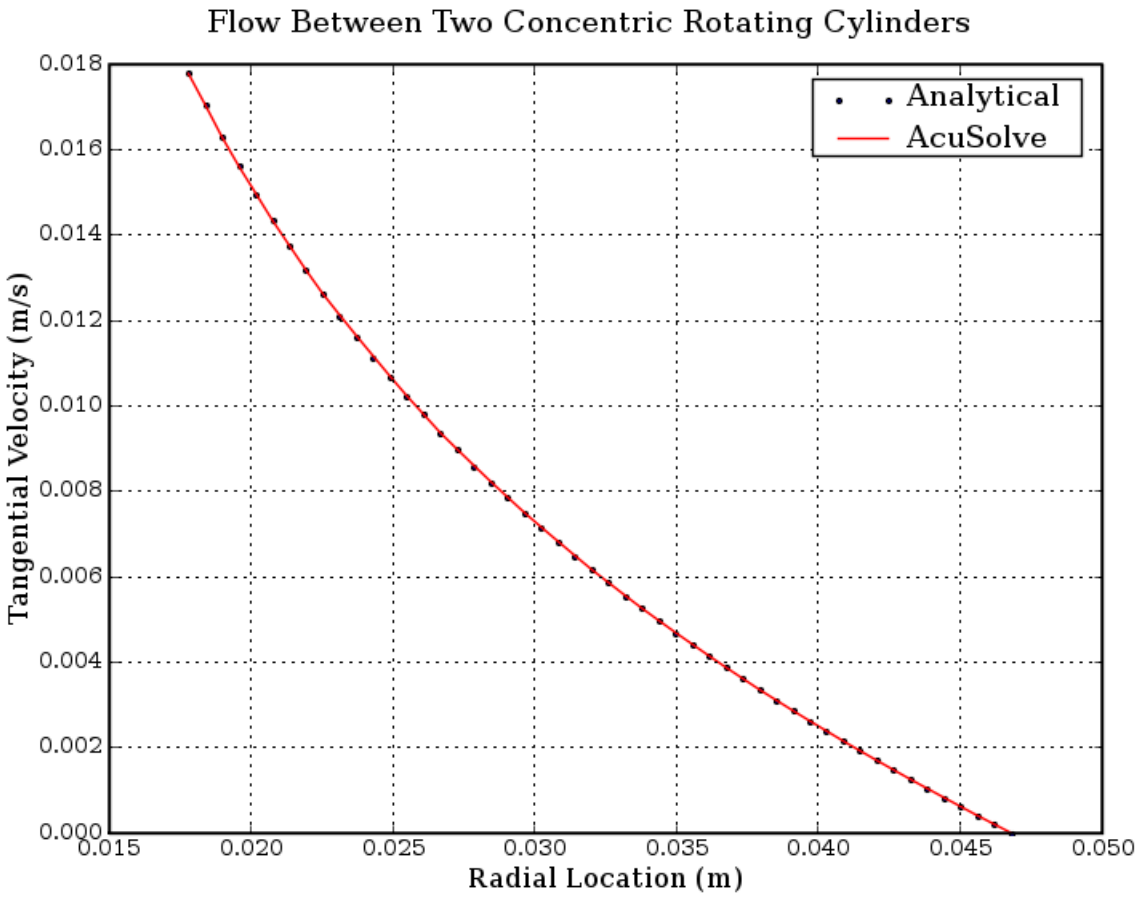


Figure 252: Tangential Velocity Plotted Against Distance from the Center of the Rotating Cylinder

Summary

The AcuSolve solution compares well with analytical results for the flow between concentric cylinders. In this application, the velocity in the annular fluid region is driven by the viscous stresses on the rotating wall. The AcuSolve tangential velocity is within 0.1 percent of the analytical solution at all radial locations.

Simulation Settings for Flow Between Concentric Cylinders

HyperMesh CFD database file: `<your working directory>\annulus_rotating\annulus_rotating.hm`

Global

- Problem Description
  - Analysis type - Steady State
  - Turbulence equation - Laminar
- Auto Solution Strategy
  - Relaxation Factor - `0.2`
- Material Model

- Water
  - Density - `1000.0` kg/m3
  - Viscosity - `0.001` kg/m-sec
- Reference Frame
  - Rotating_Cylinder
    - Rotation center
      1. X-coordinate - `0.0` m
      2. Y-coordinate - `0.0` m
      3. Z-coordinate - `0.0` m
    - Angular velocity
      1. X-component - `0.0` rad/sec
      2. Y-component - `0.0` rad/sec
      3. Z-component - `-1.0` rad/sec

Model

- Volumes
  - Volume
    - Element set
      1. Material model - Water
- Surfaces
  - Boundary1
    - Simple Boundary Condition
      1. Type - Symmetry
  - Boundary2
    - Simple Boundary Condition
      1. Type - Symmetry
  - Inner
    - Simple Boundary Condition
      1. Type - Wall
      2. Reference Frame - Rotating_Cylinder
  - Outer
    - Simple Boundary Condition
      1. Type - Wall
- Nodes
  - Fixed
    - Pressure
      1. Type - Zero

References

F. M. White. "Viscous Fluid Flow". Section 3-2.3. McGraw-Hill Book Co., Inc. New York. 1991.

Turbulent Flow Through a Pipe

In this application, turbulent flow of air through a pipe is simulated. AcuSolve results are compared with experimental results as described in White (1991) and extracted from the Moody chart. The close agreement of AcuSolve results with experimental results validates the ability of AcuSolve to model turbulent flow within pipes.

Problem Description

The problem consists of air flowing through a pipe 0.004 m in diameter and 0.02 m long, as shown in the following image, which is not drawn to scale. The AcuSolve simulation utilizes periodic boundary conditions to obtain the fully developed profile within the pipe. The defined pressure drop, applied as a body force on the fluid volume, offsets the change in pressure due to the friction created by the no-slip walls of the pipe. The Reynolds number for this problem is approximately 8,250.

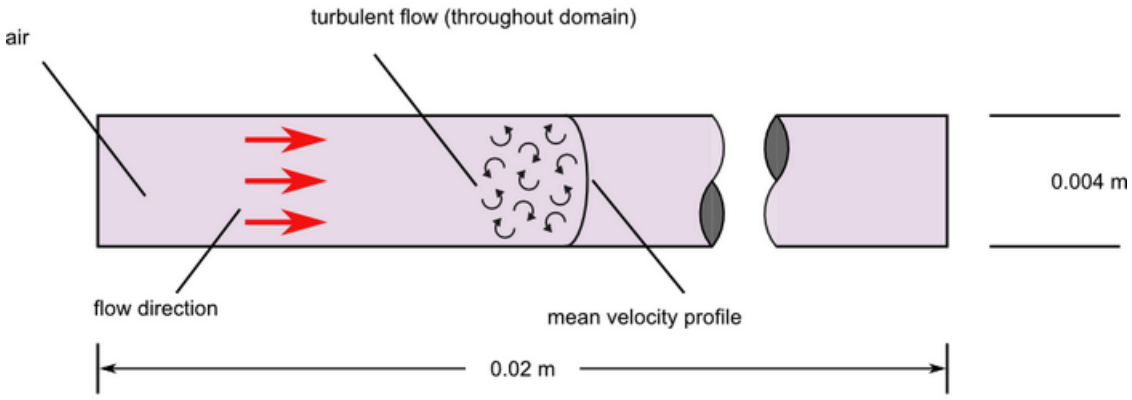


Figure 253: Critical Dimensions and Parameters for Simulating Turbulent Flow Through a Pipe

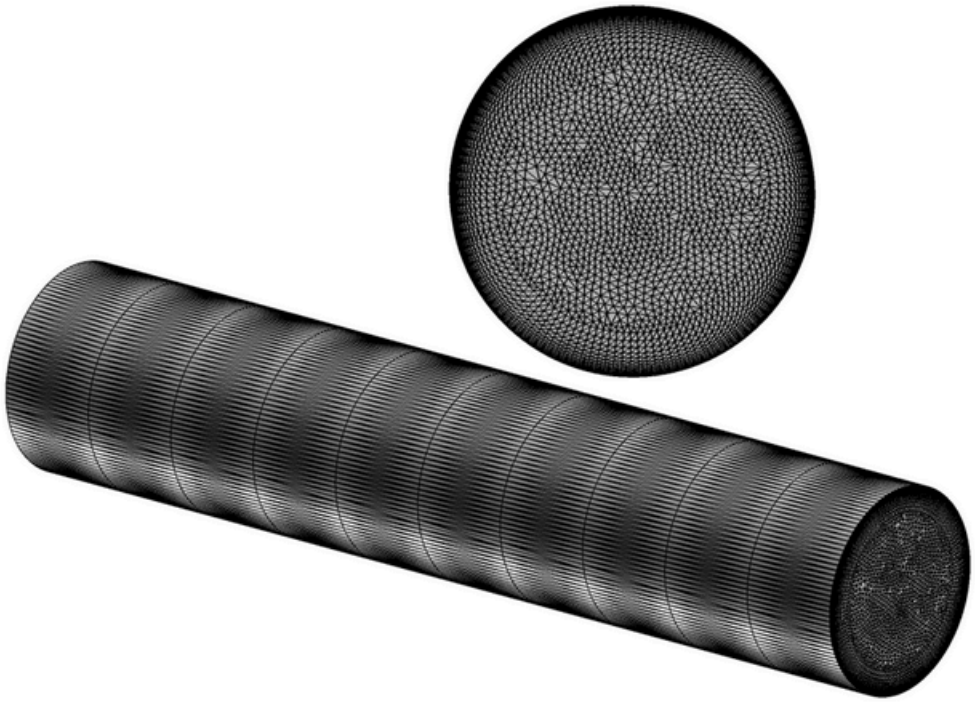


Figure 254: Mesh of a Periodic Segment Used for Simulating Turbulent Flow Through a Pipe

AcuSolve Results

The AcuSolve solution converged to a steady state and the results reflect the mean flow conditions with a turbulent velocity profile that is fully developed. The simulation was performed using the Spalart-Allmaras single-equation turbulence model. The velocity and eddy viscosity profiles are constant along the length of the pipe.

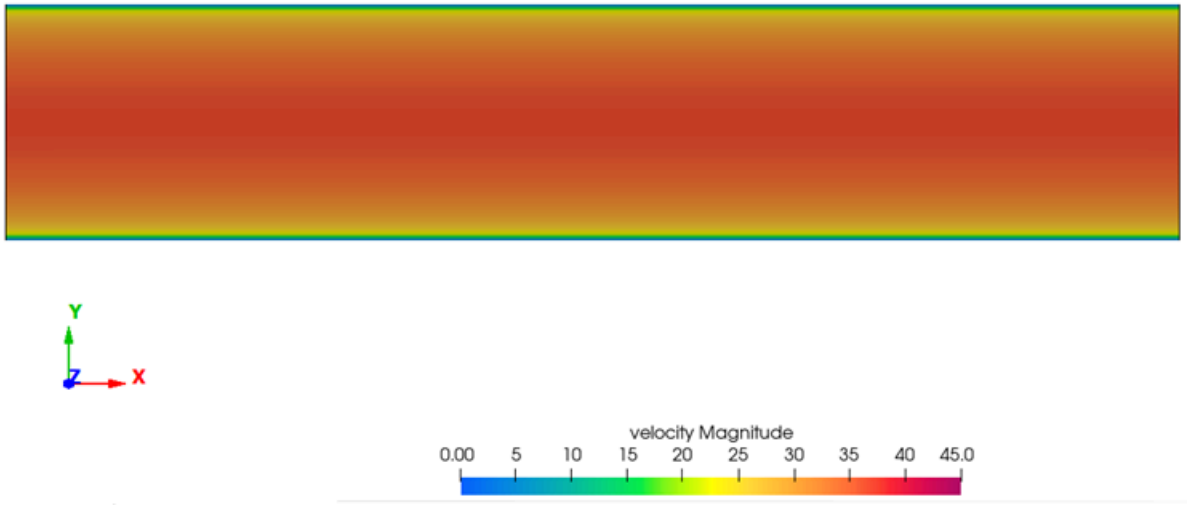


Figure 255: Velocity Contours for the Averaged Turbulent Flow

The experimental result for average velocity at the inlet is presented with the corresponding AcuSolve prediction in the following table.

Table 15:

	Experimental result	AcuSolve prediction	Percent deviation from experimental
Average inlet velocity	30.0	30.63	2.1

Summary

The AcuSolve solution compares well with the experimental result for average inlet velocity for turbulent flow through a pipe. In this application, the applied body force counteracts the change in pressure due to the viscous stresses near the pipe wall. The resulting friction factor for a smooth wall pipe and the specified Reynolds number is approximately 0.0326. With the imposed pressure drop defining the flow, the AcuSolve prediction of average inlet velocity is within 2.0 percent of the Darcy-Weisbach approximation.

Simulation Settings for Turbulent Flow Through a Pipe

SimLab database file: `<your working directory >\pipe_turbulent\pipe_turbulent.slb`.

Global

- Problem Description
  - Flow - Steady State
  - Turbulence equation - Spalart Allmaras
- Auto Solution Strategy
  - Relaxation factor - `0.4`

- Material Model
  - Air
    - Density - `1.225` kg/m3
    - Viscosity - `1.781e-05` kg/m-sec
- Body Force
  - dpdx
    - Gravity
      1. X-component - `3739.98` m/s2

  Model
- Volumes
  - Fluid
    - Element Set
      1. Material model - Air
      2. Body force - dpdx
- Surfaces
  - Inlet
    - Simple Boundary Condition - (disabled to allow for periodic conditions to be set)
  - Outlet
    - Simple Boundary Condition - (disabled to allow for periodic conditions to be set)
  - Wall
    - Simple Boundary Condition
      1. Type - Wall
      2. Roughness height - `0.0` mm
- Periodics
  - Periodic 1
    - Periodic Boundary Condition
      1. Type - Periodic

References

F. M. White. "Viscous Fluid Flow". Section 3-2.1. McGraw-Hill Book Co., Inc.. New York. 1991.

Experimental solution adapted from Darcy-Weisbach equation based on friction factor taken from the Moody chart with a Reynolds number of approximately 8,250.

Laminar Couette Flow with Imposed Pressure Gradient

In this application, AcuSolve is used to simulate the viscous flow of water between a moving and a stationary plate with an imposed pressure gradient. AcuSolve results are compared with analytical results described in White (1991). The close agreement of AcuSolve results with analytical results validates the ability of AcuSolve to model cases with imposed pressure gradients.

Problem Description

The problem consists of air between two plates in a two dimensional domain, as shown in the following image, which is not drawn to scale. The domain is 1.0 m high and 1.5 m long. The top plate moves with a constant velocity of 3.0 m/sec and the bottom plate is fixed. There is a mean-pressure gradient of -12 Pa/m applied to the bulk fluid in the streamwise direction. The problem is simulated with periodic boundaries in the streamwise direction. The induced flow field is laminar and exhibits a steady state behavior. The flow field develops from the pressure gradient, the motion of the top plate, and the viscous shear stresses near the plates.

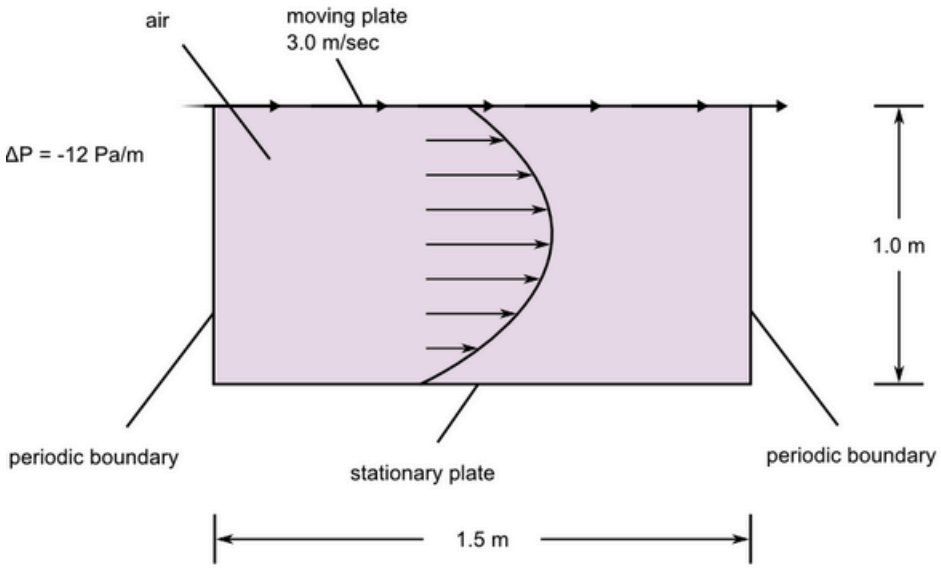


Figure 256: Critical Dimensions and Parameters for Simulating Laminar Couette Flow with an Imposed Pressure Gradient

The simulation was performed as a two dimensional problem by restricting flow in the out-of-plane direction through the use of a mesh that is one element thick.

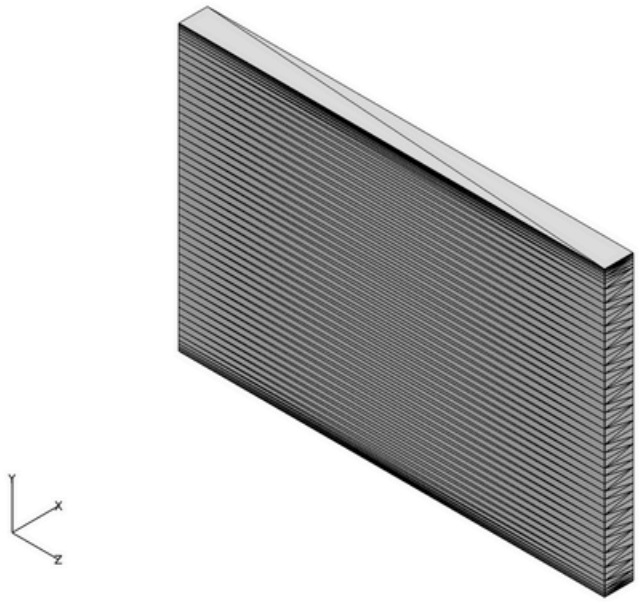


Figure 257: Mesh used for Simulating Laminar Couette Flow with an Imposed Pressure Gradient

AcuSolve Results

The AcuSolve solution converged to a steady state and the results reflect the mean flow conditions. The greatest velocity is located at approximately 40 percent of the channel height, closer to the moving plate. The flow develops as a result of the pressure gradient and the shear stress acting on the fluid near both the moving plate and the stationary plate.

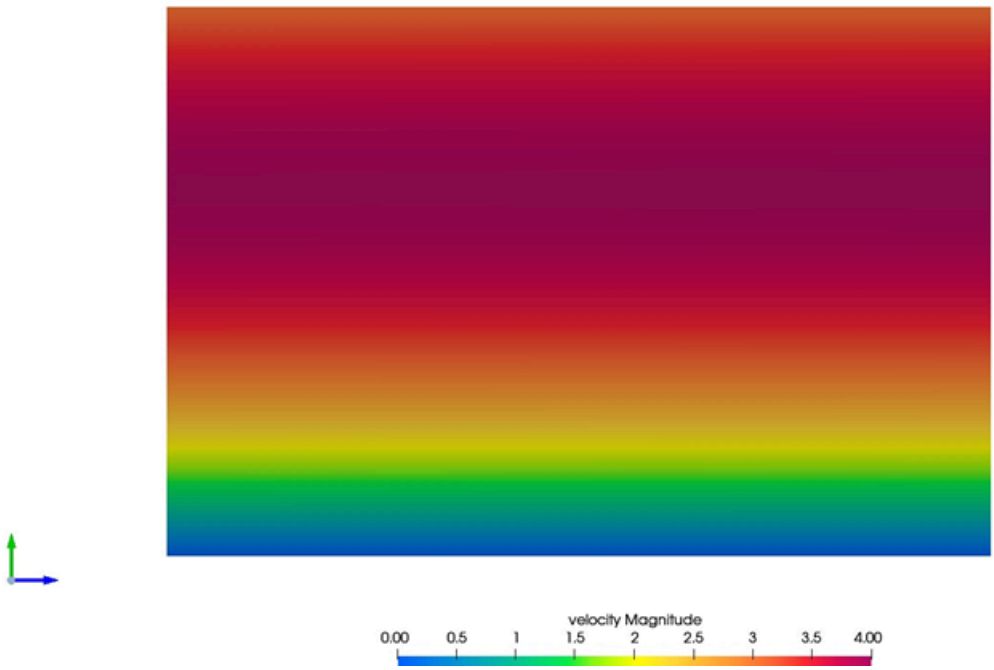


Figure 258: Z-Velocity Contours and Velocity Vectors

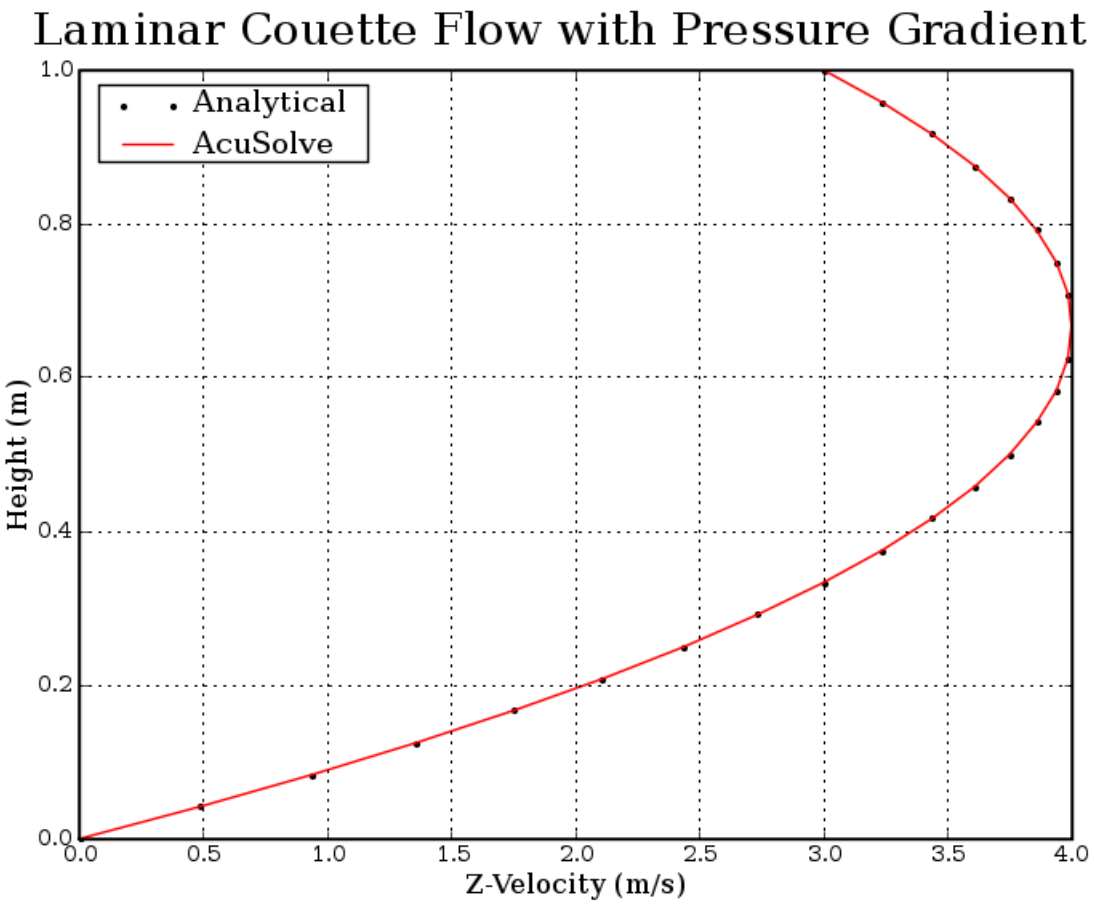


Figure 259: Z Velocity Plotted Against Height Above the Bottom of the Flow Field (Z Velocity is Presented on the X Axis to Better Represent the Velocity Profile in the Direction of Flow)

Summary

The velocity profile computed by AcuSolve agrees well with the analytical solution for this application. The velocity profile arises due to the combination of the imposed pressure gradient and the constant upper-wall velocity.

Note: The combination of these effects results in the asymmetric velocity profile that is reflected in the results.

Simulation Settings for Laminar Couette Flow with Imposed Pressure Gradient

SimLab database file: `<your working directory>\couette_flow\couette_flow.slb`

Global

- Problem Description
  - Solution Type - Steady State
  - Flow - Laminar

- Auto Solution Strategy
  - Relaxation factor - `0.2`
- Material Model
  - Air
    - Density - `1.0` kg/m3
    - Viscosity - `1.0` kg/m-sec
- Body Force
  - DP/DL
    - Gravity
      1. Z-component - `18.0` m/sec2

Model

- Volumes
  - Fluid
    - Element set
      1. Material model - Air
      2. Body force - DP/DL
- Surfaces
  - Max_X
    - Simple Boundary Condition
      1. Type - Symmetry
  - Max_Y
    - Simple Boundary Condition
      1. Type - Wall
      2. Wall velocity type - Cartesian
      3. Z-velocity - `3.0` m/s
  - Max_Z
    - Simple Boundary Condition - (disabled to allow for periodic conditions to be set)
  - Min_X
    - Simple Boundary Condition
      1. Type - Symmetry
  - Min_Y
    - Simple Boundary Condition
      1. Type - Wall
  - Min_Z
    - Simple Boundary Condition - (disabled to allow for periodic conditions to be set)
- Periodics
  - Periodic 1

- Periodic Boundary Conditions
  1. Type - Periodic

References

F. M. White. "Viscous Fluid Flow". Section 3-2.3. McGraw-Hill Book Co., Inc. New York. 1991.

Flow Inside a Rotating Cavity

In this application, AcuSolve is used to simulate the flow of air in an enclosed cylindrical cavity with a rotating top and a fixed bottom. AcuSolve results are compared with experimental data adapted from Michelsen (1986). The close agreement of AcuSolve results with experimental data validates the ability of AcuSolve to model cases containing enclosed cavities with flow induced by rotating walls.

Problem Description

The problem consists of air in an enclosed cylinder 1.0 m tall with a radius of 1.0 m, as shown in the following image, which is not drawn to scale. The top of the cylinder rotates about its center at 1 rad/s, while the bottom of the cylinder is fixed. As the container top spins, the viscous stresses on the fluid induce a circumferential (swirl) velocity throughout the height of the cylinder. To conserve mass and momentum, the fluid generates a radial velocity that changes direction based on distance away from the rotation center of the cylinder.

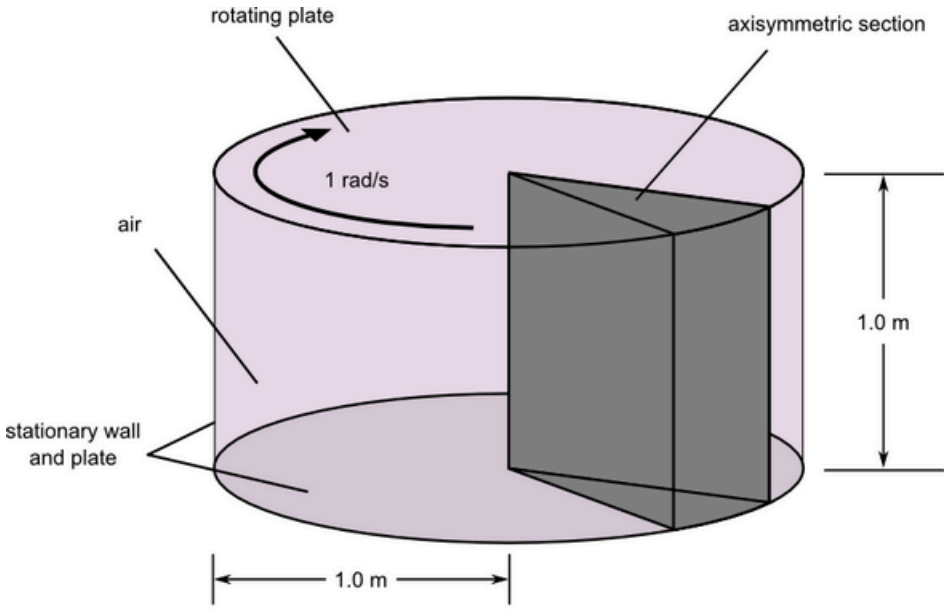


Figure 260: Critical Dimensions and Parameters for Simulating Flow Inside a Rotating Cavity

The flow domain is modeled with axisymmetric periodicity in the circumferential direction, which allows for accurate simulation of the flow while minimizing computational time.

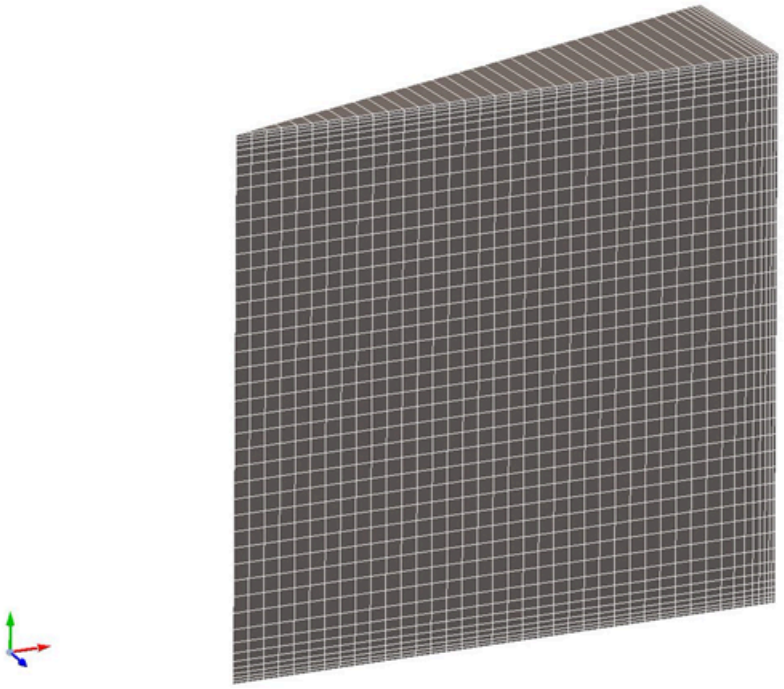


Figure 261: Mesh of Periodic Section Used for Simulating Flow Inside a Rotating Cylinder

AcuSolve Results

The AcuSolve solution converged to a steady state and the results reflect the mean flow conditions. The velocity varies with both vertical location and with distance from the rotation center. The complex flow field develops from a combination of the viscous stresses acting at the rotating cylinder top and at the stationary bottom.

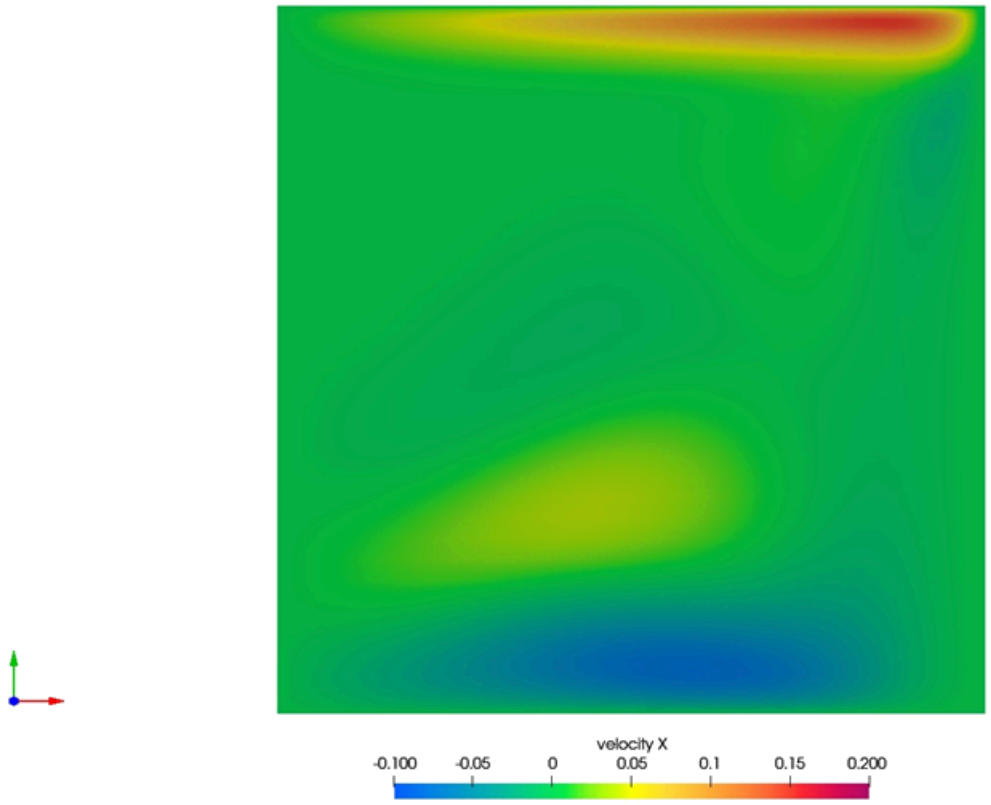


Figure 262: Contours of Radial Velocity with Velocity Vectors. This Image Shows the Front Face of the Modeled Cylinder Wedge, with the Center of Rotation on the Left Edge. The Vertical Line Represents a Radial Location 0.6 m From the Center of Rotation.

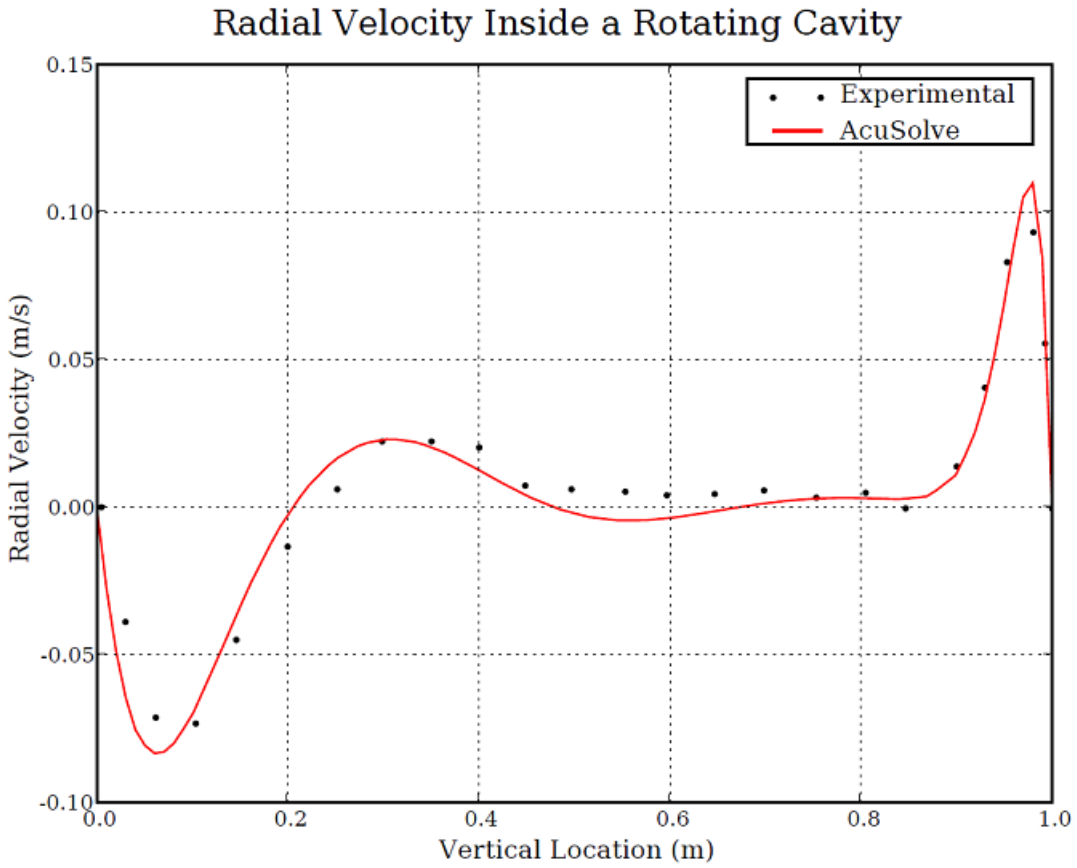


Figure 263: Radial Velocity (at 0.6 m From the Center of Rotation) as a Function of Vertical Location From Cylinder Bottom

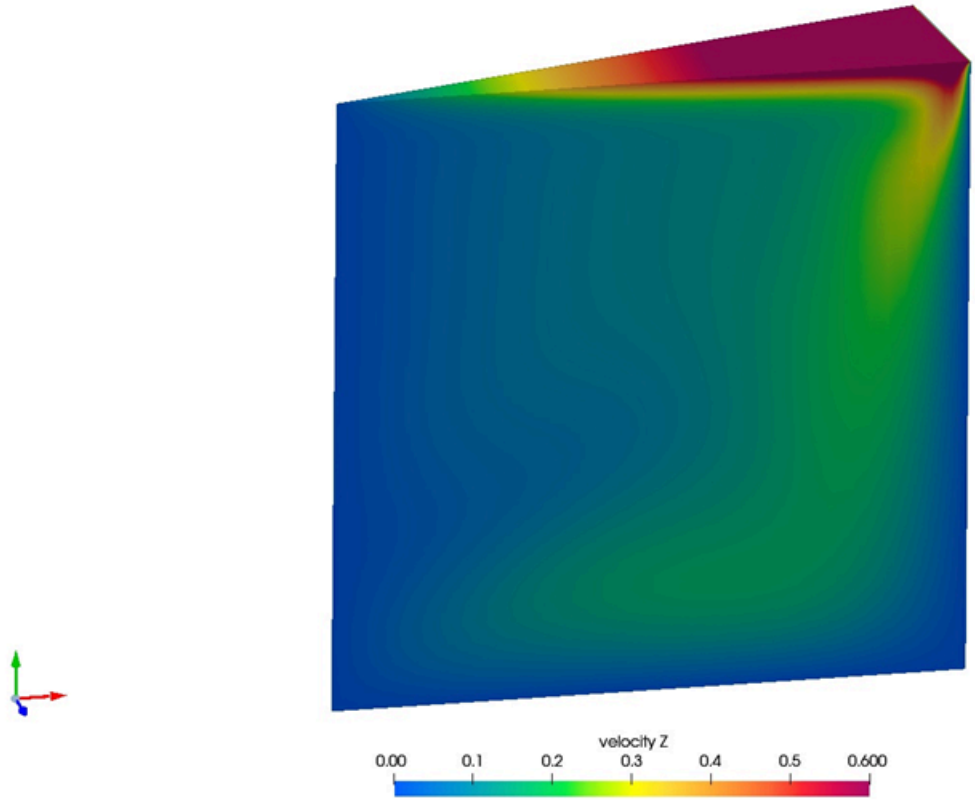


Figure 264: Contours of Swirl Velocity with Velocity Vectors

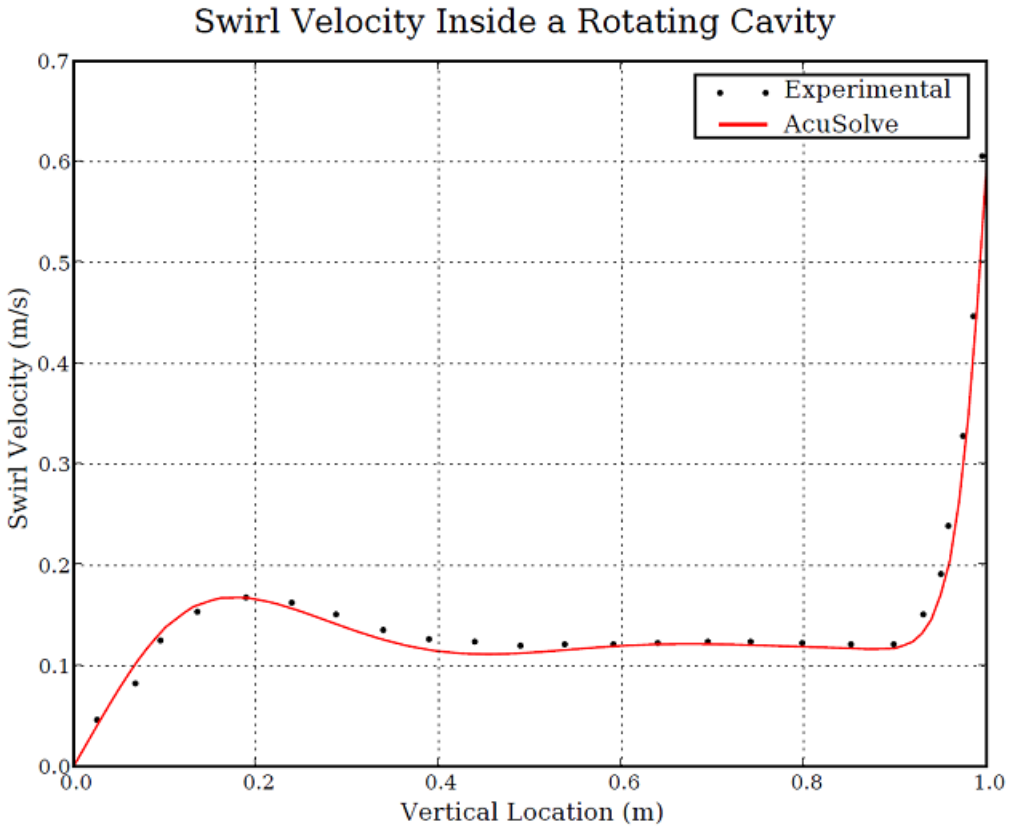


Figure 265: Swirl Velocity (at 0.6 m From Center of Rotation) as a Function of Vertical Location From the Cylinder Bottom

Summary

The AcuSolve solution compares well with the experimental data for flow induced by a rotating top of an enclosed cylinder. In this application, the flow in the fluid region is driven by the viscous stresses near the rotating top. Viscous stresses drag the fluid in a circular direction near the spinning wall. The angular velocity of the fluid decreases as distance from the top wall increases. Radial velocity develops as a result of the migration of the fluid toward the outer wall in regions of high angular velocity. The AcuSolve radial and swirl velocities compare very closely with the experimental data.

Simulation Settings for Flow Inside a Rotating Cavity

SimLab database file: `<your working directory>\cavity_rotating\cavity_rotating.slb`

Global

- Problem Description
  - Solution type - Steady State
  - Flow - Laminar
- Auto Solution Strategy
  - Relaxation Factor - `0.4`
- Material Model

- Air
  - Density - `1.0` kg/m3
  - Viscosity - `0.000556` kg/m-sec
- Reference Frame
  - Cavity Rotation
    - Rotation center
      1. X-coordinate - `0.0`
      2. Y-coordinate - `0.0`
      3. Z-coordinate - `0.0`
    - Angular velocity
      1. X-component - `0.0`
      2. Y-component - `-1.0` rad/sec
      3. Z-component - `0.0`

Model

- Volumes
  - Fluid
    - Element Set
      1. Material model - Air
- Surfaces
  - Bottom
    - Simple Boundary Condition
      1. Type - Wall
  - Max_X
    - Simple Boundary Condition
      1. Type - Wall
  - Max_Z
    - Simple Boundary Condition - (disabled to allow for periodic conditions to be set)
  - Min_Z
    - Simple Boundary Condition - (disabled to allow for periodic conditions to be set)
  - Top
    - Simple Boundary Condition
      1. Type - Wall
      2. Reference frame - Cavity Rotation
- Periodics
  - Periodic 1
    - Periodic Boundary Condition
      1. Type - Axisymmetric

2 Rotation axis
  1 point 1
    1 X-coordinate - `0.0` m
    2 Y-coordinate - `0.0` m
    3 Z-coordinate - `0.0` m
  2 point 2
    1 X-coordinate - `0.0` m
    2 Y-coordinate - `1.0` m
    3 Z-coordinate - `0.0` m

References

J. A. Michelsen. "Modeling of Laminar Incompressible Rotating Fluid Flow". AFM 86-05. Ph.D. thesis, Department of Fluid Mechanics, Technical University of Denmark. 1986.

Natural Convection in a Concentric Annulus

In this application, AcuSolve is used to simulate natural convection in the annular space between a heated inner pipe and an outer concentric pipe. AcuSolve results are compared with experimental results adapted from Kuehn and Goldstein (1978). The close agreement of AcuSolve results with experimental results validates the ability of AcuSolve to model cases with flow induced by natural convection.

Problem Description

The problem consists of two concentric cylinders with air filling the void between them, as shown in the following image, which is not drawn to scale. The radius of the inner cylinder is 0.0178 m and the radius of the outer cylinder is 0.0463 m. The inner cylinder is held at a fixed temperature of 373 K while the outer cylinder is held at 327 K. The temperature gradient drives the flow due to buoyancy effects.

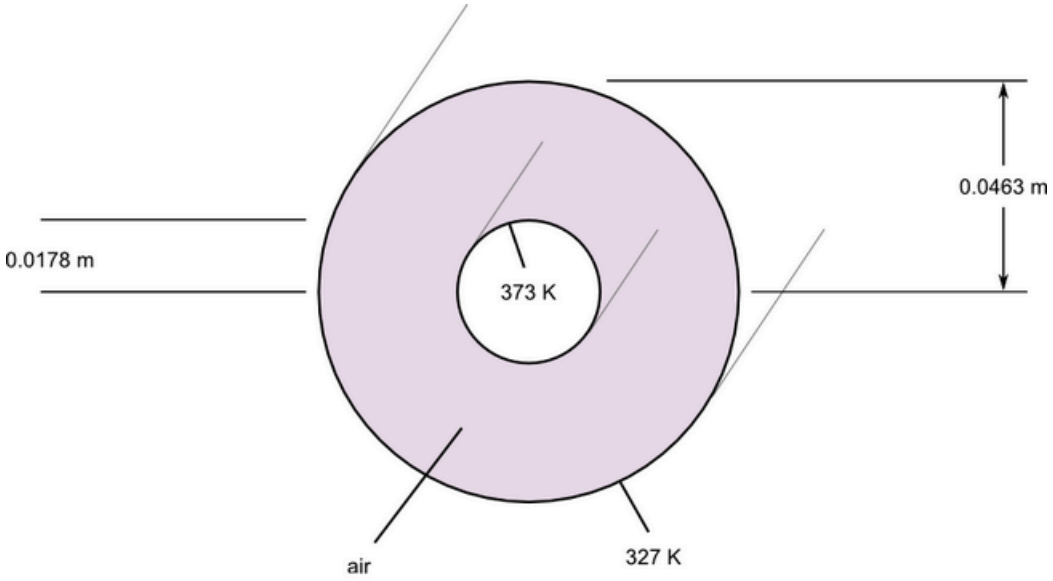


Figure 266: Critical Dimensions and Parameters for Simulating Natural Convection in a Concentric Annulus

The simulation was performed as a two dimensional problem by restricting flow in the out-of-plane direction through the use of a mesh that is one element thick. In addition, the half symmetry of the geometry is exploited to allow for modeling only half of the geometry. These characteristics allow for accurate simulation of the flow while minimizing computational time.

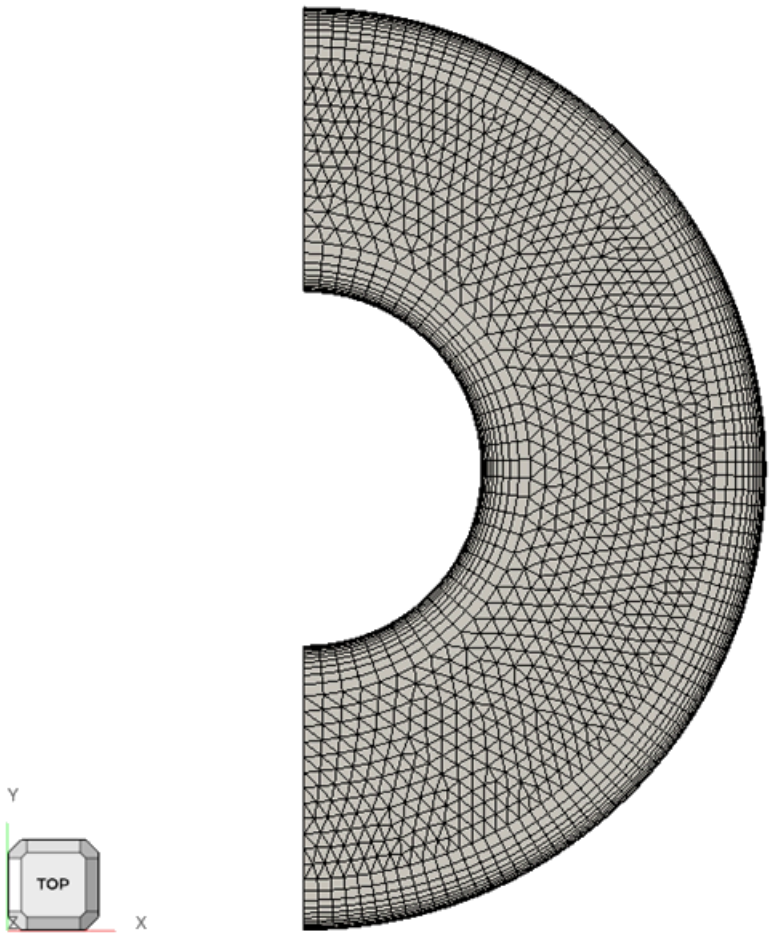


Figure 267: Mesh (Half of a Concentric Annulus) used for Simulating Natural Convection in a Concentric Annulus

AcuSolve Results

The AcuSolve solution converged to a steady state and the results reflect the mean flow conditions. Air density decreases due to heating by the inner cylinder, leading to convective currents within the annulus. As air approaches the outer cylinder, it is cooled by the outer wall, causing the density to increase. This results in heavier air sinking toward the bottom of the assembly.

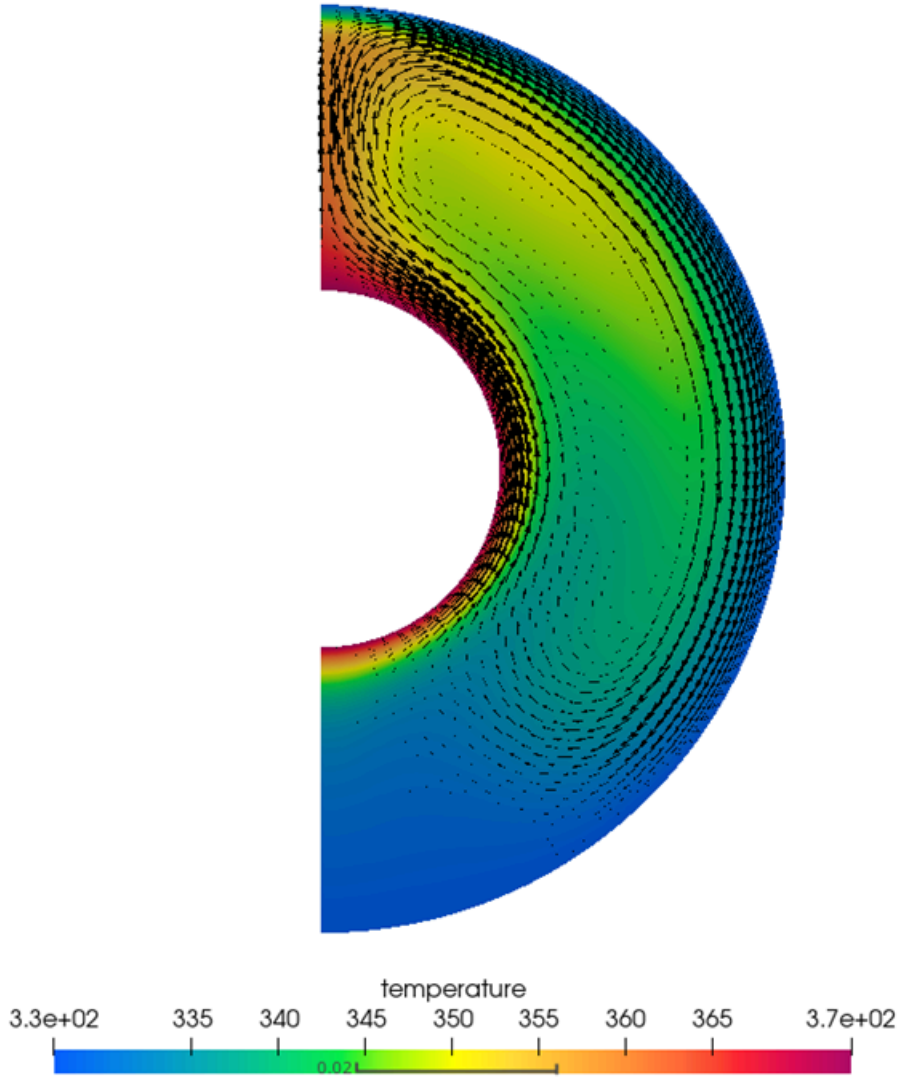


Figure 268: Temperature Contours and Velocity Vectors

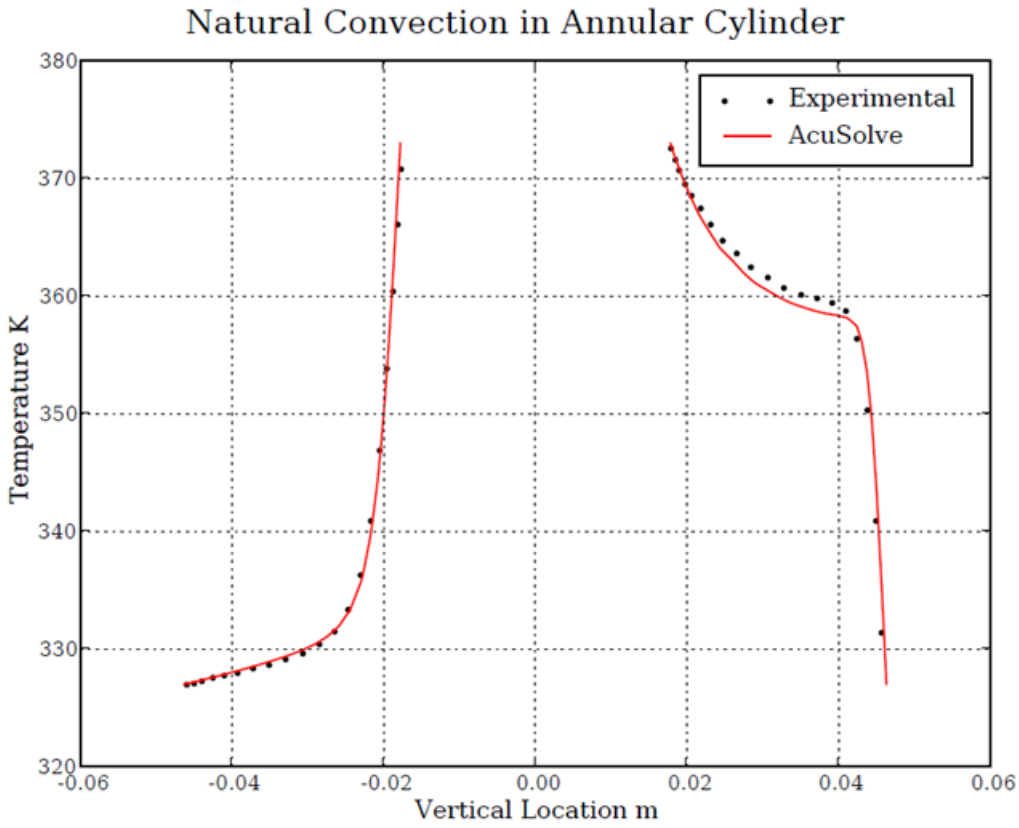


Figure 269: Temperature as a Function of Distance From the Center of the Inner Cylinder

Summary

The AcuSolve solution compares well with analytical results for natural convection in a concentric annulus. In this application, flow is driven by a decrease in density as air is heated. The local variations in density result in the higher density fluid sinking to the bottom of the annulus while the lower density fluid rises to the top. This transfer of momentum is a continuous process which results in the convective currents that are visible in the solution. The AcuSolve temperature results compare very closely with the experimental results.

Simulation Settings for Natural Convection in a Concentric Annulus

HyperMesh CFD database file: `<your working directory>\annulus_heat\annulus_heat.hm`

Global

- Problem Description
  - Analysis type - Steady State
  - Abs. pressure offset - `101325.0` N/m2
  - Temperature equation - Advective Diffusive
  - Turbulence equation - Laminar
  - Gravitational acceleration - { 0, -9.80665, 0 }
- Auto Solution Strategy

- Relaxation factor - `0.2`
- Flow - On
- Temperature - On

- Material Model
  - Air
    - Type - Boussinesq
    - Density - `1.225` kg/m3
    - Expansivity - `0.0034722` 1/K
    - Reference temperature - `288` K
    - Isothermal compressibility - `0.0` m2/N
    - Viscosity - `2.081e-5` kg/m-sec

  Model
- Volumes
  - Fluid
    - Element Set
      1. Material model - Air
  - Surfaces
    - ID
      1. Simple Boundary Condition
         1. Type - Wall
         2. Temperature BC type - Value
         3. Temperature - `373.0` K
    - Max_Z
      1. Simple Boundary Condition
      2. Type - Symmetry
    - Min_Z
      1. Simple Boundary Condition
      2. Type - Symmetry
    - OD
      1. Simple Boundary Condition
         1. Type - Wall
         2. Temperature BC type - Value
         3. Temperature - `327.0` K
    - Symmetry
      1. Simple Boundary Condition
      2. Type - Symmetry
  - Nodes
    - Node 1

1 Pressure

1 Type - Zero

References

T.H. Kuehn and R. J. Goldstein. "An Experimental Study of Natural Convection Heat Transfer in Concentric and Eccentric Horizontal Cylindrical Annuli". Journal of Heat Transfer 100:635-640. 1978.

Laminar Flow Past a 90° T-Junction

In this application, AcuSolve is used to simulate laminar flow through a channel with two outlets forming a T-junction. AcuSolve results are compared with experimental results adapted from Hayes and others (1989). The close agreement of AcuSolve results with experimental results validates the ability of AcuSolve to model cases with multiple outlet paths.

Problem Description

The problem consists of air flowing past a T-junction in a channel, as shown in the following image, which is not drawn to scale. Air enters the channel with an average velocity of 0.667 m/s and travels past the T-junction 2.0 m from the inlet. A portion of the flow will travel out of the branch of the channel due to the pressure difference between the bulk flow and the outlet of the branch.

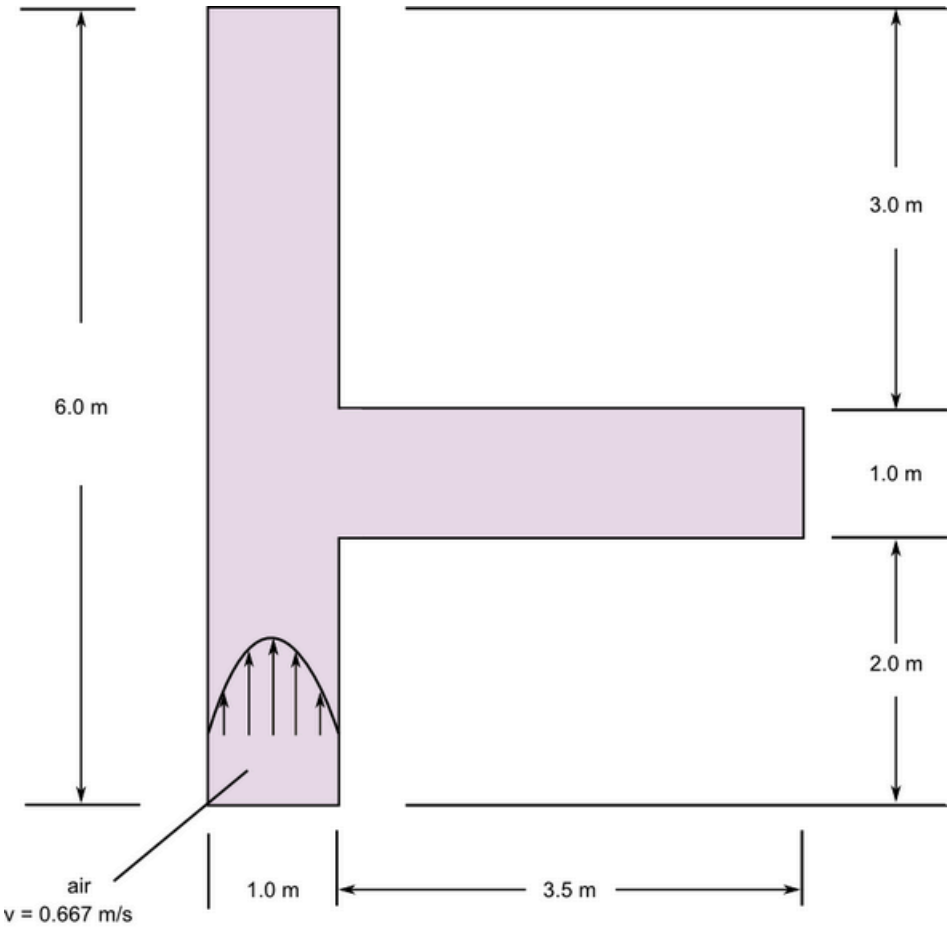


Figure 270: Critical Dimensions and Parameters for Simulating Laminar Flow Past a 90° T-Junction

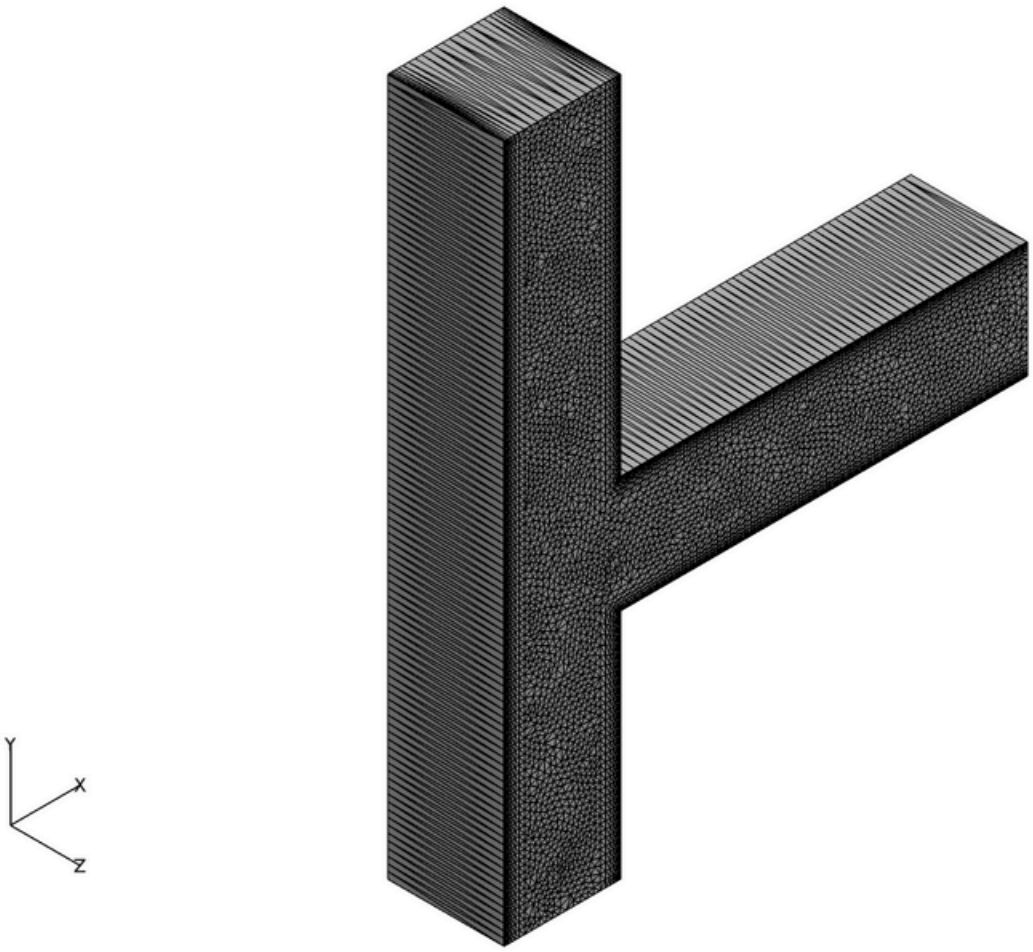


Figure 271: Mesh Used for Simulating Laminar Flow past a 90° T-Junction

AcuSolve Results

The AcuSolve solution converged to a steady state and the results reflect the mean flow conditions. As the air flows past the junction, a portion of it is diverted into the branch. A small recirculation region develops at the top of the junction and collapses before the flow exits the domain through the right branch.

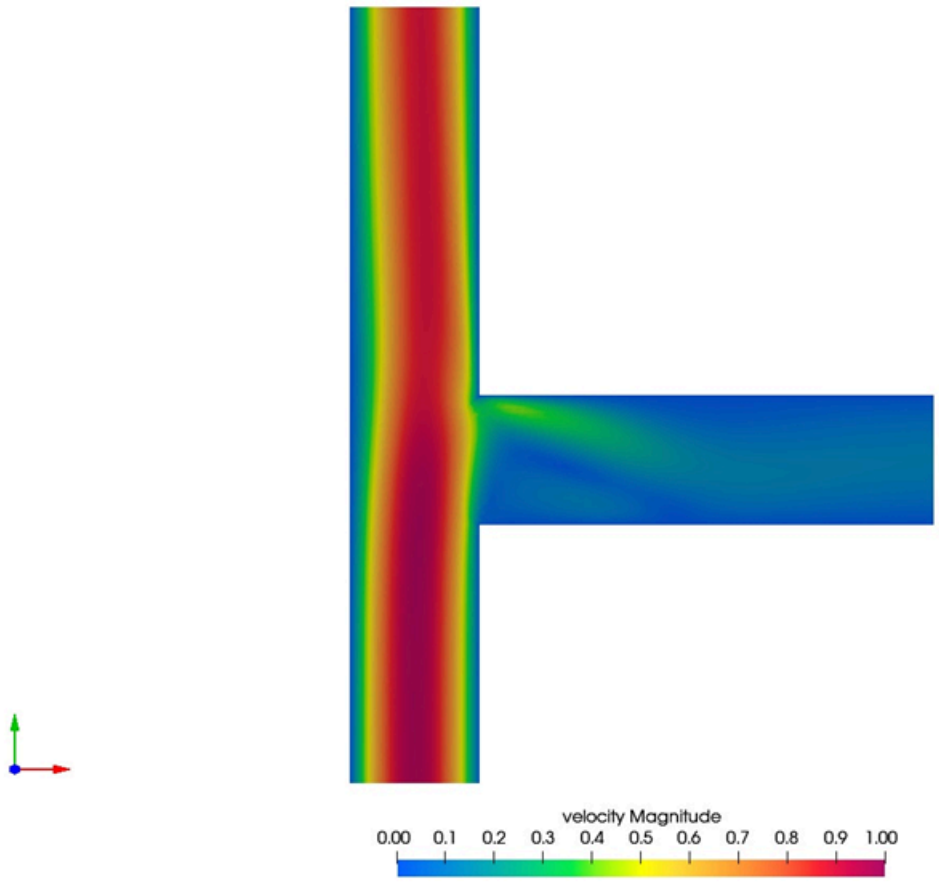


Figure 272: Velocity Contours in a T-Junction

The experimental value for the fraction of flow exiting the top branch of the channel is presented with the corresponding AcuSolve result in the following table.

Table 16:

	Experimental fractional flow	**AcuSolve fractional flow**	**Percent deviation from experimental**
Fractional flow exiting the upper branch	0.887	0.889	0.332

Summary

The AcuSolve solution compares well with experimental results for flow past a T-junction. In this application, flow is driven by a fixed flow rate at the inlet to the main branch. A portion of the flow from the main branch is diverted into the right branch of the T-junction, giving rise to recirculation just downstream of the junction. This recirculation collapses before the flow exits the side branch. The AcuSolve result for fractional flow exiting the top branch is within 0.33 percent of the experimental results.

Simulation Settings for Laminar Flow Past a 90° T-Junction

SimLab database file: `<your working directory>\T_junction_laminar\T_junction_laminar.slb`

Global

- Problem Description
  - Solution type - Steady State
  - Flow - Laminar
- Auto Solution Strategy
  - Relaxation factor - `0.2`
- Material Model
  - Air
    - Type - Constant
    - Density - `1.0` kg/m3
    - Viscosity - `0.003333` kg/m-sec

  Model
- Volumes
  - Fluid
    - Element Set
      1. Material model - Air
- Surfaces
  - Inflow
    - Simple Boundary Condition
      1. Type - Inflow
      2. Inflow type - Average Velocity
      3. Average velocity - `0.6667` m/sec
  - Max_Z
    - Simple Boundary Condition - (disabled to allow for periodic conditions to be set)
  - Min_Z
    - Simple Boundary Condition - (disabled to allow for periodic conditions to be set)
  - Outflow
    - Simple Boundary Condition
      1. Type - Outflow
  - T_Out
    - Simple Boundary Condition
      1. Type - Outflow
  - Walls
    - Simple Boundary Condition
      1. Type - Wall

- Periodics
  - Periodic 1
    - Periodic Boundary Condition
      1 Type - Periodic

References

R. E. Hayes, K. Nandkumar, and H. Nasr-El-Din. "Steady Laminar Flow in a 90 Degree Planar Branch". Computers and Fluids 17(4): 537-553. 1989.

Laminar Flow Through a Channel with Heated Walls

In this application, AcuSolve is used to simulate high Peclet number laminar flow through a channel with heated walls. AcuSolve results are compared with analytical results adapted from Hua and Pillai (2010). The close agreement of AcuSolve results with analytical results validates the ability of AcuSolve to model cases involving heat transfer to a moving fluid with a high Peclet number.

Problem Description

The problem consists of water at 20 °C flowing through a channel of infinite width with top and bottom walls heated to 75 °C. The channel is 0.2 m high and 0.8 m long, as shown in the following image, which is not drawn to scale. A centrally located slice 0.02 m wide is modeled with slip boundary conditions so that side-wall influences can be ignored. Water enters the channel with an average velocity of 0.003 m/s. As the fluid flows through the channel, it is heated by the top and bottom plates.

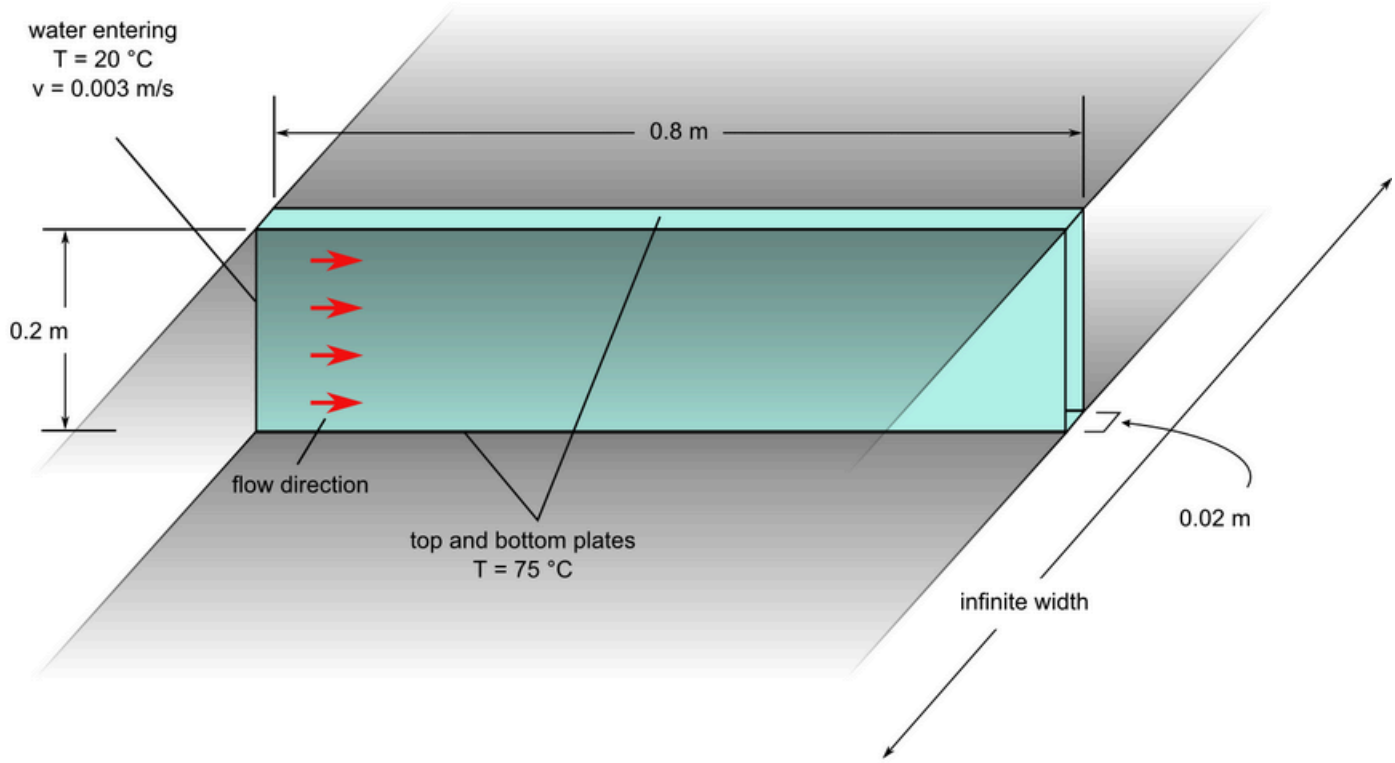


Figure 273: Critical Dimensions and Parameters for Simulating Laminar Flow Through a Channel with Heated Walls

The simulation was performed as a two dimensional problem by restricting flow in the out-of-plane direction through the use of a mesh that is one element thick. In addition, the symmetry of the geometry in the height direction is exploited to allow for modeling only half of the geometry. These characteristics allow for accurate simulation of flow while minimizing computational time.

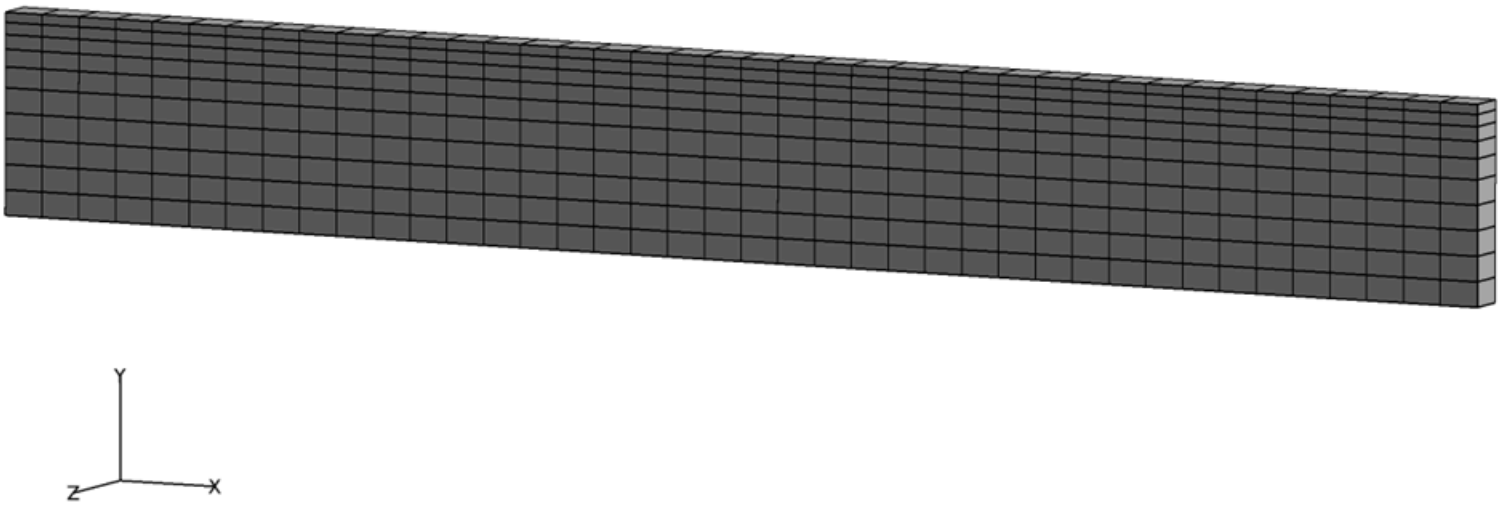


Figure 274: Mesh (Top Half of the Channel) used for Simulating Laminar Flow Through a Channel with Heated Walls

AcuSolve Results

The AcuSolve solution converged to a steady state and the results reflect the mean flow conditions. As the cool water enters the channel at temperature less than that of the walls, heat is transferred to the water by conduction. As the fluid travels along the channel, the temperature differential between the wall and the adjacent water decreases. The thermal boundary layer within the water develops as the flow propagates downstream.

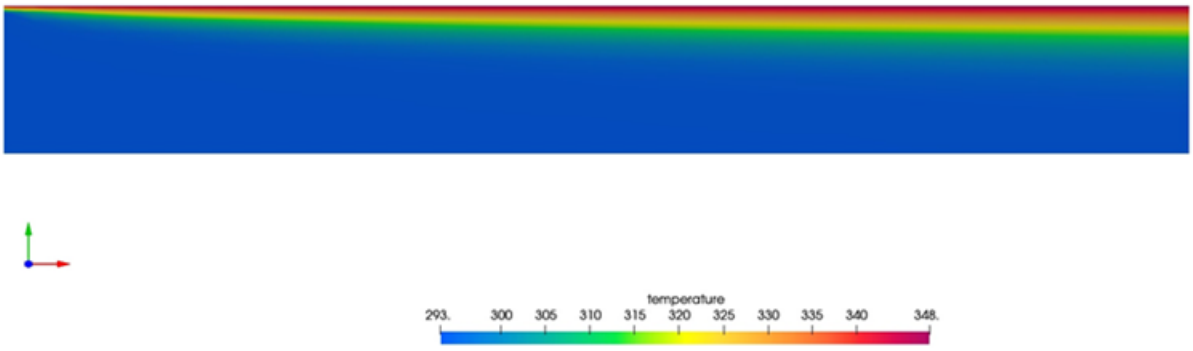


Figure 275: Temperature Contours Along the Top Half of a Heated Channel

Temperature at a specified vertical position in the channel increases along the length of the channel. The nature of that temperature change is dependent on proximity to the heated wall. Water in the center of the flow will have the least temperature change. Since this problem was solved for symmetrical flow, only the top half of the flow region was modeled. The vertical position for results shown in the following figure are based on the center of flow having a Y-position of 0.

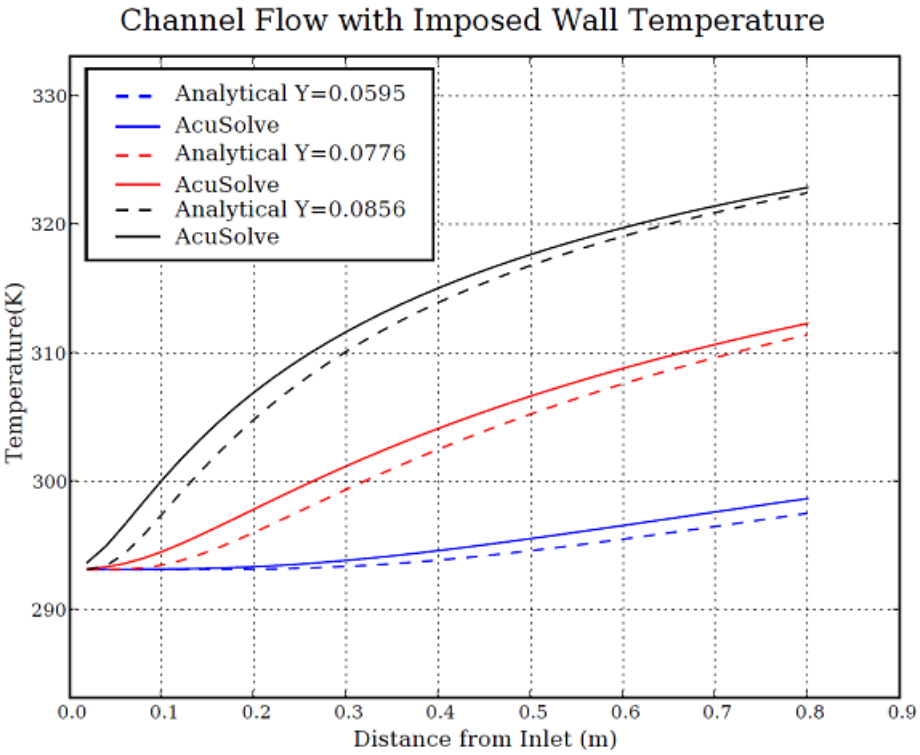


Figure 276: Temperature Plotted Against Distance from Inlet for 3 Different Heights from the Channel Center Line

Summary

The AcuSolve results compare well with the analytical results for the development of a thermal boundary layer in a heated channel. In this application, the model is set up to yield large gradients as the flow convects away from the inlet. The boundary conditions and mesh size were chosen specifically to yield a high Peclet number. The element Peclet number in the flow direction in this case is Pe=30.0, as calculated from the following equation.

$$Pe = \frac{\rho Cp|v|he}{k} \tag{9}$$

where ρ is the density, Cp the heat capacity, v the velocity, he the length, and k the thermal conductivity.

This example shows the robustness of the stabilized technique in AcuSolve when element Peclet number is high.

> **Note:** Standard Galerkin finite element formulations become unstable when the element Peclet number is greater than 1.0.

Simulation Settings for Laminar Flow Through a Channel with Heated Walls

SimLab database file: `<your working directory>\channel_laminar_heat\channel_laminar_heat.slb`

Global

- Problem Description
  - Flow - Steady State
  - Temperature equation - Advective Diffusive
  - Turbulence equation - Laminar
- Auto Solution Strategy
  - Relaxation factor - `0.4`
- Material Model
  - Fluid_Material
    - Density - `1000.0` kg/m3
    - Specific Heat - `1000` J/kg-K
    - Viscosity - `1.0e-12` kg/m-sec
    - Conductivity - 1.0 W/m-K

  Model
- Volumes
  - Fluid
    - Element Set
      1. Material model - Fluid_Material
- Surfaces
  - Inlet
    - Simple Boundary Condition
      1. Type - Inflow
      2. Inflow type - Velocity
      3. X velocity - `0.003` m/sec
      4. Temperature - `293.15` K
  - Outlet
    - Simple Boundary Condition
      1. Type - Outflow
  - Symm_MaxZ
    - Simple Boundary Condition
      1. Type - Slip
  - Symm_MinY
    - Simple Boundary Condition
      1. Type - Slip
  - Symm_MinZ
    - Simple Boundary Condition
      1. Type - Slip
  - Wall

- Simple Boundary Condition
  1. Type - Wall
  2. Temperature BC type - Value
  3. Temperature - `348.15` K

References

Hua Tan and K. M. Pillai. "Numerical Simulation of Reactive Flow in Liquid Composite Molding Using Flux-Corrected Transport (FCT) Based Finite Element/Control Volume (FE/CV) Method". International Journal of Heat and Mass Transfer. 53:2256-2271, 2010.

Turbulent Natural Convection Inside a Tall Cavity

In this application, AcuSolve is used to simulate the natural convection of a turbulent flow field within a tall rectangular cavity. AcuSolve results are compared with experimental results as described in Betts and Bokhari (2000). The close agreement of AcuSolve results with experimental results validates the ability of AcuSolve to model cases with natural convection of turbulent flow within a tall cavity.

Problem Description

The problem consists of air within a tall cavity with a hot wall and a cold wall, as shown in the following image, which is not drawn to scale. The cavity is 2.18 m tall, 0.0762 m wide, and 0.52 m deep. The cavity's vertical walls differ in temperature, causing the fluid to transfer the heat, leading to natural convection. The temperature of the hot wall is 307.85 K, while the temperature of the cold wall is 288.25 K. The horizontal walls of the cavity are adiabatic. The length-to-width ratio of 28.6 and temperature difference of 19.6 K produce a turbulent flow field within the cavity with a Rayleigh number of $8.6X10^{5}$ (Betts and Bokhari 2000). The flow medium is air, with a Boussinesq approximation for density, a specific heat of 1005 J/kg-K, and a viscosity of $1.781 X 10^{-5}$ kg/m-s. Gravity is applied globally to the volume of air.

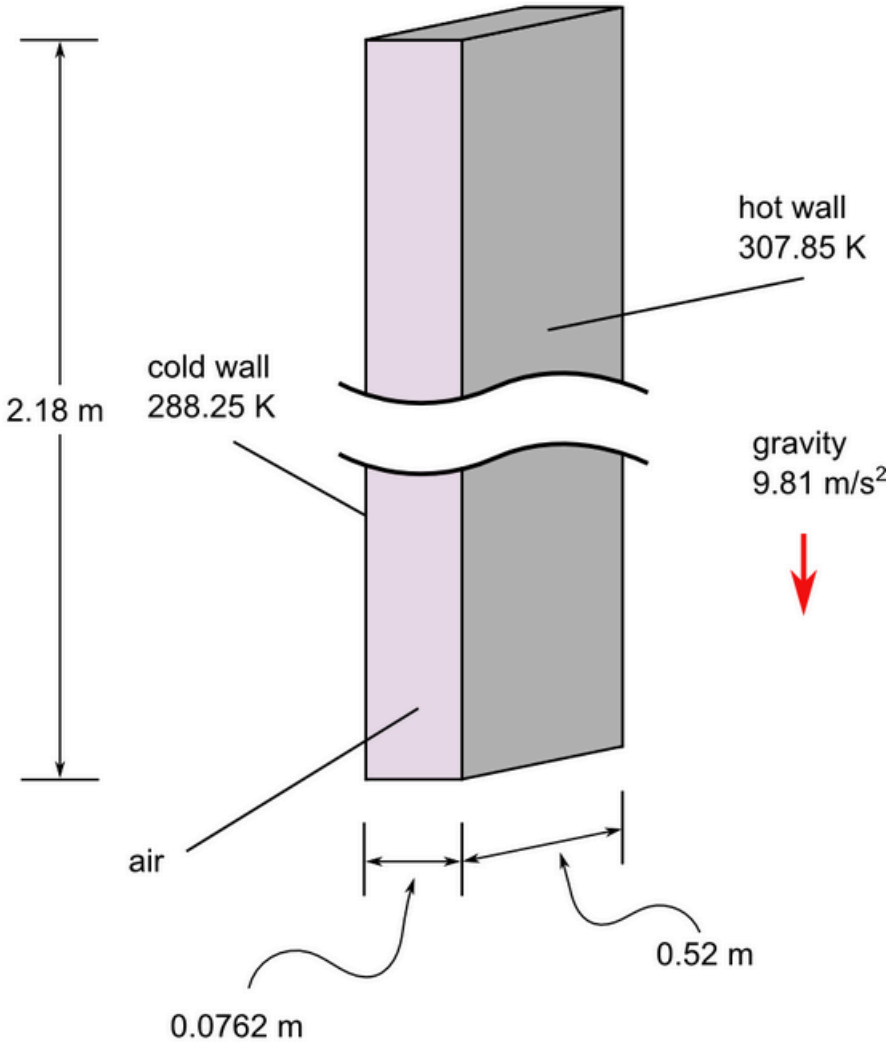


Figure 277: Critical Dimensions and Parameters for Simulating Turbulent Natural Convection in a Tall Cavity

The simulation was performed as a two dimensional problem by constructing a volume mesh that contains a single layer of elements in the extruded direction, normal to the flow plane and by imposing symmetry boundary conditions on the extruded planes.

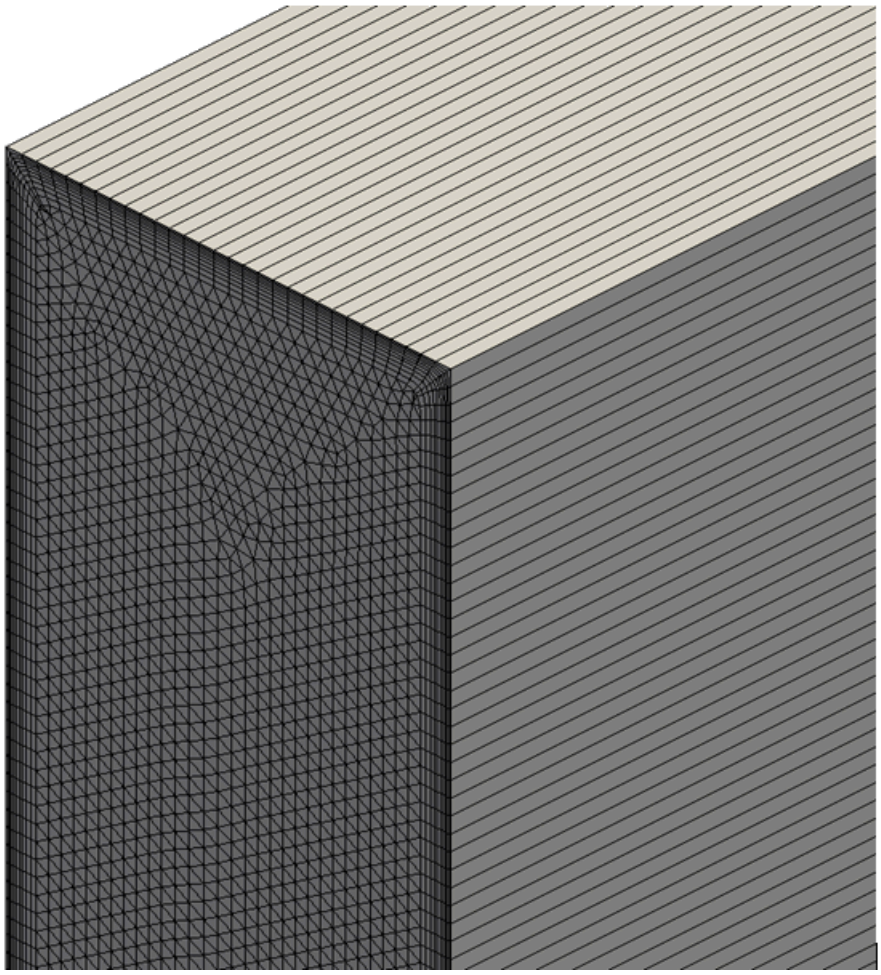


Figure 278: Mesh used for Simulating the Natural Convection of Turbulent Flow in a Tall Cavity

AcuSolve Results

The AcuSolve solution converged to a steady state and the results reflect the mean flow conditions. The natural convection of the flow is generated by heat transfer from the vertical walls to the fluid in the cavity. The temperature gradients created by this heat transfer cause differing densities within the flow region. The warmer air rises to the top of the cavity due to its lower density while the colder air sinks to the bottom of the cavity due to its higher density. This produces flow near the hot vertical wall in the positive vertical direction and flow near the cold wall in the negative vertical direction.

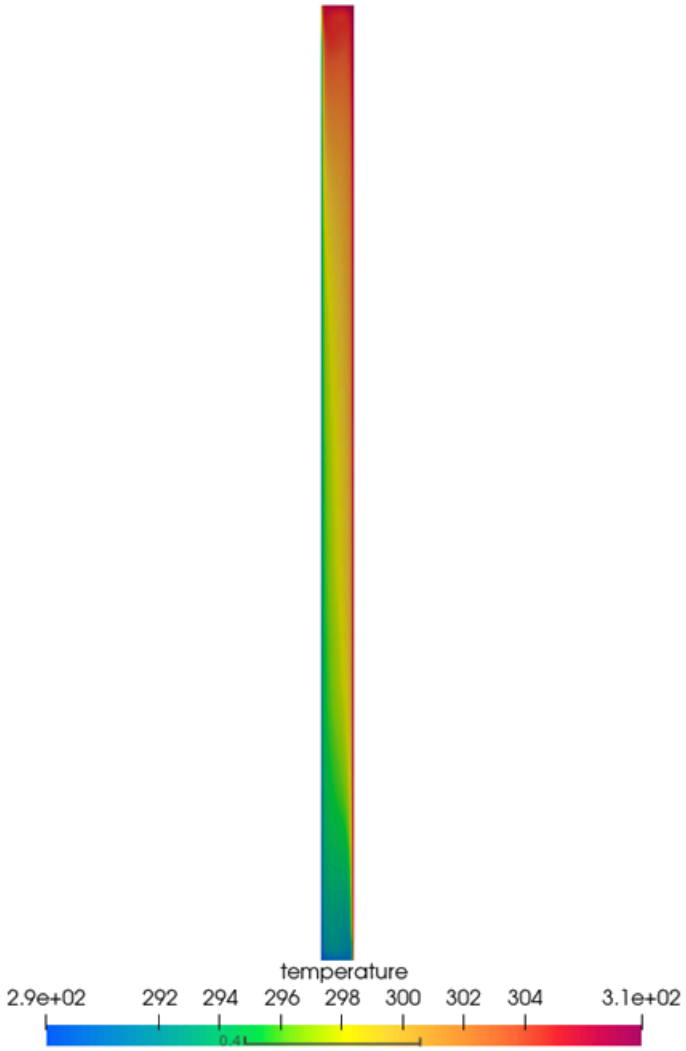


Figure 279: Temperature Contours Throughout Tall Cavity in the X-Y Plane

The AcuSolve results of the temperature and vertical velocity within the cavity are compared to the corresponding experimental values in the plots shown below. The temperature of the air is lowest near the cold vertical wall, remains relatively steady in the middle of the cavity, and then peaks near the hot vertical wall. Following a similar trend, the AcuSolve results show that the velocity is lowest near the cold vertical wall, due to the air sinking, and then steadily increases as the air begins to rise near the hot vertical wall. The velocity at the walls is zero due to the no-slip boundary condition. Additional comparisons are made to evaluate the performance of four turbulence models, Spalart-Allmaras (SA), shear stress transport (SST), K-Omega and K-ε.

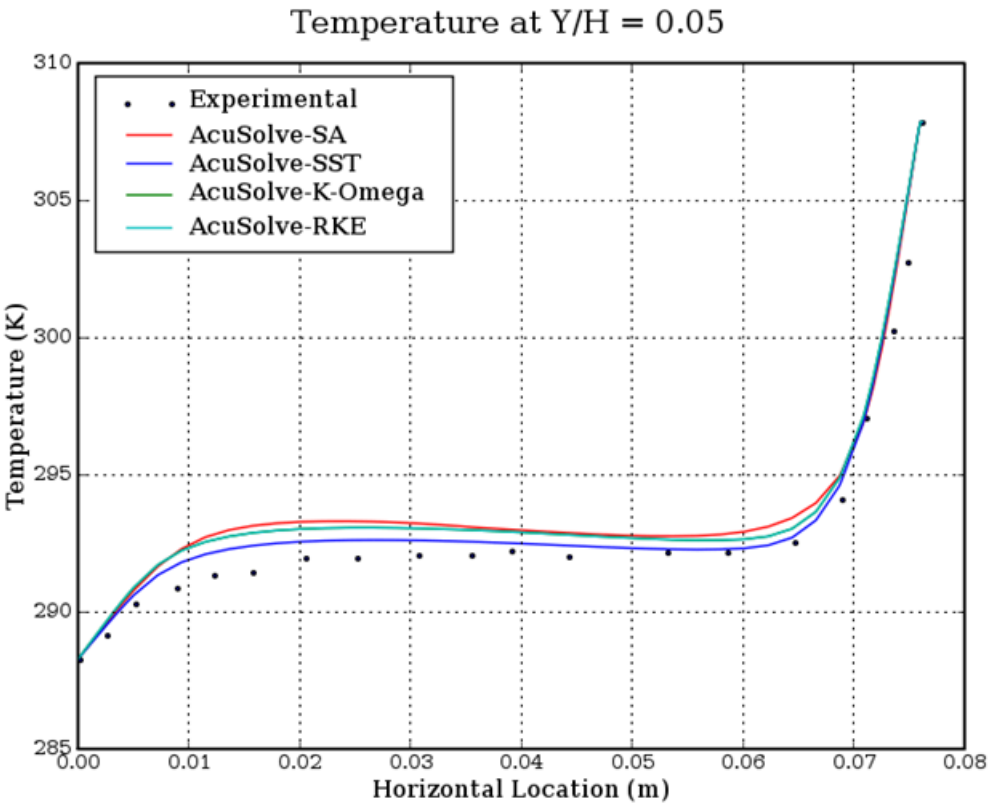


Figure 280: Temperature Plotted against Location along Horizontal at a Position of y/H=0.05 in the Cavity, where H is the Cavity Height and y is the Distance from the Bottom Wall

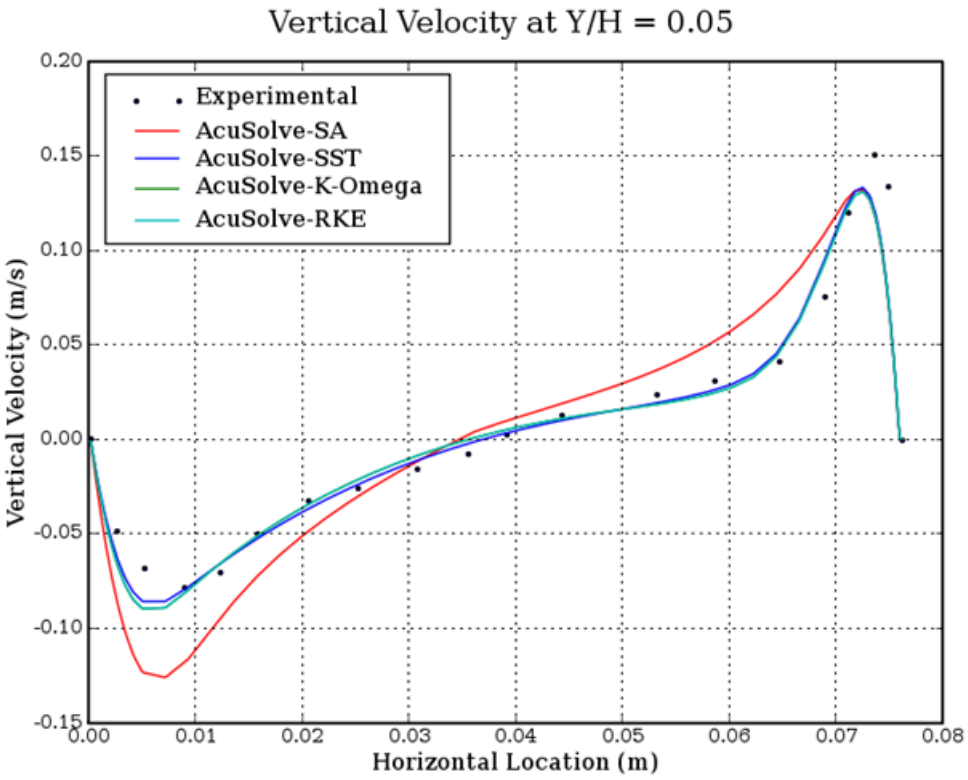


Figure 281: Vertical Velocity Plotted against Location along Horizontal at a Position of y/H=0.05 in the Cavity, where H is the Cavity Height and y is the Distance from the Bottom Wall

Summary

In this application, turbulent flow developed by natural convection, at a Rayleigh number of 8.6X105, is studied within a tall cavity. The AcuSolve results compare well with the experimental data for temperature and vertical velocity along a horizontal line at a location of y/H=0.05 in the tall cavity, with the two-equation models capturing the velocity gradient with greater accuracy. A temperature difference occurs within the flow region due to the heat transfer from the vertical walls of the cavity. The hotter, less-dense air rises to the top of the cavity while the colder, denser air sinks to the bottom, giving rise to recirculation. AcuSolve demonstrates the ability to accurately predict the natural convection of turbulent flow within a tall cavity.

Simulation Settings for Turbulent Natural Convection Inside a Tall Cavity

HyperMesh CFD database file: `<your working directory\cavity_turbulent_heat \cavity_turbulent_heat.hm`

Global

- Problem Description
  - Analysis type - Steady State
  - Turbulence equation - SST
- Auto Solution Strategy
  - Relaxation factor - `0.5`

- Convergence tolerance - `0.005`

- Material Model
  - Air
    - Type - Boussinesq
    - Density - `1.225` kg/m3
    - Specific Heat - `1005` J/kg-K
    - Viscosity - `1.781e-5` kg/m-sec

  Model
- Volumes
  - Volume
    - Element Set
      1. Material model - Air
- Surfaces
  - Back
    - Simple Boundary Condition
      1. Type - Symmetry
  - Bottom
    - **Simple Boundary Condition**
      1. Type - Wall
      2. Temperature BC type - Flux
      3. Heat Flux - `0.0` W/m2
  - Cold
    - **Simple Boundary Condition**
      1. Type - Wall
      2. Temperature BC type - Value
      3. Temperature - `288.25` K
  - Front
    - Simple Boundary Condition
      1. Type - Symmetry
  - Hot
    - Simple Boundary Condition
      1. Type - Wall
      2. Temperature BC type - Value
      3. Temperature - `307.85` K
  - Top
    - Simple Boundary Condition
      1. Type - Wall

2 Temperature BC type - Flux

3 Heat Flux - `0.0` W/m2

References

P.L. Betts and I.H. Bokhari. "Experiments on Turbulent Natural Convection in an Enclosed Tall Cavity". International Journal of Heat and Fluid Flow 21:675-683. 2000.

Turbulent Flow with Separation in an Asymmetric Diffuser

In this application, AcuSolve is used to simulate fully developed turbulent flow through an asymmetric diffuser with a divergent lower wall and a straight upper wall. AcuSolve results are compared with experimental results as described in Buice and Eaton (2000). The close agreement of AcuSolve results with experimental results validates the ability of AcuSolve to model cases with internal turbulent flow with flow separation and reattachment in an asymmetric diffuser.

Problem Description

The problem consists of air flowing through an asymmetric diffuser with a divergent lower wall and a straight upper wall, as shown in the following image, which is not drawn to scale. The diffuser inlet has a height of 1.5 cm (H) and extends 9 cm (6H) to the divergent section. The lower wall of the diffuser diverges at an angle of 10° and expands to 7.05 cm (4.7H). The divergent section has a horizontal length of 31.5 cm (21H). The expanded section of the diffuser extends 84 cm (56H) to the outlet. Air, with a density of 1.225 kg/m^3 and a viscosity of 1.8325 X 10^{-5} kg/m-s enters the diffuser through the inlet of the diffuser with a fully developed turbulent profile at a Reynolds's number of 20,000. The simulation was conducted with the Reynolds Averaged Navier-Stokes equations using four turbulence models, Spalart Allmaras, Shear Stress Transport (SST), K-ω and Realizable K-ε.

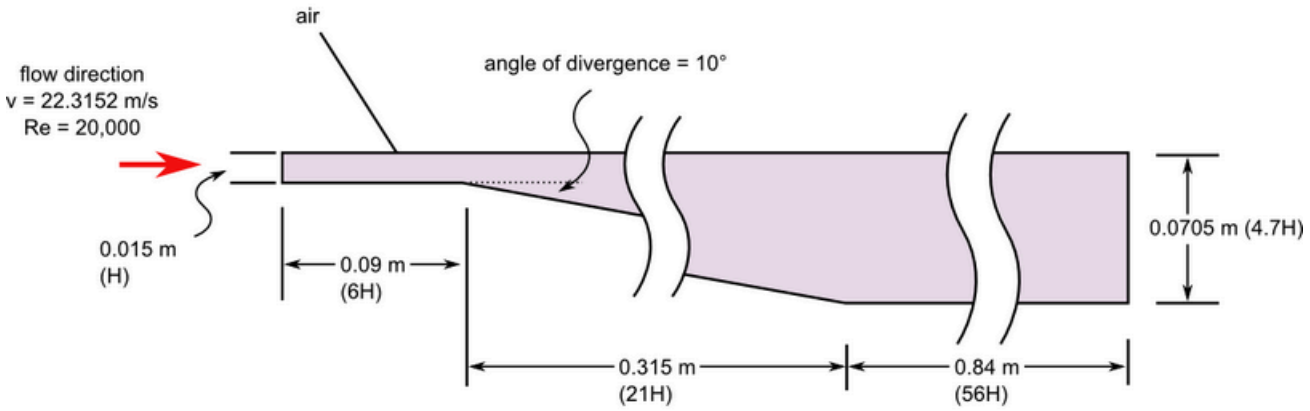


Figure 282: Critical Dimensions and Parameters for Simulating Turbulent Flow with Separation in an Asymmetric Diffuser

The simulation was performed as a two dimensional problem by constructing a volume mesh that contains a single layer of elements extruded in the cross stream direction (perpendicular to the flow plane) and by imposing symmetry boundary conditions on the extruded planes.



Figure 283: Mesh Details Near the Inlet and Divergent Section of Diffuser

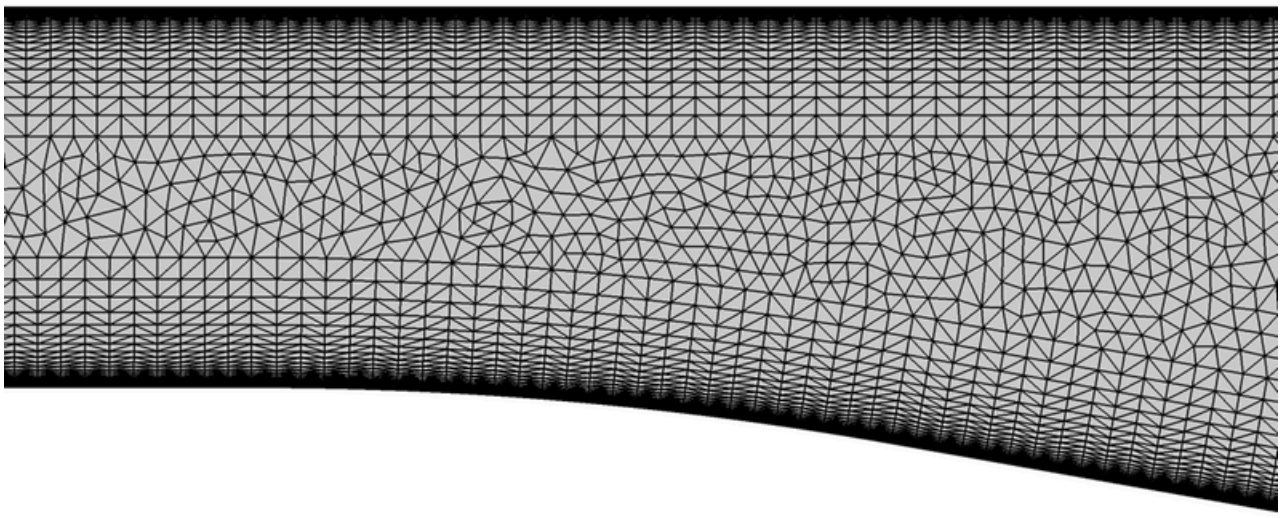


Figure 284: Mesh Details at the Beginning of the Divergence of the Lower Wall in the Diffuser

AcuSolve Results

The AcuSolve solution converged to a steady state and the results reflect the mean flow conditions. As the fully developed turbulent flow enters the divergent section, the peak velocity is maintained until the expansion of the cross-sectional height, forms an adverse pressure gradient. After the flow enters the divergent section, the velocity decreases significantly, due to the expansion of the cross-section height. This causes separation of the flow along the divergent wall and results in an area of recirculation.
The bulk of the flow above the divergent wall maintains its streamwise direction, while a portion of it reverses direction before reattaching further downstream of the divergent section. The following images show the steady state flow solution for flow within the diffuser.

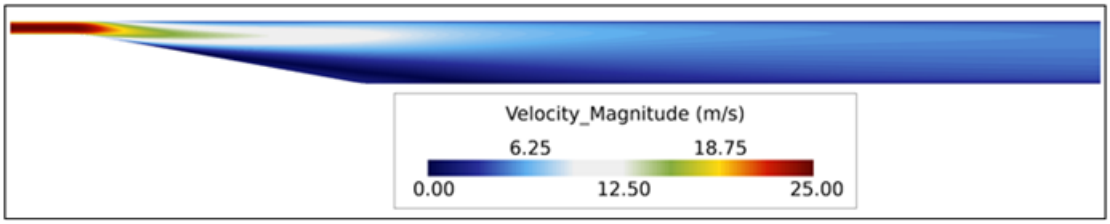


Figure 285: Velocity Contours Within the Diffuser

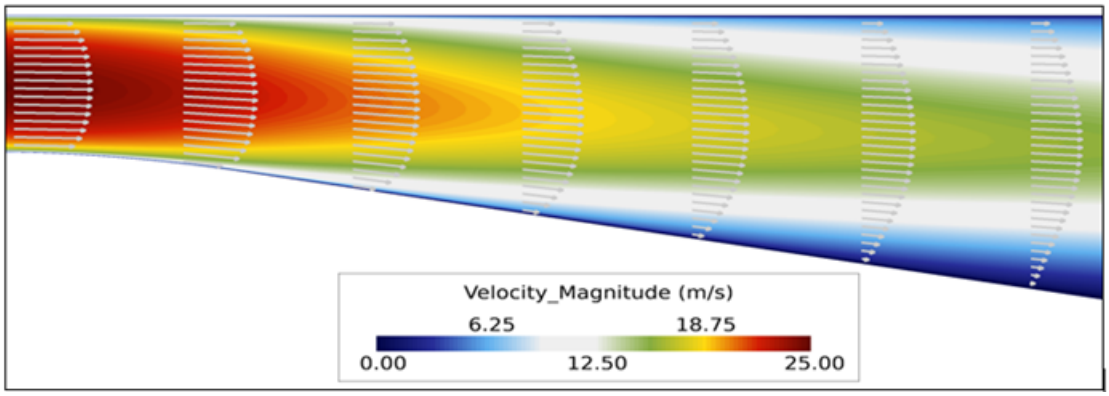


Figure 286: Close up View of Velocity Vectors and Contours of Velocity Magnitude in the Diffuser

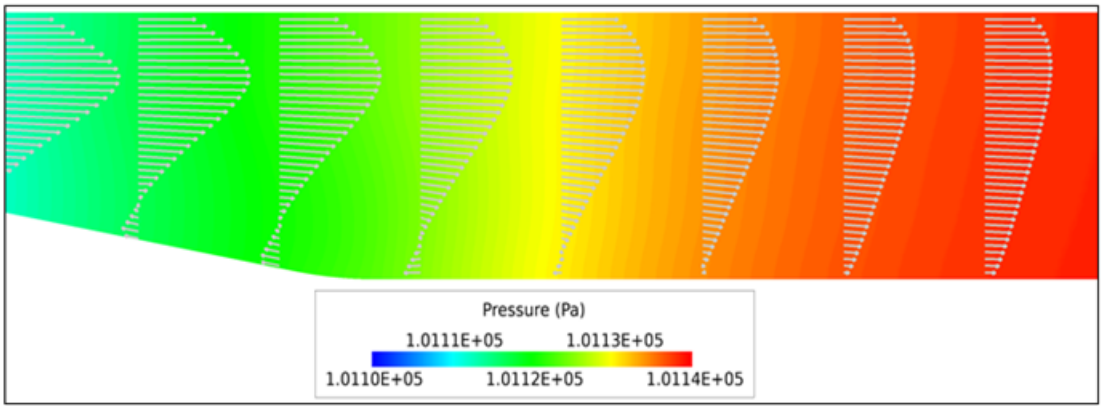


Figure 287: Close up View of Velocity Vectors and Contours of Pressure to Show Recirculation as it Approaches the Reattachment Point

Upstream of the diffuser section, the streamline velocity increases as the distance from the lower wall increases until it reaches the maximum velocity at the center of the channel. As the flow enters the divergent section of the channel, the streamwise velocity decreases near the bottom wall. The images below show the velocity profiles at three locations as measured from the midpoint of the curve where the bottom wall begins to diverge (X=0.0) for each of the tested turbulence models. The first location, where X/H = -5.944, is close to the inlet. The second location, where X/H = 13.468, is approximately 0.2 m downstream of the divergent section (~ 0.1 m from the fully expanded section). The third location, where X/H = 24.066, is approximately 0.16 m downstream of the point where the diffuser has reached the maximum height. In these plots the black circles represent the experimental measurements (Buice and Eaton 2000), the solid red lines for the prediction for the Spalart Allmaras model, solid blue lines for the prediction for the SST model, solid green lines for the prediction for the K-ω model and solid cyan lines for the K-ε model, representing the AcuSolve results. The non-dimensional height is represented by the fraction of the vertical height (Y) divided by the inlet height (H) and the velocity is normalized by the inlet velocity (Uref).

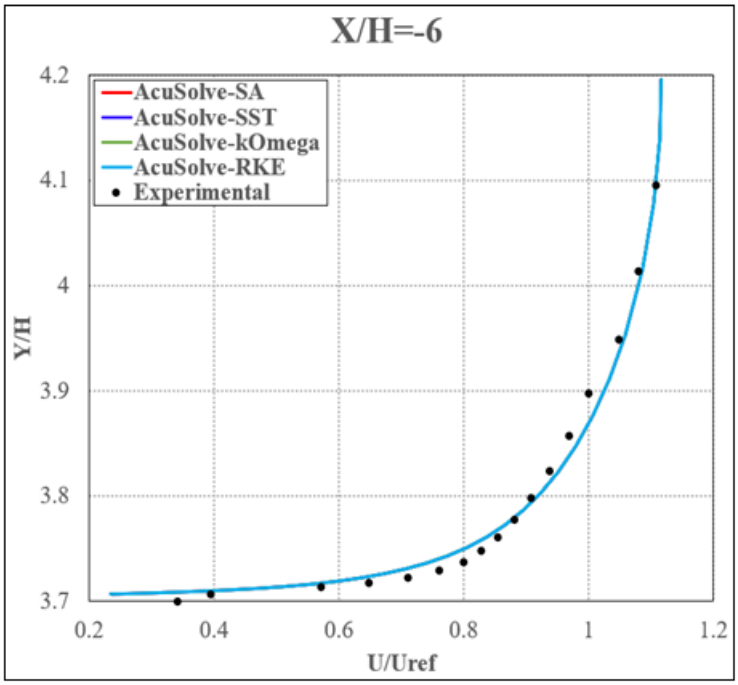


Figure 288: Non-Dimensional Streamwise Velocity Plotted Against Vertical Location Near the Inlet (X/H=-5.9442, Where the Reference Point is 6H Downstream of the Inlet)

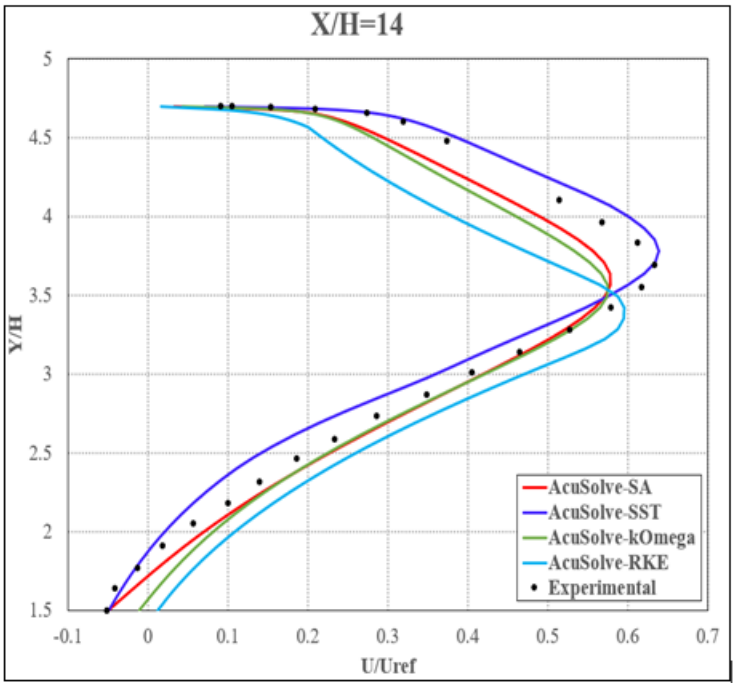


Figure 289: Non-Dimensional Streamwise Velocity Plotted Against Vertical Location Approximately 0.2 m Downstream of the Divergence (X/H = 13.468, Where the Reference Point is 6H Downstream of the Inlet)

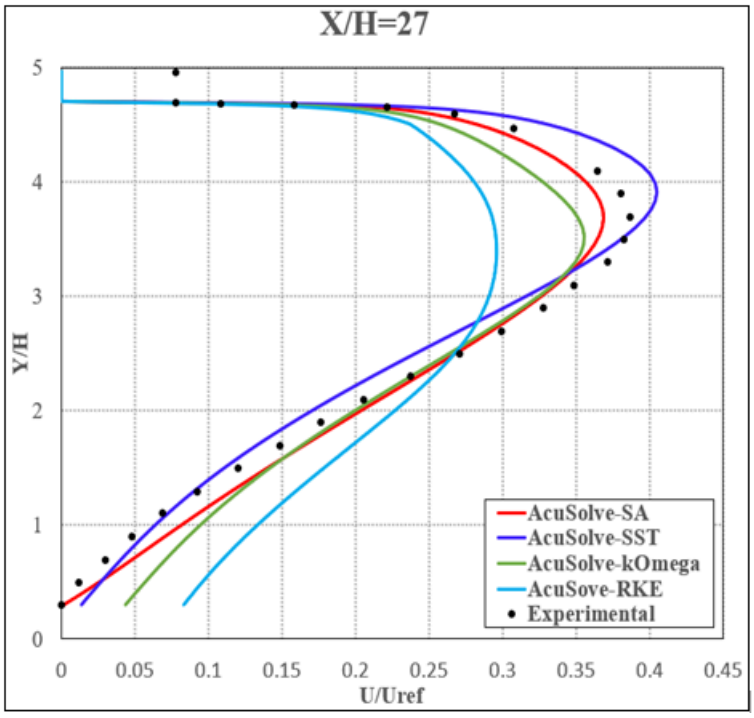


Figure 290: Non-Dimensional Streamwise Velocity Plotted Against Vertical Location Approximately 0.2 m Downstream of the Transition to the Fully Divergent Section (X/H = 27.066, Where the Reference Point is 6H Downstream of the Inlet)

The non-dimensional pressure coefficient (Cp) all along the inlet-bottom stretch of the diffuser is calculated using the reference pressure at X=-3H (at the bottom wall) and with reference velocity (Uref) at the inlet with the value of 22.3152 (m/s). The predicted non-dimensional pressure coefficients are compared to experimental results. The figure below shows Cp, along a constant vertical height, as a function of the streamwise distance from the inlet of the channel. The results demonstrate that AcuSolve is capable of accurately predicting the pressure within the diffuser within the expected range based on the type of turbulence model used. The performance of the three turbulence models were found to be consistent with previously published results for flow through the diffuser as published by Buice and Eaton (2000), with the SST model predicting the pressure distribution most accurately.

Note: The inlet of the experimental duct was 6H longer than that modeled - AcuSolve values where X/H < -6 are reported as the inlet value.

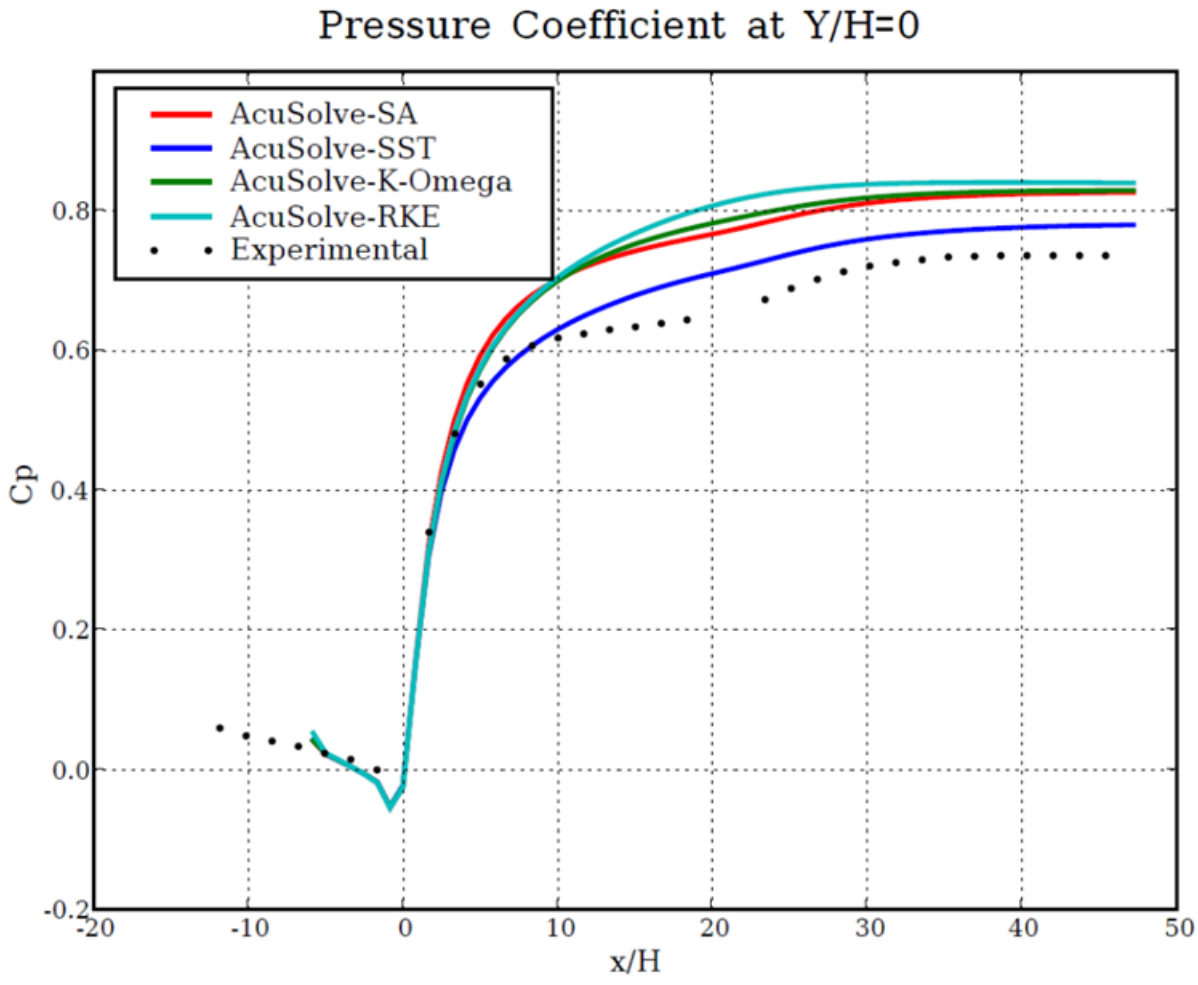


Figure 291: Non-Dimensional Pressure Coefficient (Cp) Plotted Against Relative Distance Along the Diffuser at a Constant Height Equal to the Bottom of the Inlet

Summary

In this application, a fully developed turbulent flow at a Reynolds number of 20,000 is studied. Due to the adverse pressure gradient, separation of flow occurs and causes recirculation in the divergent

section of the diffuser. The results were found to be consistent with previously published computational studies and experimental data. The results of this validation demonstrate the ability of AcuSolve to accurately predict the separation point, the recirculation that occurs along the divergent wall, and the reattachment point in the straight section of the diffuser.

Simulation Settings for Turbulent Flow with Separation in an Asymmetric Diffuser

HyperMesh CFD database file: `<your working directory>\asymmetric_diffuser_turbulent\asymmetric_diffuser_turbulent.hm`

Global

- Problem Description
  - Analysis type - Steady State
  - Turbulence equation - Spalart Allmaras
- Auto Solution Strategy
  - Max time steps - `150`
  - Relaxation Factor - `0.4`
- Material Model
  - Air
    - Density - `1.225.0` kg/m3
    - Viscosity - `1.8325e-5` kg/m-sec

  Model
- Volume
  - Volume
    - Element Set
      1. Material model - Air
- Surfaces
  - Bottom
    - Simple Boundary Condition
      1. Type - Wall
  - Inlet
    - Simple Boundary Condition (disabled to allow for nodal boundary conditions to be set)
    - Advanced Options
      1. Nodal Boundary Conditions
         1. X-Velocity
            1. Type - Linear
            2. Precedence - `2`
            3. Curve fit variable - Y coordinate
            4. Curve fit values (included in database)
         2. Y-Velocity

1 Type - Linear
2 Precedence - 2
3 Curve fit variable - Y coordinate
4 Curve fit values (included in database)

3 Eddy Viscosity
1 Type - Linear
2 Precedence - 2
3 Curve fit variable - Y coordinate
4 Curve fit values (included in database)

- Outlet
  - Simple Boundary Condition
    1 Type - Outflow - 101139.0 Pa
- Side 1
  - Simple Boundary Condition
    1 Type - Symmetry
- Side 2
  - Simple Boundary Condition
    1 Type - Symmetry
- Top
  - Simple Boundary Condition
    1 Type - Wall

References

C.U. Buice, and J.K., Eaton. "Experimental Investigation of Flow Through an Asymmetric Plane Diffuser". Journal of Fluids Engineering 122:433-435. June 2000.

S. Obi, K. Aoki and S. Masuda. "Experimental and Computational Study of Turbulent Separating Flow in an Asymmetric Plane Diffuser". Ninth Symposium on Turbulent Shear Flows. p. 305. Kyoto, Japan. August 16-19, 1993.

Turbulent Flow Over a Backward-Facing Step

In this application, AcuSolve is used to simulate fully developed turbulent flow over a backward-facing step. AcuSolve results are compared with experimental results as described in Driver (1985) and on the NASA Langley Research Center Turbulence Modeling Resource web page. The close agreement of AcuSolve results with experimental data and reference turbulence model performance validates the ability of AcuSolve to model cases with turbulent flow that forms a shear layer, recirculates and then reattaches downstream of the divergent step.

Problem Description

The problem consists of a fluid with material properties close to air flowing through a channel containing a sharp expansion, as shown in the following image, which is not drawn to scale. The step causes the flow to recirculate before reattaching downstream of the step. The inlet height of the channel is 8.0 m and expands as a step function to 9.0 m at a distance 20.0 m downstream of the inlet. This expanded section of the channel extends 50 m downstream of the step. The inflow of the channel is defined as fully developed at a Reynolds number (Re) of 36,000, based on the step height to match the experimental conditions. The density of the flow medium is 1.1837 kg/m^3 and the dynamic viscosity is 1.457 X 10^{-3} kg/m-s. The simulation was conducted with the Reynolds Averaged Navier-Stokes equations using four turbulence models, Spalart Allmaras, Shear Stress Transport (SST), K-ω and K-ε.

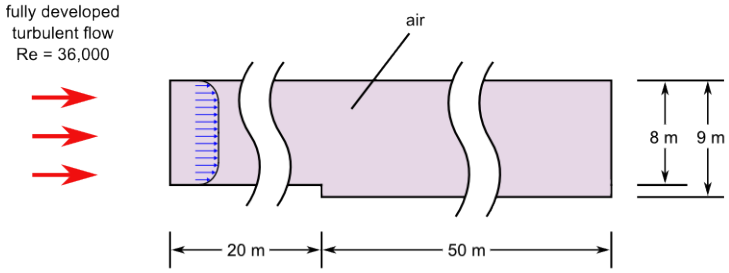


Figure 292: Critical Dimensions and Parameters for Simulating Turbulent Flow Through a Channel with a Backward-Facing Step

The simulation was performed as a two-dimensional problem by constructing a volume mesh that contains a single layer of elements extruded in the cross-stream direction, normal to the flow plane and by imposing symmetry boundary conditions on the extruded planes. The upper and lower walls are specified as no-slip, the inlet velocity and eddy viscosity are specified to match the conditions in the experiment (Driver 1985) at a distance of 20 m upstream of the step.

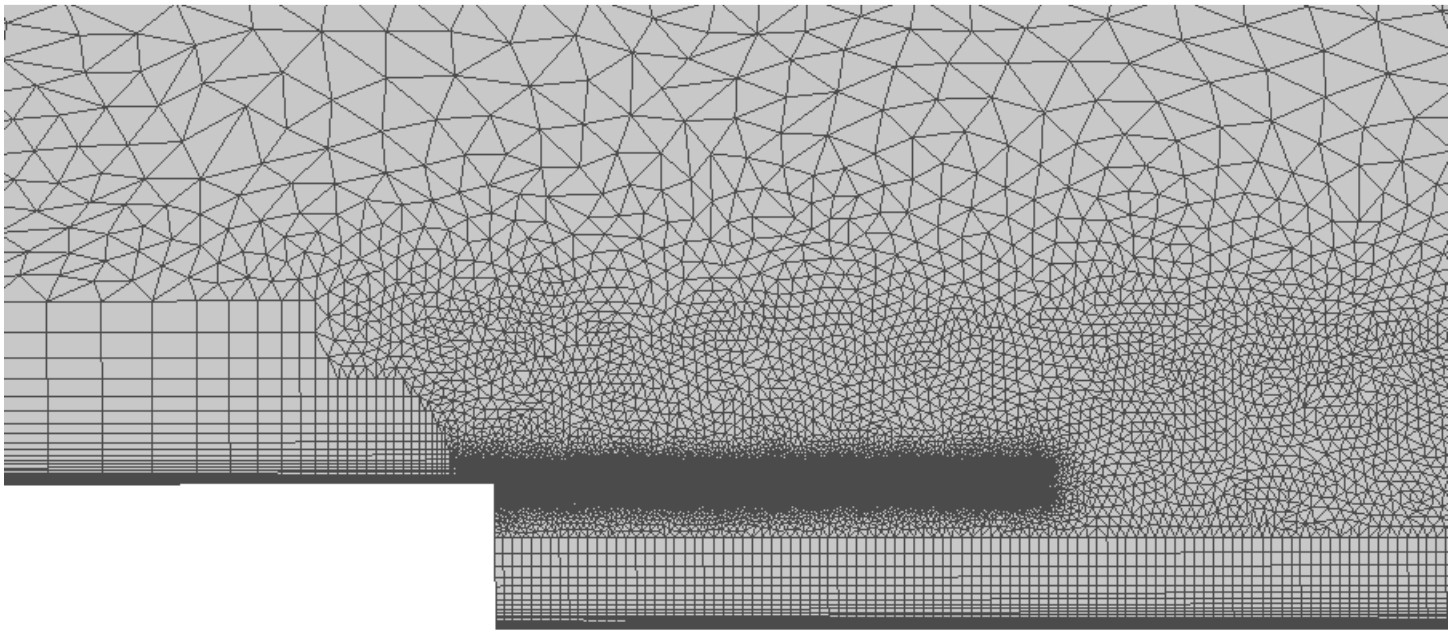


Figure 293: Detail of Mesh Near the Backward-Facing Step

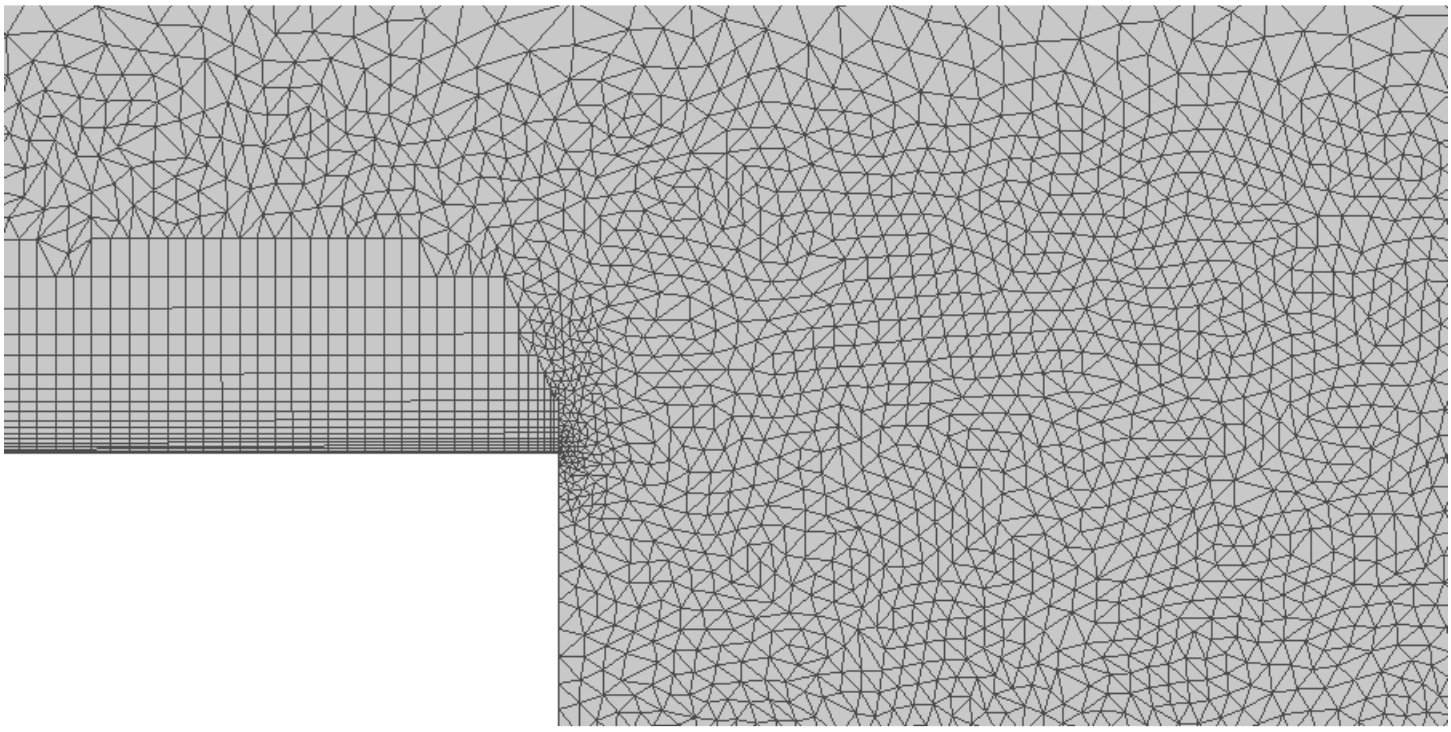


Figure 294: Finer Detail of Mesh Near the Backward-Facing Step

AcuSolve Results

The AcuSolve solution converged to a steady state and the results reflect the mean flow conditions. As the fully developed turbulent flow enters the divergent section, the expansion of the cross-sectional height causes a shear layer to develop above the lower wall. The expansion causes two recirculation zones; one immediately near the step wall and one that extends further downstream near the lower wall. The recirculation region eventually recovers downstream and the flow reattaches. The following images show the flow solution within the channel, demonstrating the recirculation region and reattachment point.

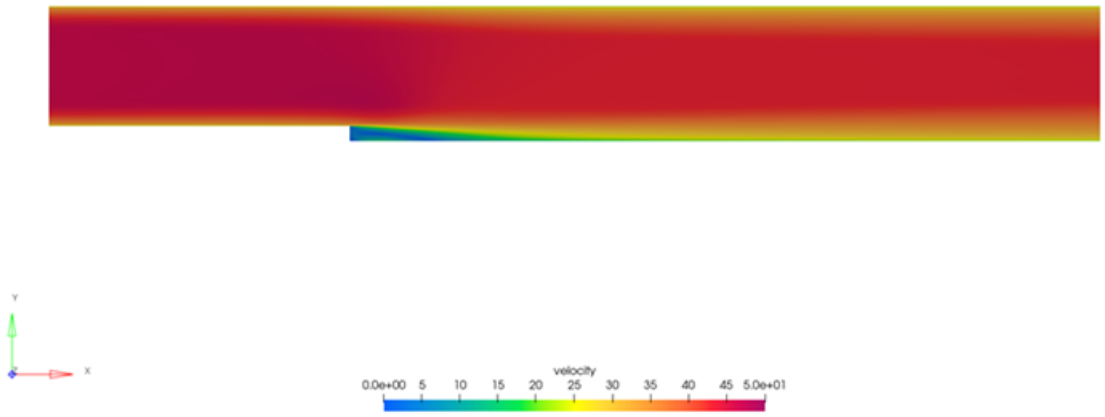


Figure 295: Velocity Contours Showing Low Velocity Near the Step Wall

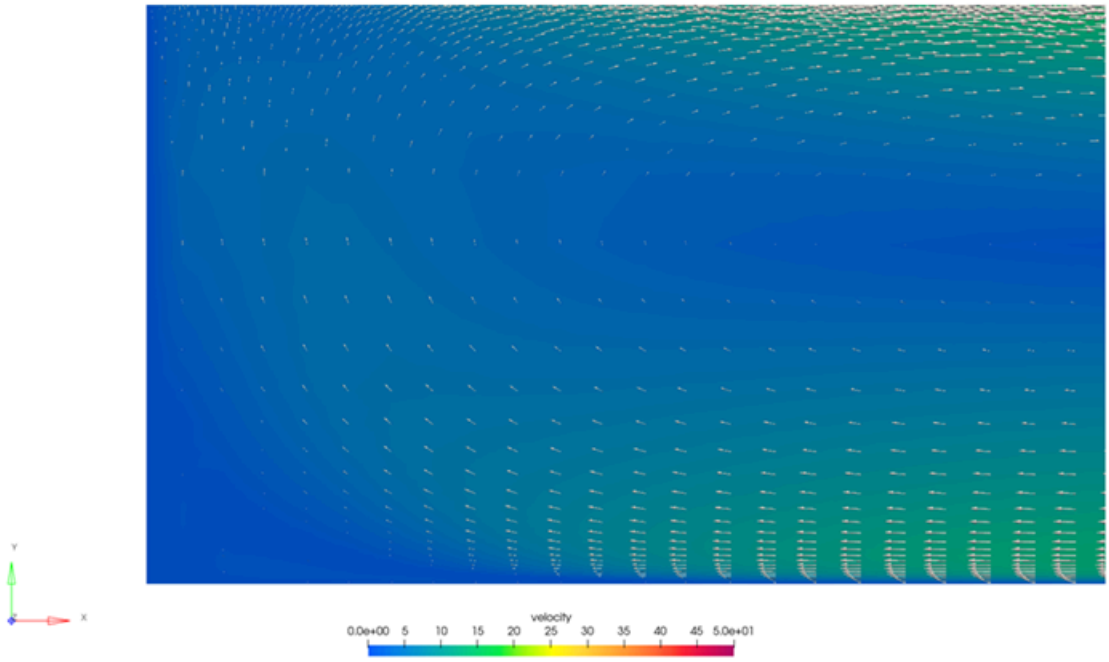


Figure 296: Close-Up View of Velocity Vectors and Contours in the Cross-Stream Plane Directly After the Step

Upstream of the expansion section, the streamwise velocity increases as the distance from the lower wall increases until it reaches the centerline of the channel and then begins decreasing until it reaches zero at the top wall. As the flow passes the step, it expands into the region directly downstream of the step wall, separating from the wall and recirculating until it recovers further downstream. The image below shows the coefficient of pressure along the lower wall of the step compared against experimental results. The coefficient of pressure is calculated using the reference velocity (Uref) obtained at x/H=-4 (centre of the channel) with the reference pressure (Pref) extracted at x/H = 40 (at the wall) so that Cp becomes 0 at x/H=40. The image shows black circles representing the experimental measurements (Driver 1985), a solid red line for the SA model, a solid blue line for the SST model, a solid green line for the K-ω model and a solid cyan line for the K-ε model, representing the AcuSolve results. The resulting pressure coefficient within the channel demonstrates minor differences between the three

turbulence models. The SA model predicts a slightly larger recirculation region and does not reach the peak pressure in the wake of the step, compared to the SST model.

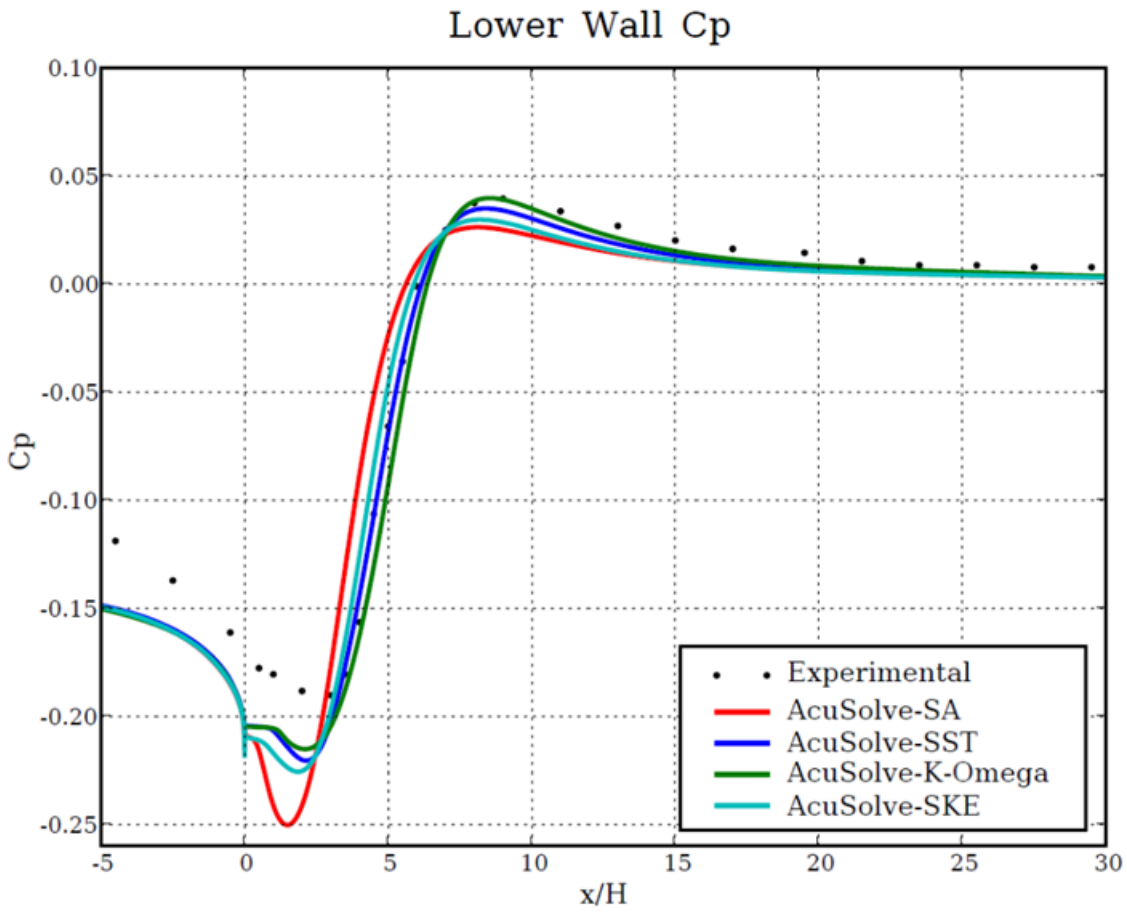


Figure 297: Coefficient of Pressure Plotted Against Location Along the Lower Wall Before and After the Step

Summary

In this application, a fully developed turbulent flow at a Reynolds number of 36,000 is studied and compared against experimental data. The AcuSolve results compare well with the experimental data for pressure coefficient. The performance of the Spalart Allmaras turbulence model was found to be consistent with previously published results for flow over a backward facing step (NASA 2015). The K-ω model appears to perform the best out of the three, predicting the reattachment and pressure distribution most accurately. AcuSolve demonstrates the ability to predict the shear layer in this type of application, the recirculation that occurs downstream of the step, as well as the reattachment point within the channel.

Simulation Settings for Turbulent Flow over a Backward-Facing Step

HyperMesh CFD database file: `<your working directory>\backstep_turbulent\backstep_turbulent.hm`

Global

- Problem Description
  - Analysis type - Steady State

- Turbulence equation - Shear Stress Transport
- Auto Solution Strategy
  - Max time steps - `100`
  - Relaxation Factor - `0.5`
- Material Model
  - Air
    - Density - `1.183` kg/m3
    - Viscosity - `1.4575e-3` kg/m-sec

  Model
- Volume
  - Fluid
    - Element Set
      1. Material model - Air
- Surfaces
  - +Z
    - Simple Boundary Condition
      1. Type - Slip
  - -Z
    - Simple Boundary Condition
      1. Type - Slip
  - Inlet
    - Simple Boundary Condition - (disabled to allow for nodal boundary conditions to be set)
    - Advanced Options
      1. Nodal Boundary Conditions
         1. X-Velocity
            1. Type - Linear
            2. Precedence - Always
            3. Curve fit variable - Y reference coordinate
            4. Curve fit values - (included in database)
         2. Y-Velocity
            1. Type - Linear
            2. Precedence - Always
            3. Curve fit variable - Y reference coordinate
            4. Curve fit values - (included in database)
         3. Z-Velocity
            1. Type - Zero
         4. Kinetic Energy

1. Type - Linear
2. Precedence - Always
3. Curve fit variable - Y reference coordinate
4. Curve fit values - (included in database)

5. Eddy Frequency
    1. Type - Linear
    2. Precedence - Always
    3. Curve fit variable - Y reference coordinate
    4. Curve fit values - (included in database)

- Outlet
    - Simple Boundary Condition
        1. Type - Outflow
- Wall - Lower - Downstream
    - Simple Boundary Condition
        1. Type - Wall
        2. Turbulence wall type - Low Reynolds Number
- Wall - Lower - Upstream
    - Simple Boundary Condition
        1. Type - Wall
        2. Turbulence wall type - Low Reynolds Number
- Wall - Step
    - Simple Boundary Condition
        1. Type - Wall
        2. Turbulence wall type - Wall Function
- Wall - Upper
    - Simple Boundary Condition
        1. Type - Wall
        2. Turbulence wall type - Low Reynolds Number

References

D. M. Driver and H. L. Seegmiller. "Features of Reattaching Turbulent Shear Layer in Divergent Channel Flow". AIAA Journal, 23(2): 163-171. Feb 1985.

NASA Langley Research Center Turbulence Modeling Resource webpage. http://turbmodels.larc.nasa.gov/backstep_val.html. Accessed June 2021.

Turbulent Flow Past a Convex Curve in a Channel

In this application, AcuSolve is used to simulate fully developed turbulent flow through a channel containing a convex curve in the lower wall. AcuSolve results are compared with experimental results as described in Smits (1979) and on the NASA Langley Research Center Turbulence Modeling Resource webpage. The close agreement of AcuSolve results with experimental data and reference turbulence model performance validates the ability of AcuSolve to model cases with turbulent flow moving past a convex curved wall.

Problem Description

The problem consists of a fluid with material properties close to air flowing through a channel containing a 30° swept wall, with a lower convex wall. The inlet channel height and remaining duct height is 0.127 m. The bulk velocity (v) normal to the inlet is 31.9 m/s and an integrated outflow pressure is specified to allow the flow to pass through the channel. The flow develops into fully turbulent flow at a Reynolds's number (Re) of 2,100,000. The density of the flow medium is 1.225 kg/m3 and the dynamic viscosity is 1.8608 X 10-5 kg/m-s. The simulation is conducted with the Reynolds Averaged Navier-Stokes equations using the Spalart Allmaras, Shear Stress Transport (SST), K-ω and Realizable K-ε turbulence models. The flow conditions are compared against experimental data and the current state-of-the-art performance for coefficient of pressure and coefficient of friction.

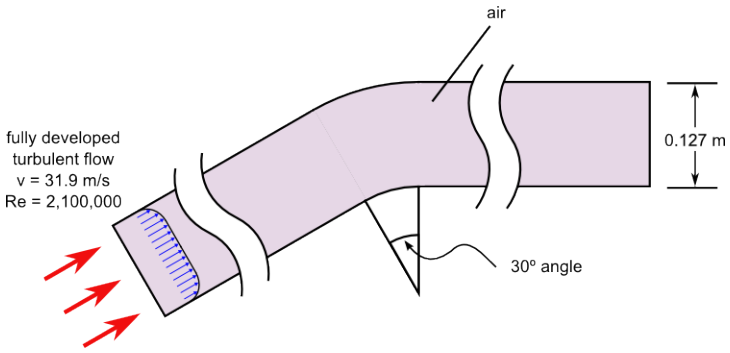


Figure 298: Critical Dimensions and Parameters for Simulating Turbulent Flow Through a Convex Channel

The simulation was performed as a two dimensional problem by restricting flow in the out-of-plane direction through the use of a mesh that is one element thick. The upper and lower walls are specified as no-slip, the inlet velocity and eddy viscosity are specified normal to the inlet face to match the experimental Reynolds Number.

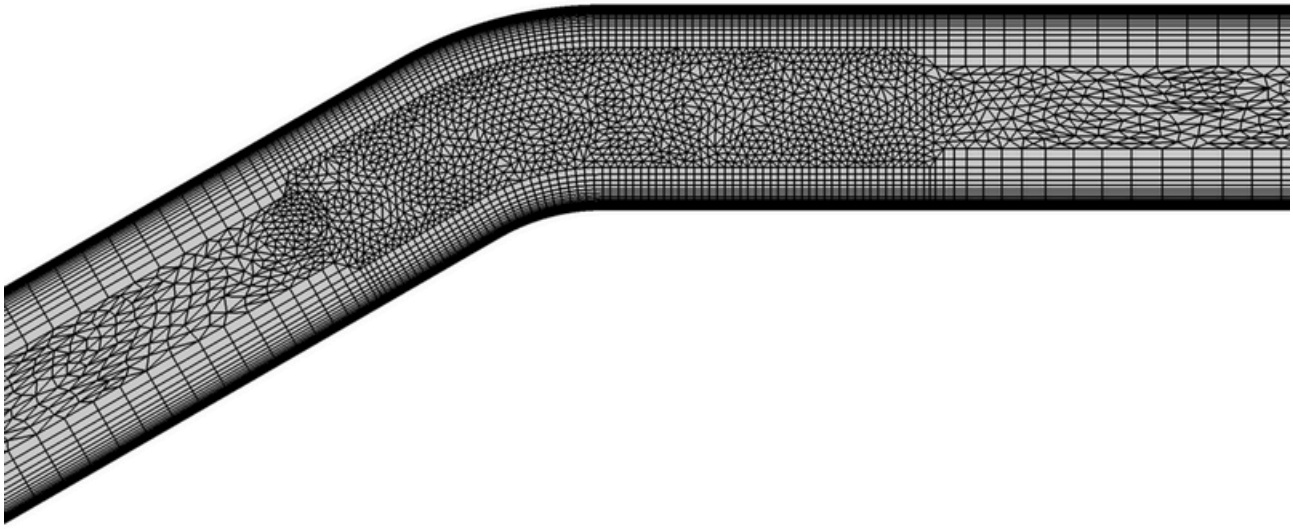


Figure 299: Detail of the Mesh used for Simulating Turbulent Flow Through a Convex Channel

AcuSolve Results

The AcuSolve solution converged to a steady state and the results reflect the mean flow conditions within the channel. As the fluid enters the channel it develops into fully turbulent flow exhibiting a steep parabolic velocity profile across the width of the channel. The flow begins to accelerate near the lower wall and decelerate near the top wall as it approaches the 30° bend. The results show that the upper (concave) wall destabilizes the boundary layer, increasing the eddy viscosity and forcing the flow velocity to decrease. The following figures show the flow conditions within the channel.

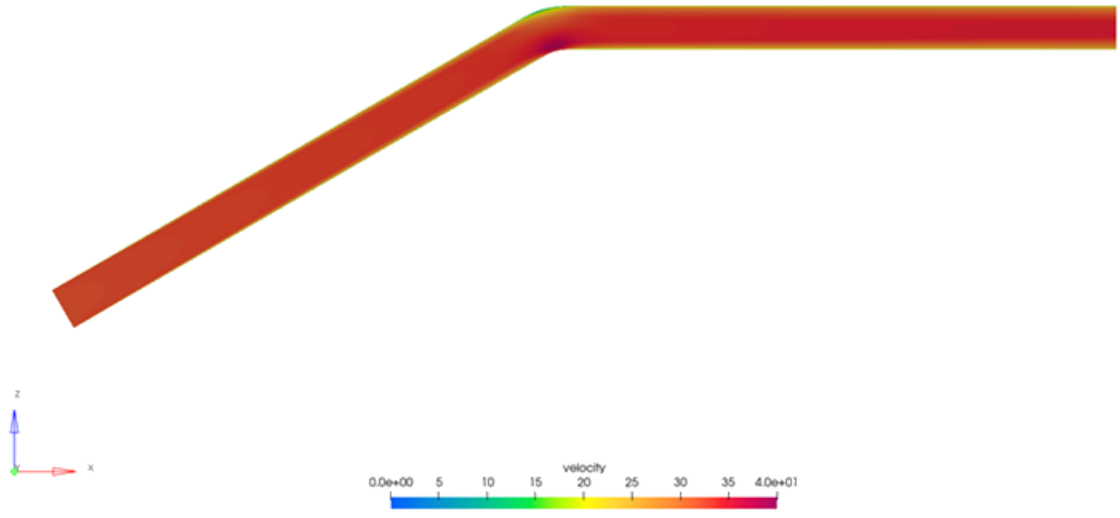


Figure 300: Velocity Contours in the Streamwise Plane

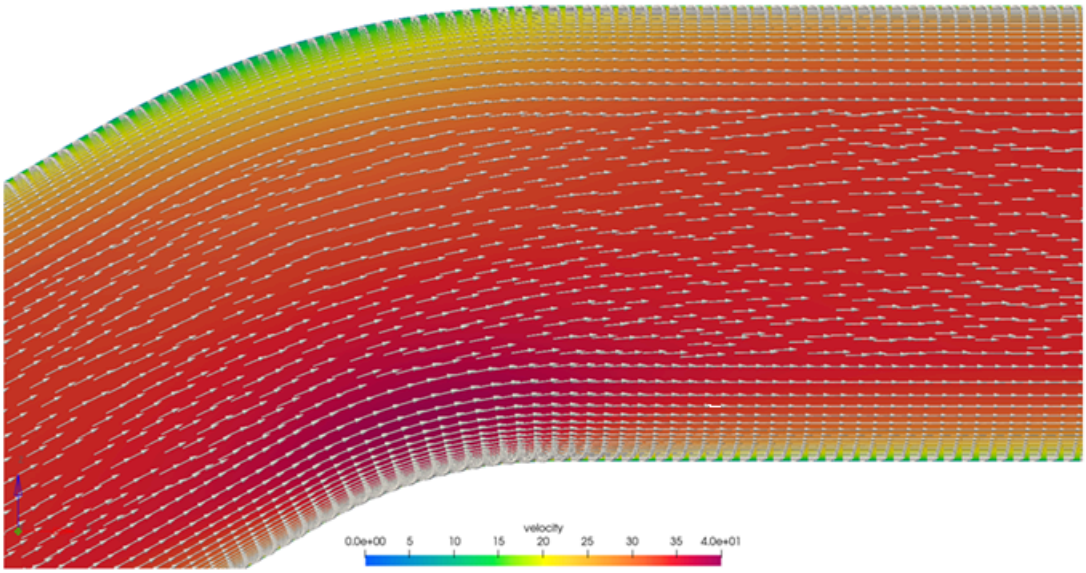


Figure 301: Close up View of Velocity Vectors and Velocity Contours at the 30° Bend

Upstream of the curved section of the channel, the flow normal to the channel opening increases as the distance from the lower wall increases until it reaches the centerline of the channel and then begins decreasing until it reaches zero at the top wall. As the flow approaches the curved section, it begins to accelerate, requiring that the flow velocity near the upper wall decrease to conserve momentum. The relatively low angle of curvature in the channel does not cause the accelerated fluid to recirculate. The images below show the coefficient of pressure (Cp) and coefficient of skin friction (Cf) along the lower wall of the channel. The images show black circles representing the experimental measurements (Smiths 1979), solid red lines for the SA model, solid blue lines for the SST model, solid green lines for the K-ω model and a solid cyan line for the K-ε model, representing the AcuSolve results. The coefficient of pressure within the channel is predicted nearly identically compared to the experiment for each of the turbulence models. It appears that the SST and K-ε models capture the low velocity region with the best accuracy, demonstrating that the flow velocity decreases significantly, but does not recirculate within the channel. This is shown in the friction coefficient plot, where the coefficient of friction, and subsequently the wall shear stress, does not decrease below zero.

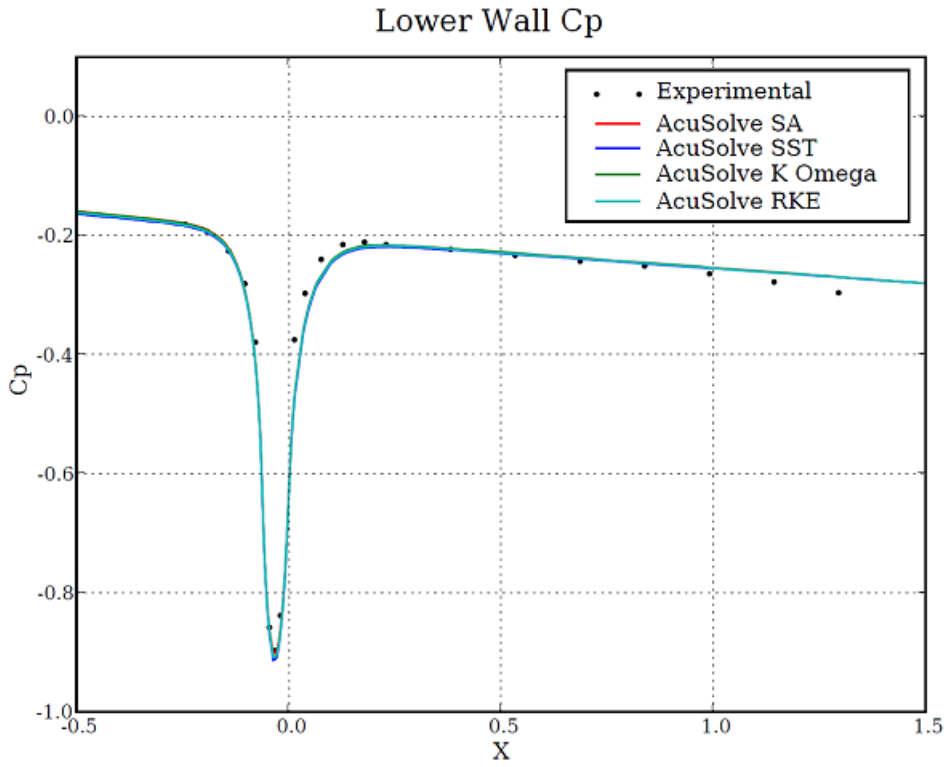


Figure 302: Coefficient of Pressure Plotted Against Relative Distance Along the Lower Wall from the Curve

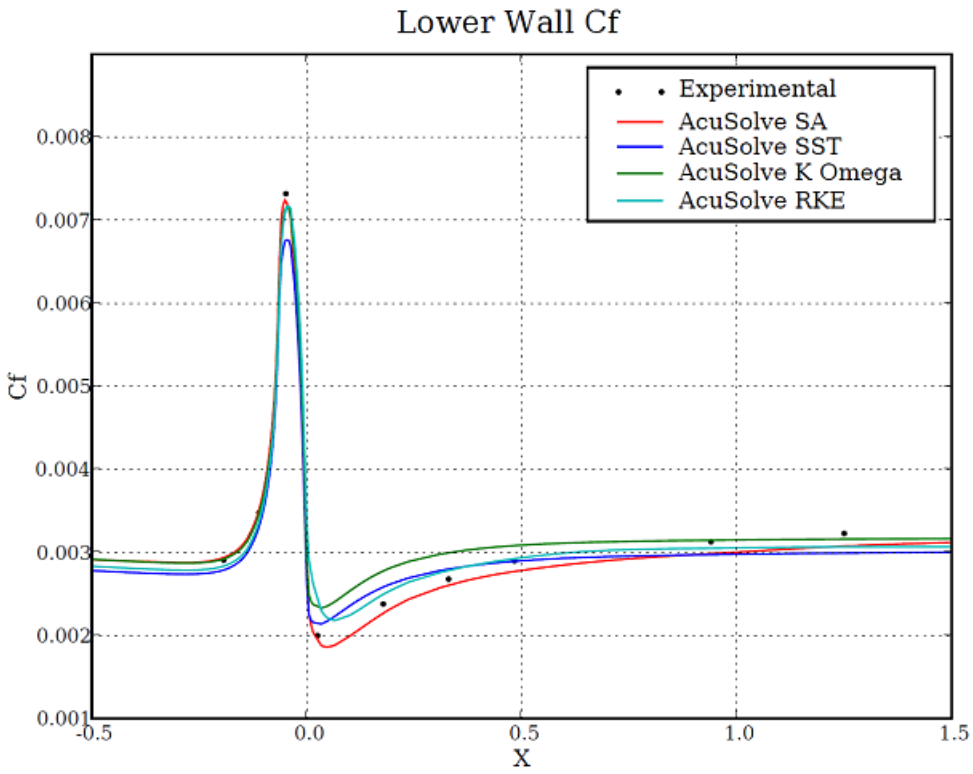


Figure 303: Skin Friction Coefficient Plotted Against Relative Distance Along the Lower Wall from the Curve

Summary

In this application, a turbulent flow through a curved channel at a Reynolds number of 2,100,000 is simulated and compared against experimental data. The AcuSolve results compare well with the experimental data for pressure coefficient and skin friction coefficient within the channel. The performance of the Spalart Allmaras turbulence model was found to be consistent with previously published results for flow through a convex-curved channel (NASA 2015) and the SST turbulence model appears to predict the shear stress on the lower wall most accurately. AcuSolve demonstrates the ability to predict the complex boundary layers resulting from the curvature of the channel and accurately predicts the propagation of the flow further downstream.

Simulation Settings for Turbulent Flow past a Convex Curve in a Channel

HyperMesh CFD database file: `<your working directory>\convex_curvature_turbulent \convex_curvature_turbulent.hm`

Global

- Problem Description
  - Analysis type - Steady State
  - Turbulence equation - Spalart Allmaras
- Auto Solution Strategy
  - Max time steps - `100`
  - Convergence tolerance - `0.0001`

    - Relaxation factor - `0.4`
- Material Model
    - Fluid
        - Density - `1.225` kg/m3
        - Viscosity - `1.8603e-5` kg/m-sec

  Model
- Volumes
    - Fluid - elbow
        - Element Set
            1. Material model - Fluid
    - Fluid - inlet
        - Element Set
            1. Material model - Fluid
    - Fluid - outlet
        - Element Set
            1. Material model - Fluid
- Surfaces
    - -Y
        - Simple Boundary Condition
            1. Type - Slip
    - +Y
        - 1. Type - Slip
    - Inlet
        - Simple Boundary Condition
            1. Type - Inflow
            2. Inflow type - Velocity
            3. Inflow velocity type - Normal
            4. Normal velocity - `31.9` m/sec
            5. Turbulence input type - Direct
            6. Eddy viscosity - `1.3671e-7` m2/sec
- Internal
    - Simple Boundary Condition - (disabled)
- Lower Wall
    - Simple Boundary Condition
        - Type - Wall
        - Turbulence wall type - Low Reynolds Number
- Outlet

    - Simple Boundary Condition
        - Type - Outflow
- Upper Wall
    - Simple Boundary Condition
        - Type - Wall
        - Turbulence wall type - Low Reynolds Number

References

A. J. Smits, S. T. B. Young, and P. Bradshaw. "The Effect of Short Regions of High Surface Curvature on Turbulent Boundary Layers". Journal of Fluid Mechanics. 94(2):209-242. 1979

NASA Langley Research Center Turbulence Modeling Resource webpage. http://turbmodels.larc.nasa.gov/smitscurve_val.html. Accessed May 2021.

Heat Transfer Between Radiating Concentric Cylinders

In this application, AcuSolve is used to simulate the heat transfer due to radiation between concentric cylinders. The inner and outer cylinders are held at constant temperature and are defined to be radiation surfaces. AcuSolve results are compared with analytical results for temperature as described in Incropera (2006). The close agreement of AcuSolve results with analytical results validates the ability of AcuSolve to model cases with radiation heat transfer requiring view factor computation.

Problem Description

The problem consists of a fluid with arbitrary material properties between two infinitely long concentric cylinders, as shown in the following image, which is not drawn to scale. The radius of the outer cylinder is 0.0468 m and the radius of the inner cylinder is 0.0178 m. The inner cylinder is defined to have a constant wall temperature at 773.0 K (500 °C). The outer cylinder is defined to have a constant wall temperature at 300.0 K (27 °C). Both cylinders are specified to radiate as grey bodies, with emissivity set to 0.03778.

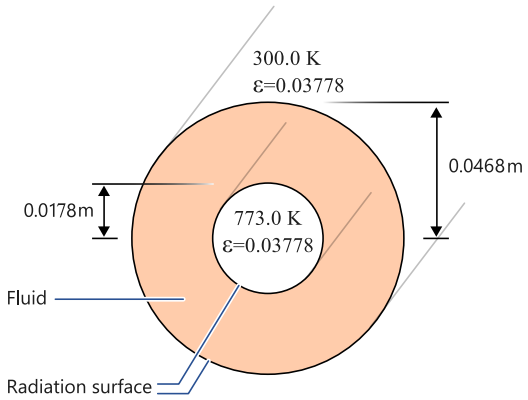


Figure 304: Critical Dimensions and Parameters Used for Simulating Radiation Between Two Concentric Cylinders

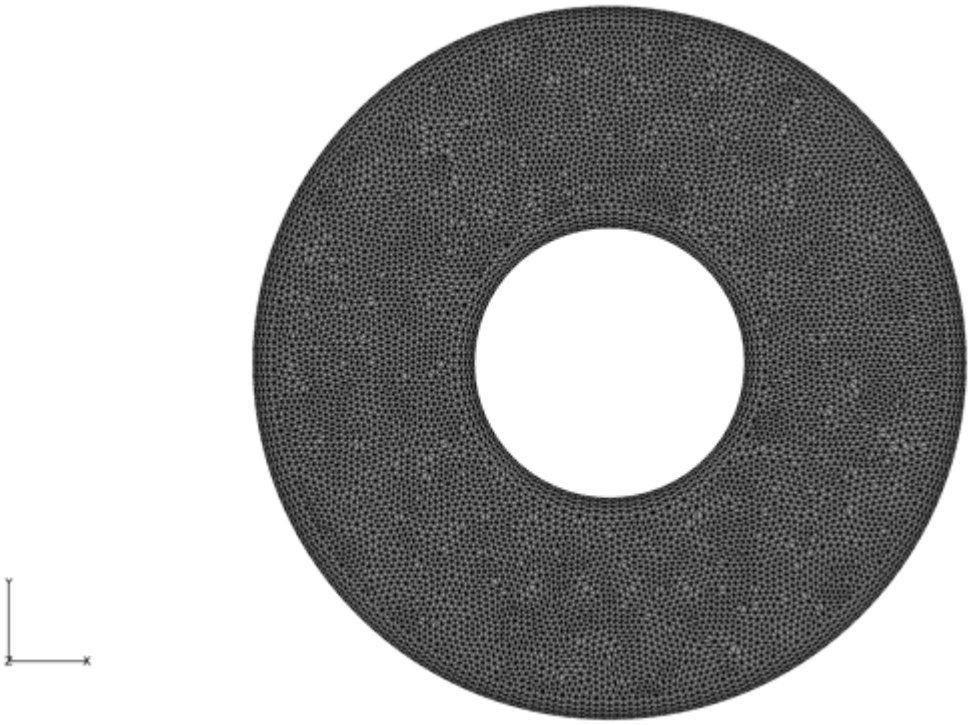


Figure 305: Mesh used for Simulating Radiation Between Two Concentric Cylinders

The simulation was performed as a two-dimensional problem by constructing a volume mesh that contains a single layer of elements normal to the radial and circumferential directions.

AcuSolve Results

The AcuSolve solution converges to a steady state and the results reflect the mean temperature distribution. As the inner diameter is considerably hotter than the outer, a heat flux, due to radiation, is present between the cylinders. The temperature within the medium reduces logarithmically as a function of the radius. The following images show the temperature with the medium as a function of radius from the center. The temperature is compared with the analytical solution as described in Incropera (2006). The image below shows black circles representing the analytical solution and a solid red line for the AcuSolve results.

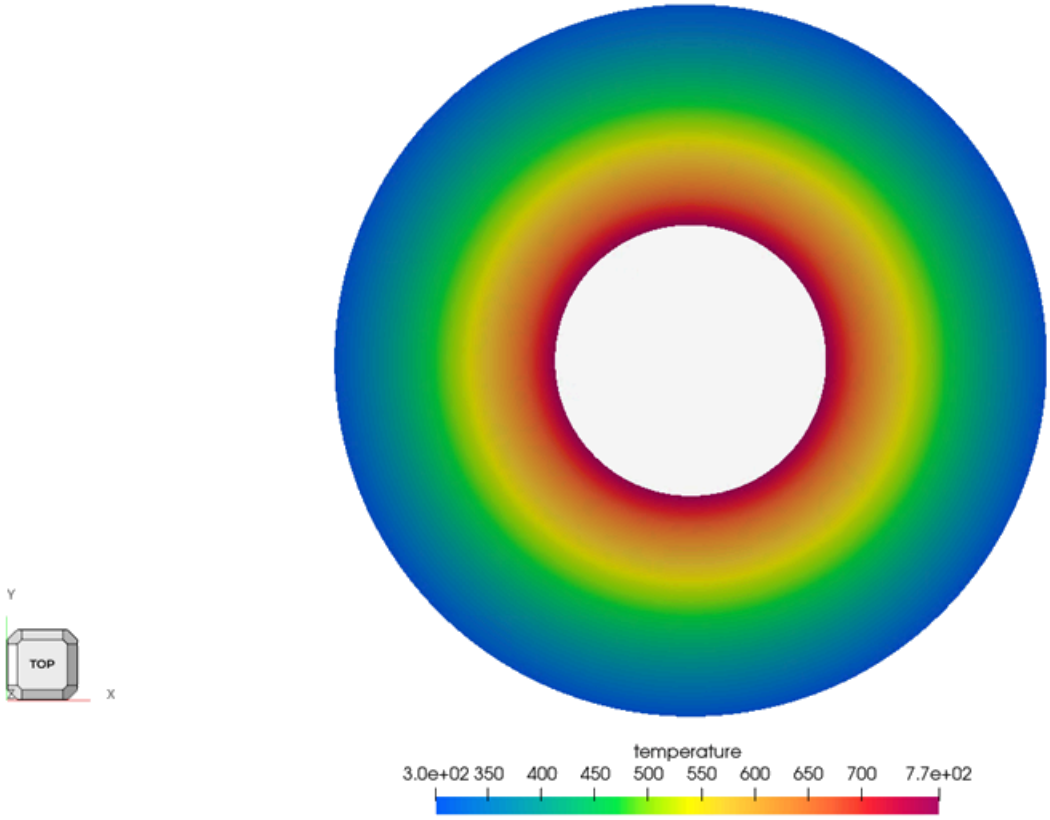


Figure 306: Contours of Temperature Between the Concentric Cylinders

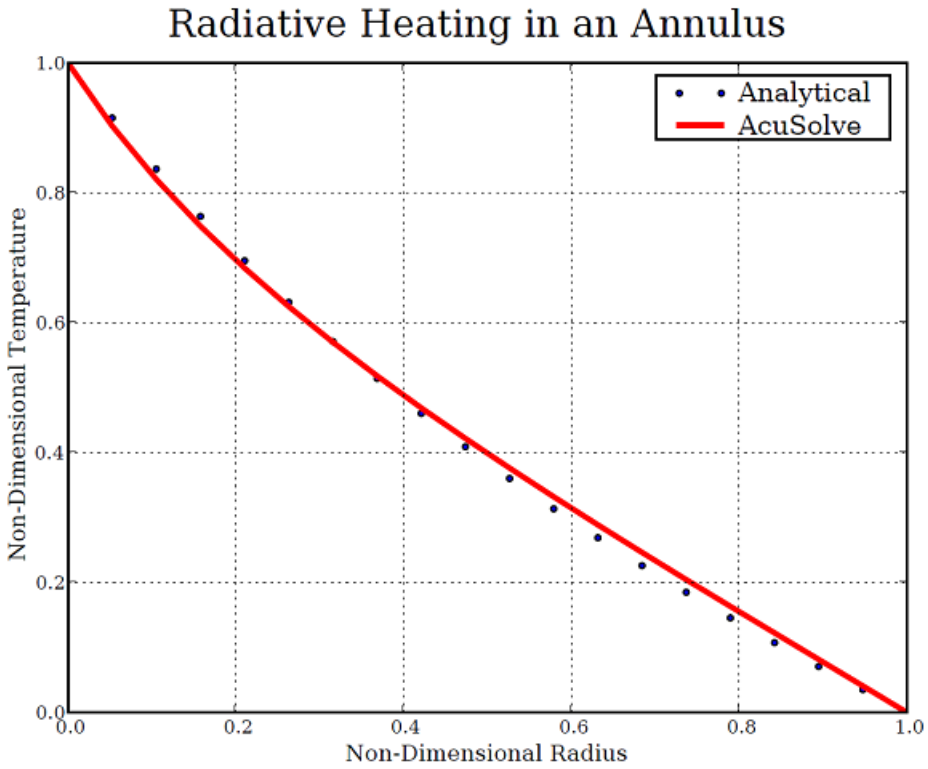


Figure 307: Non Dimensional Temperature Distribution Within the Annulus as a Function of Non Dimensional Radius

Summary

The AcuSolve solution compares well with analytical results for heat transfer due to radiation between two concentric cylinders. In this application, an arbitrary material is subjected to a heat flux that is calculated based on the view factors within the model. As a result of radiative heat flux a temperature distribution between the two cylinders develops. The AcuSolve solution for the temperature as a function of radius matches well compared to the analytical solution.

Heat Transfer Between Radiating Concentric Cylinders

HyperMesh CFD database file: `<your working directory>\annulus_radiation \annulus_radiation.hm`

Global

- Problem Description
  - Analysis type - Steady State
  - Temperature equation - Advective Diffusive
  - Radiation equation- Enclosure
- Auto Solution Strategy
  - Convergence tolerance - `0.0001`
  - Relaxation Factor- `0.4`
  - Flow- off

    - Enclosure radiation- on
- Material Model
    - Material
        - Conductivity
            1. Type - Constant
            2. Conductivity- `1.0`
- Emissivity Model
    - Grey Body
        - Emissivity- `0.03778`
    - Black Body
        - Emissivity- `1.0`

  Model
- Volumes
    - Medium
        - Element Set
            1. Medium - Fluid
            2. Material model- Material
- Surfaces
    - ID
        - Simple Boundary Condition
            1. Type- Wall
            2. Temperature BC type- Value
            3. Temperature- `773.0` K
        - Radiation Surface
            1. Type- Wall
            2. Emissivity model- Grey Body
    - Max_Z
        - Simple Boundary Condition
            1. Type- Symmetry
        - Radiation Surface
            1. Type- Wall
            2. Emissivity model- Black Body
    - Min_Z
        - Simple Boundary Condition
            1. Type- Symmetry
        - Radiation Surface
            1. Type- Wall

2. Emissivity model- Black Body

- OD
  - Simple Boundary Condition
    1. Type- Wall
    2. Temperature BC type- Value
    3. Temperature- `300.0` K
  - Radiation Surface
    1. Type- Wall
    2. Emissivity model- Grey Body

References

F. P. Incropera and D. P. DeWitt. "Fundamentals of Heat Transfer - Sixth Edition". John Wiley & Sons. New York. 2006.

Turbulent Flow Through a 180 Degree Curved Channel

In this application, AcuSolve is used to simulate turbulent flow through a strongly curved two dimensional 180 degree U-duct channel. AcuSolve results are compared with experimental results adapted from Rumsey et al. (2000). The close agreement of AcuSolve results with experimental results validates the ability of AcuSolve to model turbulent cases with strong curvature effects.

Problem Description

The problem consists of a fluid with properties similar to air flowing through a curved channel, as shown in the following image, which is not drawn to scale. The inlet channel height and remaining duct height is 0.0381 m. The bulk velocity (v) normal to the inlet is 31.1 m/s and an integrated outflow pressure is specified to allow the flow to pass through the channel. The flow develops into fully turbulent flow at a Reynolds's number (Re) of approximately 1,000,000. The density of the flow medium is 1.0 kg/m3 and the dynamic viscosity is 1.1818 X 10-6 kg/m-s. The simulation is conducted with the Reynolds Averaged Navier-Stokes equations using the Spalart Allmaras, Shear Stress Transport (SST), K-ω and Realizable K-ε turbulence models. The velocity field from the simulations is compared against experimental data at select measurement locations.

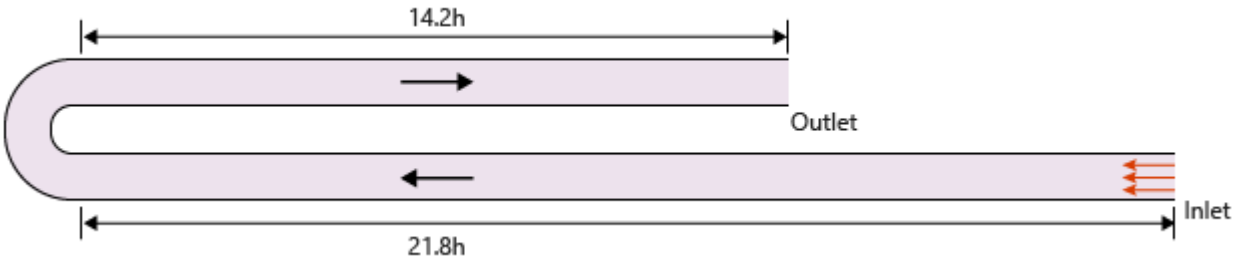
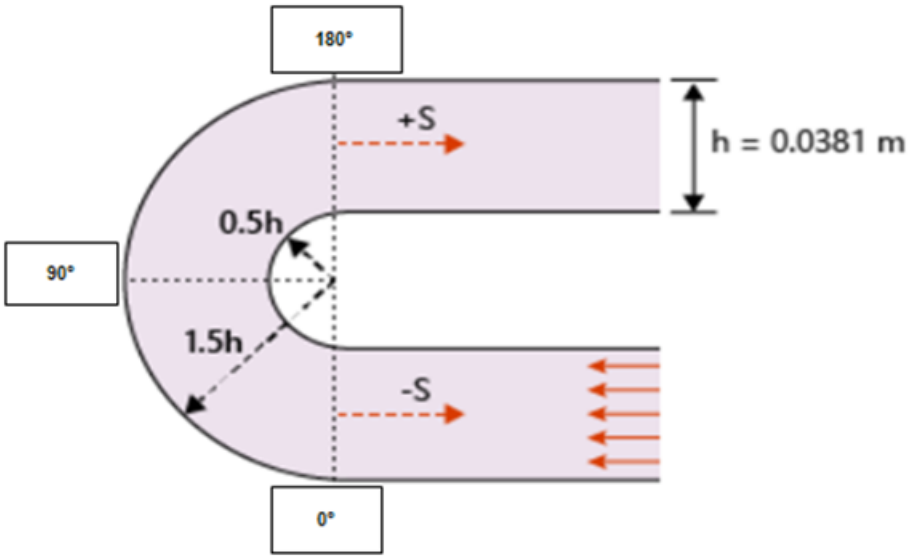


Figure 308: Critical Dimensions and Parameters for Simulating Turbulent Flow in the 180 degree U-Duct



The simulation was performed as a two dimensional problem by restricting flow in the out-of-plane direction through the use of a mesh that is one element thick. The upper and lower walls are specified as no-slip, the inlet velocity and eddy viscosity are specified normal to the inlet face to match the experimental Reynolds Number.

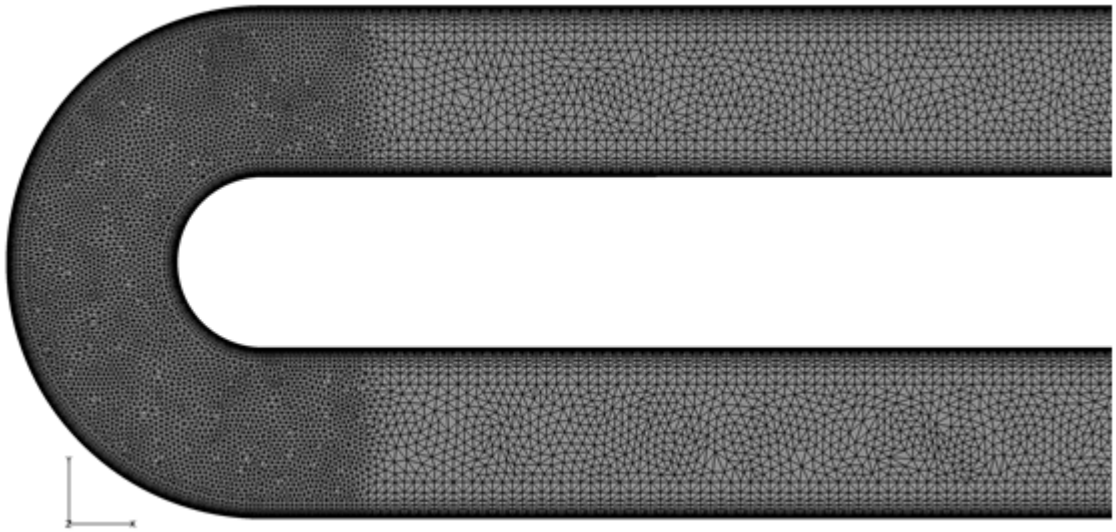


Figure 309: Mesh Used for Simulating Turbulent Flow in the 180 Degree U-Duct

AcuSolve Results

The AcuSolve solution converged to a steady state and the results reflect the mean flow conditions. As the flow passes the inner convex wall it begins to accelerate before decelerating directly past the curved section due to the adverse pressure gradient that eventually leads to a local recirculation zone. On the outer concave wall, the flow remains attached, but is influenced by the adverse pressure gradient above the recirculation region.

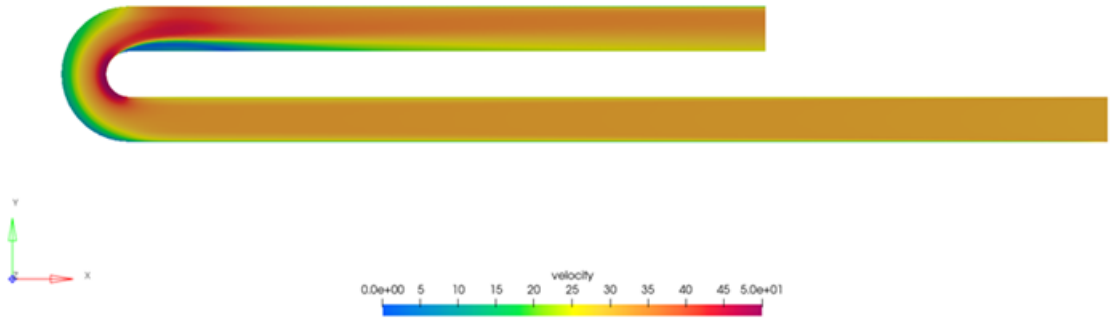


Figure 310: Velocity Contours in Stream Wise Plane

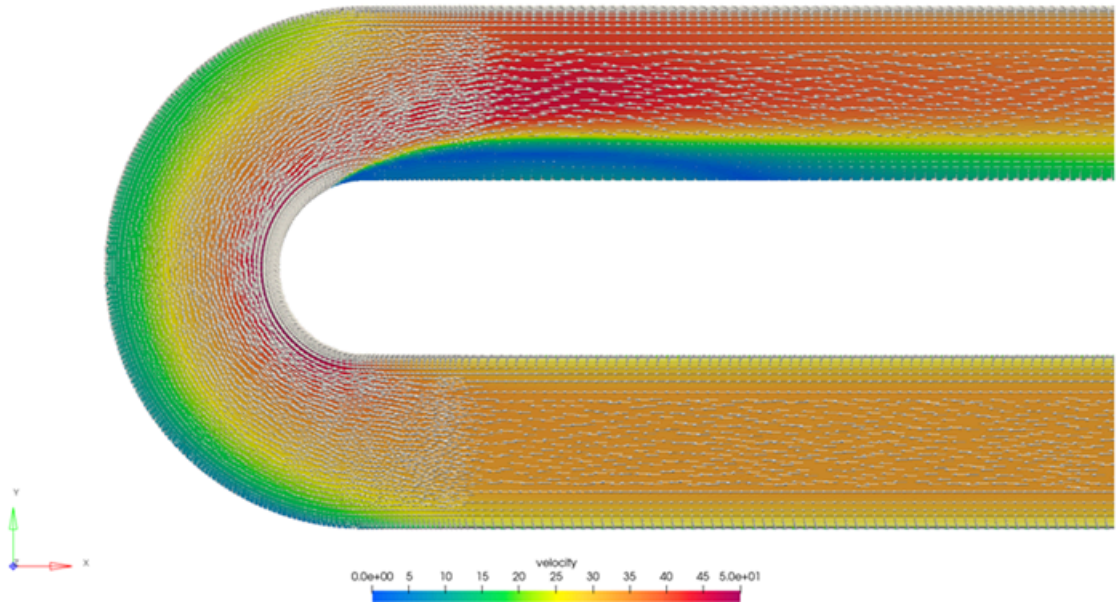


Figure 311: Close up View of Velocity Vectors and Velocity Contours at 180 Degree Bend

The experimental value for the ratio of Velocity magnitude (Vm) to inlet bulk velocity (Vb=31.1 m/s) at different sections of the U-duct is presented with the corresponding AcuSolve result for each of the turbulence models tested in the following images. The images show black circles representing the experimental measurements (Rumsey 2000), solid red lines for the SA model, solid blue lines for the SST model, solid green lines for the K-ω model and solid cyan lines for the K-ε model.

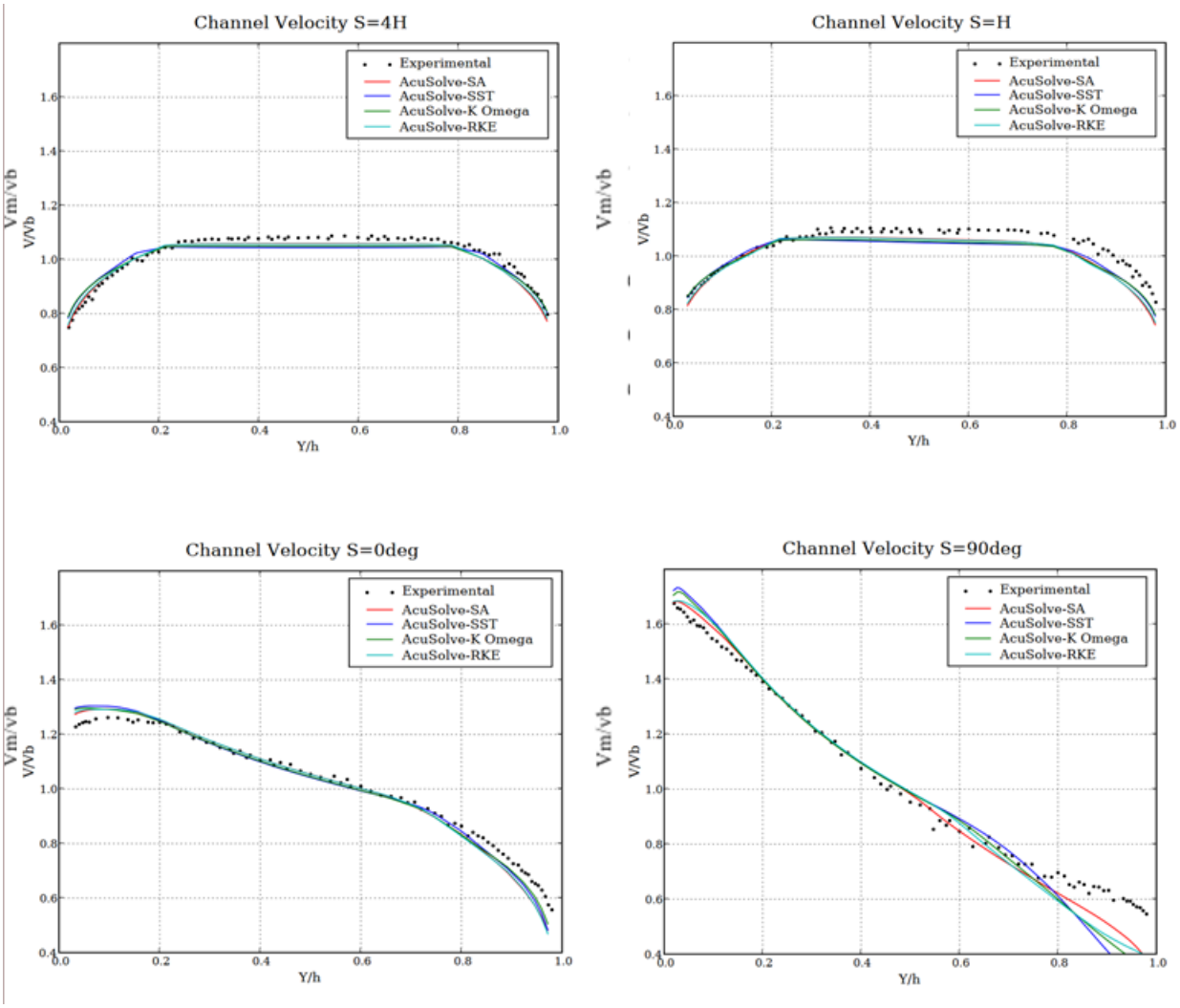


Figure 312:

Summary

The AcuSolve solution compares well with experimental results for flow past the 180 degree U-duct. The experimental value for the ratio of Velocity magnitude to inlet bulk velocity at different sections of the U-duct is presented with the corresponding AcuSolve result for various turbulence models. The performance of the Spalart Allmaras turbulence model was found to improve when the rotation curvature correction is included in the numerical formulation (enabled by default). In this application, AcuSolve demonstrates the ability to predict the complex boundary layer separation and reattachment resulting from the curvature of the channel.

Simulation Settings for Turbulent Flow Through a 180 Degree Curved Channel

HyperMesh CFD database file: `<your working directory>\curved_channel_simple_turbulent \curved_channel_simple_turbulent.hm`

Global

- Problem Description

- Analysis type - Steady State
- Turbulence equation - Realizable K-Epsilon

- Auto Solution Strategy
  - Relaxation factor - `0.4`
- Material Model
  - Air
    - Type- Constant
    - Density- `1.0` kg/m3
    - Viscosity- `1.1818e-006` kg/m-sec

  Model
- Volumes
  - Fluid
    - Element Set
      1. Material model- Air
- Surfaces
  - Inlet
    - Simple Boundary Condition
      1. Type- Wall
      2. Inflow type- Velocity
      3. Inflow velocity type- Normal
      4. Normal velocity- `31.1` m/sec
      5. Turbulence input type- Direct
      6. Eddy viscosity- `3.5547e-06` m2/sec
  - ext1
    - Simple Boundary Condition- Symmetry
  - ext2
    - Simple Boundary Condition- Symmetry
  - Outlet
    - Simple Boundary Condition
      1. Type- Outflow
  - wall-bottom
    - Simple Boundary Condition
      1. Type- Wall
      2. Turbulence wall type- Low Reynolds Number
  - wall-top
    - Simple Boundary Condition
      1. Type- Wall

2 Turbulence wall type- Low Reynolds Number

References

Christopher L. Rumsey, Thomas B. Gatski, and Joseph H. Morrison. "Turbulence Model Predictions of Strongly Curved Flow in a U-Duct", AIAA Journal, Vol. 38, No. 8 (2000), pp. 1394-1402.

Circumferential Flow in a Cylinder Induced by a Rotating Solid

In this application, AcuSolve is used to simulate the flow of air between concentric cylinders that is initiated by the rotation of the solid inner cylinder. The outer cylinder is held stationary while the inner cylinder rotates with a constant speed. AcuSolve results are compared with analytical results as described in White (1991). The close agreement of AcuSolve results with analytical results validates the ability of AcuSolve to maintain a continuous velocity across a non-conformal guide surface interface.

Problem Description

The problem consists of a fluid with material properties of a viscous fluid with the density of air rotating between two infinitely long concentric cylinders, as shown in the following image, which is not drawn to scale. The radius of the outer cylinder is 3.0 m and the radius of the inner cylinder is 1.5 m. The inner cylinder is defined as a solid medium and rotates at 1 rad/sec. The inner cylinder's surface velocity is mapped to the adjacent surface within the fluid medium, while the outer cylinder is fixed. The induced flow is laminar and exhibits a steady state behavior after running for a short period of physical time. The rotation of the inner cylinder causes the fluid to rotate due to viscous shearing near the wall. As the outer cylinder is fixed, a velocity gradient is generated as a function of radius within the flow domain.

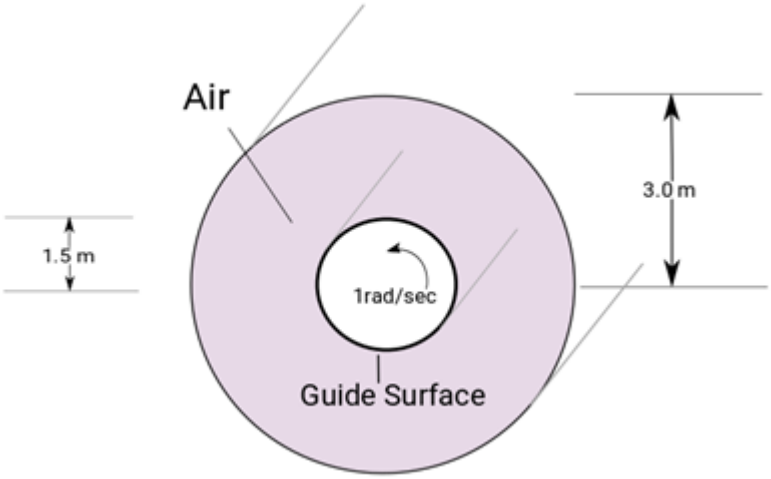


Figure 313: Critical Dimensions and Parameters Used for Simulating Flow Between Two Concentric Cylinders Split with a Guide Surface

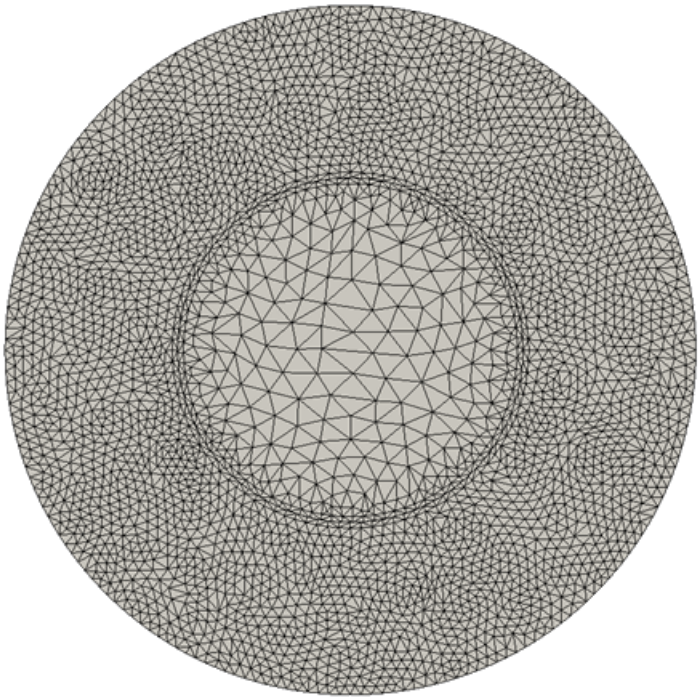


Figure 314: Mesh Used for Simulating Flow Between Two Concentric Cylinders

The simulation was performed as a two dimensional problem by constructing a volume mesh that contains a single layer of elements in the extruded direction, normal to the flow plane and by imposing slip flow and mesh boundary conditions on the extruded planes.

AcuSolve Results

The AcuSolve solution reaches a quasi-static result with the velocity between the two cylinders reaching a steady state at the simulation end time. As the solid inner cylinder rotates, it acts as a guide surface for the fluid elements to track and inherit the two velocity components. The velocity at the edge of the inner cylinder is equal to exactly the rotational speed multiplied by the radius. As the radius increases, the flow velocity reduces until it reaches zero at the outer diameter. The following images show the tangential velocity within the fluid as a function of radius from the center. The tangential velocity is compared with the analytical solution. The image below shows black circles representing the analytical solution and a solid red line for the AcuSolve results.

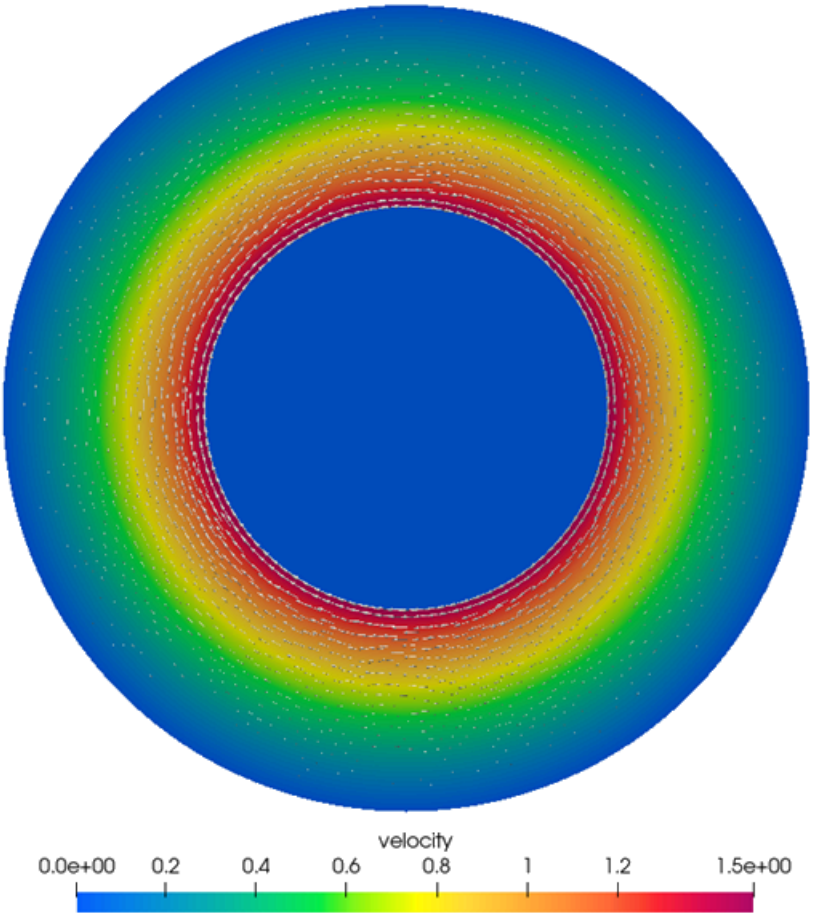


Figure 315: Contours and Vectors of Velocity Between the Concentric Cylinders

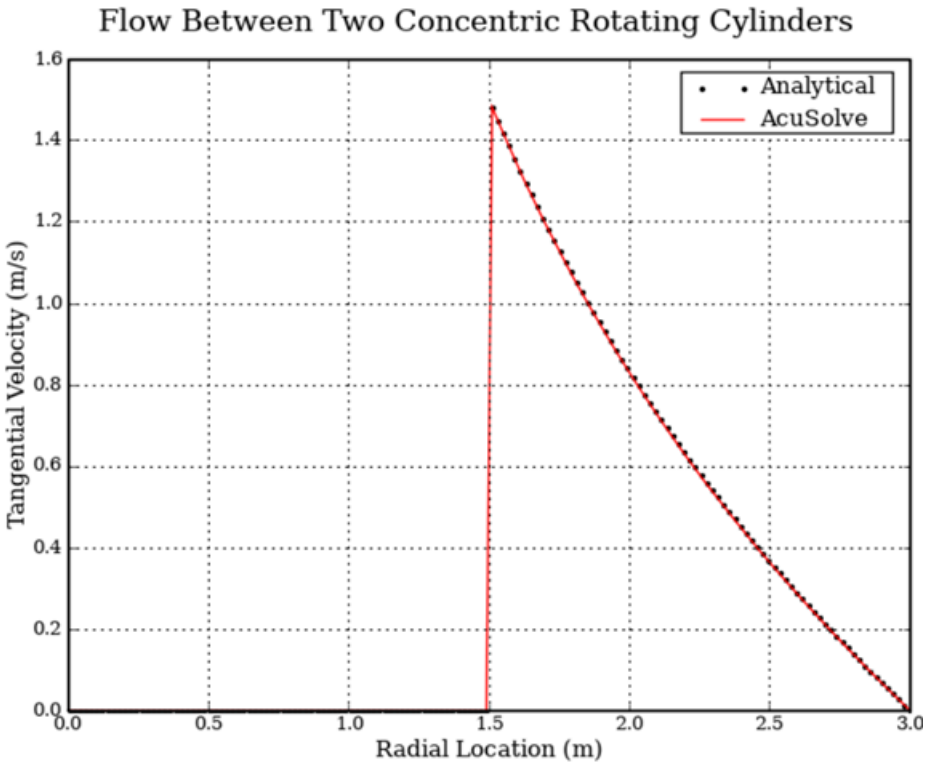


Figure 316: Tangential Velocity Within the Solid and Fluid as a Function of Radial Distance from the Center at the Final Timestep

Summary

The AcuSolve solution compares well with analytical results for laminar flow between concentric cylinders, where the inner cylinder guides the adjacent fluid elements. In this application, a fluid initially at rest inherits the angular velocity from the inner cylinder while the outer cylinder does not rotate. As a result of the inherited velocity and viscosity of the fluid, flow develops between the two cylinders. The AcuSolve solution for the tangential velocity as a function of radius matches exactly with the analytical results.

Simulation Settings for Flow Between Concentric Split Cylinders

HyperMesh CFD database file: `<your working directory>\annulus_split_rotating \annulus_split_rotating.hm`

- Problem Description
  - Analysis type - Transient
  - Flow equation - Navier Stokes
  - Turbulence equation - Laminar
  - Mesh type - Arbitrary Mesh Movement (ALE)
- Auto Solution Strategy
  - Max time steps - `40`
  - Initial time increment- `0.02` sec

- Convergence tolerance - `0.001`
- Min stagger iterations - `2`
- Max stagger iterations - `4`

- Material Model
  - Air
    - Density
      1. Type - Constant
      2. Density - `1.225` kg/m3
    - Viscosity
      1. Type - Constant
      2. Viscosity - `1.781` kg/m-sec
- Mesh Motion
  - Rotation
    - Rotation Center
      1. X-coordinate - `2.0` m
      2. Y-coordinate - `0.0` m
      3. Z-coordinate - `0.0` m
    - Angular velocity
      1. X-component - `1.0` rad/sec
      2. Y-component- `0.0` rad/sec
      3. Z-component - `0.0` rad/sec

  Model
- Volumes
  - CylinderInner
    - Element Set
      1. Medium - Solid
      2. Material model - Aluminum
  - CylinderOuter
    - Element Set
      1. Medium - Fluid
      2. Material model - Air
- Surfaces
  - InBottom
    - Simple Boundary Condition
      1. Type- Slip
      2. Mesh displacement type- Slip
  - InInterf

        - Simple Boundary Condition
            1. Type- Wall
            2. Mesh displacement type- Fixed
            3. Mesh motion- Rotation
        - Guide Surface
            1. Type- Faceted
    - InTop
        - Simple Boundary Condition
            1. Type- Slip
            2. Mesh displacement type- Slip
    - OutBottom
        - Simple Boundary Condition
            1. Type- Slip
            2. Mesh displacement type- Slip
    - OutInterf
        - Simple Boundary Condition
            1. Type- Wall
            2. Wall velocity type- Match Mesh Velocity
            3. Mesh displacement type- Guide surface
            4. Guide surface- InInterf
    - OutTop
        - Simple Boundary Condition
            1. Type- Slip
            2. Mesh displacement type- Slip
    - OutWall
        - Simple Boundary Condition
            1. Type- Wall
            2. Mesh displacement type- Fixed
- Nodes
    - PressurePoint
        - Pressure
            1. Type- Zero

References

F. M. White. "Viscous Fluid Flow". Section 3-2.3. McGraw-Hill Book Co., Inc. New York. 1991.

Heat Transfer Between Radiating Concentric Spheres

In this application, AcuSolve is used to simulate the heat transfer due to conduction and radiation between concentric spheres. The inside surface of the inner and the outside surface of the outer sphere are both held at constant temperature, while the gap between them radiates the heat from one sphere to the other.

AcuSolve results are compared with analytical results for temperature and heat flux as described in Incropera (2006) and Salazar, et al. (2016). The close agreement of AcuSolve results with analytical results validates the ability of AcuSolve to model cases with radiation heat transfer and conjugate heat transfer with enclosure radiation modeling and the discrete ordinate (DO) radiation model.

Problem Description

The problem consists of a fluid region with arbitrary material properties between two concentric spheres with surfaces held at fixed temperature, as shown in the following image, which is not drawn to scale. The radius of the outer sphere is 0.04 m and the radius of the inner sphere is 0.01 m. The inner surface of the inner sphere is defined to have a constant wall temperature at 300.0 K (27 ºC). The outer surface of the outer sphere is defined to have a constant wall temperature at 1300.0 K (1027 ºC). The fluid within the spheres is defined as a non-conducting material, allowing heat to transfer via radiation only. The solid and fluid regions equilibrate to a steady temperature and can be compared with a semi-analytical solution for the temperature and heat flux at the fluid boundaries.

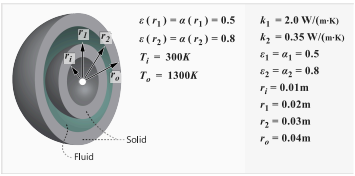


Figure 317: Critical Dimensions and Parameters used for Simulating Conduction and Radiation Between two Concentric Spheres



Figure 318: Mesh used for Simulating Radiation Between two Concentric Spheres

The simulation was performed as a three dimensional problem by constructing a volume mesh that contains a layer of boundary elements normal to the radial direction.

AcuSolve Results

The AcuSolve solution converges to a steady state and the results reflect the mean temperature distribution within the spheres. As the outer diameter is considerably hotter than the inner, a heat flux is present between the spheres. The temperature within the mediums increases as a function of the radius, with a slope corresponding to the temperature difference and the specified emissivity of the shells. The following image shows the temperature contour within the spheres along with the two-dimensional plot of the temperature versus radius in the solid mediums. The temperature and heat flux at the radiation surfaces are compared with the analytical solution as described in Salazar, et al. (2016).

Table 17: The Analytical Solution for the Temperature and Heat Flux at r1 and r2 are Presented with the Corresponding AcuSolve Results for the Enclosure (Surface to Surface) Model and the DO

	T(r1) (K)	T(r2) (K)	Q(r1) (W)	Q(r2) (W)
Analytical	578.2	1035.0	-27822.5	12365.6
AcuSolve (Enclosure)	578.4	1035.1	-27827	12364.2
AcuSolve (DO)	561.8	1023.6	-26175	12897.0
Percent Difference (Enclosure)	0.034%	0.010%	-0.015%	-0.011%
Percent Difference (DO)	2.8%	-1.11%	5.92%	4.3%

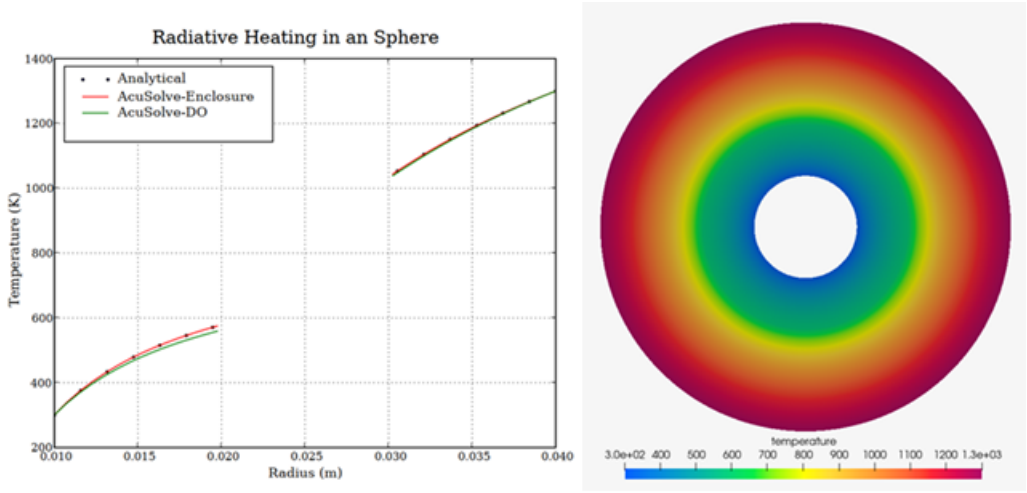


Figure 319: Two-Dimensional Plot and Contours of Temperature Between the Concentric Spheres

Summary

The AcuSolve solution compares well with analytical results for heat transfer due to conduction and radiation between two concentric spheres. In this application, an arbitrary material is subjected to a heat flux that is calculated based on the view factors or the DO model within the simulation. As a result of the conjugate heat transfer and the radiative heat flux a temperature distribution between the two spheres develops. The AcuSolve solution for the temperature and heat flux at the radiation surfaces matches well compared to the analytical solution with only a minor difference for the enclosure radiation model. The enclosure radiation model was found to have a higher accuracy for this application compared to the DO model, as expected due to the relatively low optical thickness in this simulation.

Heat Transfer Between Radiating Concentric Spheres

HyperMesh CFD database file: `<your working directory>\sphere_radiation\sphere_radiation.hm`.

Global

- Problem Description
  - Analysis type - Steady State
  - Temperature equation - Advective Diffusive
  - Radiation equation - Enclosure
- Auto Solution Strategy
  - Convergence tolerance - `1.0e-5`
  - Relaxation Factor - `0.4`
  - Flow - off
  - Enclosure radiation - on
- Material Model
  - Inner
  - Conductivity
    - Type - Constant

        - Conductivity - `2.0`
    - Outer
    - Conductivity
        - Type - Constant
        - Conductivity - `0.35`
    - Radiating
    - Conductivity
        - Type - Constant
        - Conductivity - `1.0e-6`
- Emissivity Model
- Inner
    - Emissivity - `0.5`
- Outer
    - Emissivity - `0.8`

  Model
- Volumes
    - Inner
        - Element Set
            1. Medium- Solid
            2. Material model - Inner
        - Outer
            1. Element Set
                1. Medium - Solid
                2. Material model - Outer
        - Radiating
            1. Element Set
                1. Medium - Fluid
                2. Material model - Radiating
- Surfaces
    - Inner_Inner_r1
        - Simple Boundary Condition - (disabled to allow for heat flux)
    - Inner_Inner_ri
        - Simple Boundary Condition
            1. Type - Wall
            2. Temperature BC type - Value
            3. Temperature - `300.0` K
    - Inner_Radiating_r1

        - Simple Boundary Condition (disabled to allow for heat flux)
        - Radiation Surface
            1. Type - Wall
            2. Emissivity model - Inner
    - Outer_Outer_r2
        - Simple Boundary Condition (disabled to allow for heat flux)
    - Inner_Outer_ro
        - Simple Boundary Condition
            1. Type - Wall
            2. Temperature BC type - Value
            3. Temperature - `1300.0` K
    - Outer_Radiating_r2
        - Simple Boundary Condition (disabled to allow for heat flux)
        - Radiation Surface
            1. Type - Wall
            2. Emissivity model - Outer

References

F. P. Incropera and D. P. DeWitt. "Fundamentals of Heat Transfer – Sixth Edition". John Wiley & Sons. New York. 2006.

Salazar, G., Droba, J., Oliver, B., & Amar, A. J. (2016). Development and Verification of Enclosure Radiation Capabilities in the CHarring Ablator Response (CHAR) code. 46th AIAA Thermophysics Conference.

Two-Phase Nucleate Boiling in a Cylindrical Pipe

In this application, AcuSolve is used to simulate the changes in wall temperature due to two-phase nucleate boiling at the heated walls of a pipe with water flowing through it. AcuSolve results are compared with experimental results adapted from Koncar and others (2015). The close agreement of AcuSolve results with experimental results validates the ability of AcuSolve to model two-phase nucleate boiling problems.

Problem Description

The problem consists of a pipe with heated surrounding walls, as shown in the following image, which is not drawn to scale. The length of the pipe is 2 m and the radius is 0.0017 m. Mass flux at the inlet is 900 kg/m^2 and the temperature of the fluid entering the pipe is 473 K. A heat flux of 570,000 W/m^2 is applied on the walls. The preheated water enters the inlet and heat is transferred to the fluid from the walls. The heat causes sub-cooled boiling to occur in the region close to the wall and leads to the formation of bubbles at nucleation sites.

During sub-cooled boiling flow, heat and mass exchange between the phases takes place on the heated wall and in sub-cooled liquid flow. On the heated surface the vapor bubbles are generated and as they move through the sub-cooled liquid they condense and release the latent heat.

The AcuSolve simulation is set up to model transient state heat transfer to determine the temperature along the centerline of the pipe and along the heated pipe walls of the model. AcuSolve computes the two-phase nucleate boiling by simulating the three-dimensional flow in a heated pipe for two-phase boiling flow, as described in Koncar (2005). The temperatures along the centerline of the pipe and along the pipe walls are compared against the experimental measurements, as described in Koncar, et al. (2005).

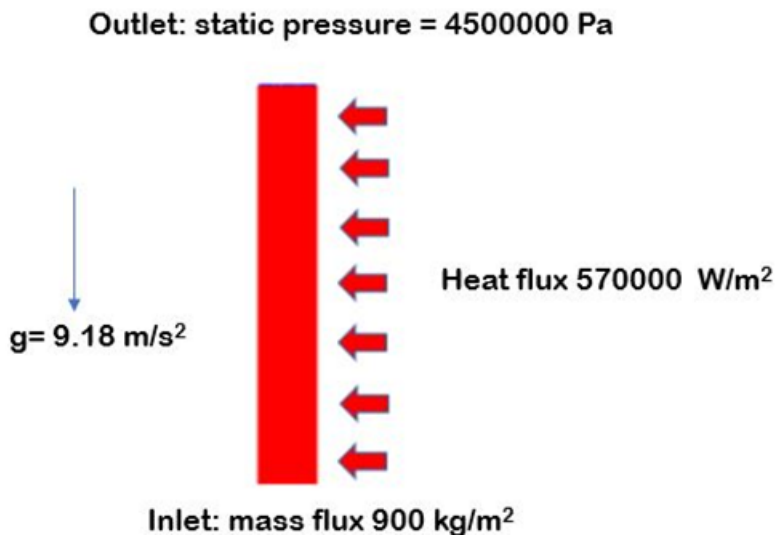


Figure 320: Parameters for Simulating a Two-Phase Nucleate Boiling Problem of a Pipe

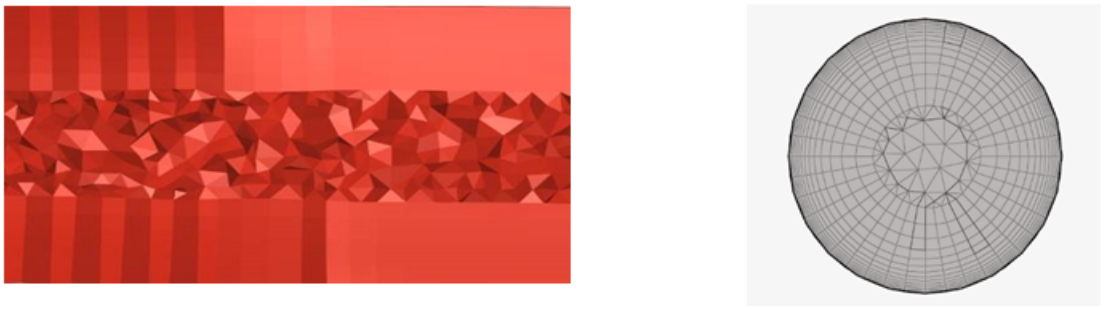


Figure 321: Mesh used for Simulating Two-Phase Flow in a Pipe

AcuSolve Results

The AcuSolve solution is run for a heat flux of 570,000 W/m^2 and the results are presented in the following image. The experimental values of wall temperature are presented with the corresponding AcuSolve results along the centerline of the pipe and along the pipe wall. The AcuSolve results show good agreement with the experimental results for the temperature, indicating that the two-phase nucleate boiling is properly captured.

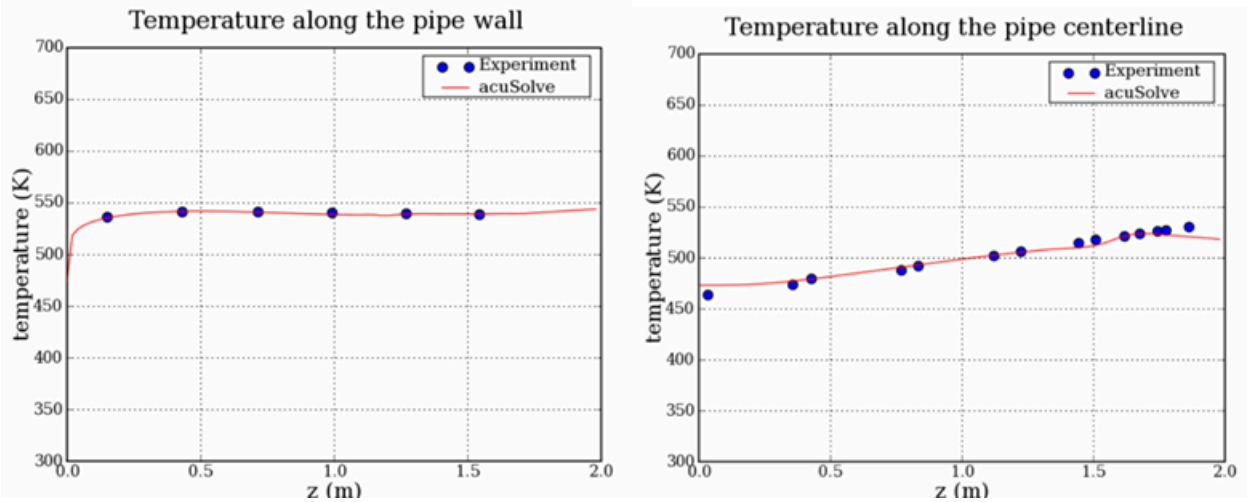


Figure 322: Temperature Values for Varying Streamwise Distance Compared to Experimental Data

Summary

The AcuSolve solution compares well with experimental results for two-phase nucleate boiling simulations. In this application, the temperature of the wall as the onset of boiling approaches are simulated with AcuSolve using the nucleate boiling feature and the SA turbulence model. The experimental values of temperature are presented with the corresponding AcuSolve results. A good agreement of simulation results with the experiment validates the ability to solve two-phase nucleate boiling using the nucleate boiling capabilities of AcuSolve.

Simulation Settings for Two-Phase Nucleate Boiling in a Cylindrical Pipe

HyperMesh CFD database file: `<your working directory>\pipe_two_phase_boiling \pipe_two_phase_boiling.hm`.

Global

- Problem Description
  - Analysis type – Transient
  - Turbulence equation – SA
  - Temperature equation – Advective Diffusive
- Auto Solution Strategy
  - Maximum time steps – `500`
  - Initial time increment – `0.003`
  - Convergence Tolerance – `0.001` sec
  - Relaxation factor – `0.3`
- Surface Tension Model (“Water_NB-Vapor_NB”)
  - Type – Constant
  - Surface Tension – `0.02382`
- Material Model
  - Vapor_NB
    - Type – Constant
    - Density – `23.75` kg/m^3
    - Viscosity – `1.79e-05` kg/m-sec
    - Specific Heat – `4225` J/kg-K
    - Latent Heat – `1675570`
    - Latent Heat Temperature – `530.55` K
    - Conductivity – `0.02528` W/m-K
  - Water_NB
    - Type – Constant
    - Density – `800` kg/m3
    - Viscosity – `0.0001339` kg/m-sec
    - Specific Heat – `4500` J/kg-K
    - Conductivity – `0.65` W/m-K
- Multifield parameter (Field interaction model)
  - Type – Algebraic Eulerian
  - Phase change type – Wall Boiling
  - Carrier field - Water
  - Disperse field – Vapor
  - Disperse field diameter type – Boiling kurul exponential
  - Drag model – Ishii zuber
  - Lift Model – Legendre Magnaudet

Model

- Volumes
  - Fluid
    - Material – Vapor_Water
- Surfaces
  - Inflow
    - Simple Boundary Condition – Inflow
    - Inflow type – Mass Flux Rate
    - Mass Flux Rate – `0.167634` kg/sec
    - Temperature – `473` K
  - Outflow
    - Simple Boundary Condition – Outflow
    - Pressure – `4500000` N/m2
  - Wall
    - Simple Boundary Condition – Wall
    - Temperature type – Flux
    - Heat Flux – `570000` W/m2

References

B. Koncar, E. Krapper, Y. Egorov, 2005, "CFD MODELING OF SUBCOOLED FLOW BOILING FOR NUCLEAR ENGINEERING APPLICATIONS", International Conference Nuclear Energy for New Europe 2005, Bled, Slovenia, September 5-8,2005.

Single-Phase Nucleate Boiling in a Rectangular Channel

In this application, AcuSolve is used to simulate the wall heat flux due to nucleate boiling at a heated wall inside a rectangular channel with water flow. Results are compared with experimental heat flux measurements as reported by Steiner, et al. (2005). The close agreement of AcuSolve results with experimental results validates the ability of AcuSolve to model single phase nucleate boiling problems.

Problem Description

The problem consists of a channel with a heated wall at the bottom. The temperature of the wall is selected to onset the nucleate boiling at the heated wall. The dimensions of the inlet are 0.03 x 0.04 m; the inlet velocity (v) is 0.39 m/s and the temperature (T) of the fluid entering the inlets is varied from 373.15 K (100 C) to 406.15 (133 C)), while the atmospheric pressure is specified to be 2 bar. The pre-heated water enters the inlets and heat is transferred into the fluid from the heated walls. The heat causes sub-cooled boiling to occur in the region close to the wall and leads to the formation of bubbles at nucleation sites. The surface tension and vapor phase models are specified to emulate the physical process of water changing state to water vapor.

The heat transfer in this regime is dominated by two effects, the macro convection due to the motion of the bulk liquid and the latent heat transport associated with the evaporation of the liquid micro-layer between the bubble and the heated wall. Each of these effects are modeled with AcuSolve and the prediction of their processes is demonstrated in the following results.

The AcuSolve simulation is prepared as a steady state heat transfer simulation to determine the temperature and heat flux on the heated walls of the model. AcuSolve computes the single-phase nucleate boiling by employing Chen’s model for two-phase boiling flow described in Chen (1966). The heat flux values for different wall temperatures are compared against the experimental measurements, as described in Steiner, et al. (2005).

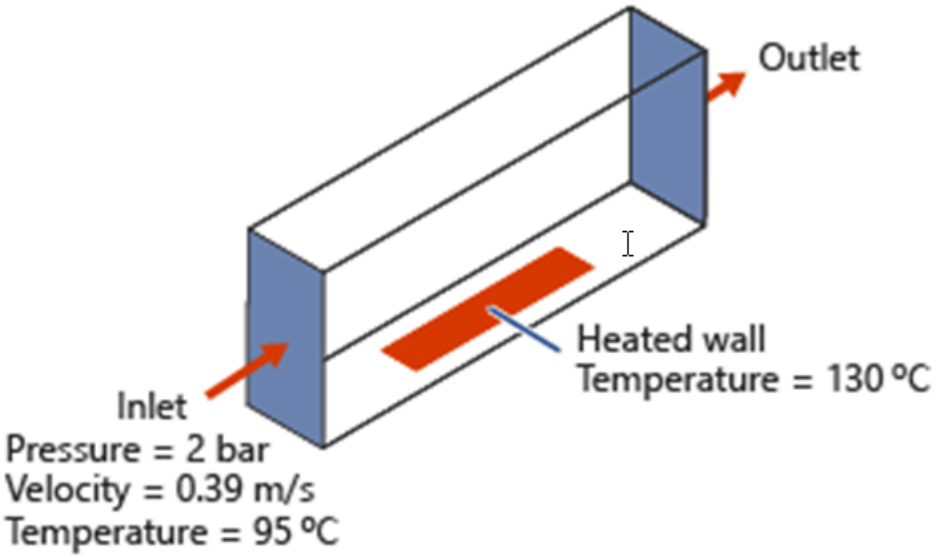


Figure 323: Critical Dimensions and Parameters for Simulating a Single-Phase Nucleate Boiling in a Rectangular Channel

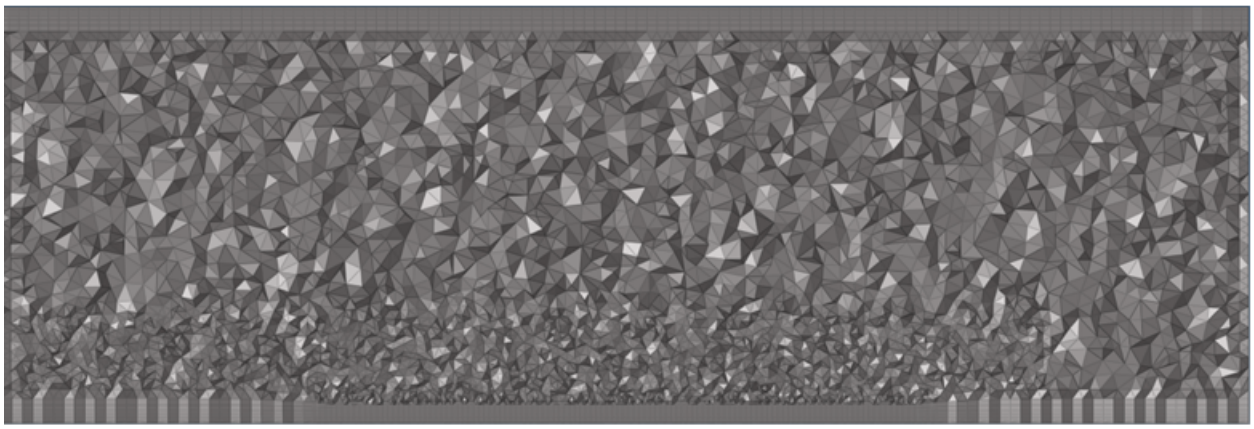


Figure 324: Mesh Used for Simulating a Single-Phase Nucleate Boiling in a Rectangular Channel

AcuSolve Results

The AcuSolve solution is run for heated wall temperature values of 100 C, 105 C, 110 C, 115 C, 120 C, 125 C, 130 C, 133 C and the results presented reflect the heat flux from the wall as the temperature nears the saturation temperature. The experimental values of heat flux (MW/m2) and wall temperature are presented with the corresponding AcuSolve results at seven temperature values. The AcuSolve results show good agreement with the experimental results for the heat flux, indicating that the single-phase nucleate boiling is properly captured.

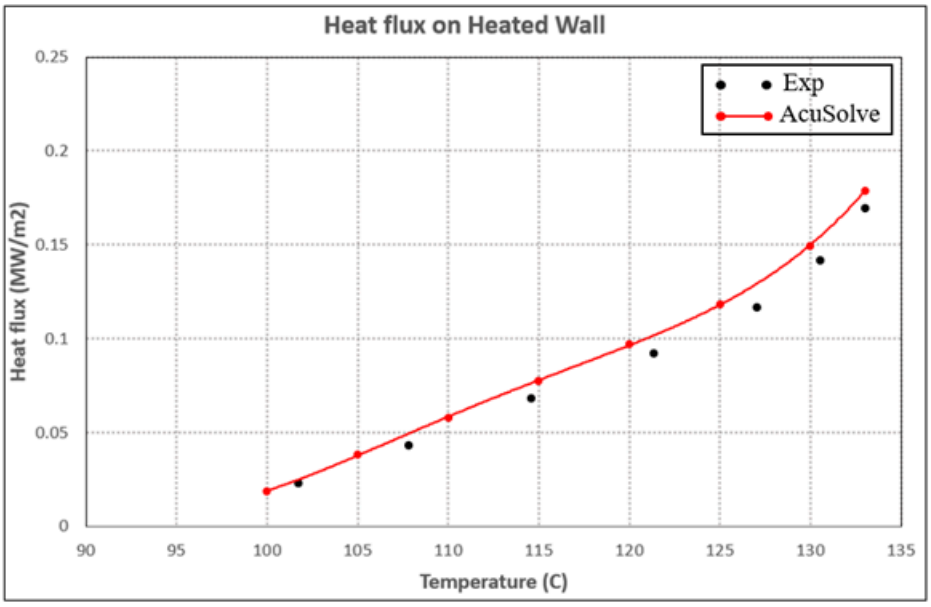


Figure 325: Heat Flux Values for Varying Wall Temperatures Compared to Experimental Data

Summary

The AcuSolve solution compares well with experimental results for single-phase nucleate boiling simulations. In this application, heat flux generated by the wall as the onset of boiling approaches are simulated with AcuSolve using the nucleate boiling feature and the RKE turbulence model. The experimental values of heat flux for the wall temperature range are presented with the corresponding AcuSolve results. A good agreement of simulation results with the experiment validates the ability to solve single-phase nucleate boiling using the nucleate boiling capabilities of AcuSolve.

Simulation Settings for Single-Phase Nucleate Boiling in a Rectangular Channel

HyperMesh CFD database file: `<your working directory>\channel_single_phase_boiling \channel_single_phase_boiling.hm`.

Global

- Problem Description
  - Analysis type – Steady
  - Turbulence equation – RKE
  - Temperature equation – Advective Diffusive
  - Nucleate Boiling Single Phase – On
- Auto Solution Strategy
  - Convergence Tolerance – `0.001`
  - Relaxation factor – `0.4`
- Surface Tension Model (“Water-srfTns”)
  - Type – Constant
  - Surface Tension – `0.07`

- Material Model
  - Vapor
    - Type – Constant
    - Density – `1.128` kg/m^3
    - Viscosity – `1.29e-5` kg/m-sec
    - Specific Heat – `2174.59` J/kg-K
    - Latent Heat – `2256000`
    - Latent Heat Temperature – `393.45` K
    - Conductivity – `0.02749` W/m-K
    - Turbulent Prandtl number – `1.0`
  - Water
    - Type – Constant
    - Density – `965.36` kg/m^3
    - Viscosity – `0.000314` kg/m-sec
    - Specific Heat – `4204.8` J/kg-K
    - Conductivity – `0.675` W/m-K
    - Turbulent Prandtl number – `0.91`
    - Vapor phase model – Vapor
    - Surface Tension model – Water-srfTns

Model

- Volumes
  - Fluid
    - Material– Water
- Surfaces
  - Inflow
    - Simple Boundary Condition – Inflow
    - Inflow type – Average Velocity
    - Average Velocity – `0.39` m/sec
    - Temperature – `368.15` K
  - Outflow
    - Simple Boundary Condition – Outflow
    - Back flow condition – On
    - Temperature back flow type – Mass flux average
    - Kinetic energy back flow type – Mass flux average
    - Dissipation rate back flow type – Mass flux average
  - Bottom
    - Simple Boundary Condition – Wall
  - Top

        - Simple Boundary Condition – Wall
    - Side_MinY
        - Simple Boundary Condition – Wall
    - Side_MaxY
        - Simple Boundary Condition – Wall
    - Heated Wall
        - Simple Boundary Condition – Wall
        - Temperature type – Value
        - Temperature – [373.15, 378.15, 383.15, 388.15, 393.15, 398.15, 403.15, 406.15] K

References

Helfried Steiner, Alexander Kobor, Ludwig Gebhard, 2005, "A wall heat transfer model for subcooled boiling flow", International Journal of Heat and Mass Transfer, Vol 48, pp. 4161- 4173.

Chen, J.C., 1966, "Correlation for Boiling Heat Transfer to Saturated Fluids in Convective Flow", United States: N. p., 1962. Web. doi:10.2172/4636495.

Supersonic Flow Through a Converging-Diverging Nozzle

In this application, AcuSolve is used to simulate the high-speed turbulent flow in a converging and then diverging nozzle. The flow within the nozzle enters as subsonic, reaches sonic at the throat and shortly after develops a normal shock. AcuSolve results are compared with experimental results adapted from Bogar and Sajben (1983). The close agreement of AcuSolve results to experimental measurements validates the ability of AcuSolve to simulate internal supersonic flows where normal shocks are present.

Problem Description

The problem consists of a converging and then diverging nozzle represented as an extruded planar surface, as shown in the image below, which is not drawn to scale. The length of the domain is 0.213 m with a throat height of 0.044 m. The stagnation pressure and static temperature are constrained at the inlet to 135,000 Pa and 265.98 K, respectively. The static pressure is defined using the outflow boundary condition, where P_{static}=97216.08 Pa. The flow in the diffuser has an inlet Reynolds number of $6.5x10^5$. The upper and lower walls are set to no-slip and the side walls are set to slip, while the exterior walls are specified to be adiabatic. Images of the numerical mesh are shown below.

The AcuSolve simulation is prepared to model the pseudo-transient state to determine the shock location and corresponding scalar quantities within the diffuser. AcuSolve computes the flow and thermal solution by simulating a planar, two-dimensional flow problem with physical dimensions and input quantities as described in the Sajben Diffuser case presented by Bogar and Sajben (1983). The gas in the simulation domain enters at subsonic conditions and is forced to accelerate beyond Mach=1.0 as it passes through the throat. After reaching supersonic speed a normal shock wave develops causing the flow speed to reduce back below sonic. The pressure along the bottom wall of the diffuser is compared against experimental measurements to demonstrate the solver's capability to solve supersonic cases.

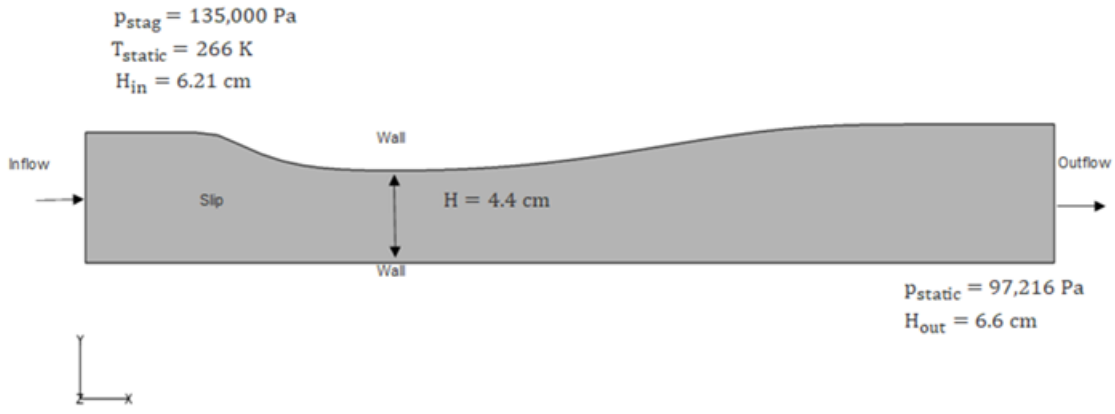


Figure 326: Parameters for Simulating Compressible Flow within a Converging-Diverging Nozzle

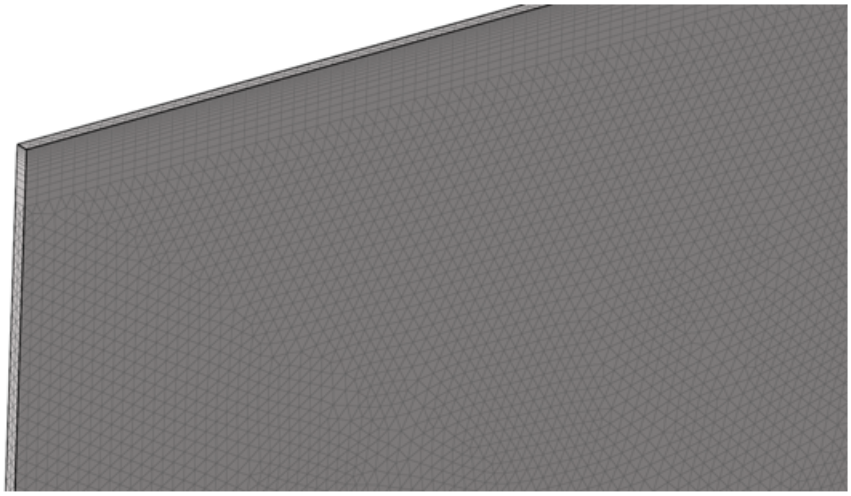


Figure 327: Mesh used for Simulating Compressible Flow in a Converging-Diverging Nozzle

AcuSolve Results

The AcuSolve solution is run for 0.025 seconds (6,250 timesteps with dt=4.0x10^{-6}sec) and converges to a pseudo-steady solution. The change in pressure from the inlet to outlet causes the flow to accelerate within the throat of the diffuser until it reaches approximately Mach=1.35. A normal shock is present just downstream of where the cross-sectional area of the nozzle increases, as shown in the image below. The numerical solution can be compared with the reference after normalizing the pressure along the wall by the inlet stagnation pressure (135 kPa) and the distance along the bottom wall by the nozzle throat height (0.044 m). The image below shows the normalized pressure versus normalized distance in comparison to NASA reference and experimental results. The image shows black circles representing the experimental measurements (Bogar and Sajben 1983), a dashed blue line representing the SA solution as obtained through NASA publication (Mohler 2005) and a solid red line representing the AcuSolve results with the Spalart-Allmaras turbulence model. The non-dimensional pressure within the diffuser agrees well with the reference data, demonstrating the correct physical location of the normal shock and expected moderate flow speed reduction within the constant cross-section diffuser portion of the nozzle.

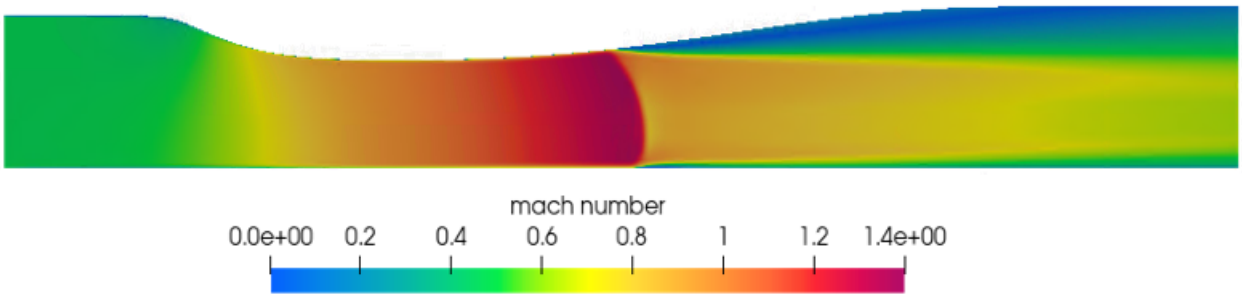


Figure 328: Contours of Mach Number within a Converging-Diverging Nozzle

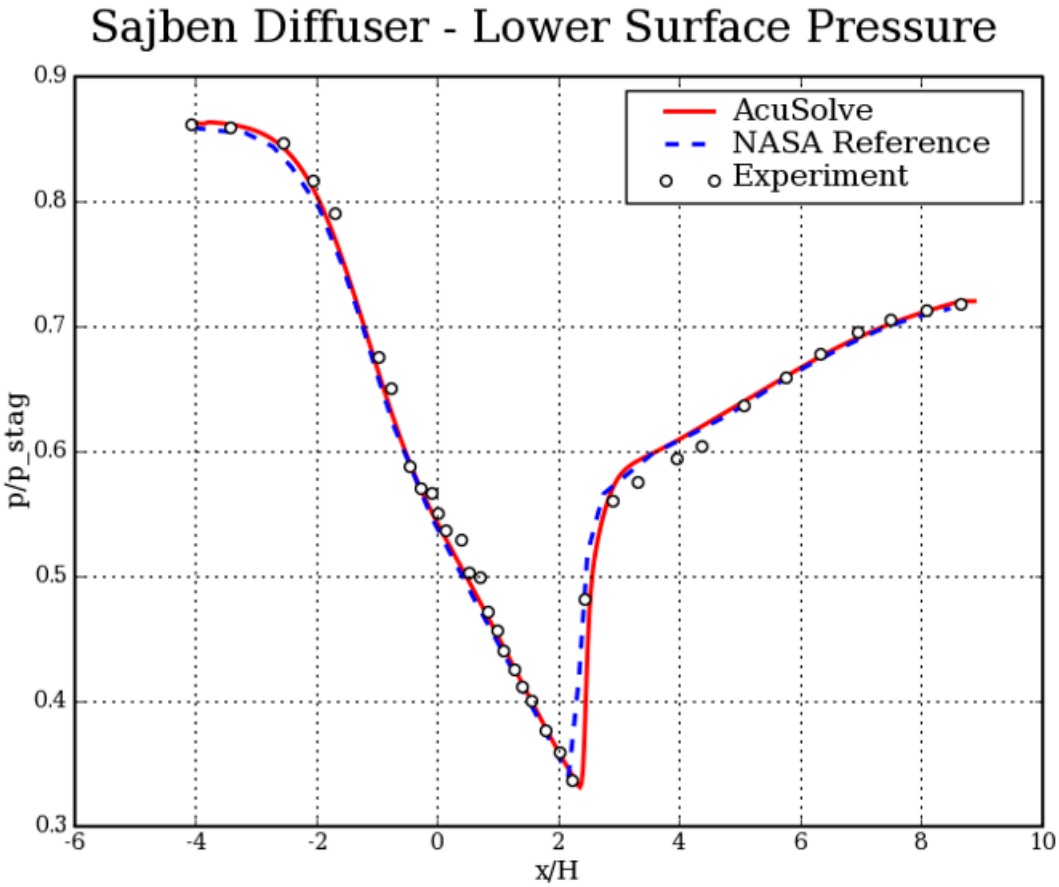


Figure 329: Normalized Pressure Versus Normalized Distance in Comparison to NASA Reference and Experimental Results

Summary

The AcuSolve solution compares well with experimental and numerical results for the described simulation. In this application, compressibility effects are accounted for using the coupled compressible flow solver with the ideal gas material definition. The thermal and momentum exchange within the nozzle is computed with AcuSolve using the compressible Navier-Stokes solver with the Spalart-Allmaras turbulence model. The experimental values of pressure are presented with the corresponding AcuSolve results and show good agreement, validating the ability to solve compressible cases with the presence of normal shocks. The results indicate that AcuSolve is able to properly predict the peak pressure magnitude and location within the diffuser while maintaining the normal shock when the time-step is selected to result in a maximum CFL of approximately 30.

Simulation Settings for Supersonic Flow Through a Converging-Diverging Nozzle

HyperMesh CFD database file: `<your working directory>\diffuser_compressible\diffuser_compressible.hm`

Global

- Problem Description

    - Flow – Compressible Navier Stokes
    - Analysis type – Transient
    - Turbulence equation – SA
    - Temperature equation – Advective Diffusive
- Auto Solution Strategy
    - Initial time increment – `4.0E-6`
    - Final time – `0.025` sec
    - Convergence Tolerance – `0.001` sec
    - Relaxation factor – `0.5`
- Material Model
    - Air-Ideal Gas
        - Type – Ideal_Gas
        - Viscosity – `1.781e-05` kg/m-sec
        - Specific Heat – `1005` J/kg-K
        - Conductivity – `0.02521` W/m-K
        - Gas Constant – `287.058` J/kg-K

Model

- Volumes
    - Fluid
        - Material – Air-Ideal Gas
- Surfaces
    - Inflow
        - Simple Boundary Condition – Inflow
        - Inflow type – Stagnation Pressure
        - Stagnation Pressure – `135000.0` N/m2
        - Turbulence_input_type – Direct
        - Eddy Viscosity – `1e-6` m^2/s
        - Temperature – `265.98` K
    - Outflow
        - Simple Boundary Condition – Outflow
        - Pressure – `97216.08` N/m2
    - Wall_1
        - Simple Boundary Condition – Wall
        - Type – auto_wall
    - Wall_2
        - Simple Boundary Condition – Wall
        - Type – auto_wall
    - Slip_1

        - Simple Boundary Condition – Slip
    - Slip_2
        - Simple Boundary Condition – Slip

References

Bogar, T. J., Sajben, M., and Kroutil, J. C. (1983) "Characteristic Frequencies of Transonic Diffuser Flow Oscillations," AIAA Journal, Vol. 21, No. 9, pp. 1232-1240.

Mohler, S.R., "Wind-US Unstructured Flow Solutions for a Transonic Diffuser," NASA CR-2005-213417, January 2005.

Turbulent Flow Past a Wall-Mounted Hump

In this application, AcuSolve is used to simulate fully developed turbulent flow past a smooth hump on the lower wall of a flow domain. AcuSolve results are compared with experimental results as described in Seifert and Pack (2002) and on the NASA Langley Research Center Turbulence Modeling Resource web page. The close agreement of AcuSolve results with experimental data and reference turbulence model performance validates the ability of AcuSolve to model cases with turbulent flow moving past a wall protrusion resulting in flow separation and recovery.

Problem Description

The problem consists of a fluid with material properties close to air flowing through a flow domain containing a well-defined smooth hump with a slit opening at approximately 65 percent of the hump chord. The inlet of the domain is defined with an inflow velocity in the streamwise direction that develops into fully turbulent flow at a Reynolds number (Re) of 936,000, based on the hump chord length of 1.0 m. The density of the flow medium is 1.0 kg/m^3 and the dynamic viscosity is 1.0684 X 10^{-6} kg/m-s. The simulation is conducted with the Reynolds Averaged Navier-Stokes equations using the Spalart Allmaras turbulence model, shear stress transport (SST) model, the K-ω model and Realizable K-ε model to evaluate the performance of the turbulence models. The flow predictions from AcuSolve are compared against experimental data and previously published turbulence model performance for pressure and friction coefficients within the domain.

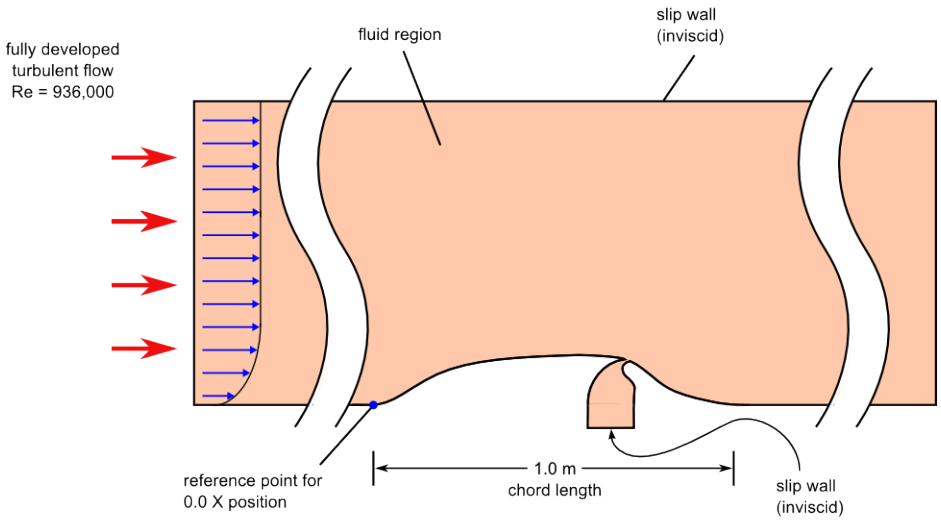


Figure 330: Critical Dimensions and Parameters for Simulating Turbulent Flow Through a Domain with a Wall-Mounted Hump

The upper walls of the domain are specified as slip (inviscid) and the lower walls are specified as no-slip. The inlet velocity and appropriate turbulence parameters are specified in the streamwise direction to match the desired Reynolds Number of 936,000. The outflow pressure is set to zero, and the lower wall on cavity below the hump is set to slip. The problem is simulated as two dimensional with a single layer of elements extruded in the cross stream direction and by defining the side walls as slip.

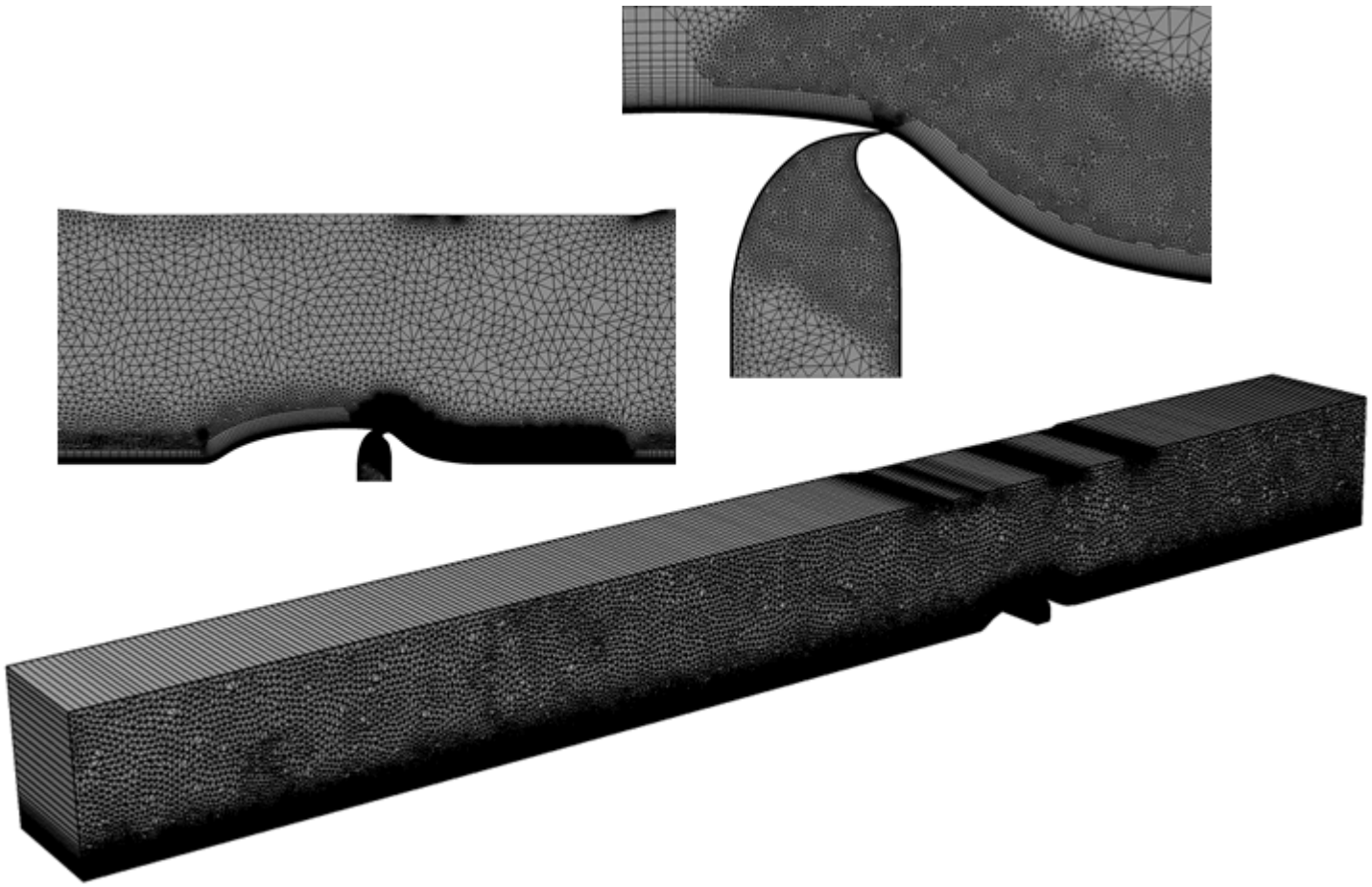


Figure 331: Three Views of the Mesh Used for Simulating Turbulent Flow over a Wall-Mounted Hump (Full Mesh is Shown on the Bottom, with Increased Resolution in Clockwise Views)

AcuSolve Results

The AcuSolve solution converged to a steady state and the results reflect the mean flow conditions within the domain. The images below show contours of velocity within the domain as well as the recirculation region directly downstream of the hump. As the flow enters the domain with a bulk velocity, it begins to develop a turbulent boundary layer near the lower wall prior to reaching the hump. As the flow approaches the hump section, the velocity near the lower wall decreases, but does not recirculate in front of the hump. It then accelerates over the top of the hump and separates immediately after reaching the cavity opening. The recirculation region propagates downstream, before the flow recovers and reattaches to the lower wall.

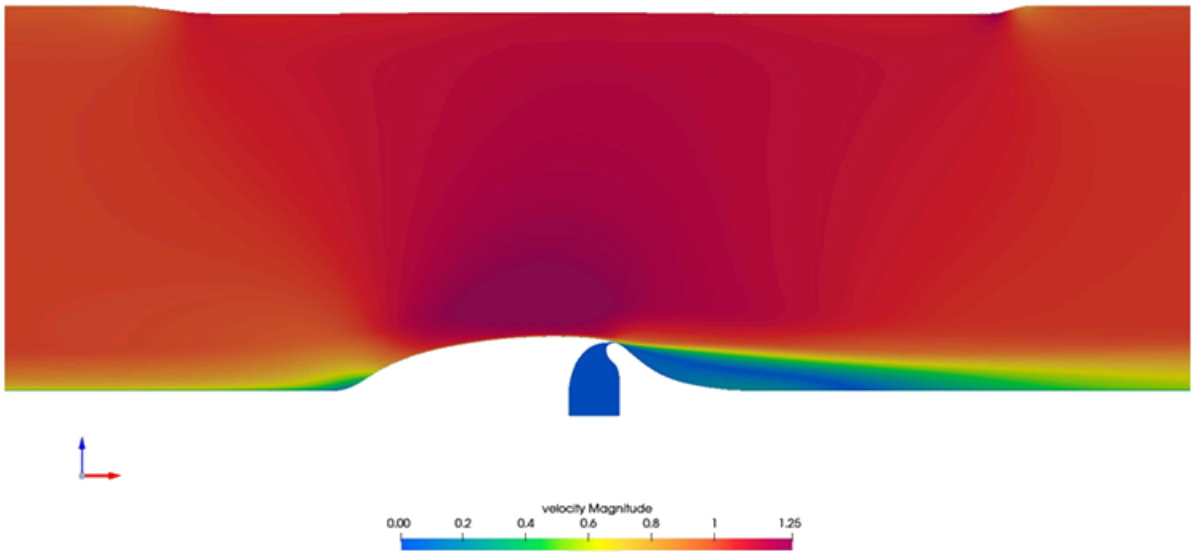


Figure 332: Velocity Contours on the Boundaries of the Domain, Showing Velocity Magnitude

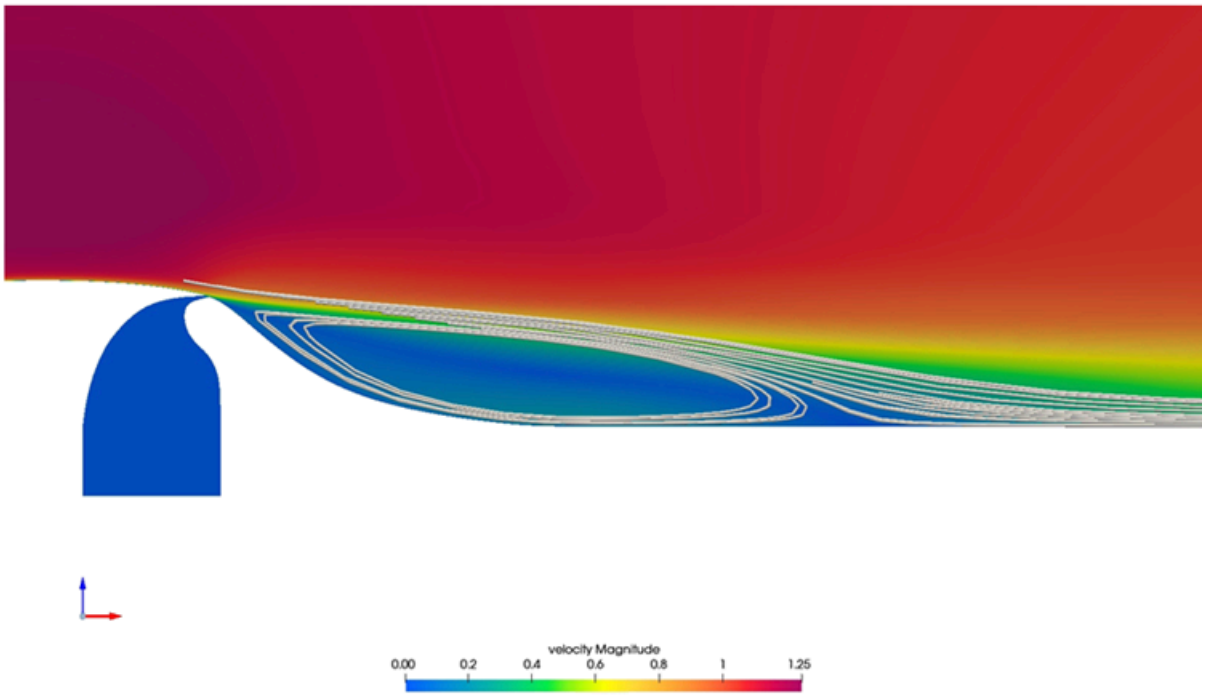


Figure 333: Close up View of Velocity Contours Showing the Recirculation Region with Streamlines (White Lines) Representing the Region of Backflow

The images below show the coefficient of pressure and coefficient of skin friction along the lower wall of the flow domain plotted with experimental results. The non-dimensional values are defined by the integrated inlet pressure and the magnitude of the inlet velocity. The images show black circles representing the experimental measurements (Seifert and Pack 2002), solid red lines for the SA model, solid blue lines for the SST model, solid green lines for the K-ω model and solid cyan lines for the Realizable K-ε model, representing the AcuSolve results. The resulting pressure coefficient within the domain demonstrates that there are minor differences between the four turbulence models. All four

models are shown to perform accurately in predicting the increase in surface pressure on the front of the hump but tend to over predict the skin friction in the wake of the hump, leading to a minor over prediction of the reattachment location. The SA model predicts a slightly larger recirculation region and does not meet the expected recovery pressure compared to SST, K- ω and K-ε models. This performance was found to be consistent with comparisons to other one equation models (NASA 2015).

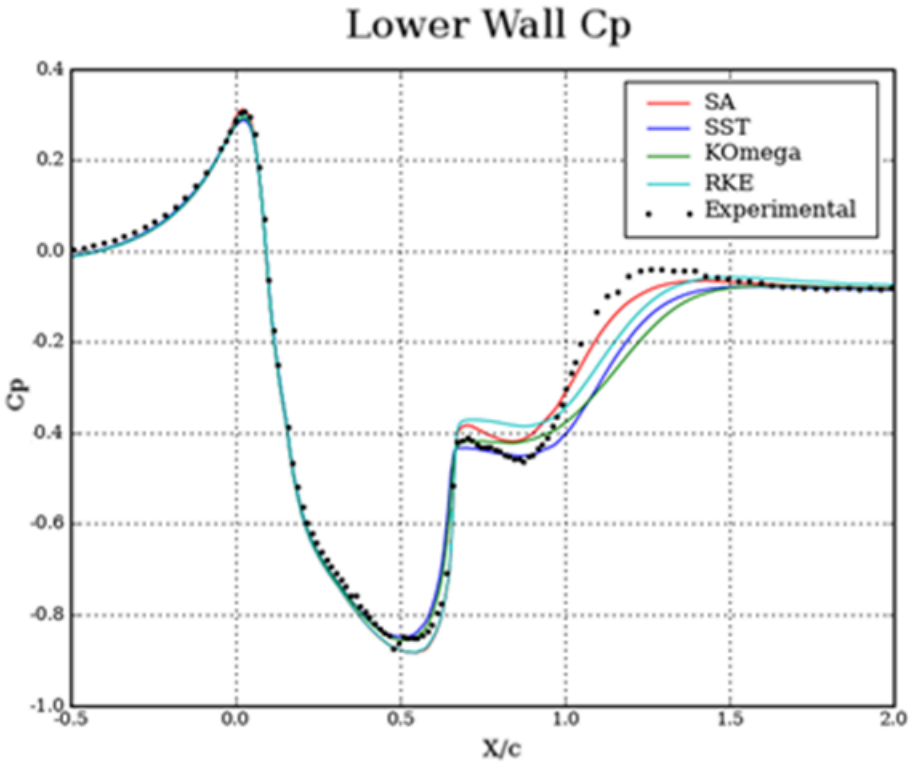


Figure 334: Coefficient of Pressure Along the Lower Wall as the Flow Moves Past the Hump, Where c is the Hump Chord Length and 0.0 is the Reference Location at the Front of the Hump in the X-Direction (Streamwise)

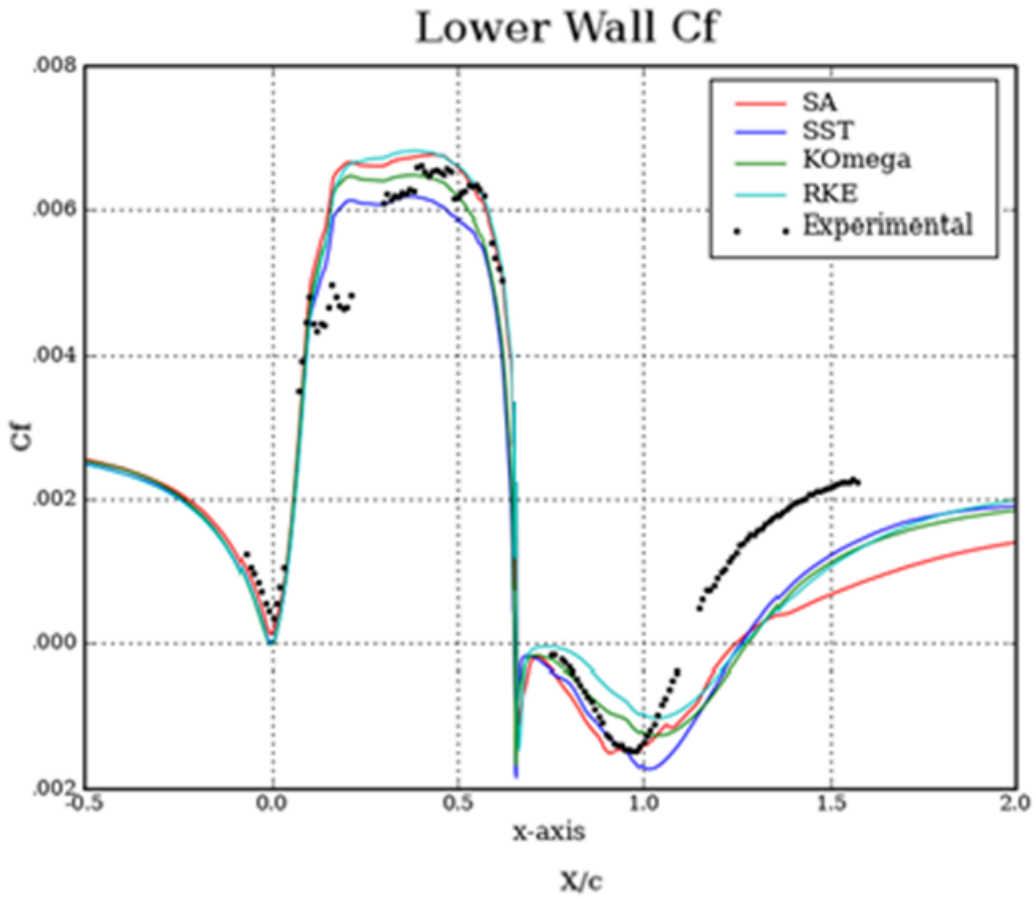


Figure 335: Skin Friction Coefficient Along the Lower Wall as the Flow Moves Past the Hump, Where c is the Hump Chord Length and 0.0 is the Reference Location at the Front of the Hump in the X-Direction (Streamwise)

Summary

In this application, a bulk turbulent flow at a Reynolds number of 936,000 within a flow domain containing a wall-mounted hump is studied and compared against experimental data. The AcuSolve results compare well with the experimental data for pressure coefficient and skin friction coefficient near the hump and downstream. The performance of the four turbulence models were found to be consistent with previously published results for flow over a wall-mounted hump (NASA 2015). For this application, the two equation models appear to outperform the one equation turbulence model, with better agreement for the downstream pressure on the wall. This application demonstrates AcuSolve's ability to predict the distribution of pressure and shear stress on protruding bodies within a turbulent flow field and serves to validate current turbulence modeling capabilities.

Simulation Settings for Turbulent Flow past a Wall-Mounted Hump

SimLab database file: `<your working directory>\wall_mounted_hump_turbulent\wall_mounted_hump_turbulent.slb`

Global

- Problem Description

    - Flow - Steady State
    - Turbulence equation - Spalart Allmaras
- Auto Solution Strategy
    - Max time steps - `100`
    - Convergence tolerance - `0.001`
    - Relaxation factor - `0.4`
- Material Model
    - Fluid
        - Density - `1.0` kg/m3
        - Viscosity - `1.0684e-6` kg/m-sec

  Model
- Volumes
    - Fluid
        - Element Set
            1. Material model - Fluid
- Surfaces
    - +Y
        - Simple Boundary Condition
            1. Type - Slip
    - -Y
        - Simple Boundary Condition
            1. Type - Slip
    - Cavity walls
        - Simple Boundary Condition
            1. Type - Wall
            2. Turbulence wall type - Wall Function
    - Hump walls
        - Simple Boundary Condition
            1. Type - Wall
            2. Turbulence wall type - Wall Function
    - Hump walls - downstream
        - Simple Boundary Condition
            1. Type - Wall
            2. Turbulence wall type - Wall Function
    - Inlet
        - Simple Boundary Condition
            1. Type - Inflow

2. Inflow type - Velocity
3. Inflow velocity type - Cartesian
4. X Velocity - `1.0` m/sec
5. Turbulence input type - Direct
6. Kinetic energy 1.2615e-5 m^2/s^2
7. Dissipation rate 0.00106 m^2/s^3

- Lower slip
  - Simple Boundary Condition
    1. Type - Slip
- Lower wall
  - Simple Boundary Condition
    1. Type - Wall
    2. Turbulence wall type - Wall Function
- Nozzle walls
  - Simple Boundary Condition
    1. Type - Wall
    2. Turbulence wall type - Wall Function

- Outlet
  - Simple Boundary Condition
    - Type - Outflow
- Slip
  - Simple Boundary Condition
    - Type - Slip

References

A Seifert and L.G. Pack. "Active Flow Separation Control on Wall-Mounted Hump at High Reynolds Numbers". AIAA Journal. 40(7). 2002.

NASA Langley Research Center Turbulence Modeling Resource web page. http://turbmodels.larc.nasa.gov/nasahump_val.html. Accessed June 2015.

Laminar Couette Flow with Imposed Pressure Gradient and Heated Walls

In this application, AcuSolve is used to simulate the flow of a highly viscous fluid between a moving and a stationary plate with an imposed pressure gradient and fixed temperature on the walls. AcuSolve results are compared with analytical results described in White (1991). The close agreement of AcuSolve results with analytical results validates the ability of AcuSolve to model cases with imposed pressure gradients and viscous heating.

Problem Description

The problem consists of a viscous fluid between two plates in a two-dimensional domain, as shown in the following image, which is not drawn to scale. The domain is 1.0 m high and 1.5 m long. The top plate moves with a constant velocity of 3.0 m/sec and the bottom plate is fixed. To simulate a fully developed flow with a relatively short length domain there is a mean-pressure gradient of -12 Pa/m applied to the fluid in the streamwise direction, defined as a body force acting on the entire fluid. The lower wall is held at a fixed temperature of 273.0 K, while the upper wall is held at a fixed temperature of 274.0 K. The problem is simulated with periodic boundaries in the streamwise direction. The Reynolds number of the flow, based on the distance between the plates is 0.3, indicating laminar flow. The flow field develops from the pressure gradient, the motion of the top plate, and the viscous shear stresses near the plates. The shear stress within the domain causes the temperature to increase within the channel.

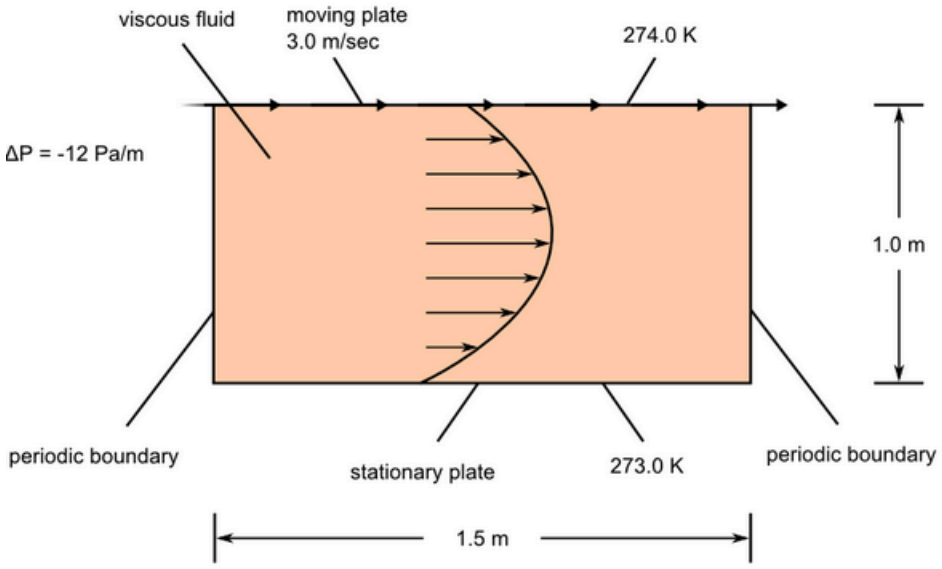


Figure 336: Critical Dimensions and Parameters for Simulating Laminar Couette Flow with an Imposed Pressure Gradient and Heated Walls

The simulation was performed as a two dimensional problem by constructing a volume mesh that contains a single layer of elements extruded in the cross stream direction, normal to the flow plane and by imposing symmetry boundary conditions on the extruded planes. Due to the periodic natural of the flow, a single element extrusion in the streamwise direction is used to reduce the model size.

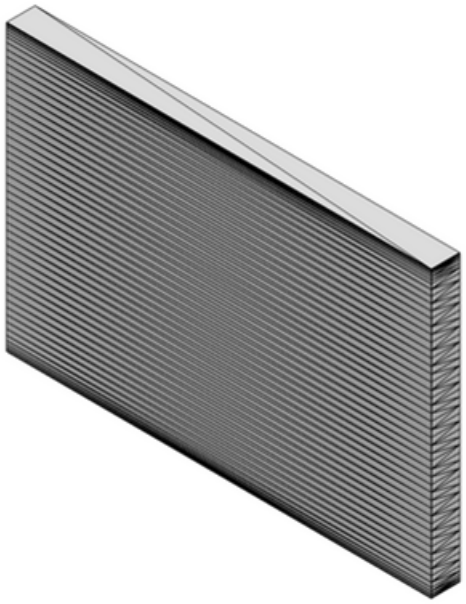


Figure 337: Mesh used for Simulating Laminar Couette Flow with an Imposed Pressure Gradient and Heated Walls

AcuSolve Results

The AcuSolve solution converged to a steady state and the results reflect the mean flow conditions. The simulation results show a flow field with a nearly linear distribution of velocity, with the peak at the top wall. The flow develops primarily because of the shear stress acting on the fluid near both the moving plate and the stationary plate. The temperature variation between the two plates develops due to the viscous heating effects that increase the temperature within the channel, with the maximum near the central height of the domain. The following figure shows the temperature distribution between the two plates and velocity vectors indicating the velocity profile.

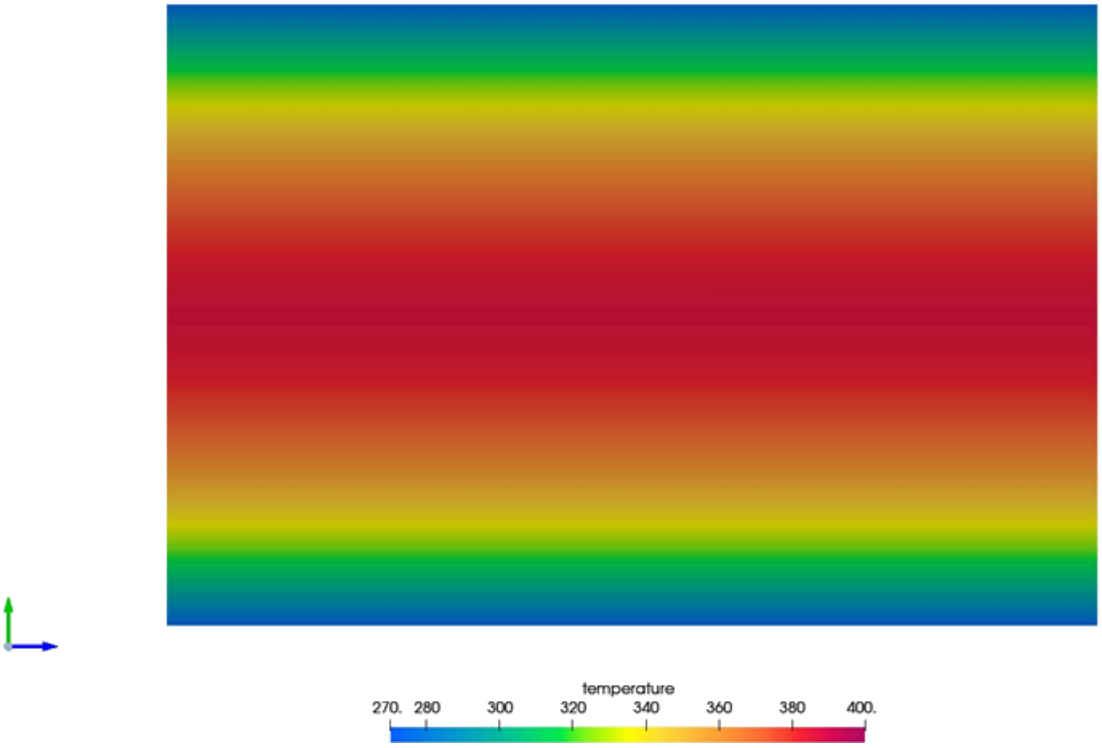


Figure 338: Contours of Temperature Between the Plates, with Velocity Vectors

The following image demonstrates the accuracy of the solution compared to the analytical results as computed by the solution for viscous heating within a channel with a moving upper boundary.

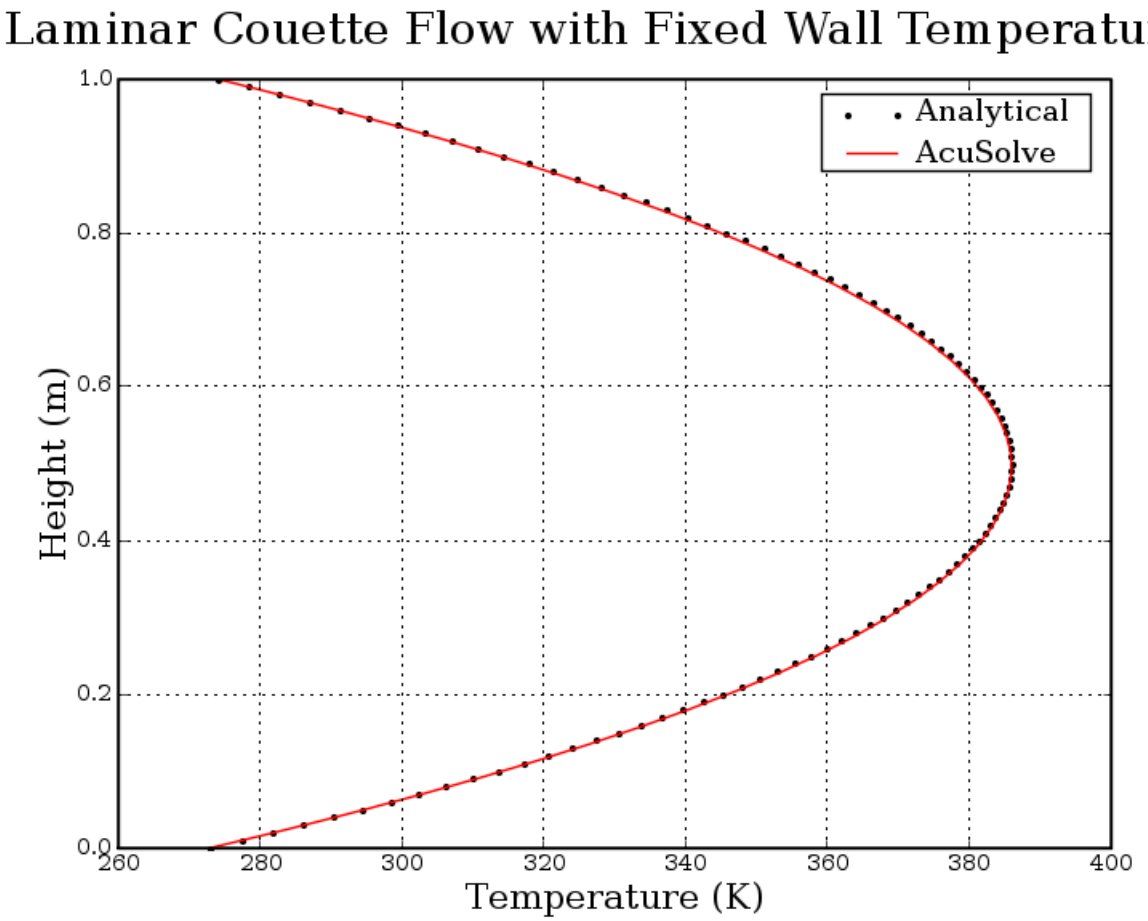


Figure 339: Temperature Plotted Against Height above the Bottom of the Flow Field (Temperature is Presented on the X Axis to Better Represent the Distribution Between the Plates in the Streamwise Direction)

Summary

In this application, a fully developed laminar flow between two plates with fixed temperature is studied and compared against analytical data. The AcuSolve results compare well with the analytical data for the temperature distribution between the two plates. The simulation indicates that the velocity profile arises due to the combination of the viscous shearing and the velocity of the upper plate. The velocity and temperature profiles computed by AcuSolve demonstrate how highly viscous fluids tend to direct the flow regime. AcuSolve demonstrates the ability to predict the analytical solution for viscous heating between two flat plates with moving and stationary boundaries and an imposed pressure gradient.

Simulation Settings for Laminar Couette Flow with Imposed Pressure Gradient and Heated Walls

SimLab database file: `<your working directory>\couette_laminar_heat\couette_laminar_heat.slb`

Global

- Problem Description

    - Flow - Steady State
    - Temperature equation - Advective Diffusive
    - Turbulence equation - Laminar
- Auto Solution Strategy
    - Relaxation factor - `0.2`
- Material Model
    - Fluid
        - Density - `1.0` kg/m3
        - Specific Heat - `1.0` J/kg-K
        - Viscosity - `100.0` kg/m-sec
- Body Force
    - DP/DL
        - Gravity
            1. Z-component - `18.0` m/sec2

Model

- Volumes
    - Fluid
        - Element set
            1. Material model - Fluid
            2. Body force - DP/DL
            3. Viscous heating - on
- Surfaces
    - Max_X
        - Simple Boundary Condition
            1. Type - Symmetry
    - Max_Y
        - Simple Boundary Condition
            1. Type - Wall
            2. Wall velocity type - Cartesian
            3. Z-velocity - `3.0` m/s
            4. Temperature - `274.0` K
    - Max_Z
        - Simple Boundary Condition - (disabled to allow for periodic conditions to be set)
    - Min_X
        - Simple Boundary Condition
            1. Type - Symmetry
    - Min_Y

        - Simple Boundary Condition
            1. Type - Wall
            2. Temperature - `273.0` K
    - Min_Z
        - Simple Boundary Condition - (disabled to allow for periodic conditions to be set)
- Periodics
    - Periodic 1 all
        - Periodic Boundary Conditions
            1. Type - Periodic

References

F. M. White. "Viscous Fluid Flow". Section 3-3.2. McGraw-Hill Book Co., Inc. New York. 1991.

External Flow

6

This section includes validation cases that consider unbounded simulation domains where external flow is present over solid bodies, leading to free boundary layer development.

This chapter covers the following:

- Turbulent Flow Behind an Open-Slit V (p. 451)
- Turbulent Flow Over a NACA 0012 Airfoil (p. 458)
- Oscillating Laminar Flow Around a Circular Cylinder (p. 466)
- Separated Laminar Flow Over a Blunt Plate (p. 471)
- Turbulent Mixing Layers in an Open Channel (p. 478)
- Laminar to Turbulent Transition Over an Airfoil (p. 483)
- Turbulent Flow Over an Oscillating Rigid Body Assembly (p. 488)
- Turbulent Flow Through a Heated Periodic Channel (p. 495)

Turbulent Flow Behind an Open-Slit V

In this application, AcuSolve is used to simulate turbulent flow of air through and behind a two dimensional open-slit V. AcuSolve results are compared with experimental results adapted from Yang and Tsai (1993). The close agreement of AcuSolve results with experimental results validates the ability of AcuSolve to model the Coandă effect.

Problem Description

The problem consists of air flowing through and past an open-slit V positioned within a flow domain, as shown in the following image, which is not drawn to scale. The flow domain is 0.3 m long and 0.1 m high. The narrow end of the V is positioned 0.05 m from the domain inlet. The slit in the V is 0.002 m high. The V widens to 0.022 m at 0.075 m from the domain inlet. Air enters the domain with a constant velocity of 20 m/s. The upper and lower limits of the domain are defined as no-slip boundary conditions.

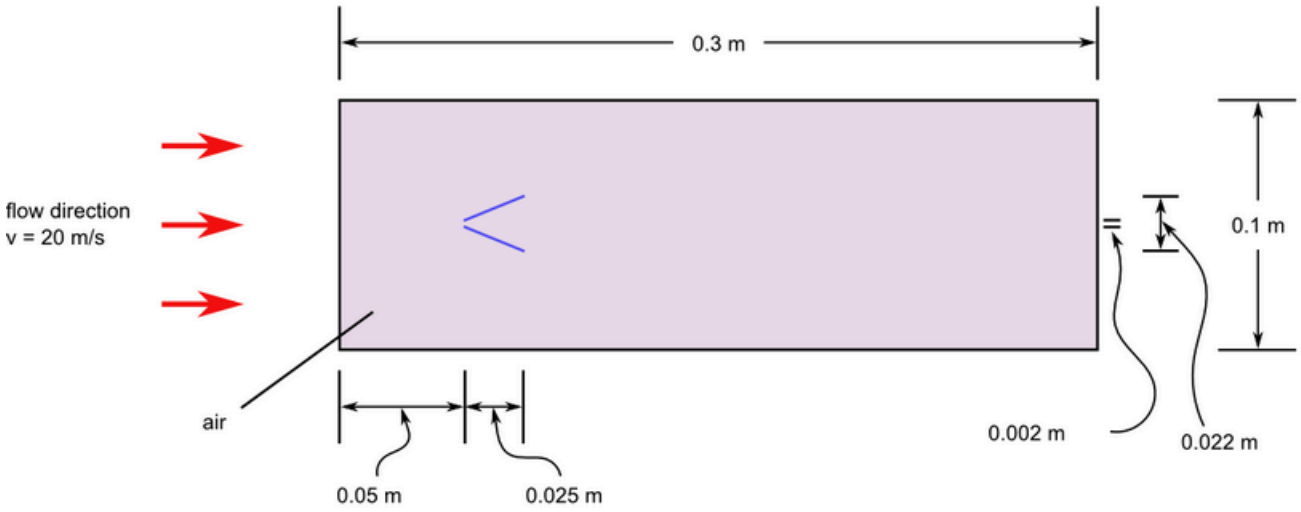


Figure 340: Critical Dimensions and Parameters for Simulating Turbulent Flow Behind an Open-Slit V

The simulation was performed as a two dimensional problem by restricting flow in the out-of-plane direction through the use of a mesh that is one element thick. A coarse mesh is used throughout much of the domain, with mesh refinement closer to the V.

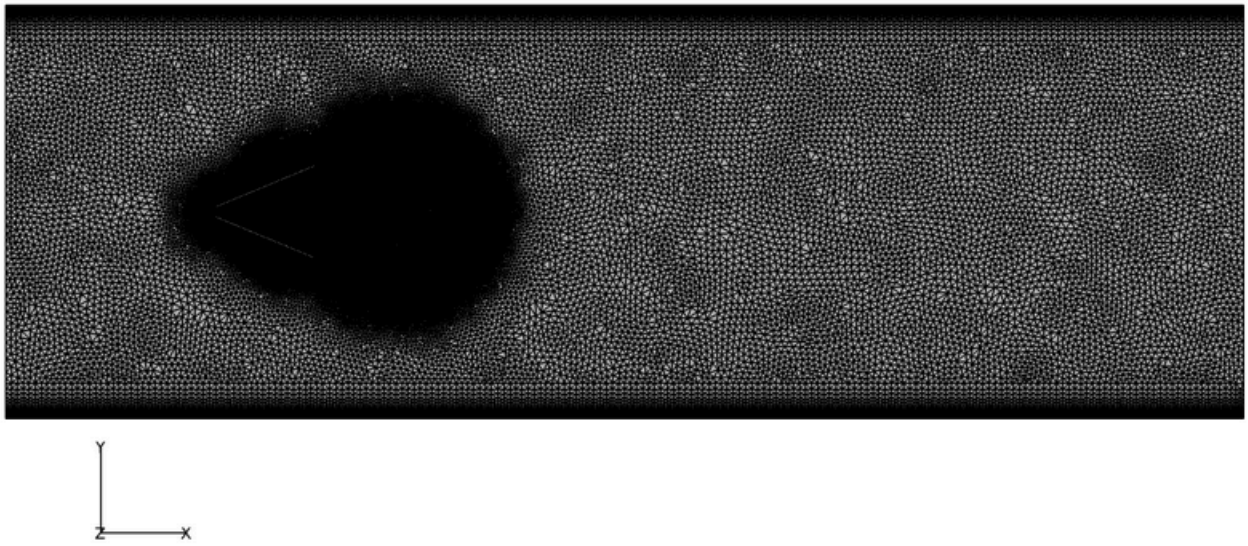


Figure 341: Mesh used for Simulating Turbulent Flow Behind an Open-Slit V (the V Lies Within the Dense Area of the Mesh)

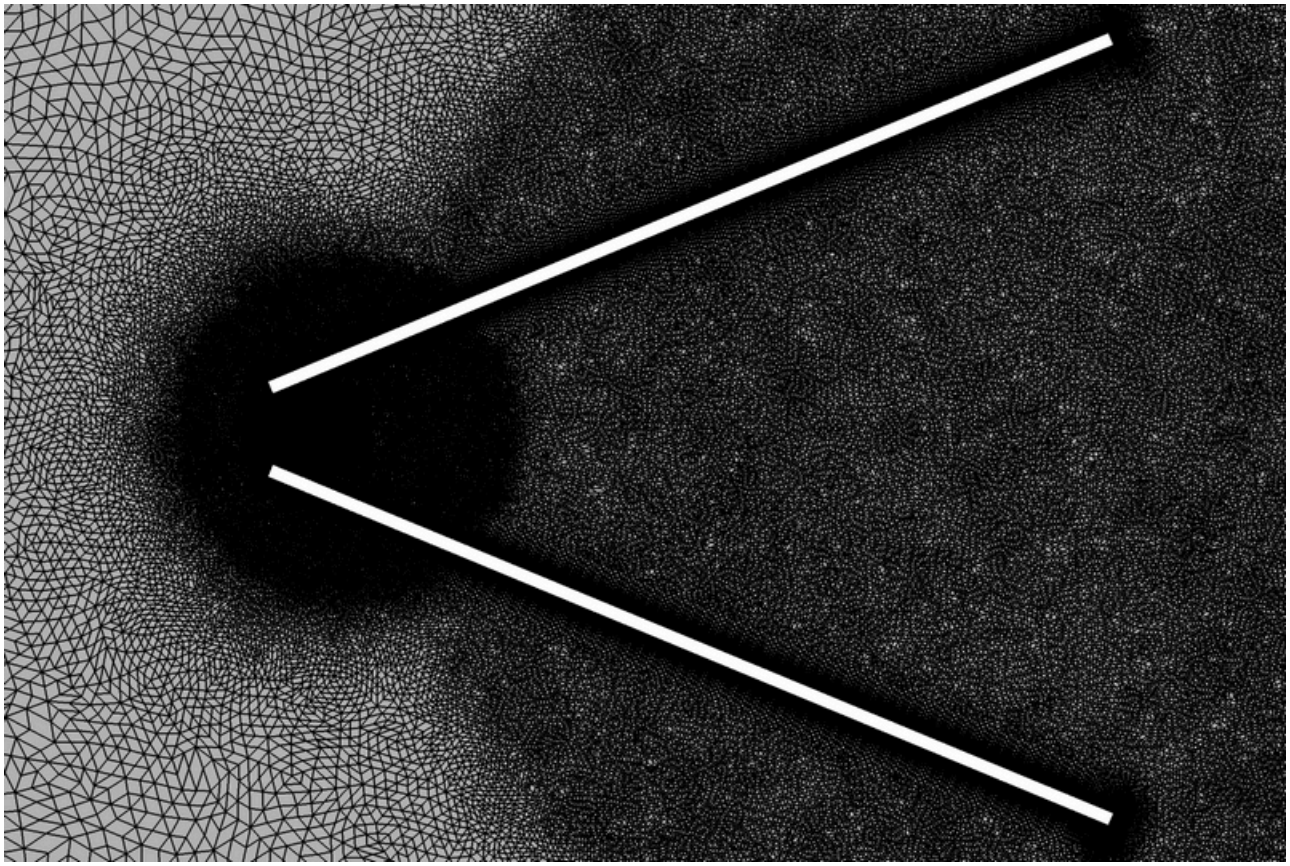


Figure 342: Mesh Surrounding the Open-Slit V

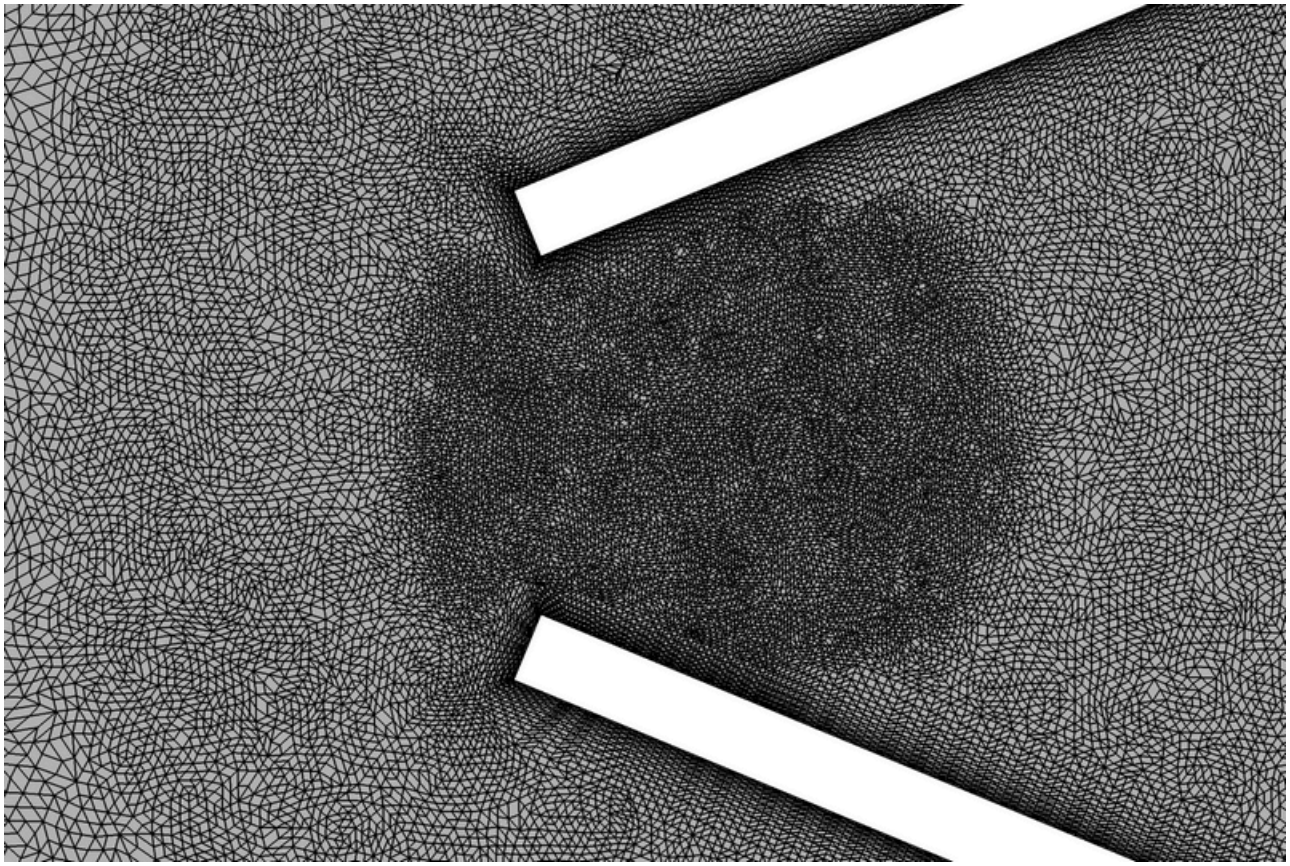


Figure 343: Mesh Near the Open Slit

AcuSolve Results

The AcuSolve solution converged to a steady state and the results reflect the mean flow conditions. Air flows through the open slit in the V and accelerates while being forced to one side due to the Coandă effect. As air encounters the exterior of the widening gutter, velocity increases and the wake induces recirculation near the exit of the V. The recirculation zone extends downstream of the V gutter.

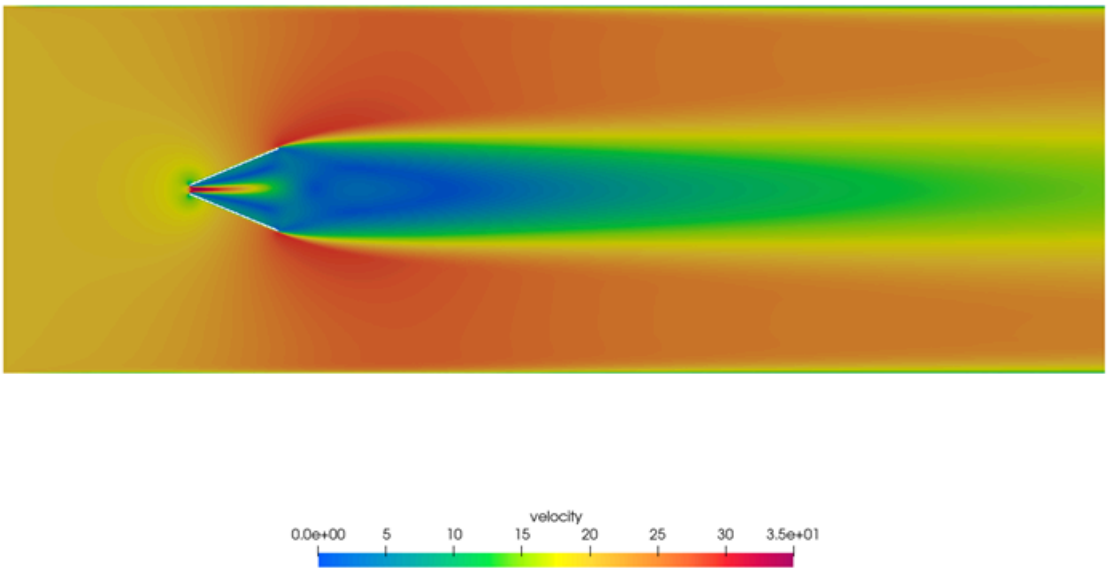


Figure 344: Contours of X-Velocity of Flow Through and Around an Open-Slit V (the Vertical Line Represents the Location, 0.022 m Downstream from the V exit, at Which Experimental Data is Compared to AcuSolve Results)

AcuSolve results were compared to experimental results at different heights 0.022 m behind the V exit. X-velocity is near zero at the bottom of the domain (height = -0.05 m), rising steeply with distance from the wall. The velocity gradient decreases until approximately 0.018 m below the center line of the domain, which is slightly below the bottom of the V exit. The velocity behind the V drops sharply with an increase in height, due to the blockage caused by the presence of the slanted walls. The lowest velocity is just above the center line of the domain.

The slight asymmetry in the velocity profile in the wake of the V is expected due to the Coandă effect.

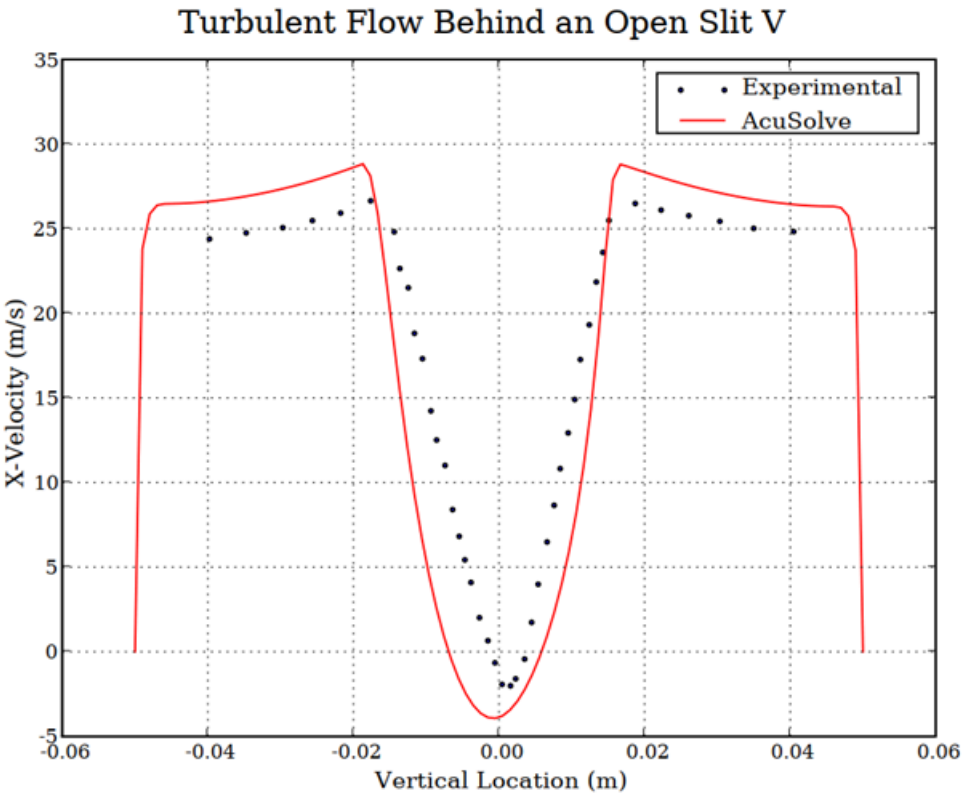


Figure 345: X-Velocity Plotted Against Vertical Location 0.0022 m Downstream of the V Exit

Summary

The AcuSolve results compare well with the experimental results for flow through and around an open-slit V. In this application, the V-shaped geometry diverts flow towards the side walls of the channel and also creates a high-velocity jet through the slit. The low pressure associated with the jet causes a deflection towards the walls of the V, resulting in an asymmetric flow field within the V shape. This application illustrates the ability of AcuSolve to accurately predict the Coandă effect. The acceleration of the flow due to the deflection along the V-shaped walls and the momentum deficit in the wake of the V is captured accurately.

Simulation Settings for Turbulent Flow Behind an Open-Slit V

HyperMesh CFD database file: `<your working directory>\v_gutter_turbulent \v_gutter_turbulent.hm`

Global

- Problem Description
  - Analysis type - Steady State
  - Turbulence equation - Spalart Allmaras
- Auto Solution Strategy
  - Relaxation factor - `0.5`
- Material Model

- Air
  - Density - `1.0` kg/m3
  - Viscosity - `1.8333e-05` kg/m-sec

Model

- Volumes
  - Fluid
    - Element Set
      1. Material model - Air
- Surfaces
  - Inlet
    - Simple Boundary Condition
      1. Type - Inflow
      2. Inflow type - Velocity
      3. X velocity - `20.0` m/sec
      4. Eddy viscosity - `0.000800426` m2/sec
  - LE_TE
    - Simple Boundary Condition
      1. Type - Wall
  - Outlet
    - Simple Boundary Condition
      1. Type - Outflow
  - Symm_MaxZ
    - Simple Boundary Condition
      1. Type - Slip
  - Symm_MinZ
    - Simple Boundary Condition
      1. Type - Slip
  - V_Walls
    - Simple Boundary Condition
      1. Type - Wall
  - Walls
    - Simple Boundary Condition
      1. Type - Wall

References

J.-T. Yang and G.-L. Tsai. "Near-wake flow of a v-gutter with slit bleed". Journal of Fluid Engineering. 115:13-20. March, 1993.

Turbulent Flow Over a NACA 0012 Airfoil

In this application, AcuSolve is used to simulate turbulent flow of a fluid over a NACA 0012 airfoil at 3 angles of attack, 0 degrees, 10 degrees, and 15 degrees. AcuSolve results are compared with experimental results for coefficients of pressure, lift, and drag reported by NASA. The close agreement of AcuSolve results with experimental results validates the ability of AcuSolve to model external aerodynamics.

Problem Description

The problem consists of a NACA 0012 airfoil located in the center of a cylindrical domain, as shown in the following image, which is not drawn to scale. Fluid enters the domain with a velocity of 1.0 m/s. The domain edges are distant, 500 chord lengths, from the airfoil to minimize any far field effects. The problem is set up to simulate high Reynolds number flow, with Re = 6,000,000.

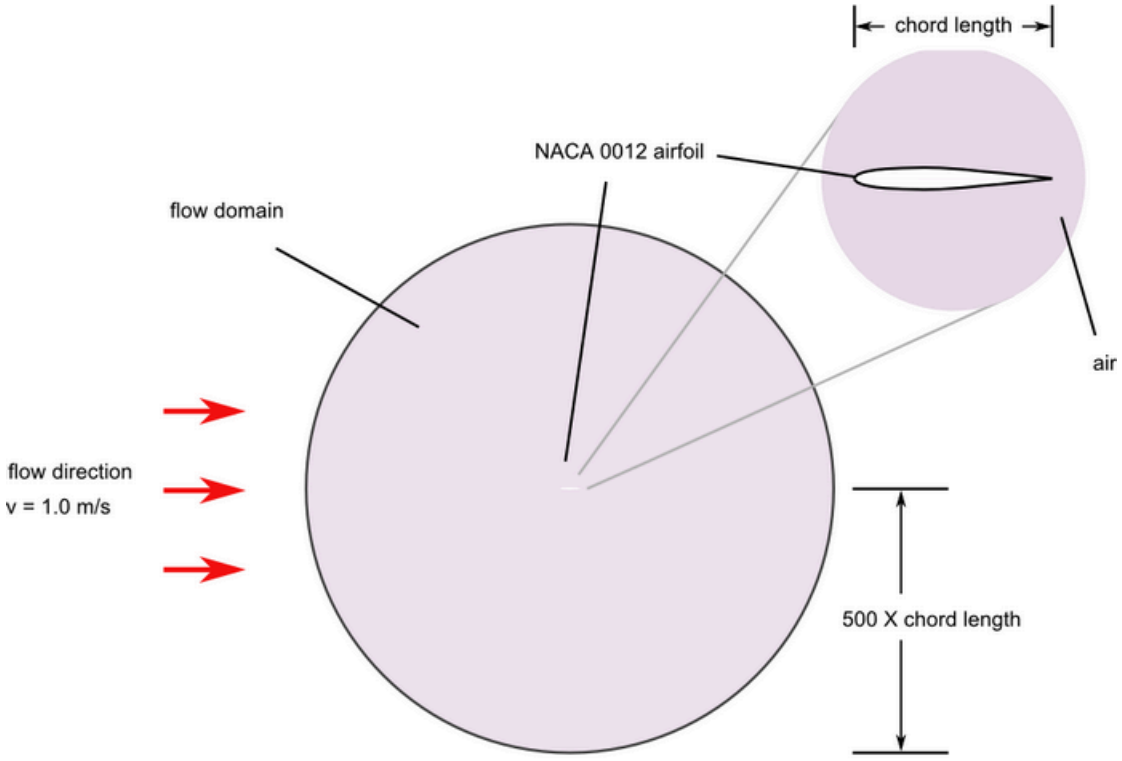


Figure 346: Critical Dimensions and Parameters for Simulating Turbulent Flow over a NACA 0012 Airfoil

The simulation was performed as a two dimensional problem by restricting flow in the out-of-plane direction through the use of a mesh that is one element thick.

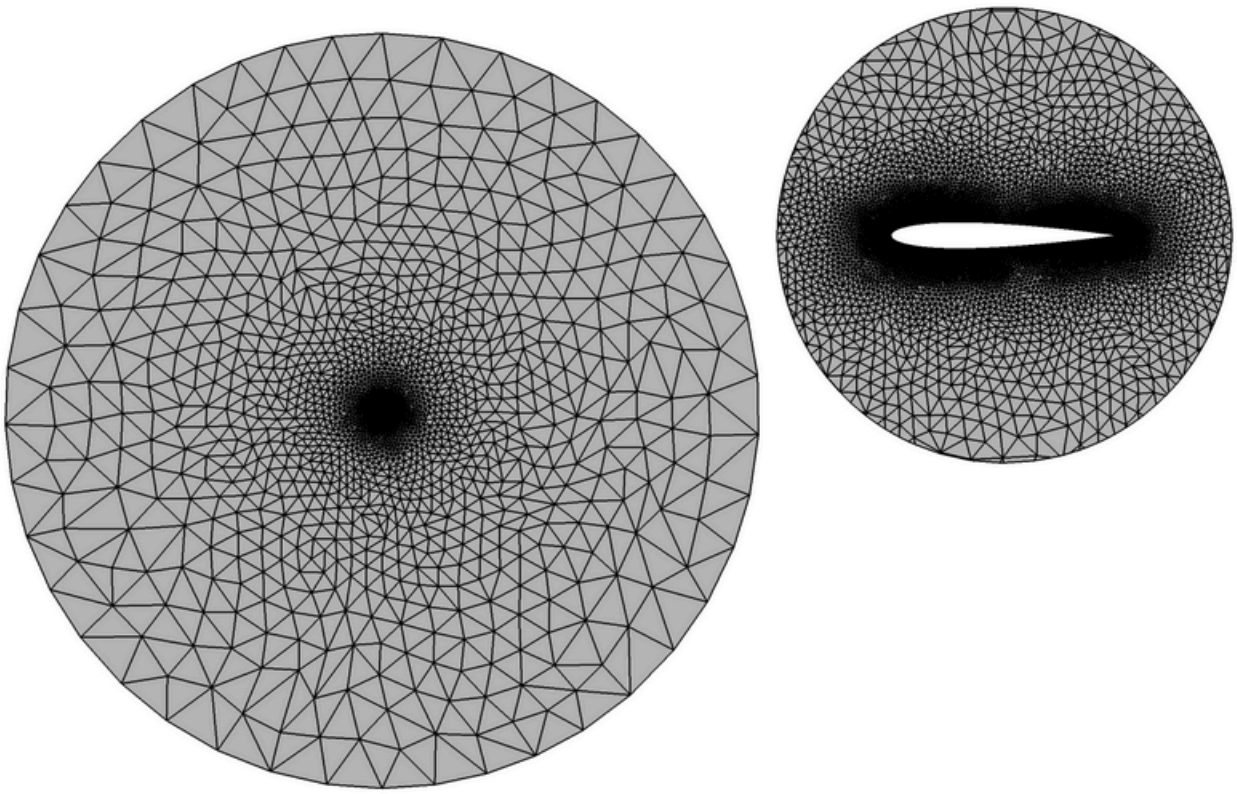


Figure 347: Mesh Used for Simulating Turbulent Flow over a NACA 0012 Airfoil (the Image on the Left Represents the Full Mesh, the Image on the Right Represents Mesh Details near the Airfoil)

AcuSolve Results

The AcuSolve solution converged to a steady state and the results reflect the mean flow conditions for each of the three angles of attack, 0 degrees, 10 degrees, and 15 degrees. For each case, the angle of attack was varied by changing the angle of the incident flow.

> **Note:** This enables the use of a single mesh for all of the simulations.

With a 0 degree angle of attack, the flow field is symmetric as the fluid flows over and under the airfoil. The airfoil impedes the flow, causing stagnation at the leading edge. As the fluid passes over and under the airfoil, velocity increases. As the fluid passes over the blunt trailing edge, a minor amount of flow separation occurs. The flow reattaches shortly after it passes the trailing edge and recovers the mean velocity in the distant far field.

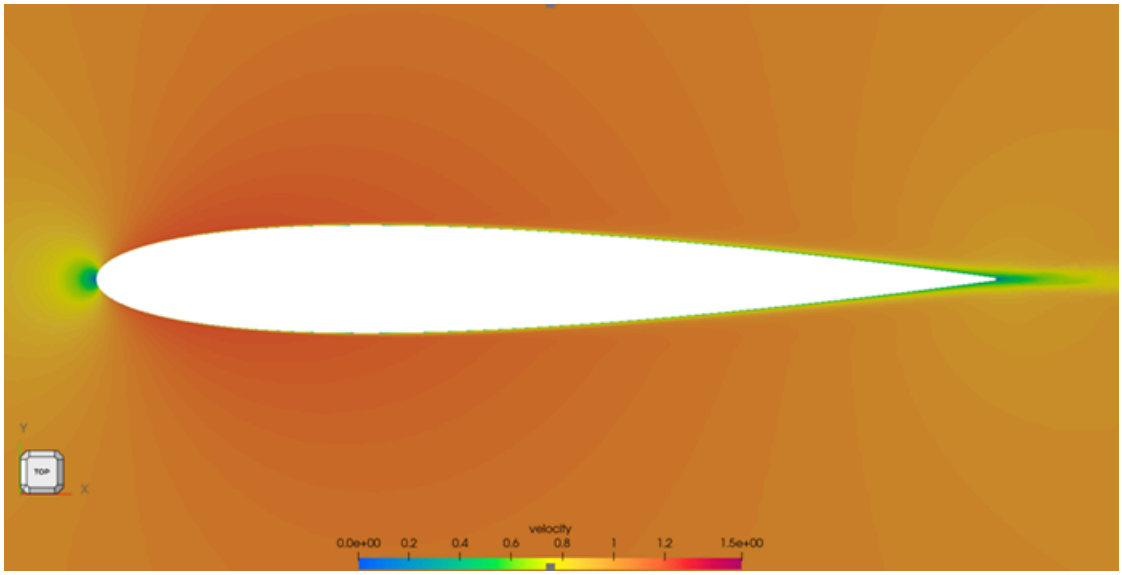


Figure 348: Contours of Velocity Magnitude Where Angle of Attack = 0 Degrees

With a 10 degree angle of attack, the stagnation point is shifted downward (relative to the airfoil), reflective of the shifted angle of attack. Fluid velocity above the airfoil is markedly different than that below the airfoil. A small low-velocity region is evident on the suction side of the airfoil, indicating some separation toward the trailing edge.

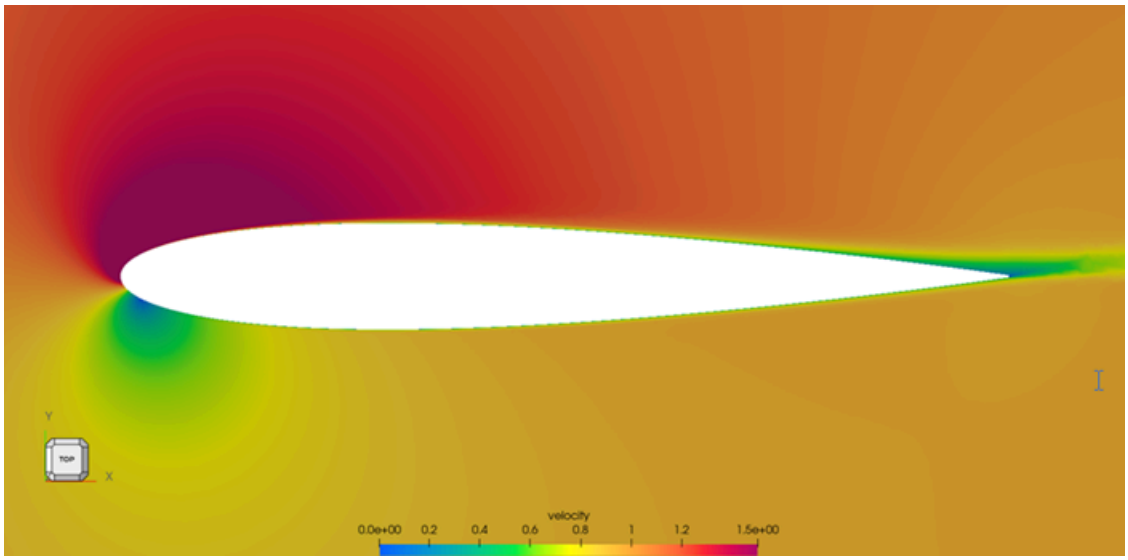


Figure 349: Contours of Velocity Magnitude Where Angle of Attack = 10 degrees

With a 15 degree angle of attack, the stagnation at the front of the airfoil is shifted even farther downward (relative to the airfoil), reflective of the shifted angle of attack. Additionally, the low-velocity wake increases in size, reflecting separation along the suction surface of the airfoil.

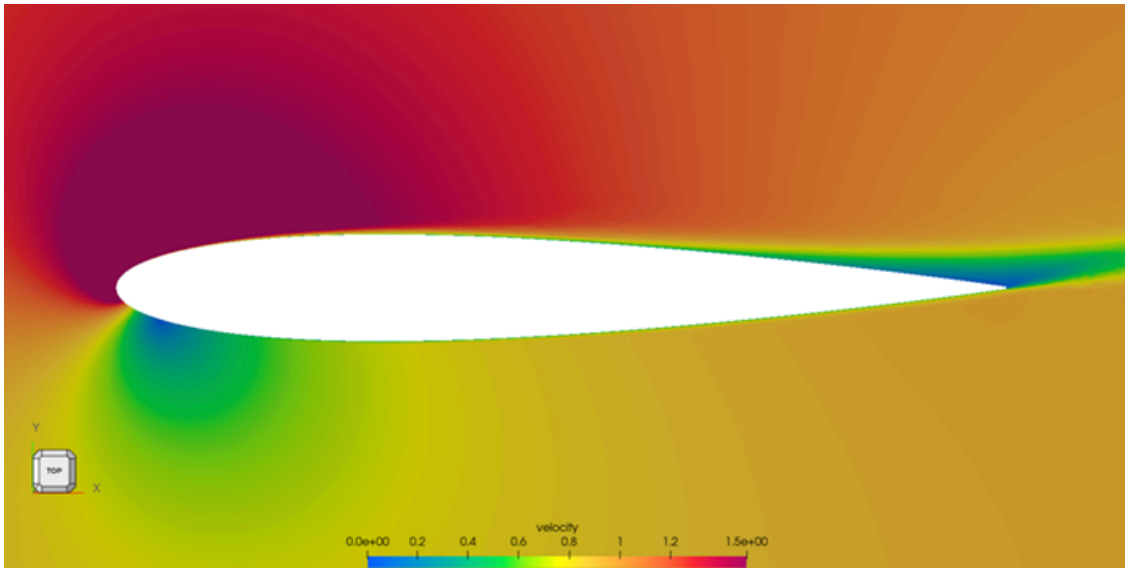


Figure 350: Contours of Velocity Magnitude Where Angle of Attack = 15 Degrees

Experimental values of coefficient of lift (CL) at angles of attack (α) of 10 degrees and 15 degrees and values of drag coefficient (cd) at angles of attack (α) of 0 degrees,10 degrees, and 15 degrees are presented with the corresponding AcuSolve results in the following table.

Table 18:

	CL (α=10)	**CL (α=15)**	**cd (α=0)**	**cd (α=10)**	**cd (α=15)**
Experimental	1.0941	1.5576	0.0082	0.0123	0.0207
AcuSolve	1.0905	1.5428	0.0081	0.0124	0.0208
Percent deviation from experimental	0.33	0.95	1.22	0.81	0.48

AcuSolve values for coefficient of pressure are plotted against experimental results for angles of attack (α) of 0 degrees, 10 degrees, and 15 degrees in the following plots. The results are presented for normalized distance along the airfoil, given by x/c, where x is the distance from the leading edge and c is the chord length.

For each case, AcuSolve is able to predict the flow characteristics at each point along the airfoil surface.

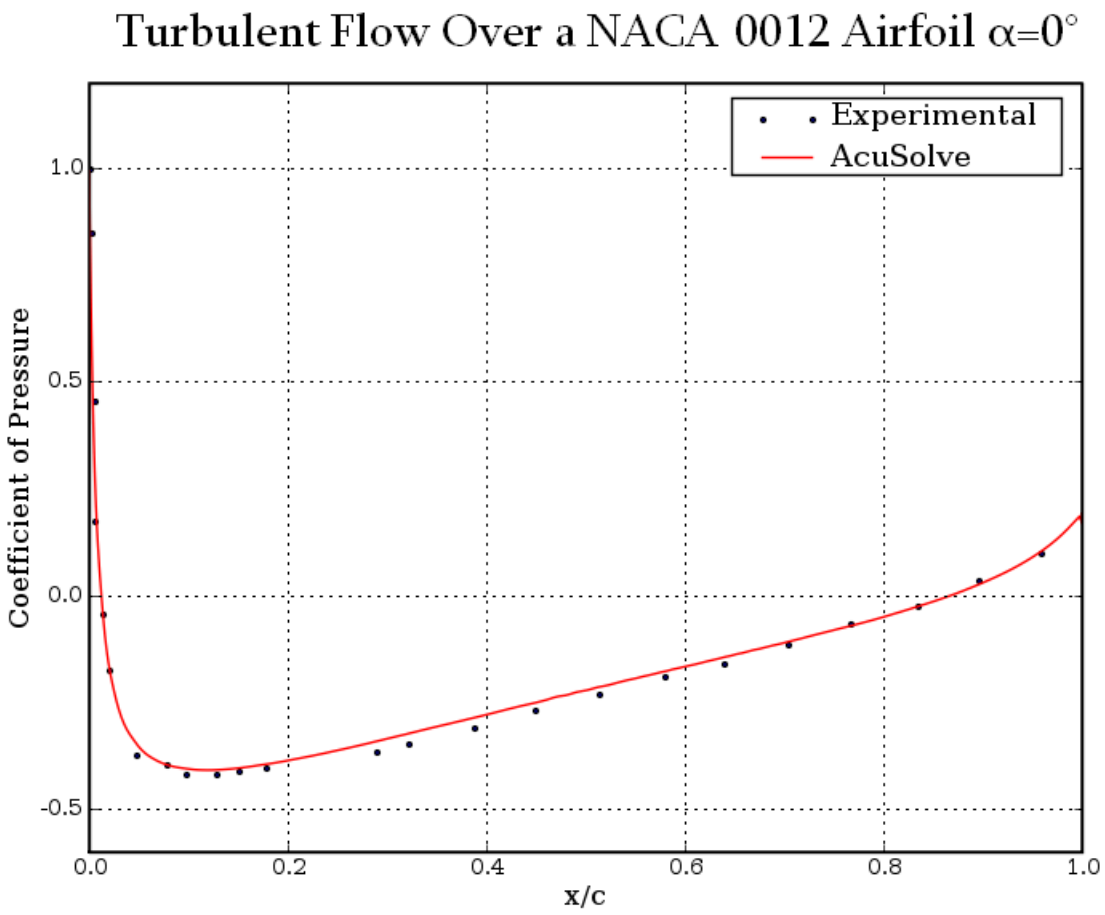


Figure 351: Coefficient of Pressure Plotted Against Normalized Distance Along the Airfoil for Angle of Attack (a) = 0 Degrees

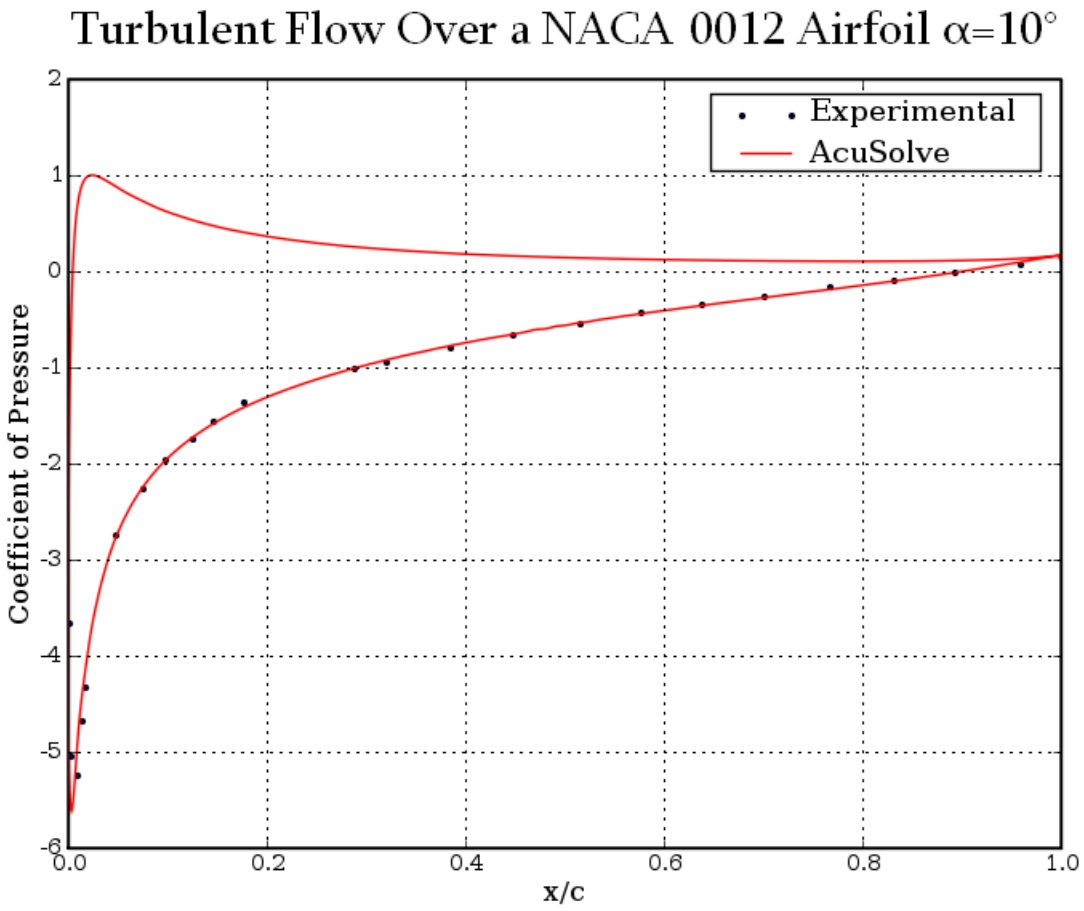


Figure 352: Coefficient of Pressure Plotted Against Normalized Distance Along the Airfoil For Angle of Attack (a) = 10 Degrees

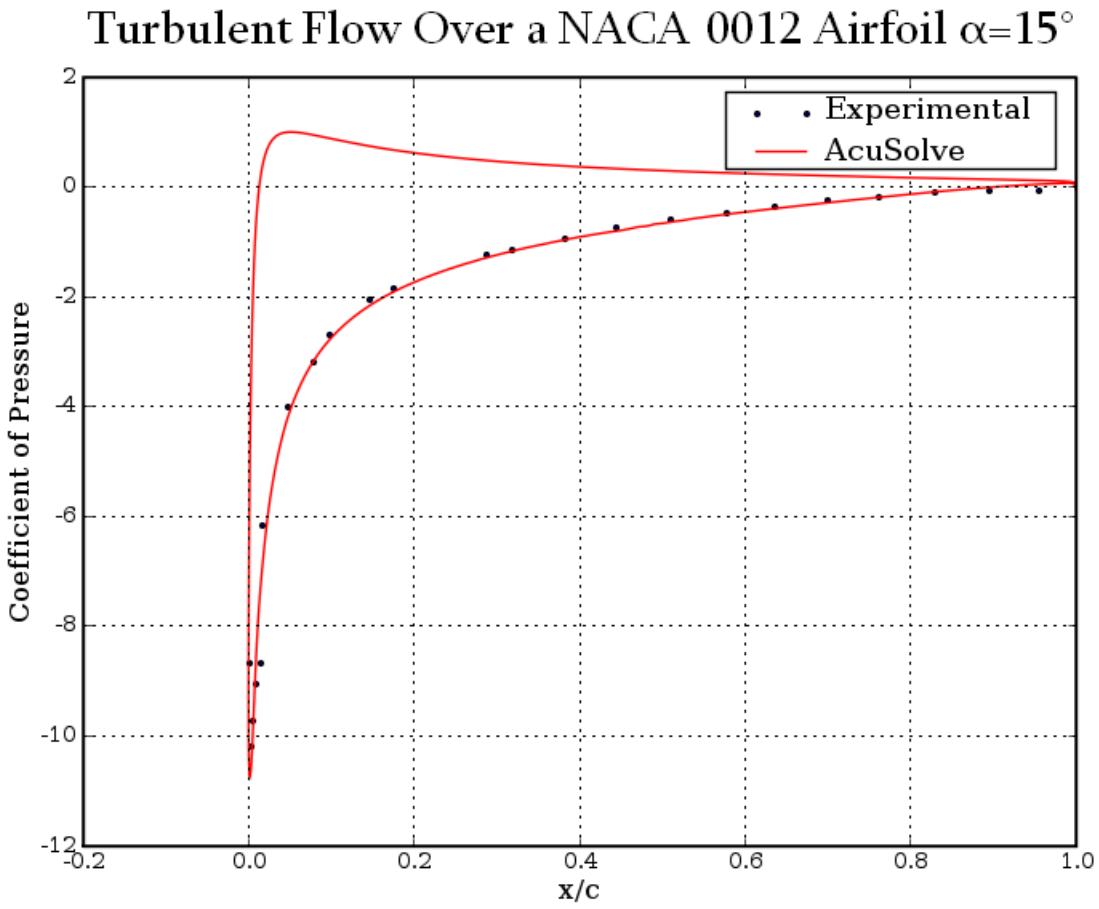


Figure 353: Coefficient of Pressure Plotted Against Normalized Distance Along the Airfoil for Angle of Attack (a) = 15 Degrees

Summary

The AcuSolve results compare well with the experimental results for flow over a NACA 0012 airfoil. In this application, a constant-velocity flow field impinges on the airfoil surface. As the flow convects in the streamwise direction along the airfoil surface, a boundary layer develops. The rate at which the boundary layer develops has significant impact on the viscous stresses present on the airfoil surface. At low angles of attack these stresses dominate the drag on the airfoil. As the angle of attack increases, the flow over the airfoil is no longer symmetric, which leads to the generation of lift. For non-zero angles of attack, the asymmetric pressure distribution on the airfoil creates another source of drag that is combined with the viscous stresses to determine the total drag on the airfoil. The AcuSolve results for coefficients of lift and drag at the 15 percent angle of attack are within 0.91 percent and 0.5 percent of experimental values, respectively. AcuSolve results for coefficient of pressure closely agree with experimental results along the length of the airfoil for all three angles of attack that were investigated.

Simulation Settings for Turbulent Flow Over a NACA0012 Airfoil

HyperMesh CFD database file: `<your working directory>\airfoil_turbulent\airfoil_turbulent.hm`

Global

- Problem Description
  - Analysis type - Steady State
  - Turbulence equation - Spalart Allmaras
- Auto Solution Strategy
  - Convergence tolerance - `0.0001`
  - Relaxation factor - `0.4`
- Material Model
  - Fluid
    - Density - `1.0` kg/m3
    - Viscosity - `1.667e-7` kg/m-sec

  Model
- Volumes
  - Fluid
    - Element Set
      1. Material model - Fluid
- Surfaces
  - +z slip
    - Simple Boundary Condition
      1. Type - Slip
  - -z slip
    - Simple Boundary Condition
      1. Type - Slip
  - airfoil surface
    - Simple Boundary Condition
      1. Type - Wall
  - farfield
    - Simple Boundary Condition
      1. Type - Far Field
      2. X velocity - cos(α) m/sec
      3. Y velocity - sin(α) m/sec
- Eddy viscosity - `1.0e-9` m2/sec

References

NASA - Langley Research Center. http://turbmodels.larc.nasa.gov/naca0012_val_sa.html

Oscillating Laminar Flow Around a Circular Cylinder

In this application, AcuSolve is used to simulate two dimensional, laminar flow over a cylinder to predict separation of flow from the cylinder surface and the flow in the wake area. AcuSolve results are compared with experimental results as described in Tritton (1959). The close agreement of AcuSolve results with experimental results validates the ability of AcuSolve to model cases with unsteady oscillating vortex streets.

Problem Description

The problem consists of a cylinder located in a rectangular domain, as shown in the following image, which is not drawn to scale. A fluid enters the domain with a low velocity (v) of 0.5 m/s. The diameter (D) of the cylinder is 20 cm. The domain extends 10 X D upstream of the cylinder center, 5D above and below the cylinder center, and 40D downstream of the cylinder center. The density of the working fluid is 1 kg/m^3 and the viscosity is 0.001 kg/m-s. The Reynolds number for this problem is 100.

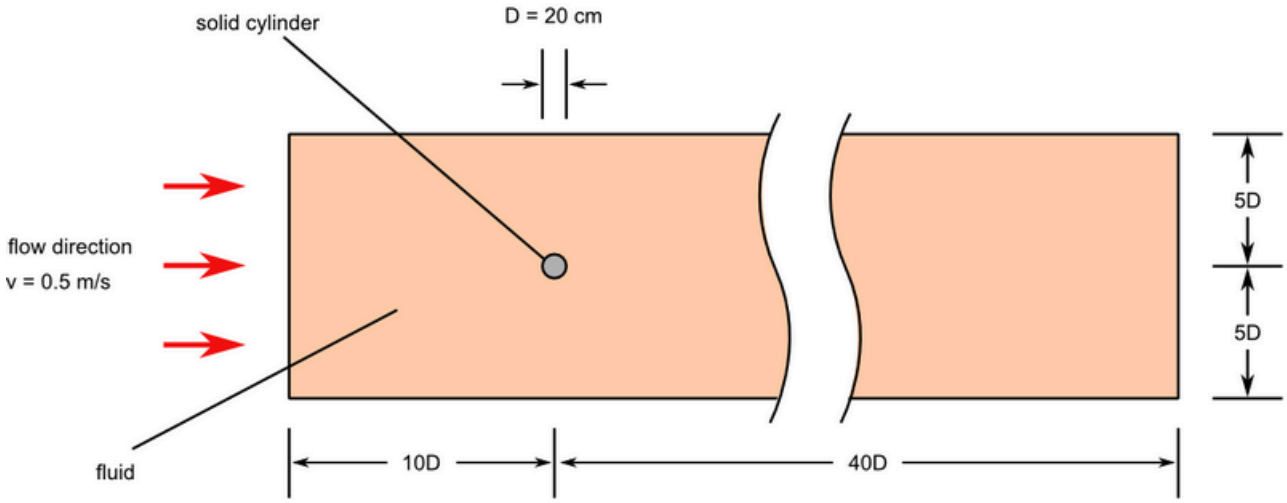


Figure 354: Critical Dimensions and Parameters for Simulating Oscillating Laminar Flow Around a Circular Cylinder

The simulation was performed as a two dimensional problem by constructing a volume mesh that contains a single layer of elements in the extruded direction, normal to the flow plane, and by imposing symmetry boundary conditions on the extruded planes.

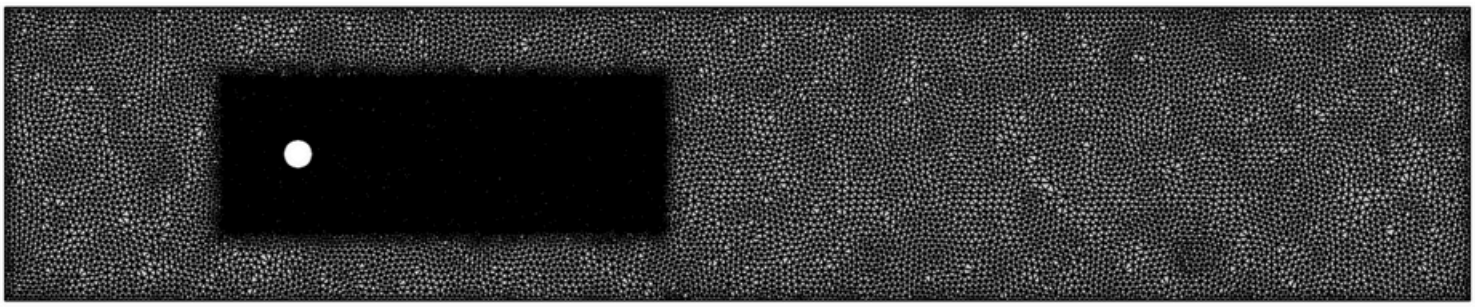


Figure 355: Mesh used for Simulating Oscillating Laminar Flow Around a Circular Cylinder

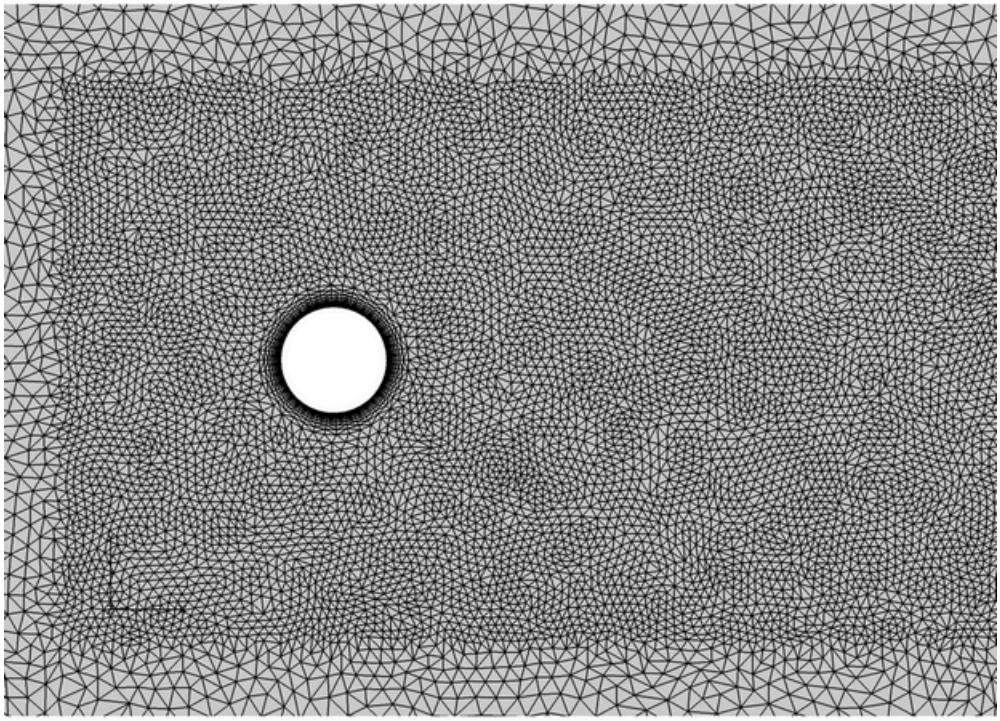


Figure 356: Details of the Mesh Showing Refinement Zone Around the Cylinder

AcuSolve Results

The simulation was run as transient for a time record sufficient to ensure that the vortex shedding in the wake reached a stabilized oscillation frequency. The AcuSolve solution shows an unsteady, oscillating flow field with flow around the cylinder separating from the cylinder surface. A wake area is developed downstream of the cylinder with alternating vortices shedding at a regular frequency from the top and bottom of the cylinder surface. This results in oscillating lift forces that act on the cylinder as shown in the following images.

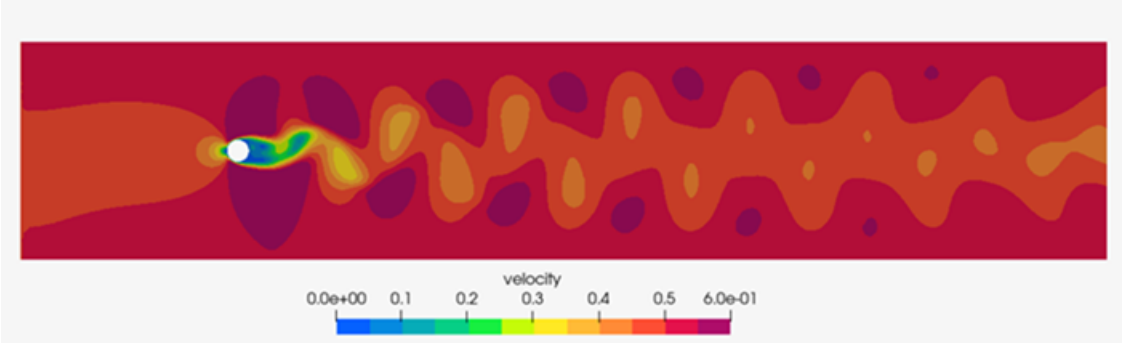


Figure 357: Contours of Velocity Magnitude

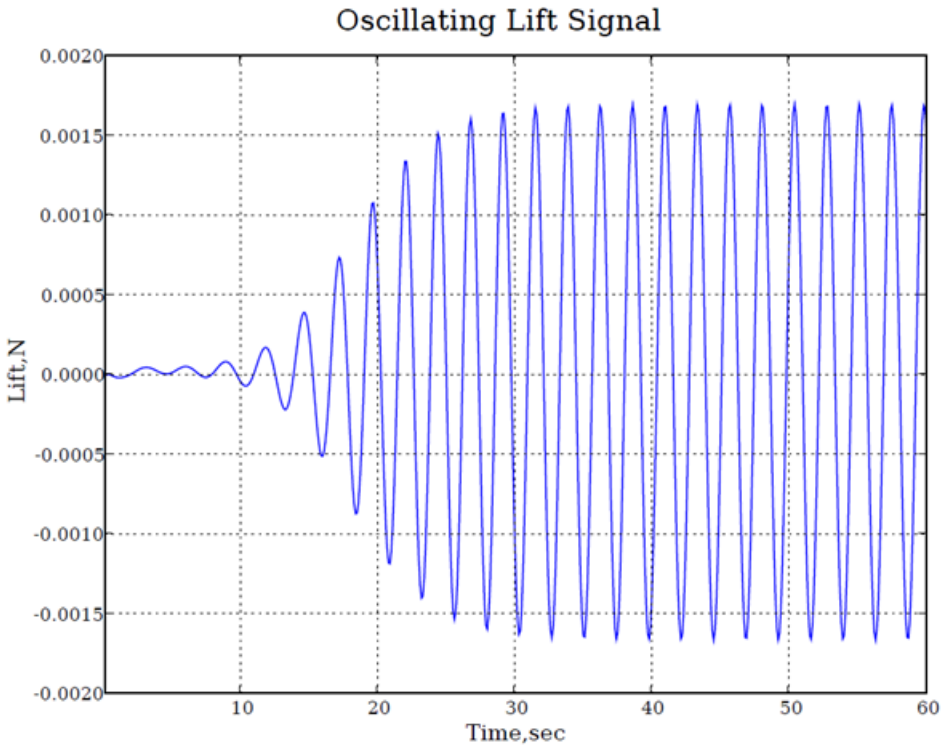


Figure 358: Lift Coefficient (lift force perpendicular to flow) plotted against time. Simulation was run for 600 time steps for a duration of 60 s

The Strouhal number for this simulation, a dimensionless number describing oscillating flows, is used to validate AcuSolve results. The experimental Strouhal number for this problem is given by

$$St = \frac{\omega * L}{V} = 0.165 \qquad (10)$$

where ω is the dominant frequency of oscillations, L is the diameter of the cylinder, and v is the flow velocity.

The peak frequency of the oscillating lift force was computed by transforming the time dependent data into frequency space with a Fourier transform. From the Fourier transform, the AcuSolve-based Strouhal number was calculated. The table below shows the comparison of the Strouhal number provided by the AcuSolve prediction and the measurement given by Tritton (1959).

Table 19:

	Experimental	**AcuSolve**
Strouhal number	0.165	0.173

Summary

In this application, two dimensional flow over a cylinder is achieved by enforcing symmetry conditions on the front and back surfaces of the flow domain. The laminar, unsteady simulation shows the flow separation that leads to alternating vortex shedding. Frequency of the lift force acting on the cylinder is calculated to evaluate the Strouhal number. The AcuSolve solution compares well with results reported by Tritton (1959), differing slightly from the experimental results. In this application, AcuSolve demonstrates the ability to accurately predict oscillating laminar flow around a circular cylinder.

Simulation Settings for Oscillating Laminar Flow Around a Circular Cylinder

HyperMesh CFD database file: `<your working directory>\cylinder_laminar\cylinder_laminar.hm`

Global

- Problem Description
  - Analysis type - Transient
  - Turbulence equation - Laminar
- Auto Solution Strategy
  - Analysis type - Transient
  - Max time - `600` sec
  - Initial time increment - `0.1` sec
- Material Model
  - Fluid
    - Density - `1.0` kg/m3
    - Viscosity - `1.0e-3` kg/m-sec

  Model
- Volumes
  - Volume
    - Element Set
      1. Material model - Fluid
- Surfaces
  - Back
    - Simple Boundary Condition
      1. Type - Symmetry
  - Base

- Simple Boundary Condition
  1. Type - Slip
- Front
  - Simple Boundary Condition
    1. Type - Symmetry
- Inflow
  - Simple Boundary Condition
    1. Type - Inflow
    2. Inflow Type - Average velocity
    3. Average Velocity - `0.5` m/sec
- Outflow
  - Simple Boundary Condition
    1. Type - Outflow
- Top
  - Simple Boundary Condition
    1. Type - Slip

References

D.J. Tritton. "Experiments on the Flow around a Circular Cylinder at Low Reynolds Number". Journal of Fluid Mech. 6(04):547-567. 1959

Separated Laminar Flow Over a Blunt Plate

In this application, AcuSolve is used to simulate the separation of laminar flow over a blunt plate. AcuSolve results are compared with experimental results as described in J.C. Lane and R.I. Loehrke (1980). The close agreement of AcuSolve results with the experimental results validates the ability of AcuSolve to model cases with external laminar flow including separation.

Problem Description

The problem consists of external, laminar flow over a blunt plate 1.5 m long and 0.09 m thick, as shown in the following image, which is not drawn to scale. The fluid flows with a uniform horizontal velocity (v) of 0.045133 m/s. The fluid material used for the simulation has a density of 1.0 kg/m^3 and a dynamic viscosity of 1.7894 X 10^{-5} kg/m-s. The resulting Reynolds number for the flow, based on the plate thickness, is approximately 227. This indicates that the flow over the plate is laminar. As the fluid flows past the leading edge of the plate, the pressure decreases, resulting in a separation region downstream of the leading edge. At some distance downstream from the leading edge, the pressure gradient decreases, and viscous forces cause the recirculation zone to dissipate, allowing the flow to reattach to the plate.

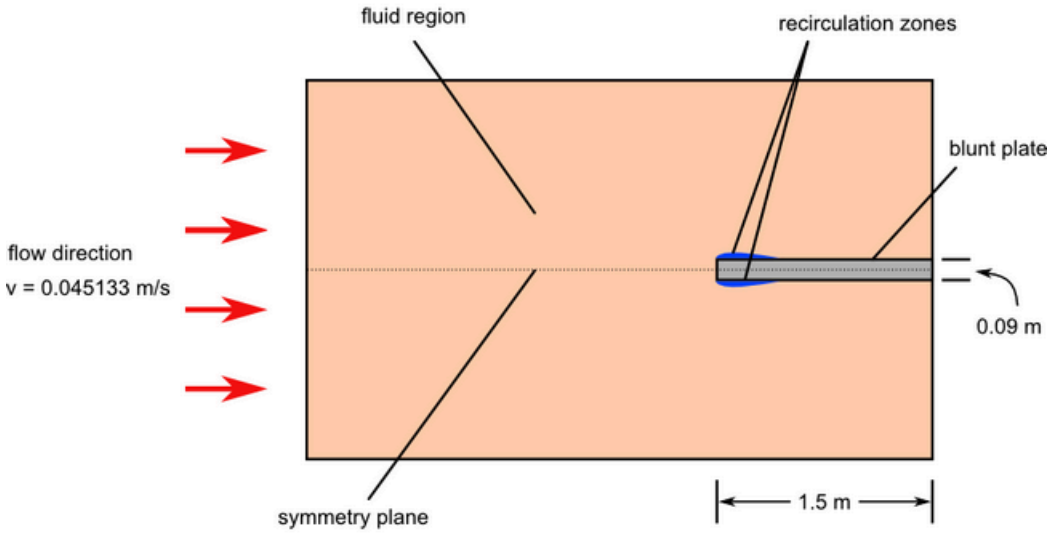


Figure 359:

The simulation was performed as a two dimensional problem by constructing a volume mesh that contains a single layer of elements in the extruded direction, normal to the flow plane, and by imposing symmetry boundary conditions on the extruded planes. In addition, the half symmetry of the geometry was exploited to allow for modeling only the top half of the geometry. These characteristics allow for accurate simulation of the flow while minimizing computational time. The following images show the mesh distribution and a refined mesh zone around the blunt plate.

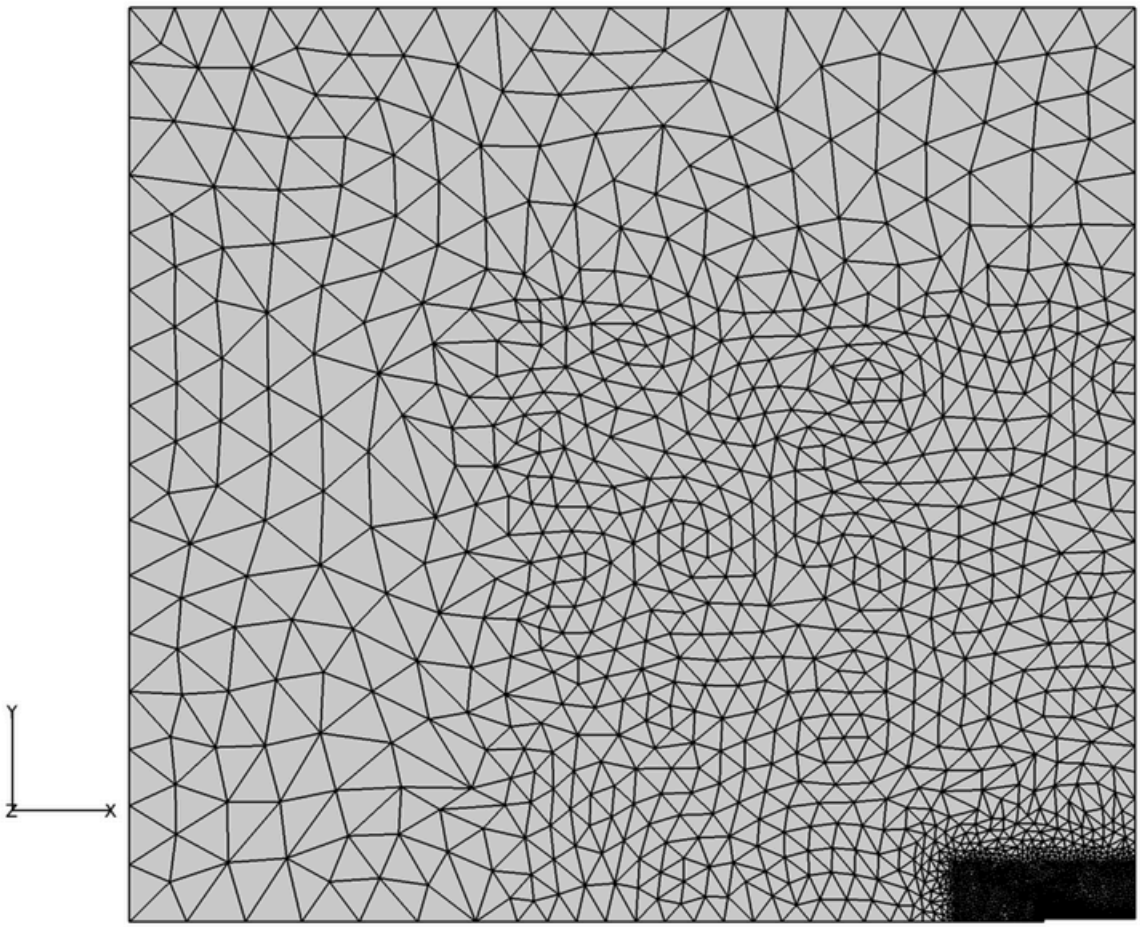


Figure 360: Mesh used for Simulating Separated Laminar Flow over a Blunt Plate

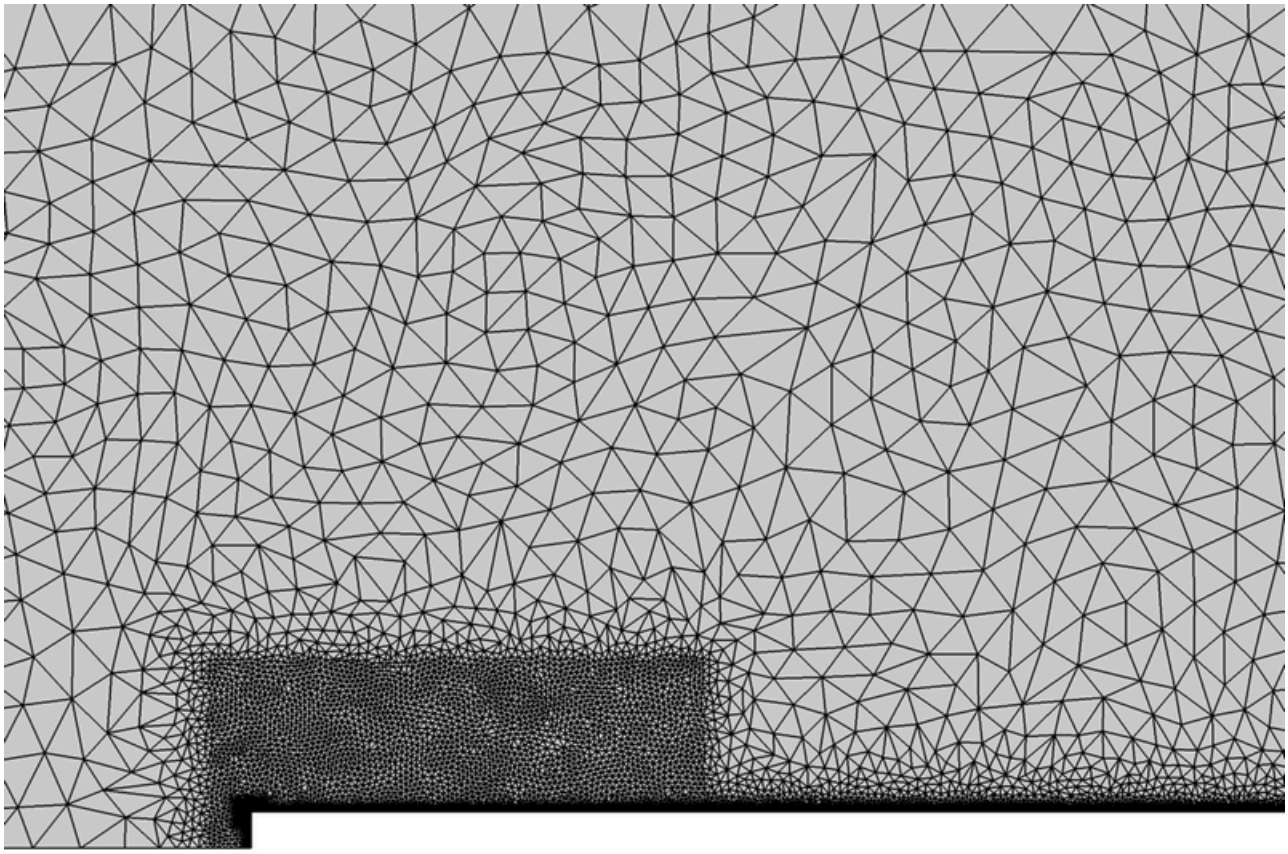


Figure 361: Mesh Detail Showing Refinement Zones at the Leading Edge of the Blunt Plate

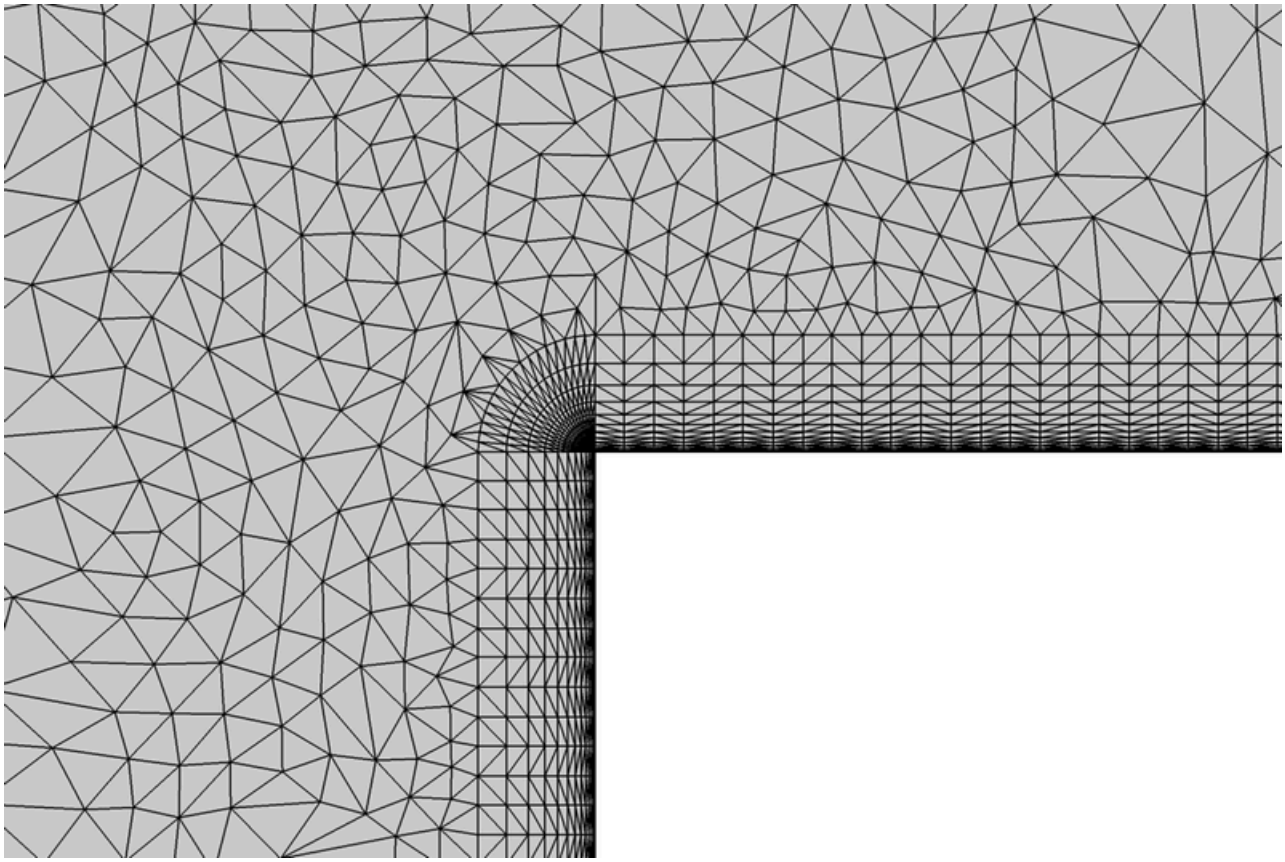


Figure 362: Mesh Detail Showing Mesh Elements Near the Leading Edge of the Blunt Plate

AcuSolve Results

The AcuSolve solution converged to a steady state and the results reflect the mean flow conditions over the blunt plate. The flow velocity is reduced to zero at the leading face, forming a stagnation point at the center. The flow reaches a maximum velocity as it flows around the leading edges and separates from the plate. Flow separation (shear stress parallel to the wall becomes negative) occurs downstream of the leading edge, leading to a recirculation zone. The flow reattaches 0.37 m downstream of the leading edge. The velocity in the laminar boundary layer increases from zero at the wall to free-stream velocity at the boundary layer edge. Along the plate length, the boundary layer slowly grows in thickness. The following image shows the contours of the flow velocity parallel to the streamwise direction and the recirculation region in the wake of the plate edge.

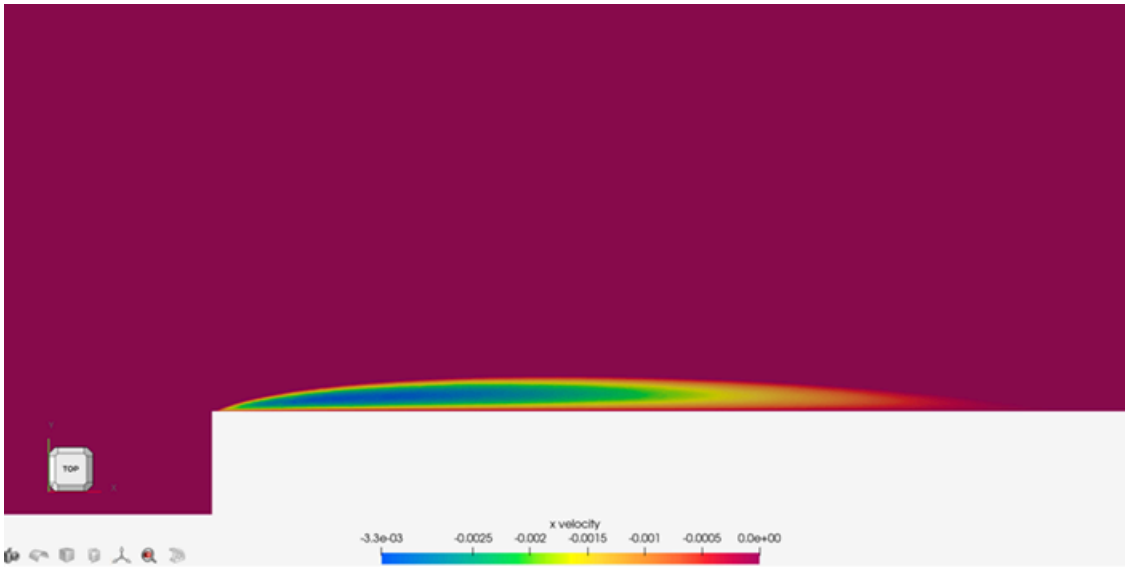


Figure 363: X-Velocity Contours Near the Leading Edge of the Blunt Plate

Downstream of the leading edge, the flow eventually reattaches to the plate at the point where the shear stress parallel to the wall passes from negative through zero to positive. The reattachment point is 0.37 m from the leading edge of the plate and corresponds to the trailing edge of the contours.

The results for the predicted and experimental reattachment length (xreattach) are presented in the table below. T represents the plate thickness.

Table 20:

AcuSolve xreattach	AcuSolve xreattach/T	Experimental xreattach/T	Percent error (%)
0.37	4.11	4.0	2.8

Summary

In this application, a constant flow inlet velocity and symmetric boundary conditions were used to model 2D flow over a blunt plate. The AcuSolve solution compares well with experimental results for the separation of laminar flow over a blunt plate. The non-dimensional reattachment length obtained from the AcuSolve steady state solution compares well with the experimental solution, with an error of less than 3.0 percent. The results of this simulation validate the ability of AcuSolve to accurately predict the reattachment point in cases with external, laminar flow with separation.

Simulation Settings for Separated Laminar Flow over a Blunt Plate

HyperMesh CFD database file: `<your working directory>\blunt_plate_laminar\blunt_plate_laminar.hm`

Global

- Problem Description

    - Analysis type - Steady State
    - Turbulence equation - Laminar
- Auto Solution Strategy
    - Relaxation Factor - `0.2`
- Material Model
    - Fluid
        - Density - `1.0` kg/m3
        - Viscosity - `1.7894e-005` kg/m-sec

  Model
- Volumes
    - Fluid
        - Element Set
            1. Material model - Fluid
- Surfaces
    - Back
        - Simple Boundary Condition
            1. Type - Symmetry
    - Freestream
        - Simple Boundary Condition
            1. Type - Slip
    - Front
        - Simple Boundary Condition
            1. Type - Symmetry
    - Inlet
        - Simple Boundary Condition
            1. Type - Inflow
            2. Inflow type - Velocity
            3. Inflow velocity type - Cartesian
            4. X Velocity - `0.045133` m/s
    - Outflow
        - Simple Boundary Condition
            1. Type - Outflow
    - Plate
        - Simple Boundary Condition
            1. Type - Wall
    - Symmetry
        - Simple Boundary Condition

1 Type - Symmetry

References

J.C. Lane and R.I. Loehrke. "Leading Edge Separation from a Blunt Plate at Low Reynolds Number". Journal of Fluids Engineering. 102(4):494-496. 1980.

Turbulent Mixing Layers in an Open Channel

In this application, AcuSolve is used to simulate the mixing of two streams of fluid with different velocities moving past a splitter plate. AcuSolve results are compared with experimental results as described in J. Delville, et al. (1989). The close agreement of AcuSolve results with the experimental results validates the ability of AcuSolve to model mixing layers in the turbulent flow regime.

Problem Description

The problem consists of two streams of fluid having material properties of standard air with density of 1.2 kg /m^3 and molecular viscosity of 1.7189 kg/m-sec. The two fluid streams enter an open channel separated by a splitter plate at two streamwise locations with differing velocities. The length of the channel is 1.8 m for the top portion and 1.5 m for the bottom portion. The inlet velocity of the top section is 41.54 m/s, producing a Reynolds's number of 2900, based on l=1.0 mm, while the inlet velocity of the lower section is 22.4 m/s, giving a Reynolds's number of 1200, as shown in the following image, which is not drawn to scale. The model is simulated as steady state with constant inflow conditions, using the Spalart Allmaras (SA) turbulence model. The velocity profile is computed for several locations downstream of the splitter plate and compared against the experimental data, as described in Delville, 1989.

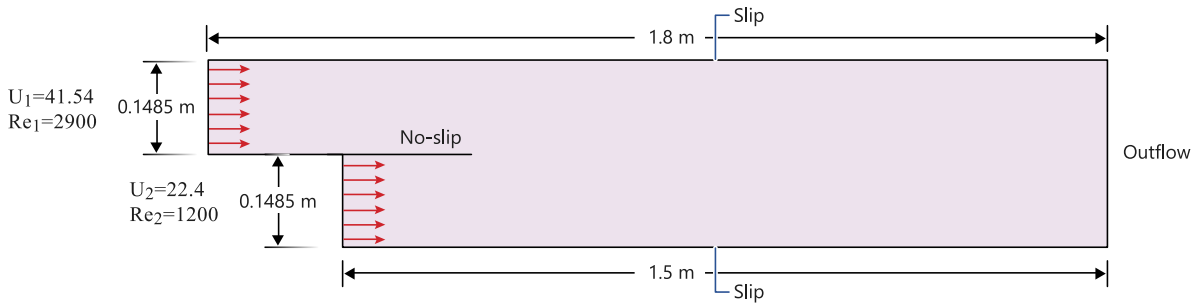


Figure 364: Critical Dimensions and Parameters Used for Simulating the Turbulent Mixing Layer

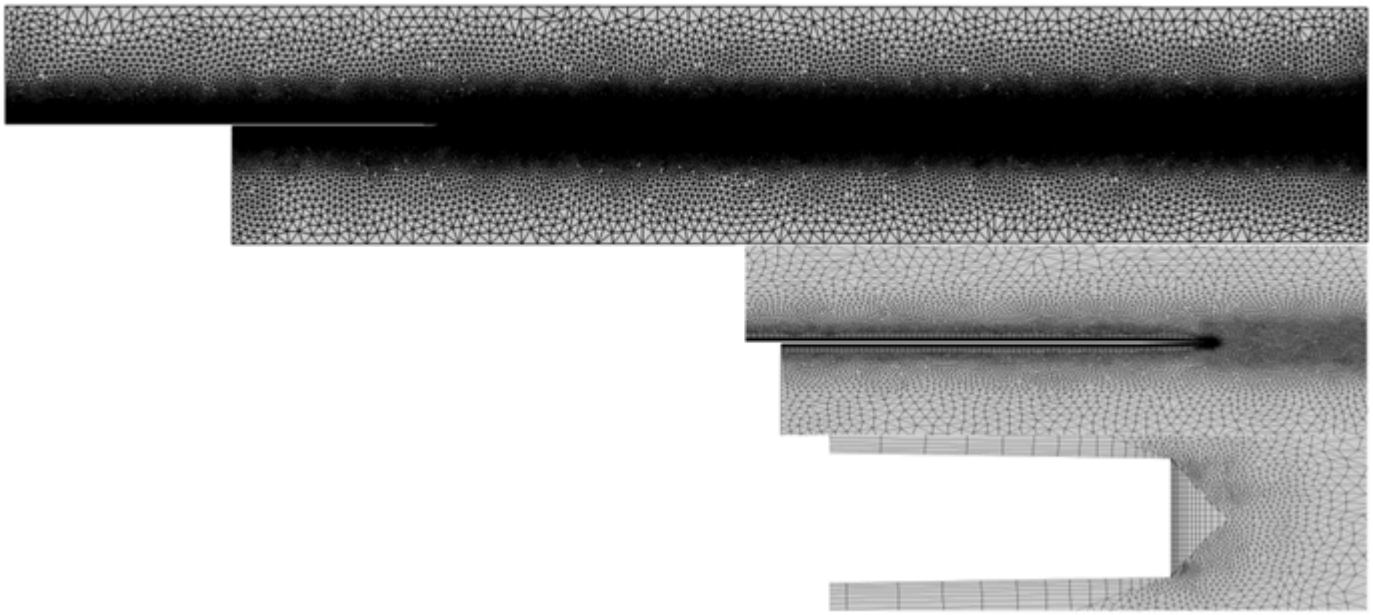


Figure 365: Mesh used for Simulating the Turbulent Mixing Layer Showing Close up Images Near the Trailing Edge of the Plate

The simulation was performed as a two dimensional problem by constructing a volume mesh that contains a single layer of elements extruded in the cross stream direction, normal to the flow plane and by imposing symmetry boundary conditions on the extruded planes. The upper and lower walls are specified as slip, the splitter plate is specified as no-slip and the inlet velocity and eddy viscosity are prescribed as constant values.

AcuSolve Results

The AcuSolve solution converged to a steady state and the results reflect the mean flow conditions within the open channel. The simulation result shows a developing flow field with the fluids fully separated as they pass the edge of the splitter plate. As the fluid travels downstream of the splitter plate, the dissimilar velocity fields produce a shear layer that results in momentum exchange between the two streams. The shear layer diffuses as the fluid travels further downstream. The relative velocity as a function of the normalized boundary layer height is computed from AcuSolve and compared with experimental data at three measurement stations, 0.2 m, 0.65 m and 0.95 m away from the trailing edge of the plate, as described in Delville, 1989. The image below shows black circles representing the experimental data and a solid red line for the AcuSolve results.

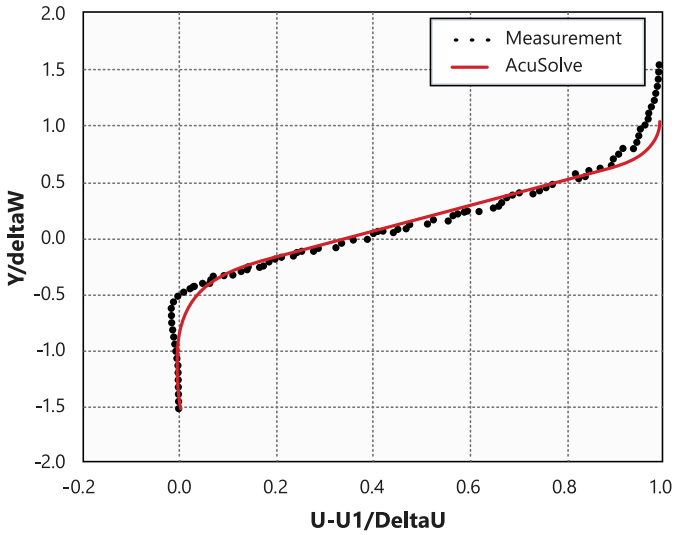


Figure 366: Relative Velocity within the Channel Compared Against Experimental Data Showing Experimental and Simulated Results for the SA Turbulence Model

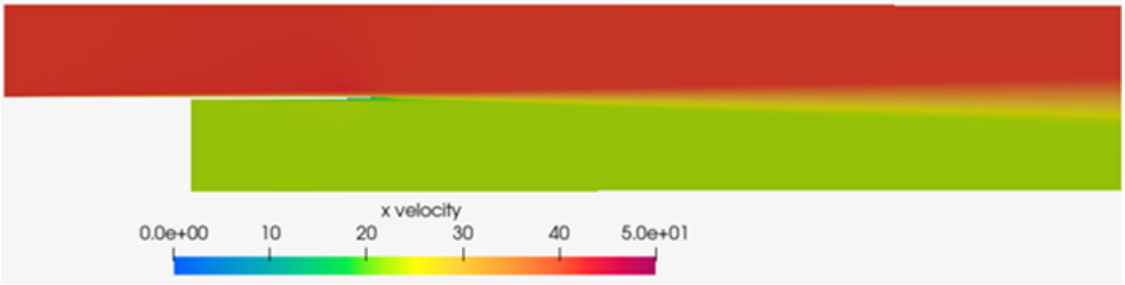


Figure 367: Velocity Magnitude Within the Channel

Summary

The AcuSolve solution compares well with experimental data for turbulent mixing within an open channel. In this application, the shear layer resulting from the dissimilar velocities of the incoming fluid streams results in an exchange of momentum within the channel. The amount of numerical dissipation from the grid is kept to a minimum to produce a good agreement with the experimental data. The good agreement with experimental results for the simulated turbulence model compares well with the measurement and previously published results, demonstrating that AcuSolve is capable of predicting turbulent mixing layers with relatively modest grid levels and the one equation turbulence model.

Simulation Settings for Turbulent Mixing Layers in an Open Channel

HyperMesh CFD database file: `<your working directory>\mixing_layer_turbulent \mixing_layer_turbulent.hm`

Global

- Problem Description
  - Analysis type - Steady State
  - Turbulence equation - Spalart Allmaras

- Auto Solution Strategy
  - Max time steps - `100`
  - Convergence tolerance - `0.001`
  - Relaxation Factor- `0.4`
- Material Model
  - Air
    - Type - Constant
    - Density - `1.2` kg/m3
    - Viscosity - `1.7189e-5` kg/m*sec

  Model
- Volumes
  - Volume
    - Element Set
      1. Material model - Air
- Surfaces
  - Back
    - Simple Boundary Condition
      1. Type- Symmetry
  - Front
    - Simple Boundary Condition
      1. Type- Symmetry
  - InletLower
    - Simple Boundary Condition
      1. Type- Inflow
      2. Inflow type- Velocity
      3. X Velocity- `22.4` m/sec
      4. Turbulence input type- Direct
      5. Eddy Viscosity- `0.0001432`
  - InletUpper
    - Simple Boundary Condition
      1. Type- Inflow
      2. Inflow type- Velocity
      3. X Velocity- `41.54` m/sec
      4. Turbulence input type- Direct
      5. Eddy Viscosity- `0.0001432`
  - Outlet
    - Simple Boundary Condition
      1. Type - Outflow

- Slip
  - Simple Boundary Condition
    1. Type- Slip
- SplitterPlate
  - Simple Boundary Condition
    1. Type - Wall
- TE
  - Simple Boundary Condition
    1. Type- Wall

References

Delville, J., Bellin, S., Garem, J. H., and Bonnet J. P., "Analysis of Structures in a Turbulent, Plane Mixing Layer by Use of a Pseudo Flow Visualization Method Based on Hot-Wire Anemometry," in: Advances in Turbulence 2, eds: H.-H. Fernholz and H. E. Fiedler, Proceedings of the Second European Turbulence Conference, Berlin, Aug. 30-Sept. 2, 1988, Springer Verlag, Berlin, 1989, pp. 251-256.

Laminar to Turbulent Transition Over an Airfoil

In this application, AcuSolve is used to solve for the flow field around a high lift airfoil with inflow conditions that lead to transitional flow on the pressure and suction side of the airfoil's surface. The moderate level of turbulence intensity at the inlet, low angle of attack and shape of the airfoil induce a transition to turbulent flow after a separation bubble develops on the surface. The coefficient of pressure is compared against experimental data from laboratory experiments.

Problem Description

The problem consists of a fluid having material properties close to air with density of 1.0 kg /m3 and molecular viscosity specified to produce a Reynolds number of 2.0e6, assuming a chord length of 1.0 m and an inlet velocity of 1.0 m/s, as is shown in the following image, which is not drawn to scale. The inflow velocity is oriented to simulate a 1 degree angle of attack. The model is simulated as steady state with constant inflow conditions using the farfield boundary condition. The two-equation gamma-ReTheta (γ- Reθ) transition model, used with the one equation Spalart Allmaras turbulence model, is validated against experimental data obtained from the experimental studies conducted by Somers, 1997.

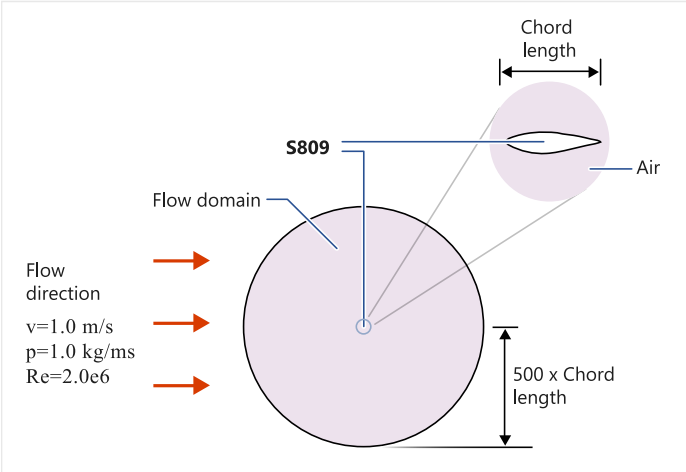


Figure 368: Critical Dimensions and Parameters used for Simulating Transitional Flow over the S809 Airfoil

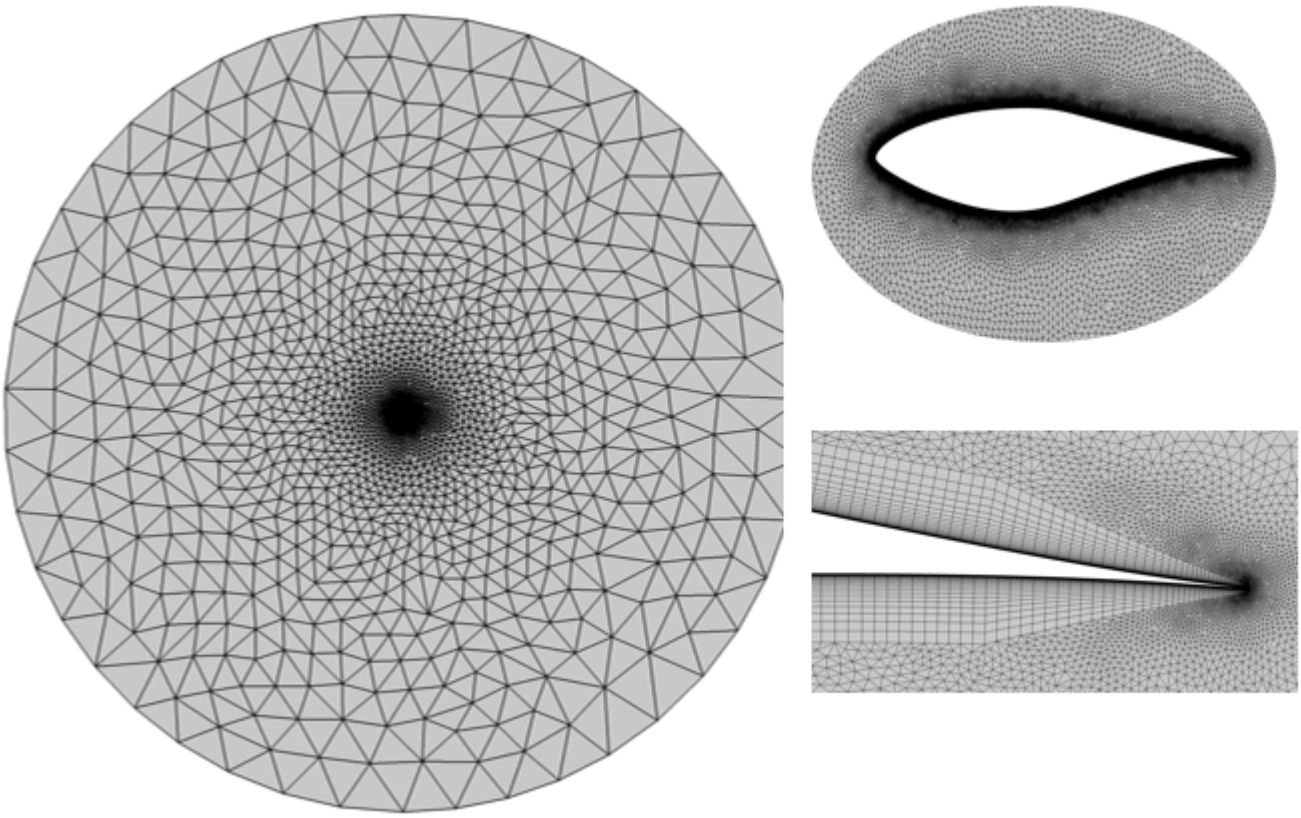


Figure 369: Mesh Used for Simulating Transitional over the S809 Airfoil

The simulation was performed as a two-dimensional problem by constructing a volume mesh that contains a single layer of elements extruded in the cross-stream direction, normal to the flow plane and by imposing symmetry boundary conditions on the extruded planes. The airfoil walls are specified as no-slip and the inlet velocity and eddy viscosity are specified at the farfield boundary.

AcuSolve Results

The AcuSolve solution converged to a steady state and the results reflect the mean flow conditions over the airfoil. The simulation results show that the flow field is laminar at the leading edge until approximately 50 percent chord on the pressure side and until approximately 55 percent on the suction side, then transitions to turbulent as it moves further downstream. The onset is caused by small separation bubbles at these locations. The following images show the negative pressure coefficient (-Cp) on the surface of the airfoil. The mean pressure at a reference point upstream of the airfoil is subtracted from the surface pressure and divided by the inlet velocity and air density to arrive at Cp. The Cp computed from AcuSolve is compared with experimental data, as described in Somers, 1997. The image shows black circles representing the experimental data and a solid red line for the AcuSolve results. Additional plots show contours of intermittency that illustrate the transition from laminar to turbulent flow.

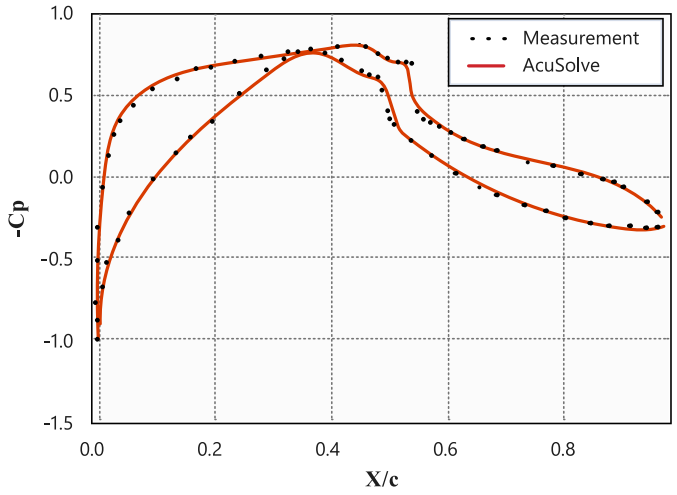


Figure 370: Negative pressure coefficient on the airfoil surface showing experimental and simulated results for the SA two equation (γ- Reθ) transition model

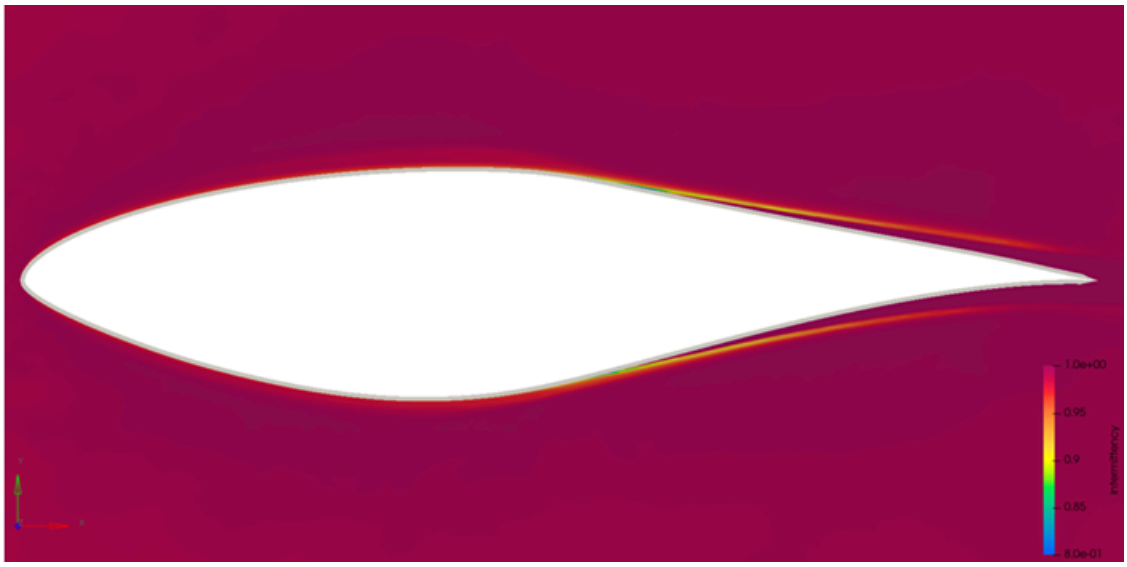


Figure 371: Contours of Intermittency Demonstrate the Onset Location from Laminar to Turbulent over the Airfoil

Summary

The AcuSolve solution compares well with experimental data for transitional flow over the S809 airfoil at a low angle of attack. Additional simulations and measurements for the full drag polar have been tested and compare well with considerably better accuracy when transition closure is included into the RANS solution. The good agreement with experimental results for the transition location and magnitude of expected pressure demonstrate that AcuSolve can predict the transition onset location for flow over surfaces with mild to moderate pressure gradients.

Simulation Settings for Laminar to Turbulent Transition Over an Airfoil

HyperMesh CFD database file: `<your working directory>\airfoil_transition\airfoil_transition.hm`

Global

- Problem Description
  - Analysis type - Steady State
  - Turbulence equation - Spalart Allmaras
  - Turbulence transition model- Gamma-ReTheta
- Auto Solution Strategy
  - Max time steps - `100`
  - Convergence tolerance - `0.0001`
  - Relaxation Factor- `0.5`
  - Turbulence transition- on
- Material Model
  - Air
    - Type - Constant
    - Density - `1.0` kg/m3
    - Viscosity - `5.0e-7` kg/m*sec

  Model
- Volumes
  - Fluid
    - Element Set
      1. Material model - Air
- Surfaces
  - +z slip
    - Simple Boundary Condition
      1. Type- Slip
  - -z slip
    - Simple Boundary Condition
      1. Type- Slip
  - farfield
    - Simple Boundary Condition
      1. Type- Far Field
      2. X velocity = `1.0` *cos(α), where α is the angle of attack in radians
      3. Y velocity = `1.0` *sin(α), where α is the angle of attack in radians
      4. Turbulence input type- Auto
      5. Turbulence intensity type- Value
      6. Turbulence intensity percent- `0.025`
  - airfoil surface
    - Simple Boundary Condition

1 Type- Wall

References

Somers, D., Design and Experimental Results for the S809 Airfoil. NREL/SR-440-6918. 1997

Turbulent Flow Over an Oscillating Rigid Body Assembly

In this application, AcuSolve is used to simulate the fluid-structure interaction of a fluid moving over a cylinder/plate assembly. AcuSolve results are compared with experimental results as described in Gomes and Lienhart (2009). The close agreement of AcuSolve results with the experimental results validates the ability of AcuSolve to model cases in which the fluid forces lead to structural motions.

Problem Description

The problem consists of a fluid having material properties of standard water with density of 998 kg / m^3 and kinematic viscosity of 0.97e-6 m^2/sec through a two dimensional channel over a cylinder and plate assembly. The diameter of the cylinder is 0.022 m and the plate length is 0.042 m, while the inlet velocity is specified to match experimental conditions with a max velocity of 1.07 m/sec, as is shown in the following image, which is not drawn to scale. The model is simulated as transient with constant inflow conditions, allowing an oscillatory motion of the assembly to develop. The Shear Stress Transport (SST) turbulence model is used to model the turbulent portion of the flow and AcuSolve's internal rigid body motion is used to capture the motion of the oscillating assembly.

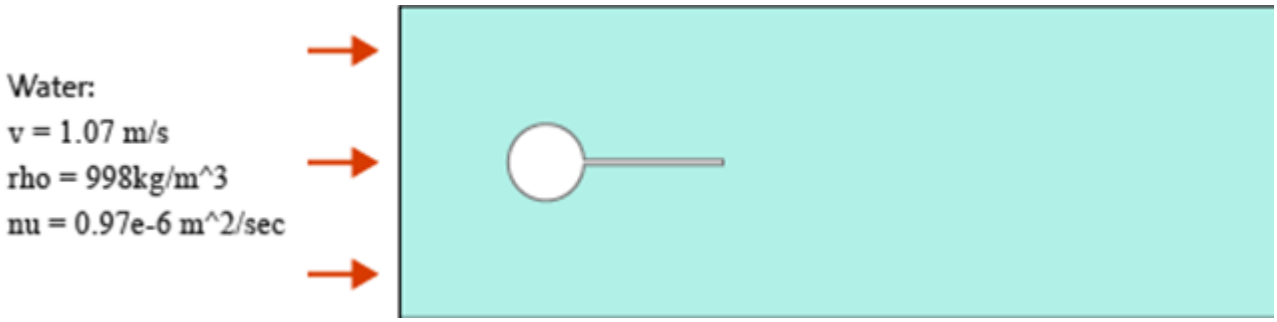


Figure 372: Critical Dimensions and Parameters used for Simulating Rigid Body Motion of Flow Past a Cylinder/Plate Assembly

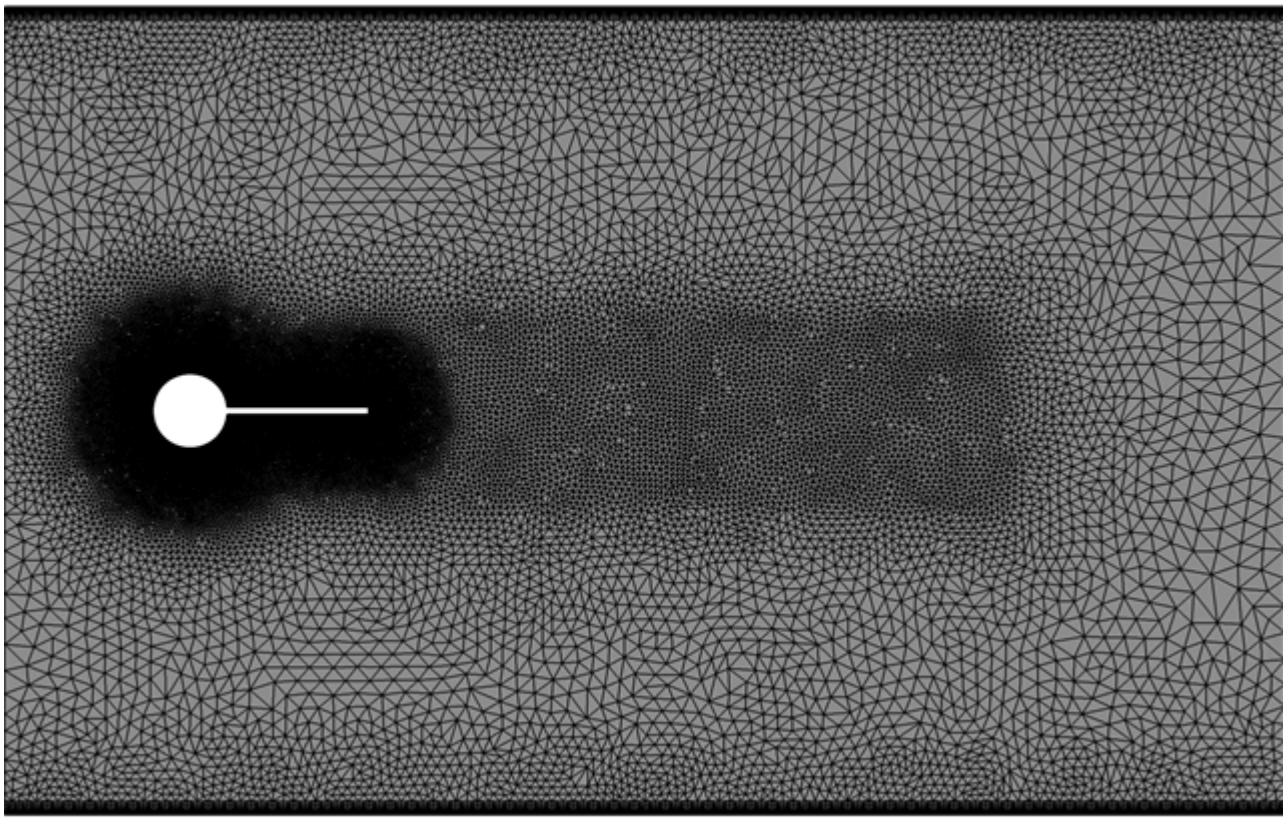


Figure 373: Mesh used for Simulating Rigid Body Motion of Flow Past a Cylinder/Plate Assembly

The simulation was performed as a two dimensional problem by constructing a volume mesh that contains a single layer of elements extruded in the cross stream direction, normal to the flow plane and by imposing symmetry boundary conditions on the extruded planes. The upper and lower walls are specified as no-slip and the inlet velocity is specified to match the conditions of the experiment (Gomes and Lienhart 2009).

AcuSolve Results

The AcuSolve solution reached a regularly repeating oscillatory state and the simulation was allowed to proceed for 10 seconds of physical time to obtain enough cycles for statistical analysis. The motion of the cylinder/plate assembly is directly attributed to the vortices shedding in its wake. The fluctuating loads on the assembly that result from the vortex shedding lead to a repeating cycle of structural rotation. The dominant oscillation frequency from the simulation was found to match well with the experimental measurements, within approximately 3.5 percent. The images below show the rigid body displacement of the assembly as it oscillates within the flow. Contours of velocity magnitude demonstrate the forcing on the assembly, while the mesh motion around the structure is captured and plotted for a single time step. Two dimensional plots showing the angular displacement demonstrate the motion, showing a single red line for the AcuSolve results.

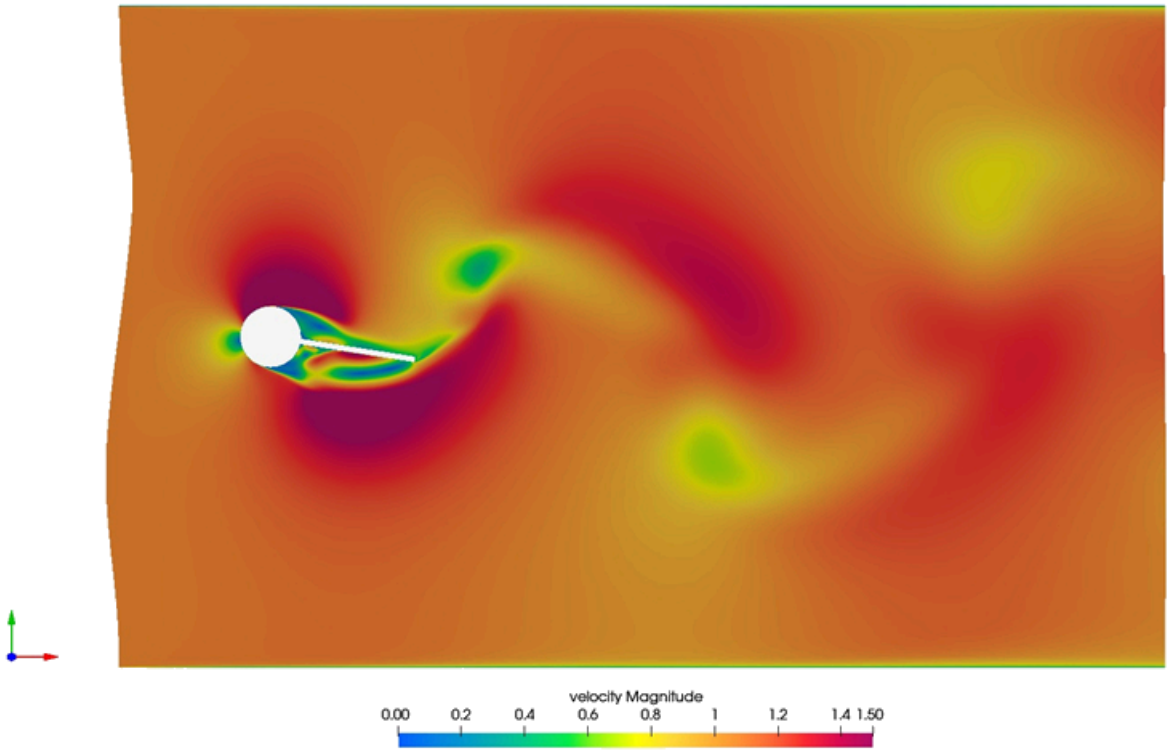


Figure 374: Velocity Contours Near the Assembly for a Single Time Step During the Simulation

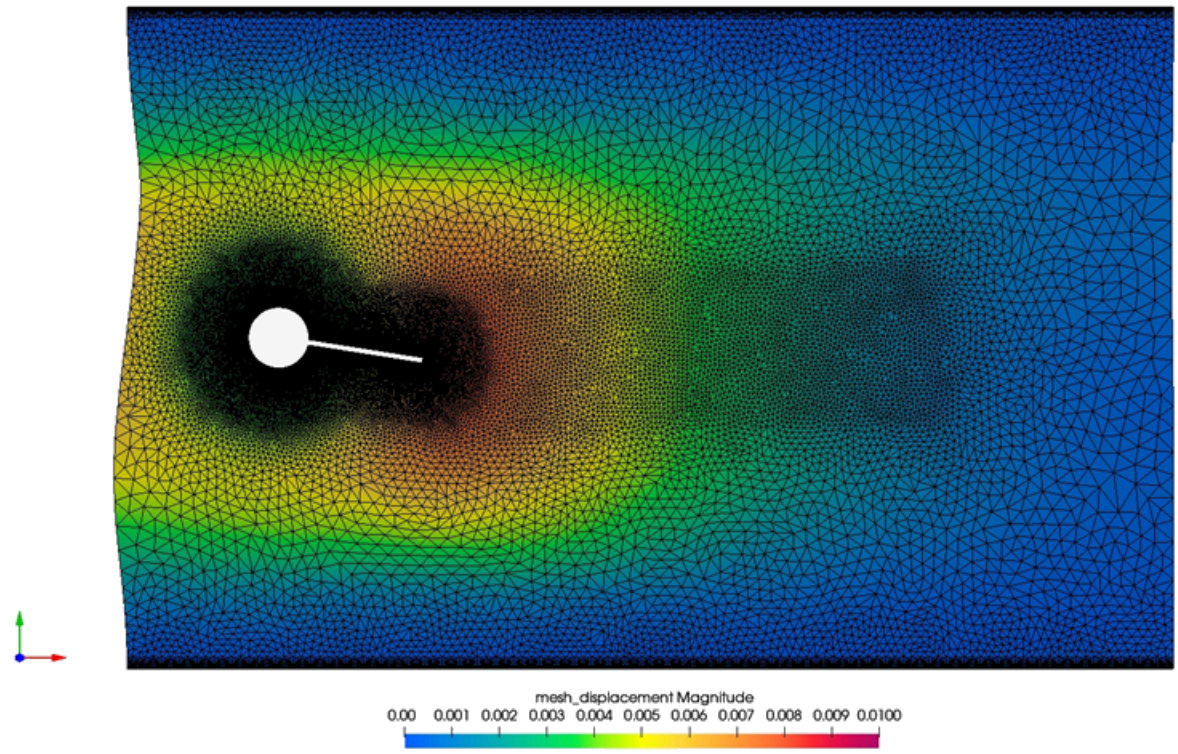


Figure 375: Mesh Displacement Contours Near the Assembly for a Single Time Step During the Simulation

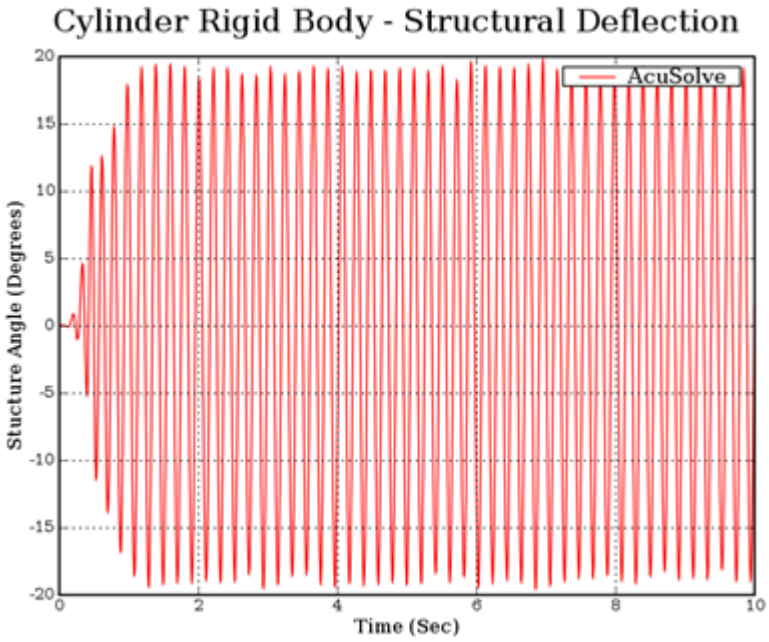


Figure 376: Rigid Body Displacement of the Assembly as a Function of Time, Showing the Oscillation Develop into the Pseudo-Steady Motion

The dominant frequency of the oscillation is easily identified in the Fast Fourier Transform (FFT) of the deflection angle, shown in the plot below.

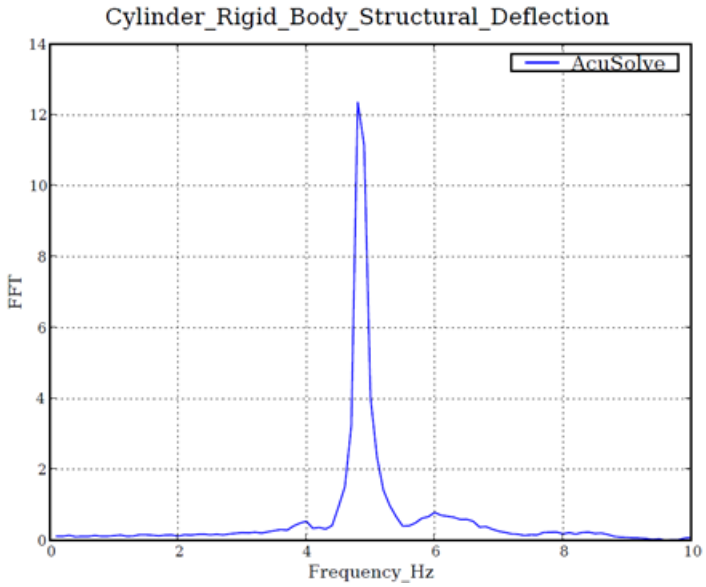


Figure 377: FFT of the Rigid Body Displacement Angle, Showing Power Spectral Density as a Function of Frequency

Summary

The AcuSolve solution compares well with experimental data for flow past an oscillating cylinder/plate assembly. In this application, water moves over the cylinder/plate assembly, giving rise to unsteady

loading that causes the body to rotate as a rigid body. The good agreement with the natural frequency of oscillation compared to the experimental data demonstrates that AcuSolve is capable of predicting fluid forced motion with an internal rigid body dynamic solver.

Simulation Settings for Turbulent Flow Over an Oscillating Rigid Body Assembly

SimLab database file: `<your working directory>\cylinder_rigidbody_turbulent\cylinder_rigidbody_turbulent.slb`

Global

- Problem Description
  - Flow - Transient
  - Turbulence equation - SST
  - Moving Mesh - Computed
- Auto Solution Strategy
  - Final Time - `10.0`
  - Initial Time Increment- `0.005`
  - Convergence tolerance- `0.001`
  - Max stagger iterations- `3`
- Material Model
  - Water
    - Type- Constant
    - Density- `998.0` kg/m3
    - Viscosity- `0.00096806` kg/m*sec
- Mesh Motion
  - RigidBody
    - Type- Rigid Body Dynamic
      1. Z rotation- Active
      2. Mass- `0.2089` kg
      3. Dyadic
         1. X-X - `3.7 e-5` kg-m2
         2. Y-Y- `3.7 e-5` kg-m2
         3. Z-Z - `3.7 e-5` kg-m2

  Model
- Volumes
  - Volume
    - Element Set
      1. Material model- Water
- Surfaces
  - Body

- Simple Boundary Condition
  1. Type- Wall
  2. Mesh displacement BC type- Fixed
  3. Mesh motion- RigidBody
- Interpolated Motion Surface

- Bottom
  - Simple Boundary Condition
    1. Type- Wall
    2. Mesh displacement BC type- Fixed
  - Interpolated Motion Surface
- Inflow
  - Simple Boundary Condition
    1. Type- Inflow
    2. Inflow type- Velocity
    3. X Velocity- `1.07` m/sec
    4. Turbulence input type- Auto
    5. Turbulence intensity type- High
  - Advanced Options
    1. Nodal Boundary Conditions
    2. X-velocity
       1. Type- Linear
       2. Precedence- `2`
       3. Curve fit variable- Y coordinate
       4. Curve fit values- Provided
    3. Y-velocity
       1. Type- Zero
    4. Z-velocity
       1. Type- Zero
- Bottom
  - Simple Boundary Condition
    1. Type- Wall
    2. Mesh displacement BC type- Fixed
    3. Mesh motion- RigidBody
- Outflow
  - Simple Boundary Condition
    1. Type- Outflow
- Top
  - Simple Boundary Condition

1 Type- Wall
2 Mesh displacement BC type- Fixed

- maxZ
  - Simple Boundary Condition
    1 Type- Slip
- minZ
  - Simple Boundary Condition
    1 Type- Slip

References

Gomes, J. P. and Lienhart, H. (2009) Experimental Benchmark: Self-excited Fluid-structure Interaction Test Cases, in Fluid-Structure Interaction II: Modeling, Simulation, Optimization, Bungartz, H. J., Mehl, M., Schafer, M. (eds.), 383-412, Springer-Verlag.Ryhming.

Turbulent Flow Through a Heated Periodic Channel

In this application, AcuSolve is used to solve for the flow and temperature field within a channel containing a heated wall. The wall is maintained at a constant temperature, inducing heat flux into the fluid, to predict the thermal law of the wall. The non-dimensional temperature versus the non-dimensional height above the wall is compared to the analytical correlation provided by Kader.

Problem Description

The problem consists of a fluid having material properties close to air with a density of 1.0 kg/m^3, molecular viscosity of 0.0001 kg/m-s, specific heat of 1005.0 J/kg-K and thermal conductivity of 0.139 W/m-K. The properties are specified to obtain a Prandtl number of 0.72. The velocity is defined as periodic and is driven by a constant acceleration body force equal to 2.0 m/s^2. The temperature is specified as periodic+unknown ratio allowing it to develop until it reaches a steady solution. The simulation description is shown in the following image, which is not drawn to scale. The model is simulated using the one equation Spalart Allmaras turbulence model along with the advective-diffusive temperature equation. The thermal wall distribution is validated against correlation data published by Kader 1981.

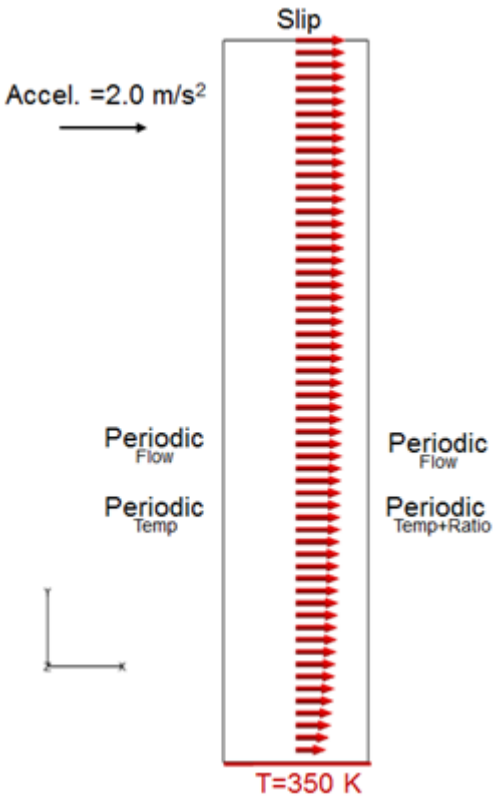


Figure 378: Critical Parameters used For Simulating Periodic Flow Within a Heated Channel

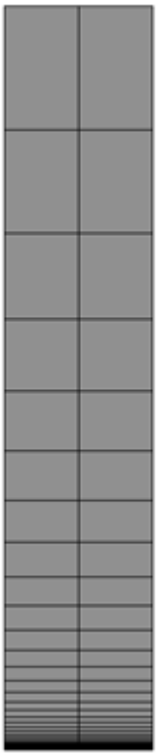


Figure 379: Mesh used For Simulating Periodic Flow Within a Heated Channel

The simulation was performed as a two-dimensional problem by constructing a volume mesh that contains a single layer of elements extruded in the cross-stream direction, normal to the flow plane and by imposing periodic boundary conditions on the extruded planes. The streamwise direction contains two elements allowing the flow and temperature solution to develop. Only the lower half of the channel is modeled, assuming the solution is mirror across the top slip plane.

AcuSolve Results

The AcuSolve solution converged to a steady state and the results reflect the mean flow conditions within the channel. The simulation results demonstrate that the channel wall induces a thermal flux into the flow field, producing a temperature distribution dependent on the distance from the wall. The thermal law of the wall computed from the AcuSolve results is compared with correlation data for the corresponding Prandtl number, as demonstrated in Kader 1981. The plot shown below gives the non-dimensional value of T+ as a function of Y+, where T+ and Y+ are computed per the following relationships:

$$T+ = \frac{(Tw - T)\rho C p u_\tau}{\dot{Q}} T \tag{11}$$

$$Y+ = \frac{y u_\tau}{v} \tag{12}$$

$$u_\tau = \sqrt{\tau w / \rho} \tag{13}$$

Where $T+$, Tw is the fixed wall temperature, T is the temperature away from the wall, ρ is the fluid density, Cp is the fluid specific heat, uT is computed from the magnitude of the shear stress and $\dot{Q}_i$ is the local surface heat flux.

The image below shows black circles representing the correlation data and a solid red line for the AcuSolve results. The results demonstrate that the temperature distribution away from the wall is resolved properly and compares well with the correlation. Since an empirical relationship for T+ is used for comparison, there will be minor discrepancies compared with the simulation results. Additional comparisons have been made against DNS results for T+ from Kawamura et al. 1998.

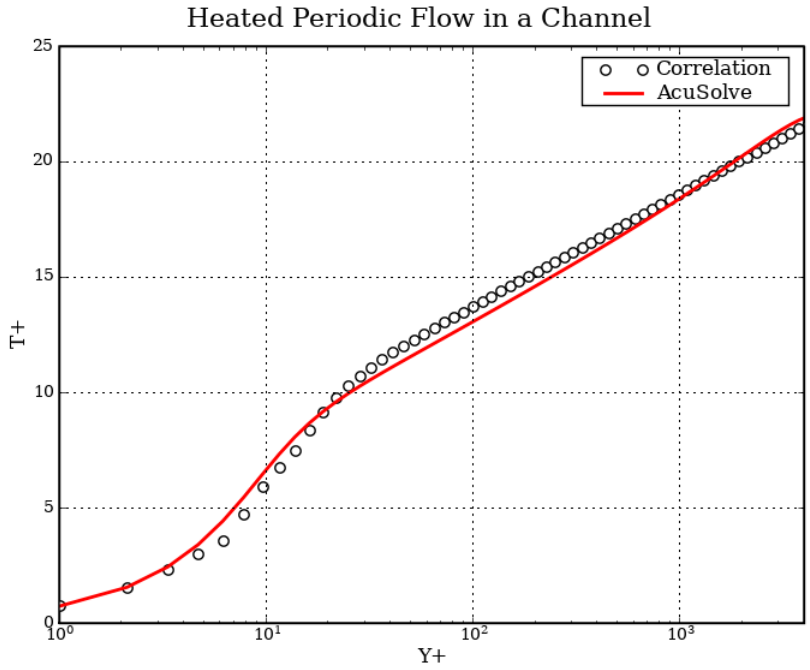


Figure 380: Thermal Boundary Layer Within the Heated Channel Compared Against the Correlation Data

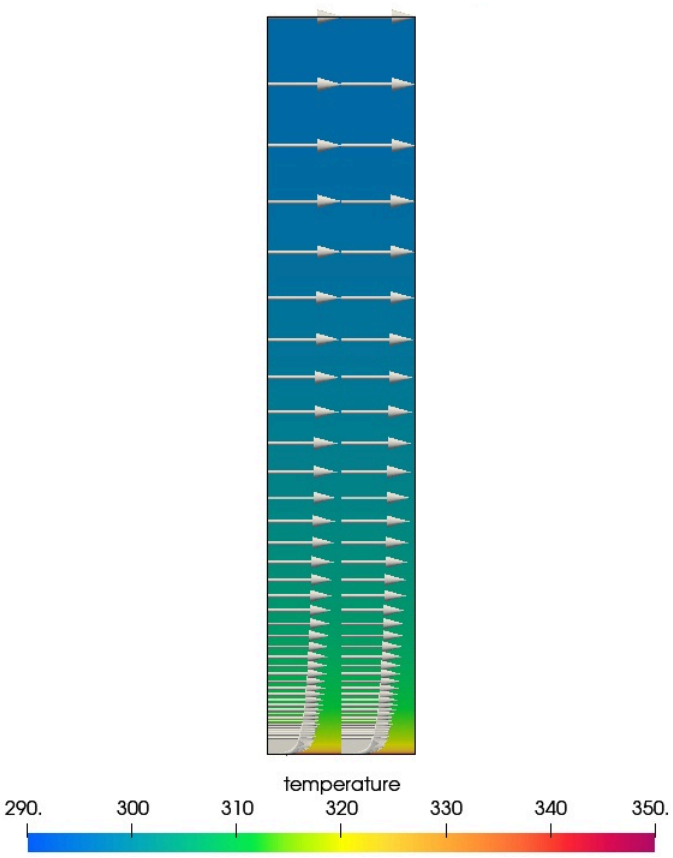


Figure 381: Contours of Temperature and Vectors Representing the Fluid Velocity Within the Channel

Summary

The AcuSolve solution compares well with the correlation data for turbulent flow within a heated channel. In this application, the constant temperature wall induces a surface heat flux, giving rise to a temperature gradient within the channel. AcuSolve can capture the correct temperature gradient at any location above the wall if an appropriate first layer height is selected to resolve a Y+ value of 1.0. The good agreement with correlation data for T+ demonstrates that AcuSolve can predict the locally varying temperature distribution within a turbulent channel.

Simulation Settings for Turbulent Flow Through a Heated Periodic Channel

SimLab database file: `<your working directory>\channel_periodic_heat\channel_periodic_heat.slb`

Global

- Problem Description
  - Flow type - Steady State
  - Temperature equation - Advective Diffusive
  - Turbulence equation - Spalart Allmaras
- Auto Solution Strategy
  - Max time steps - `50`

    - Convergence tolerance - `0.0001`
    - Relaxation Factor - `0.4`
    - Temperature - On
- Material Model
    - Fluid
        - Type - Constant
        - Density - `1.0` kg/m3
        - Viscosity - `1.0e-4` kg/m*sec
        - Specific Heat - `1005.0` J/kg*K
        - Conductivity - `0.139` W/m*K
- Body Force
    - BodyForce
        - Gravity
            1. X-component - `2.0` m/sec2

Model

- Volumes
    - Fluid
        - Element Set
            1. Material model - Fluid
            2. Body force - BodyForce
- Surfaces
    - Symmetry_1
        - Simple Boundary Condition - (disabled to allow for periodic conditions to be set)
    - Symmetry_2
        - Simple Boundary Condition - (disabled to allow for periodic conditions to be set)
    - Inflow
        - Simple Boundary Condition - (combination of integrated BC and periodic BC set)
        - Advanced Options
            1. Integrated Boundary Conditions - Temperature - `300.0` K
    - Outflow
        - Simple Boundary Condition - (disabled to allow for periodic conditions to be set)
    - Slip_surface
        - Simple Boundary Condition
            1. Type- Slip
    - Wall_surface
        - Simple Boundary Condition
            1. Type- Wall

2 Temperature BC type - Value
3 Temperature - `350.0` K

- Periodics
  - 2D
    - Periodic Boundary Conditions
      1 Type - Periodic
  - Flow
    - Periodic Boundary Conditions
      1 Type - Periodic
  - Temperature
    - Individual Periodic BCs
      1 Temperature: Type - Single Unknown Ratio
- Nodes
  - Zero_z-velocity
    - Z-Velocity: Type - Zero

References

B.A. Kader, "Temperature and concentration profiles in fully turbulent boundary layers", International Journal of Heat and Mass Transfer, Volume 24, Issue 9, 1981, Pages 1541-1544.

H. Kawamura, K. Ohsaka, H. Abe and K. Yamamoto, "DNS of turbulent heat transfer in channel flow with low to medium-high Prandtl number fluid", International Journal of Heat and Mass Transfer, 19:482-491, 1998.

Transitional Flow

7

This section includes validation cases containing conditions producing laminar to turbulent flow that are simulated with a turbulence transition model.

This chapter covers the following:

- Laminar to Turbulent Transition Over an Airfoil (p. 502)

Laminar to Turbulent Transition Over an Airfoil

In this application, AcuSolve is used to solve for the flow field around a high lift airfoil with inflow conditions that lead to transitional flow on the pressure and suction side of the airfoil's surface. The moderate level of turbulence intensity at the inlet, low angle of attack and shape of the airfoil induce a transition to turbulent flow after a separation bubble develops on the surface. The coefficient of pressure is compared against experimental data from laboratory experiments.

Problem Description

The problem consists of a fluid having material properties close to air with density of 1.0 kg /m3 and molecular viscosity specified to produce a Reynolds number of 2.0e6, assuming a chord length of 1.0 m and an inlet velocity of 1.0 m/s, as is shown in the following image, which is not drawn to scale. The inflow velocity is oriented to simulate a 1 degree angle of attack. The model is simulated as steady state with constant inflow conditions using the farfield boundary condition. The two-equation gamma-ReTheta (γ- Reθ) transition model, used with the one equation Spalart Allmaras turbulence model, is validated against experimental data obtained from the experimental studies conducted by Somers, 1997.

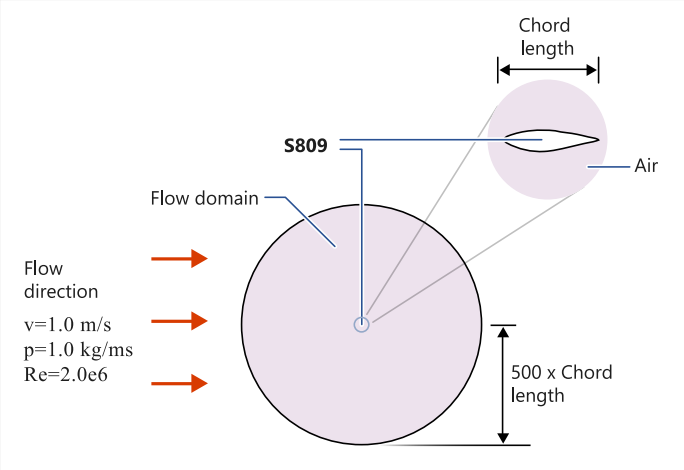


Figure 382: Critical Dimensions and Parameters used for Simulating Transitional Flow over the S809 Airfoil

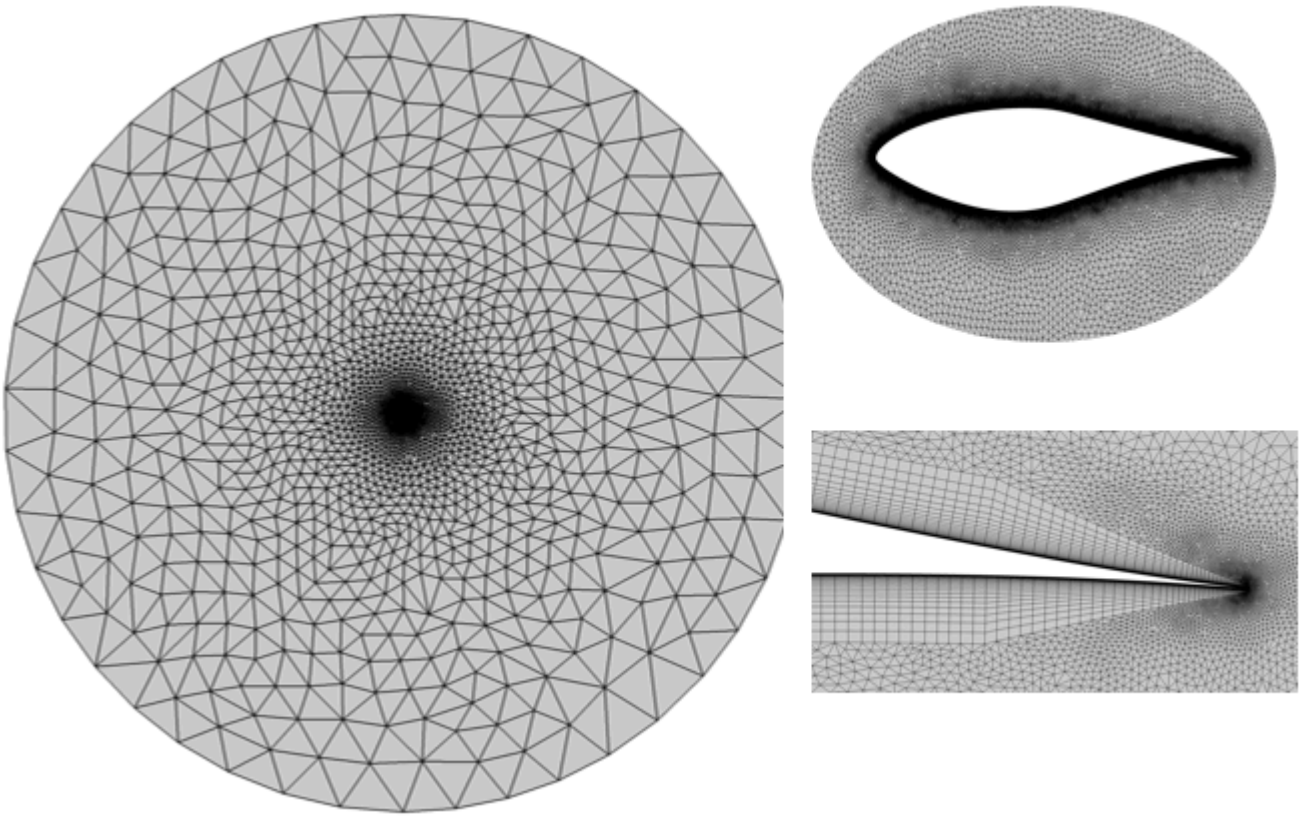


Figure 383: Mesh Used for Simulating Transitional over the S809 Airfoil

The simulation was performed as a two-dimensional problem by constructing a volume mesh that contains a single layer of elements extruded in the cross-stream direction, normal to the flow plane and by imposing symmetry boundary conditions on the extruded planes. The airfoil walls are specified as no-slip and the inlet velocity and eddy viscosity are specified at the farfield boundary.

AcuSolve Results

The AcuSolve solution converged to a steady state and the results reflect the mean flow conditions over the airfoil. The simulation results show that the flow field is laminar at the leading edge until approximately 50 percent chord on the pressure side and until approximately 55 percent on the suction side, then transitions to turbulent as it moves further downstream. The onset is caused by small separation bubbles at these locations. The following images show the negative pressure coefficient (-Cp) on the surface of the airfoil. The mean pressure at a reference point upstream of the airfoil is subtracted from the surface pressure and divided by the inlet velocity and air density to arrive at Cp. The Cp computed from AcuSolve is compared with experimental data, as described in Somers, 1997. The image shows black circles representing the experimental data and a solid red line for the AcuSolve results. Additional plots show contours of intermittency that illustrate the transition from laminar to turbulent flow.

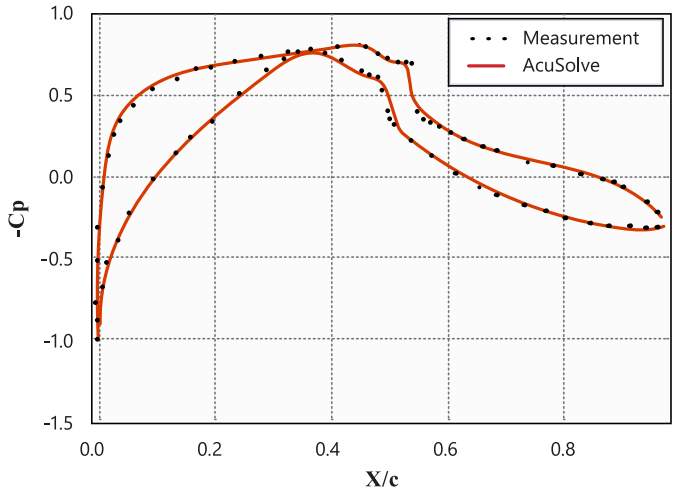


Figure 384: Negative pressure coefficient on the airfoil surface showing experimental and simulated results for the SA two equation (γ- Reθ) transition model

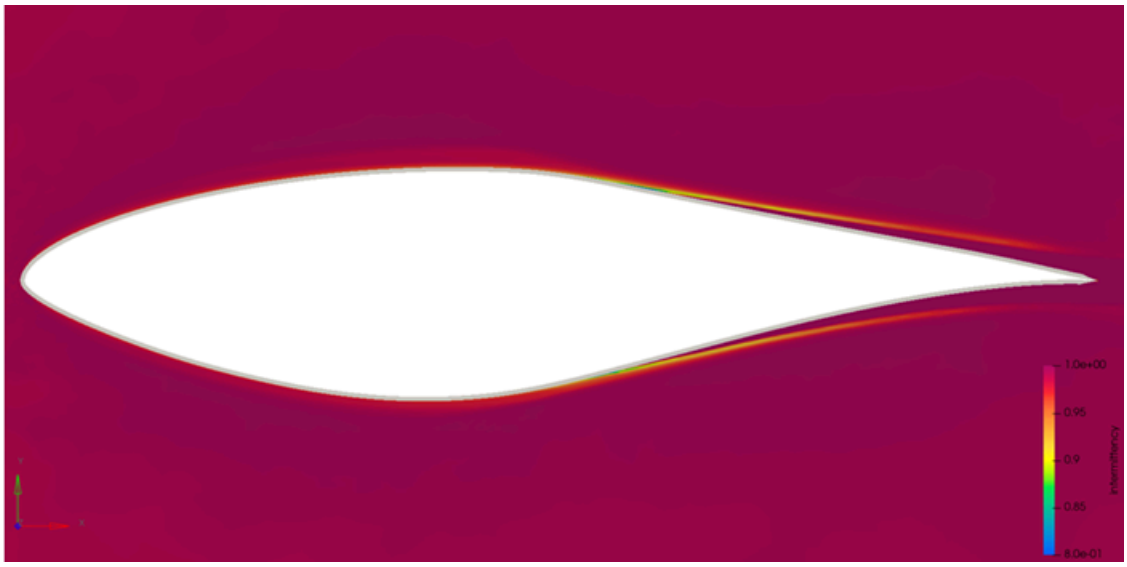


Figure 385: Contours of Intermittency Demonstrate the Onset Location from Laminar to Turbulent over the Airfoil

Summary

The AcuSolve solution compares well with experimental data for transitional flow over the S809 airfoil at a low angle of attack. Additional simulations and measurements for the full drag polar have been tested and compare well with considerably better accuracy when transition closure is included into the RANS solution. The good agreement with experimental results for the transition location and magnitude of expected pressure demonstrate that AcuSolve can predict the transition onset location for flow over surfaces with mild to moderate pressure gradients.

Simulation Settings for Laminar to Turbulent Transition Over an Airfoil

HyperMesh CFD database file: `<your working directory>\airfoil_transition\airfoil_transition.hm`

Global

- Problem Description
  - Analysis type - Steady State
  - Turbulence equation - Spalart Allmaras
  - Turbulence transition model- Gamma-ReTheta
- Auto Solution Strategy
  - Max time steps - `100`
  - Convergence tolerance - `0.0001`
  - Relaxation Factor- `0.5`
  - Turbulence transition- on
- Material Model
  - Air
    - Type - Constant
    - Density - `1.0` kg/m3
    - Viscosity - `5.0e-7` kg/m*sec

  Model
- Volumes
  - Fluid
    - Element Set
      1. Material model - Air
- Surfaces
  - +z slip
    - Simple Boundary Condition
      1. Type- Slip
  - -z slip
    - Simple Boundary Condition
      1. Type- Slip
  - farfield
    - Simple Boundary Condition
      1. Type- Far Field
      2. X velocity = `1.0` *cos(α), where α is the angle of attack in radians
      3. Y velocity = `1.0` *sin(α), where α is the angle of attack in radians
      4. Turbulence input type- Auto
      5. Turbulence intensity type- Value
      6. Turbulence intensity percent- `0.025`
  - airfoil surface
    - Simple Boundary Condition

1 Type- Wall

References

Somers, D., Design and Experimental Results for the S809 Airfoil. NREL/SR-440-6918. 1997

Transient Flow

8

This section includes validation cases that consider time dependent flow simulations.

This chapter covers the following:

- Oscillating Laminar Flow Around a Circular Cylinder (p. 508)
- Circumferential Flow in a Cylinder Induced by a Rotating Solid (p. 513)
- Two-Phase Nucleate Boiling in a Cylindrical Pipe (p. 519)
- Supersonic Flow Through a Converging-Diverging Nozzle (p. 523)
- Turbulent Flow Over an Oscillating Rigid Body Assembly (p. 528)
- Ideal Gas Compression in an Actuating Piston (p. 535)

Oscillating Laminar Flow Around a Circular Cylinder

In this application, AcuSolve is used to simulate two dimensional, laminar flow over a cylinder to predict separation of flow from the cylinder surface and the flow in the wake area. AcuSolve results are compared with experimental results as described in Tritton (1959). The close agreement of AcuSolve results with experimental results validates the ability of AcuSolve to model cases with unsteady oscillating vortex streets.

Problem Description

The problem consists of a cylinder located in a rectangular domain, as shown in the following image, which is not drawn to scale. A fluid enters the domain with a low velocity (v) of 0.5 m/s. The diameter (D) of the cylinder is 20 cm. The domain extends 10 X D upstream of the cylinder center, 5D above and below the cylinder center, and 40D downstream of the cylinder center. The density of the working fluid is 1 kg/m^3 and the viscosity is 0.001 kg/m-s. The Reynolds number for this problem is 100.

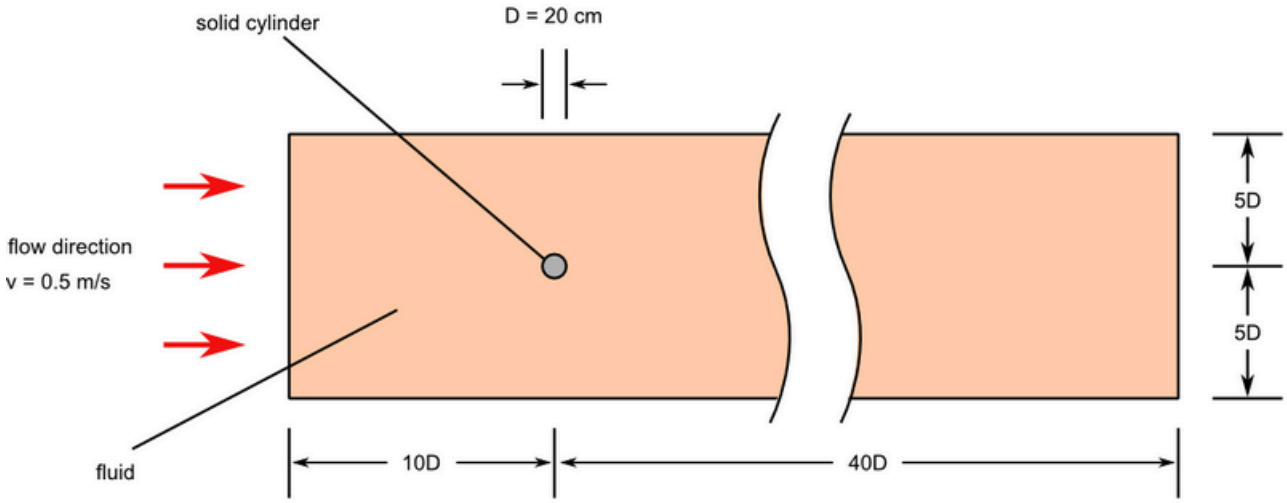


Figure 386: Critical Dimensions and Parameters for Simulating Oscillating Laminar Flow Around a Circular Cylinder

The simulation was performed as a two dimensional problem by constructing a volume mesh that contains a single layer of elements in the extruded direction, normal to the flow plane, and by imposing symmetry boundary conditions on the extruded planes.

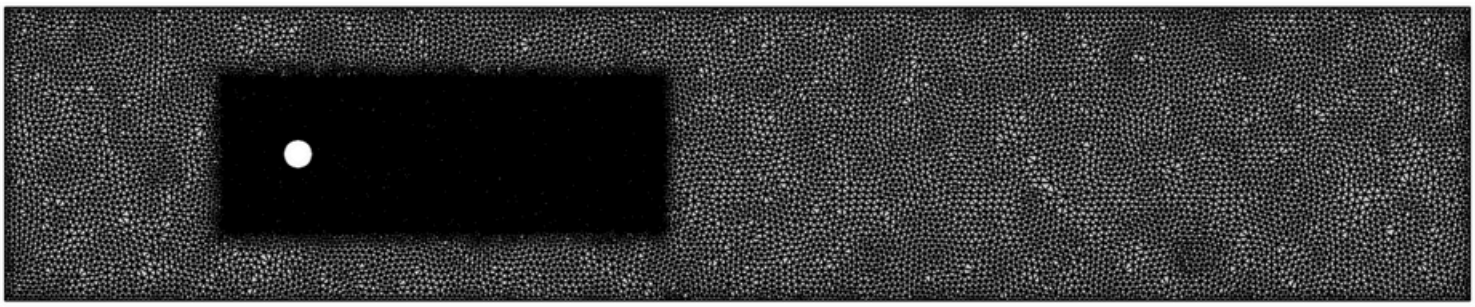


Figure 387: Mesh used for Simulating Oscillating Laminar Flow Around a Circular Cylinder

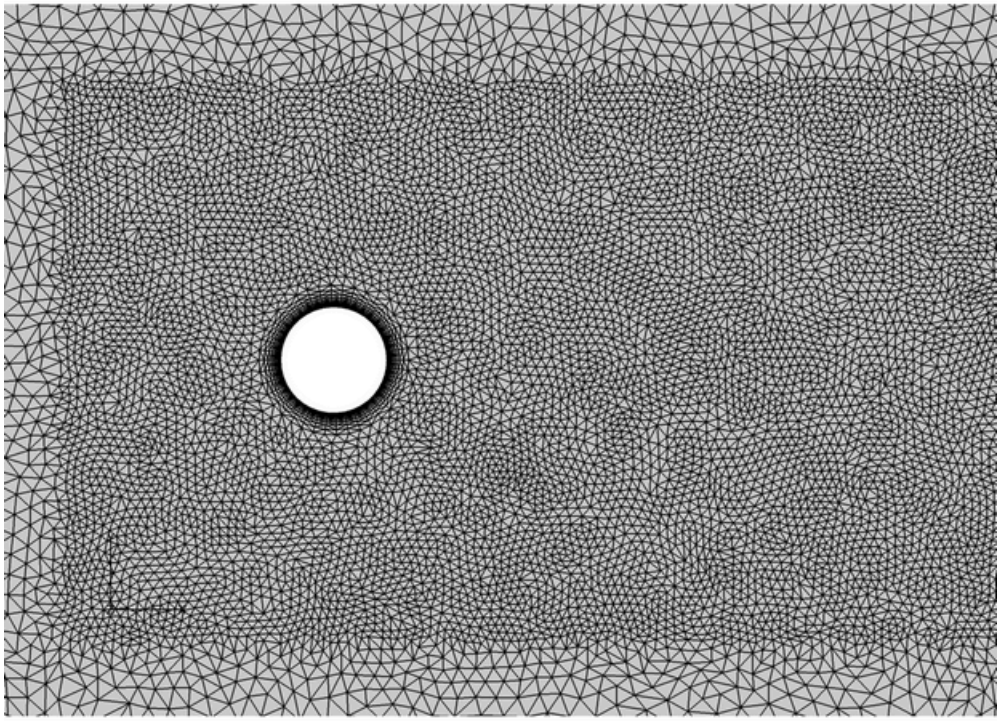


Figure 388: Details of the Mesh Showing Refinement Zone Around the Cylinder

AcuSolve Results

The simulation was run as transient for a time record sufficient to ensure that the vortex shedding in the wake reached a stabilized oscillation frequency. The AcuSolve solution shows an unsteady, oscillating flow field with flow around the cylinder separating from the cylinder surface. A wake area is developed downstream of the cylinder with alternating vortices shedding at a regular frequency from the top and bottom of the cylinder surface. This results in oscillating lift forces that act on the cylinder as shown in the following images.

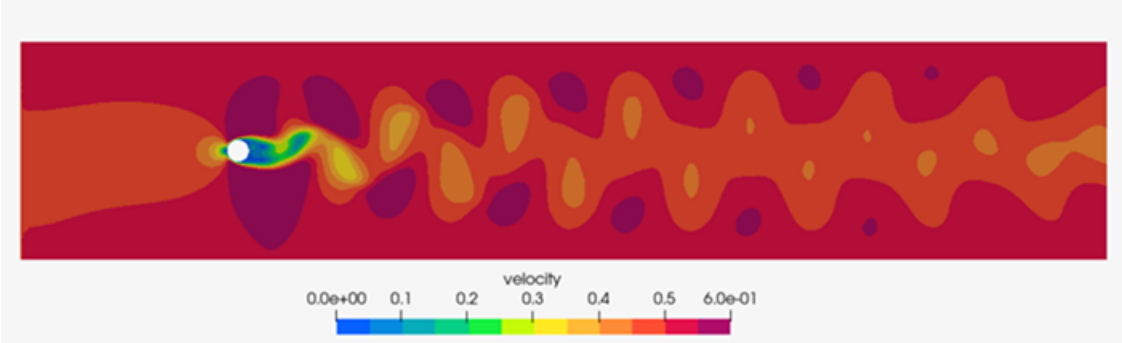


Figure 389: Contours of Velocity Magnitude

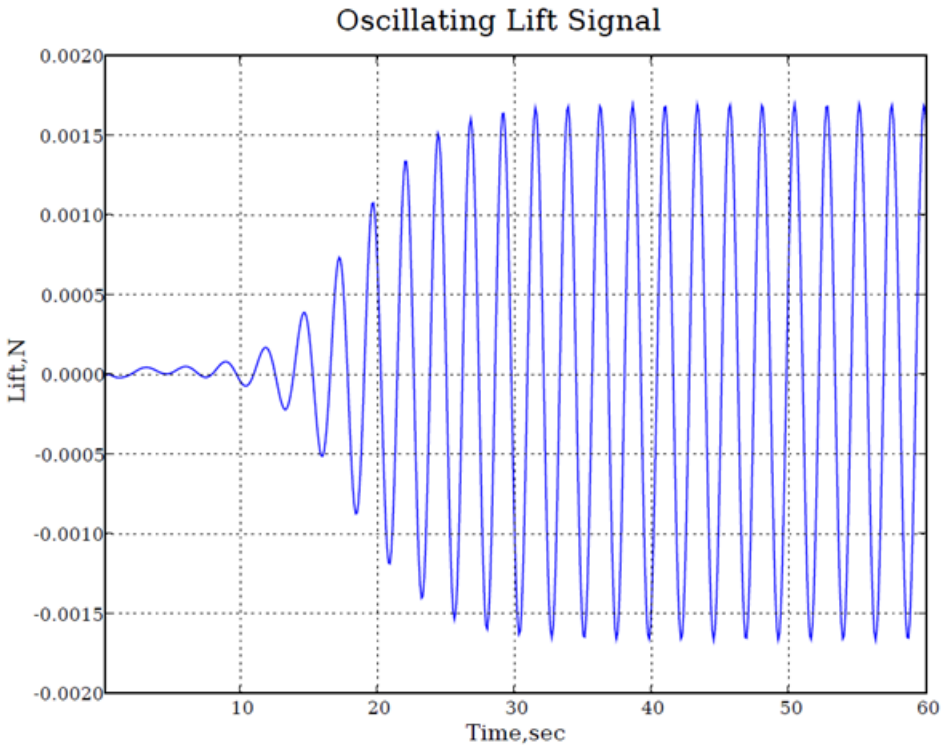


Figure 390: Lift Coefficient (lift force perpendicular to flow) plotted against time. Simulation was run for 600 time steps for a duration of 60 s

The Strouhal number for this simulation, a dimensionless number describing oscillating flows, is used to validate AcuSolve results. The experimental Strouhal number for this problem is given by

$$St = \frac{\omega * L}{V} = 0.165 \qquad (14)$$

where ω is the dominant frequency of oscillations, L is the diameter of the cylinder, and v is the flow velocity.

The peak frequency of the oscillating lift force was computed by transforming the time dependent data into frequency space with a Fourier transform. From the Fourier transform, the AcuSolve-based Strouhal number was calculated. The table below shows the comparison of the Strouhal number provided by the AcuSolve prediction and the measurement given by Tritton (1959).

Table 21:

	Experimental	**AcuSolve**
Strouhal number	0.165	0.173

Summary

In this application, two dimensional flow over a cylinder is achieved by enforcing symmetry conditions on the front and back surfaces of the flow domain. The laminar, unsteady simulation shows the flow separation that leads to alternating vortex shedding. Frequency of the lift force acting on the cylinder is calculated to evaluate the Strouhal number. The AcuSolve solution compares well with results reported by Tritton (1959), differing slightly from the experimental results. In this application, AcuSolve demonstrates the ability to accurately predict oscillating laminar flow around a circular cylinder.

Simulation Settings for Oscillating Laminar Flow Around a Circular Cylinder

HyperMesh CFD database file: `<your working directory>\cylinder_laminar\cylinder_laminar.hm`

Global

- Problem Description
  - Analysis type - Transient
  - Turbulence equation - Laminar
- Auto Solution Strategy
  - Analysis type - Transient
  - Max time - `600` sec
  - Initial time increment - `0.1` sec
- Material Model
  - Fluid
    - Density - `1.0` kg/m3
    - Viscosity - `1.0e-3` kg/m-sec

  Model
- Volumes
  - Volume
    - Element Set
      1. Material model - Fluid
- Surfaces
  - Back
    - Simple Boundary Condition
      1. Type - Symmetry
  - Base

- Simple Boundary Condition
  1. Type - Slip
- Front
  - Simple Boundary Condition
    1. Type - Symmetry
- Inflow
  - Simple Boundary Condition
    1. Type - Inflow
    2. Inflow Type - Average velocity
    3. Average Velocity - `0.5` m/sec
- Outflow
  - Simple Boundary Condition
    1. Type - Outflow
- Top
  - Simple Boundary Condition
    1. Type - Slip

References

D.J. Tritton. "Experiments on the Flow around a Circular Cylinder at Low Reynolds Number". Journal of Fluid Mech. 6(04):547-567. 1959

Circumferential Flow in a Cylinder Induced by a Rotating Solid

In this application, AcuSolve is used to simulate the flow of air between concentric cylinders that is initiated by the rotation of the solid inner cylinder. The outer cylinder is held stationary while the inner cylinder rotates with a constant speed. AcuSolve results are compared with analytical results as described in White (1991). The close agreement of AcuSolve results with analytical results validates the ability of AcuSolve to maintain a continuous velocity across a non-conformal guide surface interface.

Problem Description

The problem consists of a fluid with material properties of a viscous fluid with the density of air rotating between two infinitely long concentric cylinders, as shown in the following image, which is not drawn to scale. The radius of the outer cylinder is 3.0 m and the radius of the inner cylinder is 1.5 m. The inner cylinder is defined as a solid medium and rotates at 1 rad/sec. The inner cylinder's surface velocity is mapped to the adjacent surface within the fluid medium, while the outer cylinder is fixed. The induced flow is laminar and exhibits a steady state behavior after running for a short period of physical time. The rotation of the inner cylinder causes the fluid to rotate due to viscous shearing near the wall. As the outer cylinder is fixed, a velocity gradient is generated as a function of radius within the flow domain.

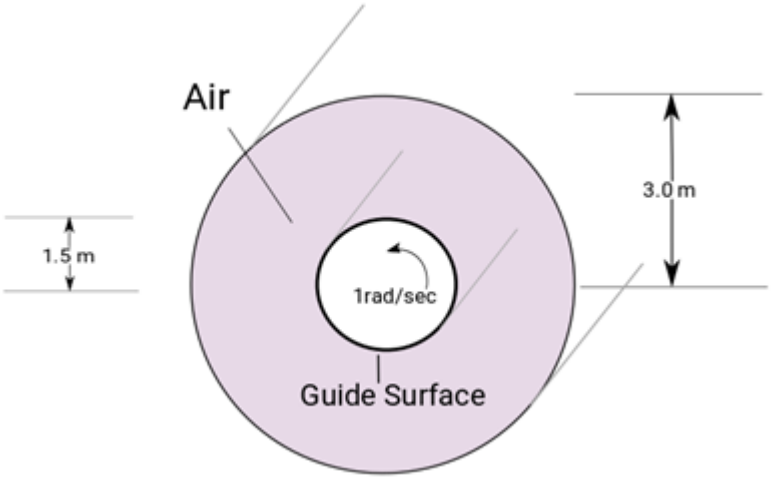


Figure 391: Critical Dimensions and Parameters Used for Simulating Flow Between Two Concentric Cylinders Split with a Guide Surface

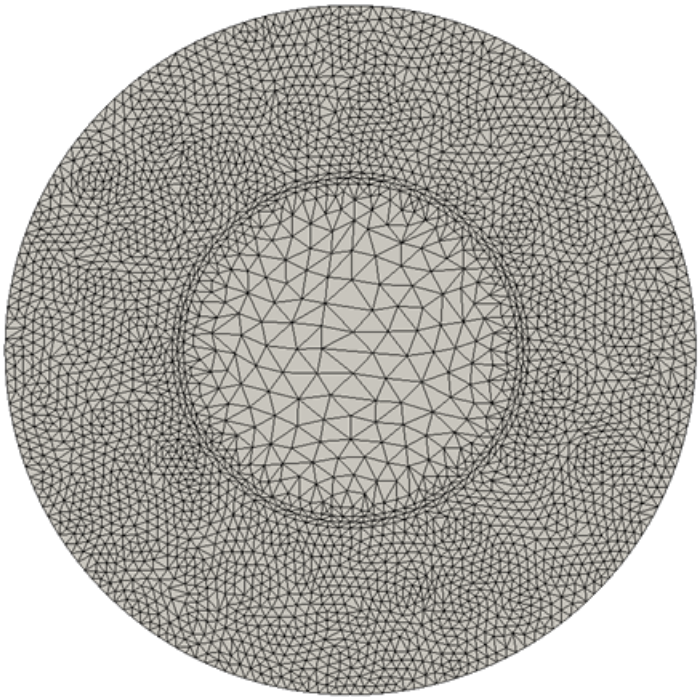


Figure 392: Mesh Used for Simulating Flow Between Two Concentric Cylinders

The simulation was performed as a two dimensional problem by constructing a volume mesh that contains a single layer of elements in the extruded direction, normal to the flow plane and by imposing slip flow and mesh boundary conditions on the extruded planes.

AcuSolve Results

The AcuSolve solution reaches a quasi-static result with the velocity between the two cylinders reaching a steady state at the simulation end time. As the solid inner cylinder rotates, it acts as a guide surface for the fluid elements to track and inherit the two velocity components. The velocity at the edge of the inner cylinder is equal to exactly the rotational speed multiplied by the radius. As the radius increases, the flow velocity reduces until it reaches zero at the outer diameter. The following images show the tangential velocity within the fluid as a function of radius from the center. The tangential velocity is compared with the analytical solution. The image below shows black circles representing the analytical solution and a solid red line for the AcuSolve results.

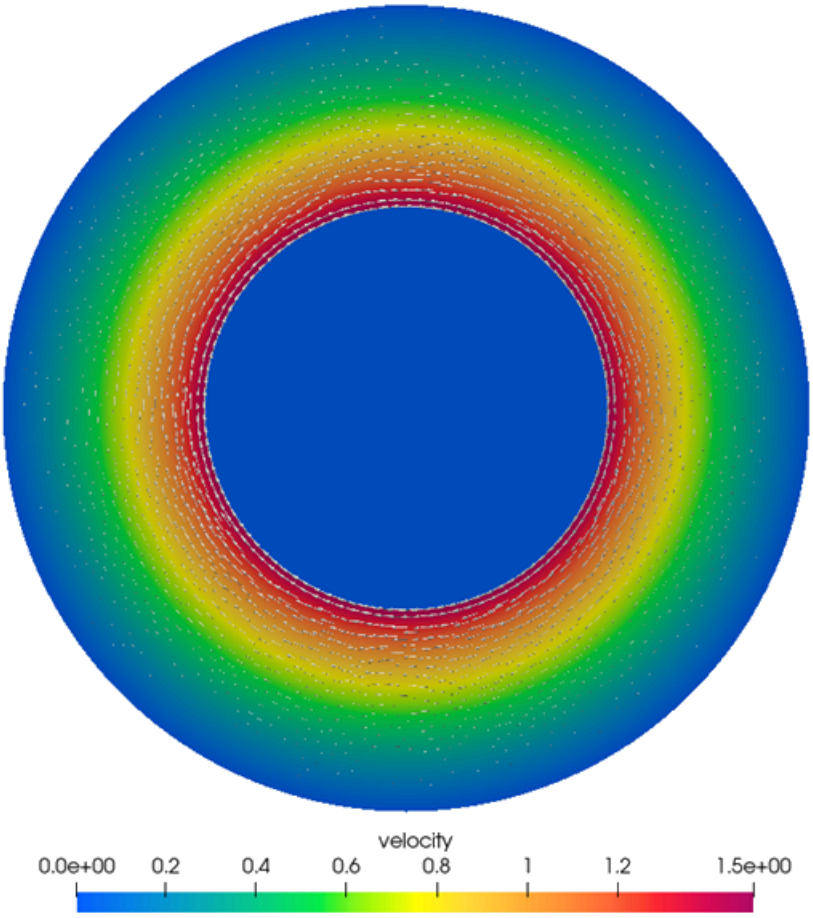


Figure 393: Contours and Vectors of Velocity Between the Concentric Cylinders

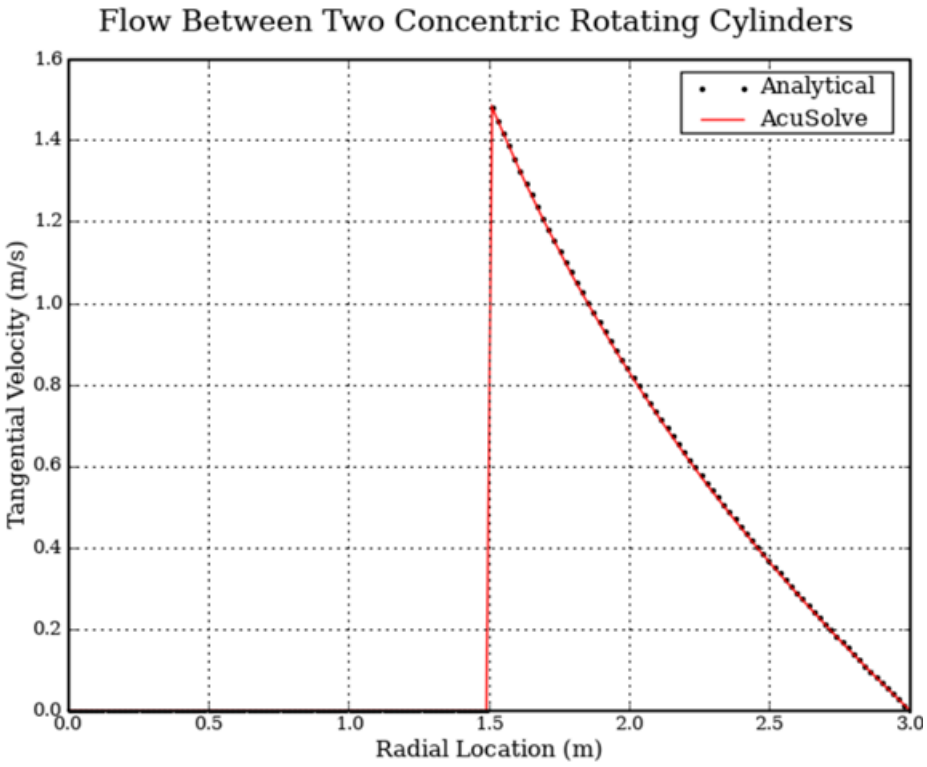


Figure 394: Tangential Velocity Within the Solid and Fluid as a Function of Radial Distance from the Center at the Final Timestep

Summary

The AcuSolve solution compares well with analytical results for laminar flow between concentric cylinders, where the inner cylinder guides the adjacent fluid elements. In this application, a fluid initially at rest inherits the angular velocity from the inner cylinder while the outer cylinder does not rotate. As a result of the inherited velocity and viscosity of the fluid, flow develops between the two cylinders. The AcuSolve solution for the tangential velocity as a function of radius matches exactly with the analytical results.

Simulation Settings for Flow Between Concentric Split Cylinders

HyperMesh CFD database file: `<your working directory>\annulus_split_rotating \annulus_split_rotating.hm`

- Problem Description
  - Analysis type - Transient
  - Flow equation - Navier Stokes
  - Turbulence equation - Laminar
  - Mesh type - Arbitrary Mesh Movement (ALE)
- Auto Solution Strategy
  - Max time steps - `40`
  - Initial time increment- `0.02` sec

    - Convergence tolerance - `0.001`
    - Min stagger iterations - `2`
    - Max stagger iterations - `4`
- Material Model
    - Air
        - Density
            1. Type - Constant
            2. Density - `1.225` kg/m3
        - Viscosity
            1. Type - Constant
            2. Viscosity - `1.781` kg/m-sec
- Mesh Motion
    - Rotation
        - Rotation Center
            1. X-coordinate - `2.0` m
            2. Y-coordinate - `0.0` m
            3. Z-coordinate - `0.0` m
        - Angular velocity
            1. X-component - `1.0` rad/sec
            2. Y-component- `0.0` rad/sec
            3. Z-component - `0.0` rad/sec

    Model
- Volumes
    - CylinderInner
        - Element Set
            1. Medium - Solid
            2. Material model - Aluminum
    - CylinderOuter
        - Element Set
            1. Medium - Fluid
            2. Material model - Air
- Surfaces
    - InBottom
        - Simple Boundary Condition
            1. Type- Slip
            2. Mesh displacement type- Slip
    - InInterf

        - Simple Boundary Condition
            1. Type- Wall
            2. Mesh displacement type- Fixed
            3. Mesh motion- Rotation
        - Guide Surface
            1. Type- Faceted
    - InTop
        - Simple Boundary Condition
            1. Type- Slip
            2. Mesh displacement type- Slip
    - OutBottom
        - Simple Boundary Condition
            1. Type- Slip
            2. Mesh displacement type- Slip
    - OutInterf
        - Simple Boundary Condition
            1. Type- Wall
            2. Wall velocity type- Match Mesh Velocity
            3. Mesh displacement type- Guide surface
            4. Guide surface- InInterf
    - OutTop
        - Simple Boundary Condition
            1. Type- Slip
            2. Mesh displacement type- Slip
    - OutWall
        - Simple Boundary Condition
            1. Type- Wall
            2. Mesh displacement type- Fixed
- Nodes
    - PressurePoint
        - Pressure
            1. Type- Zero

References

F. M. White. "Viscous Fluid Flow". Section 3-2.3. McGraw-Hill Book Co., Inc. New York. 1991.

Two-Phase Nucleate Boiling in a Cylindrical Pipe

In this application, AcuSolve is used to simulate the changes in wall temperature due to two-phase nucleate boiling at the heated walls of a pipe with water flowing through it. AcuSolve results are compared with experimental results adapted from Koncar and others (2015). The close agreement of AcuSolve results with experimental results validates the ability of AcuSolve to model two-phase nucleate boiling problems.

Problem Description

The problem consists of a pipe with heated surrounding walls, as shown in the following image, which is not drawn to scale. The length of the pipe is 2 m and the radius is 0.0017 m. Mass flux at the inlet is 900 kg/m^2 and the temperature of the fluid entering the pipe is 473 K. A heat flux of 570,000 W/m^2 is applied on the walls. The preheated water enters the inlet and heat is transferred to the fluid from the walls. The heat causes sub-cooled boiling to occur in the region close to the wall and leads to the formation of bubbles at nucleation sites.

During sub-cooled boiling flow, heat and mass exchange between the phases takes place on the heated wall and in sub-cooled liquid flow. On the heated surface the vapor bubbles are generated and as they move through the sub-cooled liquid they condense and release the latent heat.

The AcuSolve simulation is set up to model transient state heat transfer to determine the temperature along the centerline of the pipe and along the heated pipe walls of the model. AcuSolve computes the two-phase nucleate boiling by simulating the three-dimensional flow in a heated pipe for two-phase boiling flow, as described in Koncar (2005). The temperatures along the centerline of the pipe and along the pipe walls are compared against the experimental measurements, as described in Koncar, et al. (2005).

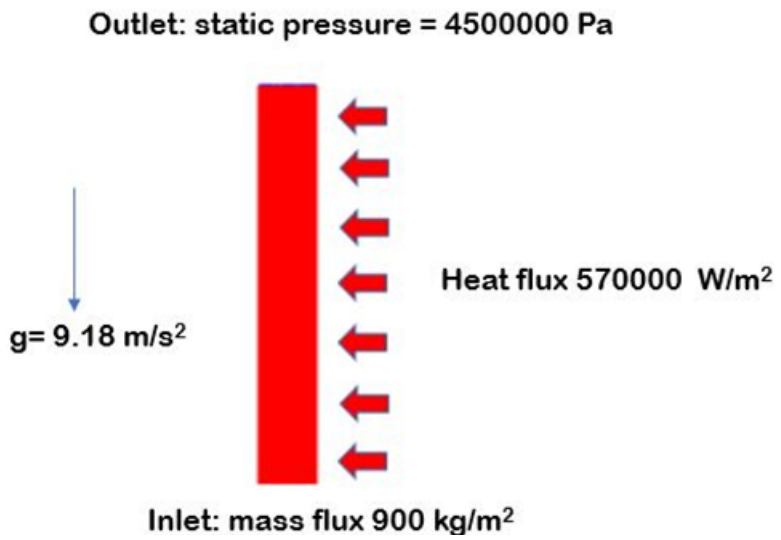


Figure 395: Parameters for Simulating a Two-Phase Nucleate Boiling Problem of a Pipe

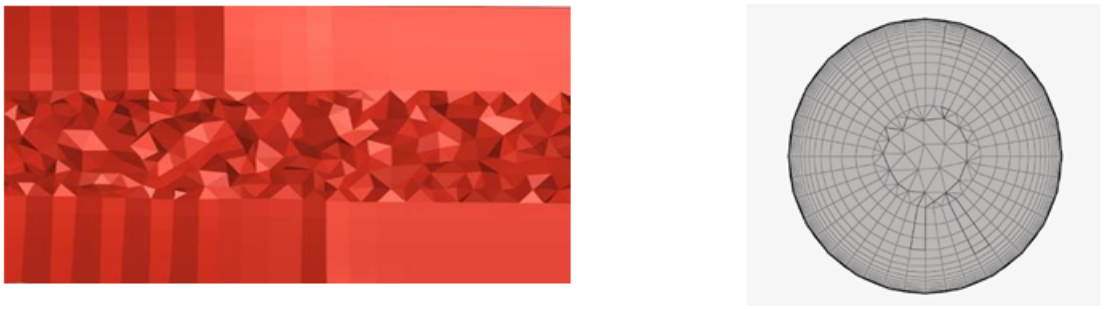


Figure 396: Mesh used for Simulating Two-Phase Flow in a Pipe

AcuSolve Results

The AcuSolve solution is run for a heat flux of 570,000 W/m^2 and the results are presented in the following image. The experimental values of wall temperature are presented with the corresponding AcuSolve results along the centerline of the pipe and along the pipe wall. The AcuSolve results show good agreement with the experimental results for the temperature, indicating that the two-phase nucleate boiling is properly captured.

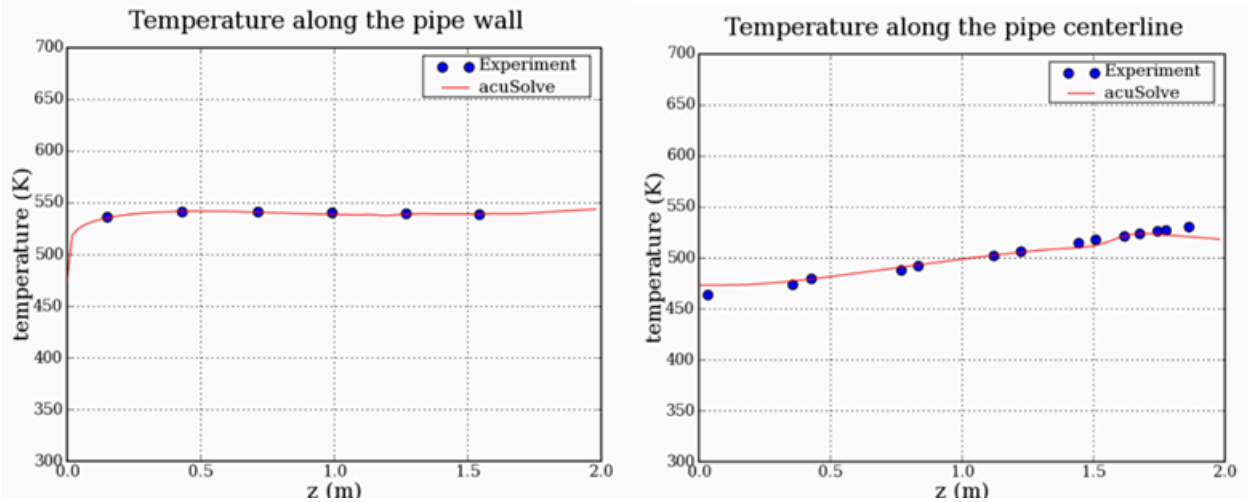


Figure 397: Temperature Values for Varying Streamwise Distance Compared to Experimental Data

Summary

The AcuSolve solution compares well with experimental results for two-phase nucleate boiling simulations. In this application, the temperature of the wall as the onset of boiling approaches are simulated with AcuSolve using the nucleate boiling feature and the SA turbulence model. The experimental values of temperature are presented with the corresponding AcuSolve results. A good agreement of simulation results with the experiment validates the ability to solve two-phase nucleate boiling using the nucleate boiling capabilities of AcuSolve.

Simulation Settings for Two-Phase Nucleate Boiling in a Cylindrical Pipe

HyperMesh CFD database file: `<your working directory>\pipe_two_phase_boiling \pipe_two_phase_boiling.hm`.

Global

- Problem Description
  - Analysis type – Transient
  - Turbulence equation – SA
  - Temperature equation – Advective Diffusive
- Auto Solution Strategy
  - Maximum time steps – `500`
  - Initial time increment – `0.003`
  - Convergence Tolerance – `0.001` sec
  - Relaxation factor – `0.3`
- Surface Tension Model (“Water_NB-Vapor_NB”)
  - Type – Constant
  - Surface Tension – `0.02382`
- Material Model
  - Vapor_NB
    - Type – Constant
    - Density – `23.75` kg/m^3
    - Viscosity – `1.79e-05` kg/m-sec
    - Specific Heat – `4225` J/kg-K
    - Latent Heat – `1675570`
    - Latent Heat Temperature – `530.55` K
    - Conductivity – `0.02528` W/m-K
  - Water_NB
    - Type – Constant
    - Density – `800` kg/m3
    - Viscosity – `0.0001339` kg/m-sec
    - Specific Heat – `4500` J/kg-K
    - Conductivity – `0.65` W/m-K
- Multifield parameter (Field interaction model)
  - Type – Algebraic Eulerian
  - Phase change type – Wall Boiling
  - Carrier field - Water
  - Disperse field – Vapor
  - Disperse field diameter type – Boiling kurul exponential
  - Drag model – Ishii zuber
  - Lift Model – Legendre Magnaudet

Model

- Volumes
  - Fluid
    - Material – Vapor_Water
- Surfaces
  - Inflow
    - Simple Boundary Condition – Inflow
    - Inflow type – Mass Flux Rate
    - Mass Flux Rate – `0.167634` kg/sec
    - Temperature – `473` K
  - Outflow
    - Simple Boundary Condition – Outflow
    - Pressure – `4500000` N/m2
  - Wall
    - Simple Boundary Condition – Wall
    - Temperature type – Flux
    - Heat Flux – `570000` W/m2

References

B. Koncar, E. Krapper, Y. Egorov, 2005, "CFD MODELING OF SUBCOOLED FLOW BOILING FOR NUCLEAR ENGINEERING APPLICATIONS", International Conference Nuclear Energy for New Europe 2005, Bled, Slovenia, September 5-8,2005.

Supersonic Flow Through a Converging-Diverging Nozzle

In this application, AcuSolve is used to simulate the high-speed turbulent flow in a converging and then diverging nozzle. The flow within the nozzle enters as subsonic, reaches sonic at the throat and shortly after develops a normal shock. AcuSolve results are compared with experimental results adapted from Bogar and Sajben (1983). The close agreement of AcuSolve results to experimental measurements validates the ability of AcuSolve to simulate internal supersonic flows where normal shocks are present.

Problem Description

The problem consists of a converging and then diverging nozzle represented as an extruded planar surface, as shown in the image below, which is not drawn to scale. The length of the domain is 0.213 m with a throat height of 0.044 m. The stagnation pressure and static temperature are constrained at the inlet to 135,000 Pa and 265.98 K, respectively. The static pressure is defined using the outflow boundary condition, where P_{static}=97216.08 Pa. The flow in the diffuser has an inlet Reynolds number of $6.5x10^5$. The upper and lower walls are set to no-slip and the side walls are set to slip, while the exterior walls are specified to be adiabatic. Images of the numerical mesh are shown below.

The AcuSolve simulation is prepared to model the pseudo-transient state to determine the shock location and corresponding scalar quantities within the diffuser. AcuSolve computes the flow and thermal solution by simulating a planar, two-dimensional flow problem with physical dimensions and input quantities as described in the Sajben Diffuser case presented by Bogar and Sajben (1983). The gas in the simulation domain enters at subsonic conditions and is forced to accelerate beyond Mach=1.0 as it passes through the throat. After reaching supersonic speed a normal shock wave develops causing the flow speed to reduce back below sonic. The pressure along the bottom wall of the diffuser is compared against experimental measurements to demonstrate the solver's capability to solve supersonic cases.

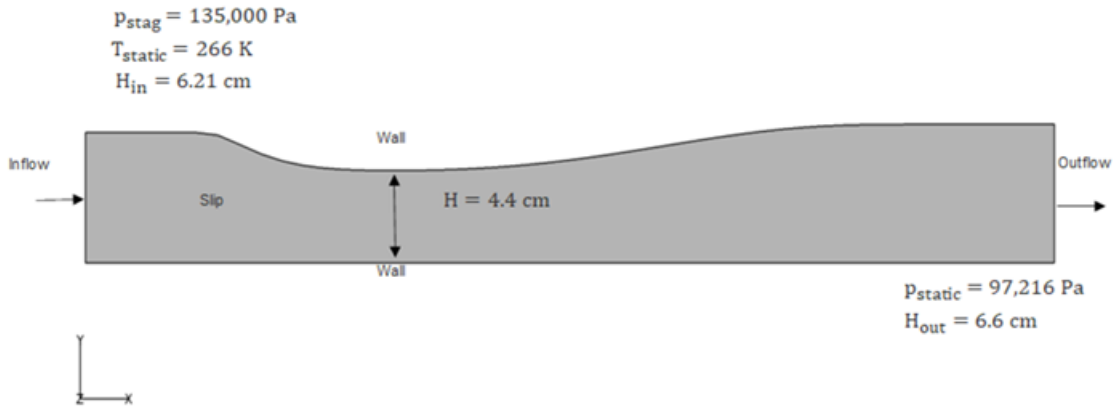


Figure 398: Parameters for Simulating Compressible Flow within a Converging-Diverging Nozzle

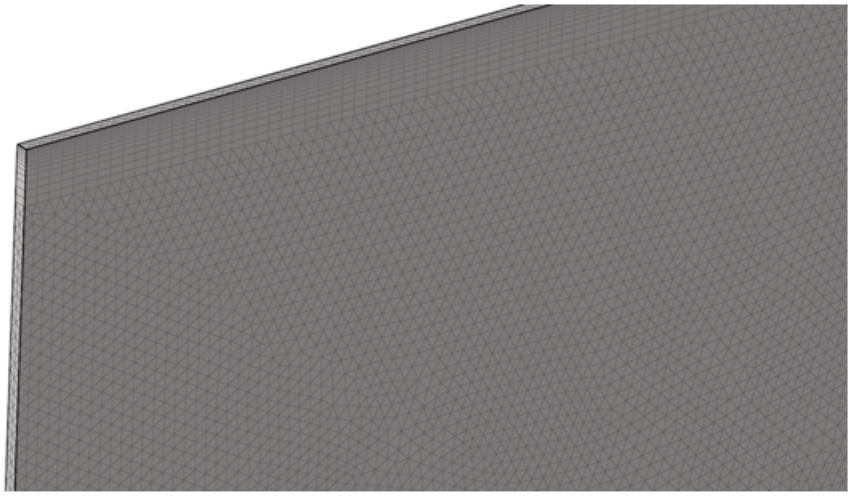


Figure 399: Mesh used for Simulating Compressible Flow in a Converging-Diverging Nozzle

AcuSolve Results

The AcuSolve solution is run for 0.025 seconds (6,250 timesteps with dt=4.0x10^{-6}sec) and converges to a pseudo-steady solution. The change in pressure from the inlet to outlet causes the flow to accelerate within the throat of the diffuser until it reaches approximately Mach=1.35. A normal shock is present just downstream of where the cross-sectional area of the nozzle increases, as shown in the image below. The numerical solution can be compared with the reference after normalizing the pressure along the wall by the inlet stagnation pressure (135 kPa) and the distance along the bottom wall by the nozzle throat height (0.044 m). The image below shows the normalized pressure versus normalized distance in comparison to NASA reference and experimental results. The image shows black circles representing the experimental measurements (Bogar and Sajben 1983), a dashed blue line representing the SA solution as obtained through NASA publication (Mohler 2005) and a solid red line representing the AcuSolve results with the Spalart-Allmaras turbulence model. The non-dimensional pressure within the diffuser agrees well with the reference data, demonstrating the correct physical location of the normal shock and expected moderate flow speed reduction within the constant cross-section diffuser portion of the nozzle.

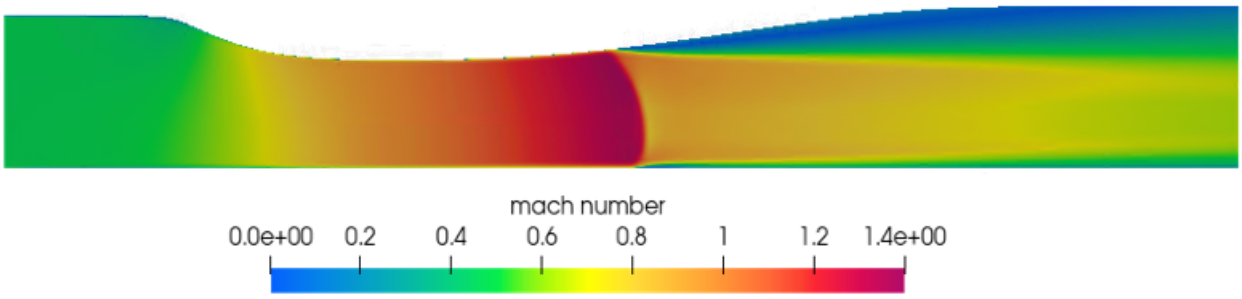


Figure 400: Contours of Mach Number within a Converging-Diverging Nozzle

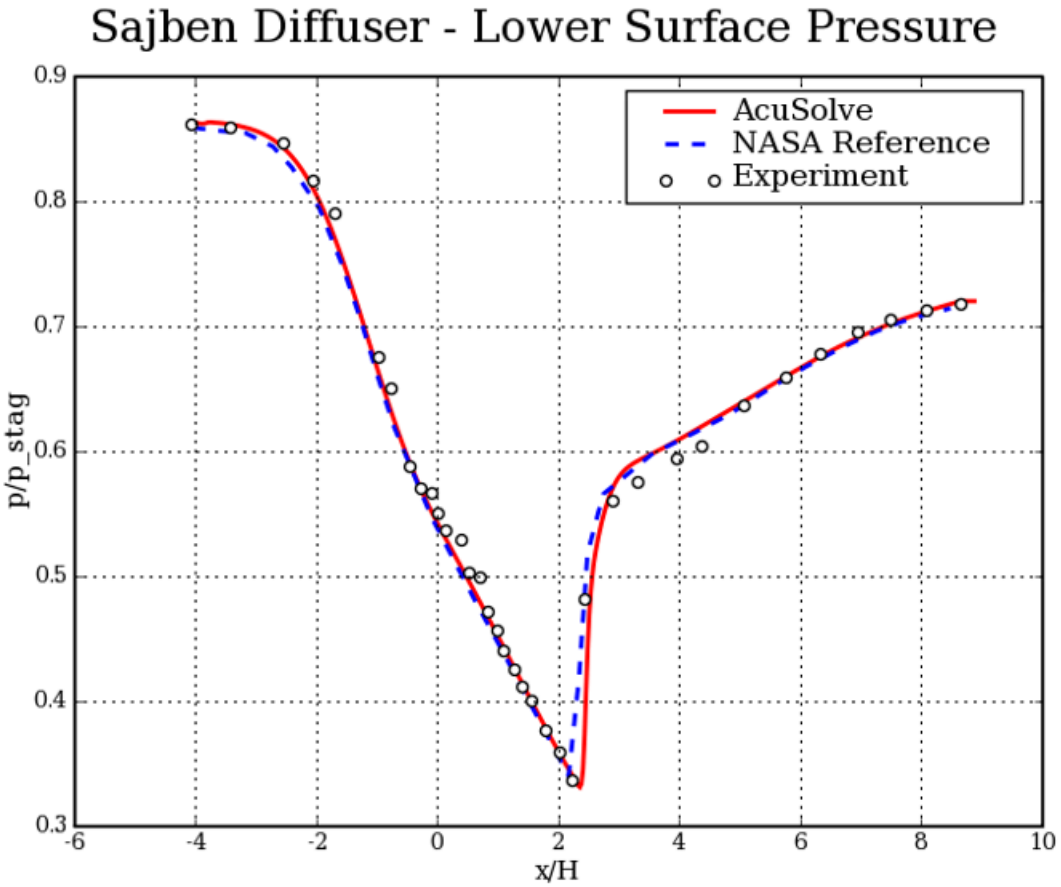


Figure 401: Normalized Pressure Versus Normalized Distance in Comparison to NASA Reference and Experimental Results

Summary

The AcuSolve solution compares well with experimental and numerical results for the described simulation. In this application, compressibility effects are accounted for using the coupled compressible flow solver with the ideal gas material definition. The thermal and momentum exchange within the nozzle is computed with AcuSolve using the compressible Navier-Stokes solver with the Spalart-Allmaras turbulence model. The experimental values of pressure are presented with the corresponding AcuSolve results and show good agreement, validating the ability to solve compressible cases with the presence of normal shocks. The results indicate that AcuSolve is able to properly predict the peak pressure magnitude and location within the diffuser while maintaining the normal shock when the time-step is selected to result in a maximum CFL of approximately 30.

Simulation Settings for Supersonic Flow Through a Converging-Diverging Nozzle

HyperMesh CFD database file: `<your working directory>\diffuser_compressible\diffuser_compressible.hm`

Global

- Problem Description

    - Flow – Compressible Navier Stokes
    - Analysis type – Transient
    - Turbulence equation – SA
    - Temperature equation – Advective Diffusive
- Auto Solution Strategy
    - Initial time increment – `4.0E-6`
    - Final time – `0.025` sec
    - Convergence Tolerance – `0.001` sec
    - Relaxation factor – `0.5`
- Material Model
    - Air-Ideal Gas
        - Type – Ideal_Gas
        - Viscosity – `1.781e-05` kg/m-sec
        - Specific Heat – `1005` J/kg-K
        - Conductivity – `0.02521` W/m-K
        - Gas Constant – `287.058` J/kg-K

Model

- Volumes
    - Fluid
        - Material – Air-Ideal Gas
- Surfaces
    - Inflow
        - Simple Boundary Condition – Inflow
        - Inflow type – Stagnation Pressure
        - Stagnation Pressure – `135000.0` N/m2
        - Turbulence_input_type – Direct
        - Eddy Viscosity – `1e-6` m^2/s
        - Temperature – `265.98` K
    - Outflow
        - Simple Boundary Condition – Outflow
        - Pressure – `97216.08` N/m2
    - Wall_1
        - Simple Boundary Condition – Wall
        - Type – auto_wall
    - Wall_2
        - Simple Boundary Condition – Wall
        - Type – auto_wall
    - Slip_1

        - Simple Boundary Condition – Slip
    - Slip_2
        - Simple Boundary Condition – Slip

References

Bogar, T. J., Sajben, M., and Kroutil, J. C. (1983) "Characteristic Frequencies of Transonic Diffuser Flow Oscillations," AIAA Journal, Vol. 21, No. 9, pp. 1232-1240.

Mohler, S.R., "Wind-US Unstructured Flow Solutions for a Transonic Diffuser," NASA CR-2005-213417, January 2005.

Turbulent Flow Over an Oscillating Rigid Body Assembly

In this application, AcuSolve is used to simulate the fluid-structure interaction of a fluid moving over a cylinder/plate assembly. AcuSolve results are compared with experimental results as described in Gomes and Lienhart (2009). The close agreement of AcuSolve results with the experimental results validates the ability of AcuSolve to model cases in which the fluid forces lead to structural motions.

Problem Description

The problem consists of a fluid having material properties of standard water with density of 998 kg / m^3 and kinematic viscosity of 0.97e-6 m^2/sec through a two dimensional channel over a cylinder and plate assembly. The diameter of the cylinder is 0.022 m and the plate length is 0.042 m, while the inlet velocity is specified to match experimental conditions with a max velocity of 1.07 m/sec, as is shown in the following image, which is not drawn to scale. The model is simulated as transient with constant inflow conditions, allowing an oscillatory motion of the assembly to develop. The Shear Stress Transport (SST) turbulence model is used to model the turbulent portion of the flow and AcuSolve's internal rigid body motion is used to capture the motion of the oscillating assembly.

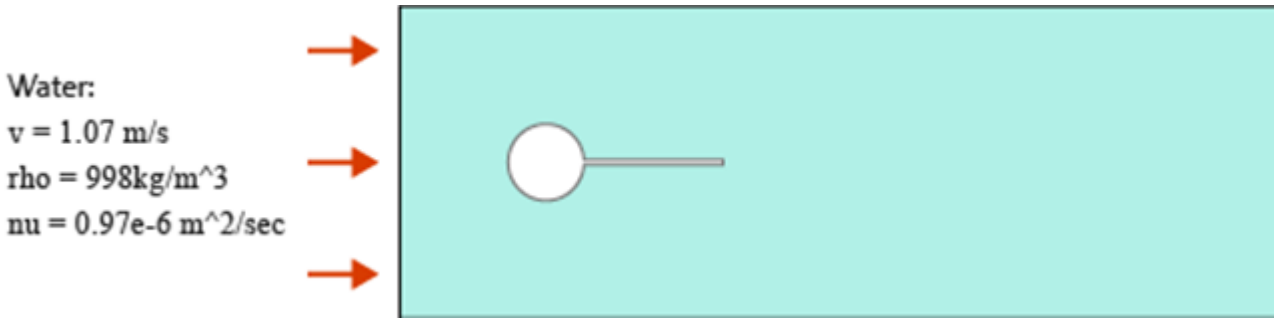


Figure 402: Critical Dimensions and Parameters used for Simulating Rigid Body Motion of Flow Past a Cylinder/Plate Assembly

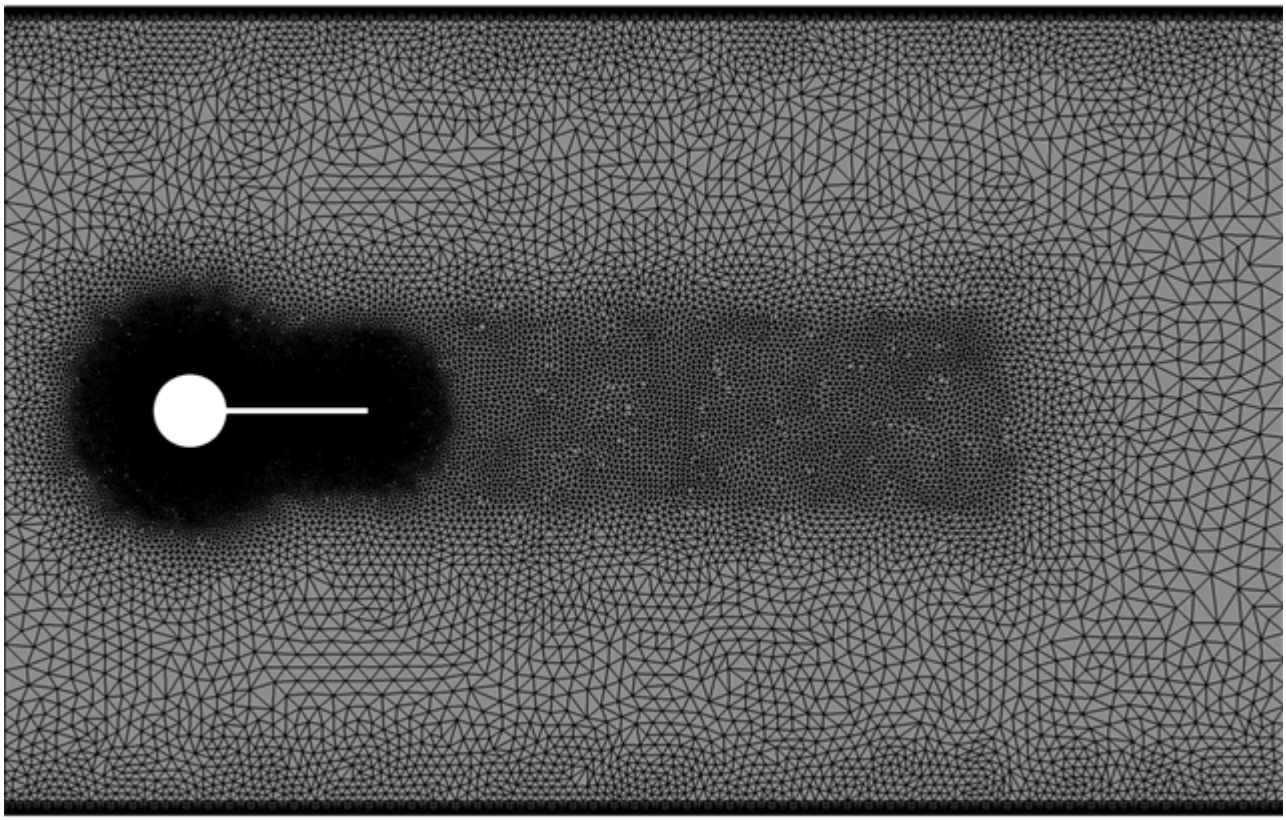


Figure 403: Mesh used for Simulating Rigid Body Motion of Flow Past a Cylinder/Plate Assembly

The simulation was performed as a two dimensional problem by constructing a volume mesh that contains a single layer of elements extruded in the cross stream direction, normal to the flow plane and by imposing symmetry boundary conditions on the extruded planes. The upper and lower walls are specified as no-slip and the inlet velocity is specified to match the conditions of the experiment (Gomes and Lienhart 2009).

AcuSolve Results

The AcuSolve solution reached a regularly repeating oscillatory state and the simulation was allowed to proceed for 10 seconds of physical time to obtain enough cycles for statistical analysis. The motion of the cylinder/plate assembly is directly attributed to the vortices shedding in its wake. The fluctuating loads on the assembly that result from the vortex shedding lead to a repeating cycle of structural rotation. The dominant oscillation frequency from the simulation was found to match well with the experimental measurements, within approximately 3.5 percent. The images below show the rigid body displacement of the assembly as it oscillates within the flow. Contours of velocity magnitude demonstrate the forcing on the assembly, while the mesh motion around the structure is captured and plotted for a single time step. Two dimensional plots showing the angular displacement demonstrate the motion, showing a single red line for the AcuSolve results.

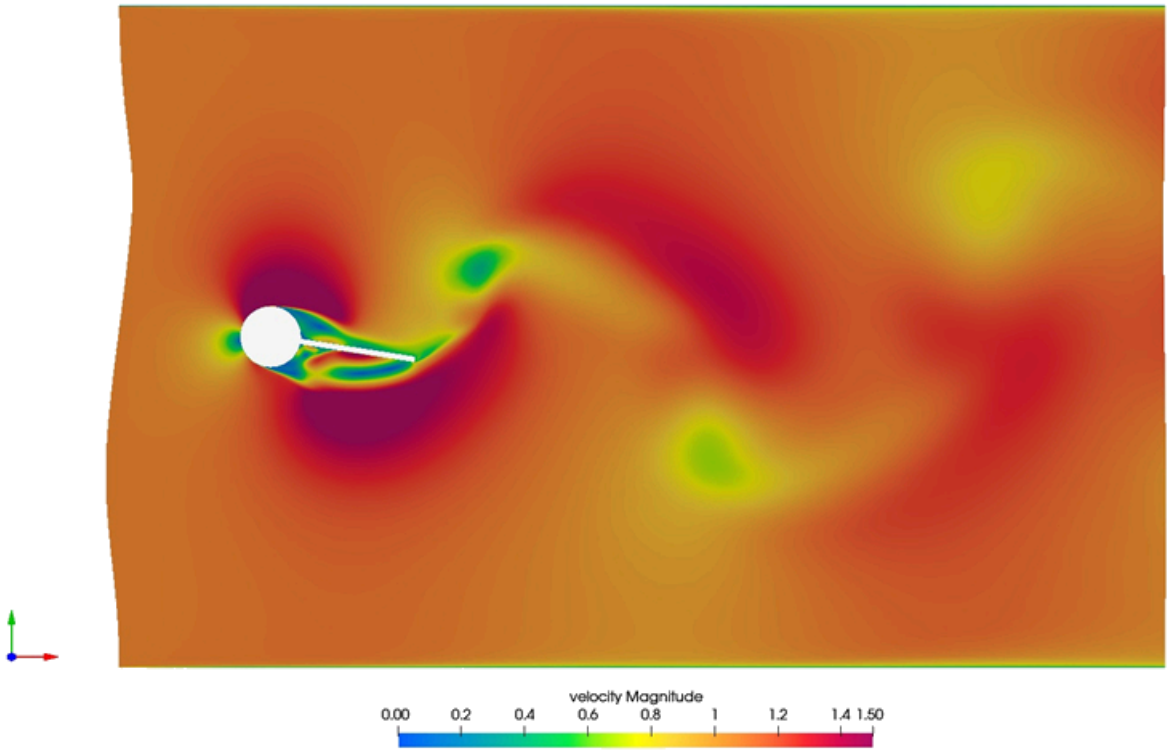


Figure 404: Velocity Contours Near the Assembly for a Single Time Step During the Simulation

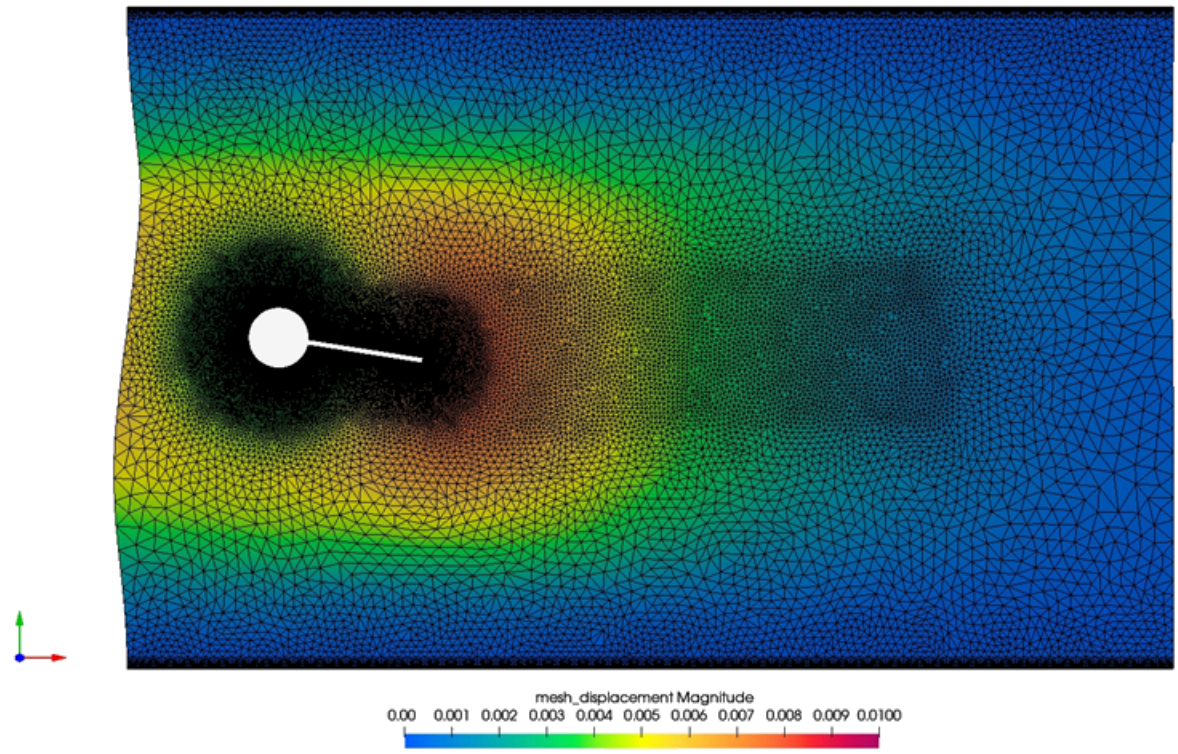


Figure 405: Mesh Displacement Contours Near the Assembly for a Single Time Step During the Simulation

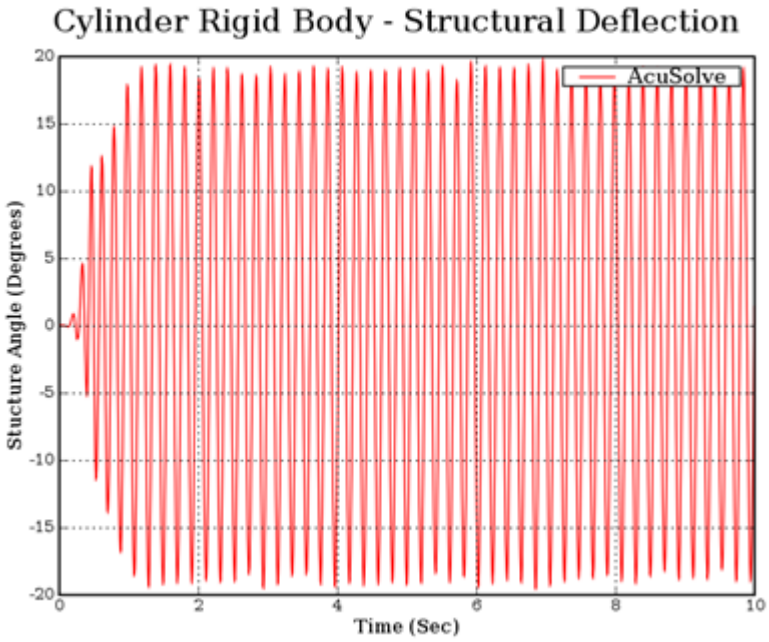


Figure 406: Rigid Body Displacement of the Assembly as a Function of Time, Showing the Oscillation Develop into the Pseudo-Steady Motion

The dominant frequency of the oscillation is easily identified in the Fast Fourier Transform (FFT) of the deflection angle, shown in the plot below.

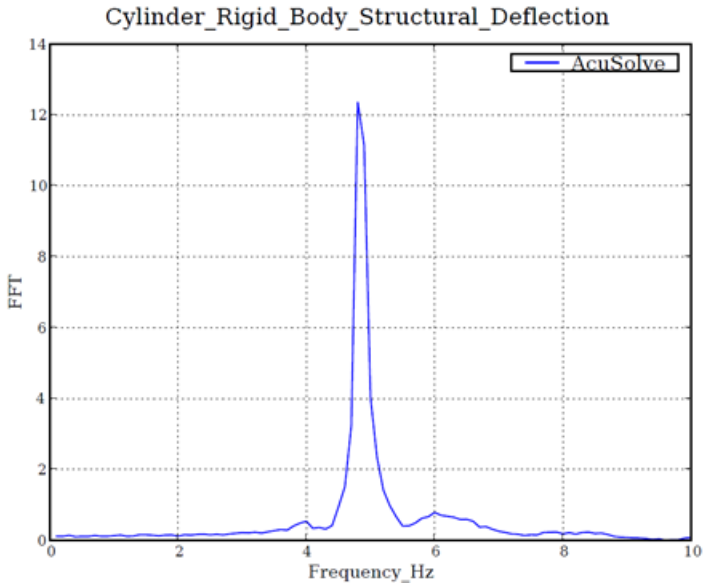


Figure 407: FFT of the Rigid Body Displacement Angle, Showing Power Spectral Density as a Function of Frequency

Summary

The AcuSolve solution compares well with experimental data for flow past an oscillating cylinder/plate assembly. In this application, water moves over the cylinder/plate assembly, giving rise to unsteady

loading that causes the body to rotate as a rigid body. The good agreement with the natural frequency of oscillation compared to the experimental data demonstrates that AcuSolve is capable of predicting fluid forced motion with an internal rigid body dynamic solver.

Simulation Settings for Turbulent Flow Over an Oscillating Rigid Body Assembly

SimLab database file: `<your working directory>\cylinder_rigidbody_turbulent\cylinder_rigidbody_turbulent.slb`

Global

- Problem Description
  - Flow - Transient
  - Turbulence equation - SST
  - Moving Mesh - Computed
- Auto Solution Strategy
  - Final Time - `10.0`
  - Initial Time Increment- `0.005`
  - Convergence tolerance- `0.001`
  - Max stagger iterations- `3`
- Material Model
  - Water
    - Type- Constant
    - Density- `998.0` kg/m3
    - Viscosity- `0.00096806` kg/m*sec
- Mesh Motion
  - RigidBody
    - Type- Rigid Body Dynamic
      1. Z rotation- Active
      2. Mass- `0.2089` kg
      3. Dyadic
         1. X-X - `3.7 e-5` kg-m2
         2. Y-Y- `3.7 e-5` kg-m2
         3. Z-Z - `3.7 e-5` kg-m2

  Model
- Volumes
  - Volume
    - Element Set
      1. Material model- Water
- Surfaces
  - Body

- Simple Boundary Condition
  1. Type- Wall
  2. Mesh displacement BC type- Fixed
  3. Mesh motion- RigidBody
- Interpolated Motion Surface

◦ Bottom
- Simple Boundary Condition
  1. Type- Wall
  2. Mesh displacement BC type- Fixed
- Interpolated Motion Surface

◦ Inflow
- Simple Boundary Condition
  1. Type- Inflow
  2. Inflow type- Velocity
  3. X Velocity- `1.07` m/sec
  4. Turbulence input type- Auto
  5. Turbulence intensity type- High
- Advanced Options
  1. Nodal Boundary Conditions
  2. X-velocity
     1. Type- Linear
     2. Precedence- `2`
     3. Curve fit variable- Y coordinate
     4. Curve fit values- Provided
  3. Y-velocity
     1. Type- Zero
  4. Z-velocity
     1. Type- Zero

◦ Bottom
- Simple Boundary Condition
  1. Type- Wall
  2. Mesh displacement BC type- Fixed
  3. Mesh motion- RigidBody

◦ Outflow
- Simple Boundary Condition
  1. Type- Outflow

◦ Top
- Simple Boundary Condition

1 Type- Wall
2 Mesh displacement BC type- Fixed

- maxZ
  - Simple Boundary Condition
    1 Type- Slip
- minZ
  - Simple Boundary Condition
    1 Type- Slip

References

Gomes, J. P. and Lienhart, H. (2009) Experimental Benchmark: Self-excited Fluid-structure Interaction Test Cases, in Fluid-Structure Interaction II: Modeling, Simulation, Optimization, Bungartz, H. J., Mehl, M., Schafer, M. (eds.), 383-412, Springer-Verlag.Ryhming.

Ideal Gas Compression in an Actuating Piston

In this application, AcuSolve is used to simulate pressure and temperature inside an actuating piston using the ideal gas relationship and fully defined mesh motion. AcuSolve results are compared with analytical results as described in Moran and Shapiro (2000). The close agreement of AcuSolve results with analytical results validates the ability of AcuSolve to model cases with material properties defined by the ideal gas law subjected to significant mesh distortion.

Problem Description

The problem consists of air compressed by a piston within a cylinder 10 m long with a diameter of π (3.14159) m, as shown in the following image, which is not drawn to scale. The piston is driven by a crankshaft 4 m long attached to a connecting rod 6 m long. The crankshaft rotates at 60o/s around a center point. At time (t) = 0.0 s the crank and piston are at top dead center (TDC) with an initial cylinder volume of 80 m^3. At t = 3.0 s the piston is at bottom dead center (BDC), at which point the volume in the cylinder is reduced to 16 m^3. The piston then moves back to TDC at t = 6.0 s. Air at atmospheric conditions, with material properties of an ideal gas and a dynamic viscosity of 1.781 X 10^5 kg/m-sec is the fluid modeled in the domain.

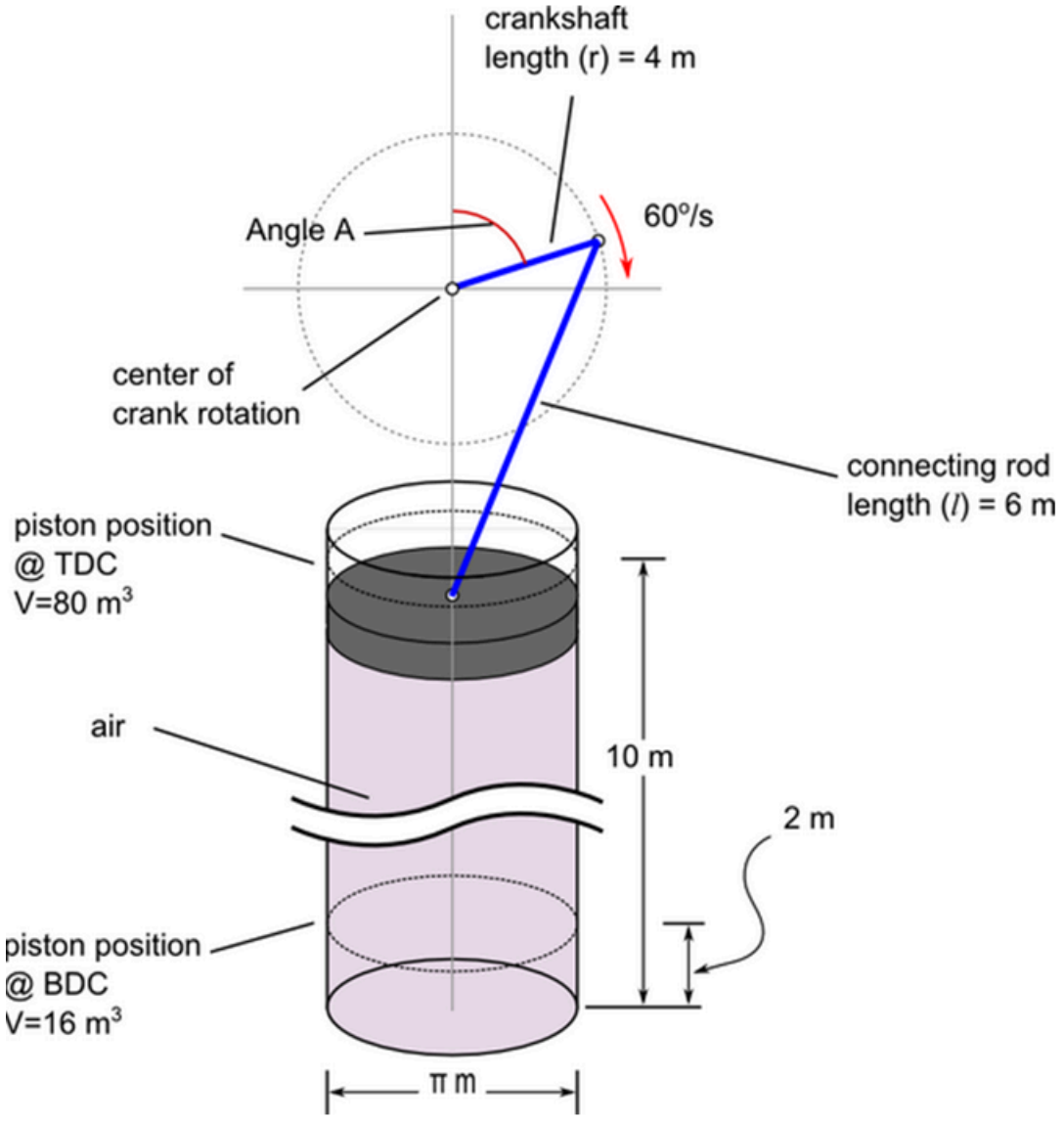


Figure 408: Critical Dimensions and Parameters for Simulating Ideal Gas Compression in an Actuating Piston

The motion of the piston is described by the following equation.

$$x = r * \cos A + \sqrt{l^2 - r^2 \sin^2 A} \qquad (15)$$

Where

- x is the distance of the piston from TDC
- r is the length of the connecting rod, 4 m
- A is the crank angle as a function of time (t)
- l is the connecting rod length, 6 m

During the simulation, the top surface of the cylinder, representing the piston, moves with an applied mesh motion that mimics the motion of the reciprocating crank, rod, and piston assembly. The ideal gas

is compressed by contracting the mesh according to the motion of that assembly and by allowing the fluid properties to change as a function of time.

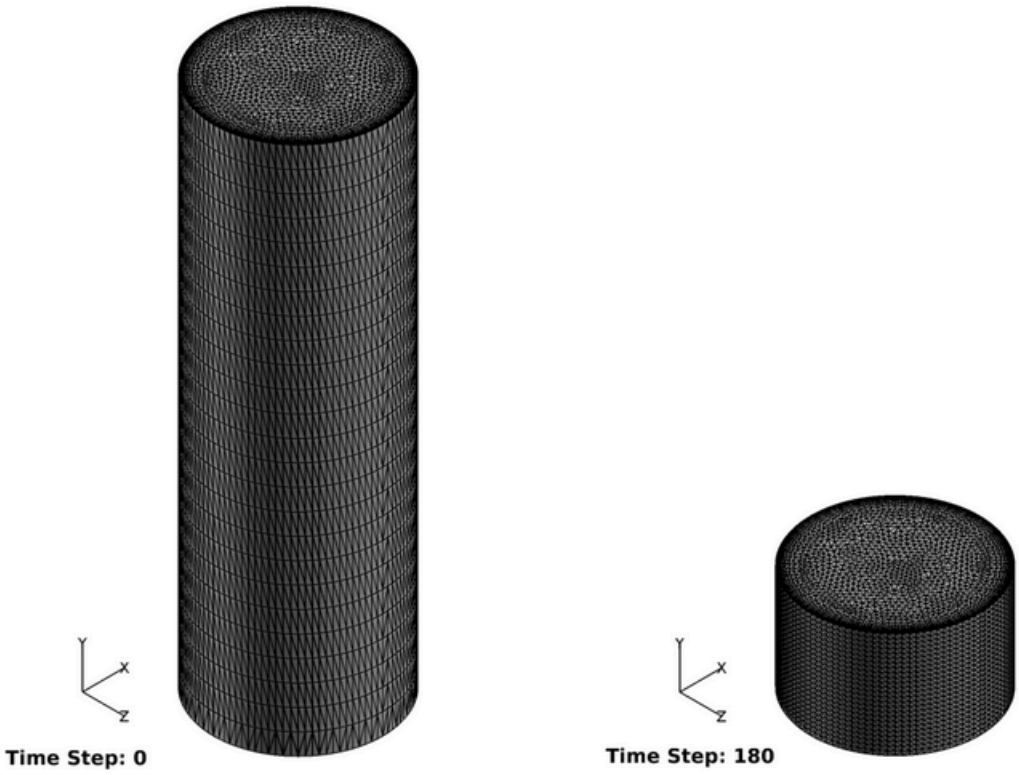


Figure 409: Mesh Used for Simulating Ideal Gas Compression in an Actuating Piston at Time Step 0 and Time Step 180 (3 s)

AcuSolve Results

The simulation was run as transient for a total of 360 time steps with a duration of 6.0 seconds. The AcuSolve solution shows time dependent pressure and temperature in a cylinder volume that compresses and expands in a 6.0 second cycle. Pressure and temperature increase as the cylinder volume decreases and returns toward initial conditions as the cylinder volume expands. The contours of pressure and temperature within the cylinder at the initial stage (t = 0.0 s) and the half cycle (t = 3.0 s) are shown in the following images.

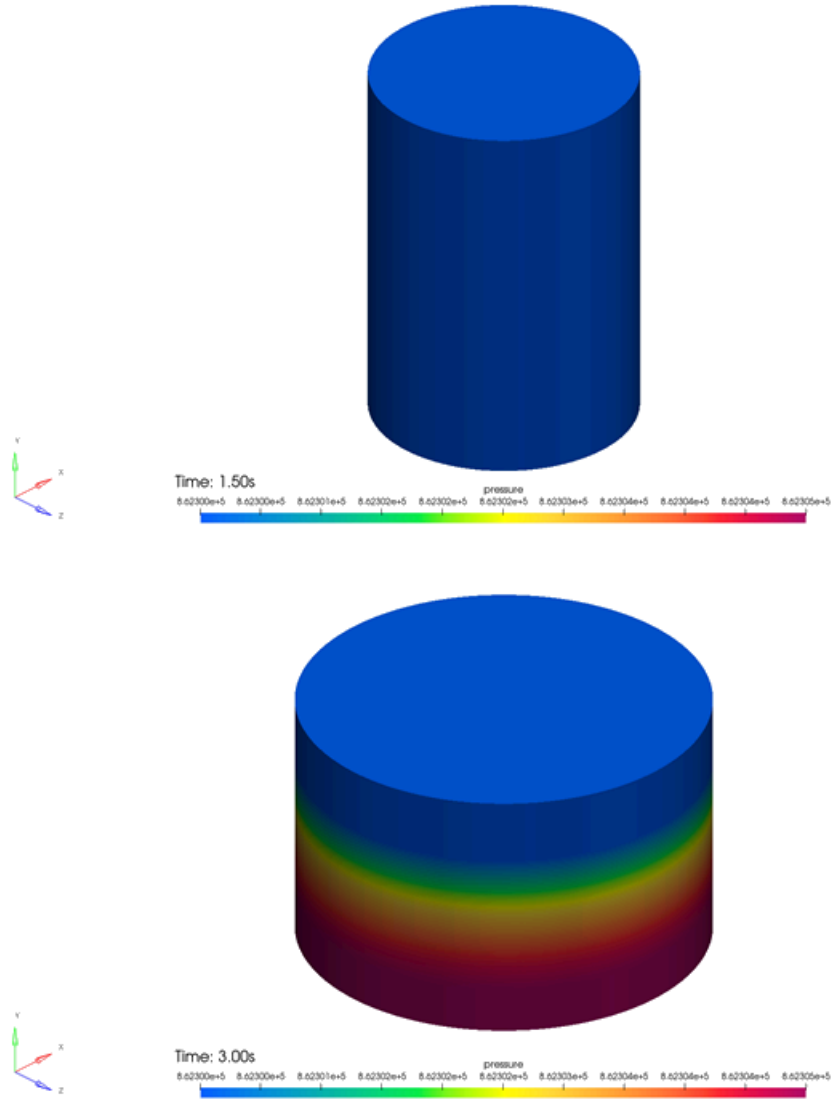


Figure 410: Pressure Distribution Within the Domain with the Piston at 1.5s and 3.0s

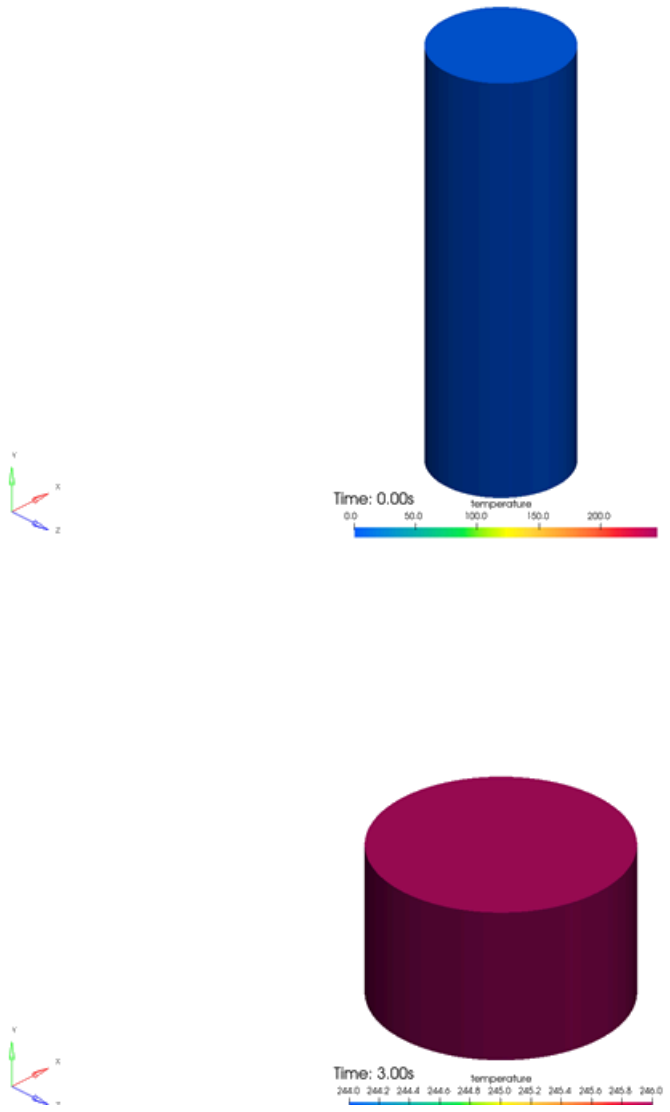


Figure 411: Temperature Distribution Within the Domain with the Piston at TDC and BDC

Comparison of time history plots of the AcuSolve and analytical solutions shows that the AcuSolve solution is nearly identical to the analytical solution. The AcuSolve computed internal pressure reaches a maximum of 8.62 X 105 Pa and the temperature reaches a maximum of 246.45 degrees C.

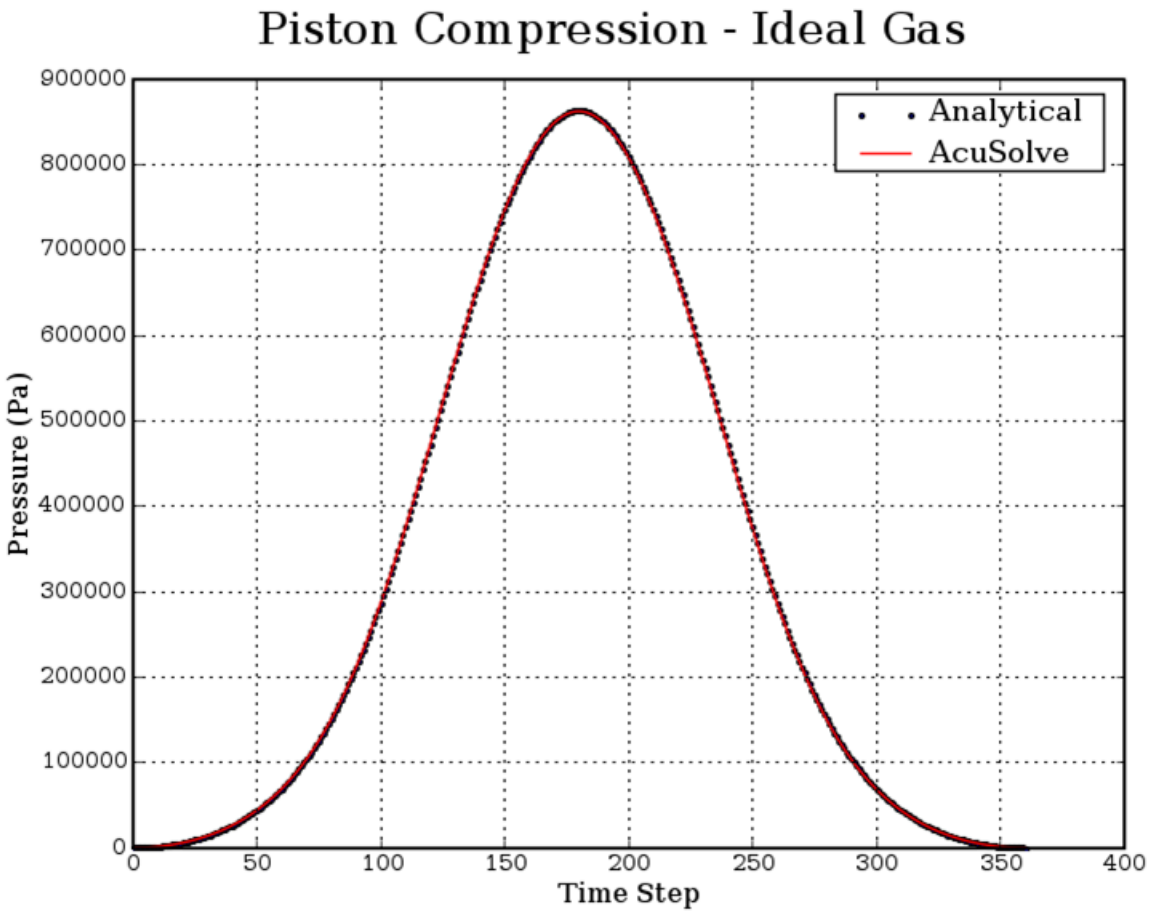


Figure 412: History Plots of Pressure for AcuSolve and Analytical Solutions

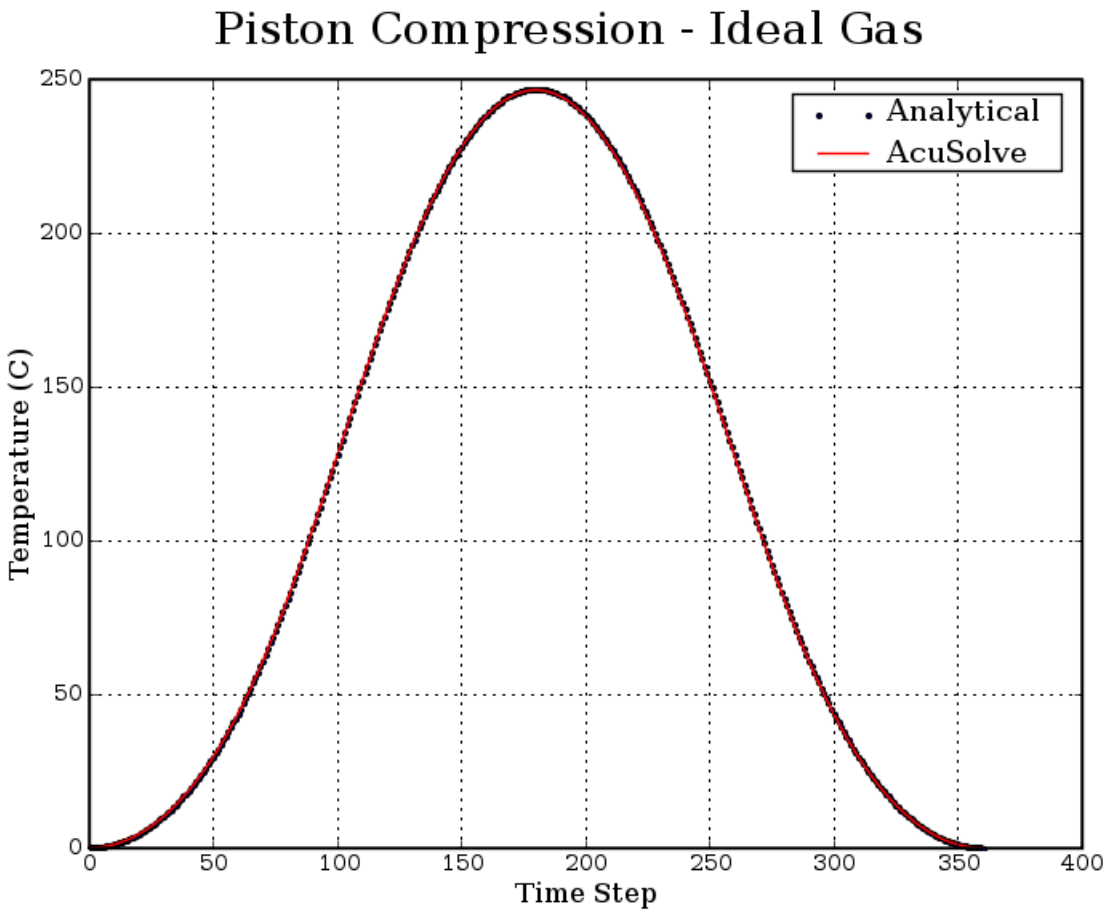


Figure 413: History Plots of Temperature for AcuSolve and Analytical Solutions

Summary

The AcuSolve solution compares well with analytical results for ideal gas compression in an actuating piston. The AcuSolve transient solution compares nearly identically with the analytical solution, with 0.1 percent and 0.16 percent error for the maximum pressure and temperature, respectively. As a result, AcuSolve demonstrates the ability to predict ideal gas compression in an idealized actuating piston.

Simulation Settings for Ideal Gas Compression in an Actuating Piston

HyperMesh CFD database file: `<your working directory>\cylinder_piston_compression\cylinder_piston_compression.hm`

Global

- Problem Description
  - Analysis type - Transient
  - Temperature equation - Advective Diffusive
  - Turbulence equation - Laminar
  - Mesh type - Fully Specified

- Auto Solution Strategy
  - Max time steps - `360`
  - Initial time increment - `0.01667` sec
  - Convergence tolerance - `1.0e-5` sec
  - Max stagger iterations - `10`
- Multiplier Function
  - Piston
    - Type - Piecewise Linear
    - Curve fit variable - Time
    - Curve fit values - (included in database as defined above)
- Material Model
  - Air
    - Density
      1. Type - Ideal Gas
      2. Gas constant - `286.9` J/kg-K
      3. Abs. pressure offset - `101325.0` N/m2
      4. Abs. temperature offset - `273.15` K
    - Viscosity - `1.781e-5` kg/m-sec
- Mesh Motion
  - Piston
    - Type - Translation
    - Translation velocity - `0.0`, `-1.0`, `0.0`
    - Velocity variable - Multiplier Function
    - Translation multiplier function - Piston

  Model
- Volumes
  - Fluid
    - Element Set
      1. Material model - Air
    - Element Output - on
- Surfaces
  - BDC
    - Simple Boundary Condition
      1. Type - Wall
      2. Wall velocity type - Match Mesh Velocity
      3. Mesh displacement BC type - Fixed
  - SideWall
    - Simple Boundary Condition

1. Type - Wall
2. Wall velocity type - Match Mesh Velocity
3. Mesh displacement BC type - Fixed

- TDC
  - Simple Boundary Condition
    1. Type - Wall
    2. Mesh displacement BC type - Fixed
    3. Mesh motion - Piston

- Nodes
  - VolumeNodes
    - Mesh X-Displacement
      1. Type - Zero
    - Mesh Y-Displacement
      1. Type - Linear
      2. Mesh motion - Piston
      3. Curve fit variable - Y reference coordinate
         1. X1 - `10.0` m
         2. Y1 - `1.0` m
         3. Y2 - `0.0` m
    - Mesh Z-Displacement
      1. Type - Zero

References

M.J. Moran and H.N Shapiro. "Fundamentals of Engineering Thermodynamics". Wiley. 4th Ed. 2000.

Heat Transfer/Radiation

9

This section includes validation cases that consider the temperature of the flow by simulating one or modes of heat transfer.

This chapter covers the following:

- Natural Convection in a Concentric Annulus (p. 545)
- Laminar Flow Through a Channel with Heated Walls (p. 551)
- Laminar Flow Through a Pipe with Constant Wall Temperature (p. 556)
- Laminar Flow Through a Pipe With Imposed Heat Flux (p. 561)
- Turbulent Natural Convection Inside a Tall Cavity (p. 566)
- Viscous Heating Inside a Rotating Annulus (p. 574)
- Heat Transfer Between Radiating Concentric Cylinders (p. 582)
- Heat Transfer Between Radiating Concentric Spheres (p. 588)
- Two-Phase Nucleate Boiling in a Cylindrical Pipe (p. 593)
- Single-Phase Nucleate Boiling in a Rectangular Channel (p. 597)
- Supersonic Flow Through a Converging-Diverging Nozzle (p. 602)
- Ideal Gas Compression in an Actuating Piston (p. 607)
- Turbulent Flow Through a Heated Periodic Channel (p. 616)
- Laminar Couette Flow with Imposed Pressure Gradient and Heated Walls (p. 622)

Natural Convection in a Concentric Annulus

In this application, AcuSolve is used to simulate natural convection in the annular space between a heated inner pipe and an outer concentric pipe. AcuSolve results are compared with experimental results adapted from Kuehn and Goldstein (1978). The close agreement of AcuSolve results with experimental results validates the ability of AcuSolve to model cases with flow induced by natural convection.

Problem Description

The problem consists of two concentric cylinders with air filling the void between them, as shown in the following image, which is not drawn to scale. The radius of the inner cylinder is 0.0178 m and the radius of the outer cylinder is 0.0463 m. The inner cylinder is held at a fixed temperature of 373 K while the outer cylinder is held at 327 K. The temperature gradient drives the flow due to buoyancy effects.

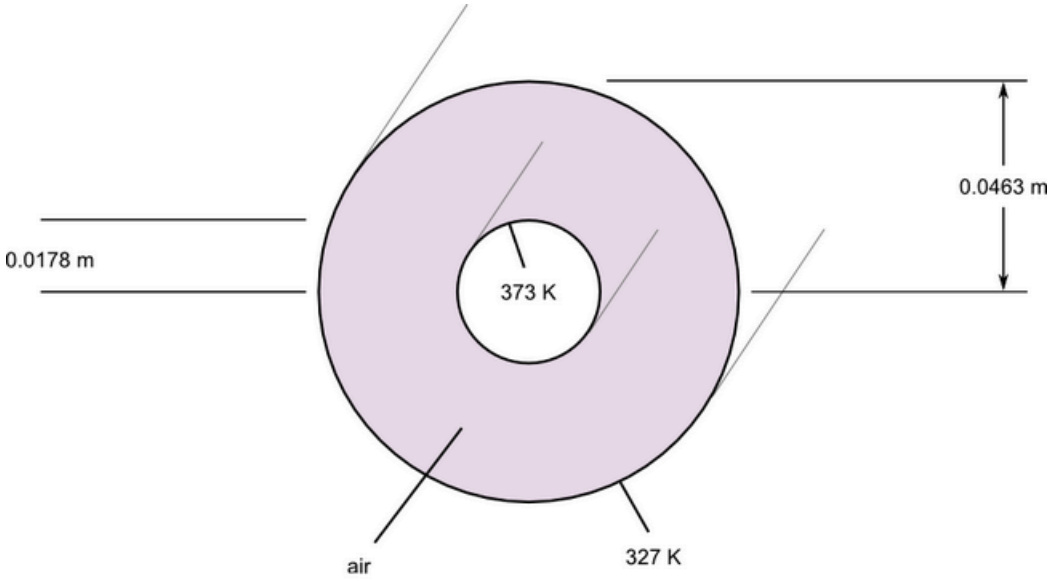


Figure 414: Critical Dimensions and Parameters for Simulating Natural Convection in a Concentric Annulus

The simulation was performed as a two dimensional problem by restricting flow in the out-of-plane direction through the use of a mesh that is one element thick. In addition, the half symmetry of the geometry is exploited to allow for modeling only half of the geometry. These characteristics allow for accurate simulation of the flow while minimizing computational time.

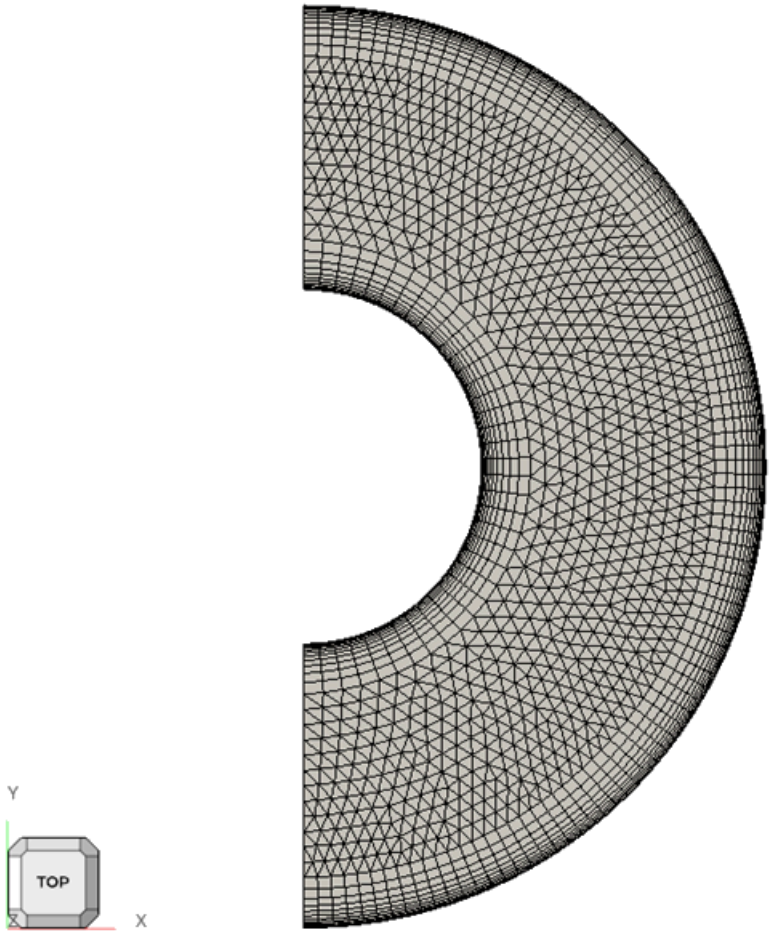


Figure 415: Mesh (Half of a Concentric Annulus) used for Simulating Natural Convection in a Concentric Annulus

AcuSolve Results

The AcuSolve solution converged to a steady state and the results reflect the mean flow conditions. Air density decreases due to heating by the inner cylinder, leading to convective currents within the annulus. As air approaches the outer cylinder, it is cooled by the outer wall, causing the density to increase. This results in heavier air sinking toward the bottom of the assembly.

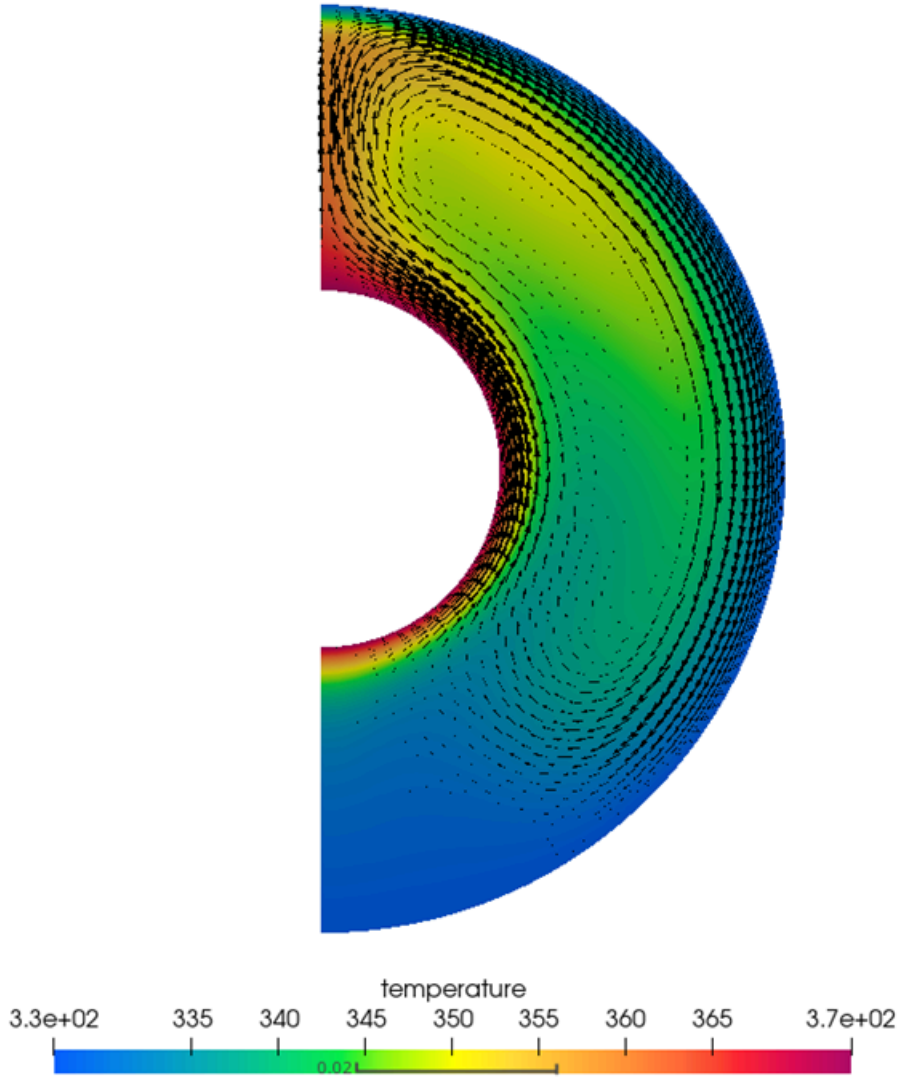


Figure 416: Temperature Contours and Velocity Vectors

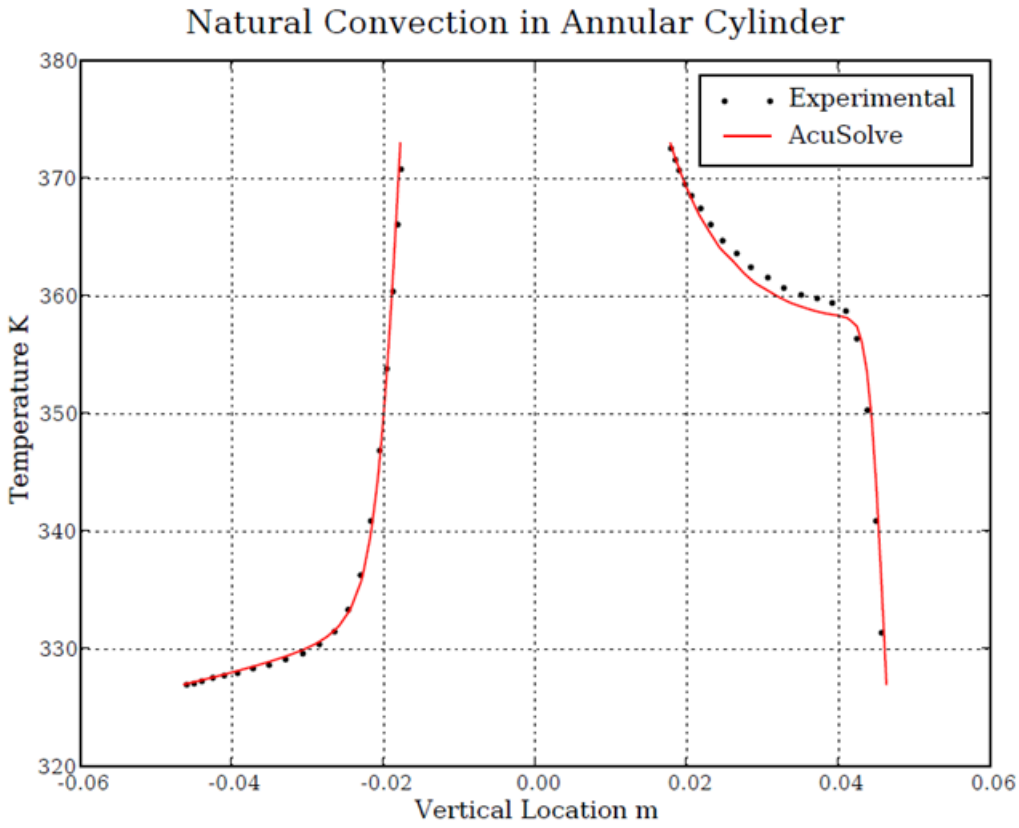


Figure 417: Temperature as a Function of Distance From the Center of the Inner Cylinder

Summary

The AcuSolve solution compares well with analytical results for natural convection in a concentric annulus. In this application, flow is driven by a decrease in density as air is heated. The local variations in density result in the higher density fluid sinking to the bottom of the annulus while the lower density fluid rises to the top. This transfer of momentum is a continuous process which results in the convective currents that are visible in the solution. The AcuSolve temperature results compare very closely with the experimental results.

Simulation Settings for Natural Convection in a Concentric Annulus

HyperMesh CFD database file: `<your working directory>\annulus_heat\annulus_heat.hm`

Global

- Problem Description
  - Analysis type - Steady State
  - Abs. pressure offset - `101325.0` N/m2
  - Temperature equation - Advective Diffusive
  - Turbulence equation - Laminar
  - Gravitational acceleration - { 0, -9.80665, 0 }
- Auto Solution Strategy

- Relaxation factor - `0.2`
- Flow - On
- Temperature - On

- Material Model
  - Air
    - Type - Boussinesq
    - Density - `1.225` kg/m3
    - Expansivity - `0.0034722` 1/K
    - Reference temperature - `288` K
    - Isothermal compressibility - `0.0` m2/N
    - Viscosity - `2.081e-5` kg/m-sec

  Model
- Volumes
  - Fluid
    - Element Set
      1. Material model - Air
  - Surfaces
    - ID
      1. Simple Boundary Condition
         1. Type - Wall
         2. Temperature BC type - Value
         3. Temperature - `373.0` K
    - Max_Z
      1. Simple Boundary Condition
      2. Type - Symmetry
    - Min_Z
      1. Simple Boundary Condition
      2. Type - Symmetry
    - OD
      1. Simple Boundary Condition
         1. Type - Wall
         2. Temperature BC type - Value
         3. Temperature - `327.0` K
    - Symmetry
      1. Simple Boundary Condition
      2. Type - Symmetry
  - Nodes
    - Node 1

1 Pressure

1 Type - Zero

References

T.H. Kuehn and R. J. Goldstein. "An Experimental Study of Natural Convection Heat Transfer in Concentric and Eccentric Horizontal Cylindrical Annuli". Journal of Heat Transfer 100:635-640. 1978.

Laminar Flow Through a Channel with Heated Walls

In this application, AcuSolve is used to simulate high Peclet number laminar flow through a channel with heated walls. AcuSolve results are compared with analytical results adapted from Hua and Pillai (2010). The close agreement of AcuSolve results with analytical results validates the ability of AcuSolve to model cases involving heat transfer to a moving fluid with a high Peclet number.

Problem Description

The problem consists of water at 20 °C flowing through a channel of infinite width with top and bottom walls heated to 75 °C. The channel is 0.2 m high and 0.8 m long, as shown in the following image, which is not drawn to scale. A centrally located slice 0.02 m wide is modeled with slip boundary conditions so that side-wall influences can be ignored. Water enters the channel with an average velocity of 0.003 m/s. As the fluid flows through the channel, it is heated by the top and bottom plates.

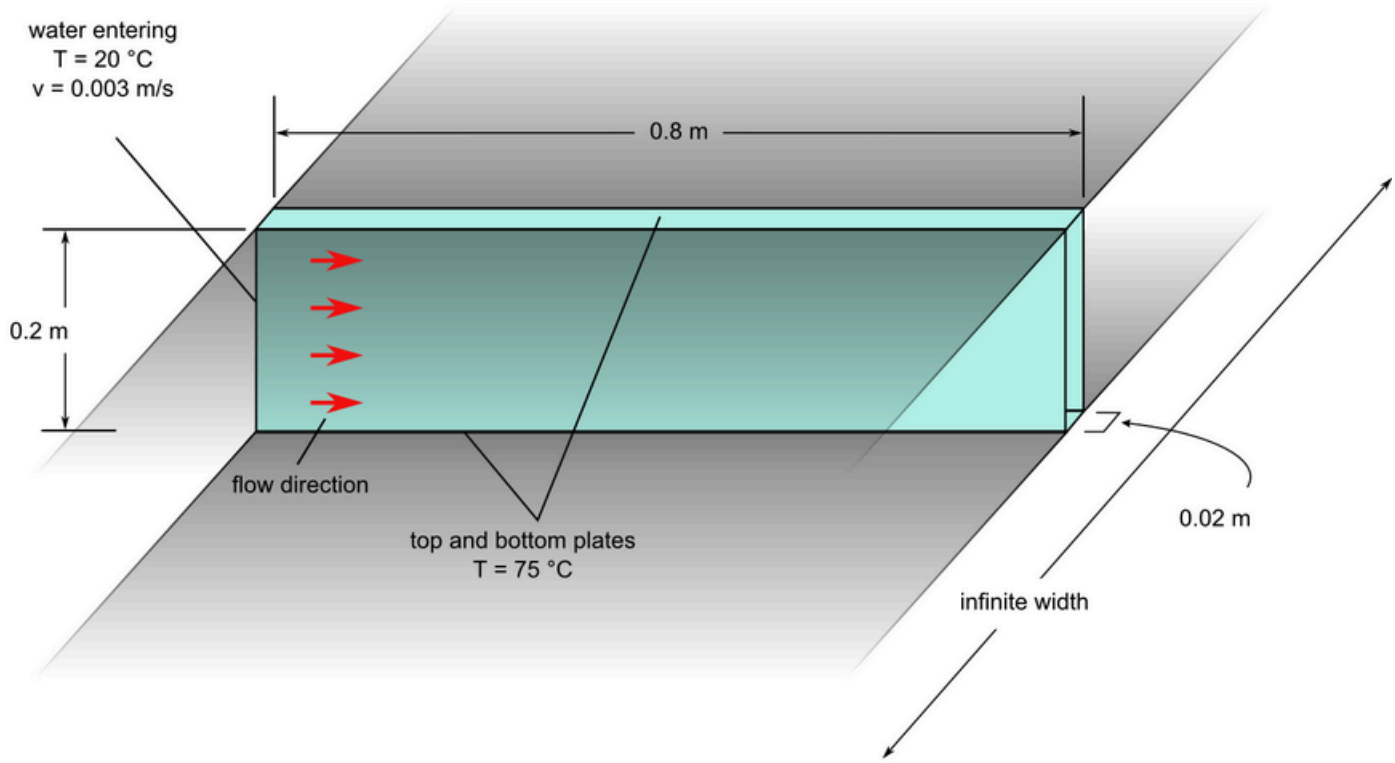


Figure 418: Critical Dimensions and Parameters for Simulating Laminar Flow Through a Channel with Heated Walls

The simulation was performed as a two dimensional problem by restricting flow in the out-of-plane direction through the use of a mesh that is one element thick. In addition, the symmetry of the geometry in the height direction is exploited to allow for modeling only half of the geometry. These characteristics allow for accurate simulation of flow while minimizing computational time.

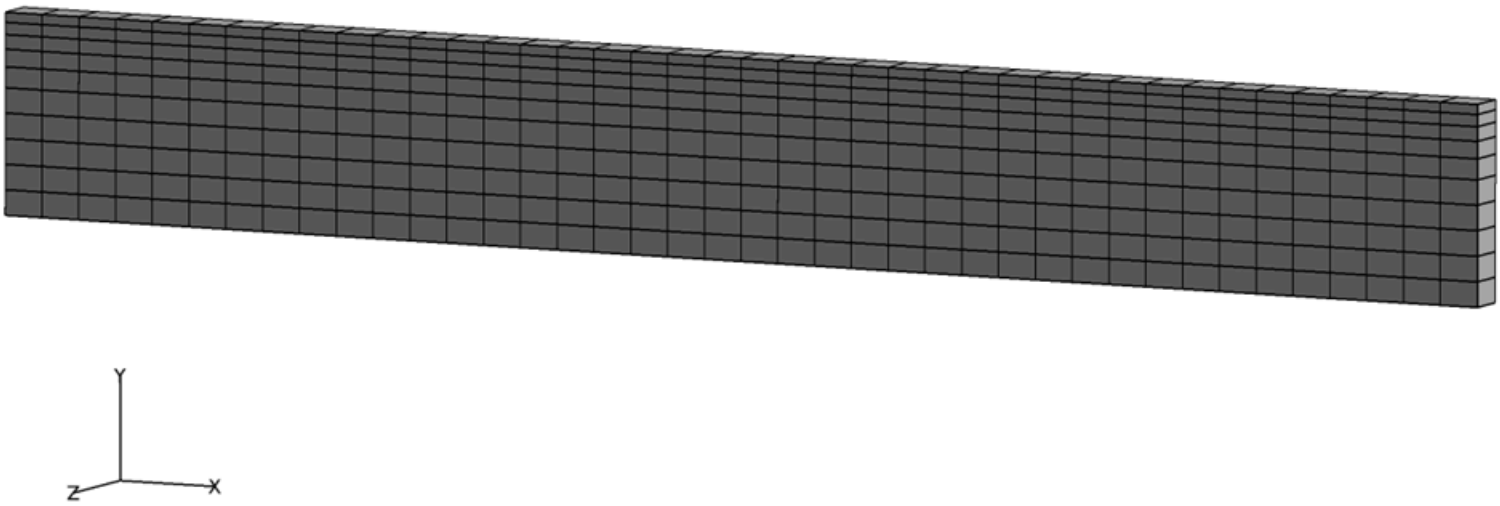


Figure 419: Mesh (Top Half of the Channel) used for Simulating Laminar Flow Through a Channel with Heated Walls

AcuSolve Results

The AcuSolve solution converged to a steady state and the results reflect the mean flow conditions. As the cool water enters the channel at temperature less than that of the walls, heat is transferred to the water by conduction. As the fluid travels along the channel, the temperature differential between the wall and the adjacent water decreases. The thermal boundary layer within the water develops as the flow propagates downstream.

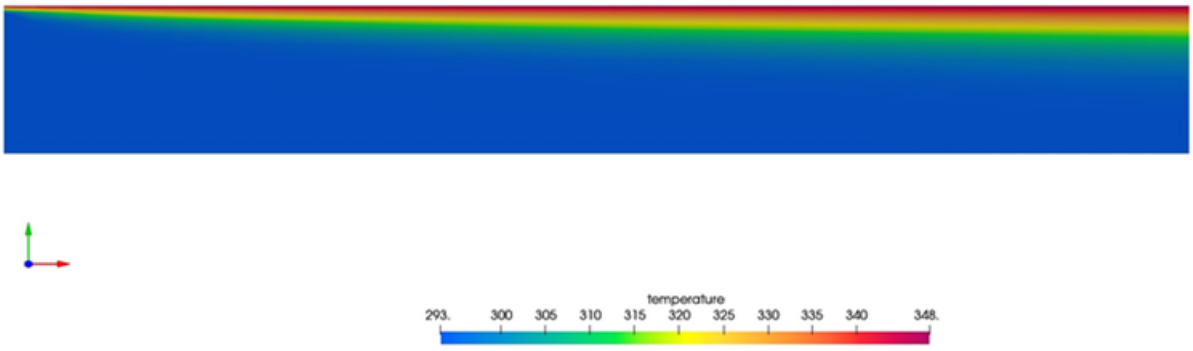


Figure 420: Temperature Contours Along the Top Half of a Heated Channel

Temperature at a specified vertical position in the channel increases along the length of the channel. The nature of that temperature change is dependent on proximity to the heated wall. Water in the center of the flow will have the least temperature change. Since this problem was solved for symmetrical flow, only the top half of the flow region was modeled. The vertical position for results shown in the following figure are based on the center of flow having a Y-position of 0.

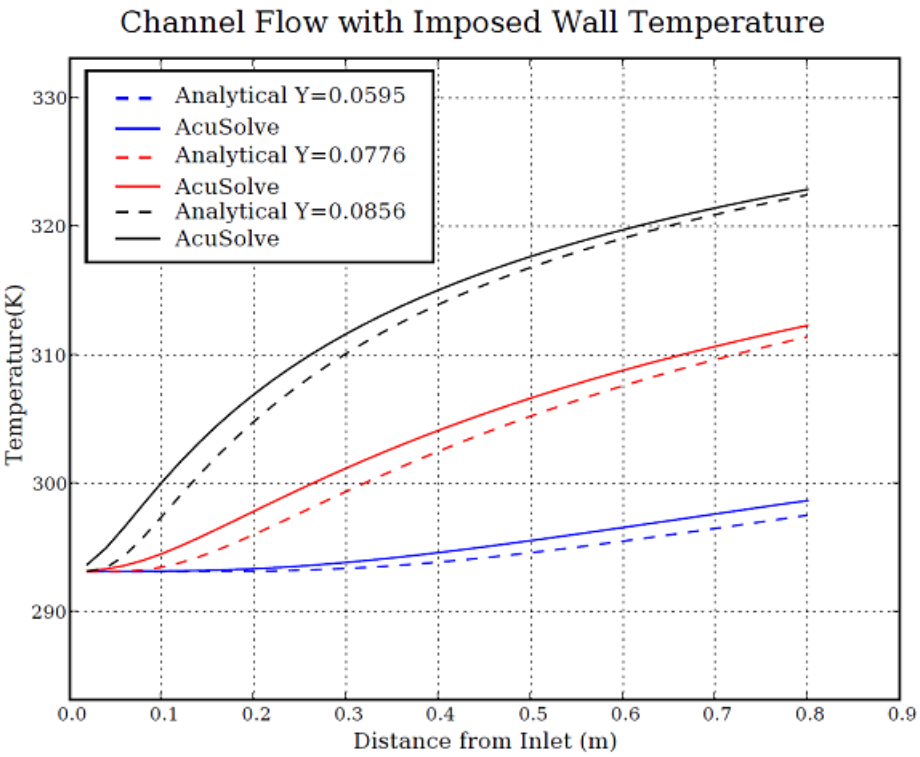


Figure 421: Temperature Plotted Against Distance from Inlet for 3 Different Heights from the Channel Center Line

Summary

The AcuSolve results compare well with the analytical results for the development of a thermal boundary layer in a heated channel. In this application, the model is set up to yield large gradients as the flow convects away from the inlet. The boundary conditions and mesh size were chosen specifically to yield a high Peclet number. The element Peclet number in the flow direction in this case is Pe=30.0, as calculated from the following equation.

$$Pe = \frac{\rho Cp|v|he}{k} \tag{16}$$

where ρ is the density, Cp the heat capacity, v the velocity, he the length, and k the thermal conductivity.

This example shows the robustness of the stabilized technique in AcuSolve when element Peclet number is high.

> **Note:** Standard Galerkin finite element formulations become unstable when the element Peclet number is greater than 1.0.

Simulation Settings for Laminar Flow Through a Channel with Heated Walls

SimLab database file: `<your working directory>\channel_laminar_heat\channel_laminar_heat.slb`

Global

- Problem Description
  - Flow - Steady State
  - Temperature equation - Advective Diffusive
  - Turbulence equation - Laminar
- Auto Solution Strategy
  - Relaxation factor - `0.4`
- Material Model
  - Fluid_Material
    - Density - `1000.0` kg/m3
    - Specific Heat - `1000` J/kg-K
    - Viscosity - `1.0e-12` kg/m-sec
    - Conductivity - 1.0 W/m-K

  Model
- Volumes
  - Fluid
    - Element Set
      1. Material model - Fluid_Material
- Surfaces
  - Inlet
    - Simple Boundary Condition
      1. Type - Inflow
      2. Inflow type - Velocity
      3. X velocity - `0.003` m/sec
      4. Temperature - `293.15` K
  - Outlet
    - Simple Boundary Condition
      1. Type - Outflow
  - Symm_MaxZ
    - Simple Boundary Condition
      1. Type - Slip
  - Symm_MinY
    - Simple Boundary Condition
      1. Type - Slip
  - Symm_MinZ
    - Simple Boundary Condition
      1. Type - Slip
  - Wall

- Simple Boundary Condition
  1. Type - Wall
  2. Temperature BC type - Value
  3. Temperature - `348.15` K

References

Hua Tan and K. M. Pillai. "Numerical Simulation of Reactive Flow in Liquid Composite Molding Using Flux-Corrected Transport (FCT) Based Finite Element/Control Volume (FE/CV) Method". International Journal of Heat and Mass Transfer. 53:2256-2271, 2010.

Laminar Flow Through a Pipe with Constant Wall Temperature

In this application, AcuSolve is used to simulate the flow of mercury through a heated pipe. The AcuSolve results are compared with analytical results for pressure drop as described in White (1991), and with temperature changes as described in Incropera and DeWitt (1981). The close agreement of AcuSolve results with analytical results validates the ability of AcuSolve to model cases with flow and imposed temperature constraints.

Problem Description

The problem consists of mercury flowing through a circular pipe that is 0.005 m in diameter and 0.1 m long, as shown in the following image, which is not drawn to scale. Mercury enters the pipe with a constant temperature of 300 K and with a fully developed velocity profile with an average velocity of 0.005 m/s. The pipe wall has a constant temperature of 500 K. These constraints impose a temperature gradient within the fluid. As the fluid moves through the pipe it is slowly heated by the wall, resulting in an increased centerline temperature. Pressure decreases along the pipe length due to the friction imposed by the viscous stresses near the pipe wall. A periodic boundary condition is imposed on the inlet and outlet to allow the pressure to change with a constant offset, while the velocity is fully periodic.

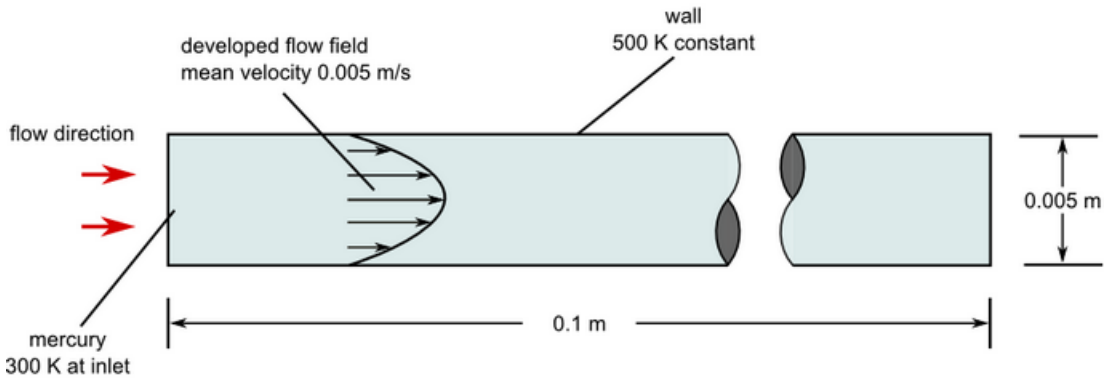


Figure 422: Critical Dimensions and Parameters for Simulating Laminar Flow through a Pipe with Constant Wall Temperature

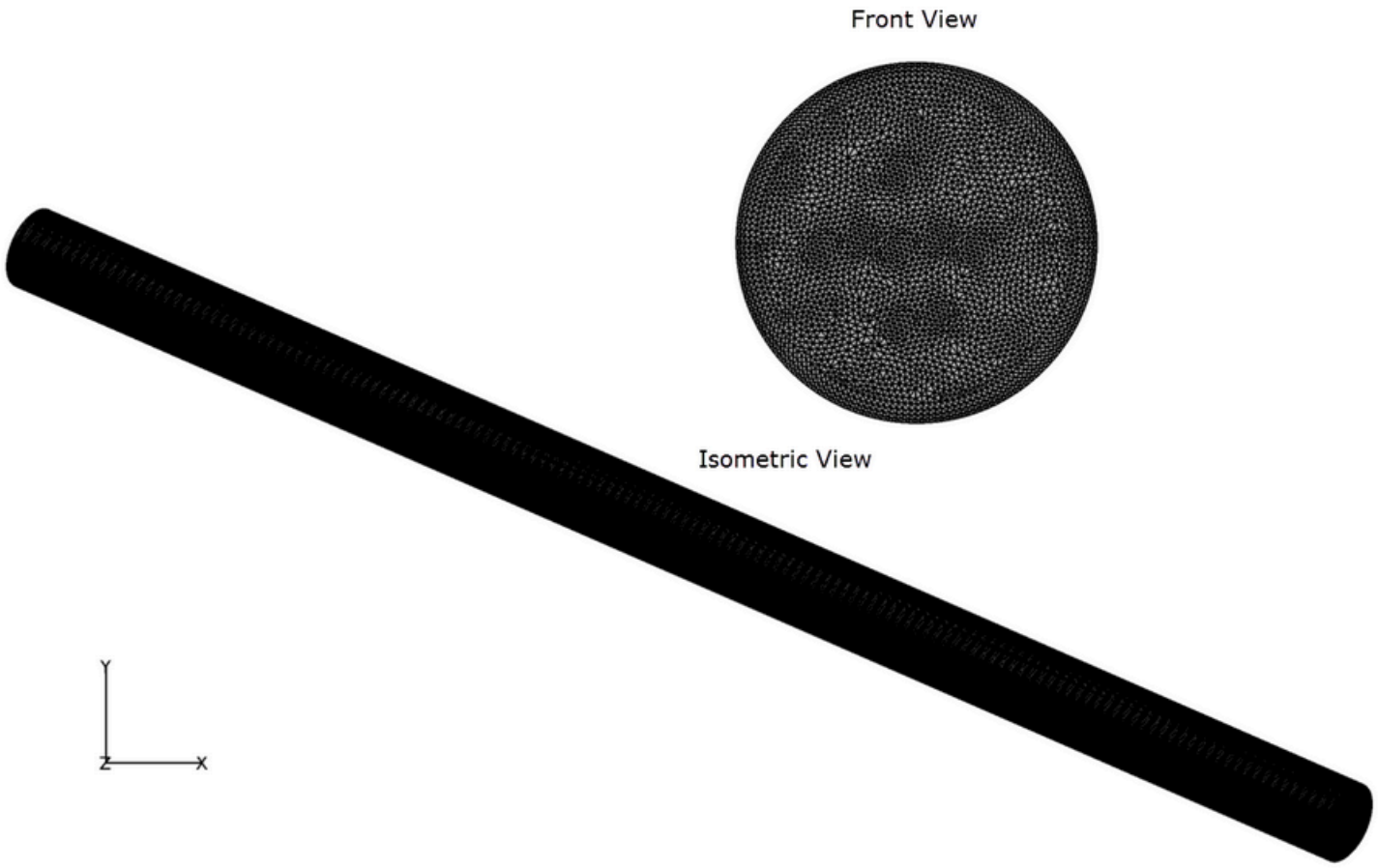


Figure 423: Mesh used for Simulating Laminar Flow Through a Pipe with Constant Wall Temperature

AcuSolve Results

The AcuSolve solution converged to a steady state and the results reflect the mean flow conditions. In this application, a fully developed laminar profile is achieved by enforcing periodic constraints on the pressure and velocity fields. The spatially developing temperature field is achieved by allowing the fluid's temperature to evolve along the full length of the model. The change in temperature along the pipe length is due to advection in the streamwise direction and heat conduction from the outer walls where the temperature is greater than the initial flow temperature. The temperature rises along the length of the pipe and the pressure drops along the length of the pipe. At the inlet, the temperature of the mercury is 300 K and the pressure is 0.496 Pa. At the outlet centerline, the temperature of the mercury has risen to 500.0 K and the pressure has dropped to -0.4965 Pa.

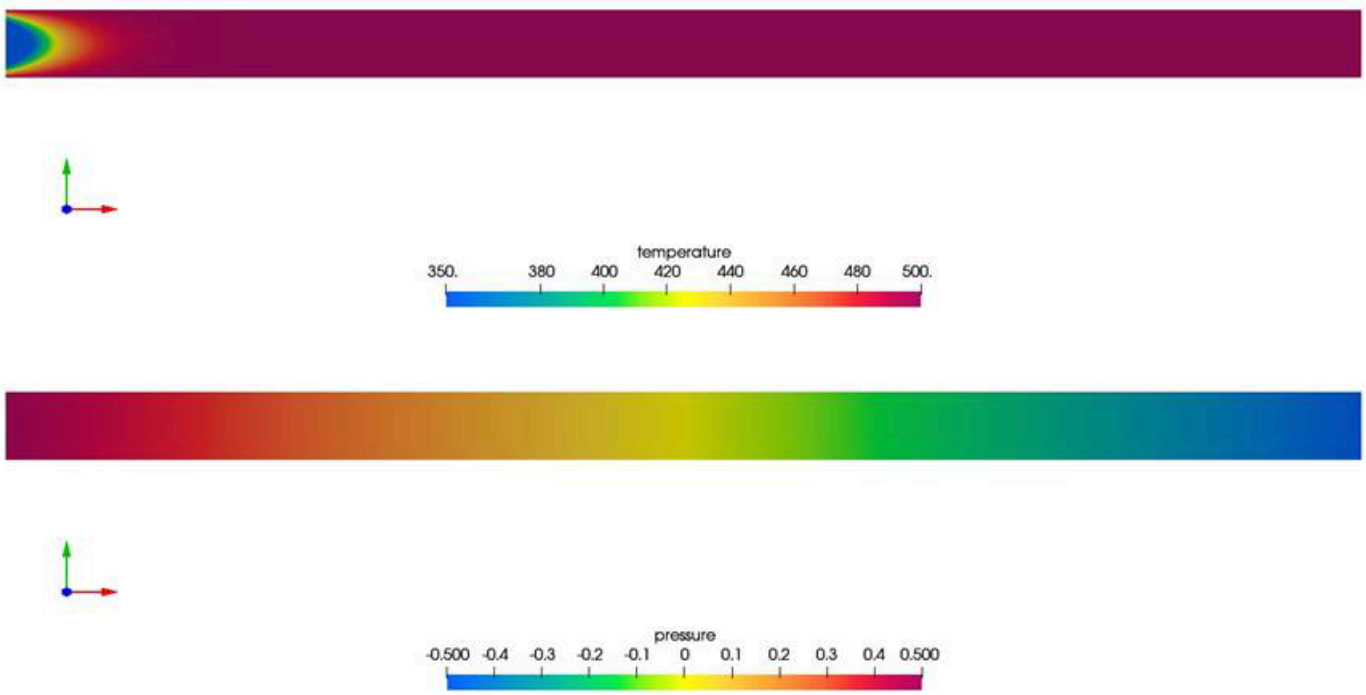


Figure 424: Temperature and Pressure Contours of Mercury Flow Through a Pipe with Prescribed Temperature Boundary

The following table shows the comparison of AcuSolve results with the analytical solutions from White (1994). Comparisons were made for the pressure drop between the inlet and outlet and the temperature at the center of the outlet.

Table 22:

	Analytical solution	**AcuSolve solution**	**% Deviation from analytical**
Pressure drop (Pa)	0.991	0.9901	0.1
Centerline temperature of flow at outlet (K)	500.0	500.0	< 0.0001

Summary

The AcuSolve solution compares well with analytical results for flow through a pipe with constant temperature boundary conditions. The AcuSolve solution for the centerline temperature is nearly identical with the analytical results and the pressure reduces as expected for the prescribed flow conditions. The results of this simulation validate the ability of AcuSolve to accurately predict the heating of fluid flowing through a pipe with constant wall temperature.

Simulation Settings for Laminar Flow Through a Pipe With Constant Wall Temperature

SimLab database file: `<your working directory>\pipe_laminar_heatDirichlet\pipe_laminar_heatDirichlet.slb`

Global

- Problem Description
  - Flow - Steady State
  - Temperature equation - Advective Diffusive
  - Turbulence equation - Laminar
- Auto Solution Strategy
  - Relaxation Factor - `0.2`
- Material Model
  - Mercury
    - Density - `13579.0` kg/m3
    - Specific Heat - `139.3` J/kg-K
    - Viscosity - `0.001548` kg/m-sec
    - Conductivity - `8.69` W/m-K

  Model
- Volume
  - Fluid
    - Element Set
      1. Material model - Mercury
- Surfaces
  - Inflow
    - Simple Boundary Condition - (disabled to allow for periodic conditions to be set)
    - Advanced Options
      1. Integrated Boundary Conditions
         1. Mass Flux
            1. Type - Constant
            2. Constant value - `1.33e-3` kg/sec
      2. Temperature
         1. Type - Constant
         2. Constant value - `300.0` K
  - Outflow
    - Simple Boundary Condition - (disabled to allow for periodic conditions to be set)
  - Wall
    - Simple Boundary Condition
      1. Type - Wall

2 Temperature BC type - Value
3 Temperature - `500.0` K

- Periodics
  - Periodic 1
    - Individual Periodic BCs
      1 Velocity
        1 Type - Periodic
      2 Pressure
        1 Type - Single Unknown Offset

References

F. M. White. "Fluid Mechanics". 3rd Edition. McGraw-Hill Book Co., Inc. New York. 1994.

F. P. Incropera and D. P. DeWitt. "Fundamentals of Heat Transfer". John Wiley & Sons. New York. 1981.

Laminar Flow Through a Pipe With Imposed Heat Flux

In this application, AcuSolve is used to simulate the flow of mercury through a heated pipe. The AcuSolve results are compared with analytical results for pressure drop as described in White (1991), and with temperature changes as described in Incropera and DeWitt (1981). The close agreement of AcuSolve results with analytical results validates the ability of AcuSolve to model cases with flow and imposed heat flux.

Problem Description

The problem consists of mercury flowing through a heated, circular pipe that is 0.005 m in diameter and 0.1 m long, as shown in the following image, which is not drawn to scale. Mercury enters the pipe with a constant temperature of 300 K. The pipe has an imposed heat flux of 2000 W/m^2. The laminar velocity field is modeled as periodic to achieve a fully developed velocity profile. As the fluid moves through the pipe it is slowly heated by the heat flux on the wall, resulting in an increased centerline temperature. Pressure decreases along the pipe length due to the friction imposed by the viscous stresses near the pipe wall.

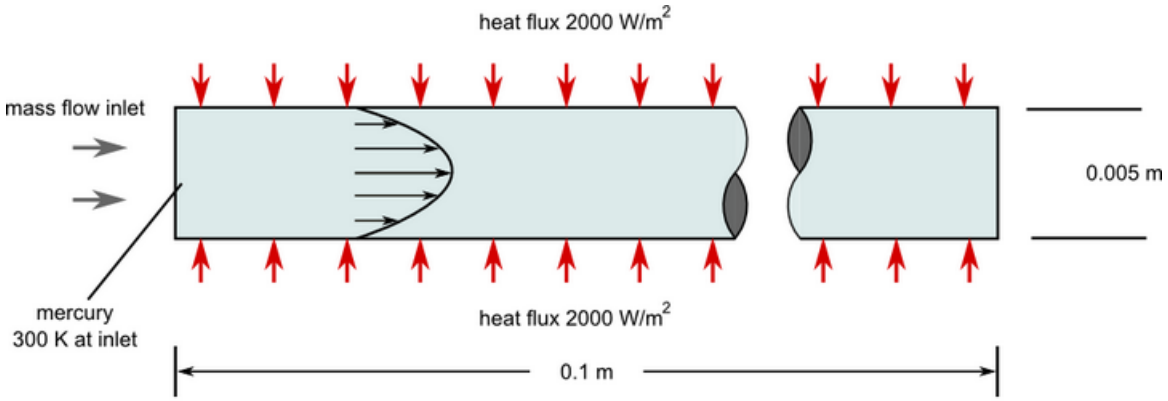


Figure 425: Critical Dimensions and Parameters for Simulating Laminar Flow through a Pipe with Imposed Heat Flux

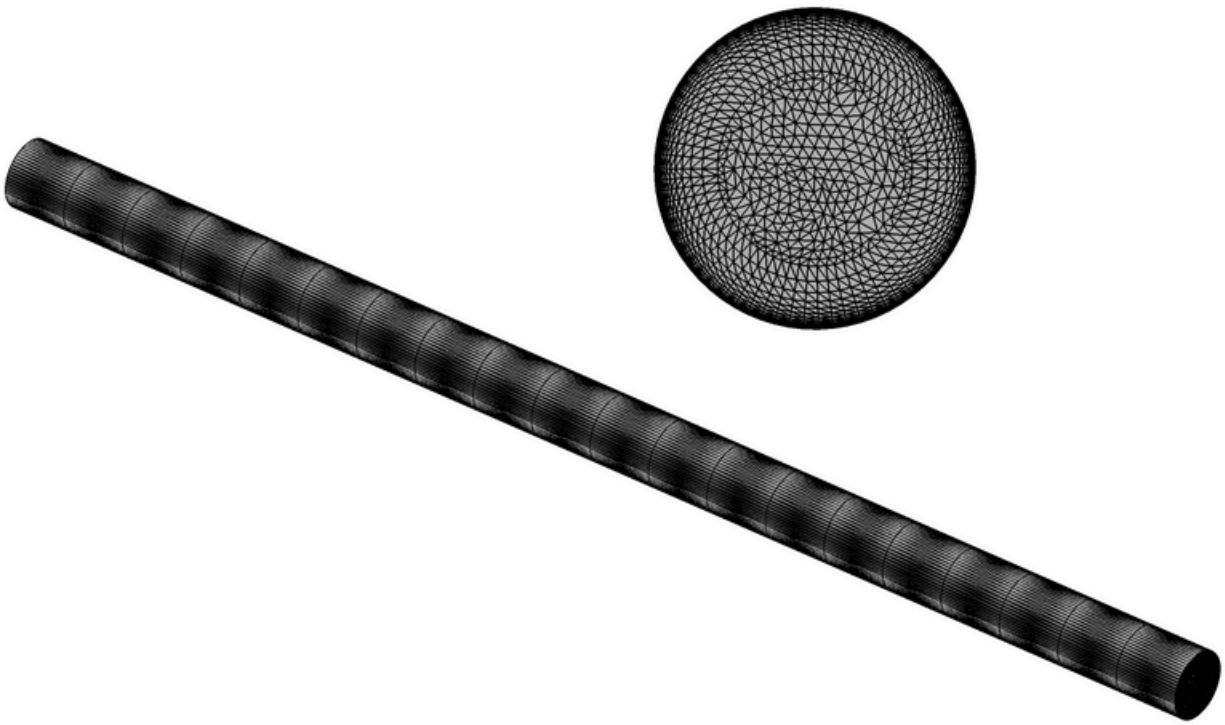


Figure 426: Mesh used for Simulating Laminar Flow Through a Pipe with Imposed Heat Flux

AcuSolve Results

The AcuSolve solution converged to a steady state and the results reflect the mean flow conditions. The greatest pressure is at the inlet, with pressure decreasing as a function of distance away from the inlet. The temperature of the mercury in the pipe increases as a function of distance from the inlet due to the impact of the heat flux on the pipe walls.

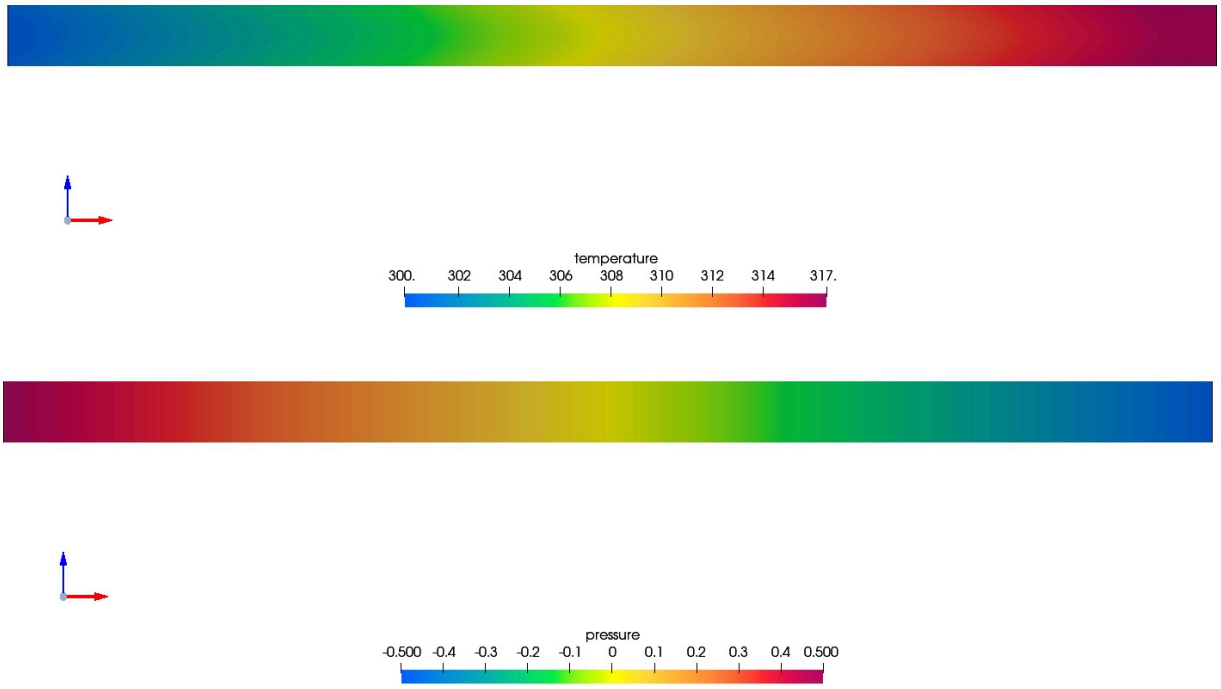


Figure 427: Temperature and Pressure Contours of Mercury Flow Through a Heated Pipe

The analytical solution for the pressure drop, between the inlet and outlet, as well as the analytical solution for the temperature of the mercury at the center of the outlet are presented with the corresponding AcuSolve results in the following table.

Table 23:

	Analytical solution	AcuSolve solution	Percent deviation from analytical
Pressure drop (Pa)	0.991	0.994	0.303
Centerline temperature of flow at outlet (K)	316.917	316.269	0.204

Summary

The AcuSolve solution compares well with analytical results for flow through a pipe with an imposed heat flux. In this application, the pressure drop in the fluid region is driven by the viscous stresses near the pipe wall. The temperature in the fluid region is influenced by the imposed heat flux on the walls. The values of pressure and temperature that are predicted by AcuSolve are within 0.3 percent of the analytical solution.

Simulation Settings for Laminar Flow Through a Pipe With Imposed Heat Flux

SimLab database file: `<your working directory>\pipe_laminar_heat\pipe_laminar_heat.slb`

Global

- Problem Description
  - Flow - Steady State
  - Temperature equation - Advective Diffusive
  - Turbulence equation - Laminar
- Auto Solution Strategy
  - Relaxation Factor - `0.2`
- Material Model
  - Mercury
    - Density - `13579.0` kg/m3
    - Viscosity - `0.001548` kg/m-sec

  Model
- Volume
  - Fluid
    - Element Set
      1. Material model - Mercury
- Surfaces
  - Inflow
    - Simple Boundary Condition - (disabled to allow for periodic conditions to be set)
    - Advanced Options
      1. Integrated Boundary Conditions
         1. Mass Flux
            1. Type - Constant
            2. Constant value - `-1.33e-3` kg/sec
         2. Temperature
            1. Type - Constant
            2. Constant value - `300.0` K
  - Outflow
    - Simple Boundary Condition - (disabled to allow for periodic conditions to be set)
  - Wall
    - Simple Boundary Condition
      1. Type - Wall
      2. Temperature BC type - Flux
      3. Heat flux - `2000.0` W/m2
- Periodics
  - Periodic 1
    - Individual Periodic BCs

1 Velocity
    1 Type - Periodic
2 Pressure
    1 Type - Single Unknown Offset
3 Temperature
    1 Type - Single Unknown Offset

References

F. M. White. "Viscous Fluid Flow". Section 3-2.1. McGraw-Hill Book Co., Inc.. New York. 1991.

F. P. Incropera and D. P. DeWitt. "Fundamentals of Heat Transfer". John Wiley & Sons. New York. 1981.

Turbulent Natural Convection Inside a Tall Cavity

In this application, AcuSolve is used to simulate the natural convection of a turbulent flow field within a tall rectangular cavity. AcuSolve results are compared with experimental results as described in Betts and Bokhari (2000). The close agreement of AcuSolve results with experimental results validates the ability of AcuSolve to model cases with natural convection of turbulent flow within a tall cavity.

Problem Description

The problem consists of air within a tall cavity with a hot wall and a cold wall, as shown in the following image, which is not drawn to scale. The cavity is 2.18 m tall, 0.0762 m wide, and 0.52 m deep. The cavity's vertical walls differ in temperature, causing the fluid to transfer the heat, leading to natural convection. The temperature of the hot wall is 307.85 K, while the temperature of the cold wall is 288.25 K. The horizontal walls of the cavity are adiabatic. The length-to-width ratio of 28.6 and temperature difference of 19.6 K produce a turbulent flow field within the cavity with a Rayleigh number of $8.6X10^{5}$ (Betts and Bokhari 2000). The flow medium is air, with a Boussinesq approximation for density, a specific heat of 1005 J/kg-K, and a viscosity of $1.781 X 10^{-5}$ kg/m-s. Gravity is applied globally to the volume of air.

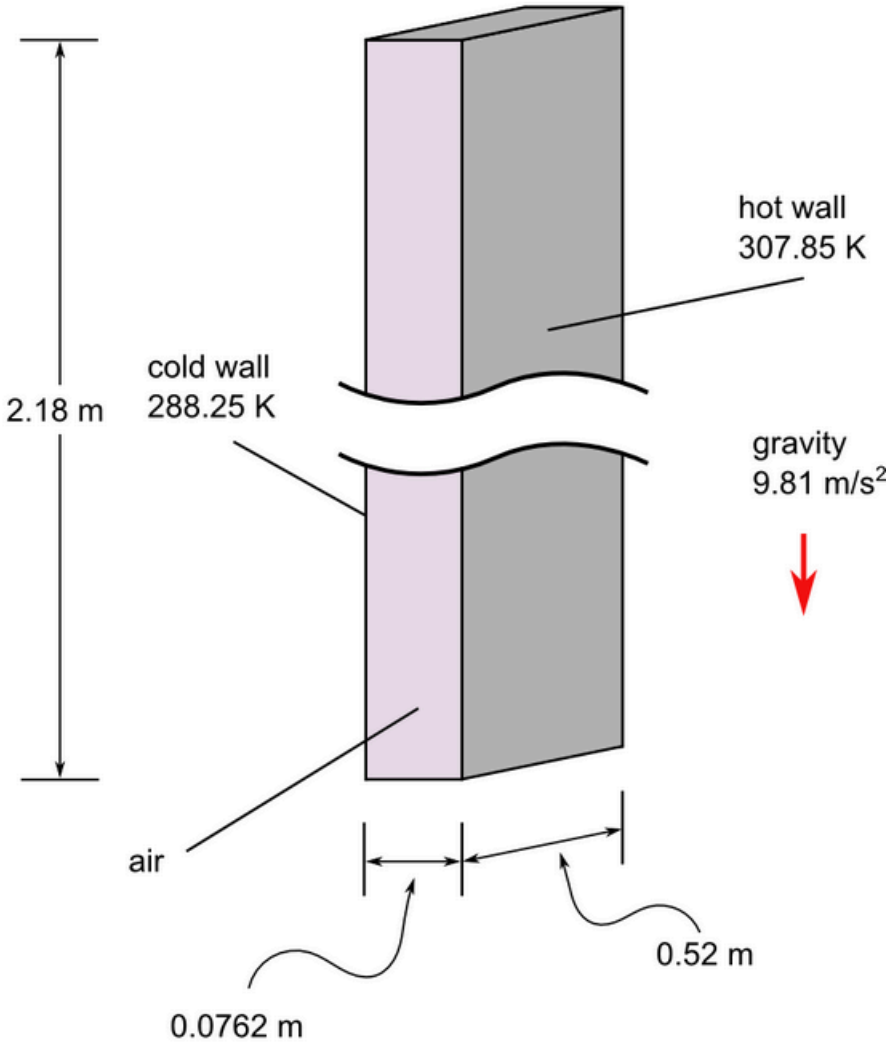


Figure 428: Critical Dimensions and Parameters for Simulating Turbulent Natural Convection in a Tall Cavity

The simulation was performed as a two dimensional problem by constructing a volume mesh that contains a single layer of elements in the extruded direction, normal to the flow plane and by imposing symmetry boundary conditions on the extruded planes.

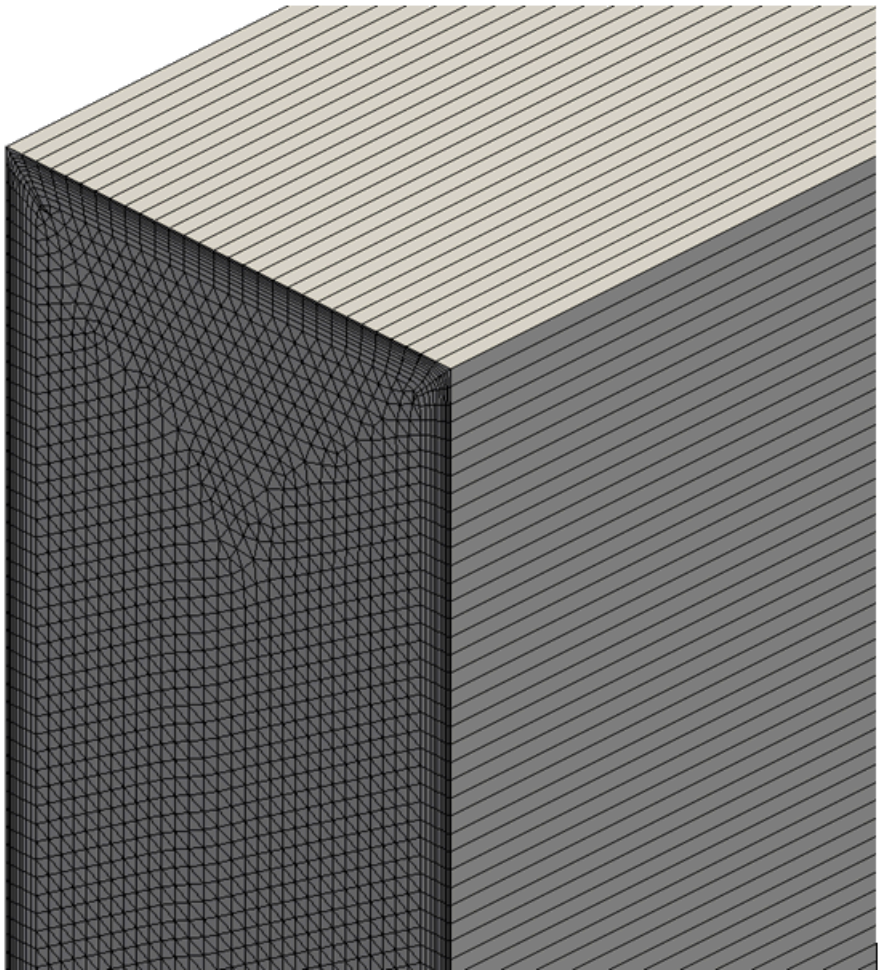


Figure 429: Mesh used for Simulating the Natural Convection of Turbulent Flow in a Tall Cavity

AcuSolve Results

The AcuSolve solution converged to a steady state and the results reflect the mean flow conditions. The natural convection of the flow is generated by heat transfer from the vertical walls to the fluid in the cavity. The temperature gradients created by this heat transfer cause differing densities within the flow region. The warmer air rises to the top of the cavity due to its lower density while the colder air sinks to the bottom of the cavity due to its higher density. This produces flow near the hot vertical wall in the positive vertical direction and flow near the cold wall in the negative vertical direction.

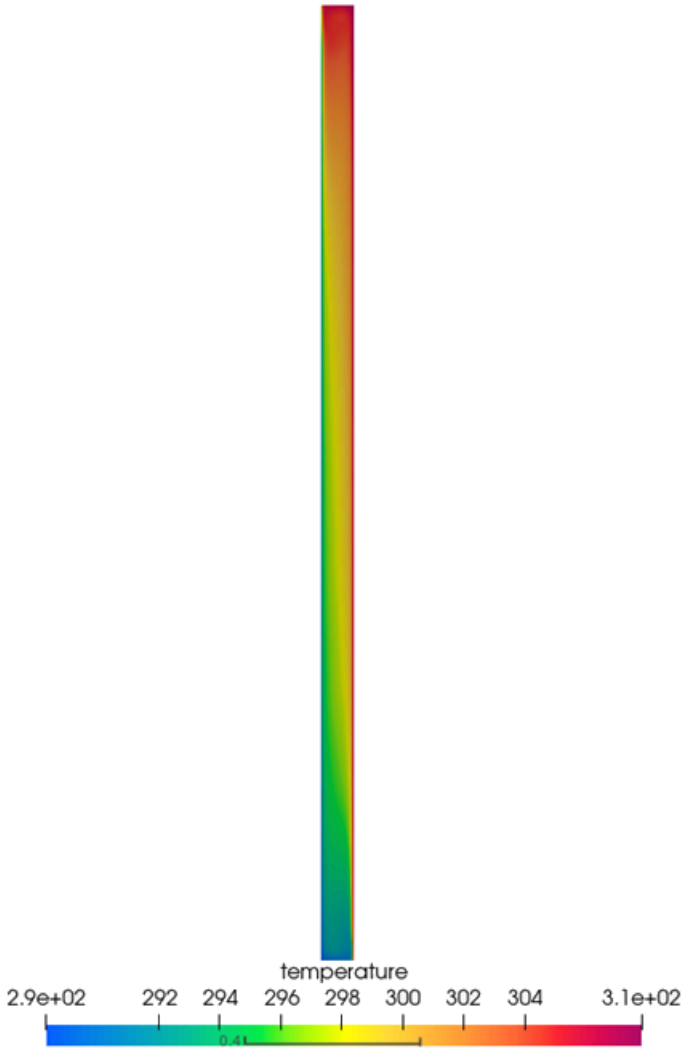


Figure 430: Temperature Contours Throughout Tall Cavity in the X-Y Plane

The AcuSolve results of the temperature and vertical velocity within the cavity are compared to the corresponding experimental values in the plots shown below. The temperature of the air is lowest near the cold vertical wall, remains relatively steady in the middle of the cavity, and then peaks near the hot vertical wall. Following a similar trend, the AcuSolve results show that the velocity is lowest near the cold vertical wall, due to the air sinking, and then steadily increases as the air begins to rise near the hot vertical wall. The velocity at the walls is zero due to the no-slip boundary condition. Additional comparisons are made to evaluate the performance of four turbulence models, Spalart-Allmaras (SA), shear stress transport (SST), K-Omega and K-ε.

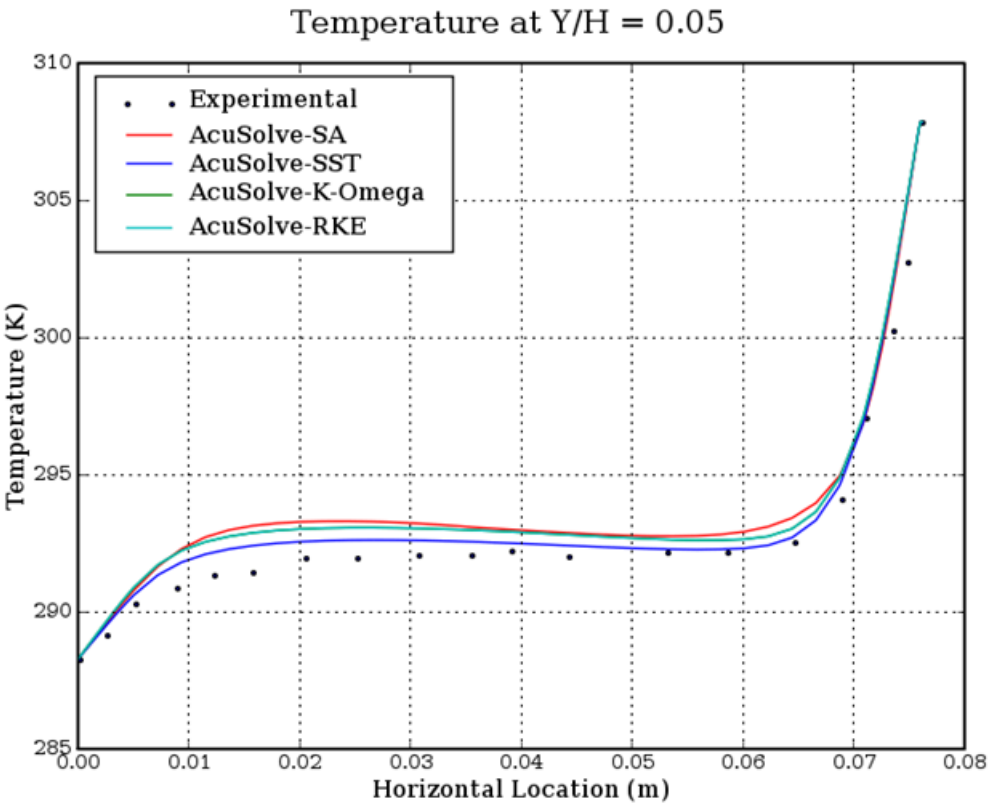


Figure 431: Temperature Plotted against Location along Horizontal at a Position of y/H=0.05 in the Cavity, where H is the Cavity Height and y is the Distance from the Bottom Wall

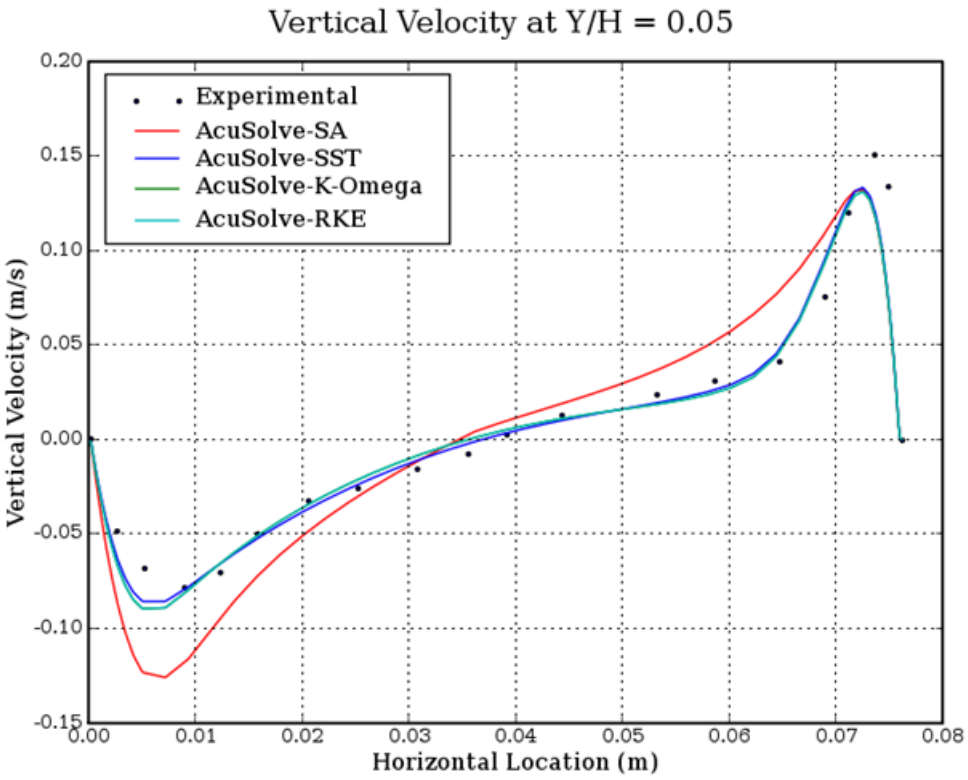


Figure 432: Vertical Velocity Plotted against Location along Horizontal at a Position of y/H=0.05 in the Cavity, where H is the Cavity Height and y is the Distance from the Bottom Wall

Summary

In this application, turbulent flow developed by natural convection, at a Rayleigh number of 8.6X105, is studied within a tall cavity. The AcuSolve results compare well with the experimental data for temperature and vertical velocity along a horizontal line at a location of y/H=0.05 in the tall cavity, with the two-equation models capturing the velocity gradient with greater accuracy. A temperature difference occurs within the flow region due to the heat transfer from the vertical walls of the cavity. The hotter, less-dense air rises to the top of the cavity while the colder, denser air sinks to the bottom, giving rise to recirculation. AcuSolve demonstrates the ability to accurately predict the natural convection of turbulent flow within a tall cavity.

Simulation Settings for Turbulent Natural Convection Inside a Tall Cavity

HyperMesh CFD database file: `<your working directory\cavity_turbulent_heat \cavity_turbulent_heat.hm`

Global

- Problem Description
  - Analysis type - Steady State
  - Turbulence equation - SST
- Auto Solution Strategy
  - Relaxation factor - `0.5`

- Convergence tolerance - `0.005`

- Material Model
  - Air
    - Type - Boussinesq
    - Density - `1.225` kg/m3
    - Specific Heat - `1005` J/kg-K
    - Viscosity - `1.781e-5` kg/m-sec

  Model
- Volumes
  - Volume
    - Element Set
      1. Material model - Air
- Surfaces
  - Back
    - Simple Boundary Condition
      1. Type - Symmetry
  - Bottom
    - **Simple Boundary Condition**
      1. Type - Wall
      2. Temperature BC type - Flux
      3. Heat Flux - `0.0` W/m2
  - Cold
    - **Simple Boundary Condition**
      1. Type - Wall
      2. Temperature BC type - Value
      3. Temperature - `288.25` K
  - Front
    - Simple Boundary Condition
      1. Type - Symmetry
  - Hot
    - Simple Boundary Condition
      1. Type - Wall
      2. Temperature BC type - Value
      3. Temperature - `307.85` K
  - Top
    - Simple Boundary Condition
      1. Type - Wall

2 Temperature BC type - Flux
3 Heat Flux - `0.0` W/m2

References

P.L. Betts and I.H. Bokhari. "Experiments on Turbulent Natural Convection in an Enclosed Tall Cavity". International Journal of Heat and Fluid Flow 21:675-683. 2000.

Viscous Heating Inside a Rotating Annulus

In this application, AcuSolve is used to simulate fluid flow and viscous heating in an annulus formed by concentric cylinders. AcuSolve results are compared with analytical results adapted from Bird and others (1960). The close agreement of AcuSolve results with analytical results validates the ability of AcuSolve to model cases with viscous heating.

Problem Description

The problem consists of a viscous fluid filling the annulus between two concentric cylinders, as shown in the following image, which is not drawn to scale. The inner cylinder has a radius of 1.0 m and is fixed in place. The outer cylinder has a radius of 2.0 m and rotates with a constant angular velocity of 0.5 rad/s. The inner cylinder is held at a constant temperature of 273 K and the outer cylinder is held at 274 K.

The rotation of the outer cylinder causes the fluid to rotate due to the viscous shearing near the wall. As the inner cylinder is fixed, a velocity gradient is generated as a function of distance from the inner cylinder center. Viscous stresses within the domain generate significant amounts of heat, leading to a substantial increase in the fluid temperature in regions of high shear.

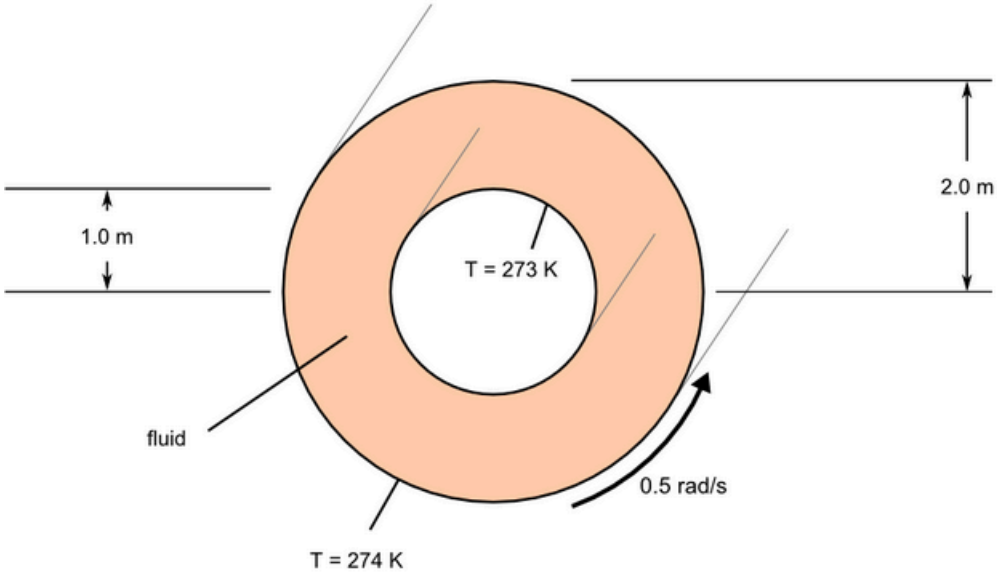


Figure 433: Critical Dimensions and Parameters for Simulating Viscous Heating Inside a Rotating Annulus

The simulation was performed as a two-dimensional problem by constructing a volume mesh that contains a single layer of elements in the extruded direction, normal to the flow plane, and by imposing symmetry boundary conditions on the extruded planes.

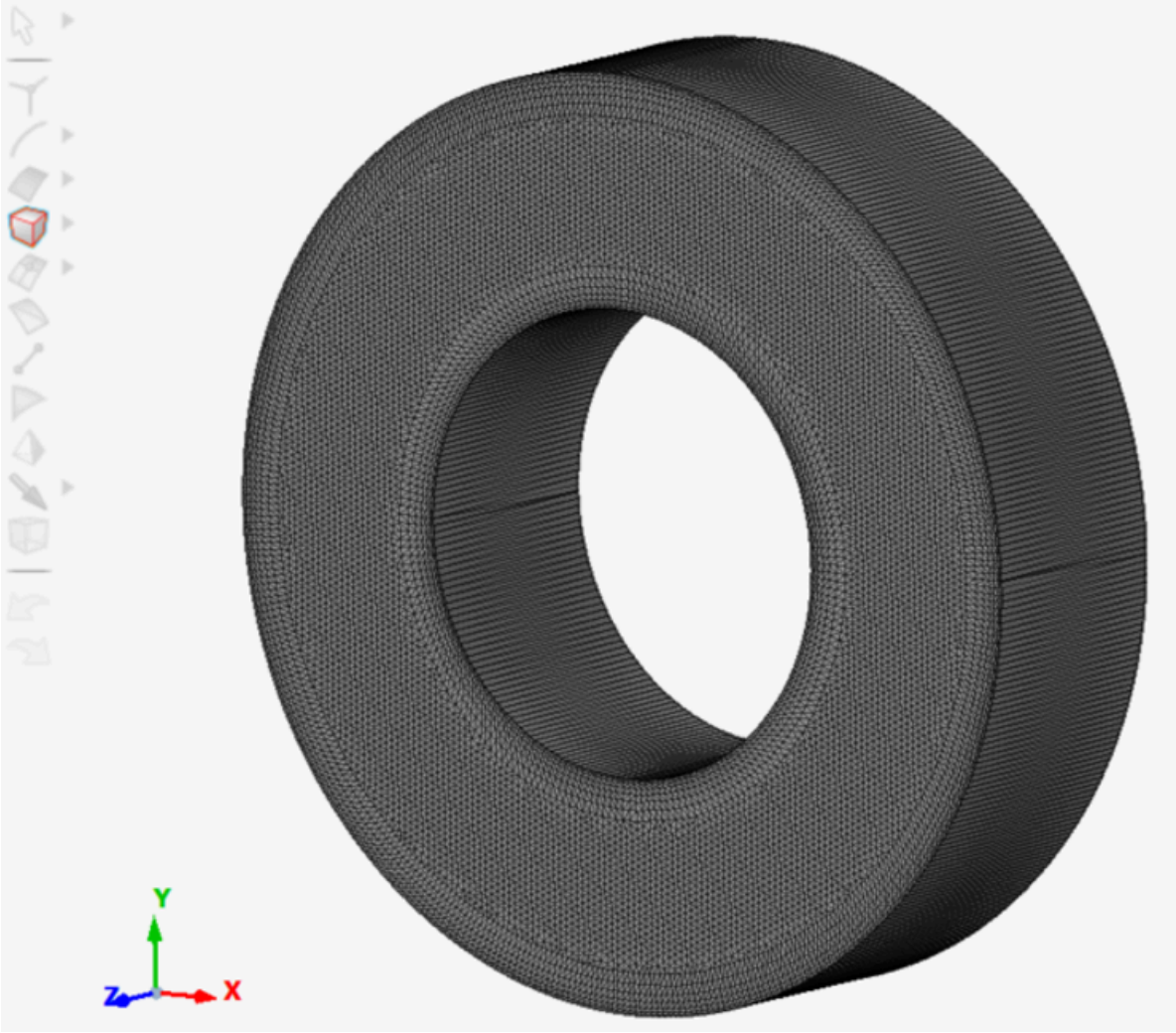


Figure 434: Mesh used for Simulating Viscous Heating Inside a Rotating Annulus

AcuSolve Results

The AcuSolve solution converged to a steady state and the results reflect the mean flow conditions. Flow is induced by the viscous shearing near the outer wall, creating a velocity gradient with the highest velocity near the moving wall.

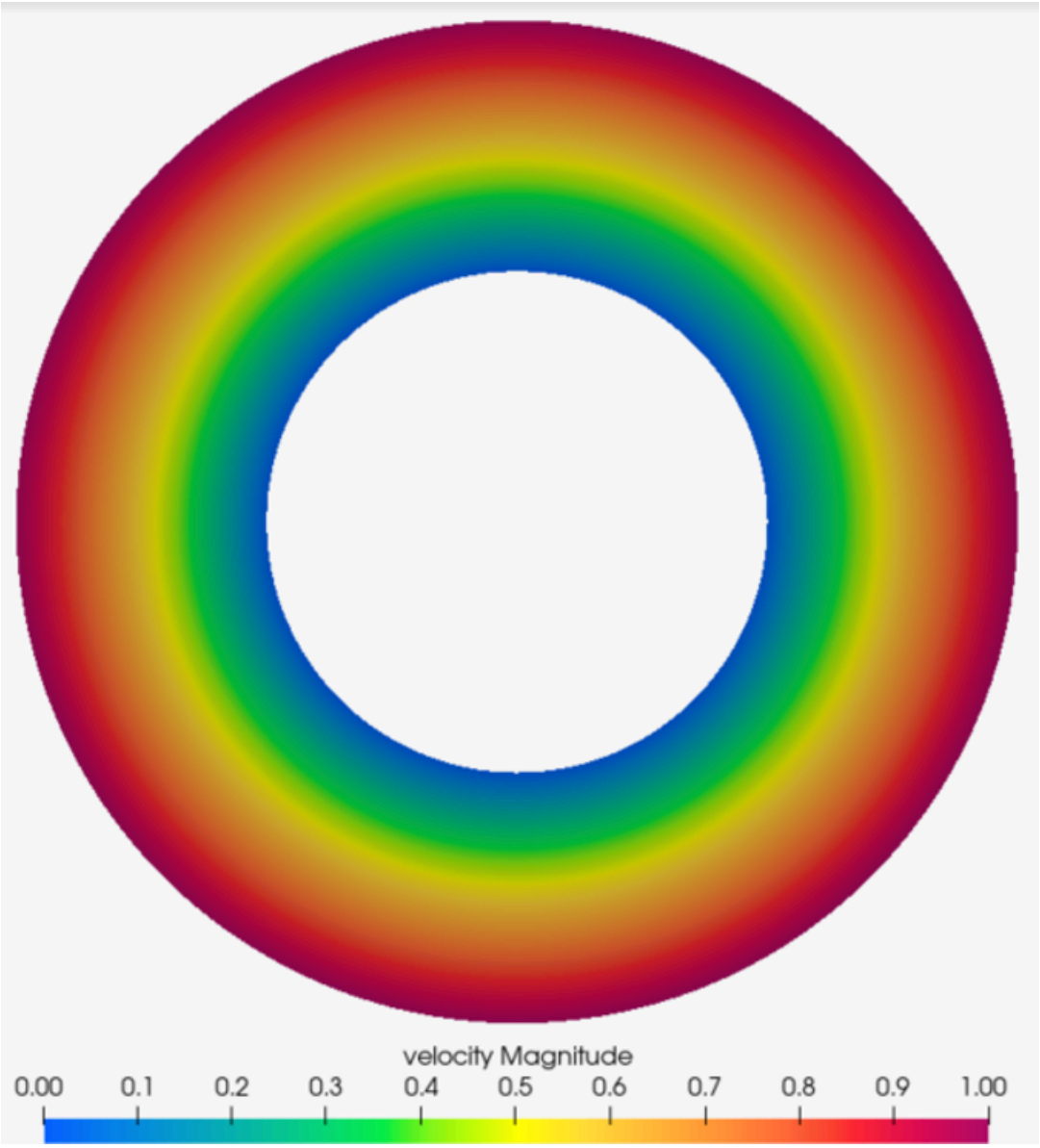


Figure 435: Contours of Velocity Magnitude (m/s)

The velocity gradient causes viscous heating, causing the fluid temperature to increase. The resulting temperature profile is nonlinear with the highest temperatures occurring in the space between the cylinders.

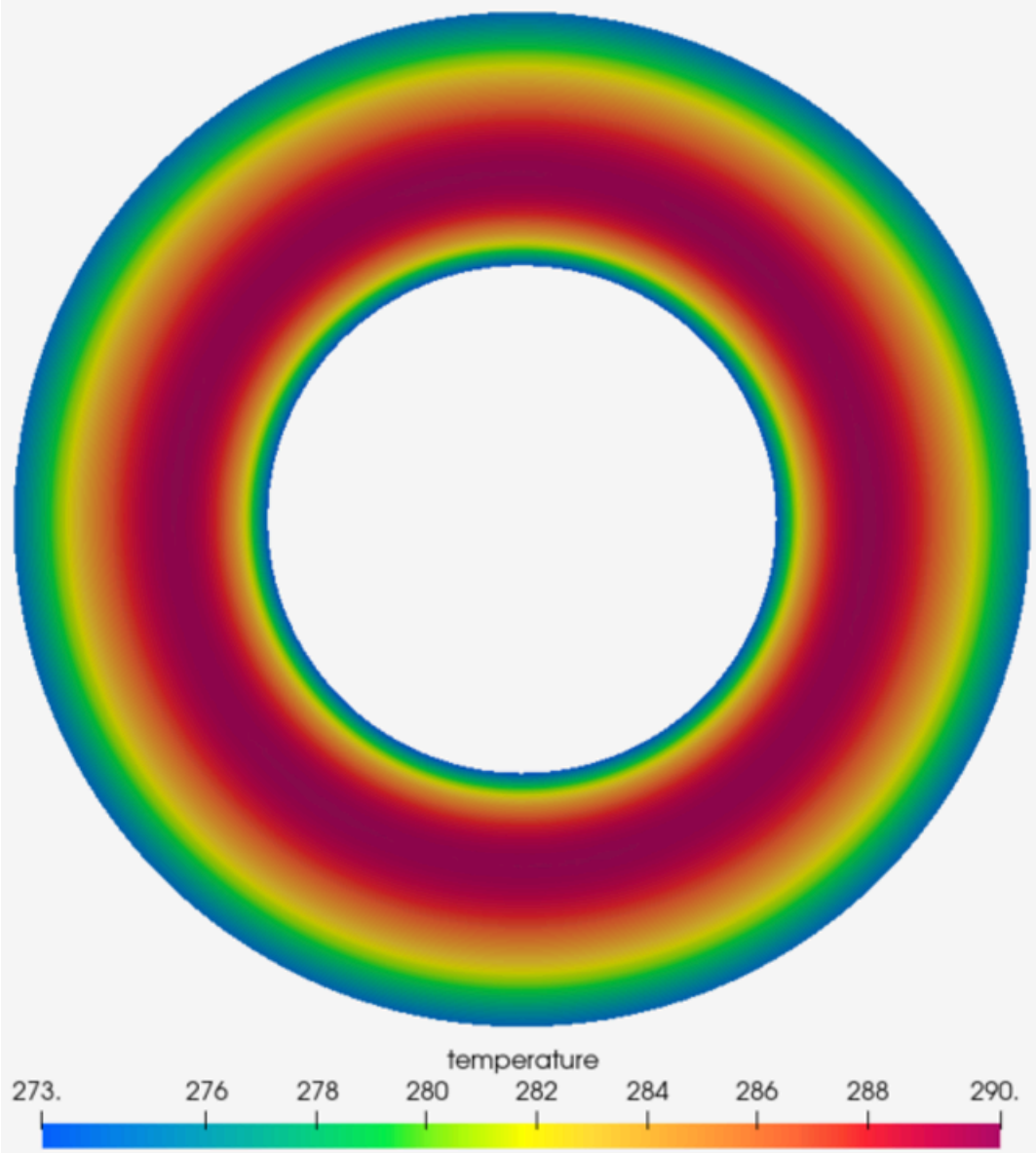


Figure 436: Contours of Temperature (K)

AcuSolve results were compared to analytical results for velocity and for temperature across a range of radial locations.

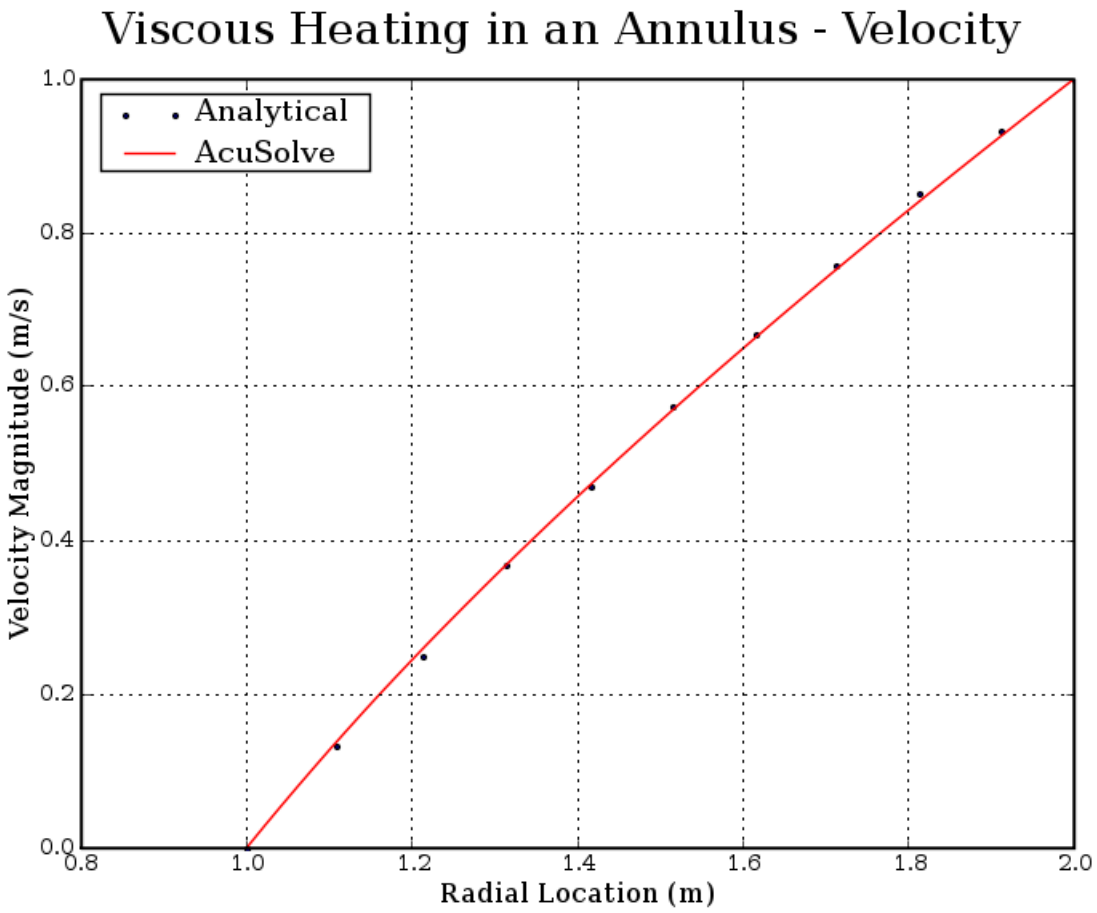


Figure 437: Velocity Magnitude Plotted Against Radial Location from the Center of the Inner Cylinder

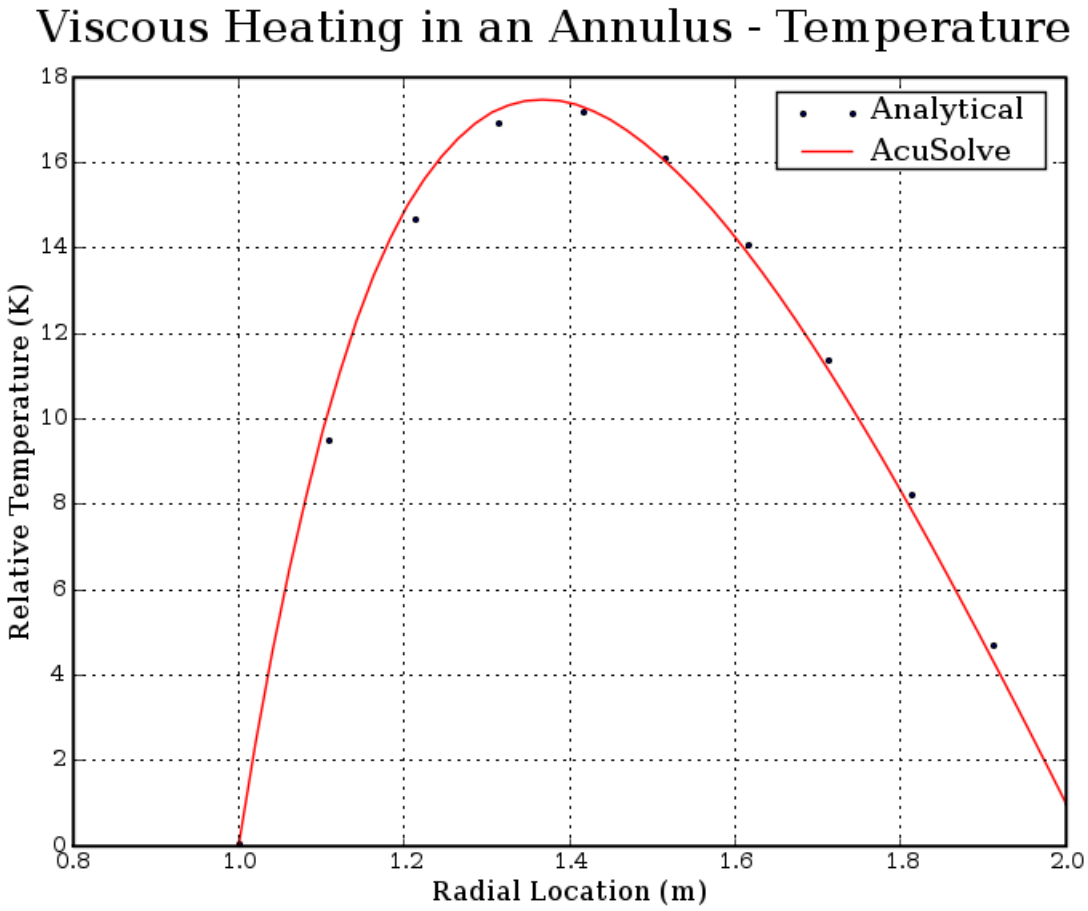


Figure 438: Temperature (Relative to the Inner Cylinder Wall Temperature) Plotted Against Radial Location from the Center of the Inner Pipe

Summary

The AcuSolve results compare well with the analytical results for both the flow field and the temperature across the annulus. In this application, flow is induced due to the viscous stresses generated by the rotation of the exterior cylinder. Velocity gradients between the cylinders give rise to shear stresses that induce frictional heating of the fluid. Due to the high viscosity of the fluid, the viscous heating is significant and leads to large increases in the temperature between the cylinders. This application validates the ability of AcuSolve to simulate flows where the viscous heating contribution is significant.

Simulation Settings for Viscous Heating Inside a Rotating Annulus

SimLab database file: `<your working directory>\annulus_rotating_heat\annulus_rotating_heat.slb`

Global

- Problem Description
  - Analysis type - Steady State
  - Temperature equation - Advective Diffusive

    - Turbulence equation - Laminar
- Auto Solution Strategy
    - Relaxation factor - `0.2`
- Material Model
    - Fluid
        - Density - `1.0` kg/m3
        - Viscosity - `300` kg/m-sec
        - Conductivity - `1.0` W/m-K
- Reference Frame
    - Outer_Rotation
        - Angular Velocity
            1. X-component - `0.0` rad/sec
            2. Y-component - `0.0` rad/sec
            3. Z-component - `0.5` rad/sec

Model

- Volumes
    - Fluid
        - Element Set
            1. Material model - Fluid
            2. Viscous heating - On
- Surfaces
    - Inner_Cylinder
        - Simple Boundary Condition
            1. Type - Wall
            2. Temperature BC type - Value
            3. Temperature - `273.0` K
    - Outer_Cylinder
        - Simple Boundary Condition
            1. Type - Wall
            2. Reference frame - Outer_Rotation
            3. Temperature BC type - Value
            4. Temperature - `274.0` K
    - Symm_MaxZ
        - Simple Boundary Condition
            1. Type - Symmetry
    - Symm_MinZ
        - Simple Boundary Condition

1 Type - Symmetry

- Nodes
  - Node 1
    - Pressure
      1 Type - Zero

References

R. B. Bird, W. E. Stewart, and E. N. Lightfoot. "Transport phenomena". New York, John Wiley and Sons, 1960

Heat Transfer Between Radiating Concentric Cylinders

In this application, AcuSolve is used to simulate the heat transfer due to radiation between concentric cylinders. The inner and outer cylinders are held at constant temperature and are defined to be radiation surfaces. AcuSolve results are compared with analytical results for temperature as described in Incropera (2006). The close agreement of AcuSolve results with analytical results validates the ability of AcuSolve to model cases with radiation heat transfer requiring view factor computation.

Problem Description

The problem consists of a fluid with arbitrary material properties between two infinitely long concentric cylinders, as shown in the following image, which is not drawn to scale. The radius of the outer cylinder is 0.0468 m and the radius of the inner cylinder is 0.0178 m. The inner cylinder is defined to have a constant wall temperature at 773.0 K (500 °C). The outer cylinder is defined to have a constant wall temperature at 300.0 K (27 °C). Both cylinders are specified to radiate as grey bodies, with emissivity set to 0.03778.

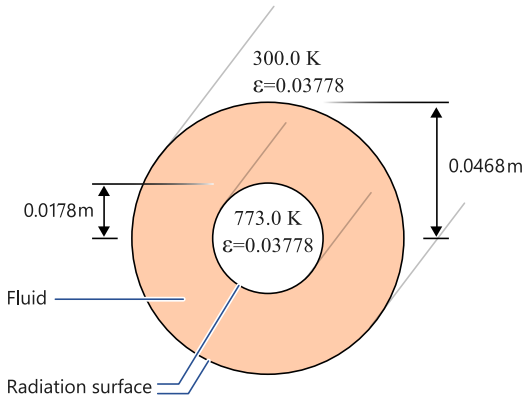


Figure 439: Critical Dimensions and Parameters Used for Simulating Radiation Between Two Concentric Cylinders

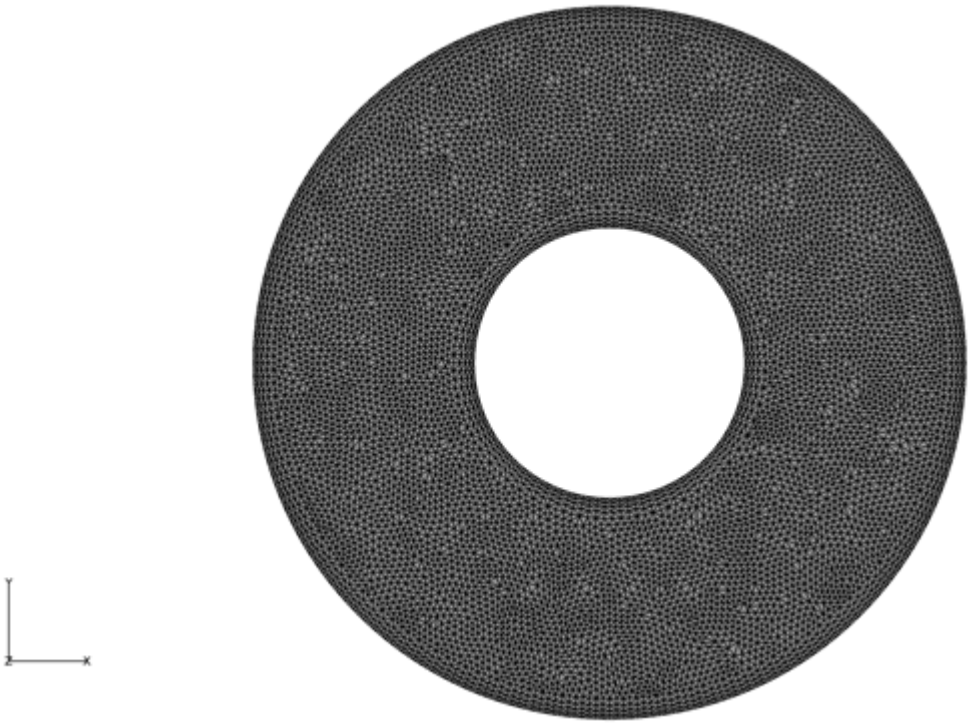


Figure 440: Mesh used for Simulating Radiation Between Two Concentric Cylinders

The simulation was performed as a two-dimensional problem by constructing a volume mesh that contains a single layer of elements normal to the radial and circumferential directions.

AcuSolve Results

The AcuSolve solution converges to a steady state and the results reflect the mean temperature distribution. As the inner diameter is considerably hotter than the outer, a heat flux, due to radiation, is present between the cylinders. The temperature within the medium reduces logarithmically as a function of the radius. The following images show the temperature with the medium as a function of radius from the center. The temperature is compared with the analytical solution as described in Incropera (2006). The image below shows black circles representing the analytical solution and a solid red line for the AcuSolve results.

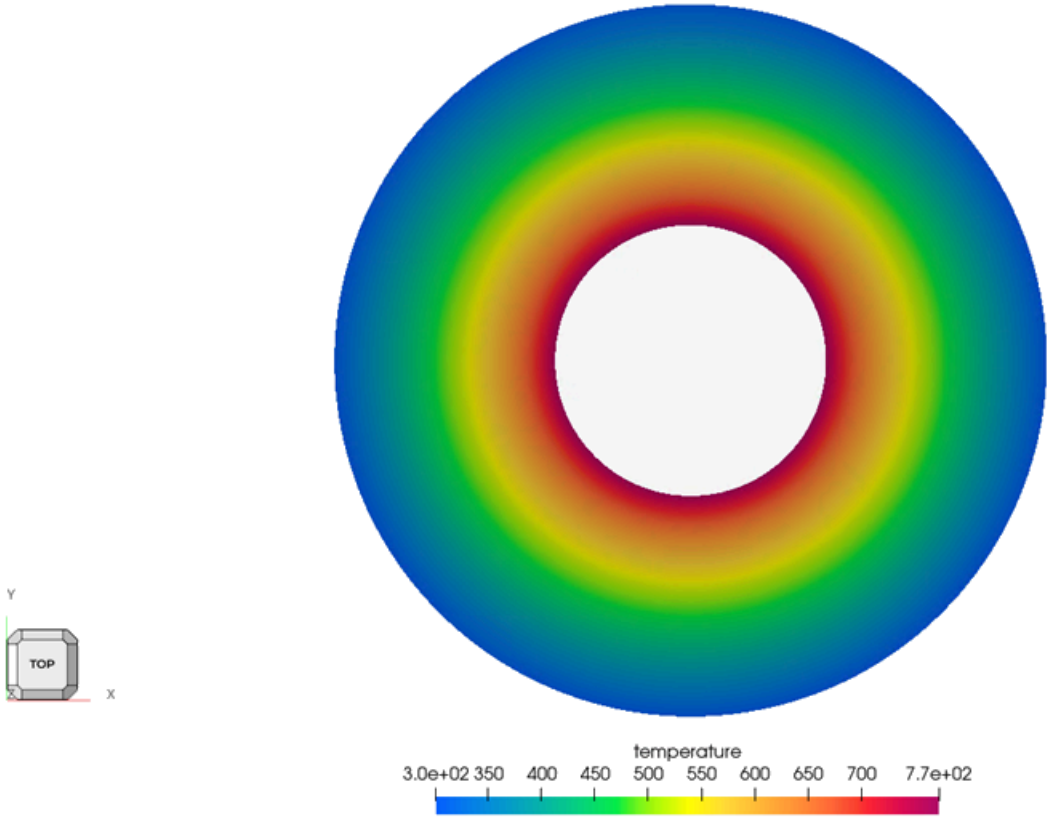


Figure 441: Contours of Temperature Between the Concentric Cylinders

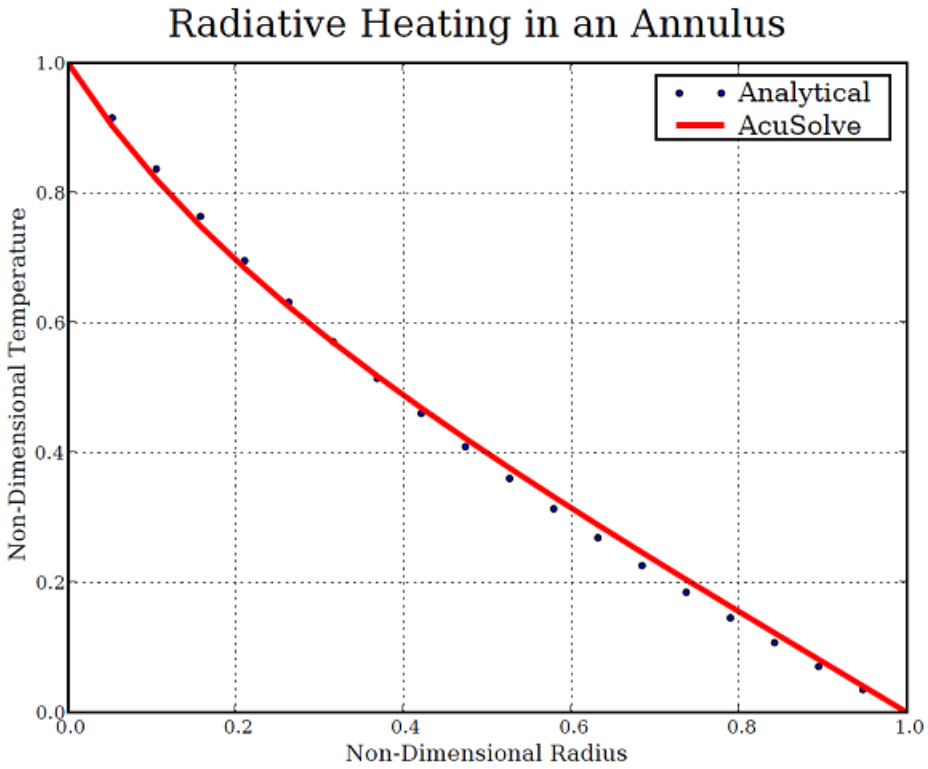


Figure 442: Non Dimensional Temperature Distribution Within the Annulus as a Function of Non Dimensional Radius

Summary

The AcuSolve solution compares well with analytical results for heat transfer due to radiation between two concentric cylinders. In this application, an arbitrary material is subjected to a heat flux that is calculated based on the view factors within the model. As a result of radiative heat flux a temperature distribution between the two cylinders develops. The AcuSolve solution for the temperature as a function of radius matches well compared to the analytical solution.

Heat Transfer Between Radiating Concentric Cylinders

HyperMesh CFD database file: `<your working directory>\annulus_radiation\annulus_radiation.hm`

Global

- Problem Description
  - Analysis type - Steady State
  - Temperature equation - Advective Diffusive
  - Radiation equation- Enclosure
- Auto Solution Strategy
  - Convergence tolerance - `0.0001`
  - Relaxation Factor- `0.4`
  - Flow- off

    - Enclosure radiation- on
- Material Model
    - Material
        - Conductivity
            1. Type - Constant
            2. Conductivity- `1.0`
- Emissivity Model
    - Grey Body
        - Emissivity- `0.03778`
    - Black Body
        - Emissivity- `1.0`

  Model
- Volumes
    - Medium
        - Element Set
            1. Medium - Fluid
            2. Material model- Material
- Surfaces
    - ID
        - Simple Boundary Condition
            1. Type- Wall
            2. Temperature BC type- Value
            3. Temperature- `773.0` K
        - Radiation Surface
            1. Type- Wall
            2. Emissivity model- Grey Body
    - Max_Z
        - Simple Boundary Condition
            1. Type- Symmetry
        - Radiation Surface
            1. Type- Wall
            2. Emissivity model- Black Body
    - Min_Z
        - Simple Boundary Condition
            1. Type- Symmetry
        - Radiation Surface
            1. Type- Wall

2. Emissivity model- Black Body

- OD
  - Simple Boundary Condition
    1. Type- Wall
    2. Temperature BC type- Value
    3. Temperature- `300.0` K
  - Radiation Surface
    1. Type- Wall
    2. Emissivity model- Grey Body

References

F. P. Incropera and D. P. DeWitt. "Fundamentals of Heat Transfer - Sixth Edition". John Wiley & Sons. New York. 2006.

Heat Transfer Between Radiating Concentric Spheres

In this application, AcuSolve is used to simulate the heat transfer due to conduction and radiation between concentric spheres. The inside surface of the inner and the outside surface of the outer sphere are both held at constant temperature, while the gap between them radiates the heat from one sphere to the other.

AcuSolve results are compared with analytical results for temperature and heat flux as described in Incropera (2006) and Salazar, et al. (2016). The close agreement of AcuSolve results with analytical results validates the ability of AcuSolve to model cases with radiation heat transfer and conjugate heat transfer with enclosure radiation modeling and the discrete ordinate (DO) radiation model.

Problem Description

The problem consists of a fluid region with arbitrary material properties between two concentric spheres with surfaces held at fixed temperature, as shown in the following image, which is not drawn to scale. The radius of the outer sphere is 0.04 m and the radius of the inner sphere is 0.01 m. The inner surface of the inner sphere is defined to have a constant wall temperature at 300.0 K (27 ºC). The outer surface of the outer sphere is defined to have a constant wall temperature at 1300.0 K (1027 ºC). The fluid within the spheres is defined as a non-conducting material, allowing heat to transfer via radiation only. The solid and fluid regions equilibrate to a steady temperature and can be compared with a semi-analytical solution for the temperature and heat flux at the fluid boundaries.

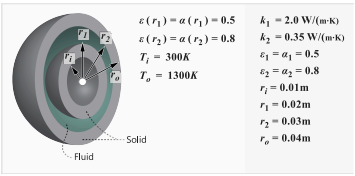


Figure 443: Critical Dimensions and Parameters used for Simulating Conduction and Radiation Between two Concentric Spheres



Figure 444: Mesh used for Simulating Radiation Between two Concentric Spheres

The simulation was performed as a three dimensional problem by constructing a volume mesh that contains a layer of boundary elements normal to the radial direction.

AcuSolve Results

The AcuSolve solution converges to a steady state and the results reflect the mean temperature distribution within the spheres. As the outer diameter is considerably hotter than the inner, a heat flux is present between the spheres. The temperature within the mediums increases as a function of the radius, with a slope corresponding to the temperature difference and the specified emissivity of the shells. The following image shows the temperature contour within the spheres along with the two-dimensional plot of the temperature versus radius in the solid mediums. The temperature and heat flux at the radiation surfaces are compared with the analytical solution as described in Salazar, et al. (2016).

Table 24: The Analytical Solution for the Temperature and Heat Flux at r1 and r2 are Presented with the Corresponding AcuSolve Results for the Enclosure (Surface to Surface) Model and the DO

	T(r1) (K)	T(r2) (K)	Q(r1) (W)	Q(r2) (W)
Analytical	578.2	1035.0	-27822.5	12365.6
AcuSolve (Enclosure)	578.4	1035.1	-27827	12364.2
AcuSolve (DO)	561.8	1023.6	-26175	12897.0
Percent Difference (Enclosure)	0.034%	0.010%	-0.015%	-0.011%
Percent Difference (DO)	2.8%	-1.11%	5.92%	4.3%

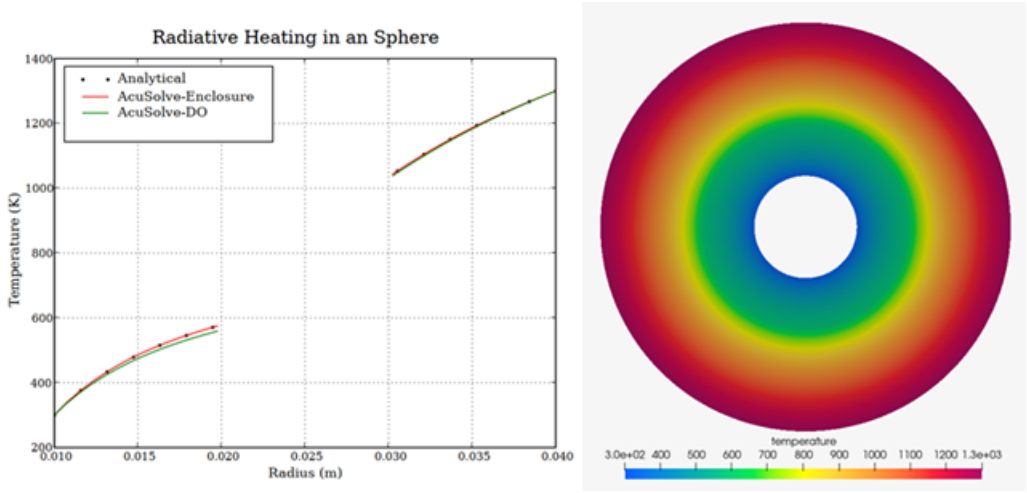


Figure 445: Two-Dimensional Plot and Contours of Temperature Between the Concentric Spheres

Summary

The AcuSolve solution compares well with analytical results for heat transfer due to conduction and radiation between two concentric spheres. In this application, an arbitrary material is subjected to a heat flux that is calculated based on the view factors or the DO model within the simulation. As a result of the conjugate heat transfer and the radiative heat flux a temperature distribution between the two spheres develops. The AcuSolve solution for the temperature and heat flux at the radiation surfaces matches well compared to the analytical solution with only a minor difference for the enclosure radiation model. The enclosure radiation model was found to have a higher accuracy for this application compared to the DO model, as expected due to the relatively low optical thickness in this simulation.

Heat Transfer Between Radiating Concentric Spheres

HyperMesh CFD database file: `<your working directory>\sphere_radiation\sphere_radiation.hm`.

Global

- Problem Description
  - Analysis type - Steady State
  - Temperature equation - Advective Diffusive
  - Radiation equation - Enclosure
- Auto Solution Strategy
  - Convergence tolerance - `1.0e-5`
  - Relaxation Factor - `0.4`
  - Flow - off
  - Enclosure radiation - on
- Material Model
  - Inner
  - Conductivity
    - Type - Constant

        - Conductivity - `2.0`
    - Outer
    - Conductivity
        - Type - Constant
        - Conductivity - `0.35`
    - Radiating
    - Conductivity
        - Type - Constant
        - Conductivity - `1.0e-6`
- Emissivity Model
- Inner
    - Emissivity - `0.5`
- Outer
    - Emissivity - `0.8`

  Model
- Volumes
    - Inner
        - Element Set
            1. Medium- Solid
            2. Material model - Inner
        - Outer
            1. Element Set
                1. Medium - Solid
                2. Material model - Outer
        - Radiating
            1. Element Set
                1. Medium - Fluid
                2. Material model - Radiating
- Surfaces
    - Inner_Inner_r1
        - Simple Boundary Condition - (disabled to allow for heat flux)
    - Inner_Inner_ri
        - Simple Boundary Condition
            1. Type - Wall
            2. Temperature BC type - Value
            3. Temperature - `300.0` K
    - Inner_Radiating_r1

- Simple Boundary Condition (disabled to allow for heat flux)
- Radiation Surface
  1. Type - Wall
  2. Emissivity model - Inner

- Outer_Outer_r2
  - Simple Boundary Condition (disabled to allow for heat flux)
- Inner_Outer_ro
  - Simple Boundary Condition
    1. Type - Wall
    2. Temperature BC type - Value
    3. Temperature - `1300.0` K
- Outer_Radiating_r2
  - Simple Boundary Condition (disabled to allow for heat flux)
  - Radiation Surface
    1. Type - Wall
    2. Emissivity model - Outer

References

F. P. Incropera and D. P. DeWitt. "Fundamentals of Heat Transfer – Sixth Edition". John Wiley & Sons. New York. 2006.

Salazar, G., Droba, J., Oliver, B., & Amar, A. J. (2016). Development and Verification of Enclosure Radiation Capabilities in the CHarring Ablator Response (CHAR) code. 46th AIAA Thermophysics Conference.

Two-Phase Nucleate Boiling in a Cylindrical Pipe

In this application, AcuSolve is used to simulate the changes in wall temperature due to two-phase nucleate boiling at the heated walls of a pipe with water flowing through it. AcuSolve results are compared with experimental results adapted from Koncar and others (2015). The close agreement of AcuSolve results with experimental results validates the ability of AcuSolve to model two-phase nucleate boiling problems.

Problem Description

The problem consists of a pipe with heated surrounding walls, as shown in the following image, which is not drawn to scale. The length of the pipe is 2 m and the radius is 0.0017 m. Mass flux at the inlet is 900 kg/m^2 and the temperature of the fluid entering the pipe is 473 K. A heat flux of 570,000 W/m^2 is applied on the walls. The preheated water enters the inlet and heat is transferred to the fluid from the walls. The heat causes sub-cooled boiling to occur in the region close to the wall and leads to the formation of bubbles at nucleation sites.

During sub-cooled boiling flow, heat and mass exchange between the phases takes place on the heated wall and in sub-cooled liquid flow. On the heated surface the vapor bubbles are generated and as they move through the sub-cooled liquid they condense and release the latent heat.

The AcuSolve simulation is set up to model transient state heat transfer to determine the temperature along the centerline of the pipe and along the heated pipe walls of the model. AcuSolve computes the two-phase nucleate boiling by simulating the three-dimensional flow in a heated pipe for two-phase boiling flow, as described in Koncar (2005). The temperatures along the centerline of the pipe and along the pipe walls are compared against the experimental measurements, as described in Koncar, et al. (2005).

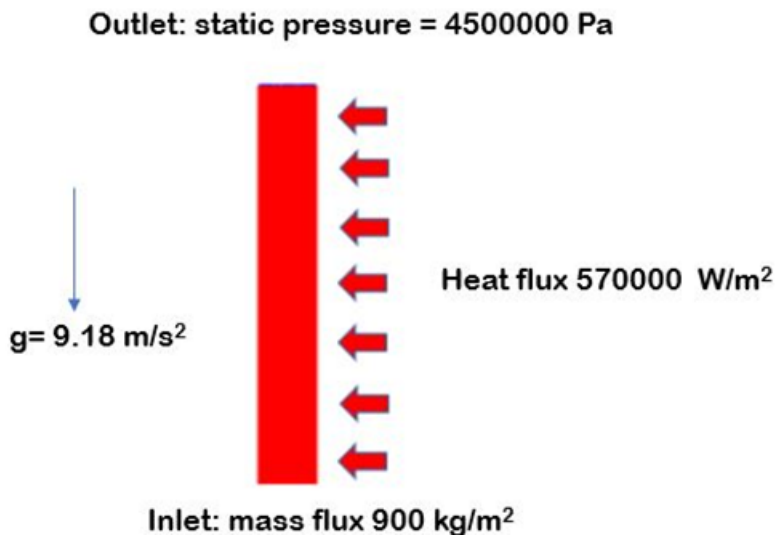


Figure 446: Parameters for Simulating a Two-Phase Nucleate Boiling Problem of a Pipe

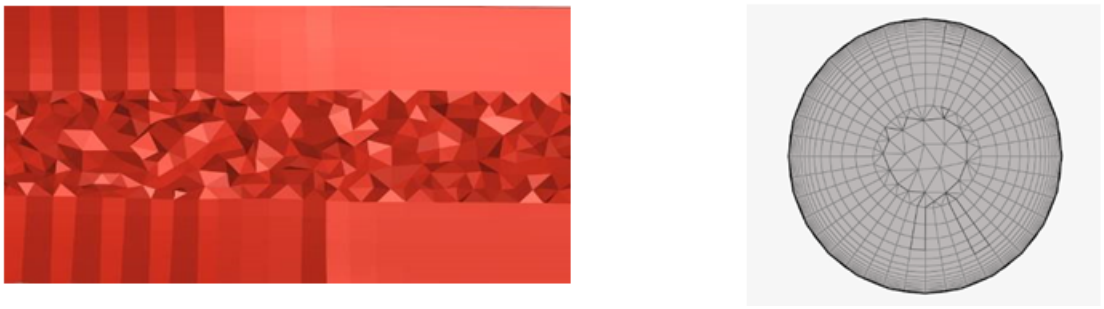


Figure 447: Mesh used for Simulating Two-Phase Flow in a Pipe

AcuSolve Results

The AcuSolve solution is run for a heat flux of 570,000 W/m^2 and the results are presented in the following image. The experimental values of wall temperature are presented with the corresponding AcuSolve results along the centerline of the pipe and along the pipe wall. The AcuSolve results show good agreement with the experimental results for the temperature, indicating that the two-phase nucleate boiling is properly captured.

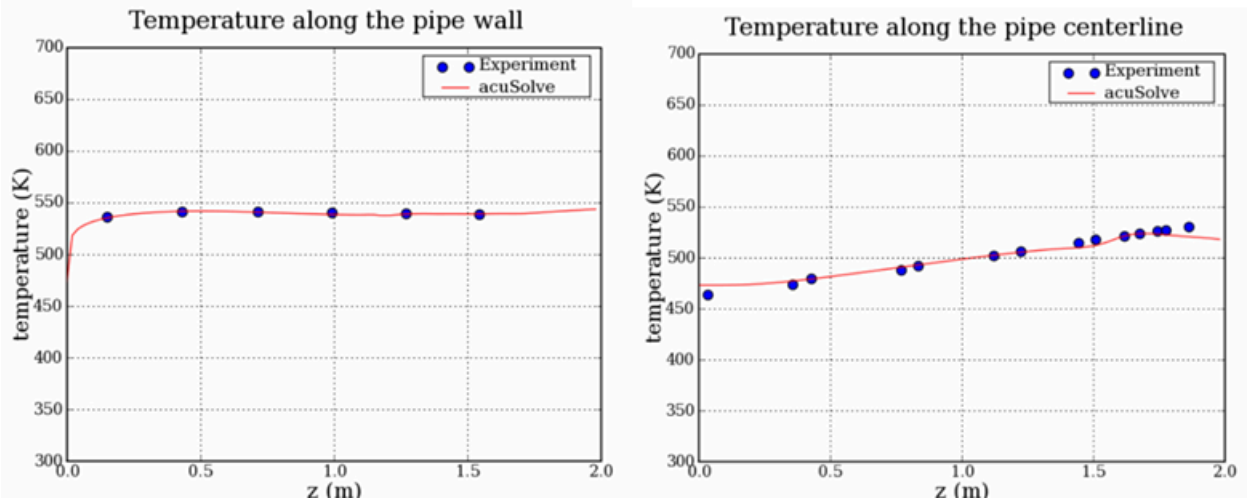


Figure 448: Temperature Values for Varying Streamwise Distance Compared to Experimental Data

Summary

The AcuSolve solution compares well with experimental results for two-phase nucleate boiling simulations. In this application, the temperature of the wall as the onset of boiling approaches are simulated with AcuSolve using the nucleate boiling feature and the SA turbulence model. The experimental values of temperature are presented with the corresponding AcuSolve results. A good agreement of simulation results with the experiment validates the ability to solve two-phase nucleate boiling using the nucleate boiling capabilities of AcuSolve.

Simulation Settings for Two-Phase Nucleate Boiling in a Cylindrical Pipe

HyperMesh CFD database file: `<your working directory>\pipe_two_phase_boiling \pipe_two_phase_boiling.hm`.

Global

- Problem Description
  - Analysis type – Transient
  - Turbulence equation – SA
  - Temperature equation – Advective Diffusive
- Auto Solution Strategy
  - Maximum time steps – `500`
  - Initial time increment – `0.003`
  - Convergence Tolerance – `0.001` sec
  - Relaxation factor – `0.3`
- Surface Tension Model (“Water_NB-Vapor_NB”)
  - Type – Constant
  - Surface Tension – `0.02382`
- Material Model
  - Vapor_NB
    - Type – Constant
    - Density – `23.75` kg/m^3
    - Viscosity – `1.79e-05` kg/m-sec
    - Specific Heat – `4225` J/kg-K
    - Latent Heat – `1675570`
    - Latent Heat Temperature – `530.55` K
    - Conductivity – `0.02528` W/m-K
  - Water_NB
    - Type – Constant
    - Density – `800` kg/m3
    - Viscosity – `0.0001339` kg/m-sec
    - Specific Heat – `4500` J/kg-K
    - Conductivity – `0.65` W/m-K
- Multifield parameter (Field interaction model)
  - Type – Algebraic Eulerian
  - Phase change type – Wall Boiling
  - Carrier field - Water
  - Disperse field – Vapor
  - Disperse field diameter type – Boiling kurul exponential
  - Drag model – Ishii zuber
  - Lift Model – Legendre Magnaudet

Model

- Volumes
  - Fluid
    - Material – Vapor_Water
- Surfaces
  - Inflow
    - Simple Boundary Condition – Inflow
    - Inflow type – Mass Flux Rate
    - Mass Flux Rate – `0.167634` kg/sec
    - Temperature – `473` K
  - Outflow
    - Simple Boundary Condition – Outflow
    - Pressure – `4500000` N/m2
  - Wall
    - Simple Boundary Condition – Wall
    - Temperature type – Flux
    - Heat Flux – `570000` W/m2

References

B. Koncar, E. Krapper, Y. Egorov, 2005, "CFD MODELING OF SUBCOOLED FLOW BOILING FOR NUCLEAR ENGINEERING APPLICATIONS", International Conference Nuclear Energy for New Europe 2005, Bled, Slovenia, September 5-8,2005.

Single-Phase Nucleate Boiling in a Rectangular Channel

In this application, AcuSolve is used to simulate the wall heat flux due to nucleate boiling at a heated wall inside a rectangular channel with water flow. Results are compared with experimental heat flux measurements as reported by Steiner, et al. (2005). The close agreement of AcuSolve results with experimental results validates the ability of AcuSolve to model single phase nucleate boiling problems.

Problem Description

The problem consists of a channel with a heated wall at the bottom. The temperature of the wall is selected to onset the nucleate boiling at the heated wall. The dimensions of the inlet are 0.03 x 0.04 m; the inlet velocity (v) is 0.39 m/s and the temperature (T) of the fluid entering the inlets is varied from 373.15 K (100 C) to 406.15 (133 C)), while the atmospheric pressure is specified to be 2 bar. The pre-heated water enters the inlets and heat is transferred into the fluid from the heated walls. The heat causes sub-cooled boiling to occur in the region close to the wall and leads to the formation of bubbles at nucleation sites. The surface tension and vapor phase models are specified to emulate the physical process of water changing state to water vapor.

The heat transfer in this regime is dominated by two effects, the macro convection due to the motion of the bulk liquid and the latent heat transport associated with the evaporation of the liquid micro-layer between the bubble and the heated wall. Each of these effects are modeled with AcuSolve and the prediction of their processes is demonstrated in the following results.

The AcuSolve simulation is prepared as a steady state heat transfer simulation to determine the temperature and heat flux on the heated walls of the model. AcuSolve computes the single-phase nucleate boiling by employing Chen’s model for two-phase boiling flow described in Chen (1966). The heat flux values for different wall temperatures are compared against the experimental measurements, as described in Steiner, et al. (2005).

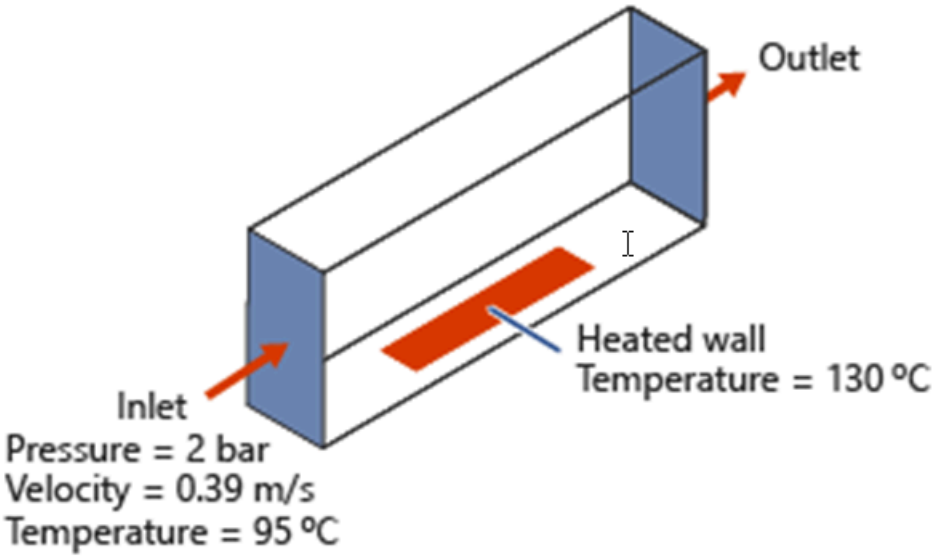


Figure 449: Critical Dimensions and Parameters for Simulating a Single-Phase Nucleate Boiling in a Rectangular Channel

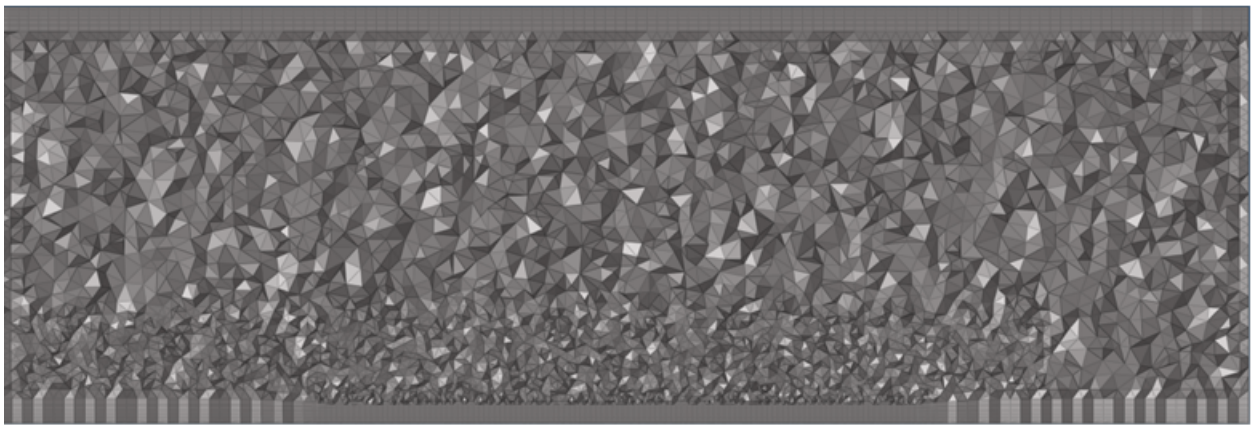


Figure 450: Mesh Used for Simulating a Single-Phase Nucleate Boiling in a Rectangular Channel

AcuSolve Results

The AcuSolve solution is run for heated wall temperature values of 100 C, 105 C, 110 C, 115 C, 120 C, 125 C, 130 C, 133 C and the results presented reflect the heat flux from the wall as the temperature nears the saturation temperature. The experimental values of heat flux (MW/m2) and wall temperature are presented with the corresponding AcuSolve results at seven temperature values. The AcuSolve results show good agreement with the experimental results for the heat flux, indicating that the single-phase nucleate boiling is properly captured.

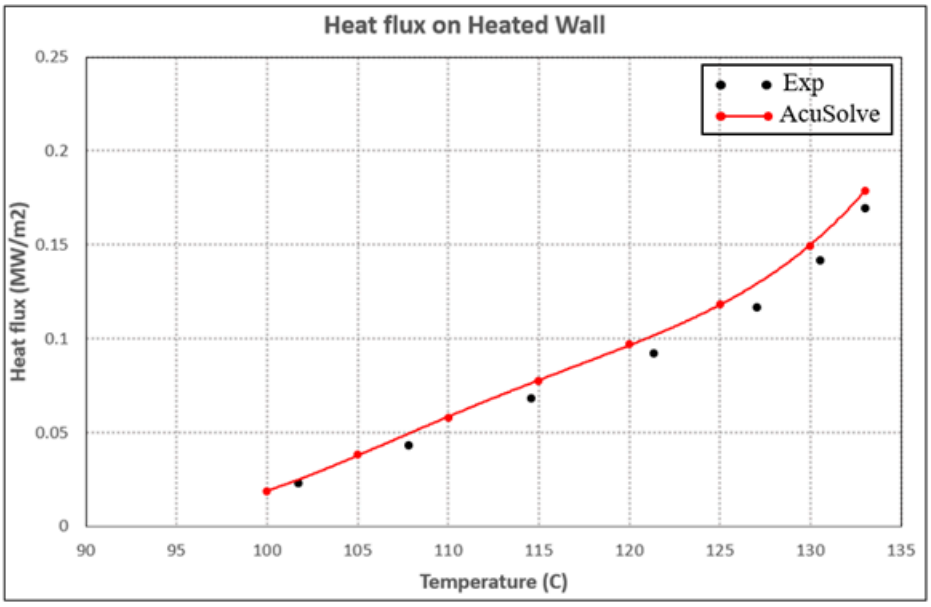


Figure 451: Heat Flux Values for Varying Wall Temperatures Compared to Experimental Data

Summary

The AcuSolve solution compares well with experimental results for single-phase nucleate boiling simulations. In this application, heat flux generated by the wall as the onset of boiling approaches are simulated with AcuSolve using the nucleate boiling feature and the RKE turbulence model. The experimental values of heat flux for the wall temperature range are presented with the corresponding AcuSolve results. A good agreement of simulation results with the experiment validates the ability to solve single-phase nucleate boiling using the nucleate boiling capabilities of AcuSolve.

Simulation Settings for Single-Phase Nucleate Boiling in a Rectangular Channel

HyperMesh CFD database file: `<your working directory>\channel_single_phase_boiling \channel_single_phase_boiling.hm`.

Global

- Problem Description
  - Analysis type – Steady
  - Turbulence equation – RKE
  - Temperature equation – Advective Diffusive
  - Nucleate Boiling Single Phase – On
- Auto Solution Strategy
  - Convergence Tolerance – `0.001`
  - Relaxation factor – `0.4`
- Surface Tension Model (“Water-srfTns”)
  - Type – Constant
  - Surface Tension – `0.07`

- Material Model
  - Vapor
    - Type – Constant
    - Density – `1.128` kg/m^3
    - Viscosity – `1.29e-5` kg/m-sec
    - Specific Heat – `2174.59` J/kg-K
    - Latent Heat – `2256000`
    - Latent Heat Temperature – `393.45` K
    - Conductivity – `0.02749` W/m-K
    - Turbulent Prandtl number – `1.0`
  - Water
    - Type – Constant
    - Density – `965.36` kg/m^3
    - Viscosity – `0.000314` kg/m-sec
    - Specific Heat – `4204.8` J/kg-K
    - Conductivity – `0.675` W/m-K
    - Turbulent Prandtl number – `0.91`
    - Vapor phase model – Vapor
    - Surface Tension model – Water-srfTns

Model

- Volumes
  - Fluid
    - Material– Water
- Surfaces
  - Inflow
    - Simple Boundary Condition – Inflow
    - Inflow type – Average Velocity
    - Average Velocity – `0.39` m/sec
    - Temperature – `368.15` K
  - Outflow
    - Simple Boundary Condition – Outflow
    - Back flow condition – On
    - Temperature back flow type – Mass flux average
    - Kinetic energy back flow type – Mass flux average
    - Dissipation rate back flow type – Mass flux average
  - Bottom
    - Simple Boundary Condition – Wall
  - Top

        - Simple Boundary Condition – Wall
    - Side_MinY
        - Simple Boundary Condition – Wall
    - Side_MaxY
        - Simple Boundary Condition – Wall
    - Heated Wall
        - Simple Boundary Condition – Wall
        - Temperature type – Value
        - Temperature – [373.15, 378.15, 383.15, 388.15, 393.15, 398.15, 403.15, 406.15] K

References

Helfried Steiner, Alexander Kobor, Ludwig Gebhard, 2005, "A wall heat transfer model for subcooled boiling flow", International Journal of Heat and Mass Transfer, Vol 48, pp. 4161- 4173.

Chen, J.C., 1966, "Correlation for Boiling Heat Transfer to Saturated Fluids in Convective Flow", United States: N. p., 1962. Web. doi:10.2172/4636495.

Supersonic Flow Through a Converging-Diverging Nozzle

In this application, AcuSolve is used to simulate the high-speed turbulent flow in a converging and then diverging nozzle. The flow within the nozzle enters as subsonic, reaches sonic at the throat and shortly after develops a normal shock. AcuSolve results are compared with experimental results adapted from Bogar and Sajben (1983). The close agreement of AcuSolve results to experimental measurements validates the ability of AcuSolve to simulate internal supersonic flows where normal shocks are present.

Problem Description

The problem consists of a converging and then diverging nozzle represented as an extruded planar surface, as shown in the image below, which is not drawn to scale. The length of the domain is 0.213 m with a throat height of 0.044 m. The stagnation pressure and static temperature are constrained at the inlet to 135,000 Pa and 265.98 K, respectively. The static pressure is defined using the outflow boundary condition, where P_{static}=97216.08 Pa. The flow in the diffuser has an inlet Reynolds number of $6.5x10^5$. The upper and lower walls are set to no-slip and the side walls are set to slip, while the exterior walls are specified to be adiabatic. Images of the numerical mesh are shown below.

The AcuSolve simulation is prepared to model the pseudo-transient state to determine the shock location and corresponding scalar quantities within the diffuser. AcuSolve computes the flow and thermal solution by simulating a planar, two-dimensional flow problem with physical dimensions and input quantities as described in the Sajben Diffuser case presented by Bogar and Sajben (1983). The gas in the simulation domain enters at subsonic conditions and is forced to accelerate beyond Mach=1.0 as it passes through the throat. After reaching supersonic speed a normal shock wave develops causing the flow speed to reduce back below sonic. The pressure along the bottom wall of the diffuser is compared against experimental measurements to demonstrate the solver's capability to solve supersonic cases.

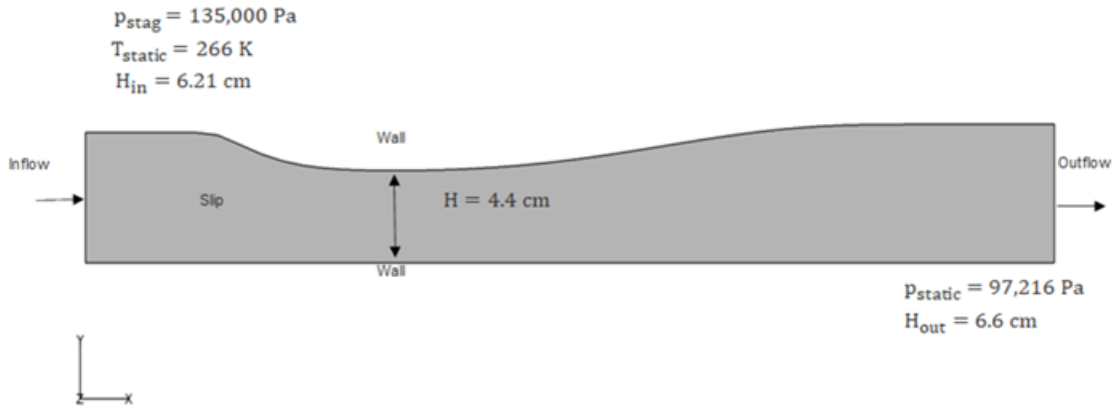


Figure 452: Parameters for Simulating Compressible Flow within a Converging-Diverging Nozzle

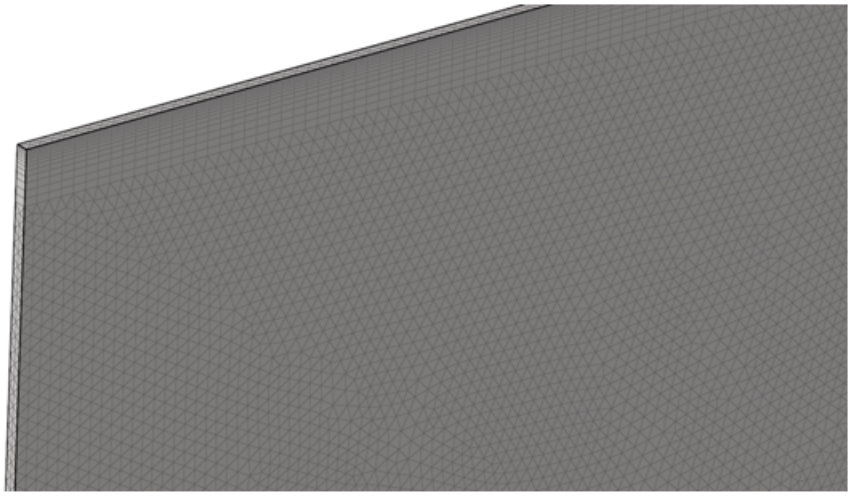


Figure 453: Mesh used for Simulating Compressible Flow in a Converging-Diverging Nozzle

AcuSolve Results

The AcuSolve solution is run for 0.025 seconds (6,250 timesteps with dt=4.0x10^{-6}sec) and converges to a pseudo-steady solution. The change in pressure from the inlet to outlet causes the flow to accelerate within the throat of the diffuser until it reaches approximately Mach=1.35. A normal shock is present just downstream of where the cross-sectional area of the nozzle increases, as shown in the image below. The numerical solution can be compared with the reference after normalizing the pressure along the wall by the inlet stagnation pressure (135 kPa) and the distance along the bottom wall by the nozzle throat height (0.044 m). The image below shows the normalized pressure versus normalized distance in comparison to NASA reference and experimental results. The image shows black circles representing the experimental measurements (Bogar and Sajben 1983), a dashed blue line representing the SA solution as obtained through NASA publication (Mohler 2005) and a solid red line representing the AcuSolve results with the Spalart-Allmaras turbulence model. The non-dimensional pressure within the diffuser agrees well with the reference data, demonstrating the correct physical location of the normal shock and expected moderate flow speed reduction within the constant cross-section diffuser portion of the nozzle.

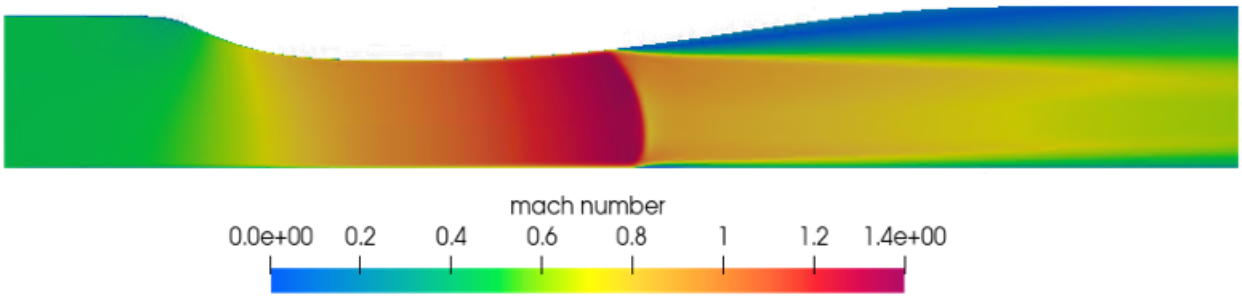


Figure 454: Contours of Mach Number within a Converging-Diverging Nozzle

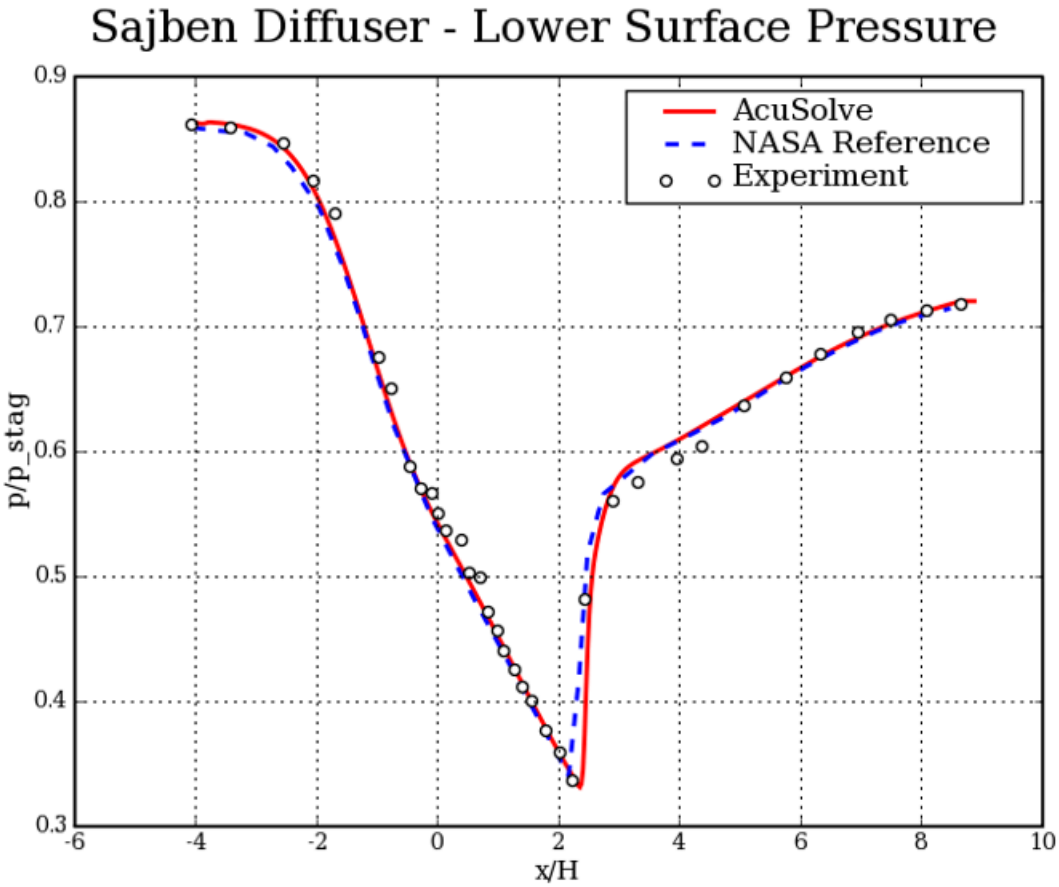


Figure 455: Normalized Pressure Versus Normalized Distance in Comparison to NASA Reference and Experimental Results

Summary

The AcuSolve solution compares well with experimental and numerical results for the described simulation. In this application, compressibility effects are accounted for using the coupled compressible flow solver with the ideal gas material definition. The thermal and momentum exchange within the nozzle is computed with AcuSolve using the compressible Navier-Stokes solver with the Spalart-Allmaras turbulence model. The experimental values of pressure are presented with the corresponding AcuSolve results and show good agreement, validating the ability to solve compressible cases with the presence of normal shocks. The results indicate that AcuSolve is able to properly predict the peak pressure magnitude and location within the diffuser while maintaining the normal shock when the time-step is selected to result in a maximum CFL of approximately 30.

Simulation Settings for Supersonic Flow Through a Converging-Diverging Nozzle

HyperMesh CFD database file: `<your working directory>\diffuser_compressible\diffuser_compressible.hm`

Global

- Problem Description

    - Flow – Compressible Navier Stokes
    - Analysis type – Transient
    - Turbulence equation – SA
    - Temperature equation – Advective Diffusive
- Auto Solution Strategy
    - Initial time increment – `4.0E-6`
    - Final time – `0.025` sec
    - Convergence Tolerance – `0.001` sec
    - Relaxation factor – `0.5`
- Material Model
    - Air-Ideal Gas
        - Type – Ideal_Gas
        - Viscosity – `1.781e-05` kg/m-sec
        - Specific Heat – `1005` J/kg-K
        - Conductivity – `0.02521` W/m-K
        - Gas Constant – `287.058` J/kg-K

Model

- Volumes
    - Fluid
        - Material – Air-Ideal Gas
- Surfaces
    - Inflow
        - Simple Boundary Condition – Inflow
        - Inflow type – Stagnation Pressure
        - Stagnation Pressure – `135000.0` N/m2
        - Turbulence_input_type – Direct
        - Eddy Viscosity – `1e-6` m^2/s
        - Temperature – `265.98` K
    - Outflow
        - Simple Boundary Condition – Outflow
        - Pressure – `97216.08` N/m2
    - Wall_1
        - Simple Boundary Condition – Wall
        - Type – auto_wall
    - Wall_2
        - Simple Boundary Condition – Wall
        - Type – auto_wall
    - Slip_1

        - Simple Boundary Condition – Slip
    - Slip_2
        - Simple Boundary Condition – Slip

References

Bogar, T. J., Sajben, M., and Kroutil, J. C. (1983) "Characteristic Frequencies of Transonic Diffuser Flow Oscillations," AIAA Journal, Vol. 21, No. 9, pp. 1232-1240.

Mohler, S.R., "Wind-US Unstructured Flow Solutions for a Transonic Diffuser," NASA CR-2005-213417, January 2005.

Ideal Gas Compression in an Actuating Piston

In this application, AcuSolve is used to simulate pressure and temperature inside an actuating piston using the ideal gas relationship and fully defined mesh motion. AcuSolve results are compared with analytical results as described in Moran and Shapiro (2000). The close agreement of AcuSolve results with analytical results validates the ability of AcuSolve to model cases with material properties defined by the ideal gas law subjected to significant mesh distortion.

Problem Description

The problem consists of air compressed by a piston within a cylinder 10 m long with a diameter of π (3.14159) m, as shown in the following image, which is not drawn to scale. The piston is driven by a crankshaft 4 m long attached to a connecting rod 6 m long. The crankshaft rotates at 60o/s around a center point. At time (t) = 0.0 s the crank and piston are at top dead center (TDC) with an initial cylinder volume of 80 m^3. At t = 3.0 s the piston is at bottom dead center (BDC), at which point the volume in the cylinder is reduced to 16 m^3. The piston then moves back to TDC at t = 6.0 s. Air at atmospheric conditions, with material properties of an ideal gas and a dynamic viscosity of 1.781 X 10^5 kg/m-sec is the fluid modeled in the domain.

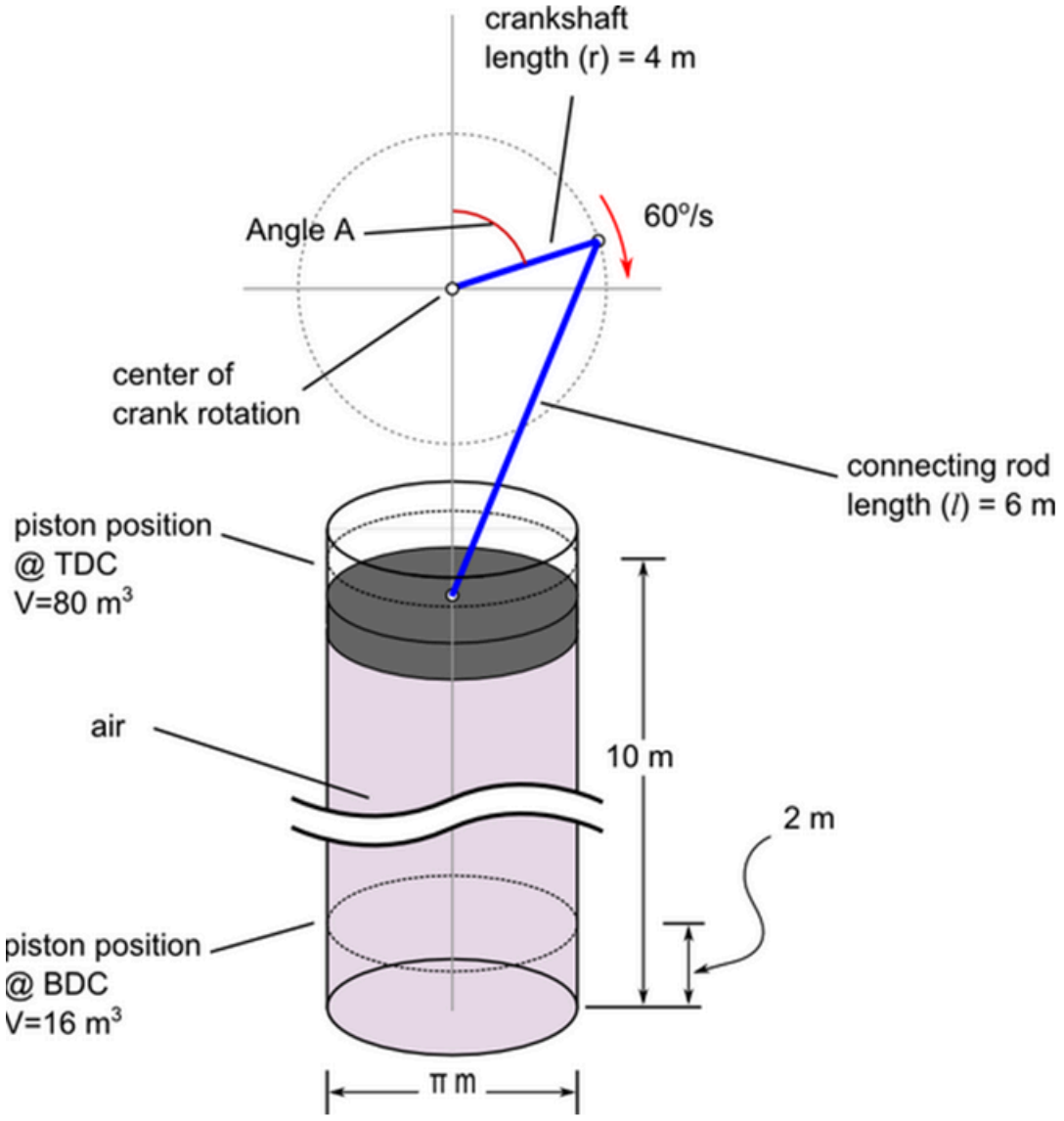


Figure 456: Critical Dimensions and Parameters for Simulating Ideal Gas Compression in an Actuating Piston

The motion of the piston is described by the following equation.

$$x = r * \cos A + \sqrt{l^2 - r^2 \sin^2 A} \tag{17}$$

Where

- x is the distance of the piston from TDC
- r is the length of the connecting rod, 4 m
- A is the crank angle as a function of time (t)
- l is the connecting rod length, 6 m

During the simulation, the top surface of the cylinder, representing the piston, moves with an applied mesh motion that mimics the motion of the reciprocating crank, rod, and piston assembly. The ideal gas

is compressed by contracting the mesh according to the motion of that assembly and by allowing the fluid properties to change as a function of time.

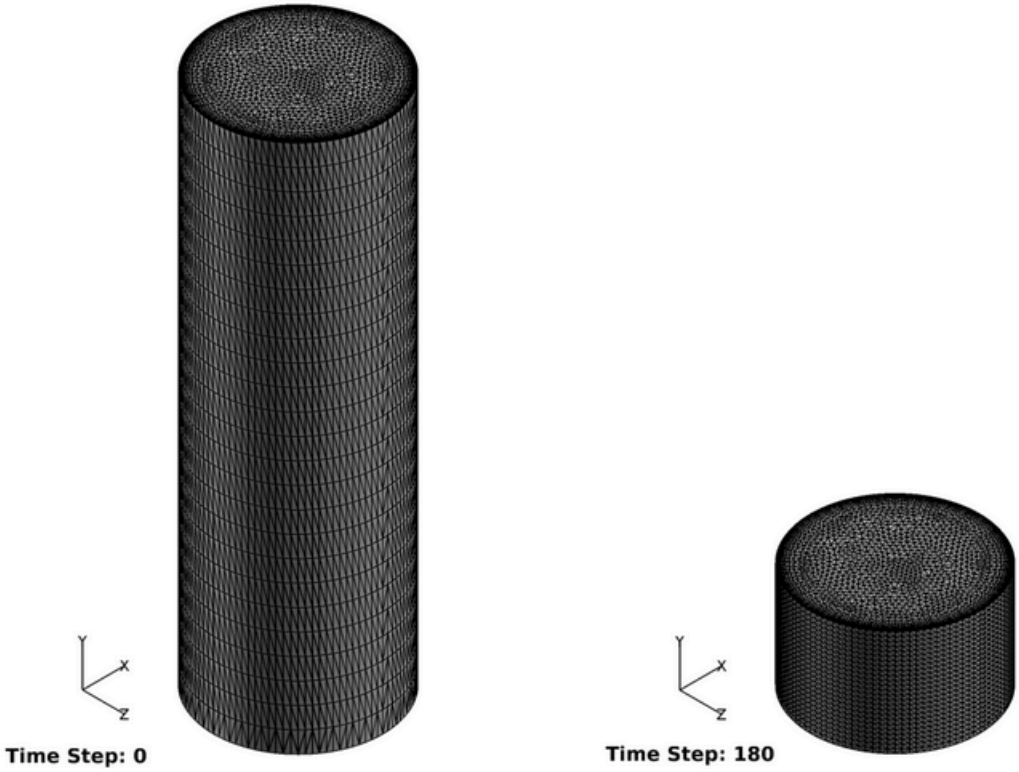


Figure 457: Mesh Used for Simulating Ideal Gas Compression in an Actuating Piston at Time Step 0 and Time Step 180 (3 s)

AcuSolve Results

The simulation was run as transient for a total of 360 time steps with a duration of 6.0 seconds. The AcuSolve solution shows time dependent pressure and temperature in a cylinder volume that compresses and expands in a 6.0 second cycle. Pressure and temperature increase as the cylinder volume decreases and returns toward initial conditions as the cylinder volume expands. The contours of pressure and temperature within the cylinder at the initial stage (t = 0.0 s) and the half cycle (t = 3.0 s) are shown in the following images.

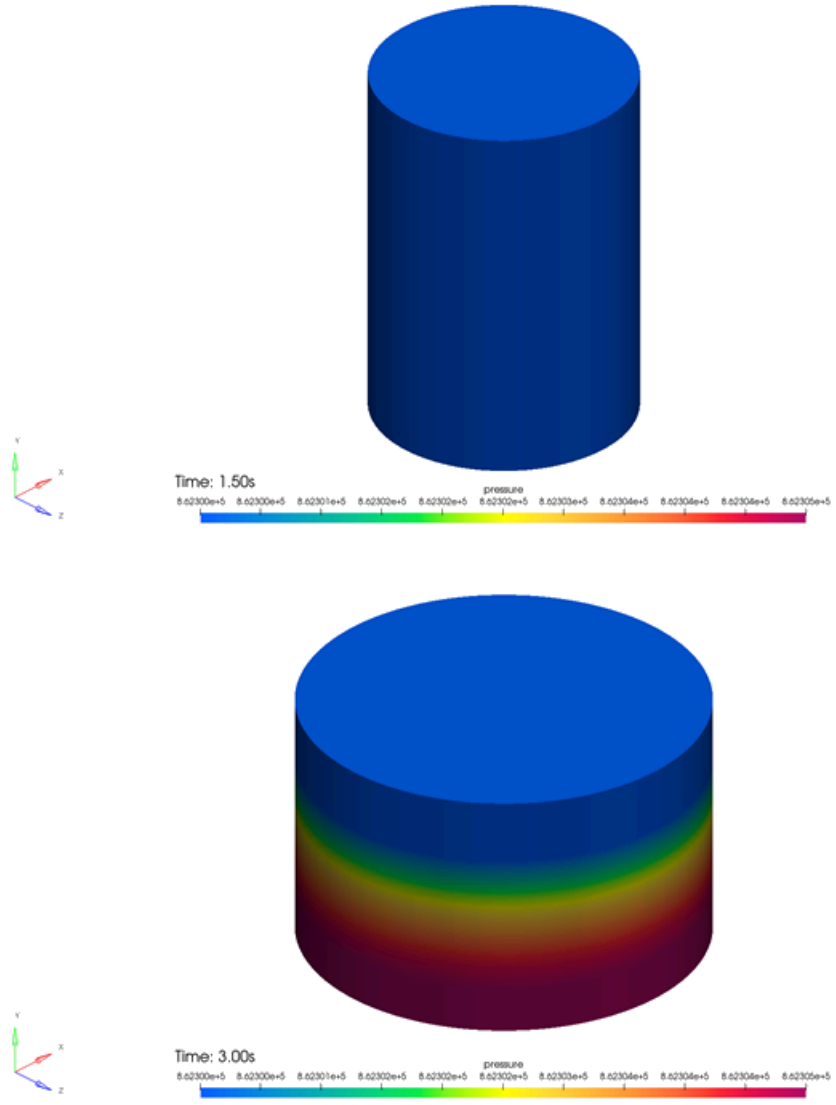


Figure 458: Pressure Distribution Within the Domain with the Piston at 1.5s and 3.0s

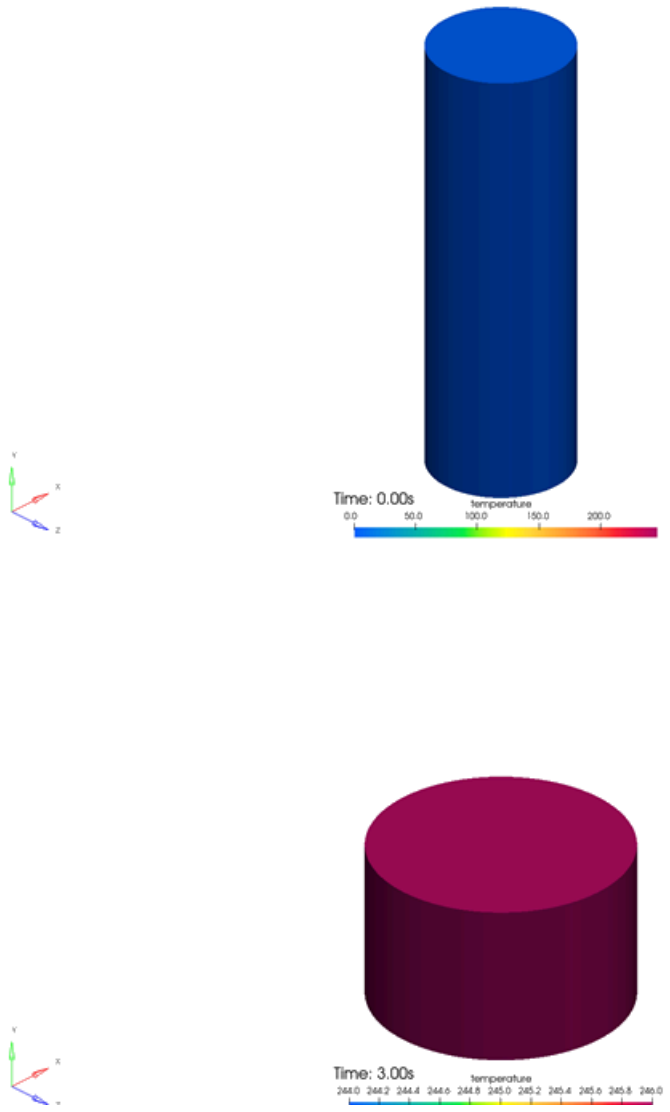


Figure 459: Temperature Distribution Within the Domain with the Piston at TDC and BDC

Comparison of time history plots of the AcuSolve and analytical solutions shows that the AcuSolve solution is nearly identical to the analytical solution. The AcuSolve computed internal pressure reaches a maximum of 8.62 X 105 Pa and the temperature reaches a maximum of 246.45 degrees C.

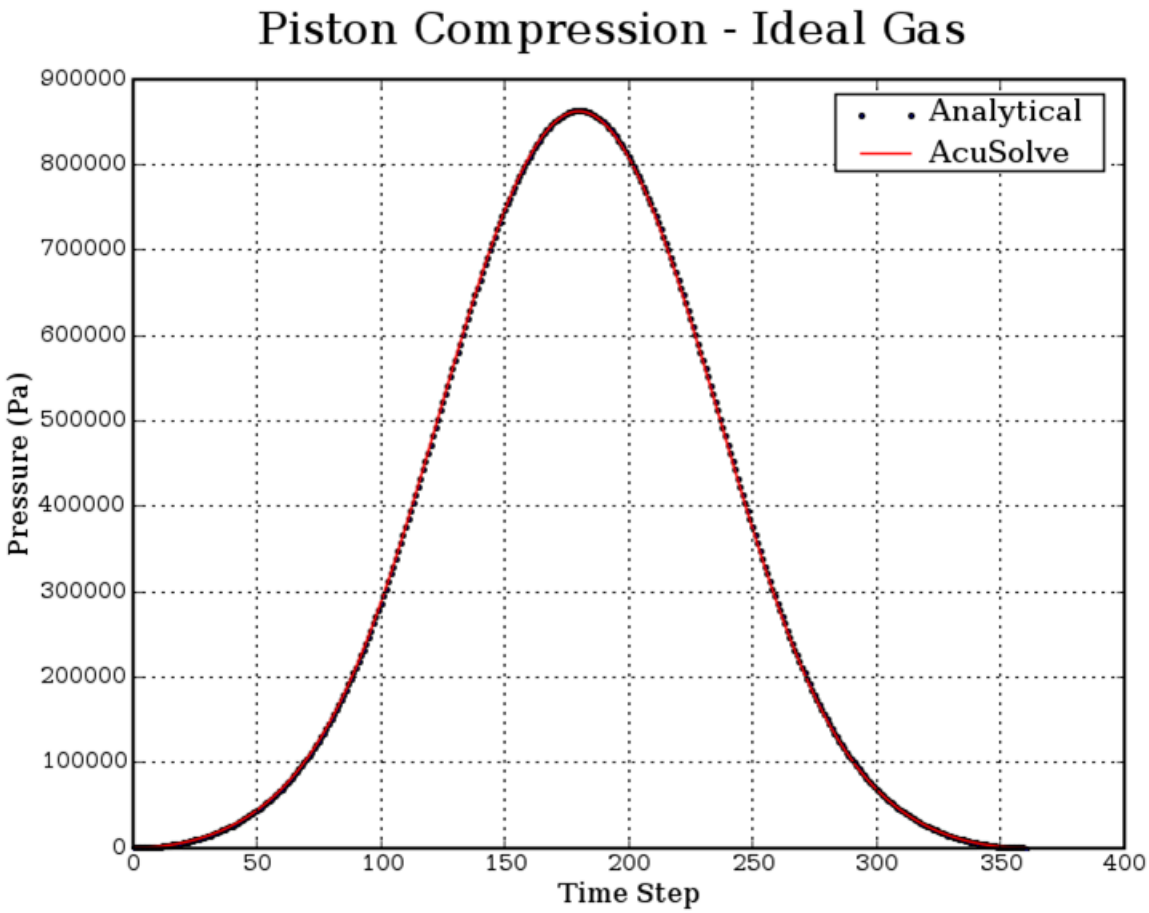


Figure 460: History Plots of Pressure for AcuSolve and Analytical Solutions

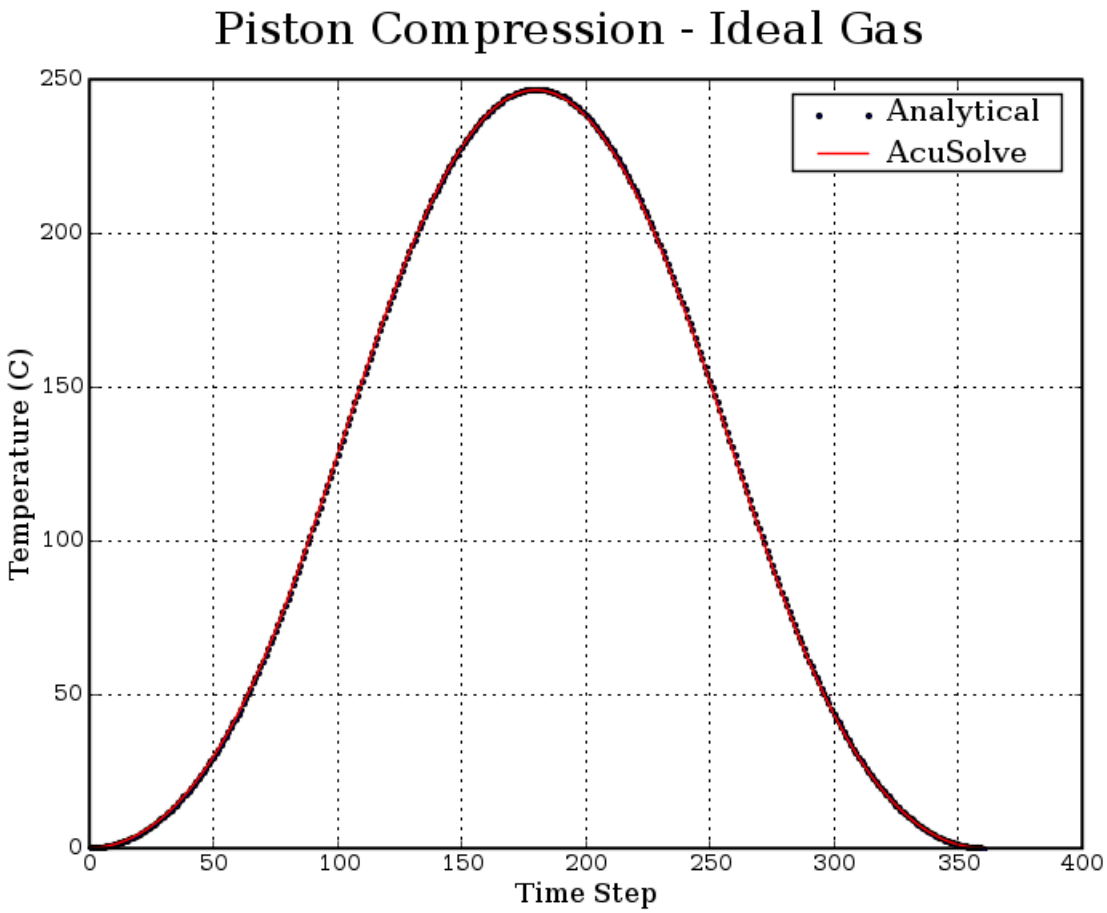


Figure 461: History Plots of Temperature for AcuSolve and Analytical Solutions

Summary

The AcuSolve solution compares well with analytical results for ideal gas compression in an actuating piston. The AcuSolve transient solution compares nearly identically with the analytical solution, with 0.1 percent and 0.16 percent error for the maximum pressure and temperature, respectively. As a result, AcuSolve demonstrates the ability to predict ideal gas compression in an idealized actuating piston.

Simulation Settings for Ideal Gas Compression in an Actuating Piston

HyperMesh CFD database file: `<your working directory>\cylinder_piston_compression\cylinder_piston_compression.hm`

Global

- Problem Description
  - Analysis type - Transient
  - Temperature equation - Advective Diffusive
  - Turbulence equation - Laminar
  - Mesh type - Fully Specified

- Auto Solution Strategy
  - Max time steps - `360`
  - Initial time increment - `0.01667` sec
  - Convergence tolerance - `1.0e-5` sec
  - Max stagger iterations - `10`
- Multiplier Function
  - Piston
    - Type - Piecewise Linear
    - Curve fit variable - Time
    - Curve fit values - (included in database as defined above)
- Material Model
  - Air
    - Density
      1. Type - Ideal Gas
      2. Gas constant - `286.9` J/kg-K
      3. Abs. pressure offset - `101325.0` N/m2
      4. Abs. temperature offset - `273.15` K
    - Viscosity - `1.781e-5` kg/m-sec
- Mesh Motion
  - Piston
    - Type - Translation
    - Translation velocity - `0.0`, `-1.0`, `0.0`
    - Velocity variable - Multiplier Function
    - Translation multiplier function - Piston

  Model
- Volumes
  - Fluid
    - Element Set
      1. Material model - Air
    - Element Output - on
- Surfaces
  - BDC
    - Simple Boundary Condition
      1. Type - Wall
      2. Wall velocity type - Match Mesh Velocity
      3. Mesh displacement BC type - Fixed
  - SideWall
    - Simple Boundary Condition

1. Type - Wall
2. Wall velocity type - Match Mesh Velocity
3. Mesh displacement BC type - Fixed

- TDC
  - Simple Boundary Condition
    1. Type - Wall
    2. Mesh displacement BC type - Fixed
    3. Mesh motion - Piston

- Nodes
  - VolumeNodes
    - Mesh X-Displacement
      1. Type - Zero
    - Mesh Y-Displacement
      1. Type - Linear
      2. Mesh motion - Piston
      3. Curve fit variable - Y reference coordinate
         1. X1 - `10.0` m
         2. Y1 - `1.0` m
         3. Y2 - `0.0` m
    - Mesh Z-Displacement
      1. Type - Zero

References

M.J. Moran and H.N Shapiro. "Fundamentals of Engineering Thermodynamics". Wiley. 4th Ed. 2000.

Turbulent Flow Through a Heated Periodic Channel

In this application, AcuSolve is used to solve for the flow and temperature field within a channel containing a heated wall. The wall is maintained at a constant temperature, inducing heat flux into the fluid, to predict the thermal law of the wall. The non-dimensional temperature versus the non-dimensional height above the wall is compared to the analytical correlation provided by Kader.

Problem Description

The problem consists of a fluid having material properties close to air with a density of 1.0 kg/m^3, molecular viscosity of 0.0001 kg/m-s, specific heat of 1005.0 J/kg-K and thermal conductivity of 0.139 W/m-K. The properties are specified to obtain a Prandtl number of 0.72. The velocity is defined as periodic and is driven by a constant acceleration body force equal to 2.0 m/s^2. The temperature is specified as periodic+unknown ratio allowing it to develop until it reaches a steady solution. The simulation description is shown in the following image, which is not drawn to scale. The model is simulated using the one equation Spalart Allmaras turbulence model along with the advective-diffusive temperature equation. The thermal wall distribution is validated against correlation data published by Kader 1981.

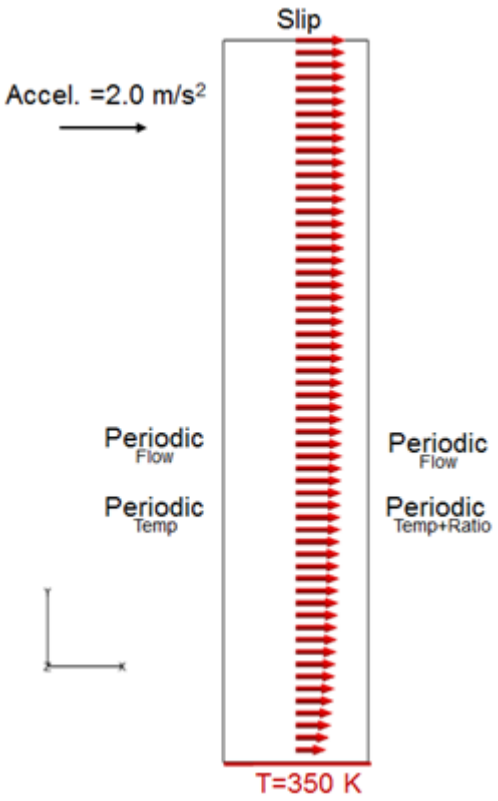


Figure 462: Critical Parameters used For Simulating Periodic Flow Within a Heated Channel

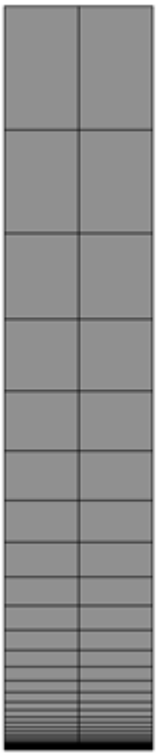


Figure 463: Mesh used For Simulating Periodic Flow Within a Heated Channel

The simulation was performed as a two-dimensional problem by constructing a volume mesh that contains a single layer of elements extruded in the cross-stream direction, normal to the flow plane and by imposing periodic boundary conditions on the extruded planes. The streamwise direction contains two elements allowing the flow and temperature solution to develop. Only the lower half of the channel is modeled, assuming the solution is mirror across the top slip plane.

AcuSolve Results

The AcuSolve solution converged to a steady state and the results reflect the mean flow conditions within the channel. The simulation results demonstrate that the channel wall induces a thermal flux into the flow field, producing a temperature distribution dependent on the distance from the wall. The thermal law of the wall computed from the AcuSolve results is compared with correlation data for the corresponding Prandtl number, as demonstrated in Kader 1981. The plot shown below gives the non-dimensional value of T+ as a function of Y+, where T+ and Y+ are computed per the following relationships:

$$T+ = \frac{(Tw - T)\rho C p u_\tau}{\dot{Q}} T \qquad (18)$$

$$Y+ = \frac{y u_\tau}{v} \qquad (19)$$

$$u_\tau = \sqrt{\tau w / \rho} \qquad (20)$$

Where $T+$, Tw is the fixed wall temperature, T is the temperature away from the wall, ρ is the fluid density, Cp is the fluid specific heat, uT is computed from the magnitude of the shear stress and $\dot{Q}_i$ is the local surface heat flux.

The image below shows black circles representing the correlation data and a solid red line for the AcuSolve results. The results demonstrate that the temperature distribution away from the wall is resolved properly and compares well with the correlation. Since an empirical relationship for T+ is used for comparison, there will be minor discrepancies compared with the simulation results. Additional comparisons have been made against DNS results for T+ from Kawamura et al. 1998.

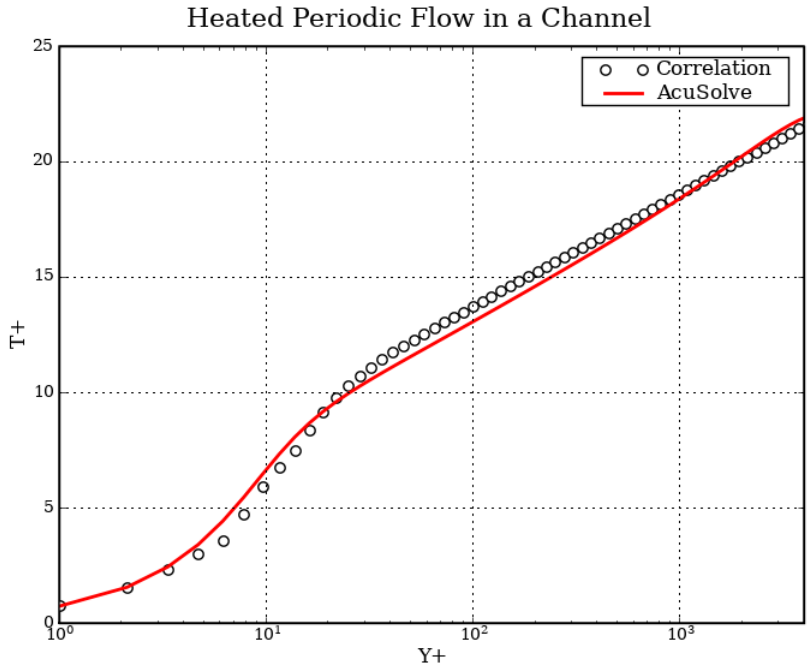


Figure 464: Thermal Boundary Layer Within the Heated Channel Compared Against the Correlation Data

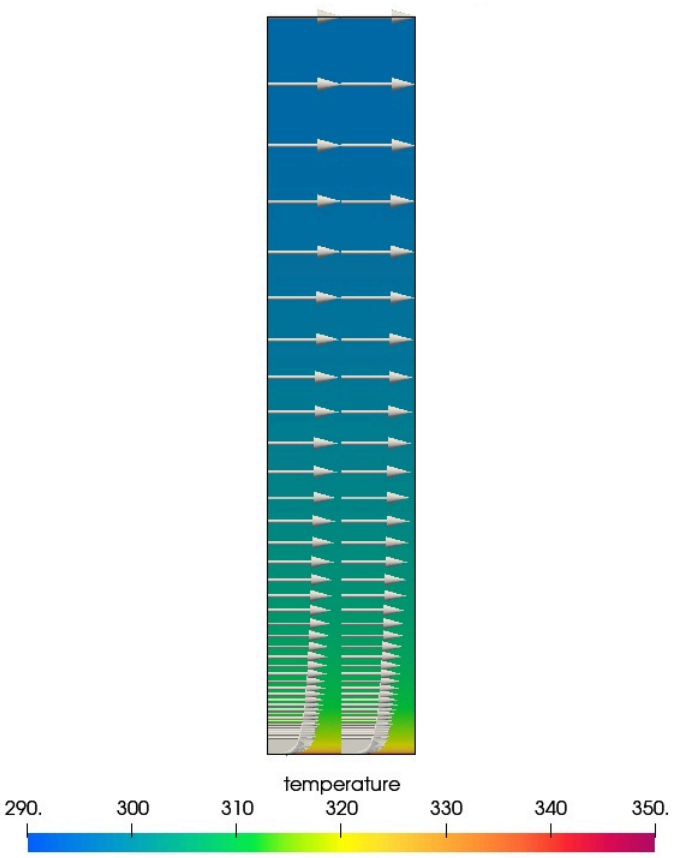


Figure 465: Contours of Temperature and Vectors Representing the Fluid Velocity Within the Channel

Summary

The AcuSolve solution compares well with the correlation data for turbulent flow within a heated channel. In this application, the constant temperature wall induces a surface heat flux, giving rise to a temperature gradient within the channel. AcuSolve can capture the correct temperature gradient at any location above the wall if an appropriate first layer height is selected to resolve a Y+ value of 1.0. The good agreement with correlation data for T+ demonstrates that AcuSolve can predict the locally varying temperature distribution within a turbulent channel.

Simulation Settings for Turbulent Flow Through a Heated Periodic Channel

SimLab database file: `<your working directory>\channel_periodic_heat\channel_periodic_heat.slb`

Global

- Problem Description
  - Flow type - Steady State
  - Temperature equation - Advective Diffusive
  - Turbulence equation - Spalart Allmaras
- Auto Solution Strategy
  - Max time steps - `50`

    - Convergence tolerance - `0.0001`
    - Relaxation Factor - `0.4`
    - Temperature - On
- Material Model
    - Fluid
        - Type - Constant
        - Density - `1.0` kg/m3
        - Viscosity - `1.0e-4` kg/m*sec
        - Specific Heat - `1005.0` J/kg*K
        - Conductivity - `0.139` W/m*K
- Body Force
    - BodyForce
        - Gravity
            1. X-component - `2.0` m/sec2

Model

- Volumes
    - Fluid
        - Element Set
            1. Material model - Fluid
            2. Body force - BodyForce
- Surfaces
    - Symmetry_1
        - Simple Boundary Condition - (disabled to allow for periodic conditions to be set)
    - Symmetry_2
        - Simple Boundary Condition - (disabled to allow for periodic conditions to be set)
    - Inflow
        - Simple Boundary Condition - (combination of integrated BC and periodic BC set)
        - Advanced Options
            1. Integrated Boundary Conditions - Temperature - `300.0` K
    - Outflow
        - Simple Boundary Condition - (disabled to allow for periodic conditions to be set)
    - Slip_surface
        - Simple Boundary Condition
            1. Type- Slip
    - Wall_surface
        - Simple Boundary Condition
            1. Type- Wall

        2 Temperature BC type - Value
        3 Temperature - `350.0` K
- Periodics
  - 2D
    - Periodic Boundary Conditions
      1 Type - Periodic
  - Flow
    - Periodic Boundary Conditions
      1 Type - Periodic
  - Temperature
    - Individual Periodic BCs
      1 Temperature: Type - Single Unknown Ratio
- Nodes
  - Zero_z-velocity
    - Z-Velocity: Type - Zero

References

B.A. Kader, "Temperature and concentration profiles in fully turbulent boundary layers", International Journal of Heat and Mass Transfer, Volume 24, Issue 9, 1981, Pages 1541-1544.

H. Kawamura, K. Ohsaka, H. Abe and K. Yamamoto, "DNS of turbulent heat transfer in channel flow with low to medium-high Prandtl number fluid", International Journal of Heat and Mass Transfer, 19:482-491, 1998.

Laminar Couette Flow with Imposed Pressure Gradient and Heated Walls

In this application, AcuSolve is used to simulate the flow of a highly viscous fluid between a moving and a stationary plate with an imposed pressure gradient and fixed temperature on the walls. AcuSolve results are compared with analytical results described in White (1991). The close agreement of AcuSolve results with analytical results validates the ability of AcuSolve to model cases with imposed pressure gradients and viscous heating.

Problem Description

The problem consists of a viscous fluid between two plates in a two-dimensional domain, as shown in the following image, which is not drawn to scale. The domain is 1.0 m high and 1.5 m long. The top plate moves with a constant velocity of 3.0 m/sec and the bottom plate is fixed. To simulate a fully developed flow with a relatively short length domain there is a mean-pressure gradient of -12 Pa/m applied to the fluid in the streamwise direction, defined as a body force acting on the entire fluid. The lower wall is held at a fixed temperature of 273.0 K, while the upper wall is held at a fixed temperature of 274.0 K. The problem is simulated with periodic boundaries in the streamwise direction. The Reynolds number of the flow, based on the distance between the plates is 0.3, indicating laminar flow. The flow field develops from the pressure gradient, the motion of the top plate, and the viscous shear stresses near the plates. The shear stress within the domain causes the temperature to increase within the channel.

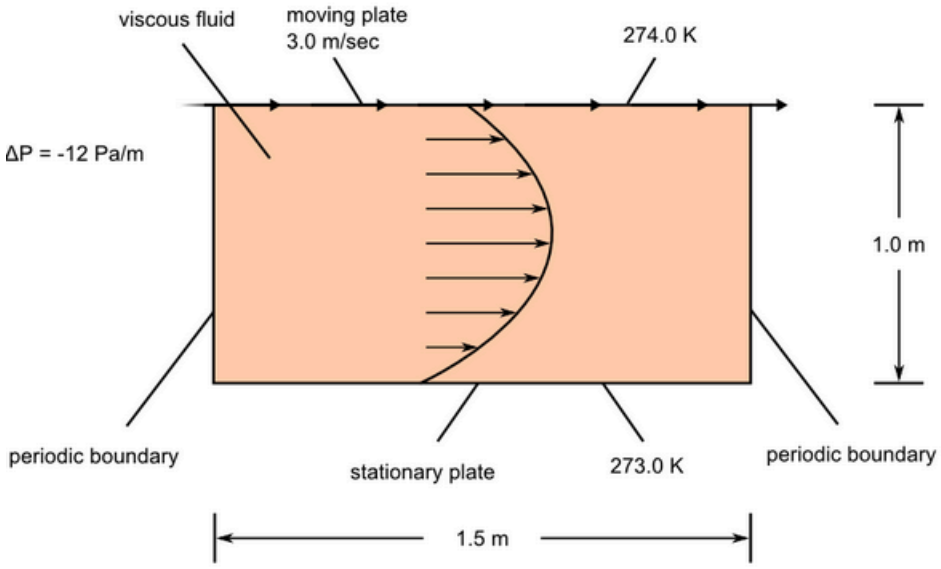


Figure 466: Critical Dimensions and Parameters for Simulating Laminar Couette Flow with an Imposed Pressure Gradient and Heated Walls

The simulation was performed as a two dimensional problem by constructing a volume mesh that contains a single layer of elements extruded in the cross stream direction, normal to the flow plane and by imposing symmetry boundary conditions on the extruded planes. Due to the periodic natural of the flow, a single element extrusion in the streamwise direction is used to reduce the model size.

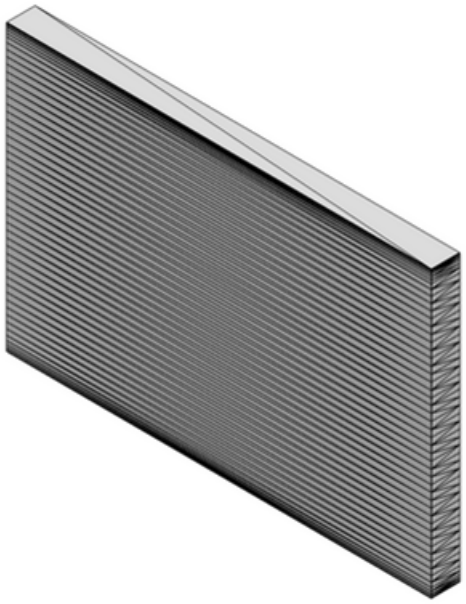


Figure 467: Mesh used for Simulating Laminar Couette Flow with an Imposed Pressure Gradient and Heated Walls

AcuSolve Results

The AcuSolve solution converged to a steady state and the results reflect the mean flow conditions. The simulation results show a flow field with a nearly linear distribution of velocity, with the peak at the top wall. The flow develops primarily because of the shear stress acting on the fluid near both the moving plate and the stationary plate. The temperature variation between the two plates develops due to the viscous heating effects that increase the temperature within the channel, with the maximum near the central height of the domain. The following figure shows the temperature distribution between the two plates and velocity vectors indicating the velocity profile.

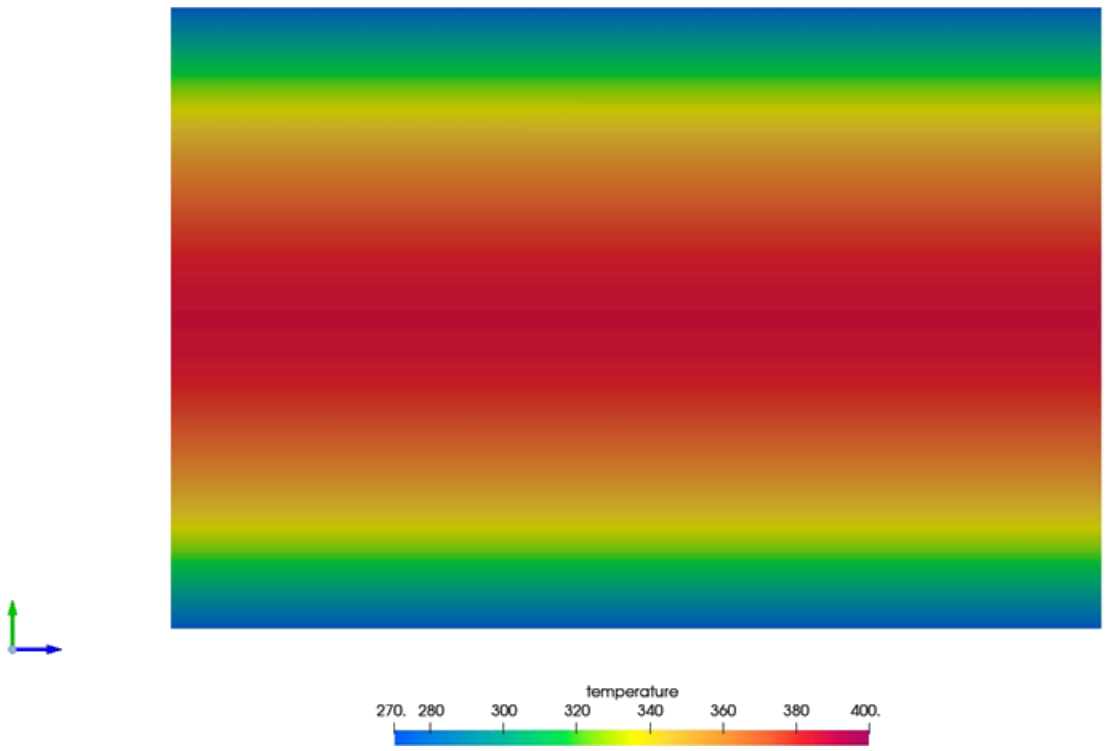


Figure 468: Contours of Temperature Between the Plates, with Velocity Vectors

The following image demonstrates the accuracy of the solution compared to the analytical results as computed by the solution for viscous heating within a channel with a moving upper boundary.

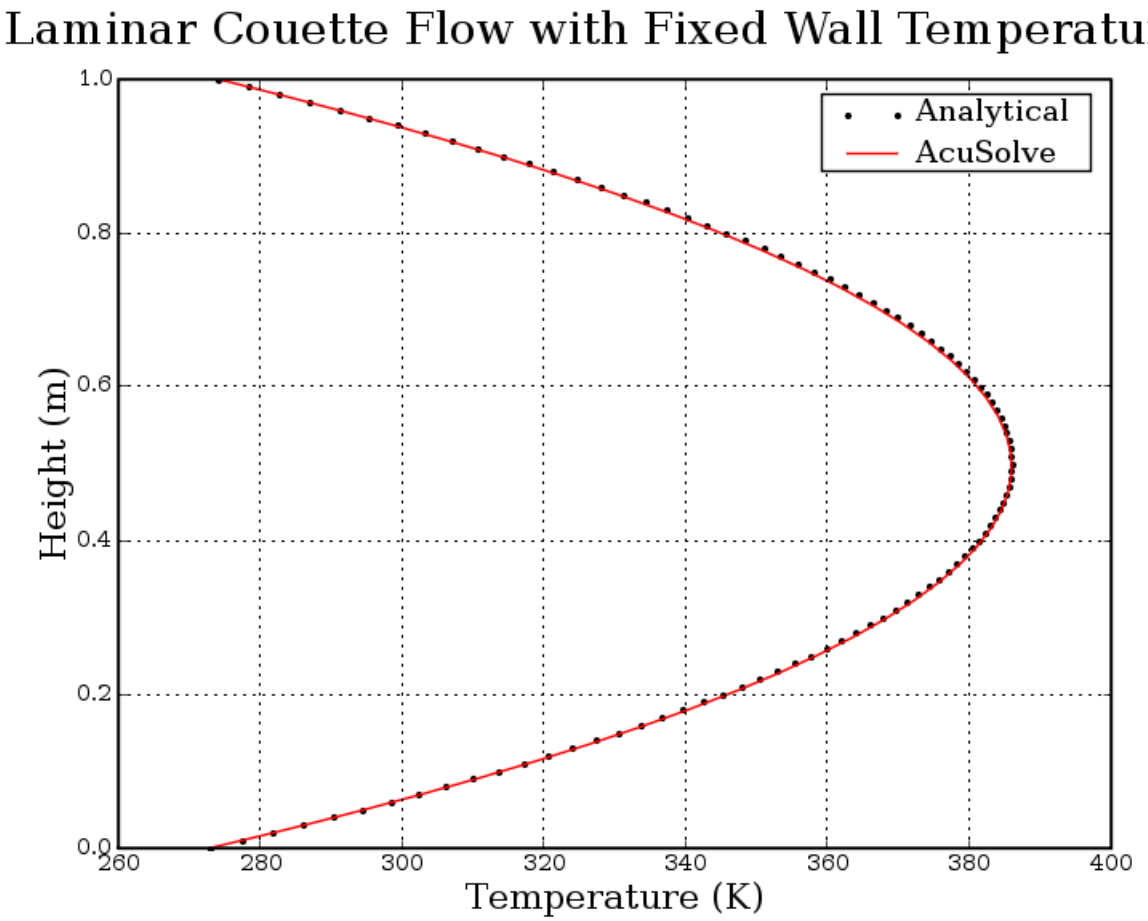


Figure 469: Temperature Plotted Against Height above the Bottom of the Flow Field (Temperature is Presented on the X Axis to Better Represent the Distribution Between the Plates in the Streamwise Direction)

Summary

In this application, a fully developed laminar flow between two plates with fixed temperature is studied and compared against analytical data. The AcuSolve results compare well with the analytical data for the temperature distribution between the two plates. The simulation indicates that the velocity profile arises due to the combination of the viscous shearing and the velocity of the upper plate. The velocity and temperature profiles computed by AcuSolve demonstrate how highly viscous fluids tend to direct the flow regime. AcuSolve demonstrates the ability to predict the analytical solution for viscous heating between two flat plates with moving and stationary boundaries and an imposed pressure gradient.

Simulation Settings for Laminar Couette Flow with Imposed Pressure Gradient and Heated Walls

SimLab database file: `<your working directory>\couette_laminar_heat\couette_laminar_heat.slb`

Global

- Problem Description

- Flow - Steady State
- Temperature equation - Advective Diffusive
- Turbulence equation - Laminar

- Auto Solution Strategy
  - Relaxation factor - `0.2`
- Material Model
  - Fluid
    - Density - `1.0` kg/m3
    - Specific Heat - `1.0` J/kg-K
    - Viscosity - `100.0` kg/m-sec
- Body Force
  - DP/DL
    - Gravity
      1. Z-component - `18.0` m/sec2

Model

- Volumes
  - Fluid
    - Element set
      1. Material model - Fluid
      2. Body force - DP/DL
      3. Viscous heating - on
- Surfaces
  - Max_X
    - Simple Boundary Condition
      1. Type - Symmetry
  - Max_Y
    - Simple Boundary Condition
      1. Type - Wall
      2. Wall velocity type - Cartesian
      3. Z-velocity - `3.0` m/s
      4. Temperature - `274.0` K
  - Max_Z
    - Simple Boundary Condition - (disabled to allow for periodic conditions to be set)
  - Min_X
    - Simple Boundary Condition
      1. Type - Symmetry
  - Min_Y

        - Simple Boundary Condition
            1. Type - Wall
            2. Temperature - `273.0` K
    - Min_Z
        - Simple Boundary Condition - (disabled to allow for periodic conditions to be set)
- Periodics
    - Periodic 1 all
        - Periodic Boundary Conditions
            1. Type - Periodic

References

F. M. White. "Viscous Fluid Flow". Section 3-3.2. McGraw-Hill Book Co., Inc. New York. 1991.

Moving Mesh

10

This section includes validation cases that consider time dependent motion within the domain, requiring that the mesh movement be modeled with a differential equation, a fully defined mesh motion or by interpolated mesh motion.

This chapter covers the following:

- Circumferential Flow in a Cylinder Induced by a Rotating Solid (p. 629)
- Turbulent Flow Over an Oscillating Rigid Body Assembly (p. 635)
- Ideal Gas Compression in an Actuating Piston (p. 642)

Circumferential Flow in a Cylinder Induced by a Rotating Solid

In this application, AcuSolve is used to simulate the flow of air between concentric cylinders that is initiated by the rotation of the solid inner cylinder. The outer cylinder is held stationary while the inner cylinder rotates with a constant speed. AcuSolve results are compared with analytical results as described in White (1991). The close agreement of AcuSolve results with analytical results validates the ability of AcuSolve to maintain a continuous velocity across a non-conformal guide surface interface.

Problem Description

The problem consists of a fluid with material properties of a viscous fluid with the density of air rotating between two infinitely long concentric cylinders, as shown in the following image, which is not drawn to scale. The radius of the outer cylinder is 3.0 m and the radius of the inner cylinder is 1.5 m. The inner cylinder is defined as a solid medium and rotates at 1 rad/sec. The inner cylinder's surface velocity is mapped to the adjacent surface within the fluid medium, while the outer cylinder is fixed. The induced flow is laminar and exhibits a steady state behavior after running for a short period of physical time. The rotation of the inner cylinder causes the fluid to rotate due to viscous shearing near the wall. As the outer cylinder is fixed, a velocity gradient is generated as a function of radius within the flow domain.

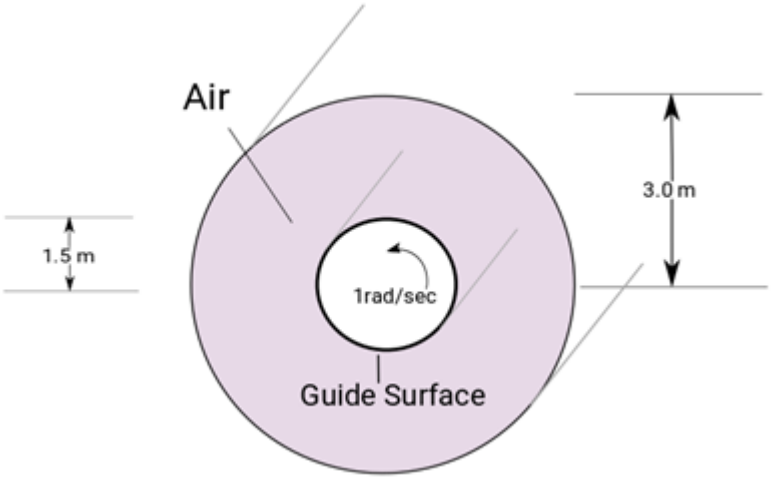


Figure 470: Critical Dimensions and Parameters Used for Simulating Flow Between Two Concentric Cylinders Split with a Guide Surface

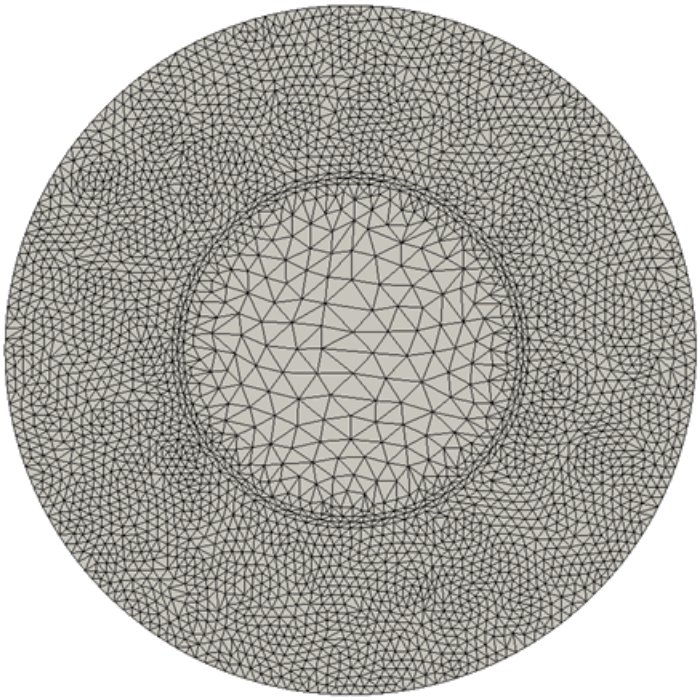


Figure 471: Mesh Used for Simulating Flow Between Two Concentric Cylinders

The simulation was performed as a two dimensional problem by constructing a volume mesh that contains a single layer of elements in the extruded direction, normal to the flow plane and by imposing slip flow and mesh boundary conditions on the extruded planes.

AcuSolve Results

The AcuSolve solution reaches a quasi-static result with the velocity between the two cylinders reaching a steady state at the simulation end time. As the solid inner cylinder rotates, it acts as a guide surface for the fluid elements to track and inherit the two velocity components. The velocity at the edge of the inner cylinder is equal to exactly the rotational speed multiplied by the radius. As the radius increases, the flow velocity reduces until it reaches zero at the outer diameter. The following images show the tangential velocity within the fluid as a function of radius from the center. The tangential velocity is compared with the analytical solution. The image below shows black circles representing the analytical solution and a solid red line for the AcuSolve results.

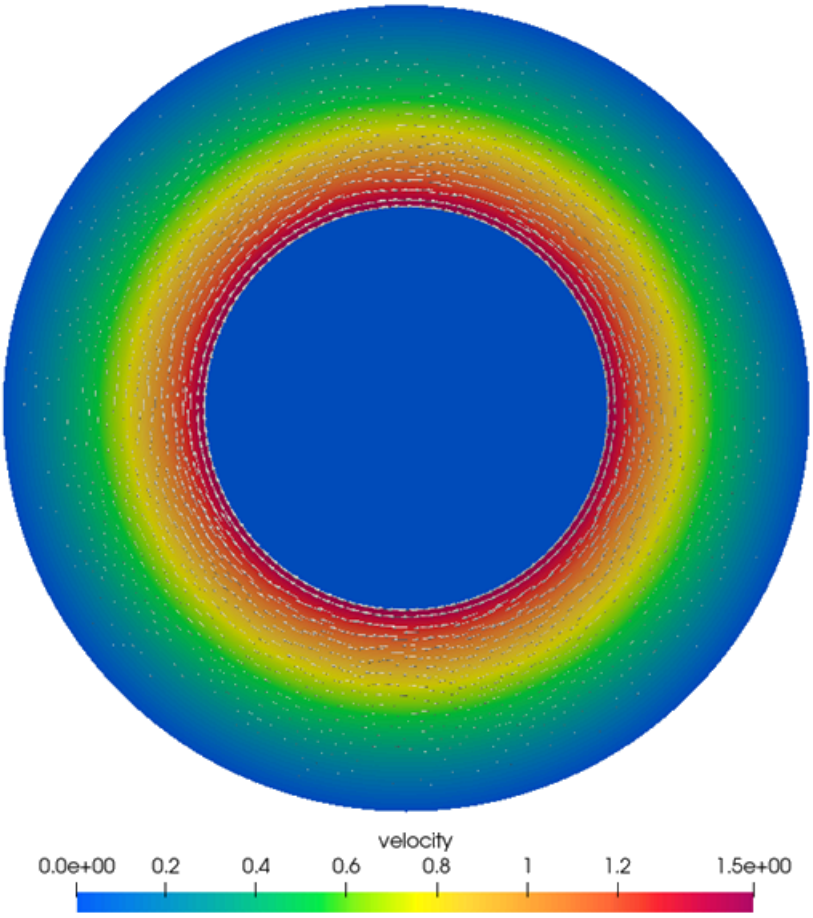


Figure 472: Contours and Vectors of Velocity Between the Concentric Cylinders

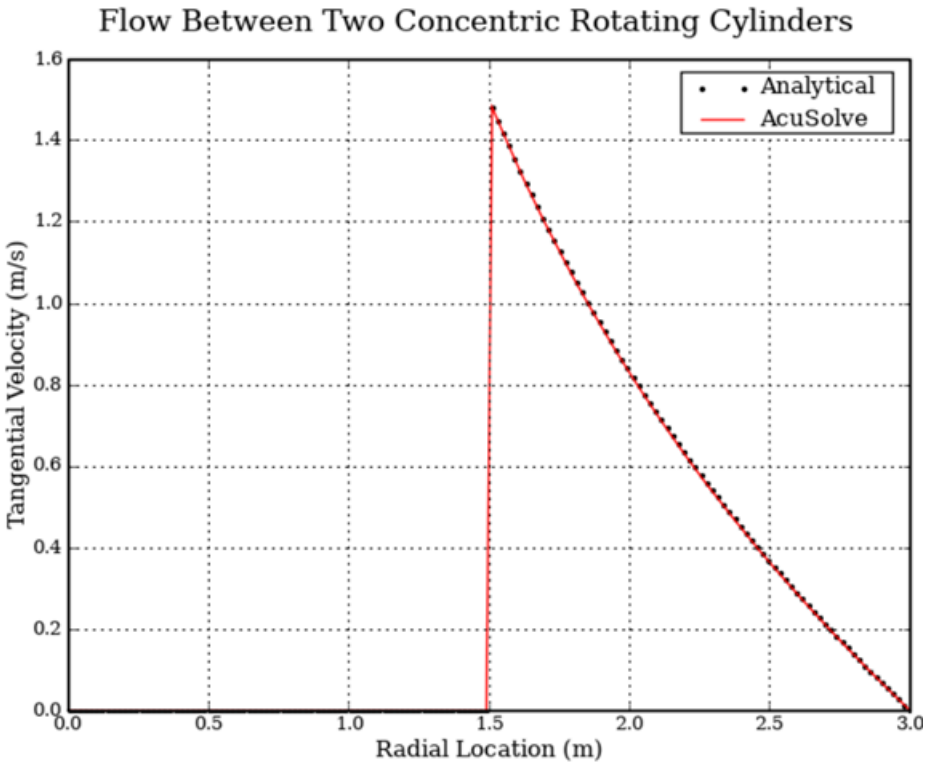


Figure 473: Tangential Velocity Within the Solid and Fluid as a Function of Radial Distance from the Center at the Final Timestep

Summary

The AcuSolve solution compares well with analytical results for laminar flow between concentric cylinders, where the inner cylinder guides the adjacent fluid elements. In this application, a fluid initially at rest inherits the angular velocity from the inner cylinder while the outer cylinder does not rotate. As a result of the inherited velocity and viscosity of the fluid, flow develops between the two cylinders. The AcuSolve solution for the tangential velocity as a function of radius matches exactly with the analytical results.

Simulation Settings for Flow Between Concentric Split Cylinders

HyperMesh CFD database file: `<your working directory>\annulus_split_rotating \annulus_split_rotating.hm`

- Problem Description
  - Analysis type - Transient
  - Flow equation - Navier Stokes
  - Turbulence equation - Laminar
  - Mesh type - Arbitrary Mesh Movement (ALE)
- Auto Solution Strategy
  - Max time steps - `40`
  - Initial time increment- `0.02` sec

- Convergence tolerance - `0.001`
- Min stagger iterations - `2`
- Max stagger iterations - `4`

- Material Model
  - Air
    - Density
      1. Type - Constant
      2. Density - `1.225` kg/m3
    - Viscosity
      1. Type - Constant
      2. Viscosity - `1.781` kg/m-sec
- Mesh Motion
  - Rotation
    - Rotation Center
      1. X-coordinate - `2.0` m
      2. Y-coordinate - `0.0` m
      3. Z-coordinate - `0.0` m
    - Angular velocity
      1. X-component - `1.0` rad/sec
      2. Y-component- `0.0` rad/sec
      3. Z-component - `0.0` rad/sec

  Model
- Volumes
  - CylinderInner
    - Element Set
      1. Medium - Solid
      2. Material model - Aluminum
  - CylinderOuter
    - Element Set
      1. Medium - Fluid
      2. Material model - Air
- Surfaces
  - InBottom
    - Simple Boundary Condition
      1. Type- Slip
      2. Mesh displacement type- Slip
  - InInterf

        - Simple Boundary Condition
            1. Type- Wall
            2. Mesh displacement type- Fixed
            3. Mesh motion- Rotation
        - Guide Surface
            1. Type- Faceted
    - InTop
        - Simple Boundary Condition
            1. Type- Slip
            2. Mesh displacement type- Slip
    - OutBottom
        - Simple Boundary Condition
            1. Type- Slip
            2. Mesh displacement type- Slip
    - OutInterf
        - Simple Boundary Condition
            1. Type- Wall
            2. Wall velocity type- Match Mesh Velocity
            3. Mesh displacement type- Guide surface
            4. Guide surface- InInterf
    - OutTop
        - Simple Boundary Condition
            1. Type- Slip
            2. Mesh displacement type- Slip
    - OutWall
        - Simple Boundary Condition
            1. Type- Wall
            2. Mesh displacement type- Fixed
- Nodes
    - PressurePoint
        - Pressure
            1. Type- Zero

References

F. M. White. "Viscous Fluid Flow". Section 3-2.3. McGraw-Hill Book Co., Inc. New York. 1991.

Turbulent Flow Over an Oscillating Rigid Body Assembly

In this application, AcuSolve is used to simulate the fluid-structure interaction of a fluid moving over a cylinder/plate assembly. AcuSolve results are compared with experimental results as described in Gomes and Lienhart (2009). The close agreement of AcuSolve results with the experimental results validates the ability of AcuSolve to model cases in which the fluid forces lead to structural motions.

Problem Description

The problem consists of a fluid having material properties of standard water with density of 998 kg / m^3 and kinematic viscosity of 0.97e-6 m^2/sec through a two dimensional channel over a cylinder and plate assembly. The diameter of the cylinder is 0.022 m and the plate length is 0.042 m, while the inlet velocity is specified to match experimental conditions with a max velocity of 1.07 m/sec, as is shown in the following image, which is not drawn to scale. The model is simulated as transient with constant inflow conditions, allowing an oscillatory motion of the assembly to develop. The Shear Stress Transport (SST) turbulence model is used to model the turbulent portion of the flow and AcuSolve's internal rigid body motion is used to capture the motion of the oscillating assembly.

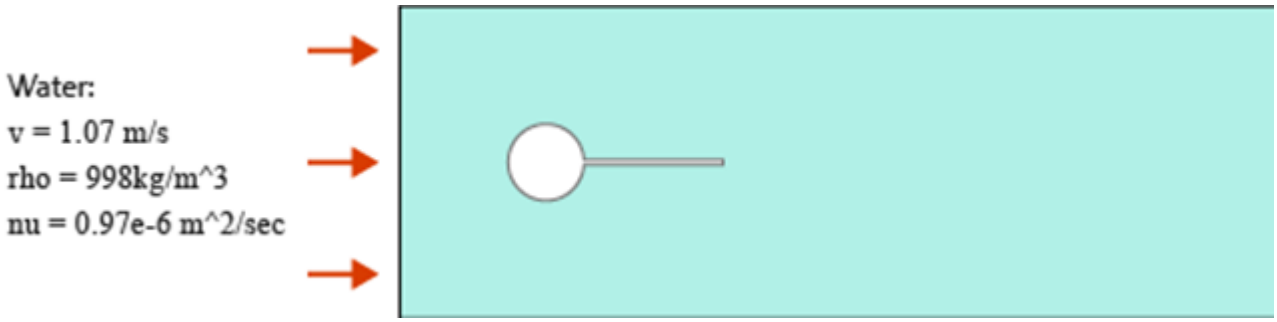


Figure 474: Critical Dimensions and Parameters used for Simulating Rigid Body Motion of Flow Past a Cylinder/Plate Assembly

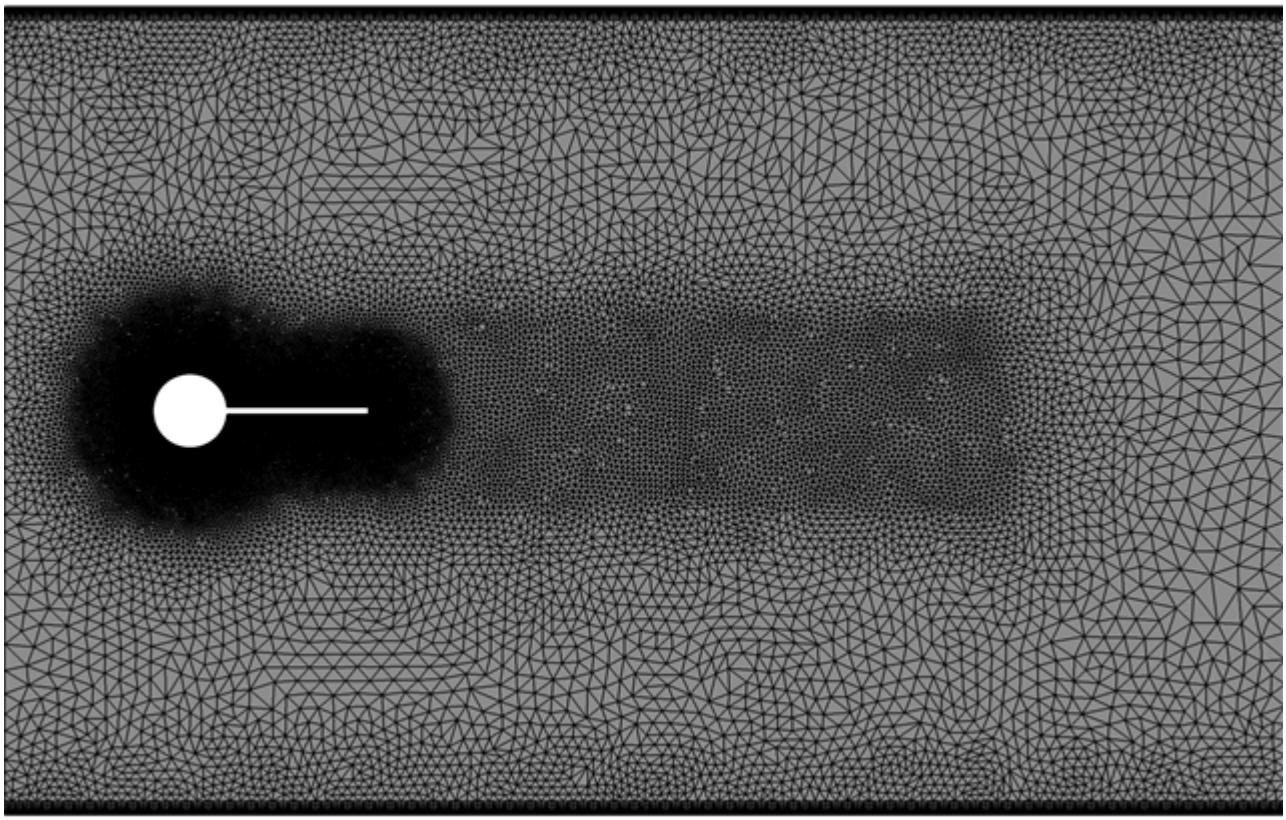


Figure 475: Mesh used for Simulating Rigid Body Motion of Flow Past a Cylinder/Plate Assembly

The simulation was performed as a two dimensional problem by constructing a volume mesh that contains a single layer of elements extruded in the cross stream direction, normal to the flow plane and by imposing symmetry boundary conditions on the extruded planes. The upper and lower walls are specified as no-slip and the inlet velocity is specified to match the conditions of the experiment (Gomes and Lienhart 2009).

AcuSolve Results

The AcuSolve solution reached a regularly repeating oscillatory state and the simulation was allowed to proceed for 10 seconds of physical time to obtain enough cycles for statistical analysis. The motion of the cylinder/plate assembly is directly attributed to the vortices shedding in its wake. The fluctuating loads on the assembly that result from the vortex shedding lead to a repeating cycle of structural rotation. The dominant oscillation frequency from the simulation was found to match well with the experimental measurements, within approximately 3.5 percent. The images below show the rigid body displacement of the assembly as it oscillates within the flow. Contours of velocity magnitude demonstrate the forcing on the assembly, while the mesh motion around the structure is captured and plotted for a single time step. Two dimensional plots showing the angular displacement demonstrate the motion, showing a single red line for the AcuSolve results.

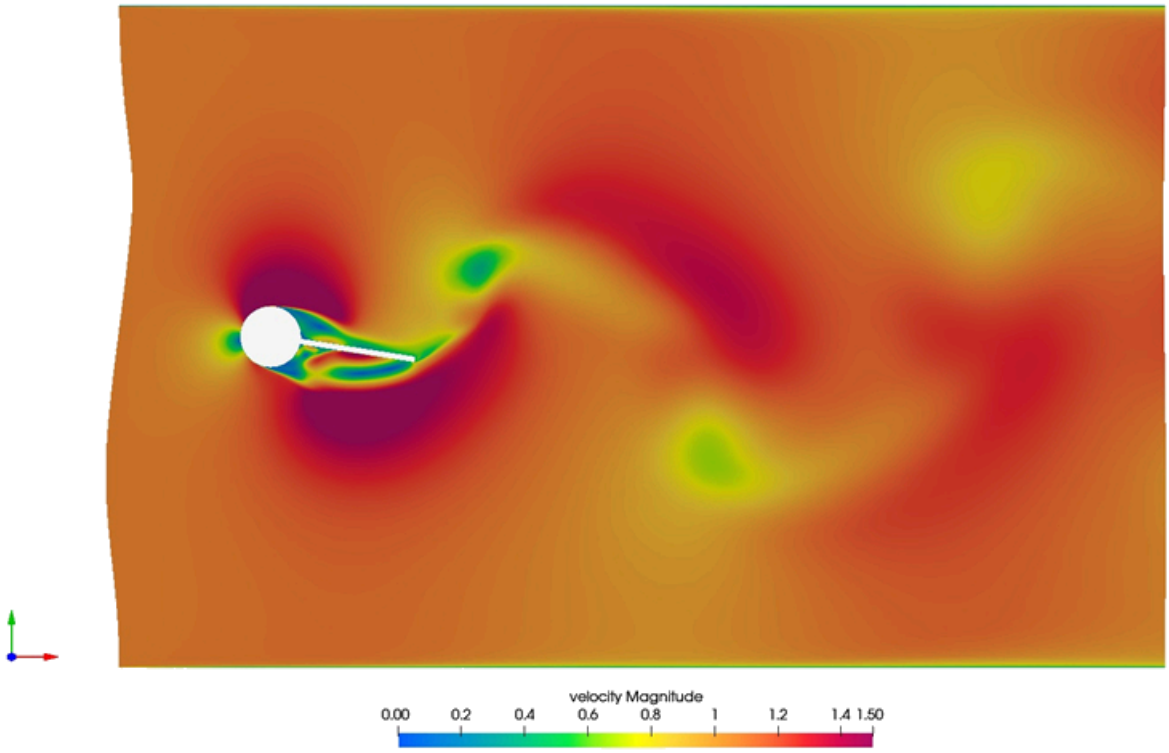


Figure 476: Velocity Contours Near the Assembly for a Single Time Step During the Simulation

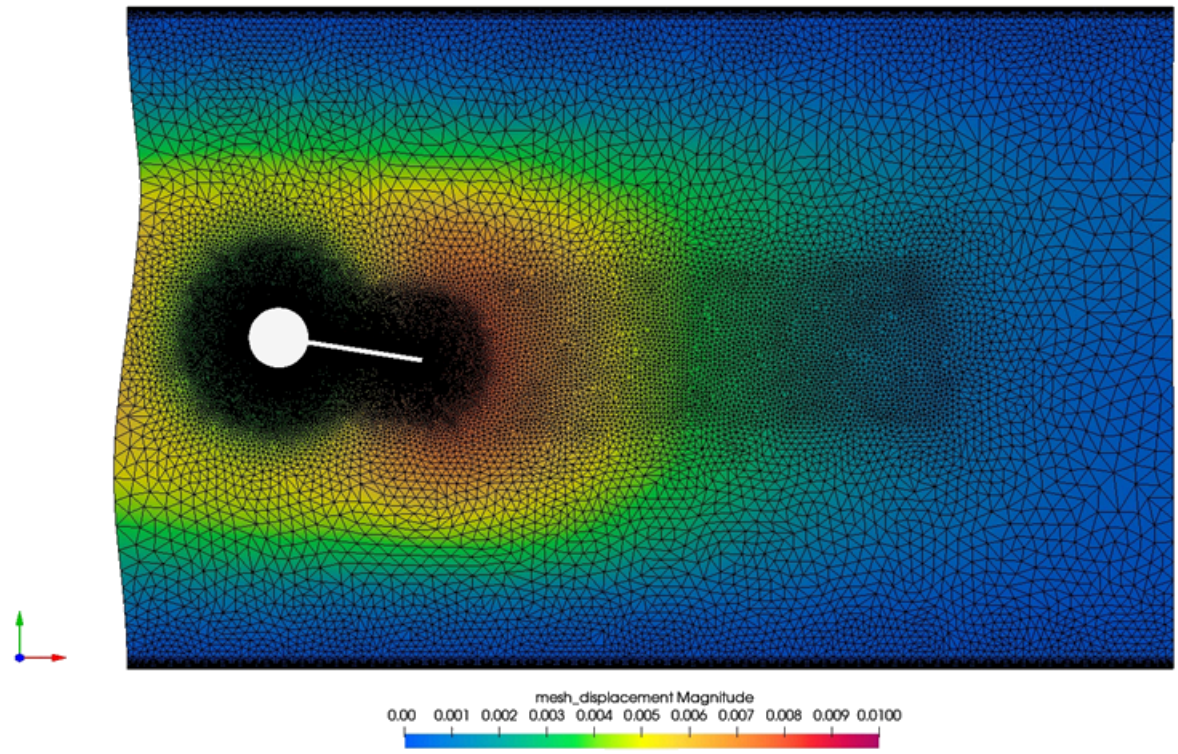


Figure 477: Mesh Displacement Contours Near the Assembly for a Single Time Step During the Simulation

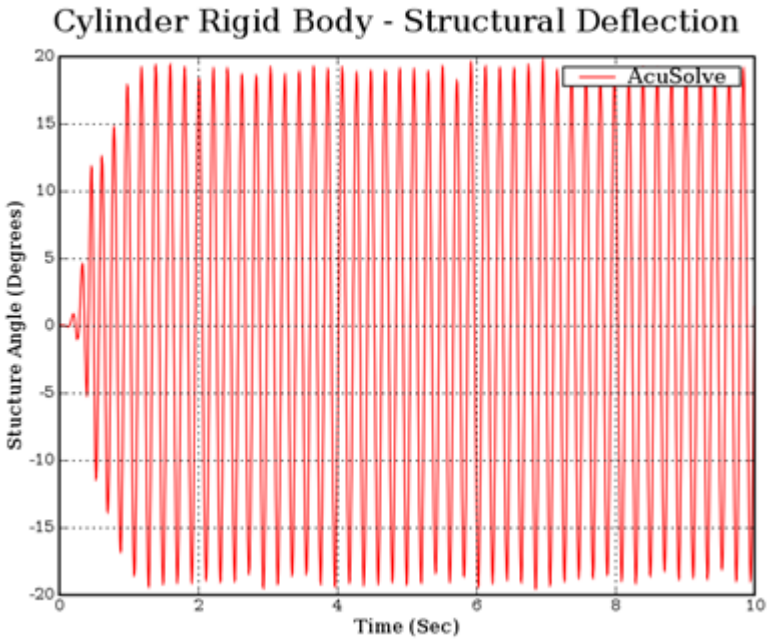


Figure 478: Rigid Body Displacement of the Assembly as a Function of Time, Showing the Oscillation Develop into the Pseudo-Steady Motion

The dominant frequency of the oscillation is easily identified in the Fast Fourier Transform (FFT) of the deflection angle, shown in the plot below.

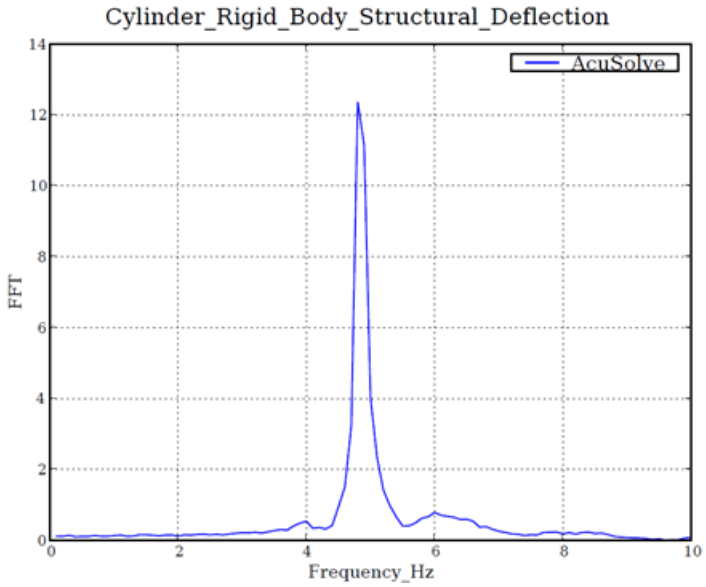


Figure 479: FFT of the Rigid Body Displacement Angle, Showing Power Spectral Density as a Function of Frequency

Summary

The AcuSolve solution compares well with experimental data for flow past an oscillating cylinder/plate assembly. In this application, water moves over the cylinder/plate assembly, giving rise to unsteady

loading that causes the body to rotate as a rigid body. The good agreement with the natural frequency of oscillation compared to the experimental data demonstrates that AcuSolve is capable of predicting fluid forced motion with an internal rigid body dynamic solver.

Simulation Settings for Turbulent Flow Over an Oscillating Rigid Body Assembly

SimLab database file: `<your working directory>\cylinder_rigidbody_turbulent\cylinder_rigidbody_turbulent.slb`

Global

- Problem Description
  - Flow - Transient
  - Turbulence equation - SST
  - Moving Mesh - Computed
- Auto Solution Strategy
  - Final Time - `10.0`
  - Initial Time Increment- `0.005`
  - Convergence tolerance- `0.001`
  - Max stagger iterations- `3`
- Material Model
  - Water
    - Type- Constant
    - Density- `998.0` kg/m3
    - Viscosity- `0.00096806` kg/m*sec
- Mesh Motion
  - RigidBody
    - Type- Rigid Body Dynamic
      1. Z rotation- Active
      2. Mass- `0.2089` kg
      3. Dyadic
         1. X-X - `3.7 e-5` kg-m2
         2. Y-Y- `3.7 e-5` kg-m2
         3. Z-Z - `3.7 e-5` kg-m2

  Model
- Volumes
  - Volume
    - Element Set
      1. Material model- Water
- Surfaces
  - Body

- Simple Boundary Condition
  1. Type- Wall
  2. Mesh displacement BC type- Fixed
  3. Mesh motion- RigidBody
- Interpolated Motion Surface

◦ Bottom
- Simple Boundary Condition
  1. Type- Wall
  2. Mesh displacement BC type- Fixed
- Interpolated Motion Surface

◦ Inflow
- Simple Boundary Condition
  1. Type- Inflow
  2. Inflow type- Velocity
  3. X Velocity- `1.07` m/sec
  4. Turbulence input type- Auto
  5. Turbulence intensity type- High
- Advanced Options
  1. Nodal Boundary Conditions
  2. X-velocity
     1. Type- Linear
     2. Precedence- `2`
     3. Curve fit variable- Y coordinate
     4. Curve fit values- Provided
  3. Y-velocity
     1. Type- Zero
  4. Z-velocity
     1. Type- Zero

◦ Bottom
- Simple Boundary Condition
  1. Type- Wall
  2. Mesh displacement BC type- Fixed
  3. Mesh motion- RigidBody

◦ Outflow
- Simple Boundary Condition
  1. Type- Outflow

◦ Top
- Simple Boundary Condition

1. Type- Wall
2. Mesh displacement BC type- Fixed

- maxZ
  - Simple Boundary Condition
    1. Type- Slip
- minZ
  - Simple Boundary Condition
    1. Type- Slip

References

Gomes, J. P. and Lienhart, H. (2009) Experimental Benchmark: Self-excited Fluid-structure Interaction Test Cases, in Fluid-Structure Interaction II: Modeling, Simulation, Optimization, Bungartz, H. J., Mehl, M., Schafer, M. (eds.), 383-412, Springer-Verlag.Ryhming.

Ideal Gas Compression in an Actuating Piston

In this application, AcuSolve is used to simulate pressure and temperature inside an actuating piston using the ideal gas relationship and fully defined mesh motion. AcuSolve results are compared with analytical results as described in Moran and Shapiro (2000). The close agreement of AcuSolve results with analytical results validates the ability of AcuSolve to model cases with material properties defined by the ideal gas law subjected to significant mesh distortion.

Problem Description

The problem consists of air compressed by a piston within a cylinder 10 m long with a diameter of π (3.14159) m, as shown in the following image, which is not drawn to scale. The piston is driven by a crankshaft 4 m long attached to a connecting rod 6 m long. The crankshaft rotates at 60o/s around a center point. At time (t) = 0.0 s the crank and piston are at top dead center (TDC) with an initial cylinder volume of 80 m^3. At t = 3.0 s the piston is at bottom dead center (BDC), at which point the volume in the cylinder is reduced to 16 m^3. The piston then moves back to TDC at t = 6.0 s. Air at atmospheric conditions, with material properties of an ideal gas and a dynamic viscosity of 1.781 X 10^5 kg/m-sec is the fluid modeled in the domain.

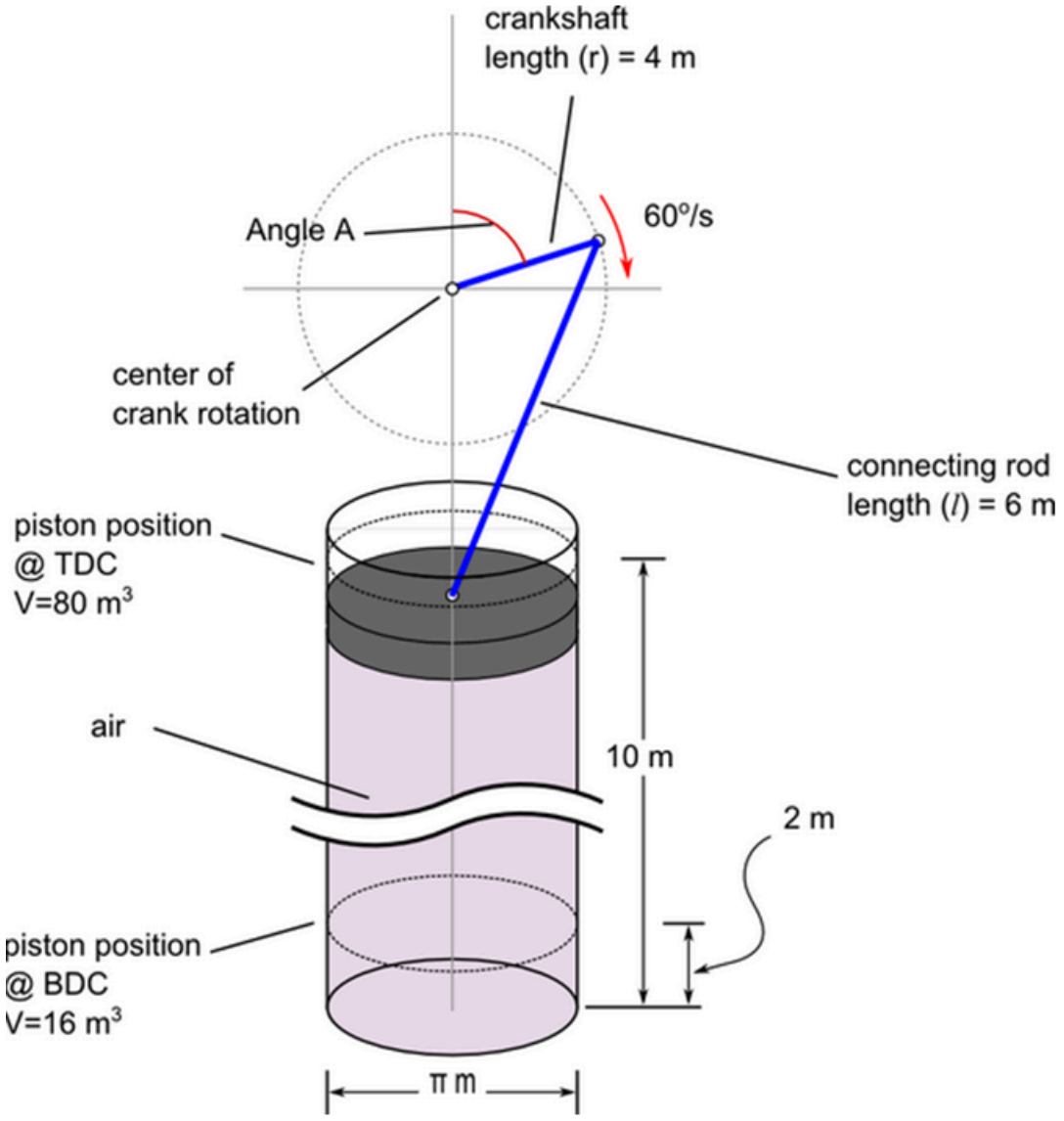


Figure 480: Critical Dimensions and Parameters for Simulating Ideal Gas Compression in an Actuating Piston

The motion of the piston is described by the following equation.

$$x = r * \cos A + \sqrt{l^2 - r^2 \sin^2 A} \qquad (21)$$

Where

- x is the distance of the piston from TDC
- r is the length of the connecting rod, 4 m
- A is the crank angle as a function of time (t)
- l is the connecting rod length, 6 m

During the simulation, the top surface of the cylinder, representing the piston, moves with an applied mesh motion that mimics the motion of the reciprocating crank, rod, and piston assembly. The ideal gas

is compressed by contracting the mesh according to the motion of that assembly and by allowing the fluid properties to change as a function of time.

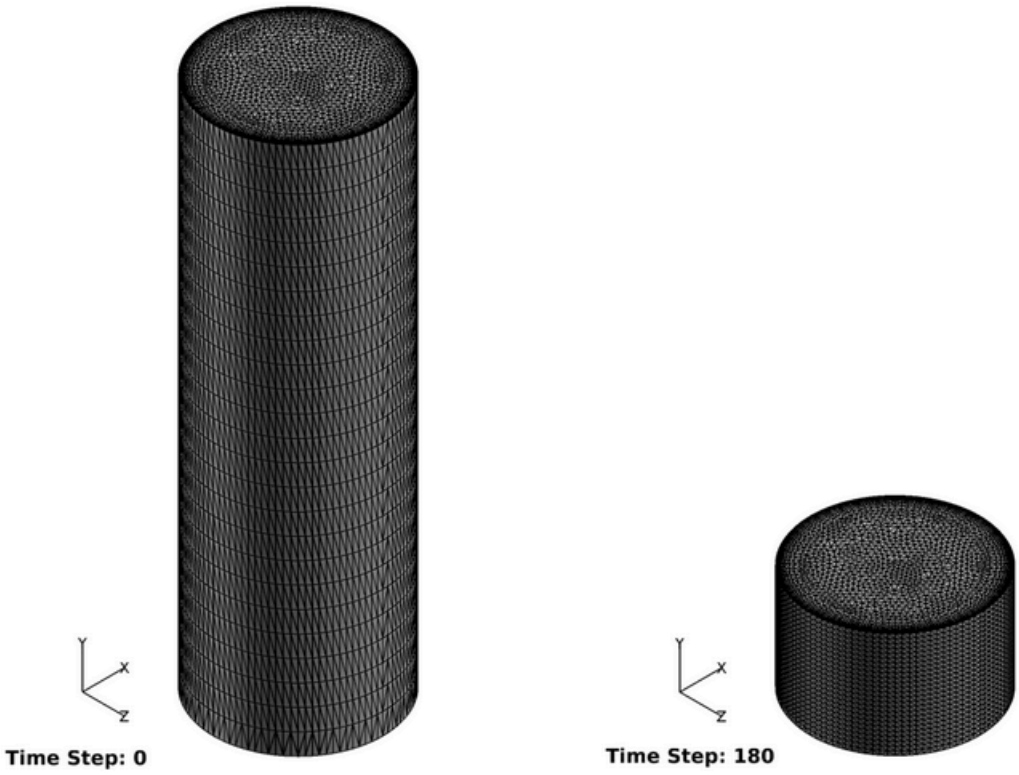


Figure 481: Mesh Used for Simulating Ideal Gas Compression in an Actuating Piston at Time Step 0 and Time Step 180 (3 s)

AcuSolve Results

The simulation was run as transient for a total of 360 time steps with a duration of 6.0 seconds. The AcuSolve solution shows time dependent pressure and temperature in a cylinder volume that compresses and expands in a 6.0 second cycle. Pressure and temperature increase as the cylinder volume decreases and returns toward initial conditions as the cylinder volume expands. The contours of pressure and temperature within the cylinder at the initial stage (t = 0.0 s) and the half cycle (t = 3.0 s) are shown in the following images.

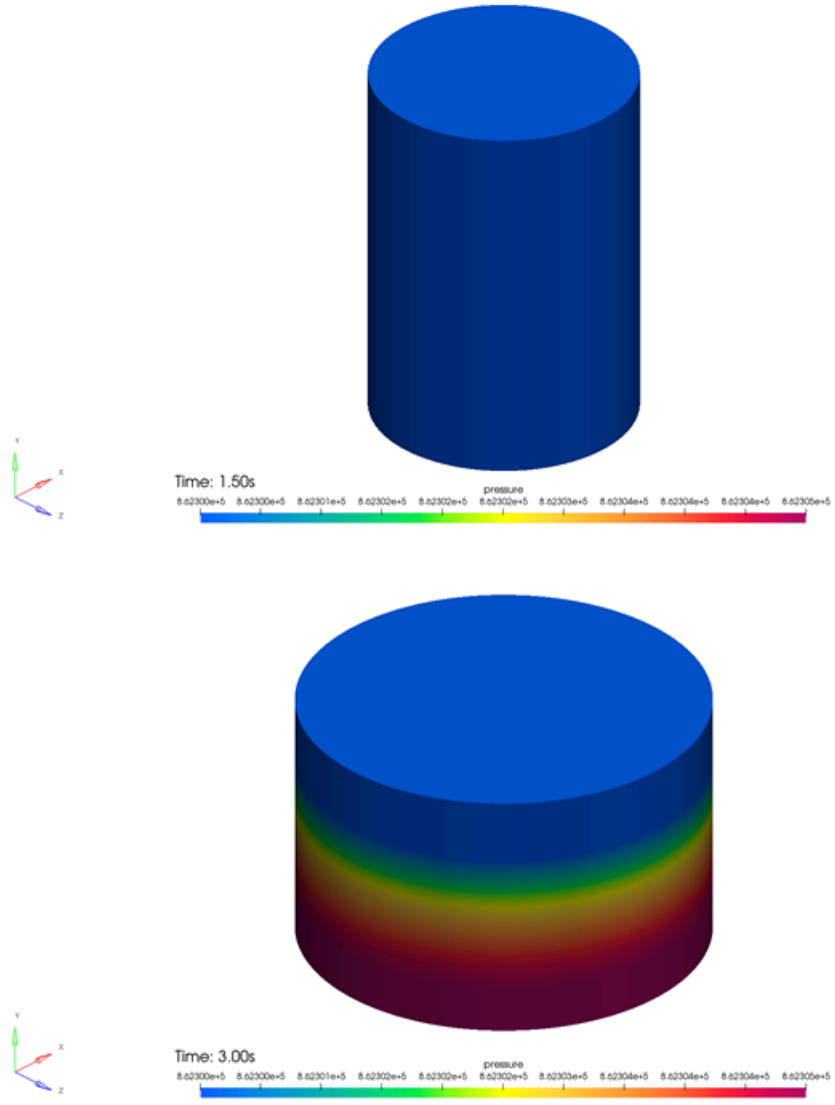


Figure 482: Pressure Distribution Within the Domain with the Piston at 1.5s and 3.0s

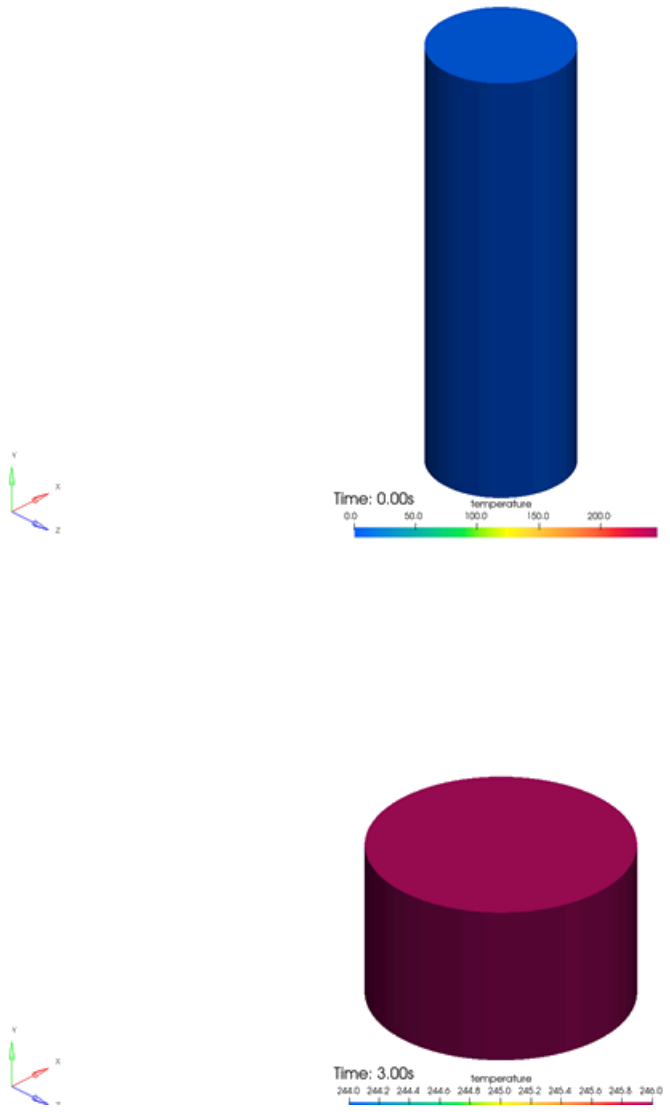


Figure 483: Temperature Distribution Within the Domain with the Piston at TDC and BDC

Comparison of time history plots of the AcuSolve and analytical solutions shows that the AcuSolve solution is nearly identical to the analytical solution. The AcuSolve computed internal pressure reaches a maximum of 8.62 X 105 Pa and the temperature reaches a maximum of 246.45 degrees C.

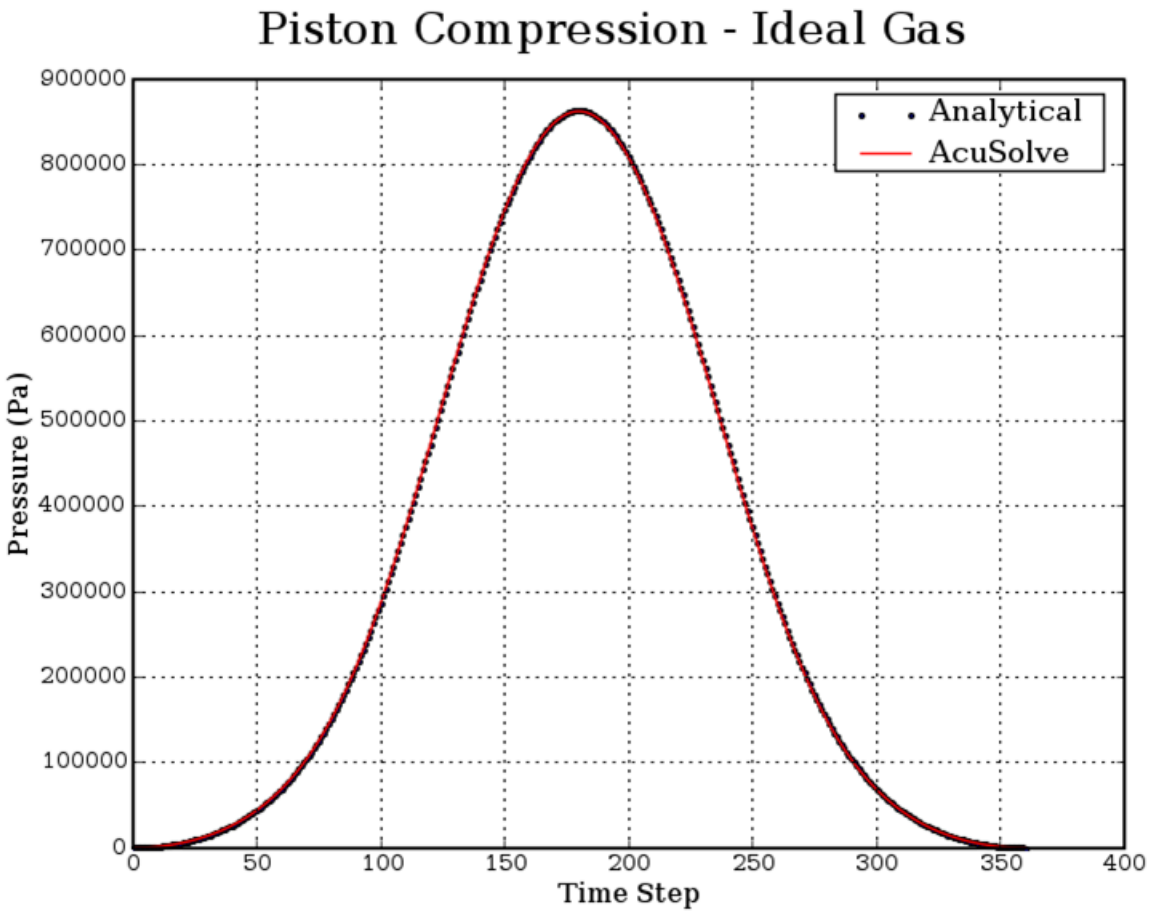


Figure 484: History Plots of Pressure for AcuSolve and Analytical Solutions

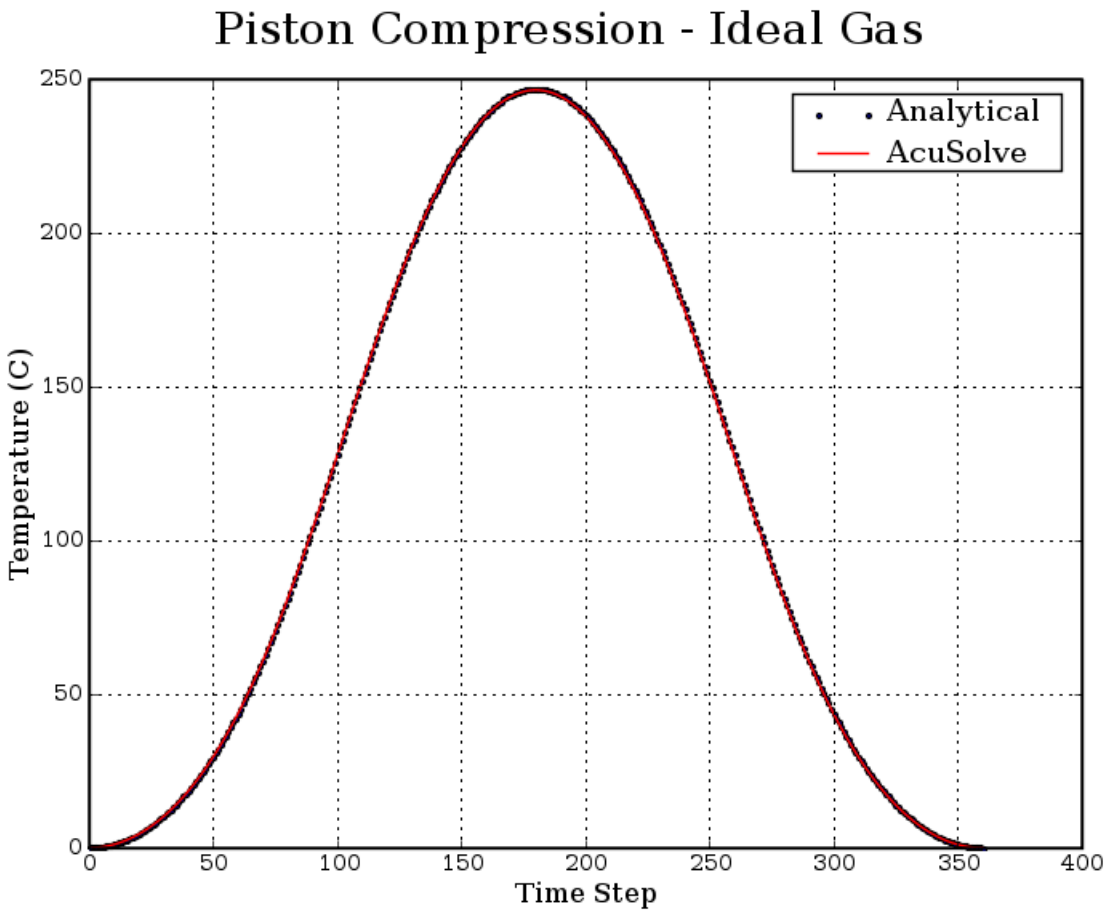


Figure 485: History Plots of Temperature for AcuSolve and Analytical Solutions

Summary

The AcuSolve solution compares well with analytical results for ideal gas compression in an actuating piston. The AcuSolve transient solution compares nearly identically with the analytical solution, with 0.1 percent and 0.16 percent error for the maximum pressure and temperature, respectively. As a result, AcuSolve demonstrates the ability to predict ideal gas compression in an idealized actuating piston.

Simulation Settings for Ideal Gas Compression in an Actuating Piston

HyperMesh CFD database file: `<your working directory>\cylinder_piston_compression\cylinder_piston_compression.hm`

Global

- Problem Description
  - Analysis type - Transient
  - Temperature equation - Advective Diffusive
  - Turbulence equation - Laminar
  - Mesh type - Fully Specified

- Auto Solution Strategy
  - Max time steps - `360`
  - Initial time increment - `0.01667` sec
  - Convergence tolerance - `1.0e-5` sec
  - Max stagger iterations - `10`
- Multiplier Function
  - Piston
    - Type - Piecewise Linear
    - Curve fit variable - Time
    - Curve fit values - (included in database as defined above)
- Material Model
  - Air
    - Density
      1. Type - Ideal Gas
      2. Gas constant - `286.9` J/kg-K
      3. Abs. pressure offset - `101325.0` N/m2
      4. Abs. temperature offset - `273.15` K
    - Viscosity - `1.781e-5` kg/m-sec
- Mesh Motion
  - Piston
    - Type - Translation
    - Translation velocity - `0.0`, `-1.0`, `0.0`
    - Velocity variable - Multiplier Function
    - Translation multiplier function - Piston

  Model
- Volumes
  - Fluid
    - Element Set
      1. Material model - Air
    - Element Output - on
- Surfaces
  - BDC
    - Simple Boundary Condition
      1. Type - Wall
      2. Wall velocity type - Match Mesh Velocity
      3. Mesh displacement BC type - Fixed
  - SideWall
    - Simple Boundary Condition

1. Type - Wall
2. Wall velocity type - Match Mesh Velocity
3. Mesh displacement BC type - Fixed

- TDC
  - Simple Boundary Condition
    1. Type - Wall
    2. Mesh displacement BC type - Fixed
    3. Mesh motion - Piston

- Nodes
  - VolumeNodes
    - Mesh X-Displacement
      1. Type - Zero
    - Mesh Y-Displacement
      1. Type - Linear
      2. Mesh motion - Piston
      3. Curve fit variable - Y reference coordinate
         1. X1 - `10.0` m
         2. Y1 - `1.0` m
         3. Y2 - `0.0` m
    - Mesh Z-Displacement
      1. Type - Zero

References

M.J. Moran and H.N Shapiro. "Fundamentals of Engineering Thermodynamics". Wiley. 4th Ed. 2000.

Reference Frame

11

This section includes validation cases that consider multiple reference frame simulations to model the effects of simplified rotational motion.

This chapter covers the following:

- Flow Between Concentric Cylinders (p. 652)
- Flow Inside a Rotating Cavity (p. 658)

Flow Between Concentric Cylinders

In this application, AcuSolve is used to simulate the flow of water between concentric cylinders. The outer cylinder is held stationary while the inner cylinder rotates with a constant speed. AcuSolve results are compared with analytical results as described in White (1991). The close agreement of AcuSolve results with analytical results validates the ability of AcuSolve to model cases containing thin annular gaps with flow induced by rotating walls.

Problem Description

The problem consists of two concentric pipes with water filling the void between them, as shown in the following image, which is not drawn to scale. The radius of the outer pipe is 0.0468 m and the radius of the inner pipe is 0.0178 m. The inner cylinder rotates at 1 rad/sec and the outer cylinder is fixed. The induced flow is laminar and exhibits a steady state behavior. The rotation of the inner cylinder causes the fluid to rotate due to viscous shearing near the wall. As the outer cylinder is fixed, a velocity gradient is generated as a function of radius within the flow domain.

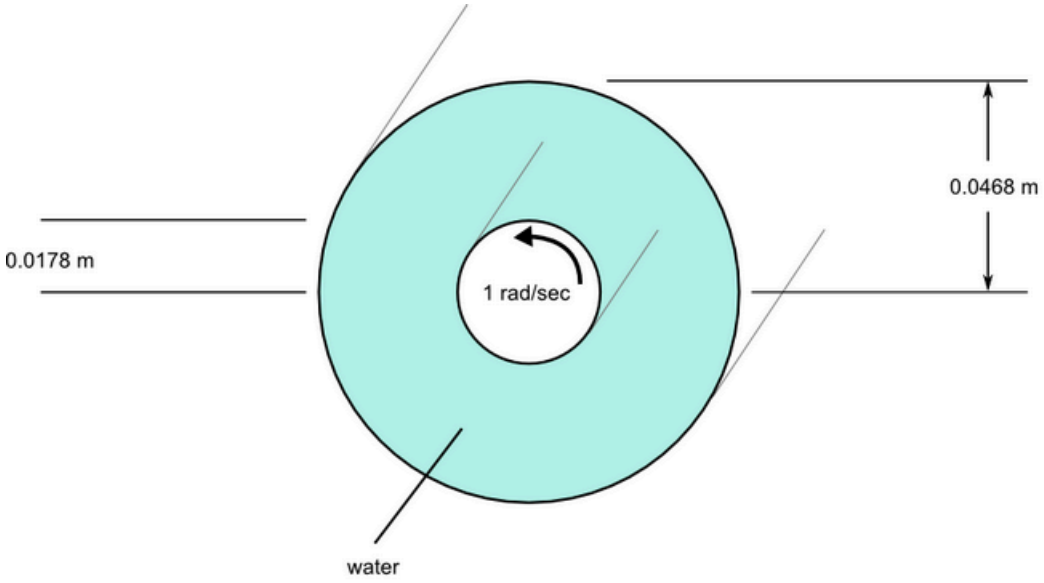


Figure 486: Critical Dimensions and Parameters for Simulating Flow Between Concentric Cylinders

The simulation was performed as a two dimensional problem by restricting flow in the out-of-plane direction through the use of a mesh that is one element thick.

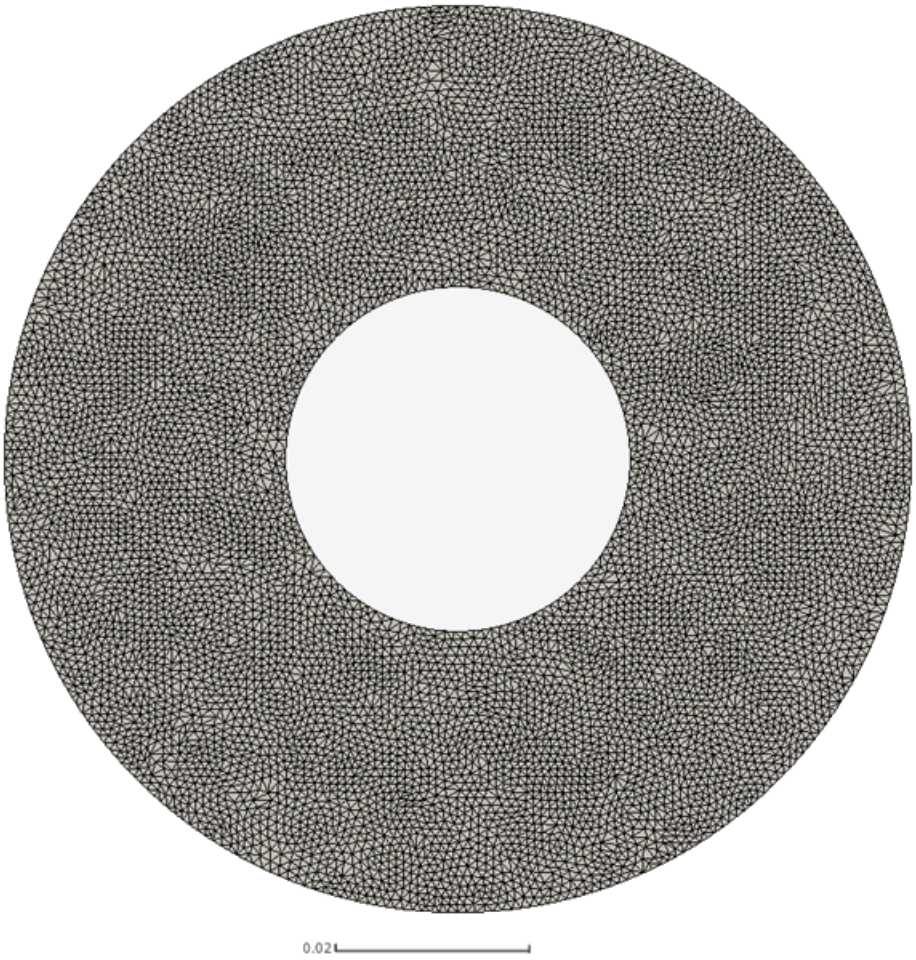


Figure 487: Mesh Used for Simulating Flow Between Concentric Cylinders

AcuSolve Results

The AcuSolve solution converged to a steady state and the results reflect the mean flow conditions. The velocity of the fluid within the cavity is greatest near the rotating inner cylinder. There is a nonlinear decrease in velocity as a function of distance away from the inner cylinder.

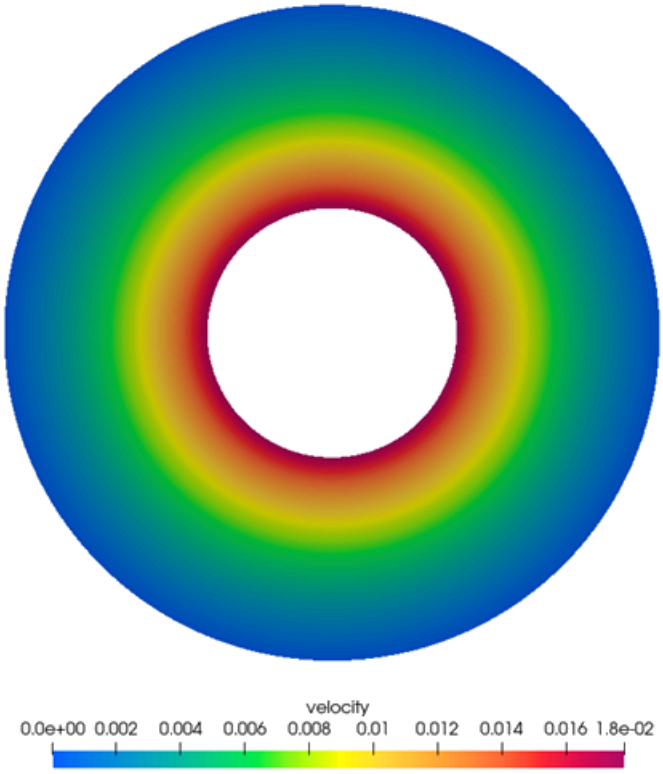


Figure 488: Contours of Tangential Velocity Between the Concentric Cylinders

Analytical tangential velocity at four distances away from the center of the rotating inner cylinder are presented with the corresponding AcuSolve results in the following table.

Table 25:

Distance from the center of rotating cylinder (m)	Analytical tangential velocity (m/s)	AcuSolve tangential velocity (m/s)	Percent deviation from analytical
0.020	0.01514	0.01514	0.04
0.025	0.01059	0.01058	0.10
0.030	0.00727	0.00727	0.06
0.035	0.00466	0.00466	0.10

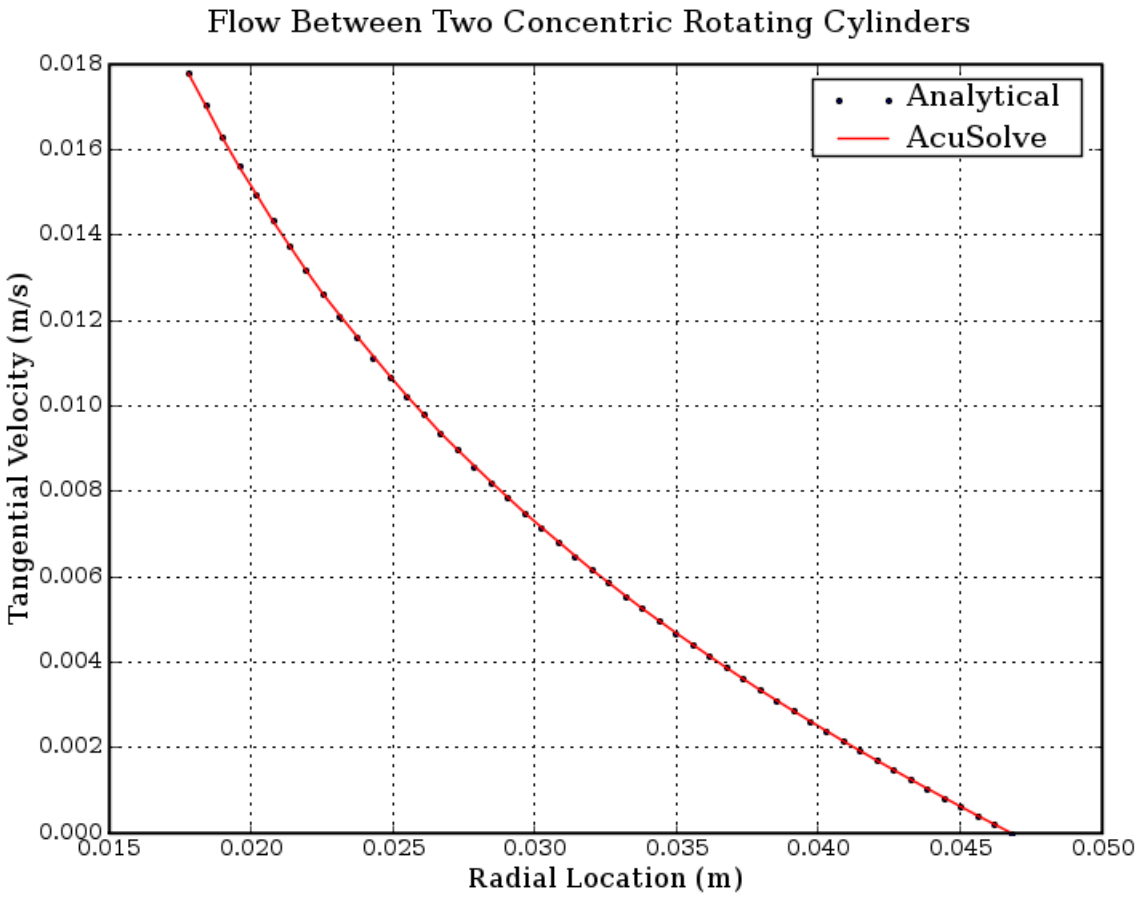


Figure 489: Tangential Velocity Plotted Against Distance from the Center of the Rotating Cylinder

Summary

The AcuSolve solution compares well with analytical results for the flow between concentric cylinders. In this application, the velocity in the annular fluid region is driven by the viscous stresses on the rotating wall. The AcuSolve tangential velocity is within 0.1 percent of the analytical solution at all radial locations.

Simulation Settings for Flow Between Concentric Cylinders

HyperMesh CFD database file: `<your working directory>\annulus_rotating\annulus_rotating.hm`

Global

- Problem Description
  - Analysis type - Steady State
  - Turbulence equation - Laminar
- Auto Solution Strategy
  - Relaxation Factor - `0.2`
- Material Model

- Water
  - Density - `1000.0` kg/m3
  - Viscosity - `0.001` kg/m-sec
- Reference Frame
  - Rotating_Cylinder
    - Rotation center
      1. X-coordinate - `0.0` m
      2. Y-coordinate - `0.0` m
      3. Z-coordinate - `0.0` m
    - Angular velocity
      1. X-component - `0.0` rad/sec
      2. Y-component - `0.0` rad/sec
      3. Z-component - `-1.0` rad/sec

Model

- Volumes
  - Volume
    - Element set
      1. Material model - Water
- Surfaces
  - Boundary1
    - Simple Boundary Condition
      1. Type - Symmetry
  - Boundary2
    - Simple Boundary Condition
      1. Type - Symmetry
  - Inner
    - Simple Boundary Condition
      1. Type - Wall
      2. Reference Frame - Rotating_Cylinder
  - Outer
    - Simple Boundary Condition
      1. Type - Wall
- Nodes
  - Fixed
    - Pressure
      1. Type - Zero

References

F. M. White. "Viscous Fluid Flow". Section 3-2.3. McGraw-Hill Book Co., Inc. New York. 1991.

Flow Inside a Rotating Cavity

In this application, AcuSolve is used to simulate the flow of air in an enclosed cylindrical cavity with a rotating top and a fixed bottom. AcuSolve results are compared with experimental data adapted from Michelsen (1986). The close agreement of AcuSolve results with experimental data validates the ability of AcuSolve to model cases containing enclosed cavities with flow induced by rotating walls.

Problem Description

The problem consists of air in an enclosed cylinder 1.0 m tall with a radius of 1.0 m, as shown in the following image, which is not drawn to scale. The top of the cylinder rotates about its center at 1 rad/s, while the bottom of the cylinder is fixed. As the container top spins, the viscous stresses on the fluid induce a circumferential (swirl) velocity throughout the height of the cylinder. To conserve mass and momentum, the fluid generates a radial velocity that changes direction based on distance away from the rotation center of the cylinder.

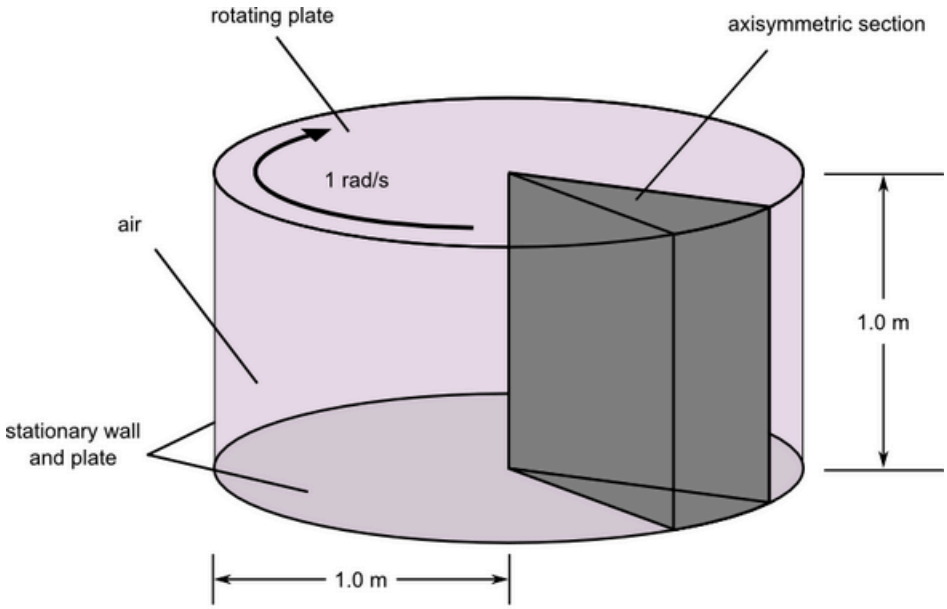


Figure 490: Critical Dimensions and Parameters for Simulating Flow Inside a Rotating Cavity

The flow domain is modeled with axisymmetric periodicity in the circumferential direction, which allows for accurate simulation of the flow while minimizing computational time.

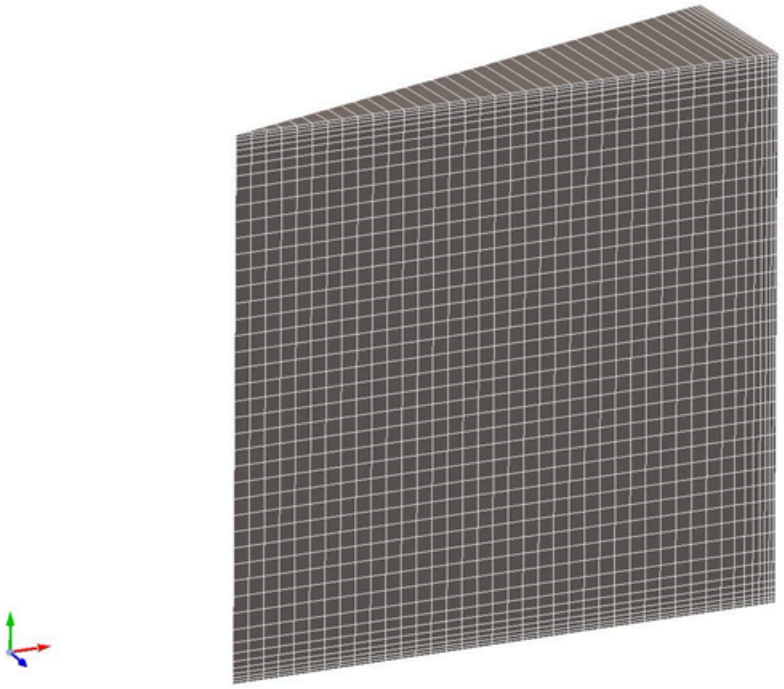


Figure 491: Mesh of Periodic Section Used for Simulating Flow Inside a Rotating Cylinder

AcuSolve Results

The AcuSolve solution converged to a steady state and the results reflect the mean flow conditions. The velocity varies with both vertical location and with distance from the rotation center. The complex flow field develops from a combination of the viscous stresses acting at the rotating cylinder top and at the stationary bottom.

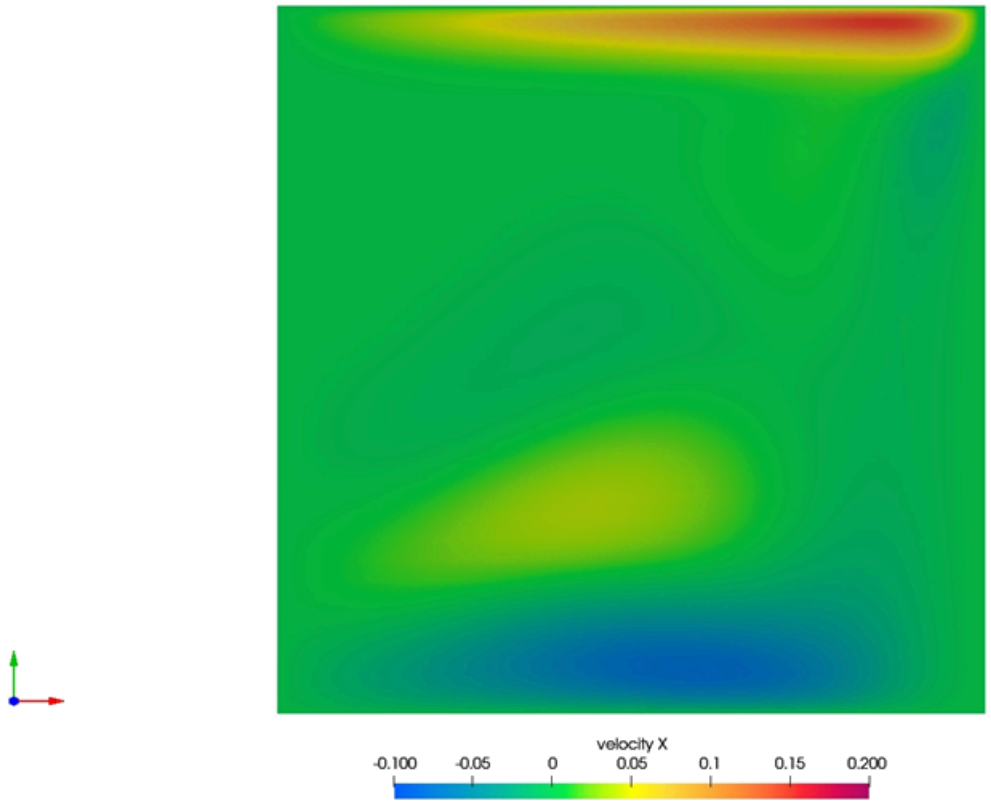


Figure 492: Contours of Radial Velocity with Velocity Vectors. This Image Shows the Front Face of the Modeled Cylinder Wedge, with the Center of Rotation on the Left Edge. The Vertical Line Represents a Radial Location 0.6 m From the Center of Rotation.

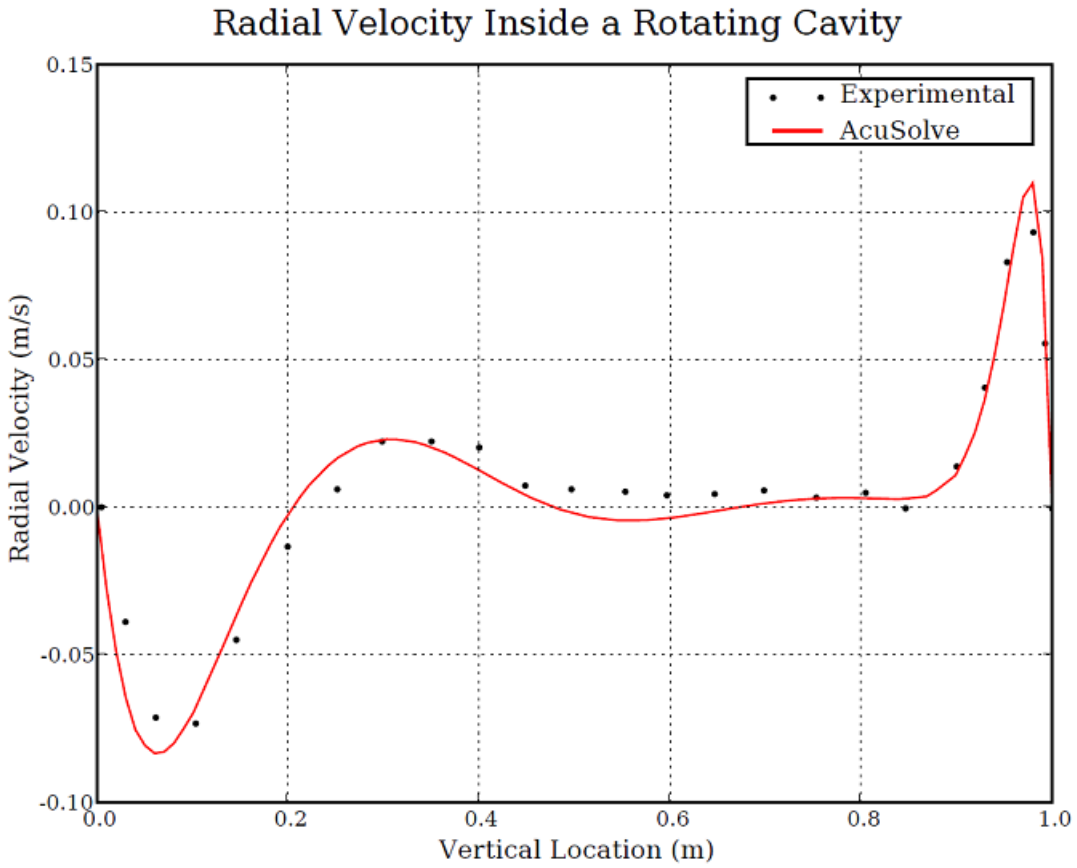


Figure 493: Radial Velocity (at 0.6 m From the Center of Rotation) as a Function of Vertical Location From Cylinder Bottom

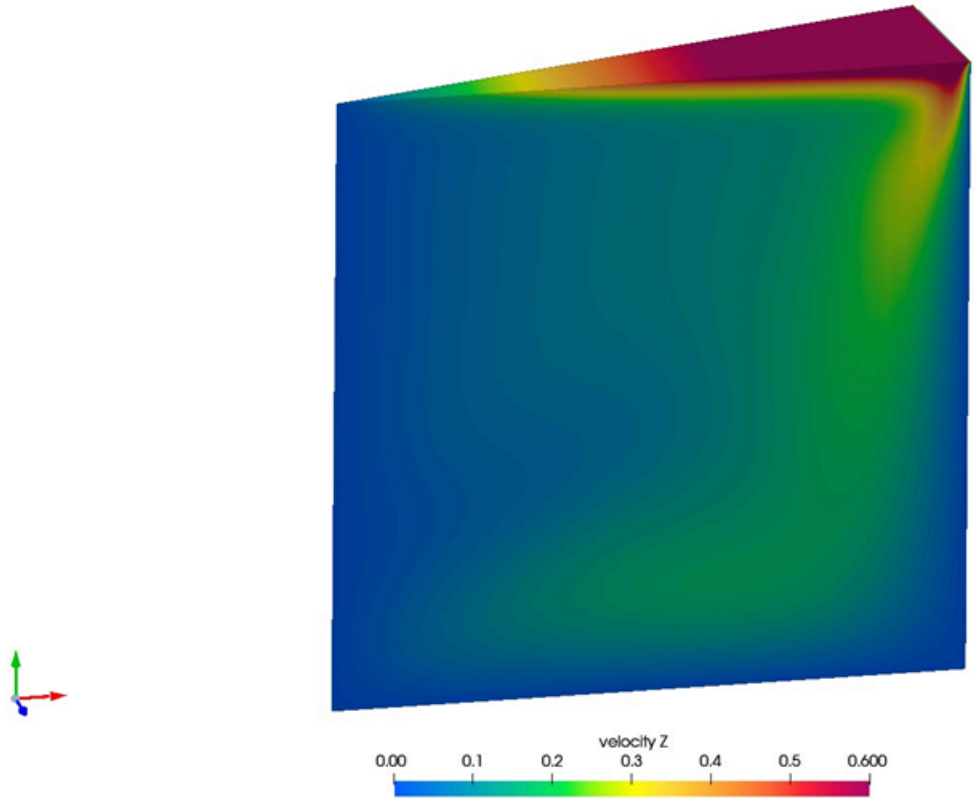


Figure 494: Contours of Swirl Velocity with Velocity Vectors

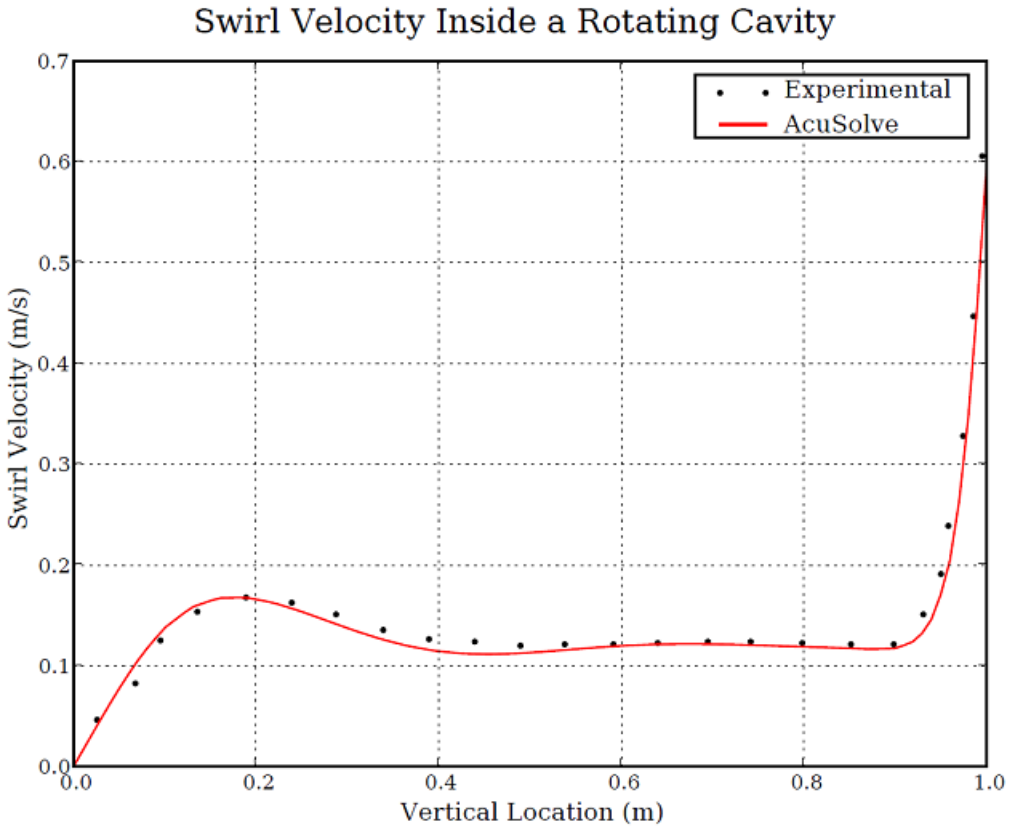


Figure 495: Swirl Velocity (at 0.6 m From Center of Rotation) as a Function of Vertical Location From the Cylinder Bottom

Summary

The AcuSolve solution compares well with the experimental data for flow induced by a rotating top of an enclosed cylinder. In this application, the flow in the fluid region is driven by the viscous stresses near the rotating top. Viscous stresses drag the fluid in a circular direction near the spinning wall. The angular velocity of the fluid decreases as distance from the top wall increases. Radial velocity develops as a result of the migration of the fluid toward the outer wall in regions of high angular velocity. The AcuSolve radial and swirl velocities compare very closely with the experimental data.

Simulation Settings for Flow Inside a Rotating Cavity

SimLab database file: `<your working directory>\cavity_rotating\cavity_rotating.slb`

Global

- Problem Description
  - Solution type - Steady State
  - Flow - Laminar
- Auto Solution Strategy
  - Relaxation Factor - `0.4`
- Material Model

- Air
  - Density - `1.0` kg/m3
  - Viscosity - `0.000556` kg/m-sec
- Reference Frame
  - Cavity Rotation
    - Rotation center
      1. X-coordinate - `0.0`
      2. Y-coordinate - `0.0`
      3. Z-coordinate - `0.0`
    - Angular velocity
      1. X-component - `0.0`
      2. Y-component - `-1.0` rad/sec
      3. Z-component - `0.0`

Model

- Volumes
  - Fluid
    - Element Set
      1. Material model - Air
- Surfaces
  - Bottom
    - Simple Boundary Condition
      1. Type - Wall
  - Max_X
    - Simple Boundary Condition
      1. Type - Wall
  - Max_Z
    - Simple Boundary Condition - (disabled to allow for periodic conditions to be set)
  - Min_Z
    - Simple Boundary Condition - (disabled to allow for periodic conditions to be set)
  - Top
    - Simple Boundary Condition
      1. Type - Wall
      2. Reference frame - Cavity Rotation
- Periodics
  - Periodic 1
    - Periodic Boundary Condition
      1. Type - Axisymmetric

2 Rotation axis
  1 point 1
    1 X-coordinate - `0.0` m
    2 Y-coordinate - `0.0` m
    3 Z-coordinate - `0.0` m
  2 point 2
    1 X-coordinate - `0.0` m
    2 Y-coordinate - `1.0` m
    3 Z-coordinate - `0.0` m

References

J. A. Michelsen. "Modeling of Laminar Incompressible Rotating Fluid Flow". AFM 86-05. Ph.D. thesis, Department of Fluid Mechanics, Technical University of Denmark. 1986.

Multiphase

12

This section includes validation cases that consider the immiscible multiphase interaction of two fluids.

This chapter covers the following:

- Multiphase Flow of a 2D Dam Break (p. 667)
- Two-Phase Nucleate Boiling in a Cylindrical Pipe (p. 671)

Multiphase Flow of a 2D Dam Break

In this application, AcuSolve is used to simulate the collapse of a water column surrounded by air. AcuSolve results are compared with experimental results adapted from Rodriguez and others (2013). The close agreement of AcuSolve results with experimental results validates the ability of AcuSolve to model multiphase flow problems.

Problem Description

The problem consists of a column of water being held in place by a membrane in a box of air, as shown in the following image, which is not drawn to scale, where a = 0.05715 m. At t = 0, the membrane is broken, allowing the water column to collapse.

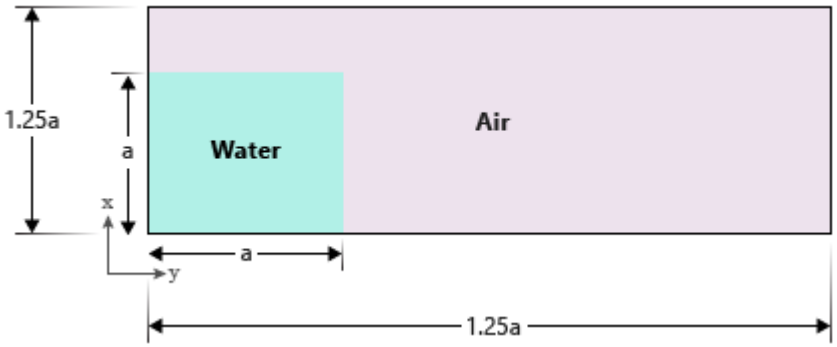


Figure 496: Critical Dimensions and Parameters for Simulating a 2D Dam Break Problem

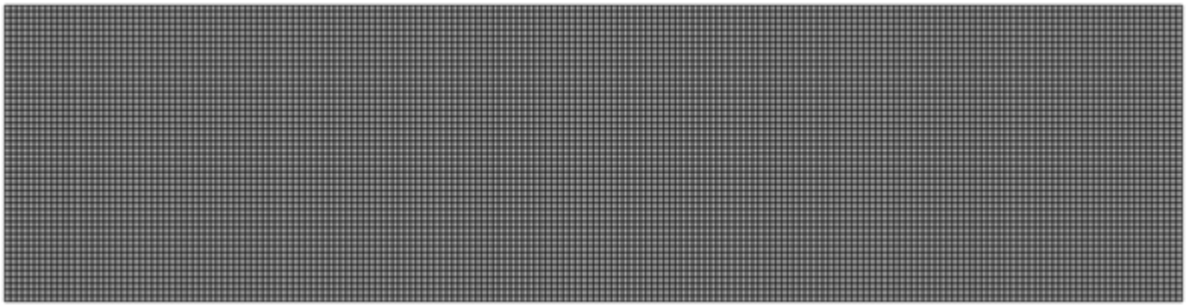


Figure 497: Mesh used for Simulating Multiphase Flow of a 2D Dam Break Problem

AcuSolve Results

The AcuSolve solution is run for a time t = 0.4 sec and the results reflect the transient motion of water column.

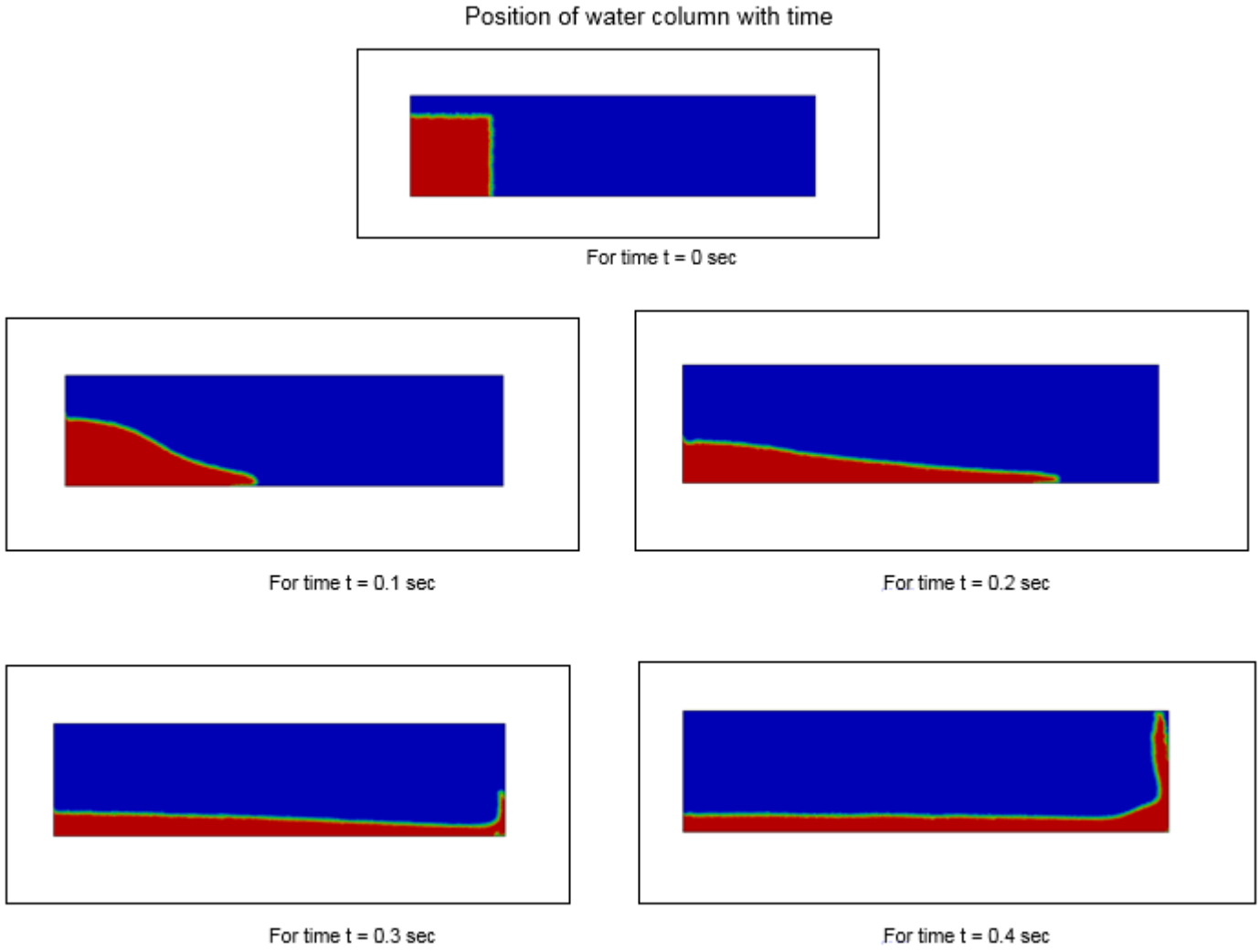


Figure 498:

The experimental values of normalized surge front positions (x/a) and normalized column height (y/a) is presented below with the corresponding AcuSolve results. The AcuSolve results show good agreement with the experimental results.

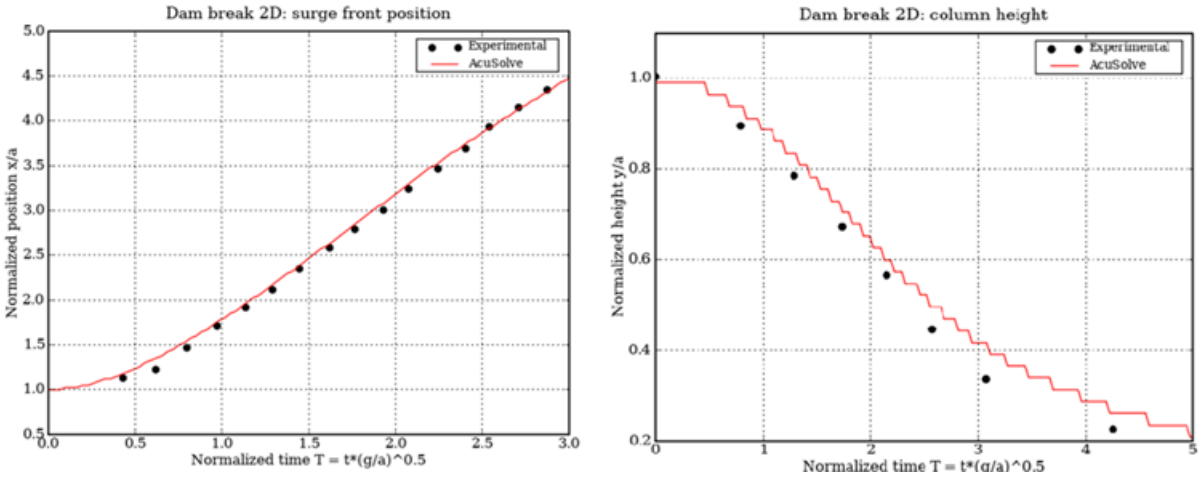


Figure 499: Surge Front Position and Column Height Compared to Experimental Results for Simulating Multiphase Flow of a 2D Dam Break

Summary

The AcuSolve solution compares well with experimental results for a dam break problem. In this application, multiphase flow simulation of the collapse of a water column is performed. The experimental value for the normalized column height and normalized surge front positions is presented with the corresponding AcuSolve results. A good agreement of simulation results with the experiment validates the multiphase capability of AcuSolve.

Simulation Settings for Multiphase Flow of a 2D Dam Break

HyperMesh CFD database file: `<your working directory>\dambreak_multiphase\damnbreak_multiphase.hm`

Global

- Problem Description
  - Analysis type - Transient
  - Multifluid - Level Set
  - Gravitational acceleration - { 0, -9.81, 0 }
- Auto Solution Strategy
  - Final Time - `0.4` sec
  - Initial time increment - `0.0005` sec
  - Fluid 1 - Water
  - Fluid 2 - Air
- Time Integration
  - Time integration order – “second”
- Material Model
  - Air
    - Type - Constant

        - Density - `1.2` kg/m3
        - Viscosity - `1.1818e-006` kg/m-sec
    - Water
        - Type - Constant
        - Density - `1000` kg/m3
        - Viscosity - `0.001` kg/m-sec
- Multifield Parameters → Field Interaction Model
    - Field 1 - Water
    - Field 2 - Air
    - Thickness type - Number of elements
    - Number of elements - `3`
    - Fluid 2 - Air

  Model
- Volumes
    - Fluid
        - Element Set
            1. Medium - Multi Field
            2. Multi field model - Water-Air
- Surfaces
    - +Z
        - Simple Boundary Condition - Slip
    - -Z
        - Simple Boundary Condition - Slip
    - Bottom wall
        - Simple Boundary Condition - Wall
    - Left wall
        - Simple Boundary Condition - Wall
    - Right wall
        - Simple Boundary Condition - Wall
    - Top wall
        - Simple Boundary Condition - Wall

References

Joseph M. Rodriguez, Onkar Sahni, Richard T. Lahey Jr., Kenneth E. Jansen. "A parallel adaptive mesh method for the numerical simulation of multiphase flows", Computers and Fluids, Vol. 87, 2013, pp. 115-131.

Two-Phase Nucleate Boiling in a Cylindrical Pipe

In this application, AcuSolve is used to simulate the changes in wall temperature due to two-phase nucleate boiling at the heated walls of a pipe with water flowing through it. AcuSolve results are compared with experimental results adapted from Koncar and others (2015). The close agreement of AcuSolve results with experimental results validates the ability of AcuSolve to model two-phase nucleate boiling problems.

Problem Description

The problem consists of a pipe with heated surrounding walls, as shown in the following image, which is not drawn to scale. The length of the pipe is 2 m and the radius is 0.0017 m. Mass flux at the inlet is 900 kg/m^2 and the temperature of the fluid entering the pipe is 473 K. A heat flux of 570,000 W/m^2 is applied on the walls. The preheated water enters the inlet and heat is transferred to the fluid from the walls. The heat causes sub-cooled boiling to occur in the region close to the wall and leads to the formation of bubbles at nucleation sites.

During sub-cooled boiling flow, heat and mass exchange between the phases takes place on the heated wall and in sub-cooled liquid flow. On the heated surface the vapor bubbles are generated and as they move through the sub-cooled liquid they condense and release the latent heat.

The AcuSolve simulation is set up to model transient state heat transfer to determine the temperature along the centerline of the pipe and along the heated pipe walls of the model. AcuSolve computes the two-phase nucleate boiling by simulating the three-dimensional flow in a heated pipe for two-phase boiling flow, as described in Koncar (2005). The temperatures along the centerline of the pipe and along the pipe walls are compared against the experimental measurements, as described in Koncar, et al. (2005).

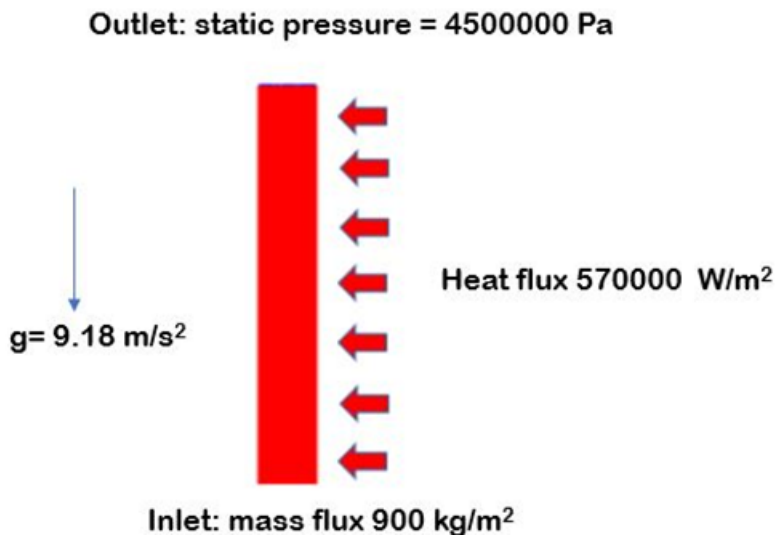


Figure 500: Parameters for Simulating a Two-Phase Nucleate Boiling Problem of a Pipe

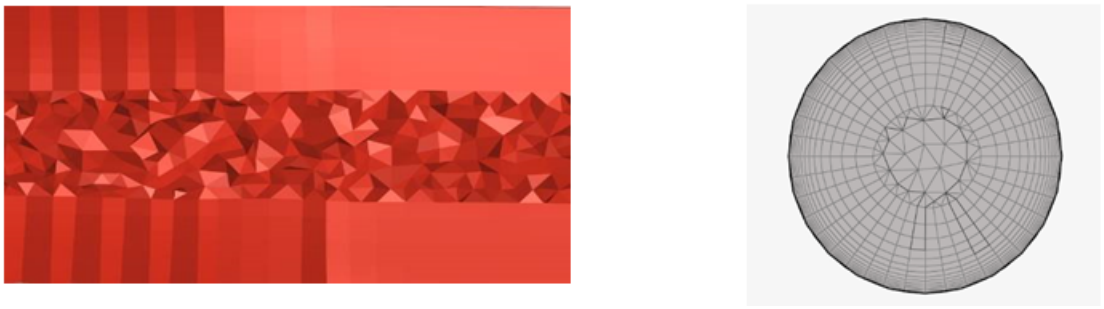


Figure 501: Mesh used for Simulating Two-Phase Flow in a Pipe

AcuSolve Results

The AcuSolve solution is run for a heat flux of 570,000 W/m^2 and the results are presented in the following image. The experimental values of wall temperature are presented with the corresponding AcuSolve results along the centerline of the pipe and along the pipe wall. The AcuSolve results show good agreement with the experimental results for the temperature, indicating that the two-phase nucleate boiling is properly captured.

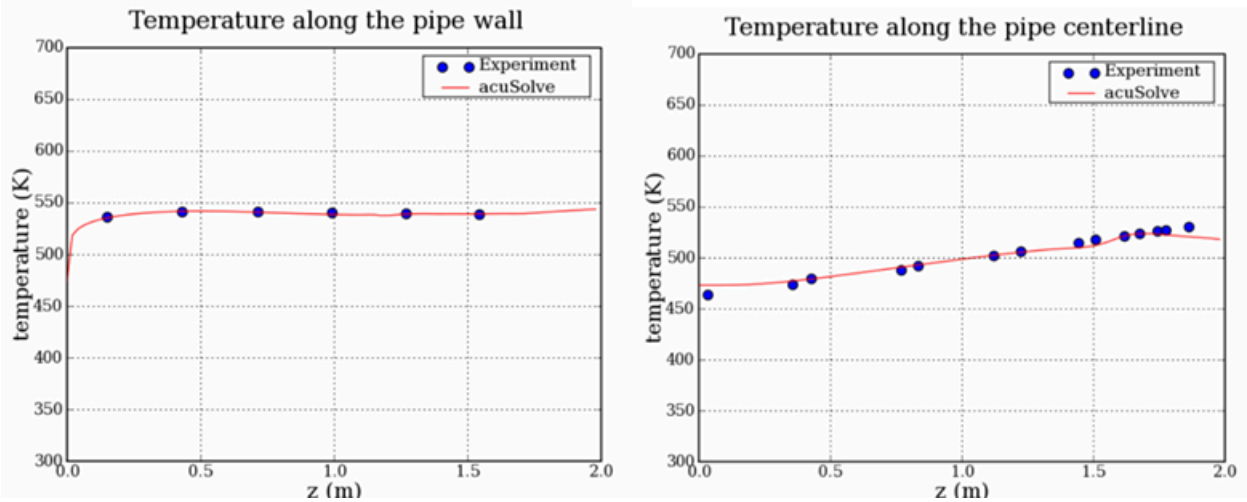


Figure 502: Temperature Values for Varying Streamwise Distance Compared to Experimental Data

Summary

The AcuSolve solution compares well with experimental results for two-phase nucleate boiling simulations. In this application, the temperature of the wall as the onset of boiling approaches are simulated with AcuSolve using the nucleate boiling feature and the SA turbulence model. The experimental values of temperature are presented with the corresponding AcuSolve results. A good agreement of simulation results with the experiment validates the ability to solve two-phase nucleate boiling using the nucleate boiling capabilities of AcuSolve.

Simulation Settings for Two-Phase Nucleate Boiling in a Cylindrical Pipe

HyperMesh CFD database file: `<your working directory>\pipe_two_phase_boiling\pipe_two_phase_boiling.hm`.

Global

- Problem Description
  - Analysis type – Transient
  - Turbulence equation – SA
  - Temperature equation – Advective Diffusive
- Auto Solution Strategy
  - Maximum time steps – `500`
  - Initial time increment – `0.003`
  - Convergence Tolerance – `0.001` sec
  - Relaxation factor – `0.3`
- Surface Tension Model (“Water_NB-Vapor_NB”)
  - Type – Constant
  - Surface Tension – `0.02382`
- Material Model
  - Vapor_NB
    - Type – Constant
    - Density – `23.75` kg/m^3
    - Viscosity – `1.79e-05` kg/m-sec
    - Specific Heat – `4225` J/kg-K
    - Latent Heat – `1675570`
    - Latent Heat Temperature – `530.55` K
    - Conductivity – `0.02528` W/m-K
  - Water_NB
    - Type – Constant
    - Density – `800` kg/m3
    - Viscosity – `0.0001339` kg/m-sec
    - Specific Heat – `4500` J/kg-K
    - Conductivity – `0.65` W/m-K
- Multifield parameter (Field interaction model)
  - Type – Algebraic Eulerian
  - Phase change type – Wall Boiling
  - Carrier field - Water
  - Disperse field – Vapor
  - Disperse field diameter type – Boiling kurul exponential
  - Drag model – Ishii zuber
  - Lift Model – Legendre Magnaudet

Model

- Volumes
  - Fluid
    - Material – Vapor_Water
- Surfaces
  - Inflow
    - Simple Boundary Condition – Inflow
    - Inflow type – Mass Flux Rate
    - Mass Flux Rate – `0.167634` kg/sec
    - Temperature – `473` K
  - Outflow
    - Simple Boundary Condition – Outflow
    - Pressure – `4500000` N/m2
  - Wall
    - Simple Boundary Condition – Wall
    - Temperature type – Flux
    - Heat Flux – `570000` W/m2

References

B. Koncar, E. Krapper, Y. Egorov, 2005, "CFD MODELING OF SUBCOOLED FLOW BOILING FOR NUCLEAR ENGINEERING APPLICATIONS", International Conference Nuclear Energy for New Europe 2005, Bled, Slovenia, September 5-8,2005.

Compressible

13

This section includes validation cases that consider the compressibility of the fluid using a variable material model.

This chapter covers the following:

- Supersonic Flow Through a Converging-Diverging Nozzle (p. 676)
- Ideal Gas Compression in an Actuating Piston (p. 681)

Supersonic Flow Through a Converging-Diverging Nozzle

In this application, AcuSolve is used to simulate the high-speed turbulent flow in a converging and then diverging nozzle. The flow within the nozzle enters as subsonic, reaches sonic at the throat and shortly after develops a normal shock. AcuSolve results are compared with experimental results adapted from Bogar and Sajben (1983). The close agreement of AcuSolve results to experimental measurements validates the ability of AcuSolve to simulate internal supersonic flows where normal shocks are present.

Problem Description

The problem consists of a converging and then diverging nozzle represented as an extruded planar surface, as shown in the image below, which is not drawn to scale. The length of the domain is 0.213 m with a throat height of 0.044 m. The stagnation pressure and static temperature are constrained at the inlet to 135,000 Pa and 265.98 K, respectively. The static pressure is defined using the outflow boundary condition, where P_{static}=97216.08 Pa. The flow in the diffuser has an inlet Reynolds number of $6.5x10^5$. The upper and lower walls are set to no-slip and the side walls are set to slip, while the exterior walls are specified to be adiabatic. Images of the numerical mesh are shown below.

The AcuSolve simulation is prepared to model the pseudo-transient state to determine the shock location and corresponding scalar quantities within the diffuser. AcuSolve computes the flow and thermal solution by simulating a planar, two-dimensional flow problem with physical dimensions and input quantities as described in the Sajben Diffuser case presented by Bogar and Sajben (1983). The gas in the simulation domain enters at subsonic conditions and is forced to accelerate beyond Mach=1.0 as it passes through the throat. After reaching supersonic speed a normal shock wave develops causing the flow speed to reduce back below sonic. The pressure along the bottom wall of the diffuser is compared against experimental measurements to demonstrate the solver's capability to solve supersonic cases.

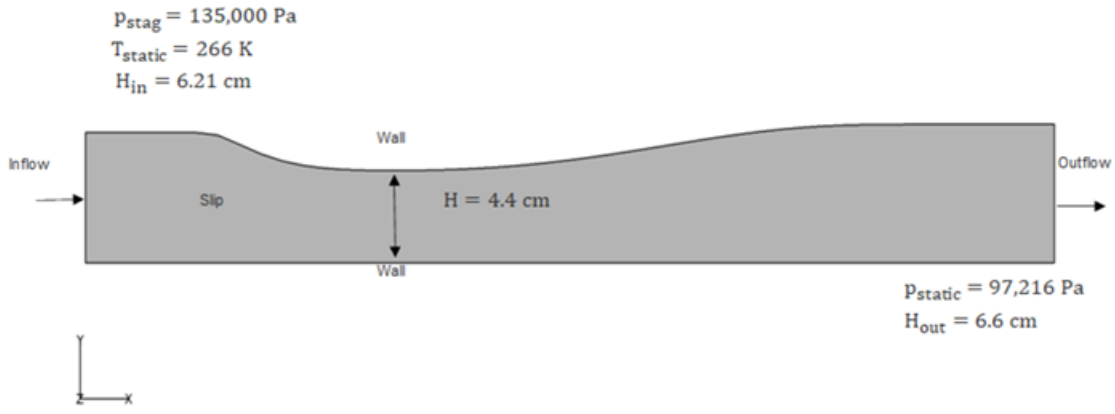


Figure 503: Parameters for Simulating Compressible Flow within a Converging-Diverging Nozzle

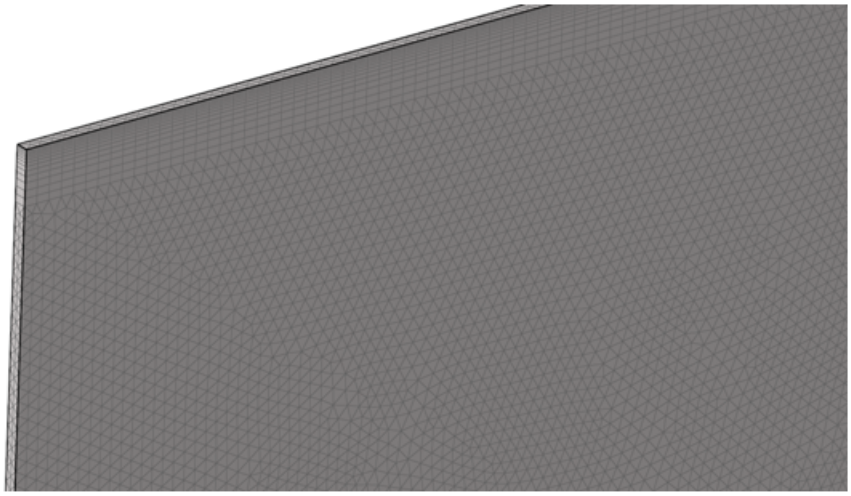


Figure 504: Mesh used for Simulating Compressible Flow in a Converging-Diverging Nozzle

AcuSolve Results

The AcuSolve solution is run for 0.025 seconds (6,250 timesteps with dt=4.0x10^{-6}sec) and converges to a pseudo-steady solution. The change in pressure from the inlet to outlet causes the flow to accelerate within the throat of the diffuser until it reaches approximately Mach=1.35. A normal shock is present just downstream of where the cross-sectional area of the nozzle increases, as shown in the image below. The numerical solution can be compared with the reference after normalizing the pressure along the wall by the inlet stagnation pressure (135 kPa) and the distance along the bottom wall by the nozzle throat height (0.044 m). The image below shows the normalized pressure versus normalized distance in comparison to NASA reference and experimental results. The image shows black circles representing the experimental measurements (Bogar and Sajben 1983), a dashed blue line representing the SA solution as obtained through NASA publication (Mohler 2005) and a solid red line representing the AcuSolve results with the Spalart-Allmaras turbulence model. The non-dimensional pressure within the diffuser agrees well with the reference data, demonstrating the correct physical location of the normal shock and expected moderate flow speed reduction within the constant cross-section diffuser portion of the nozzle.

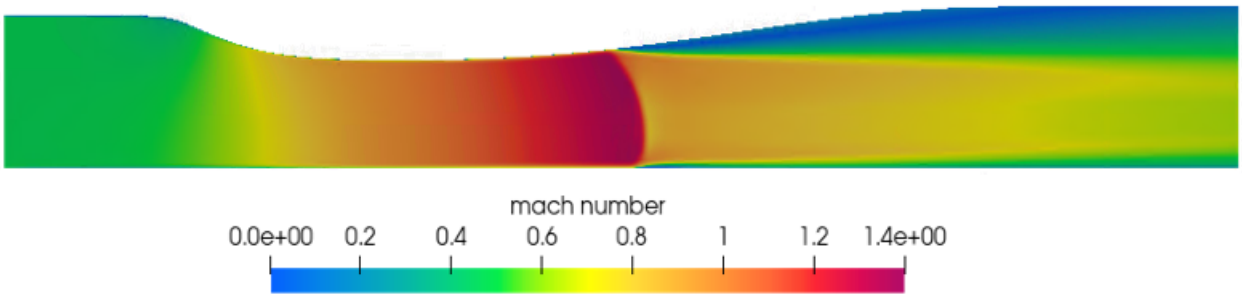


Figure 505: Contours of Mach Number within a Converging-Diverging Nozzle

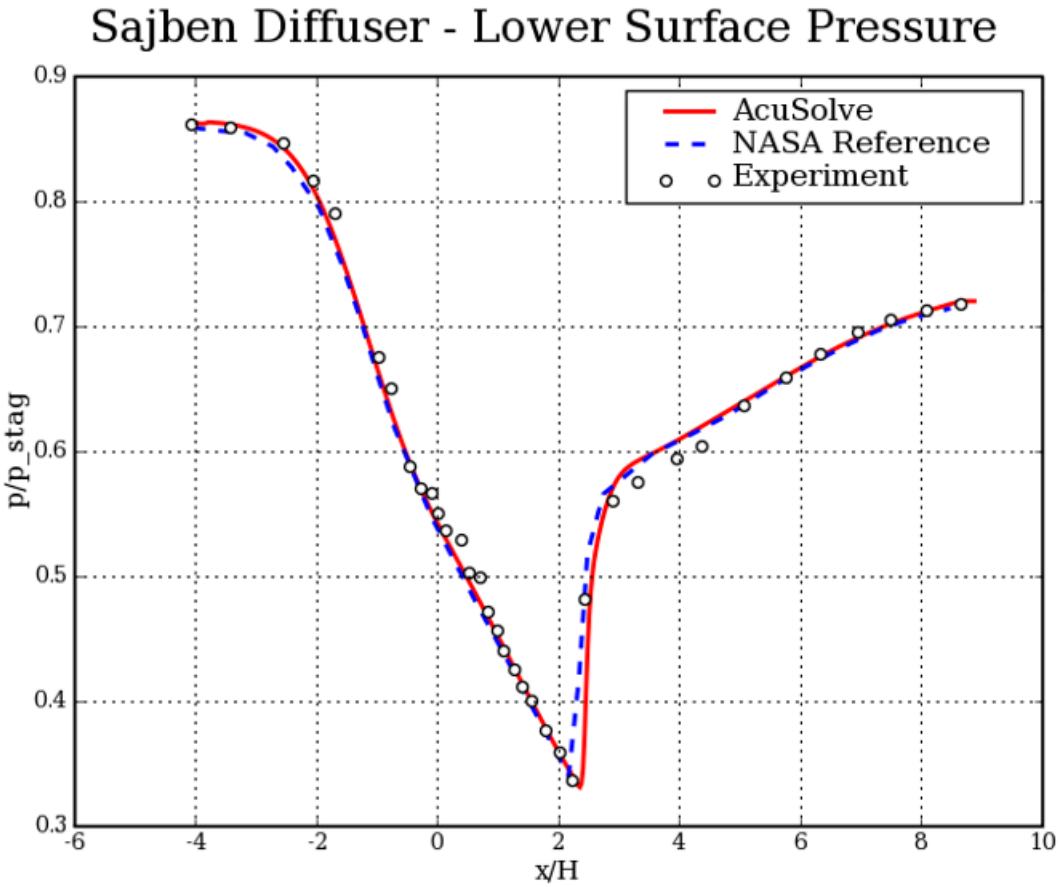


Figure 506: Normalized Pressure Versus Normalized Distance in Comparison to NASA Reference and Experimental Results

Summary

The AcuSolve solution compares well with experimental and numerical results for the described simulation. In this application, compressibility effects are accounted for using the coupled compressible flow solver with the ideal gas material definition. The thermal and momentum exchange within the nozzle is computed with AcuSolve using the compressible Navier-Stokes solver with the Spalart-Allmaras turbulence model. The experimental values of pressure are presented with the corresponding AcuSolve results and show good agreement, validating the ability to solve compressible cases with the presence of normal shocks. The results indicate that AcuSolve is able to properly predict the peak pressure magnitude and location within the diffuser while maintaining the normal shock when the time-step is selected to result in a maximum CFL of approximately 30.

Simulation Settings for Supersonic Flow Through a Converging-Diverging Nozzle

HyperMesh CFD database file: `<your working directory>\diffuser_compressible\diffuser_compressible.hm`

Global

- Problem Description

    - Flow – Compressible Navier Stokes
    - Analysis type – Transient
    - Turbulence equation – SA
    - Temperature equation – Advective Diffusive
- Auto Solution Strategy
    - Initial time increment – `4.0E-6`
    - Final time – `0.025` sec
    - Convergence Tolerance – `0.001` sec
    - Relaxation factor – `0.5`
- Material Model
    - Air-Ideal Gas
        - Type – Ideal_Gas
        - Viscosity – `1.781e-05` kg/m-sec
        - Specific Heat – `1005` J/kg-K
        - Conductivity – `0.02521` W/m-K
        - Gas Constant – `287.058` J/kg-K

Model

- Volumes
    - Fluid
        - Material – Air-Ideal Gas
- Surfaces
    - Inflow
        - Simple Boundary Condition – Inflow
        - Inflow type – Stagnation Pressure
        - Stagnation Pressure – `135000.0` N/m2
        - Turbulence_input_type – Direct
        - Eddy Viscosity – `1e-6` m^2/s
        - Temperature – `265.98` K
    - Outflow
        - Simple Boundary Condition – Outflow
        - Pressure – `97216.08` N/m2
    - Wall_1
        - Simple Boundary Condition – Wall
        - Type – auto_wall
    - Wall_2
        - Simple Boundary Condition – Wall
        - Type – auto_wall
    - Slip_1

- Simple Boundary Condition – Slip
- Slip_2
  - Simple Boundary Condition – Slip

References

Bogar, T. J., Sajben, M., and Kroutil, J. C. (1983) "Characteristic Frequencies of Transonic Diffuser Flow Oscillations," AIAA Journal, Vol. 21, No. 9, pp. 1232-1240.

Mohler, S.R., "Wind-US Unstructured Flow Solutions for a Transonic Diffuser," NASA CR-2005-213417, January 2005.

Ideal Gas Compression in an Actuating Piston

In this application, AcuSolve is used to simulate pressure and temperature inside an actuating piston using the ideal gas relationship and fully defined mesh motion. AcuSolve results are compared with analytical results as described in Moran and Shapiro (2000). The close agreement of AcuSolve results with analytical results validates the ability of AcuSolve to model cases with material properties defined by the ideal gas law subjected to significant mesh distortion.

Problem Description

The problem consists of air compressed by a piston within a cylinder 10 m long with a diameter of π (3.14159) m, as shown in the following image, which is not drawn to scale. The piston is driven by a crankshaft 4 m long attached to a connecting rod 6 m long. The crankshaft rotates at 60o/s around a center point. At time (t) = 0.0 s the crank and piston are at top dead center (TDC) with an initial cylinder volume of 80 m^3. At t = 3.0 s the piston is at bottom dead center (BDC), at which point the volume in the cylinder is reduced to 16 m^3. The piston then moves back to TDC at t = 6.0 s. Air at atmospheric conditions, with material properties of an ideal gas and a dynamic viscosity of 1.781 X 10^5 kg/m-sec is the fluid modeled in the domain.

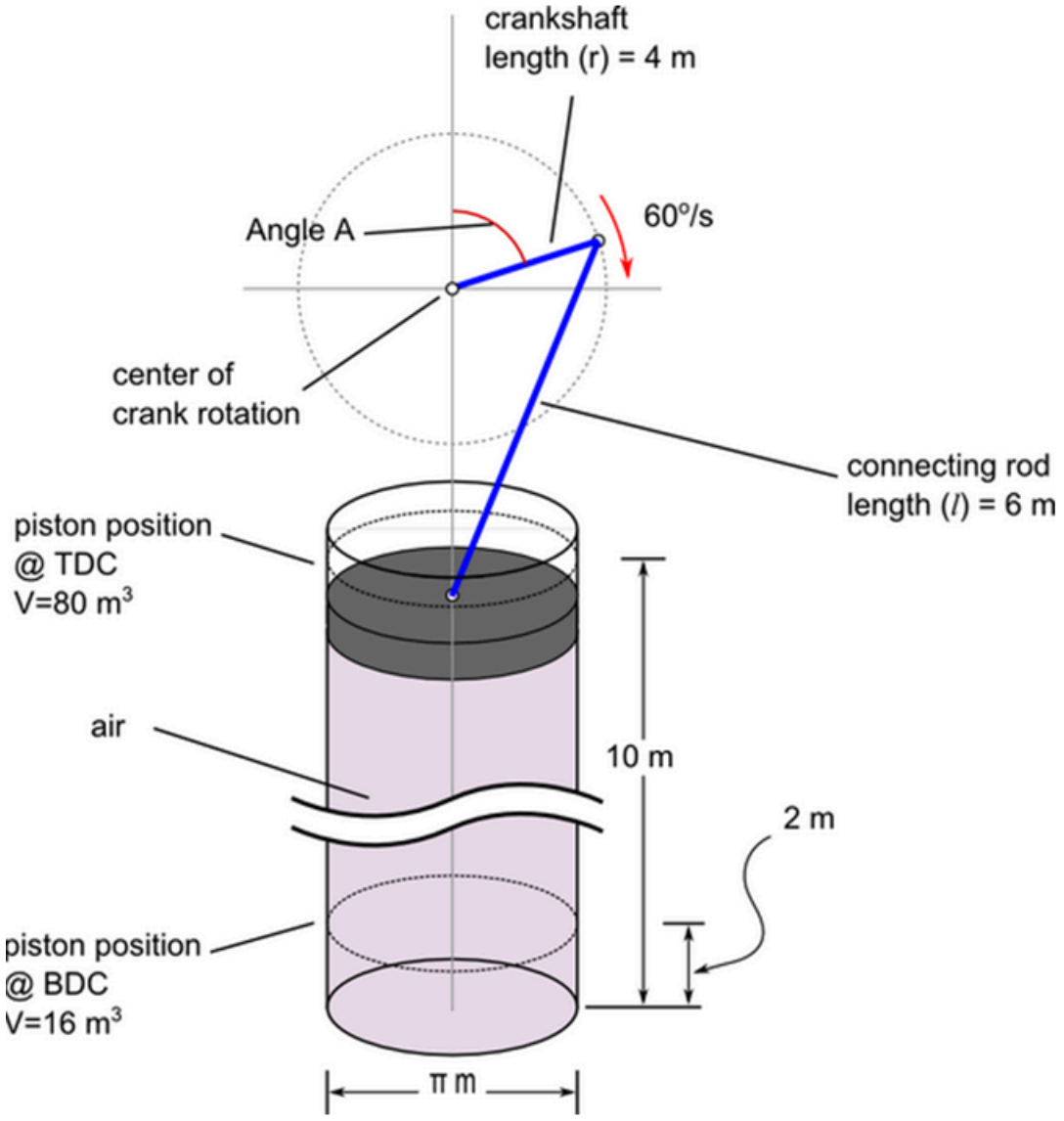


Figure 507: Critical Dimensions and Parameters for Simulating Ideal Gas Compression in an Actuating Piston

The motion of the piston is described by the following equation.

$$x = r * \cos A + \sqrt{l^2 - r^2 \sin^2 A} \tag{22}$$

Where

- x is the distance of the piston from TDC
- r is the length of the connecting rod, 4 m
- A is the crank angle as a function of time (t)
- l is the connecting rod length, 6 m

During the simulation, the top surface of the cylinder, representing the piston, moves with an applied mesh motion that mimics the motion of the reciprocating crank, rod, and piston assembly. The ideal gas

is compressed by contracting the mesh according to the motion of that assembly and by allowing the fluid properties to change as a function of time.

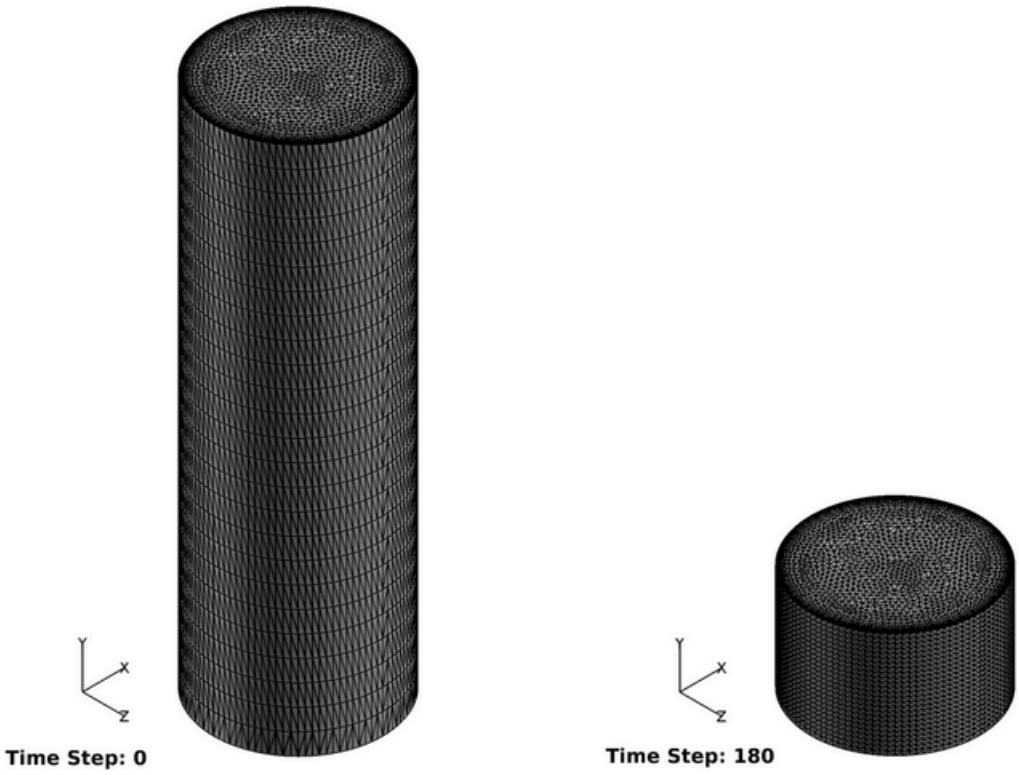


Figure 508: Mesh Used for Simulating Ideal Gas Compression in an Actuating Piston at Time Step 0 and Time Step 180 (3 s)

AcuSolve Results

The simulation was run as transient for a total of 360 time steps with a duration of 6.0 seconds. The AcuSolve solution shows time dependent pressure and temperature in a cylinder volume that compresses and expands in a 6.0 second cycle. Pressure and temperature increase as the cylinder volume decreases and returns toward initial conditions as the cylinder volume expands. The contours of pressure and temperature within the cylinder at the initial stage (t = 0.0 s) and the half cycle (t = 3.0 s) are shown in the following images.

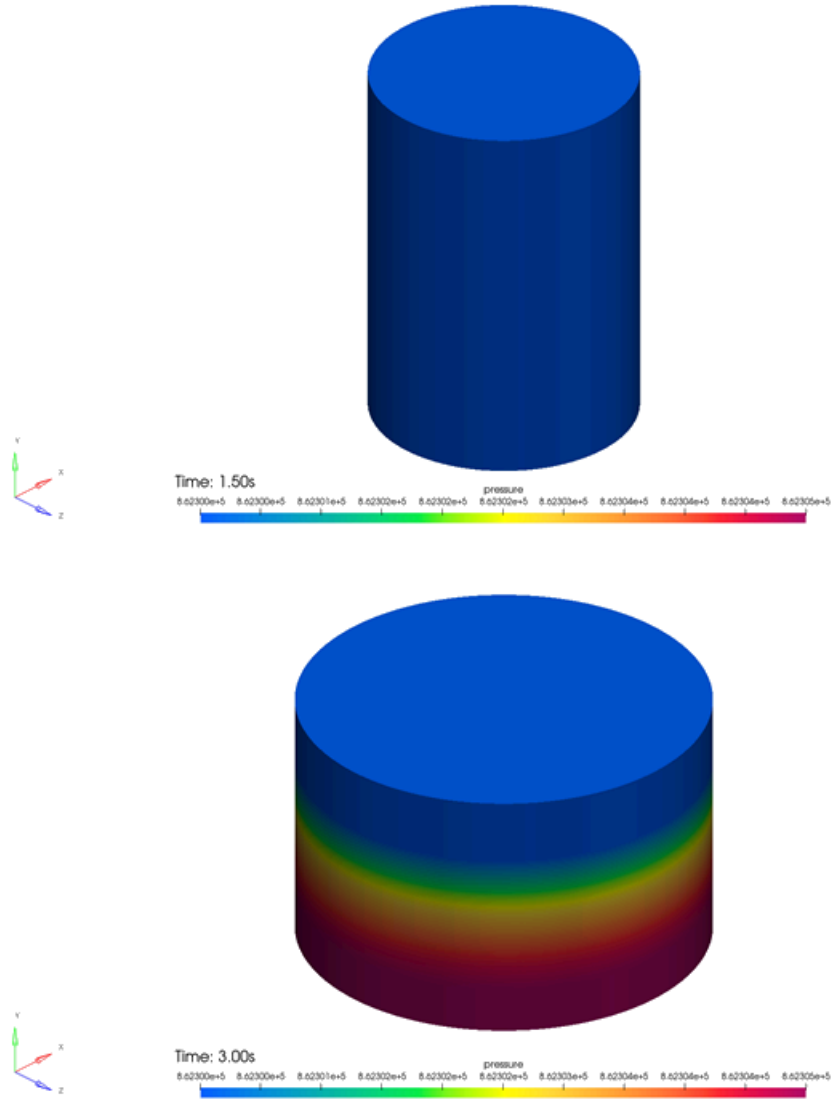


Figure 509: Pressure Distribution Within the Domain with the Piston at 1.5s and 3.0s

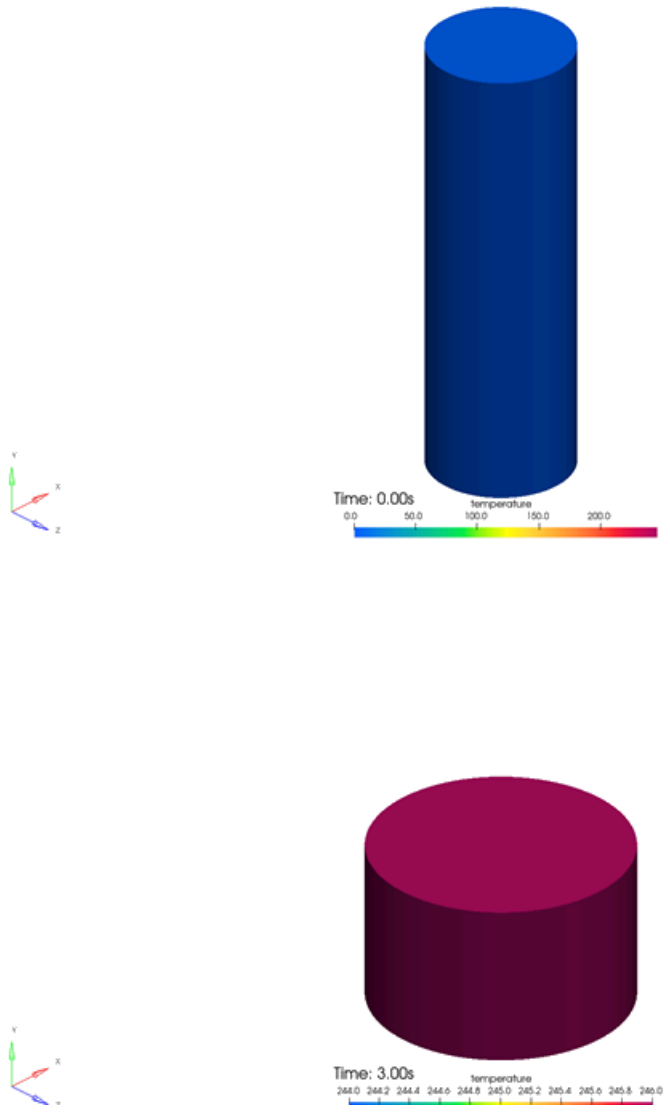


Figure 510: Temperature Distribution Within the Domain with the Piston at TDC and BDC

Comparison of time history plots of the AcuSolve and analytical solutions shows that the AcuSolve solution is nearly identical to the analytical solution. The AcuSolve computed internal pressure reaches a maximum of 8.62 X 105 Pa and the temperature reaches a maximum of 246.45 degrees C.

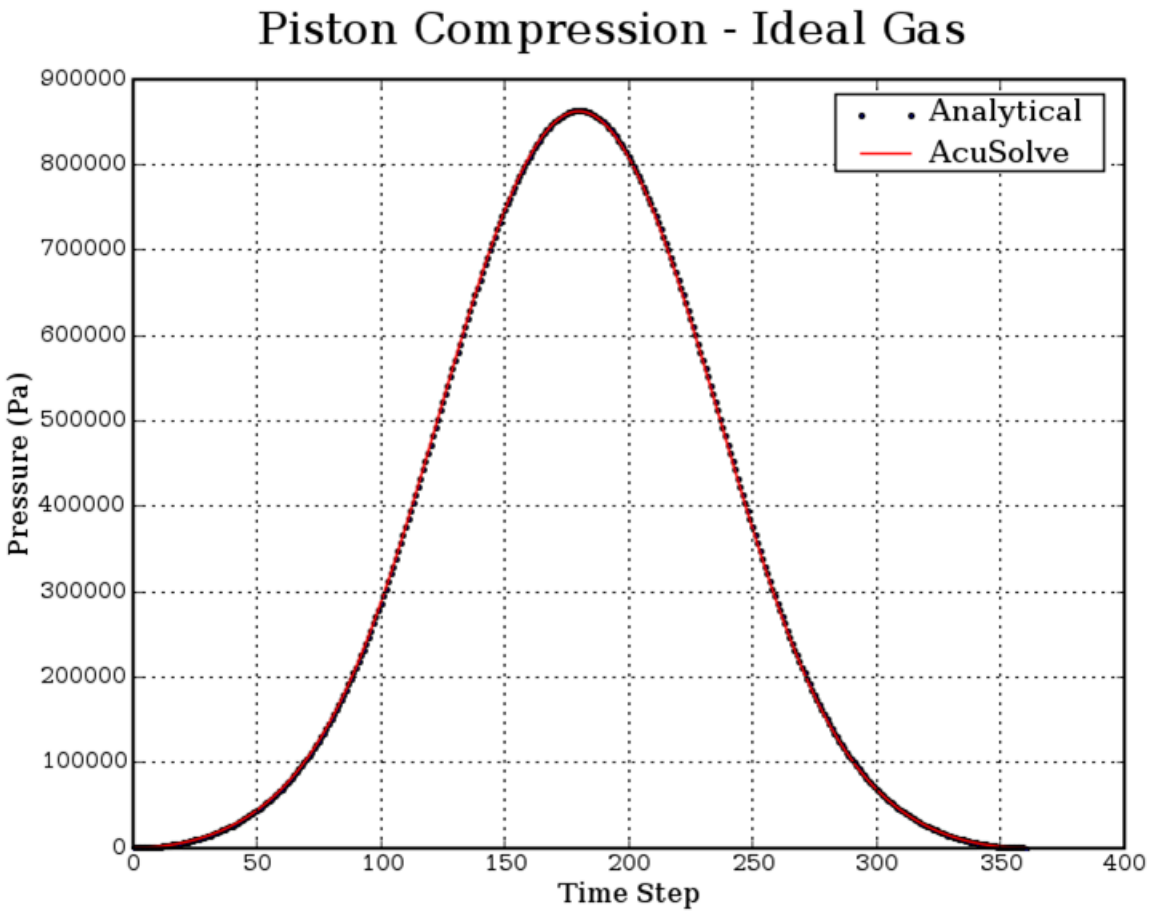


Figure 511: History Plots of Pressure for AcuSolve and Analytical Solutions

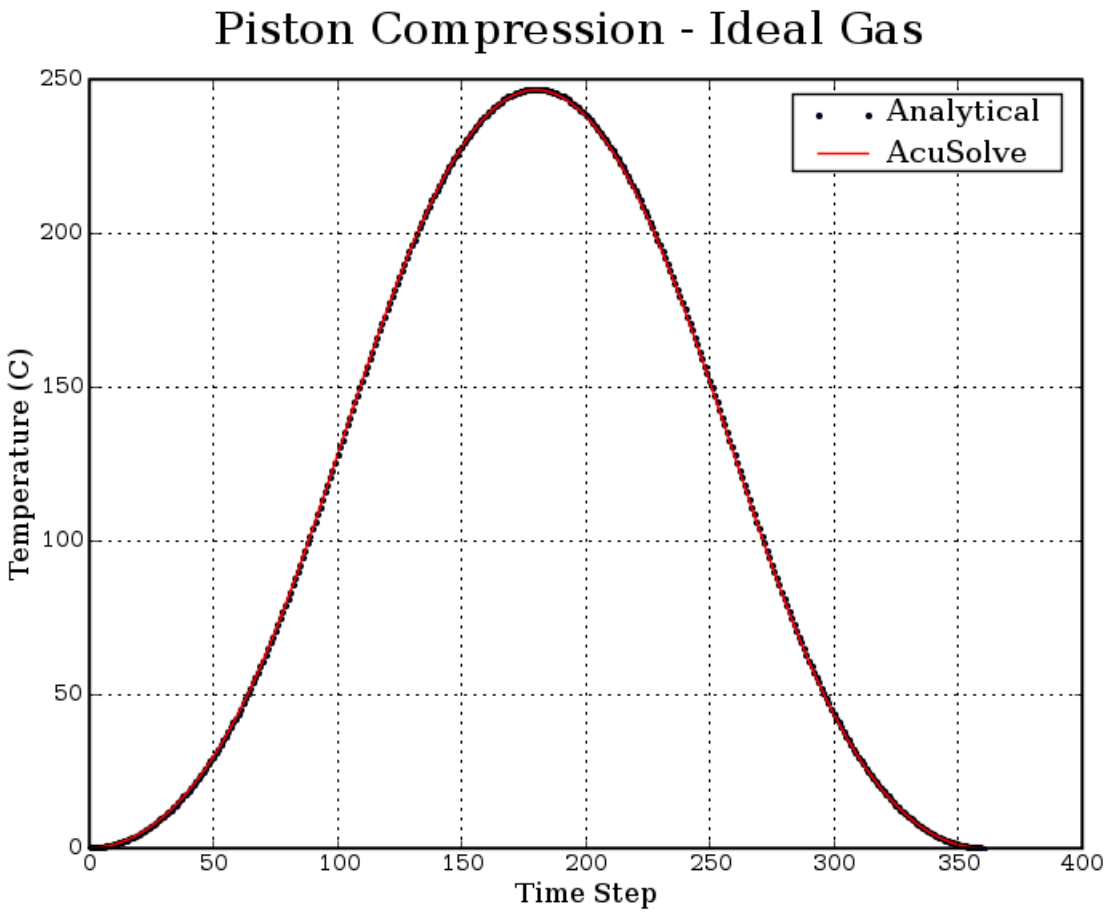


Figure 512: History Plots of Temperature for AcuSolve and Analytical Solutions

Summary

The AcuSolve solution compares well with analytical results for ideal gas compression in an actuating piston. The AcuSolve transient solution compares nearly identically with the analytical solution, with 0.1 percent and 0.16 percent error for the maximum pressure and temperature, respectively. As a result, AcuSolve demonstrates the ability to predict ideal gas compression in an idealized actuating piston.

Simulation Settings for Ideal Gas Compression in an Actuating Piston

HyperMesh CFD database file: `<your working directory>\cylinder_piston_compression\cylinder_piston_compression.hm`

Global

- Problem Description
  - Analysis type - Transient
  - Temperature equation - Advective Diffusive
  - Turbulence equation - Laminar
  - Mesh type - Fully Specified

- Auto Solution Strategy
  - Max time steps - `360`
  - Initial time increment - `0.01667` sec
  - Convergence tolerance - `1.0e-5` sec
  - Max stagger iterations - `10`
- Multiplier Function
  - Piston
    - Type - Piecewise Linear
    - Curve fit variable - Time
    - Curve fit values - (included in database as defined above)
- Material Model
  - Air
    - Density
      1. Type - Ideal Gas
      2. Gas constant - `286.9` J/kg-K
      3. Abs. pressure offset - `101325.0` N/m2
      4. Abs. temperature offset - `273.15` K
    - Viscosity - `1.781e-5` kg/m-sec
- Mesh Motion
  - Piston
    - Type - Translation
    - Translation velocity - `0.0`, `-1.0`, `0.0`
    - Velocity variable - Multiplier Function
    - Translation multiplier function - Piston

  Model
- Volumes
  - Fluid
    - Element Set
      1. Material model - Air
    - Element Output - on
- Surfaces
  - BDC
    - Simple Boundary Condition
      1. Type - Wall
      2. Wall velocity type - Match Mesh Velocity
      3. Mesh displacement BC type - Fixed
  - SideWall
    - Simple Boundary Condition

1. Type - Wall
2. Wall velocity type - Match Mesh Velocity
3. Mesh displacement BC type - Fixed

- TDC
  - Simple Boundary Condition
    1. Type - Wall
    2. Mesh displacement BC type - Fixed
    3. Mesh motion - Piston

- Nodes
  - VolumeNodes
    - Mesh X-Displacement
      1. Type - Zero
    - Mesh Y-Displacement
      1. Type - Linear
      2. Mesh motion - Piston
      3. Curve fit variable - Y reference coordinate
         1. X1 - `10.0` m
         2. Y1 - `1.0` m
         3. Y2 - `0.0` m
    - Mesh Z-Displacement
      1. Type - Zero

References

M.J. Moran and H.N Shapiro. "Fundamentals of Engineering Thermodynamics". Wiley. 4th Ed. 2000.

Intellectual Property Rights Notice

Copyright © 1986-2024 Altair Engineering Inc. All Rights Reserved.

This Intellectual Property Rights Notice is exemplary, and therefore not exhaustive, of the intellectual property rights held by Altair Engineering Inc. or its affiliates. Software, other products, and materials of Altair Engineering Inc. or its affiliates are protected under laws of the United States and laws of other jurisdictions.

In addition to intellectual property rights indicated herein, such software, other products, and materials of Altair Engineering Inc. or its affiliates may be further protected by patents, additional copyrights, additional trademarks, trade secrets, and additional other intellectual property rights. For avoidance of doubt, copyright notice does not imply publication. Copyrights in the below are held by Altair Engineering Inc. or its affiliates. Additionally, all non-Altair marks are the property of their respective owners. If you have any questions regarding trademarks or registrations, please contact marketing and legal.

This Intellectual Property Rights Notice does not give you any right to any product, such as software, or underlying intellectual property rights of Altair Engineering Inc. or its affiliates. Usage, for example, of software of Altair Engineering Inc. or its affiliates is governed by and dependent on a valid license agreement.

Altair® HyperWorks®, a Design & Simulation Platform

Altair® AcuSolve® ©1997-2024

Altair® Activate® ©1989-2024

Altair® Automated Reporting Director™ ©2008-2022

Altair® Battery Damage Identifier™ ©2019-2024

Altair® CFD™ ©1990-2024

Altair Compose® ©2007-2024

Altair® ConnectMe™ ©2014-2024

Altair® DesignAI™ ©2022-2024

Altair® DSim™ ©2024

Altair® EDEM™ ©2005-2024

Altair® EEvision™ ©2018-2024

Altair® ElectroFlo™ ©1992-2024

Altair Embed® ©1989-2024

Altair Embed® SE ©1989-2024

Altair Embed®/Digital Power Designer ©2012-2024

Altair Embed®/eDrives ©2012-2024

Altair Embed® Viewer©1996-2024

Altair® e-Motor Director™©2019-2024

Altair® ESAComp® ©1992-2024

Altair® expertAI™ ©2020-2024

Altair® Feko® ©1999-2024

Altair® FlightStream® ©2017-2024

Altair® Flow Simulator™ ©2016-2024

Altair® Flux® ©1983-2024

Altair® FluxMotor® ©2017-2024

Altair® GateVision PRO™ ©2002-2024

Altair® Geomechanics Director™ ©2011-2022

Altair® HyperCrash® ©2001-2023

Altair® HyperGraph® ©1995-2024

Altair® HyperLife® ©1990-2024

Altair® HyperMesh® ©1990-2024

Altair® HyperMesh® CFD ©1990-2024

Altair® HyperMesh ® NVH ©1990-2024

Altair® HyperSpice™ ©2017-2024

Altair® HyperStudy® ©1999-2024

Altair® HyperView® ©1999-2024

Altair® HyperView Player® ©2022-2024

Altair® HyperWorks® ©1990-2024

Altair® HyperWorks® Design Explorer ©1990-2024

Altair® HyperXtrude® ©1999-2024

Altair® Impact Simulation Director™ ©2010-2022

Altair® Inspire™ ©2009-2024

Altair® Inspire™ Cast ©2011-2024

Altair® Inspire™ Extrude Metal ©1996-2024

Altair® Inspire™ Extrude Polymer ©1996-2024

Altair® Inspire™ Form ©1998-2024

Altair® Inspire™ Mold ©2009-2024

Altair® Inspire™ PolyFoam ©2009-2024

Altair® Inspire™ Print3D ©2021-2024

Altair® Inspire™ Render ©1993-2024

Altair® Inspire™ Studio ©1993-2024

Altair® Material Data Center™ ©2019-2024

Altair® Material Modeler™ ©2019-2024

Altair® Model Mesher Director™ ©2010-2024

Altair® MotionSolve® ©2002-2024

Altair® MotionView® ©1993-2024

Altair® Multi-Disciplinary Optimization Director™ ©2012-2024

Altair® Multiscale Designer® ©2011-2024

Altair® newFASANT™ ©2010-2020

Altair® nanoFluidX® ©2013-2024

Altair® NLVIEW® ©2018-2024

Altair® NVH Director™ ©2010-2024

Altair® NVH Full Vehicle™ ©2022-2024

Altair® NVH Standard™ ©2022-2024

Altair® OmniV™ ©2015-2024

Altair® OptiStruct® ©1996-2024

Altair® physicsAI™ ©2021-2024

Altair® PollEx™ ©2003-2024

Altair® PollEx™ for ECAD ©2003-2024

Altair® PSIM™ ©1994-2024

Altair® Pulse™ ©2020-2024

Altair® Radioss® ©1986-2024

Altair® romAI™ ©2022-2024

Altair® RTLvision PRO™ ©2002-2024

Altair® S-CALC™ ©1995-2024

Altair® S-CONCRETE™ ©1995-2024

Altair® S-FRAME® ©1995-2024

Altair® S-FOUNDATION™ ©1995-2024

Altair® S-LINE™ ©1995-2024

Altair® S-PAD™ ©1995-2024

Altair® S-STEEL™ ©1995-2024

Altair® S-TIMBER™ ©1995-2024

Altair® S-VIEW™ ©1995-2024

Altair® SEAM® ©1985-2024

Altair® shapeAI™ ©2021-2024

Altair® signalAI™ ©2020-2024

Altair® Silicon Debug Tools™ ©2018-2024

Altair® SimLab® ©2004-2024

Altair® SimLab® ST ©2019-2024

Altair® SimSolid® ©2015-2024

Altair® SpiceVision PRO™ ©2002-2024

Altair® Squeak and Rattle Director™ ©2012-2024

Altair® StarVision PRO™ ©2002-2024

Altair® Structural Office™ ©2022-2024

Altair® Sulis™ ©2018-2024

Altair® Twin Activate® ©1989-2024

Altair® UDE™ ©2015-2024

Altair® ultraFluidX® ©2010-2024

Altair® Virtual Gauge Director™ ©2012-2024

Altair® Virtual Wind Tunnel™ ©2012-2024

Altair® Weight Analytics™ ©2013-2022

Altair® Weld Certification Director™ ©2014-2024

Altair® WinProp™ ©2000-2024

Altair® WRAP™ ©1998-2024

Altair® HPCWorks®, a HPC & Cloud Platform

Altair® Allocator™ ©1995-2024

Altair® Access™ ©2008-2024

Altair® Accelerator™ ©1995-2024

Altair® Accelerator™ Plus ©1995-2024

Altair® Breeze™ ©2022-2024

Altair® Cassini™ ©2015-2024

Altair® Control™ ©2008-2024

Altair® Desktop Software Usage Analytics™ (DSUA) ©2022-2024

Altair® FlowTracer™ ©1995-2024

Altair® Grid Engine® ©2001, 2011-2024

Altair® InsightPro™ ©2023-2024

Altair® Hero™ ©1995-2024

Altair® Liquid Scheduling™ ©2023-2024

Altair® Mistral™ ©2022-2024

Altair® Monitor™ ©1995-2024

Altair® NavOps® ©2022-2024

Altair® PBS Professional® ©1994-2024

Altair® PBS Works™ ©2022-2024

Altair® Simulation Cloud Suite (SCS) ©2024

Altair® Software Asset Optimization (SAO) ©2007-2024

Altair® Unlimited™ ©2022-2024

Altair® Unlimited Data Analytics Appliance™ ©2022-2024

Altair® Unlimited Virtual Appliance™ ©2022-2024

Altair® RapidMiner®, a Data Analytics & AI Platform

Altair® AI Hub ©2023-2024

Altair® AI Edge™ ©2023-2024

Altair® AI Cloud ©2022-2024

Altair® AI Studio ©2023-2024

Altair® Analytics Workbench™ ©2002-2024

Altair® Graph Lakehouse™ ©2013-2024

Altair® Graph Studio™ ©2007-2024

Altair® Knowledge Hub™ ©2017-2024

Altair® Knowledge Studio® ©1994-2024

Altair® Knowledge Studio® for Apache Spark ©1994-2024

Altair® Knowledge Seeker™ ©1994-2024

Altair® IoT Studio™ ©2002-2024

Altair® Monarch® ©1996-2024

Altair® Monarch® Classic ©1996-2024

Altair® Monarch® Complete™ ©1996-2024

Altair® Monarch® Data Prep Studio ©2015-2024

Altair® Monarch Server™ ©1996-2024

Altair® Panopticon™ ©2004-2024

Altair® Panopticon™ BI ©2011-2024

Altair® SLC™ ©2002-2024

Altair® SLC Hub™ ©2002-2024

Altair® SmartWorks™ ©2002-2024

Altair® RapidMiner® ©2001-2024

Altair One® ©1994-2024

Altair® CoPilot™ ©2023-2024

Altair® License Utility™ ©2010-2024

Altair® TheaRender® ©2010-2024

OpenMatrix™ ©2007-2024

OpenPBS® ©1994-2024

OpenRadioss™ ©1986-2024

October 7, 2024

Technical Support

Altair's support resources include engaging learning materials, vibrant community forums, intuitive online help resources, how-to guides, and a user-friendly support portal.

Visit Customer Support to learn more about our support offerings.

Index

A

AcuSolve validation manual introduction *6*

C

circumferential flow in a cylinder induced by a rotating solid *264*, *412*, *513*, *629*
compressible *675*

E

external flow *450*

F

flow between concentric cylinders *112*, *311*, *330*, *652*
flow inside a rotating cavity *128*, *276*, *346*, *658*

H

heat transfer between radiating concentric cylinders *212*, *317*, *400*, *582*
heat transfer between radiating concentric spheres *234*, *418*, *588*
heat transfer/radiation *544*

I

ideal gas compression in an actuating piston *535*, *607*, *642*, *681*
internal flow *329*

L

laminar couette flow with imposed pressure gradient *122*, *270*, *340*
laminar couette flow with imposed pressure gradient and heated walls *257*, *323*, *444*, *622*
laminar flow *263*
laminar flow past a 90 degree t-junction *142*, *284*, *360*
laminar flow past a 90° t-junction *142*, *284*, *360*
laminar flow through a channel with heated walls *147*, *365*, *551*
laminar flow through a pipe with constant wall temperature *556*
laminar flow through pipe, imposed heat flux *561*
laminar poiseuille flow through a pipe *289*
laminar to turbulent transition over an airfoil *223*, *483*, *502*

M

moving mesh *628*
multiphase *666*
multiphase flow of a 2d dam break *667*

N

natural convection in a concentric annulus *136*, *305*, *354*, *545*

O

oscillating laminar flow around a circular cylinder *293*, *466*, *508*

R

reference frame *651*

S

separated laminar flow over a blunt plate *183*, *298*, *471*
single-phase nucleate boiling in rectangular channel *9*, *239*, *427*, *597*
steady flow *111*
supersonic flow through converging-diverging nozzle *92*, *432*, *523*, *602*, *676*

T

transient flow *507*
transitional flow *501*
turbulent flow *8*
turbulent flow behind open-slit v *18*, *152*, *451*
turbulent flow over backward-facing step *33*, *198*, *386*
turbulent flow over naca 0012 airfoil *55*, *159*, *458*
turbulent flow over oscillating rigid body assembly *104*, *488*, *528*, *635*
turbulent flow past convex curve in channel *40*, *205*, *393*
turbulent flow past wall-mounted hump *97*, *244*, *437*
turbulent flow through 180 degree curved channel *63*, *228*, *406*
turbulent flow through heated periodic channel *77*, *251*, *495*, *616*
turbulent flow through pipe *14*, *118*, *336*
turbulent flow through wavy channel *69*
turbulent flow with separation in an asymmetric diffuser *25*, *190*, *378*
turbulent mixing layers in open channel *83*, *218*, *478*
turbulent natural convection inside tall cavity *47*, *167*, *370*, *566*
two-phase nucleate boiling in cylindrical pipe *88*, *423*, *519*, *593*, *671*

V

viscous heating inside a rotating annulus *175*, *574*